Seventh International Visual Field
Symposium, Amsterdam, September 1986

Documenta Ophthalmologica Proceedings Series

Seventh International Visual Field
Symposium, Amsterdam, September 1986

Edited by E.L. Greve and A. Heijl

Copyright

Contents

Obituary

Charles Dexter Phelps, M.D. (1937–1985)

It was with great regret that we heard that Charles Phelps died on the 13th of September, 1985, three days prior to his 48th birthday He played a prominent role in the affairs of the International Perimetric Society and was Chairman of the Glaucoma Group at the time of his death.

Charles Phelps was born on the 16th of September, 1937. He was the son of an Iowa Opthalmologist. He obtained his medical degree at the University of Iowa, interned at the Boston City Hospital and then took his residency training in Ophthalmology in Iowa City. He followed this with a glaucoma fellowship at Washington University in St. Louis and was invited to return back to the University of Iowa to take over the Glaucoma Department which he led for 13 years.

Dr. Phelps was greatly admired as an outstanding human being He was friendly, charming, gracious, had a profound knowledge of his subject and a good deal of common sense. He was witty and was an engaging public speaker. He made many contributions to all areas of glaucoma research and many of his investigations have included perimetry.

Although Charles was already considered one of the leading glaucoma experts he was still so young that the would have undoubtedly made many more contributions to the field of glaucoma and perimetry.

Charles is survived by his wife and companion Dorsey Phelps, two sons, two daughters, his parents, and three brothers. All of us who have known him are poorer for his passing and the International Perimetric Society has lost one of its outstanding members, a prolific contributor, an exceptionally honest, warm human being and above all a great friend.

Stephen M Drance, M.D

Introduction

The Seventh International Visual Field Symposium organized by the International Perimetric Society was held in Amsterdam, The Netherlands, September 6–10, 1986. In many respects it was an exciting and fruitful meeting The number of participants was greater than ever. The number of papers was too great to accommodate all of them. The quality of the papers reflects the continuously rising interest in perimetry in general and in automated perimetry in particular Last but not least the social programme was organized in the, by now, almost classical friendly, enjoyable and humouristic style of the International Perimetric Society. This created an atmosphere of openness and free exchange of information which was clearly also felt in the scientific sessions.

The scientific part was divided in seven sessions with 44 spoken papers and a separate postersession during which the 46 posters were discussed. The major themes of the meeting were 'The influence of media-disturbances on the visual field' and 'Advances in perimetry in glaucoma with special emphasis on progression'.

The session on 'media' provided interesting information on how the visual field was effected by preretinal filters. The authors either studied the influence of lens- or corneal opacities or simulated opacities by special filters placed in front of the eye. In two papers the effect of cataract was qualified by photography or straylight measurements.

In the glaucoma-sessions several papers dealt with the correlation between the optic disc and the visual field. Part of these studies included longterm comparisons of optic disc- and visual field parameters The different distribution of visual field defects (a subject also discussed in 1982) was approached from a different point of view in three papers. This time the authors agreed that a diffuse reduction of sensitivity is more often seen in glaucomapatients with high intra-ocular pressures while more localized defects tend to be associated with lower intra-ocular pressures.

The effect of treatment of glaucoma on the visual field was considered The interesting concept of the safe level of intra-ocular pressure was discussed in two

papers. These papers reflect the general feeling that there is no magic number of intra-ocular pressures below which the visual field will not progress. It would be advantageous if this level could be determined in the individual case. The scala of low-tension glaucomas was extended by the so-called vasospastic syndrome. Migraine-patients show damage that many resemble low-tension glaucoma. The relatively frequent occurence of migraine in glaucoma has been reported separately in the literature.

A special session was devoted to variability of perimetric results. Short- and long-term fluctuation, fatigue, reliability parameters etc. were considered in several highly interesting papers. The present main trend in visual field research is the statistical analysis of the results of automated perimetry Several parameters have been proposed to indicate the characteristics of a visual field defect. The papers in this meeting have brought us again closer to the understanding of the factors that influence fluctuation and in particular have provided new ways for dealing with these factors clinically

A special session was devoted to ergoperimetry. An extensive report was presented on the method used in many countries to express visual disability. A plea was made for the use of a common language in automated perimetry. Indeed, we have strayed far from the standard offered by manual Goldmann-type kinetic perimetry. There are many different examination strategies, statistical analyses, printouts and even different types of automated perimeters. The aim should be to come to a more standardized way of examining and analysing normal fields using automated perimetry It looks as if the first steps in that direction have been made.

The effect of chiasmal tumours on the visual field was discussed in three papers. Neuro-ophthalmological perimetry will be the subject of the next meeting of the IPS in 1988 in Vancouver.

A number of interesting papers dealt with so-called special methods, i.e. methods that do not use the classical set-up of a perimeter measuring the differential threshold. Fundus perimetry, although not widely used, presents interesting possibilities for direct correlation of fundus – characteristics and lightsensitivity. One paper described the correlation between lightsensitivity and the peripapillary changes. Foveal thresholds, multi-flash presentations, pattern discrimination, computer graphics, fatigue were among the other special methods presented in this meeting. Each of these will have to show that it provides more information than carefull examination of the differential threshold without increasing the difficulty of the patients task.

Several new automated perimeters were introduced and existing perimeters were evaluated.

This introduction can only describe some headlines of the many subjects that were presented during this succesfull meeting of the IPS. We look forward to an even more memorable meeting in 1988.

The organization of the IPS was and is in the able hands of Anders Heijl. His

dedicated enthousiasm has provided a smoothly scientific programme The local organization was headed by Erik Greve with the assistance of Dorine de Jong, Douwe Bakker, At Zeilstra, Marjoleine Raakman, Els Mutsaerts, Stella Ompi and Marianne Wagemans.

Vivat, crescat, floreat IPS.

The editors

Section I
Influence of media opacities on the visual field

I.1 Influence of ocular media on perimetric results: effect of IOL implantation

PH. HENDRICKSON, D. EICHENBERGER, B GLOOR and Y. ROBERT
Zürich, Switzerland

Abstract

Improvement in Octopus G-1 perimetric results following cataract surgery and intraocular lens implantation was compared with improvement in the Contrast Transfer Ratio (CTR) The latter provides an objective measurement of the imaging quality of the ocular media. All examinations were performed prior to surgery, as well as one and six weeks post-operatively.

This investigation afforded evaluation of how well the Contrast Transfer Ratio can serve to discriminate loss of light sensitivity caused by opacification of the refractive media from that caused by disease of the retina or of the optic nerve. Although visual acuity improved between one and six weeks following the lens implantation, this was much more obviously seen in appropriate improvement in the visual acuity and the CTR than in the visual field parameters, such as Mean and Central Sensitivity. In view of the strict inclusion criteria for the subjects in this study, the CTR is seen to demonstrate the actual ability of the ocular media to transfer contrast, that is, how well the ocular media perform.

Introduction

If the aging lens, in becoming more and more opaque, acts as a diffuser, not only will the image falling onto the retina become worse but also there will be a deterioration in visual performance as a whole, seen, for example, in the results of visual field examination. Looking through the ocular media the other way around, that is, ophthalmoscopically, bright and dark features of the ocular fundus will be less well transfered as such through the eye to a viewer in front. The greater the extent of opacification, the less will be the contrast difference between those two features. Recently [2] we reported the corroboration of this idea by means of the photopapillometer. This instrument [3, 4] measures the brightness of any chosen spot on the retina, such as the papilla or the macula, which then

conveniently serve as distinct targets differing considerably in their brightness. The resulting 'Contrast Transfer Ratio (CTR)' serves as a measure of the ability of the ocular media to transfer contrast, determining objectively that which cataract surgeons can only subjectively estimate before every operation.

Seen in the results of our investigations on the effects of simulated cataract (using orthoptic occlusion material from the Ryser Company, St. Gallen, Switzerland) on performance in visual field examinations [1] the opaque lens acts as a diffuser. Therefore, in the present study, we sought to elucidate the diffuser effect in vivo with regard to influences on the performance in Octopus G-1 testing. In establishing this relationship, it might become possible in the case of combined cataract *and* glaucoma to identify and subtract the effect of the former from that of the latter in such testing Our first task was to establish a relationship between the Contrast Transfer Ratio (CTR) and the visual field in cataract patients with otherwise 'healthy' visual fields. For comparison with an old, trusted parameter, we also measured the visual acuity.

Methods

Patients who preoperatively passed the following inclusion criteria were chosen for the study:
1. no history of visual field loss (damage) with other etiology,
2. no ocular hypertension,
3. no glaucoma,
4. no vascular occlusion,
5. no retinitis pigmentosa,
6. no known macular disease.
Nine patients fulfilled these requirements. Shortly before, one week after, and six weeks after cataract removal and intraocular lens implantation surgery, visual examination with the Octopus G-1 program provided values for the Mean and Central Sensitivities At the same times, the visual acuity and the Contrast Transfer Ratio (CTR) were measured.

Results

The standard measure, visual acuity, improves in a manner like that of the CTR (Fig. 1). This is reassuring because the photopapillometer is shown to be capable of measuring objectively a property of the lens itself, here not how it *is* (density), but of obvious and much greater importance, how it *performs* (contrast transfer). The post-operative acuity improves to the same extent as does the CTR. Of further interest is the fact that subsequent improvement in the acuity between 1 and 6 weeks is accompanied by a like improvement in the CTR; the former is
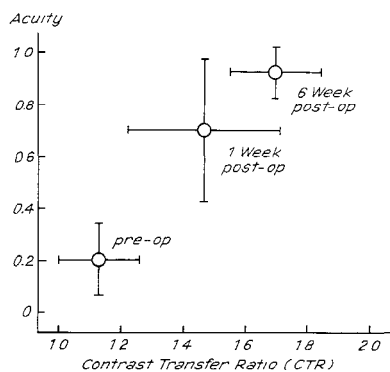
Figure 1 The relationship between acuity and Contrast Transfer Ratio is demonstrated as group mean values of the former versus group mean values of the latter The extents of the standard deviations run parallel to the respective axes Continued improvement in both parameters is seen between 1 and 6 weeks

likely provided by the latter Clinicians would probably suggest that the improvement between 1 and 6 weeks is due to a lessening of post-operative inflammation. Therefore, whenever an immediately post-operative visual acuity doesn't meet expectations, the determination of the Contrast Transfer Ratio with the photopapillometer could help demonstrate objectively the actual optical performance of the ocular media.

In Figures 2 and 3 we have plotted the group mean values for Mean Sensitivity versus the group mean values for CTR and acuity, respectively. Like improvement in both relationships is seen; however, it is obvious, indeed, that the G-1
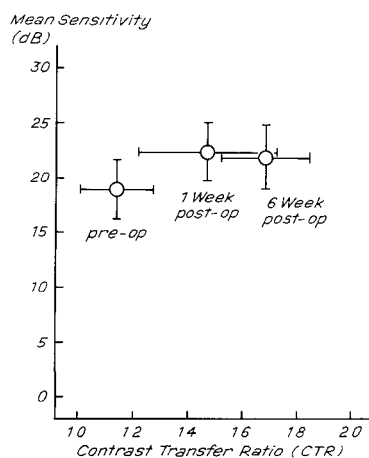
Figure 2 Improvement in Mean Sensitivity is related to the Contrast Transfer Ratio in a plot as in Figure 1 That only modest improvement occurred immediately post-operatively and not at all between 1 and 6 weeks is obvious
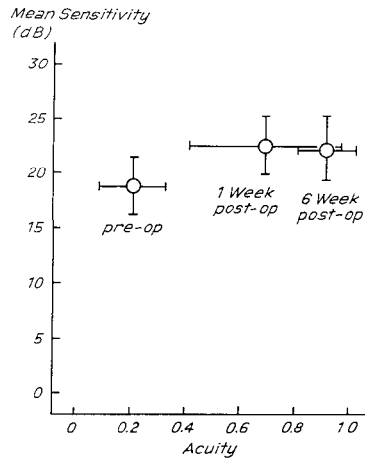
Figure 3 Mean Sensitivity versus acuity shows virtually the same modest improvement as in Figure 2

measured Mean Sensitive is not as markedly improved through implant surgery as is the visual acuity (Fig. 1). Mean Sensitivity seems more likely to be a glaucoma parameter than one of cataract This assumption obviously requires further proof

In Figures 4 and 5 the group mean values for Central Sensitivity have been plotted against the group mean values for CTR and acuity, respectively Central
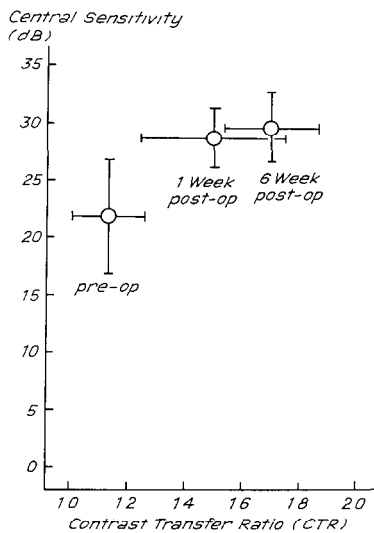
Figure 4 When Central Sensitivity is plotted versus Contrast Transfer Ratio, a slight improvement between 1 and 6 weeks is noticed, but, again, the weak correlation between these two parameters is demonstrated
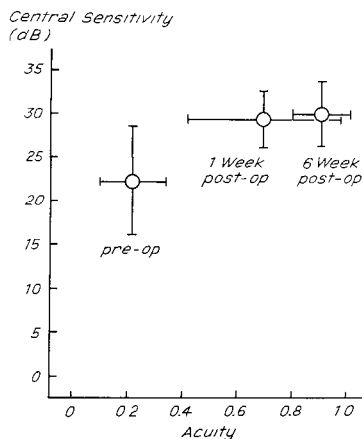
Figure 5 Improvement in Central Sensitivity with regard to acuity indicates a similar weakness of correlation as that between the two parameters (CS and CTR) in Figure 4

Sensitivity demonstrates a course over the three examination times similar to that of Mean Sensitivity (Figs 2 and 3) Visual acuity and the CTR improved between the 1- and 6-week examinations in a similar manner, while the visual field parameters remained, moreover, unchanged.

Discussion

Clinically, lens opacities have a subjective effect on the patient's visual perception: images become blurred Objectively, such blurring consists of a reduction of the maxima of dark and light in object space as well as a loss of sharpness in the boundaries between such maxima – contrast becomes diminished [2]. Until recently the visual acuity (subjective) was the only available way to estimate the optical performance of the ocular media, *but then only indirectly so* Now, by determining the Contrast Transfer Ratio, the diffuser effect can be *objectively* and *directly* quantified. Our investigations demonstrate that these parameters (acuity and CTR) behave in a like manner, as long as no other pathology is present

The differential light sensitivity, too, measured with static computerized perimetry, points in the same direction, but not to the same extent as does the CTR with regard to clearly following the recovery of visual function after IOL implantation.

Couching these statements in cautious terms, the question posed in the introduction, whether visual field damage due to glaucoma and that imparted by a cataract may be differentiated, can be answered positively. That is, namely, preoperatively the Central Sensitivity is only slightly disturbed by a cataract. If a grave disturbance occurs, it is probably due to glaucoma.

Conclusions

The introduction of the measurement of the Contrast Transfer Ratio provides us for the first time an exact, objective measure of the actual performance of the ocular media with regard to their ability to transfer contrast and, therefore, to their role in the results of visual field examination. An appropriate next step from this present study would be to determine the behavior of these same parameters (visual field, visual acuity, and CTR) in glaucoma patients.

References

1 Eichenberger D, Hendrickson Ph, Robert Y, Gloor B: Influence of ocular media on perimetric results: effect of simulated cataract Proceedings of the International Perimetric Society Meeting, Amsterdam, 6–10 September 1986
2 Hendrickson Ph, Robert Y: Klinische Bestimmung des funktionellen Trübungsgrades einer Katarakt (Pap/Mak-Verhältnis): Theorie und Technik Klin Mbl Augenheilk 188: 421–424 (1986)
3 Hendrickson Ph, Robert Y, Stöckli H-P: Principles of photometry of the papilla Arch Ophthalmol (Chicago) 102: 1704–1707 (1984)
4 Robert Y, Hendrickson Ph: Color appearance of the papilla in normal and glaucomatous eyes: a photopapillometric study Arch Ophthalmol (Chicago) 102: 1772–1775 (1984)

Author's address:
Dr phil Ph Hendrickson,
Universitäts-Augenklinik,
Rämistrasse 100, CH-8091 Zürich, Switzerland

I.2 Influence of ocular media on perimetric results: effect of simulated cataract

D. EICHENBERGER, PH. HENDRICKSON, Y. ROBERT and B GLOOR
Zürich, Switzerland

Abstract

The influence of changes of the ocular media, in the form of both image degrada-
tion and light attenuation, on the results of perimetric examination was investig-
ated in normal subjects whose visual fields were examined with the Octopus G-1
program. Degradation of the visual image was accomplished by means of dif-
fusers (orthoptic occlusion material standardized for various visual acuities). Loss
of sensitivity in examinations performed through the diffusers was correlated to
visual acuity

The effect of light attenuation, as seen clinically e g. in cataracta brunescens,
was simulated by performing further G-1 examinations through selected Kodak
neutral density filters.

Both forms of ocular media changes were subsequently compared with regard
to their influence on the Mean and Central Sensitivities as well as the Loss
Variance Considering the results of similar testing in patients before and after
lens implantation surgery, the behavior of the parameters with diffusers was seen
to be similar to that with cataract.

Introduction

In order to elucidate the effects of filtration and diffusion by lens opacities on
perimetric results, normal subjects were examined with Octopus G-1 testing
while viewing through various steps of neutral density filtration [3] and diffusion
material. The similarity between these results and those of actual in-vivo cataract
influence on visual field parameters could then be examined

Methods

Seven healthy, young (mean age = 24.7 years) volunteers underwent Octopus G-1 visual field examinations while viewing through Kodak neutral density filters (Nos. 1, 2, 3 and 4) and through orthoptic standard occlusion diffusers (acuities of 0.1, 0.3, and 0.6 – Ryser Optical Company, St. Gallen,, Switzerland). The data accumulated included Mean and Central Sensitivities, Loss Variance, and visual acuity. Between examination phases the subjects were provided with light-shielding hoods and goggles.

Results

Taking visual acuity as a guideline, the neutral density filters (Fig. 1) were seen to degrade the Mean and Central Sensitivities much more than did the diffusers (Fig. 2). One should bear in mind that neutral density filters are logarithmically scaled. On a log-log plot (decibels sensitivity vs. log-steps of filtration) a straight line was observed. More unexpected, indeed, is that the Loss Variance (Fig. 3) increased with the increasing neutral density filtration in a linear manner, contrary to the effect seen with diffusers (Fig. 4).

Discussion

When clinical Contrast Transfer Ratio (CTR) [2] data are plotted along the normal curve (Fig. 5) and these are compared with the slopes of the sensitivity
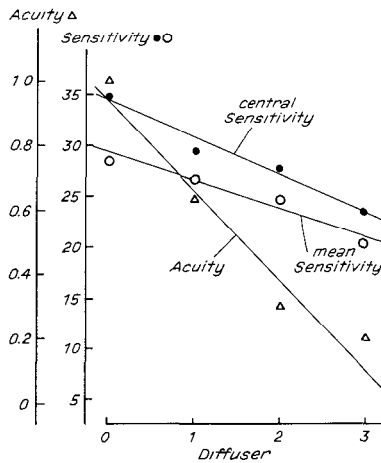
Figure 1 The behavior of the visual field parameters runs about parallel to that of visual acuity The only apparent effect of the neutral density filters seems to be that of light attenuation at the fundus
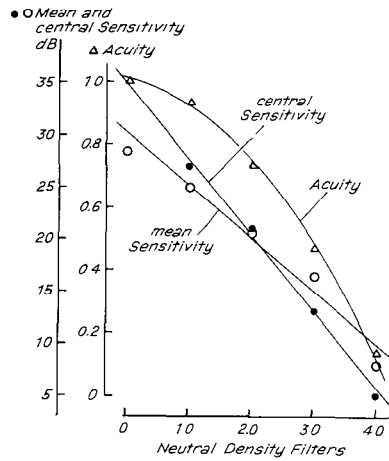
Figure 2 With increasing diffuser effect, an obvious discrepancy between the rate of visual acuity impairment and that of the visual field parameters is seen; acuity decreases more rapidly with increasing diffusion

curves in Figure 6, the similarity between cataract and diffusers is obvious

As is indicated in Figure 6, the perimetric parameter, Central Sensitivity, was considerably less affected by a diffuser being placed into the viewing system than was the case with the neutral density filters. If a cataract acts as a diffuser, one could expect its effect on the Sensitivities as well to be less pronounced than that which light attenuation has [1]. Those authors, by determining the ability of the
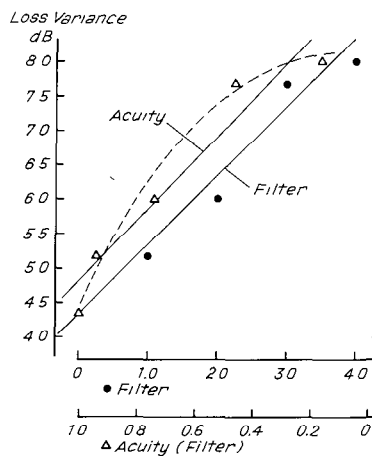
Figure 3 Increase in the Loss Variance follows the increase in neutral density filter light attenuation linearly

12
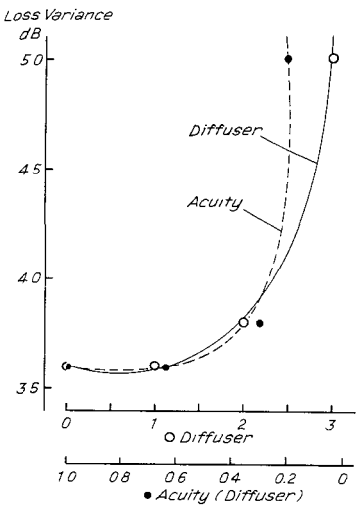
Figure 4 The unusual effect of diffusers on the Loss Variance is demonstrated with the corresponding visual acuity (measured through the diffusers)

ocular media to transfer contrast (objective Contrast Transfer Ratio), could demonstrate that a cataract has a more marked effect on the visual acuity than it does on the perimetric parameters, acting, therefore, like a diffuser.
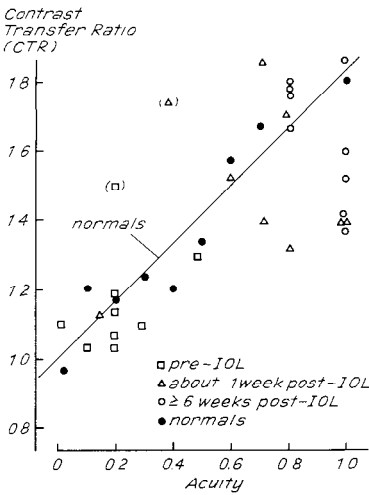
Figure 5 Superimposed onto a plot of Contrast Transfer Ratio data from otherwise normal persons at various stages of cataract development (closed circles and line) are data from cataract patients before and after cataract and implant lens surgery
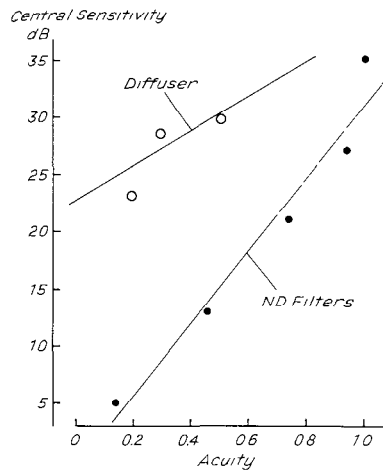
Figure 6 The effect of diffusers on the visual acuity runs parallel to the line of best fit through the clinical data seen above

References

1 Hendrickson Ph, Eichenberger D, Gloor B, Robert Y: Influence of ocular media on perimetric results: effect of IOL implantation Proceedings of the International Perimetric Society Meeting, Amsterdam, 6–10 September 1986
2 Hendrickson Ph, Robert Y: Contrast transfer ratio in normal, cataractous, and intraocular implant lenses: a clinical photopapillometric study Graefe's Arch Clin Exp Ophthalmol 224: 191–194 (1986)
3 Klewin K, Radius R: Background illumination and automated perimetry Arch Ophthalmol (Chicago) 104: 395–397 (1986)

Author's address:
Dr phil Ph Hendrickson,
Universitäts-Augenklinik,
Rämistrasse 100, CH-8091 Zürich, Switzerland

I.3 The influence of simulated media opacities on threshold measurements

D.K. HEUER, D.R. ANDERSON, W.J FEUER, R W. KNIGHTON,
M.G. GRESSEL and F.E. FANTES
Los Angeles, U S.A.

Abstract

The absorbing, scattering, and blurring effects of media opacities on Octopus 201 perimeter and/or Humphrey Field Analyzer threshold measurements were simulated in the right eyes of five subjects with randomly-ordered series of neutral density filters (NDFs), diffusers, and spherical plus overcorrections Threshold measurements were performed 0°, 5°, 10°, 15°, 20°, and 25° nasally along the 180° meridian with the F4 program on the Octopus 201 perimeter and with twice-repeated profiles on the Humphrey Field Analyzer.

A 0.6 log unit NDF, which reduces retinal illumination the equivalent of halving the pupillary diameter, decreased the mean Octopus threshhold measurements by an average of 1.7 dB and the mean Humphrey threshold measurements by an average of 1.1 dB Diffuser 4, with which visual acuities were 0.67–1.00 (mean $\pm$ SD = 0.87 $\pm$ 0.18) and with which Miller-Nadler glare disability scores were 20%–45% (mean $\pm$ SD = 35.0 $\pm$ 11.7%), decreased the Octopus threshold measurements by an average of 6.6 dB and the Humphrey threshold measurements by an average of 8.1 dB. One and two diopters spherical plus overcorrections decreased the Octopus threshold measurements by an average of 1.4 dB and 2.9 dB, respectively.

Our data suggest that even media changes that cause only negligible effects on visual acuities may influence threshold measurements

Introduction

The differential light threshold is influenced by numerous, often related factors, such as the subject's age, alertness, media clarity, ocular diseases, ocular medications, and systemic medications. We sought to better understand the influence of media opacities on threshold measurements by simulating their absorbing, scattering, and blurring effects with neutral density filters (NDFs), diffusers, and spherical plus overcorrections.

Subjects and methods

Five ocular normals, aged 30–46 (mean ± SD = 35 8 ± 7.6) years, underwent threshold measurements on their right eyes with series of randomly-ordered NDFs (0.0, 0.3, 0.6, 1 0, 1 5, 2.0, and 3.0 log unit[s]), diffusers (0.00, −0.23, −0.31, −0 38, −0.64, −0 93, and −1.24 log relative transmittance), and spherical plus overcorrections (plano, +1.00, +2 00, +3 00, +4.00, +5 00, and +6.00 diopter[s]) The subjects had cycloplegic refractive errors of +0.75 to −2.25 (mean ± SD = 0 40 ± 1 23) diopters spherical equivalent, with no more than 0 50 diopter of astigmatism (one subject's refractive error was actually −3.50 + 4 00 × 90; however, with his hard contact lens, which was worn for all threshold measurements, his cycloplegic refractive error was +0.75 diopter sphere). Each series of threshold measurements on an individual subject was completed in a single session with rest as necessary between threshold profiles, and only one series of thresholds was performed on any subject on any one day. For the series of NDFs, subjects' right pupils were dilated with either tropicamide 1% and phenylephrine hydrochloride 2.5% (Octopus 201 perimeter threshold profiles) or cyclopentolate hydrochloride 1% (Humphrey Field Analyzer threshold profiles). The NDFs were incorporated in aviator goggles to eliminate stray light that might influence retinal adaptation, and the following protocol was used to allow for dark adaptation ten minutes at the beginning of the NDF series; ten minutes whenever the NDF density was increased 1 0 log unit or more, five minutes whenever the NDF density was increased at least 0.5 log unit, but less than 1.0 log unit; and approximately three minutes whenever the NDF density was decreased or increased less than 0 5 log unit. For the series of diffusers, the subjects' pupils were not pharmacologically manipulated Immediately before the series of spherical plus overcorrections, cycloplegic refractions were performed 40 minutes after the last of three drops of 1% cyclopentolate hydrochloride (drops instilled ten minutes apart), cycloplegia was maintained during threshold testing with the administration of supplemental drops of 1% cyclopentolate hydrochloride after the cycloplegic refraction and after every other threshold profile. Optical corrections appropriate for subject age and perimeter bowl radius were provided The threshold measurements were performed with a Goldmann size III stimulus at 0°, 5°, 10°, 15°, 20°, and 25° nasally in right eyes along the 180° meridian with the F4 program (four threshold measurements at each test point) on an Octopus 201 perimeter and with a profile program (run twice) on a Humphrey Field Analyzer The F4 program for any given diffuser on the Octopus 201 perimeter was repeated in sequence if the standard deviation for the four threshold measurements at any test point was >3.0 dB; the subsequent threshold profile measurements for that diffuser were used for data analysis. The mean and standard deviation of the threshold values for the five subjects were calculated from the mean threshold values of the individual subjects at each test point for each NDF, diffuser, and spherical plus overcorrection.

Visual acuities (starting with NDF 3.0 log units, diffuser 6, or +6 00 spherical overcorrection and progressing in descending order to no NDF, no diffuser, or plano spherical ovecorrection, respectively) were measured on Diabetic Retinopathy Study Charts 1–4 with luminance of $60 \, cd/m^2$

For the diffusers, glare disabilities (starting with diffuser 6 and progressing in descending order to no diffuser) were measured with a Miller-Nadler glare tester. To determine to what extent the measured glare disability was caused by image contrast degradation rather than light scattering, glare disabilities were also measured while the bright surround on the Miller-Nadler glare tester was masked and the central Landolt C was viewed through a 2.0 cm hole

Results

The NDF threshold measurement data from the Octopus 201 perimeter and the Humphrey Field Analyzer are summarized in Tables 1 and 2, respectively The diffuser threshold measurement data from the Octopus 201 perimeter and the Humphrey Field Analyzer are summarized in Tables 3 and 4, respectively The spherical plus overcorrection threshold measurement data from the Octopus 201 perimeter are summarized in Table 5. The visual acuity data for the NDFs,

Table 1 Influence of neutral density filters on Octopus 201 perimeter threshold measurements (dB; mean ± SD)

NDF[1]	Eccentricity					
	0°	5°	10°	15°	20°	25°
None	35 4 ± 3 2	32 9 ± 1 5	31 0 ± 1 8	30 6 ± 1 9	28 5 ± 1 9	28 1 ± 2 0
0 3 log	33 9 ± 2 4	31 4 ± 1 6	30 0 ± 1 5	29 0 ± 1 5	27 8 ± 0 8	26 2 ± 1 6
0 6 log[2]	33 2 ± 3 8	30 9 ± 2 7	29 6 ± 1 9	28 9 ± 2 2	27 4 ± 2 9	26 2 ± 2 5
1 0 log[3]	*31 3 ± 2 1*	29 6 ± 2 0	28 0 ± 1 5	27 0 ± 1 1	25 4 ± 2 0	*24 1 ± 1 6*
1 5 log[4]	25 7 ± 3 1	25 2 ± 2 6	*24 3 ± 2 0*	23 4 ± 2 6	*22 5 ± 1 8*	*20 2 ± 2 3*
2 0 log	*23 3 ± 1 6*	*23 2 ± 1 8*	22 9 ± 1 6	21 9 ± 1 2	*21 0 ± 2 0*	20 7 ± 1 4
3 0 log[5] [6]	*10 6 ± 3 1*	*16 8 ± 3 3*	*17 3 ± 2 5*	*16 9 ± 2 0*	*15 9 ± 2 5*	*14 6 ± 2 4*
cv (cd)[7]	32 9 (2 5)	30 8 (2 1)	29 7 (1 3)	29 3 (1 3)	26 8 (1 7)	26 0 (2 1)

[1] NDF = neutral density filter

[2] Repeated in one subject because of 4 3 dB standard deviation of threshold measurement at 15°

[3] Repeated in one subject because aviator goggles fogged

[4] Repeated in one subject because of 3 4 dB standard deviation of threshold measurement at 10°

[5] Repeated in one subject because of 3 8 dB standard deviation of threshold measurement at 0°

[6] Repeated in one subject because of 4 2 dB standard deviation of threshold measurement at 5°

[7] cv (cd) = critical value (critical difference) from Dunnett's test (one-tailed $p = 0 \, 05$); threshold values below critical value italicized

Table 2 Influence of neutral density filters on Humphrey Field Analyzer threshold measurements (dB; mean ± SD)

NDF[1]	Eccentricity					
	0°	5°	10°	15°	20°	25°
None	37 7 ± 1 8	33 4 ± 0 9	31 4 ± 0 5	31 2 ± 1 9	28 5 ± 2 4	26 6 ± 2 4
0 3 log	36 3 ± 2 5	32 6 ± 1 5	31 4 ± 1 1	*29 2 ± 0 8*	27 6 ± 1 2	25 8 ± 1 3
0 6 log	37 0 ± 1 8	32 0 ± 1 0	30 8 ± 0 8	*29 2 ± 0 8*	27 7 ± 0 9	25 4 ± 1 5
1 0 log	35 1 ± 2 2	*31 3 ± 1 2*	29 4 ± 2 3	*28 0 ± 1 6*	26 9 ± 1 7	*24 1 ± 1 5*
1 5 log	*31 9 ± 1 9*	*29 0 ± 1 2*	27 8 ± 1 5	26 2 ± 1 3	*24 8 ± 1 5*	22 2 ± 2 6
2 0 log	*29 5 ± 1 6*	*26 6 ± 1 8*	26 2 ± 1 3	25 6 ± 0 9	*23 1 ± 2 3*	*21 0 ± 1 6*
3 0 log	*21 6 ± 1 5*	*21 5 ± 1 4*	*20 4 ± 0 9*	*19 4 ± 1 7*	*17 7 ± 2 3*	*15 8 ± 2 3*
cv (cd)[2]	34 3 (3 4)	31 8 (1 6)	29 8 (1 6)	29 4 (1 8)	26 2 (2 3)	24 2 (2 4)

[1] NDF = neutral density filter

[2] cv (cd) = critical value (critical difference) from Dunnett's test (one-tailed p = 0 05); threshold values below critical value italicized

Table 3 Influence of diffusers on Octopus 201 perimeter threshold measurements (dB; mean ± SD)

Diffuser	LRT[1]	Eccentricity					
		0°	5°	10°	15°	20°	25°
None	0 00	35 8 ± 2 3	33 3 ± 1 4	31 8 ± 0 9	31 1 ± 1 7	30 0 ± 1 8	29 1 ± 2 5
1	− 0 23	33 8 ± 3 1	*31 6 ± 0 9*	30 6 ± 1 7	30 1 ± 1 1	28 7 ± 1 8	*27 3 ± 1 8*
2	− 0 31	*32 3 ± 2 4*	29 6 ± 0 8	*28 8 ± 1 3*	*28 1 ± 1 9*	*26 9 ± 2 0*	*26 1 ± 2 1*
3	− 0 38	*31 8 ± 1 7*	29 4 ± 1 1	*28 6 ± 1 0*	*28 6 ± 1 4*	*26 7 ± 2 0*	*26 4 ± 1 7*
4	− 0 64	*29 8 ± 1 6*	*26 3 ± 1 0*	*24 7 ± 1 5*	*24 1 ± 1 9*	*23 7 ± 2 1*	*23 2 ± 2 2*
5	− 0 93	*25 8 ± 1 5*	*21 8 ± 0 9*	*20 4 ± 1 7*	*20 0 ± 1 7*	*18 3 ± 1 9*	*17 4 ± 2 2*
6	− 1 24	*18 5 ± 3 8*	*15 6 ± 1 1*	*13 7 ± 1 5*	*12 9 ± 1 3*	*11 3 ± 2 0*	*9 2 ± 1 7*
cv (cd)[2]		33 8 (2 0)	32 3 (1 0)	30 6 (1 2)	30 1 (1 0)	28 5 (1 5)	27 6 (1 5)

[1] LRT = log relative transmittance

[2] cv (cd) = critical value (critical difference) from Dunnett's test (one-tailed p = 0 05); threshold values below critical value italicized

Table 4 The influence of diffusers on Humphrey Field Analyzer threshold measurements (dB; mean ± SD)

Diffuser	LRT[1]	Eccentricity					
		0°	5°	10°	15°	20°	25°
None	0 00	39 4 ± 2 4	34 6 ± 1 1	33 6 ± 1 3	32 6 ± 2 1	31 7 ± 1 9	30 2 ± 1 1
0	− 0 06	39 4 ± 1 8	34 3 ± 1 3	33 8 ± 1 3	32 6 ± 1 5	31 8 ± 1 3	29 4 ± 0 5
1	− 0 23	*37 0 ± 1 4*	*32 6 ± 0 9*	*30 8 ± 0 8*	*29 6 ± 0 9*	*28 4 ± 1 3*	*26 6 ± 2 2*
2	− 0 31	*35 5 ± 2 6*	*31 3 ± 2 3*	*30 6 ± 0 5*	*29 6 ± 1 5*	*28 2 ± 1 8*	*27 2 ± 1 9*
3	− 0 38	*34 9 ± 1 1*	*30 6 ± 1 5*	*29 8 ± 1 5*	*28 6 ± 1 5*	*27 0 ± 0 5*	*25 0 ± 1 4*
4	− 0 64	*31 0 ± 1 8*	*26 7 ± 1 9*	*26 2 ± 1 9*	*24 8 ± 1 5*	*23 4 ± 1 6*	*21 4 ± 2 5*
5	− 0 93	*26 7 ± 2 5*	*22 6 ± 1 3*	*20 2 ± 2 2*	*20 6 ± 2 1*	*19 0 ± 2 6*	*17 6 ± 1 9*
6	− 1 24	*20 8 ± 0 8*	*16 0 ± 1 2*	*15 4 ± 0 9*	*14 6 ± 1 5*	*13 8 ± 1 3*	*11 8 ± 1 3*
cv (cd)[2]		37 4 (2 0)	32 9 (1 7)	31 8 (1 8)	31 2 (1 4)	29 7 (2 0)	28 3 (1 9)

[1] LRT = log relative transmittance

[2] cv (cd) = critical value (critical difference) from Dunnett's test (one-tailed p = 0 05); threshold values below critical value italicized

Table 5 Influence of spherical plus overcorrections on Octopus 201 perimeter threshold measurements (dB; mean ± SD)

Lens	Eccentricity					
	0°	5°	10°	15°	20°	25°
Plano	34 3 ± 1 8	32 2 ± 1 3	31 3 ± 1 7	29 5 ± 1 0	28 6 ± 2 2	27 6 ± 1 5
+1	33 8 ± 1 2	31 1 ± 1 5	*29 3 ± 1 5*	*28 1 ± 0 9*	27 0 ± 0 7	26 0 ± 1 0
+2	*31 1 ± 1 4*	*30 0 ± 1 1*	*27 7 ± 1 3*	*27 3 ± 0 6*	25 7 ± 1 0	24 3 ± 1 2
+3	*29 0 ± 1 5*	*28 7 ± 1 2*	*27 1 ± 1 0*	25 9 ± 0 4	24 4 ± 1 1	23 5 ± 0 8
+4[1]	*27 3 ± 1 6*	*26 9 ± 1 7*	*26 2 ± 1 2*	24 7 ± 0 8	23 3 ± 0 7	*21 5 ± 1 4*
+5[2]	*25 7 ± 1 8*	*26 2 ± 1 1*	*24 9 ± 1 0*	23 4 ± 0 7	22 1 ± 1 1	20 8 ± 1 4
+6	*25 1 ± 1 3*	*25 1 ± 1 2*	*23 8 ± 0 4*	23 0 ± 0 8	21 1 ± 0 5	20 1 ± 1 4
cv (cd)[3]	33 1 (1 2)	31 1 (1 1)	30 3 (1 0)	28 7 (0 8)	27 3 (1 3)	26 3 (1 3)

[1] Repeated in one subject because of 3 3 dB standard deviation of threshold measurement at 15°

[2] Repeated in one subject because of 3 3 dB standard deviation of threshold measurement at 5°

[3] cv (cd) = critical value (critical difference) from Dunnett's test (one-tailed p = 0 05); threshold values below critical value italicized

Table 6 Visual acuities and Miller-Nadler glare disabilities (mean ± SD)

NDF	VA[1]	Diffuser	VA[1]	MNGD[2] without mask (%)	MNGD[2] with mask (%)	Over-correc-tion	VA[1]
None	1 00 ± 0 00	None	1 00 ± 0 00	5 0 ± 0 0	4 6 ± 0 9	Plano	1 00 ± 0 00
0 3 log	1 00 ± 0 00	1	1 00 ± 0 00	13 2 ± 3 9	5 0 ± 0 0	+1 00	0 80 ± 0 18
0 6 log	0 93 ± 0 15	2	1 00 ± 0 00	14 8 ± 4 8	5 0 ± 0 0	+2 00	0 33 ± 0 10
1 0 log	0 93 ± 0 15	3	1 00 ± 0 00	17 8 ± 4 7	5 0 ± 0 0	+3 00	0 16 ± 0 07
1 5 log	0 74 ± 0 15	4	0 87 ± 0 18	35 0 ± 11 7	6 0 ± 2 2	+4 00	0 11 ± 0 04
2 0 log	0 64 ± 0 08	5	0 57 ± 0 15	55 0 ± 11 7	8 0 ± 2 7	+5 00	0 07 ± 0 04
3 0 log	0 24 ± 0 07	6	0 19 ± 0 03	>75 0 ± 0 0	11 6 ± 1 7	+6 00	0 04 ± 0 01

[1] VA = visual acuity
[2] MNGD = Miller-Nadler Glare Disability

diffusers, and spherical plus overcorrections, as well as the Miller-Nadler glare disability data for the diffusers, are summarized in Table 6.

Discussion

This study sought to better understand the absorbing, scattering, and blurring effects of media opacities on threshold measurements, by simulating those phenomenon in normal subjects undergoing perimetry on commercially available computerized threshold perimeters. Estimating the effect of media opacities on perimetry is a vexing clinical problem. Kinetic perimetry in cataract patients with visual acuities as low as 20/80 revealed essentially no depression of threshold sensitivity with the I3e, I4e, III4e, and V4e isopters; however, with visual acuities of less than 20/50 the I2e isopter was generally absent, and with acuities as good as 20/20 the I2e isopter was depressed [7]. Given that depression or absence of the I2e isopter with early cataracts, a depression of the threshold measurements on computerized threshold perimeters should be expected, consequently, it would be ideal if the extent to which a media opacities (particularly cataracts) would depress threshold measurements could be estimated by other psychophysical measurements and/or physical parameters.

Although cataracts usually do not cause relative afferent pupillary defects and therefore probably decrease retinal illumination by less than 1 2 log units [4], our data demonstrate that even a 0 6 log unit reduction in retinal illumination influences threshold measurements. This finding is not surprising since the background illuminations of both the Octopus 201 perimeter (4 apostilbs) and the Humphrey Field Analyzer (31.5 apostilbs) are below that at which Weber-Fechner Law is valid [1].

In glaucoma patients retinal illumination may also be altered by changes in

pupil size. Two studies of this effect in normal subjects on the Octopus 201 perimeter have reported average changes in threshold measurements of 2 5 dB [3] and 2.6 dB [5] per 1.0 log unit of change in pupillary area This study and another study [6] of the influence of background illumination on Octopus perimeter threshold measurements found 3.2 dBand 3.9 dB mean sensitivity changes, respectively, per 1 0 log unit of neutral density change within the range of 0 5 to 1.0 log units. Although the changes observed in that latter study may have influenced by stray light around the Octopus lens holder altering retinal adaptation, both studies of neutral density filters appear to overestimate the influence of background illumination compared with the effect of changes in pupillary size

Media opacity probably have their greatest influence on the differential light threshold by virtue of their lack of homogeneity, which causes light scattering In addition to seeking primarily to quantitate the influence of simulated light scattering on Octopus 201 perimeter and Humphrey Field Analyzer threshold measurements, we undertook this investigation to test our hypothesis that, because of its higher background luminance (31.5 apostilbs), threshold measurements on a Humphrey Field Analyzer might be affected to a greater extent by simulated light scattering than threshold measurements on an Octopus 201 perimeter (background luminance of 4 apostilbs) Diffuser 4, with which visual acuities were 20/20 to 20/30 and with which Miller-Nadler glare disability scores were 20% to 45%, did decrease the average Octopus threshold measurements statistically significantly less than the average Humphrey threshold measurements (Octopus 6.6 dB v Humphrey 8 1 dB; p = 0 0019, repeated measures analysis of variance); however, that difference is probably not clinically significant and may only compensate for the slightly better performance of the Humphrey Field Analyzer with the changes in retinal illumination (specifically, mean Octopus threshold decreases of 1.7 dB and 3.5 dB v mean Humphrey threshold decreases of 1 1 dB and 2.3 with 0.6 log and 1 0 log unit filters, respectively).

A recent study of two normal subjects and one subject with a small paracentral scotoma demonstrated no statistically or clinically significant change in threshold measurements from either program 31 or 61 on an Octopus 201 perimeter with ± 2 00 diopter spherical overcorrections [2]. However, another study [8] and this study have demonstrated statistically significant depression of Octopus threshold measurements with +1.00 spherical overcorrections, reporting 1 26 dB and 1 4 dB average decreases, respectively, in threshold measurements per diopter of overcorrection for +1.00 and +2.00 spherical overcorrections Consequently, the importance of accurate refraction with appropriate overcorrection for perimeter bowl radius and patient age to minimize such threshold measurement artefacts cannot be overemphasized

With respect to attempting to predict the effect of our simulated media opacities on threshold measurements, visual acuity was dissappointing; both the NDFs and diffusers seem to have greater influences on threshold measurements than might be suspected by their effects on visual acuities, while the converse appears

to be true for the spherical plus overcorrections. Our data suggest that other psychophysical measurements (such as contrast sensitivity or glare disability) or physical parameters (such as an objective measure of media light transmission or scattering) may be of more predictive value.

References

1 Aulhorn E, Harms H, Raabe M: Die Lichtunterschiedsempfinlichkeit als Funktion der Umfeldleuchtdichte Documenta Ophthalmologica 20: 537–556 (1966)
2 Benedetto MD, Cyrlin MN: The effect of blur upon static perimetric thresholds In: Heijl A, Greve EL (eds) Proceedings of the 6th International Visual Field Symposium, pp 563–567 Dr W Junk Publishers, Dordrecht, The Netherlands, 1985
3 Choplin N, Spaeth G, Steinman W: The effect of induced miosis on the visual field of normal subjects Presented at the Fourth Annual Octopus Users' Society Meeting, San Diego, CA, February 8, 1985
4 Cox TA: Pupillography of a relative afferent pupillary defect Am J Ophthalmol 101: 320–324 (1986)
5 Gressell M, Heuer D, Anderson D: Does the Octopus obey Weber's law? Presented at the Second Octopus Users' Society Meeting, Niagara Falls, NY, August 13, 1983
6 Klewin KM, Radius RL: Background illumination and automated perimetry Arch Ophthalmol 104: 395–397 (1986)
7 Radius RL: Perimetry in cataract patients Arch Ophthalmol 96: 1574–1579 (1978)
8 Weinreb RN, Perlman JP: The effect of refractive correction on automated perimetric thresholds Am J Ophthalmol 101: 706–709 (1986)

Authors' address:
Dale K Heuer, MD,
Estelle Doheny Eye Foundation Building, 1355 San Pablo Street, Los Angeles, CA 90033, U S A
(also Dept of Ophthalmology, University of Southern California School of Medicine)

D R Anderson, W J Feuer, R W Knighton, F E Fantes,
Bascom Palmer Eye Institute, Dept of Ophthalmology, University of Miami School of Medicine, Miami (FL), U S A

M G Gressel,
Dept of Ophthalmology, Lorain Community Hospital, Lorain (OH), U S A

I.4 Simulation of the influence of lens opacities on the perimetric results; investigated with orthoptic occluders

U. URNER-BLOCH
Zürich, Switzerland

Abstract

The development of cataract during perimetric follow up of glaucoma patients is a difficult, but frequent problem in the daily practice of the ophthalmologist.

By simulating media opacities with orthoptic occluders on the corrective lens, their influence on the perimetric results (using the Octopus 500E, programme G_1) was studied in a group of normal persons and a group of patients with pathological fields.

Introduction

The development of a cataract during glaucoma therapy represents a difficult problem in interpreting visual fields. It is, however also one of the most common situations in ophthalmologic practice.

Although the Octopus system initially achieved a high standard of precision and reproducibility for static perimetric techniques [3], the development of new software (delta programme, G_1 programme [2, 4] has led to further advances, particularly in the field of glaucoma diagnosis. This has been due to simplification of the representation and interpretation of results and control parameters

In programme G_1, a number of reduced data (so-called field-indices) are available together with the usual numerical tables and graphics immediately after the measurement process. These reduced data are capable of characterising the state of the visual field. Important initial experiments using the methods of data reduction in the examination of glaucoma patients have already been published [5], as well as those defining the influence of other non-glaucomatous conditions such as fluctuations or age related changes [6, 7, 9]. Little, however, is known concerning the influence of the commonly found media opacities. The comparison of perimetric results in cataract patients pre- and postoperatively to judge the media-effect is dependent on clear definition and measurement of the opacity [8, 10].

The generally advanced age of cataract patients often detracts from the reliability of the results. Concomitant illnesses such as maculopathy or glaucoma make interpretation difficult, and sometimes perimetry appears to be totally impracticable.

The imitation of a cataract with an occluder of a defined opacity, such as is used in orthoptic practice, was first used by Niesel [11, 12] with the Goldmann perimeter in the study of normals and glaucoma patients The use of tinted contact leses [13] is based on the same principle. It allows the exclusion of other influences (in the examination of normal people) and more rapid results (saving in time compared with that required for operative intervention)

In our clinical trial we combined Niesel's method with computerized static perimetry and the new software permitting data reduction.

Material and methods

For perimetry we used programme G_1 (phase 1 and 2) on the Octopus 500E perimeter

Three patient groups were studied:

a) *cataract patients about two weeks pre- and 6 to 8 weeks postoperatively* after a stable visual acuity had been reached in order to compare qualitatively the results with those of the occlusive studies: n = 9, average age 72.1 years, range 59–87 years. All had extracapsular extraction and implantation of a posterior chamber lens;

b) *people with normal visual fields* (all indices normal) with and without two occluders of varying strength on the same corrective lens (occluder 0.3 reduces the visual acuity to approximately 0.3, and occluder 0.6 reduces it to about 0.6): n = 10, average age 34 2 years, range 21–51 years;

c) *patients with varying diagnoses showing definite pathological indices* (raised MD and CLV) were subjected to perimetry with and without occluder 0 3: n = 12, average age 49 7 years, range 19–71 years; 8 glaucoma, 3 optical atrophy of which 2 of vascular origin and 1 by tumor compression; 1 partial hemi-anopsia.

The following data were collected and statistically analyzed (with the aid of the Wilcoxon-Test, Wilcoxon-Mann-Whitney-Test and regression analysis): the visual field indices MD, CLV and SF, each with and without occluders, and each pre- and postoperatively, as well as the mean sensitivities (MS) calculated for various eccentricities Corresponding MD values were not available at the time of the study, as the normal values for individual measurement points were missing.

Results

Cataract patients (see Fig. 1a)

A marked decrease in MD, as well as an increase in the CLV is present in 7 of 9 cases (in two cases the MD was higher postoperatively, in spite of a good visual acuity). The baseline values and the degree of changes with the operation, however, show large variations. Reasons for this are.
a) various types and degrees of lens opacities as well as the presence of glaucomatous defects;
b) unforeseen postoperative problems such as capsular opacity, poor corneal moistening or maculopathy.
(For two patients only the results with the programme 38 were available For these patients, the indices were calculated according to the formula provided for programme G_1, using the normal values for sensitivities provided in the basic comparitive tables. Another patient could be examined only by Phase 1 with respect to his age).

An attempt to imitate the preoperative condition in two patients with occlusives resulted in a similar but inverted course of the vectors in the MD-CLV-diagram.

Normal subjects (see Figs 1b, 2a and 2b)

A marked increase in MD was observed following application of occlusives (with occlusive 0.3, an average of 4.9 db; with occlusive 0 6, an average of 2.3 db). The difference between MD with occlusive 0 3 and MD with occlusive 0 6 is highly significant ($p<1‰$).

From our data for CLV, as well as for SF no change by the occluders could be assumed.

Patients with pathological visual fields

a) A consistent marked increase in MD and fall in CLV was caused by the occluders (see Fig. 1b).
b) In terms of the grey-scale, this corresponds to a diffuse depression of the visual field ('becomes greyer'), and a concomitant flattening out of any scotomata present. Absolute scotomata remain, although their borders to the remaining visual field are less clear ('faded appearance'). Flat scotomata almost disappear, this corresponding again numerically to the reduction of the CLV close to the normal range (see Fig. 3).
c) With increasing baseline values of MD, including data from normal visual
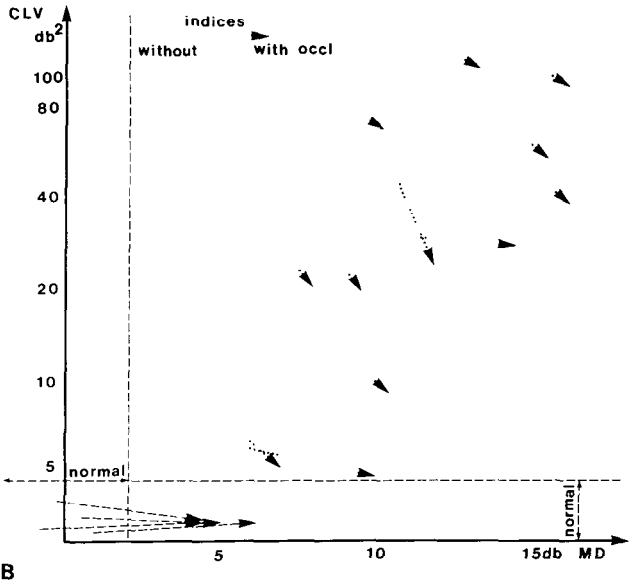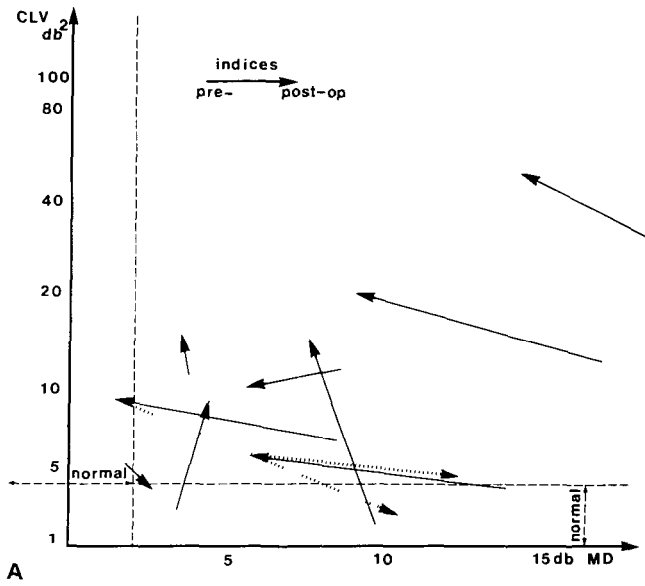
Figure 1 a MD/CLV-diagram for cataract patients (———) An attempt to imitate the preoperative condition by applying occlusives (   ) was undertaken in two cataract patients b MD/CLV-diagram for normal (– – –) (only 4 of 10 shown) and pathological visual fields (   ) similar as in Fig 1a
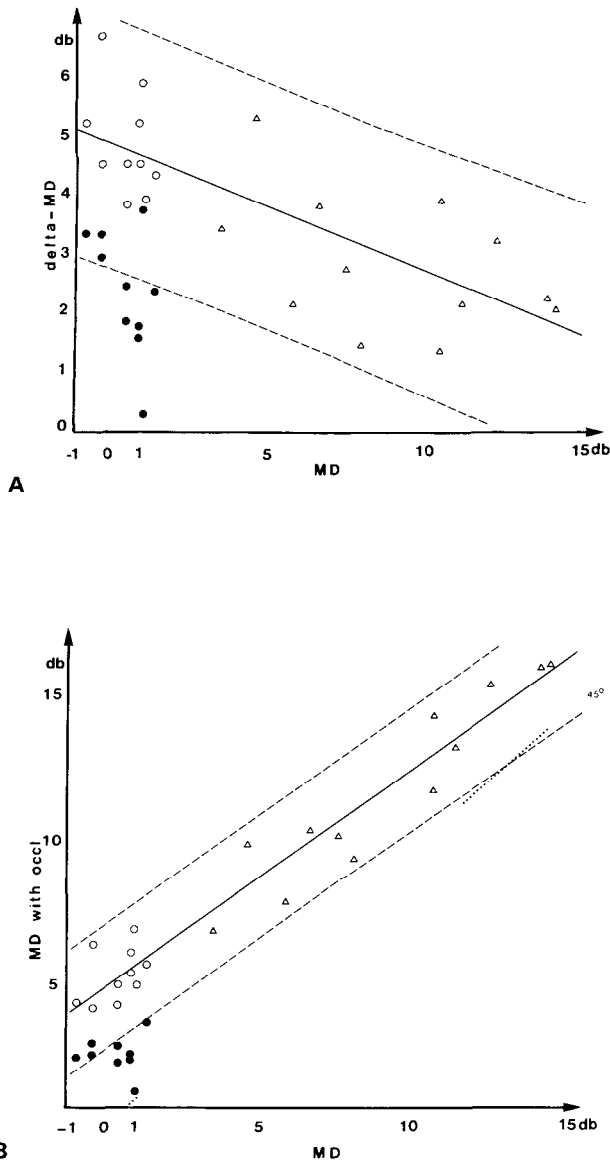
Figure 2 a MD/delta-MD-diagram for normal (with occlusive 0 3 ○ and occlusive 0 6 ●) and pathological (△) visual fields A straight line is obtained by linear regression (——) which can be used for estimating the delta-MD produced by any given initial value of MD using te occluder 0 3 b MD/MD + delta-MD-diagram: for comparison with practice, where the portion of the visual field not related to a media opacity has to be calculated from the measured values, this representation of MD without occluders compared with MD with occluders (= MD + delta-MD) is more appropriate Symbols as in Fig 2a
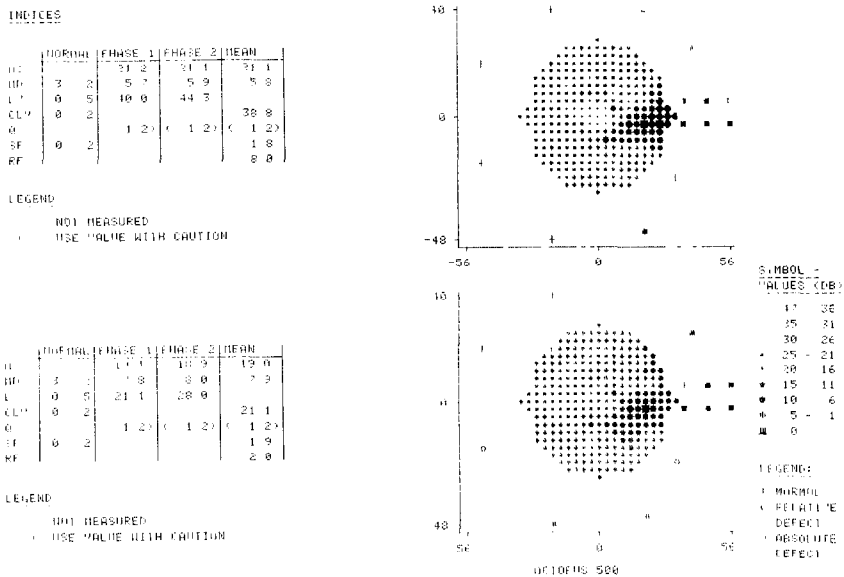
Figure 3 Example for an Octopus print-out with indices and grey scale from a glaucoma patient left without, and right with occluder 0 3

fields, a tendency to a slight decrease in the change of MD (= delta-MD) may be observed (see Fig. 2a; r = 0.756, p<0 1‰). The relationship observed for this small patient group is not marked due to the relatively large variation of the delta-MD. Other factors, however, may contribute to this variation.

For comparison with practice, where the portion of the visual field not related to media opacities has to be estimated from the measured values, the diagram of the relation of MD without occluders to MD with occluders (= MD + delta-MD) is of greater benefit (see Fig. 2b). The estimated values for MD with occluders, however, deviate quite markedly from the actual values in patients with pathological visual fields This means that the prognostic value of the influence of occluders lies for our data within a broad range of about +/−2.2 db (= 95% confidence interval)

d) Similar results are found for CLV without occluders and CLV with occluders (= CLV + delta-CLV) The higher the initial value of CLV, the greater the fall in CLV with occlusives (r = 0 972; p<0.1‰; 95% confidence interval: +/−8 db).

e) In this group, SF falls with the influence of the occlusive by at least 0.1 db (p<1‰). It is worth mentioning that there is a highly significant difference between the baseline-SF of pathological fields and that of normal visual fields (p<1‰).

Changes in mean sensitivity in relation to eccentric positions in normal and pathological visual fields

In normal fields, greater sensitivities can be measured centrally with a decrease towards the periphery ('sensitivity peak') However, the influence of the occlusives is constant over the entire visual field

In the *pathological* group, the decrease of MS (= delta-MS) is most marked between 0° an 10°. For extremely low sensitivities as can be found in this group in the middle eccentricities, a slight trend for a decrement of delta-MS can be observed. This finding supports the fore-mentioned tendency to reduction in delta-MD with increasing initial values.

Discussion and conclusion for ophthalmological practice

Assessment of glaucoma with increasing cataract

a) It may be concluded that there is probably no change in the status of the glaucomatous pathology if during routine follow-up of a glaucoma patient MD values are high and CLV values are low in comparison to the previous examination Inversely, an increase in the glaucomatous process may be inferred if CLV remains constant or even increases
b) The cataract in principle influences the entire visual field homogeneously Our model experiments indicate, however, that the extent of change is lower with severe pre-existing damage. A visual field that is already initially severly changed (with high MD) almost only shows 'paradoxical' decrease in CLV with the simulated cataract.
c) Very early glaucoma related visual field changes are more difficult to recognize in the presence of concomitant development of cataract (disappearence of relative scotomata in the grey-scale, fall of a minimally elevated CLV to the near normal range). Control of the patient using other criteria of glaucoma (pressure, optic disc if still visible) is all the more important.
Computer simulation of visual field defects is helpful in understanding this finding [1]. The results correspond well to the model experiments of Niesel and with practical experience in the long term treatment of glaucoma patients. The superiority of computer-assisted perimetry together with practical software packages in the form of programme G_1 allow relationships to be quantitatively evaluated and exact standards to be defined

The prognostic value of changes in visual field indices with known degrees of cataract opacity

a) The comparison of perimetry results from cataract patients pre- and post-operatively does not give complete information concerning the visual field changes induced Various unforeseen or poorly defined conditions can influence the result and make evaluation difficult.
b) A large number of patients with varying initial values of indices must be studied in order to allow the construction of calibration curves for a particular degree of lens opacity.
c) Estimation of the influence of a measured level of opacity will always be connected with a degree of uncertainty, as even in normal fields a variation of the media effect has to be expected.

Acknowledgements

References

1 Augustiny L, Flammer J: The influence of artificially induced visual field defects on the visual field indices Doc Ophthal Proc Series 42: 55–67 (1985)
2 Bebie H: Computerized techniques of visual field analyses In: Drance SM, Anderson DR (eds) Automated perimetry in glaucoma, pp 147–160 Grune and Stratton, New York, 1985
3 Fankhauser F: Problems related to the design of automated perimeters Doc Ophthalmol 47: 89–138 (1979)
4 Flammer J: The Octopus glaucoma program G_1 Proceedings of the Third Octopus Users' Society Meeting, 1984, p 25
5 Flammer J, Drance SM, Augustiny L, Funkhouser A: Quantification of glaucomatous visual field defects with automated perimetry Invest Ophthalmol Vis Sci 26: 176–181 (1985)
6 Flammer J: Fluctuations in the visual field In: Drance SM, Anderson DR (eds) Automated perimetry in glaucoma, pp 161–173 Grune and Stratton, New York, 1985
7 Gloor BP, Vökt BA: Long-Term fluctuation versus actual field loss in glaucoma patients In: Straub W, Gloor BP (eds) Visual fields in glaucoma patients Dev Ophthal 12, pp 48–69 Karger, Basel, 1985
8 Guthauser U, Flammer J, Lotmar W, Niesel P: Einfluss der Katarakt auf das Gesichtsfeld Klin Mbl Augenheilk 188: 409–411 (1986)
9 Haas A, Flammer J, Schneider U: Influence of age on the visual fields of normal subjects Am J Ophthalmol 101: 199–203 (1986)
10 Hendrickson PH, Robert Y: Klinische Bestimmung des funktionellen Trübungsgrades einer Katarakt (PAP/MAK-Verhältnis): Theorie und Technik Klin Mbl Augenheilk 188: 421–424 (1986)

11   Niesel P, Ramel Ch, Weidmann BOS: Das Verhalten von perimetrischen Untersuchungsbe-
     funden bei Entwicklung einer Katarakt Klin Mbl Augenheilk 172: 477–480 (1978)
12   Niesel P, Wiher Ch: Modellexperimente zum Verhalten glaukomatöser Gesichtsfeldausfälle bei
     Kataraktentwicklung Klin Mbl Augenheilk 180: 461–463 (1982)
13   Walonker AF, Diddie KR: Simulating decreased visual acuity with a contact lens system Am J
     Ophthalmol 92: (6): 863–864 (1981)

Author's address:
Dr med U Urner-Bloch,
Augenärztin FMH,
Gloriastrasse 70, CH-8044 Zürich, Switzerland

I.5 Relation between media disturbances and the visual field

T J.T P. VAN DEN BERG
Amsterdam, The Netherlands

Abstract

The effect of media disturbances on the retinal projection of the external light distribution can be described by means of the so-called point spread function (PSF). The PSF is defined as the retinal light distribution resulting from an external point source. Consequently visual field changes because of media disturbances can be understood if the PSF could be measured. These visual field changes may include sensitivity loss because of increased light scattering in lens or cornea. We have designed a new method to learn more about the pathological PSF than was possible up to now. With this method we are able to measure the part of the PSF outside 1 degree, relative to the central portions of the PSF. Using this method complemented with the help of the modulation transfer function, actual pathological PSF's were estimated. Considerable changes in the visual field were predicted for relatively mildly disturbed media

Introduction

A point source of light is projected on the retina not as a point but as a more or less widened bell shaped distribution (Fig. 1). This is called the 'point spread function'. The optical media are not perfect lenses They contain irregularities which deflect light away from the center of the image. Moreover part of the light is lost by absorption in the media. In pathological conditions of the media these two phenomena may be increased. They have distinctly different effects during visual field examination. Light loss due to absorption causes the effective light level of the perimetric measurement to decrease. This light loss has been studied by Weale [7] a.o. If severe enough it might result in mesopization of the visual field, comparable to the effect of a reduction of the overall luminance level of the perimetric instrument. This mesopization results in a decrease of sensitivity especially in the center.
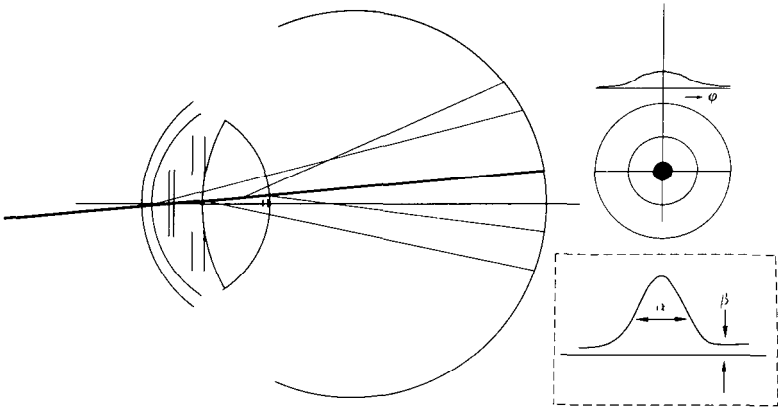
Figure 1 Schematic representation of the point spread function of the eye, assumed to be circularly symmetric The inset in the lower right corner emphasizes that our formula for the point spread function has two free parameters: α defines the width of the central peak, β defines the strength of the tail

Our study has however concentrated on the effect of widening of the point spread function (PSF). If part of the light from a perimetric stimulus is scattered away from the center of the image it may get lost for perimetric sensitivity. This will depend on how much is scattered outside the retinal integration area defined in some way or other. We were interested in the effect of this scatter, expressed in dB, on light sensitivity in practical cases.

A formula describing the normal PSF has been derived by Vos [5] as an approximation to an experimentally based numerical complete PSF [6]. We have adapted the formula to include pathological cases:

$$PSF\ (\varphi) = \frac{465 - 3.26\beta^2}{\alpha^2} \left(e^{-(\frac{\varphi}{\alpha})^2} + .125\ (\frac{\varphi}{\alpha} + 1)^{-3} \right) + \beta\ (\varphi + .9)^{-2}$$

where φ = angular distance to the point source in degrees, α = parameter defining the width of the central peak, and β = parameter defining the height of the peripheral part. The PSF can be broken down into two parts. The left two terms describe the central peak ($\varphi<1°$), the right term dominates for $\varphi>1°$. As a model for the pathological PSF we have assumed that it can be approached with the same general shape but that the central peak can be more wide and that the peripheral part can be increased Our task was to estimate the width parameter α of the central peak and the strength β of the peripheral part for actual pathological cases.

Methods

In order to measure the amount of light scattered for $\phi > 1°$ (β) we designed the following technique [4]: at a distance ϕ from the fixation point a bright flickering annulus is presented to the patient. With no light in the central test area a flicker effect is perceived there. This is caused by the light scattered over the distance ϕ from the annulus to the center. In order to determine the luminance of this scattered light a counter phase flickering light is added in the central test area. This light can be adjusted in strength. When the patient observes extinction of the flicker, by definition the compensating light equals the stray light. This measurement can be performed for angles larger then $1°$ It has been used to estimate the strength of the peripheral part of the PSF (β) for some 60 patients now with a variety of media disturbances. An important application is in glare testing.

The width of the central peak (α) was estimated on the basis of the modulation transfer function. On the one hand the actual modulation transfer functions were determined subjectively testing the patients with sinusoidal gratings These curves were compared with the mean of a normal control group If the patients suffer from disturbances in the optical media only, sensitivity losses with respect to normal can be attributed to losses in optical transfer with respect to normal

Optical transfer functions were mathematically derived from the above formula for several values of the width of the central peak (α). These functions were compared with the function for the normal eye ($\alpha = 0.02°$). For the purpose of the present study it was assumed that the differences with normal for the calculated optical transfer can be compared to that for the measured modulation transfer.

Results

Figures 2 and 3 give the results for β and α estimation respectively for a 79-year-old patient suffering from a senile cortical and nuclear cataract. In figure 2 L stands for the luminance of the central test area, ϕ^2/E being added for normalizing purposes. If L is small the patient perceives a flicker in the center due to scattered light originating from the flickering annulus at eccentricity ϕ What happens if the luminance L of the compensatory flickering light is slowly raised? When the difference between stray light and compensating light has become rather small the flicker can no longer be perceived. These are the lower crosses and circles. When L is increased further flicker becomes visible again These are the higher crosses and circles. In between the two lights are about equal For this patient the experiment was performed at 4 angular distances of the stray light annulus. The estimated value of β is about 60 for all distances. The lower broken curves show β for a control population to lie between about 3 and 10.

Figure 3 shows a series of optical modulation loss functions calculated for the indicated width's of the central peak (α) with respect to the normal value $\alpha =$
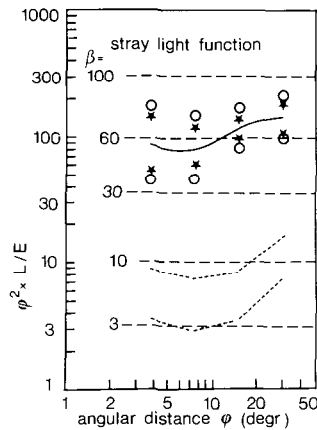
Figure 2 The straylight function for angles larger than 1° The symbols for a cataract patient indicate β to be around 60; the dashed lines below indicate β to be between 3 and 10 for the controlgroup

0.02°. The points representing the measured modulation transfer loss of this patient lie near the curves for α = 0.080° and α = 0.057°.

This set of experiments was performed for a large number of patients. Visual acuity was restricted to be better then 0.1 since only then sufficient accuracy could be obtained. For 6 of these patients also static threshold perimetry was performed. Suspicion of retinal pathology was excluded For these six patients the values for visual acuity, α and β were respectively: 0.3, 0.06, 60; 1 0, 0.03, 50; 0.33, 0.04, 100; 0.3, 0 06, 25–50; 0.8, 0 03, 12; 0.25, 0.08, 25. For this sample of patients as well as for the whole population α and β proved to be not very well
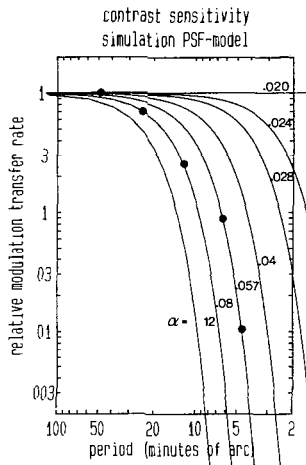
Figure 3 The modulation transfer function of the same cataract patient relative to normal (dots; normal ≡ 1), compared to the calculated optical transfer functions for indicated values of α relative to α = 0 02° (lines; (α = 0 02°) ≡ 1) For this patient α lies between 0 057° and 0 08°

related. So, increased light scatter over large angles may or may not be accompanied by increased light scatter over small angles and vice versa.

Discussion

Since β is based on a direct comparison experiment, the outcome can hardly be influenced by unknown retinal pathology or light loss in the media We must be less confident about the correctness of the α values. For the sake of argument let us assume however that both are accurate Then we know the form of the PSF of the pathological eye and we can derive the amount of light falling within retinal integration areas. Figure 4 shows the result for combinations of the normal values α = 0.02° and β = 10 and the pathological values α = 0 06° and β = 60 The curves show the fraction of the light falling within a circle with radius φ. Ranges of literature estimates of retinal integration areas are indicated for 0°, 7° and 30° eccentricity (see e.g. [2]) The normal curve (the upper most one) reaches values around 0.5 for foveal integration sizes. The pathological curves stay far below. The lower most a factor of 5 to 10 This would predict a loss of 7 to 10 dB in the foveal perimetric value. At 7° for the normal eye about 80% and for the pathological cases down to about 30% of the light remains within the retinal integration area. This would predict a loss of 4 dB. At 30° the predicted loss would be about 3 dB.

For the above 6 patients actual loss values ranged for 0°, 7° and 30° respectively as follows: 5–12, 4–10 and 2–4 dB. Also for individual comparisons the correspondence proved to be limited, actual losses being as a rule larger then predicted However we may not expect this comparison to be very successful. Important points of uncertainty are, as already mentioned, the estimation of α and potential effects of unknown retinal pathology or mesopization. Moreover criticism is possible on this way of using integration areas. Nevertheless it helps to judge the importance of light scattering in perimetry It can be read from these curves that also for other (realistic) integration sizes scatter effects can be quite considerable.

In *conclusion* the results point out that light scattering over large as well as over small angles may play a prominent role in loss of perimetric sensitivity in relatively mildly disturbed media.

From this analysis it can also be understood that these losses of perimetric sensitivity depend on target size. The present study refers to small target size. Figure 4 can however be applied directly to large target sizes. In that case the curves give the relative retinal intensity in the center of a large target as a function of the radius of the target. E.g. for a target with a 1° radius it can be read that the central intensity is dropped to about 90% (upper two curves) or about 50% (lower two curves) with respect to a situation without light scatter. Since retinal integration sizes are smaller this would be all the loss suffered because of scattering. So, the use of large targets could reduce the effects of light scatter on perimetric sensitivity considerably

38
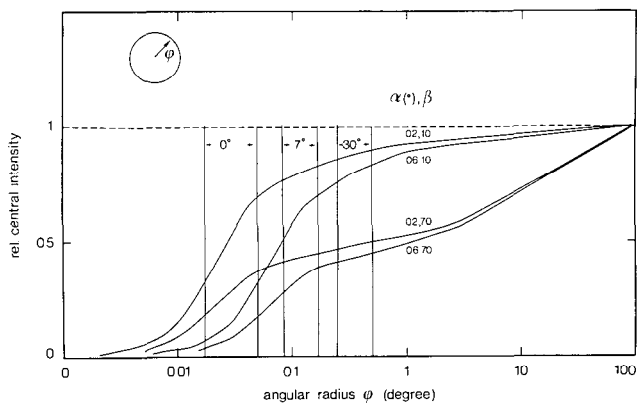
Figure 4 Integrated values for point spread functions with the indicated α's and β's as a function of φ
This shows the fraction of the light of a point source that is scattered within an area with radius
Vertical lines indicate litterature ranges for retinal integration sizes

Acknowledgements

References

1 Aulhorn E, Harms H: Visual perimetry In: Jameson D, Hurvich LM (eds) Hb of sensory physiology VII/4 Visual psychophysics, pp 102–145 Springer, Berlin, 1972
2 Brindley GS: Physiology of the retina and visual pathway Williams and Wilkin, Baltimore, 1970
3 Klewin KM, Radius RL: Background illumination and automated perimetry Arch Ophthalmol 104: 395–397 (1986)
4 Van den Berg TJPT: Importance of pathological intraocular light scatter for visual disability Doc Ophthal 61: 327–333 (1986)
5 Vos JJ: Verblinding bij tunnelingangen I De invloed van strooilicht in het oog Rapp IZF 1873 C-8 TNO (English abstract), 1983
6 Vos JJ, Walraven J, Van Meeteren A: Light profiles of the foveal image of a point source Vis Res 16: 215–219 (1976)
7 Weale RA: Physical changes due to age and cataract In: Duncan G (ed) Mechanisms of cataract formation in the human lens Academic Press, New York, 1981

Author's address:
Dr T J T P van den Berg,
The Netherlands Ophthalmic Research Institute and Laboratory of Medical Physics
of the University of Amsterdam,
Academic Medical Center,
Meibergdreef 15, 1105 AZ Amsterdam, The Netherlands

I.6 Relationship between cataract density and visual field damage

U. GUTHAUSER, J. FLAMMER and P. NIESEL
Berne, Switzerland

Abstract

The densities of cataracts were quantified with the help of computerized densitometry on a Zeiss-Scheimpflug slit-lamp measuring-system which measures the stray light scattered by the lens. In patients that underwent surgery, the visual acuities and the visual fields as well as the lens opacities were measured before surgery. Six weeks after the implantation of an intraocular lens, visual acuity and visual field measurements were repeated. The visual field changes were highly correlated with the densities of the lenses and to a lesser degree with the changes in visual acuity.

The measurement of stray light of the cataract seems, therefore, to be a good method for predicting the influence of cataracts on the visual fields

Introduction

It is well known that cataracts have a more or less diffuse influence on the visual field [3]. Also glaucoma can produce diffuse visual field damage [1]. This makes the interpretation of visual fields often quite difficult. We would like, therefore, to differentiate lens-induced visual field changes from changes due to glaucoma or other diseases. The purpose of this study was to quantify the opacity of the lens and to test whether there is a relationship with visual field changes.

Patient and methods

Included in the study were patients that underwent cataract surgery with a lens implantation. Excluded were glaucoma patients with marked damage or systemic diseases as well as patients with a postoperative visual acuity less than 0.8. Thirty eyes of thirty patients were included in the final analysis The visual field and

visual acuity were measured before surgery and two months after the implanta-
tion of an intraocular lens. The density of the lens was measured a few days
preceding surgery.

The lens opacity was quantified with the help of the Zeiss-Scheimpflug slit-
lamp measuring-system containing a computerized digital densitometry capa-
bility The visual fields were measured with the help of program G1 on the
Octopus automated perimeter

Results

In a first step we compared the visual fields before and after surgery. We found a
diffuse influence of the cataract on the visual field results. The influence was
slightly higher in the center than in the mid periphery [2]. In the next step we
correlated the improvement of the mean sensitivity after surgery with the pre-
operative density of the cataract. This revealed a good correlation ($r = 0.9$;
$p = 0.0001$) Finally we correlated the preoperative density of the lens with the
improvement of the visual acuity after surgery. This relation was weaker but still
significant ($r = n0.51$; $p = 0.004$) [2].

Discussion

Our method for quantifying lens opacity is based on the measurement of stray
light The outcome of this measurement showed a very good correlation with the
visual field changes We conclude from these results that stray light measure-
ments may be helpful for the interpretation of visual fields. It may also be of some
help for predicting the influence of cataracts on visual acuity The visual acuity,
though, is less accurate in the prediction of the visual field changes.

Based on this experience we are currently developing a simplified technique for
measuring the stray light of the lens in order to quantify lens opacity and to allow a
prediction of the influence of cataract on the visual field.

Acknowledgement

References

1 Flammer J, Eppler E, Niesel P: Die quantitative Perimetrie beim Glaukompatienten ohne lokale
  Gesichtsfelddefekte Graefe's Arch Clin Exp Ophthalmol 219: 92–94 (1982)

2 Guthauser U, Flammer J, Niesel P: How much of a visual field damage is caused by cataract? A new method to quantify cataract density (in preparation)

3 Niesel P, Ramel Ch, Weidmann BOS: Das Verhalten von perimetrischen Untersuchungsbefunden bei Entwicklung eines Katarakt Klin Mbl Augenheilk 172: 477–480 (1978)

Author's address:
Prof Dr J Flammer,
Dept of Ophthalmology,
University Eye Clinic,
CH-3010 Bern, Switzerland

I.7 A comparison of visual impairment caused by nuclear (NC) and posterior subcapsular (PSC) cataracts

P. BARALDI, J.M. ENOCH and S. RAPHAEL
Berkeley, U.S.A.

Abstract

A clear description of the major optical degradation effects caused by different types of ocular media opacities is not available at the present time. In this paper we compare results of a hyperacuity test, the 'gap function', in patients with posterior subcapsular cataract (PSC) and nuclear cataract (NC). Early posterior subcapsular opacities often have a more deleterious effect on visual acuity than roughly comparable anterior opacities or nuclear cataracts. Also, patients with PSC often report multiple images or 'starburst' effects. These effects can be greatly reduced by low spatial frequency pass-band filtering, providing a white noise background and/or use of a small pinhole held close to the eye. If these problems are not present or are adequately controlled, the hyperacuity 'gap function' shows less functional effect due to the opacity for PSC than NC in all cases tested. Visual acuity provides an insufficient description of the effects of media opacities on image formation.

Introduction

Changes in the ocular media of the eye often result in degradation of the retinal image [2, 12]. Thus, a method designed to predict potential visual acuity or other visual function after surgical intervention must take into consideration the different forms of alteration of the retinal image. Data cannot be pooled from patients who have irregularities of the ocular optical surfaces, the presence of multiple images, the existence of scattering bodies of different size and type, the presence of absorbing pigments (such as blood or the products of a bleed), etc. Each form of image degradation at each locus must be considered separately or in combination. From a body of such knowledge, one can develop a general set of perceptions relative to predictive capability of any given test(s).

We recount our experience in differentiating between nuclear and posterior

subcapsular cataract. We have been assessing hyperacuity judgments for evaluation of vision through ocular media opacities and degradations [1, 3–7, 14]. Hyperacuity includes judgments such as vernier acuity, the ability to make bisection judgments, etc. [13]. Hyperacuity differs from visual acuity in that visual acuity asks how many objects (or details of objects) one sees. In hyperacuity, it is assumed that you see more than one object (with some exceptions). In these tests, one asks where one object is relative to a second object (or more). This requires a totally different data analysis system in the central nervous system than visual acuity. As long as the individual can locate the center of a blurred/degraded image, he can finely localize that object in space. Thus, no window is needed through the cataract or other media opacity. The test is not particularly sensitive to contrast or luminance level once the two or more primary test objects are above the detection threshold

In order to improve the image quality of the PSC patients we introduced three simple maneuvers which taken individually or in combination greatly improved the visual performance of the patients These were:

1. Remove high spatial frequency components from the test target, i.e., remove the sharp borders from the stimulus. This is similar to placing a handkerchief or a piece of translucent glass just in front of a light source. A piece of Kodak ground glass was placed somewhat in front of the cathode ray tube (CRT) display of the two test points used in making the vertical alignment, vernier hyperacuity judgment. In almost every case, removing high spatial frequency components improved test performance

2. If there are *minor* perturbations due to spurious resolution or high spatial frequency noise, a generalized white background like that used on modern perimeters (in acoustical terms, a white noise background) serves to dampen the lesser peaks and disturbances Thus, contrary to general wisdom in testing individuals with cataracts, we added a low level white background on our display This served to reduce modestly the contrast of our test pattern, but helped make judgments easier.

3. Finally, the broader the light beam passing through the area of posterior subcapsular cataract, the greater the image degradation. By placing a small pinhole (about 1.0–1.5 mm) *very close* to the eye, we reduced the breadth of the light beam path passing through the posterior subcapsular cataract and markedly improved the quality of the retinal image.

It is clear that the visual loss in posterior subcapsular cataract is due largely to the equivalent of high spatial frequency noise. That is, the appearance of either extra borders, stria, or multiple images, etc., served to distract these patients from making appropriate judgments This argument applies to any test object whether it be a hyperacuity target, visual acuity display, or otherwise. When the three steps outlined above were taken, resultant visual acuity or hyperacuity improved greatly In fact, it became clear that when there was not a substantial nuclear cataract associated with the posterior subcapsular cataract, patient per-

formance following these remedial actions was far better than that encountered in an equivalent grade of nuclear cataract. In short, the diffuse scattering caused by nuclear cataract is only modestly affected by the techniques described above. Thus, the two forms of cataract have rather different effects on visual responses, and it was possible by these maneuvers to greatly improve the assessment of visual function in patients with PSC.

These same steps are applicable to hyperacuity perimetry or more conventional perimetry. In each case, the patient should be well focused on the perimeter bowl in order to minimize further interference with image formation.

These arguments may be generalized to other forms of presurgical evaluation of potential visual fuction following surgery. Further, each form of refractive/ media degradation must be separately analyzed in order to determine methods of testing which will allow assessment of optimal visual performance

Methods

Patients were referred to the laboratory by local ophthalmologists In this study, we consider only patients for whom
a) Ocular normality was verified by postoperative ophthalmological examination and
b) postoperative Snellen visual acuity (with correction) was at least 20/25, i.e., 0.8 decimal notation or better.
The reliability of measure responses was determined on each patient. The conditions of the test room were selected to optimize Snellen acuity and best refractive correction was determined. Slit lamp microscopy was conducted to classify the type and density of the cataract. The second eye was always assessed in order to verity the stability of the measurements before and after surgery. The techniques used to measure the gap and other hyperacuity tests have been described in detail elsewhere [3, 6].

Briefly, the vernier acuity stimulus consists of two bright dots (2 min arc by 1 min arc, 100 cd/m^2) presented on a CRT screen, with the top dot offset laterally by a variable amount. The patient's task is to push one of two response buttons in order to indicate the direction of the displacement of the top dot (left or right) Feedback, stimulus presentation, and response analysis were controlled by a computer (PDP 11/23). Thresholds were determined by a staircase procedure requiring an average of about 25 stimulus presentations per data point A single trial (stimulus presentation and response) typically took only 2 of 3 seconds The mean luminance of the white CRT background used with some of the patients with PSC was 32 cd/m^2

The hyperacuity perimetry test, where vernier acuity is measured at several eccentricties from fixation, was also performed In this test, we test five retinal loci in the horizontal meridian at the same time including the point of fixation ($\pm 8°$, $\pm 4°$, $0°$ eccentricity).

All the patients studied (ten total) exhibited posterior subcapsular eye lens changes classified from grade +2 to +4. (Here, the notation grades +1, +2, +3, +4 represent the percentage of the area affected, respectively 25%, 50%, 75%, 100%). A mild nuclear cataract was also present in all cases with one exception, because a pure PSC opacity is a rarity. Preoperative visual acuity of the patients tested varied from 20/70 to 20/1000 Snellen (0.29 to 0.02 in decimal notation). Informed consent was obtained.

Results

An example of the test results recorded from each patient is shown in Fig. 1. Here, the gap (Fig. 1a) and perimetry (Fig. 1b) test functions are reported before (filled cricles) and after (open circles) surgery. This patient (No. 1) exhibited bilateral cataracts. The opacity in the left eye, (results reported here) was described as being a grade +1 nuclear cataract and grade +4 posterior subcapsular cataract. The patient was 70 years old With a +2.00 D.S , he had a visual acuity of 20/200 (0.1 decimal acuity) in that eye. Test results after surgery, typical of normal subjects, indicated that the cataract was the only cause of the reduction in visual performance. Preoperatively, the perimetric profile (Fig. 1b) shows a superior response at the point of fixation and symmetric fall-off in hyperacuity vernier performance with increasing eccentricity. The minimum threshold for the gap function(corresponding to the best hyperacuity performance) lies between 4 and 8 minutes of arc (Fig. 1a). These data do *not* match data obtained from the group of otherwise normal cataractous patients having primarily nuclear opacities and whose visual acuity varied between 20/100–20/400.
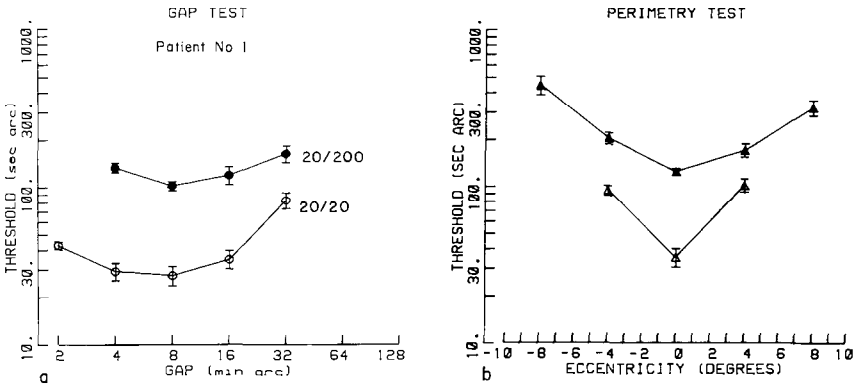
Figure 1 a Gap test results of patient No 1 affected by PSC cataract in the left eye Filled circles refer to preoperative data, open circles to post-operative data b Vernier thresholds of the same patient measured at five loci in the horizontal meridian After surgery, visual acuity was 20/20 and both the gap and the perimetry functions were normal
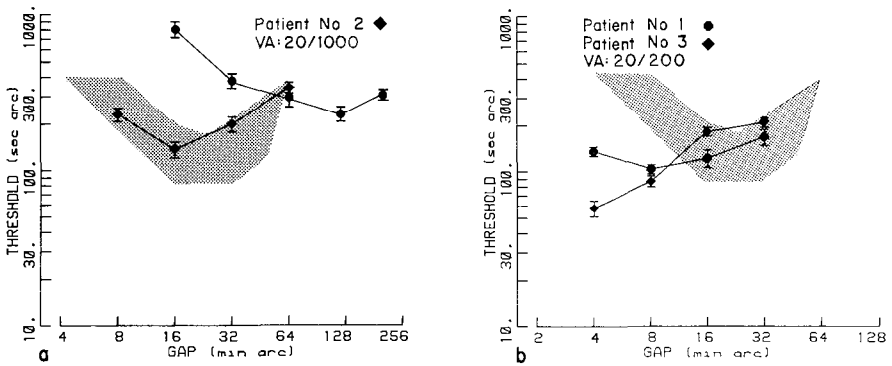
Figure 2 Results of the gap function measurements in PSC cataract patients a Gap function (filled diamonds) of patient No 2 with 20/1000 VA The data are compared with a nuclear cataract patient with the same VA (filled circles) The shaded region represents data obtained from a group of otherwise normal patients with nuclear cataract and visual acuity in the range of 20/100–20/400 b The gap test of two PSC cataract patients (No 1 and No 3) with 20/200 visual acuity (filled symbols) are compared with the data of the 'nuclear cataract group' with the same range of visual acuity The superiority of the performance in the PSC cataract patients is evident

Figure 2b displays data obtained from patient No 1 and from patient No 3, both of whom presented analogous characteristics (same visual acuity and type and grade of opacity). In this figure, both results are compared with previously obtained gap function data from the 'predominantly nuclear cataract (NC) group with visual acuity of 20/100–20/400'. The shaded area shows the range of individual curves comprising the NC group. Other examples are shown in Figures 2a and 3. They refer to patients exhibiting pre-operative visual acuity of 20/1000 and 20/70 respectively Here, we have reported

1. the 'nuclear cataract group' with matched visual acuity,
2. the gap function obtained in the PSC cataract patient, and
3 the subsequent 'nuclear cataract group' corresponding to a superior visual acuity.

It is evident that the patients with PSC opacities fit very well with the group of NC opacities with correspondingly better visual acuities

In most cases including patients whose data are not included in this report, we have had to deal with the presence of multiple images and/or the 'starburst' appearance of each target. These make the task rather hard to perform and/or result in abnormally higher hyperacuity thresholds In a majority of such cases, we were able to minimize these effects by utilizing one or more of the techniques outlined in the introduction.
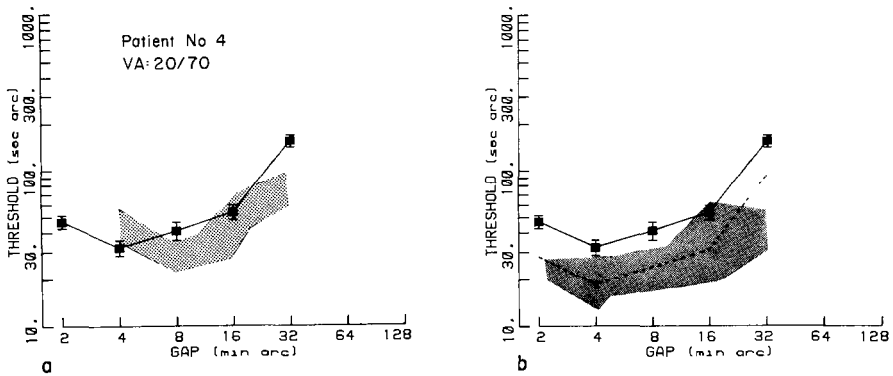
Figure 3 Gap test data obtained from patient No 4 with 20/70 VA a Comparison of the gap function with the data of the 'nuclear cataract group' in the same range of visual acuity (20/50–20/70) b Here the gap function of the same patient is compared with the gap of the 'nuclear cataract group' with visual acuity in the range 20/20–20/40 The shape of the function of the PSC cataract patient is more closely approximated by the latter group The broken line denotes the same function shifted downward and pinned on the average value of the minimum of the 'nuclear cataract group' function.

Discussion

The above results indicate that for our hyperacuity tests to successfully predict visual acuity post-operatively, we need at least two different classifications of otherwise normal cataractous patients depending upon the dominance of nuclear or cortical opacities. These results demonstrate, as in other studies [10, 11], that Snellen visual acuity is a rather poor indicator of the effect of intraocular scattering To date, a complete description of the major optical degradation effects on the retinal image caused by the different types of ocular media opacities is not available.

Using measurements of spatial contrast sensitivity, other investigators have found that both low and high spatial frequencies are affected in corneal edema and cataracts [9, 10]. An anomaly in the low spatial frequency part of the spectrum produces a more debilitating effect on the image than that predicted by visual acuity (mainly a test of high spatial frequency response). It one argues that nuclear cataracts reduce contrast sensitivity of low frequencies more than that caused by PSC opacities, then this explains why the hyperacuity gap function is less affected in the latter form of cataracts. We have shown that the effects of NC can be simulated by placing a ground-glass plate (a low spatial frequency pass-band filter) in front of the CRT [6, 14]. Fourier amplitude spectra of the stimulus showed that when the distance between the CRT and the ground glass was increased, there as a progressively lower high frequency cutoff.

If we consider only the relative positions of the NC and PSC opacities on the optic axis of the eye and the relative eye lens volume that are usually involved, we

can hypothesize a smaller degradation of the image due to scatter from the PSC opacity On the other hand, clinical studies have led to the conclusion that early PSC opacities often have a more deleterious effect on visual acuity than roughly comparable anterior or nuclear opacities [8].

Clearly, further effort is indicated to clarify the specific effects which are produced by different types of ocular media opacities These experiments do show the intrinsic value of hyperacuity methods for the assessment of vision in the presence of media opacities We recommend that clinicians use the simple experimental maneuvers (use of a pinhole, etc.) which we employed in the presence of posterior subcapsular cataract to better evaluate the performance of such patients.

Acknowledgements

References

1   Baraldi P, Enoch JM, Raphael S: Vision through nuclear and posterior subcapsular cataract Int Ophthalmol 9: 173–178 (1986)
2   Bettelheim FA: Physical basis of lens transparency In: Maisel H (ed) The ocular lens (structure, function, and pathology), pp 265–300 Marcel Dekker, New York-Basel, 1985
3   Enoch JM, Williams RA, Essock EA, Barricks M: Hyperacuity perimetry: Assessment of macular function through ocular opacities Arch Ophthalmol 102: 1164–1168 (1984)
4   Enoch JM, Williams RA, Essock EA, Fendick M: Hyperacuity: A promising means of evaluating vision through cataract In: Osborne NN, Chader GJ (eds) Progress in retinal research, Vol 4, pp 67–88 Pergamon Press, Oxford, 1985
5   Enoch JM, Baraldi P, Knowles R: New techniques in clinical application of hyperacuity tests on patients with media opacities Abstract for 1986 Annual Meeting of the Association for Research in Vision and Ophthalmology Invest Ophthalmol Vis Sci (Suppl), 27: 106 (1986)
6   Essock EA, Williams RA, Enoch JM, Raphael S: The effects of image degradation by cataract on vernier acuity Invest Ophthalmol Vis Sci 25: 1043–1050 (1984)
7   Essock EA, Enoch JM, Williams RA, Barricks M, Raphael S: Joint application of hyperacuity perimetry and gap tests to assess visual function behind cataracts: initial trials Doc Ophthalmol 60: 293–312 (1985)
8   Faye EE: Low vision aids In: Safir A (ed) Refraction and clinical optics, pp 215–228 Harper & Row Publisher, Hagerstown, 1984
9   Hess R, Garner LF: The effects of corneal edema on visual function Invest Ophthalmol Vis Sci 16: 5–13 (1978)
10 Hess R, Woo G: Vision through cataracts Invest Ophthalmol Vis Sci 17: 428–435 (1978)
11 Hirsch KP, Nadler MP, Miller D: Clinical performance of a disability glare tester Arch Ophthalmol 102: 1633–1636 (1984)
12 Tripathy RC, Tripathy BC: Lens morphology, aging and cataract J Gerontol 38: 258–270 (1983)
13 Westheimer G: The spatial sense of the eye Invest Ophthalmol Vis Sci 18: 893–912 (1979)

14   Williams RA, Enoch JM, Essock EA: The resistance of selected hyperacuity configurations to image degradations   Invest Ophthalmol Vis Sci 25: 389–399 (1984)

Authors' address:
Prof J M Enoch,
School of Optometry, University of California, Berkeley, CA 94720, U S A

P Baraldi (new address),
Clinica Oculistica, University of Modena, Modena, Italy

S Raphael,
Eye Diagnostics Lab, Castro Valley, CA, U S A

I.8 The role of intraocular light scatter in the attenuation of the perimetric response

J.M. WOOD, J.M. WILD, D.L. SMERDON and S.J. CREWS
Birmingham, United Kingdom

Abstract

The relationship between perimetric attenuation and intraocular light scatter was investigated in normal subjects using latex bead cells and in patients with uniocular media opacities. The Octopus 201 and Dicon 3000 automated perimeters were used to measure perimetric sensitivity and the Nicolet CS2000 system employed to measure contrast sensitivity with and without glare light in order to calculate intraocular light scatter. A high correlation for both samples was found between intraocular light scatter and perimetric attenuation as measured by both instruments. Attenuation was greatest at the 10 asb bowl luminance for the Dicon, and was greater at fixation than at 27.5°. For the Octopus attenuation was lowest at fixation.

Introduction

Perimetric assessment of patients with media opacities is currently confounded by the problem of separating the reduction in sensitivity arising from optical degradation from that due to neural attenuation

Several studies have qualitatively investigated the effect of cataract on the visual field profile. In manual kinetic perimetry cataracts have been shown to produce contraction of the isopters, pseudo-defects or exaggeration of existing field loss [4, 9, 15, 17, 19] while in manual static perimetry a general decrease in sensitivity is found with the central field being more depressed than the periphery [8, 9]. Clearly, it is necessary to derive a quantitative relationship between sensitivity determined by computer assisted perimetry and the degree of media opacity.

In recent years, contrast sensitivity has been shown to be a more representative measurement of visual function in the presence of cataract than Snellen acuity [11]. Furthermore, the foward intraocular light scatter arising from lenticular

opacities which produces retinal image degradation has been investigated by Paulsson and Sjostrand [18] using contrast sensitivity in the presence and in the absence of glare light Indeed, it has been recently reported that an increased glare score is related to an increase in the turbidity of the media while visual acuity correlates poorly with glare score [1].

The neuro-visual integrity of patients with cataract cannot be established with certainty. Several studies have therefore employed cataract simulations in order to investigate various psychophysical functions. These simulations include, for example, petroleum jelly spots distributed over the surface of a lens system [22] suspensions of particles $5 \mu m$ in diameter [11] varying concentrations of latex beads $10 \mu m$ in diameter [16] and ground glass [7]. In addition, a recent study has investigated the influence of 'simulated glare' produced by diffusing lenses on the differential threshold obtained with the Octopus and Humphrey perimeters [12].

We report an ongoing study the aim of which is threefold: to produce a source of intraocular light scatter; to devise a method whereby the relationship between intraocular light scatter and the perimetric attenuation of both projected stimuli and light emitting diode stimuli could be determined; and to further investigate this relationship utilizing a sample of patients with media disturbances.

Methods

The study has been divided into two sections. The sample for the first part comprised 12 clinically normal age matched subjects (mean age 24.1 years; SD 2.9 years) familiar with psychophysical techniques. Intraocular light scatter was simulated by suspending 0 01%, 0.02% and 0.025% solutions of latex beads in cells consisting of plano powered CR39 optical lenses. A bead diameter of 500 nm was selected since it has been demonstrated that the diameter of the protein aggregates producing intraocular light scatter is between 300–500 nm [2, 6] in human and calf cataractous lenses respectively. Different concentrations of beads were employed since it has also been demonstrated that interparticle separation is an important parameter in intraocular light scatter [2].

The second sample comprises patients displaying a marked asymmetry in the degree of cataract. Criteria for selection of the better eye is a distance acuity of better than or equal to 6/9 and minimal disturbance of the media. As far as can be ascertained the patients are free of other ocular or neurological pathology and of systemic disease with known serious ophthalmic complications; those in whom a fundal view cannot be obtained undergo flash E.R.G.s and V.E.R.s. Patients with marked nuclear cataracts are excluded

Contrast sensitivity for both samples is measured using the apparatus devised by Griffiths, Barnes and Drasdo [10] which utilises the Nicolet CS 2000 contrast sensitivity system in the presence and absence of narrow angle (3 5°) and wide angle (30°) glare light (Fig 1). A sine wave grating is used with a spatial frequency
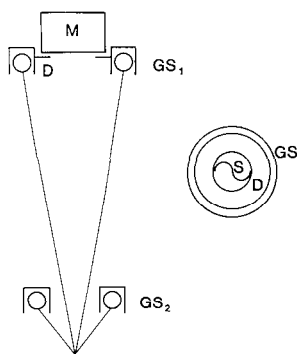
Figure 1 Diagrammatic representation of the apparatus used to derive the light scattering factor in the two experimental samples GS₁ and GS₂ denote the narrow and wide angle glare sources respectively, M is the monitor, D is the diffusing screen and S is the sine wave grating

of 1 c/deg, counter phased at a rate of 2 Hz, as this frequency is not considered to be attenuated by optical blur [5]. The viewing distance is 3 m and the screen luminance 94 cdm^{-2}. Differential light sensitivity for both samples is measured with the Dicon AP3000 (target projected diameter 0 28°; peak wavelength 580 nm) at bowl luminances of 10 asb and 45 asb and with the Octopus 201 automated perimeter. The meridional threshold and macula threshold programs of the Dicon are used along the 85° and 265° meridians at eccentricities of 0°, 1°, 3°, 5°, 7.5°, 20°, 27.5° with a stimulus presentation time of 400 ms and interstimulus duration of 1s. Octopus program 31 is used in conjunction with stimulus size 3 (projected diameter 0.431°) the standard bowl luminance of 4 asb and the stimulus presentation time of 100 ms.

Using these procedures, contrast sensitivity and the visual fields were measured in the right eye of the first sample with and without the simulated light scatter. The examinations for the second sample are undertaken on each eye of the patient. The contrast sensitivity and the Dicon examinations are determined at one session; the sequence of examination within this session is randomized. The Octopus examination is conducted at another session on a separate occasion. The order of the two sessions, the experimental condition in the case of the first sample and the order of eye examined in the case of the second sample are all randomized. Patients with no experience of automated perimetry and/or contrast sensitivity receive suitable training. Distance correction is used with the appropriate near correction for the particular viewing distance. Natural pupils are used throughout since the procedure is intended for clinical application; the changes in pupil size, however, compensate to some extent for the changes in illumination associated with the glare light.

The intraocular light scatter with and without the various concentrations of latex beads was calculated from the equation of Paulsson and Sjostrand [18]:

$$\mu = L/E \ (M_2/M_1 - 1)$$

where L = the screen luminance, E = the illuminance of the glare source and M_2 and M_1 are the contrast thresholds with and without glare light respectively In the first sample results for a given subject are presented in terms of the differences in scatter factor and in perimetric sensitivity between the eye in the normal state and in the particular experimental condition. In the second sample, a similar calculation is carried out for both eyes of a given patient and the results are presented in terms of the differences between the two eyes.

Results and discussion

The attenuation in perimetric sensitivity for the Octopus, expressed as a volumetric index derived by the Monte Carlo technique [21] due to the increasing intraocular light scatter arising from the latex bead simulations shows a linear relationship for both the narrow and wide angle glare sources (Fig. 2). The degree of scatter is less for the wide angle light source than for the narrow angle due to the line spread function of the eye.

The depression in Octopus sensitivity expressed as the mean of the 4 measure-
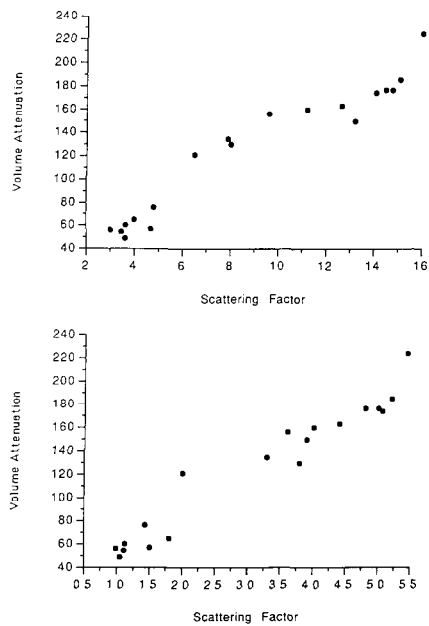
Figure 2 Scattergram illustrating the increase in volumetric attenuation (dB radian²) for Octopus Program 31 with increase in the narrow (top) and the wide angle angle (bottom) scattering factor for the normal subjects in combination with the varying concentrations of latex beads
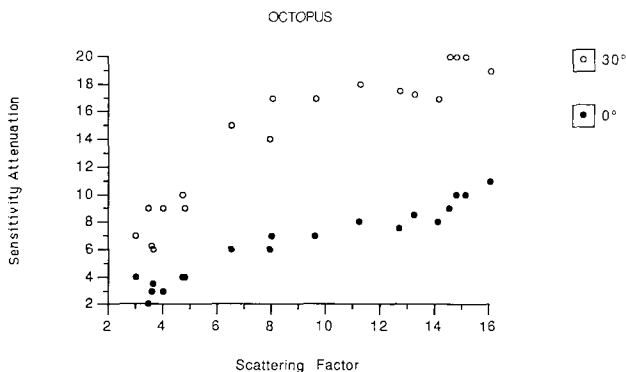
OCTOPUS

Figure 3 Scattergram illustrating attenuation of sensitivity (dB) for Octopus program 31 against narrow angle scattering factor as a function of eccentricity for the normal subjects in combination with the varying concentrations of latex beads

ments at a given eccentricity, as a function of peripheral angle, shows a greater attenuation with increasing intraocular light scatter for the peripheral eccentricities than for fixation (Fig. 3) This arises because the foveal region is saturated and therefore relatively insensitive to small changes in light intensity, for the larger targets such as Goldmann 3 at the low photopic bowl luminance of 4 asb [20] This has the effect of steepening the normal sensitivity gradient within the central field (Fig 4) and has also been reported to occur with age [13]. The depression in sensitivity, expressed as the mean of 2 measurements at each eccentricity, with increasing intraocular light scatter for the Dicon also demonstrates a linear relationship for both glare sources. The attenuation is greater at the lower bowl luminance of 10 asb than at 45 asb bowl luminance and is due to the greater increase in Weber's Fraction at lower luminances (Fig 5). This is in accord with Greve [8] and is compatible with the conclusions of a recent study [14]. In contrast to the results from the Octopus, the attenuation for the Dicon is greater centrally than peripherally at both bowl luminances (Fig. 6) and arises for
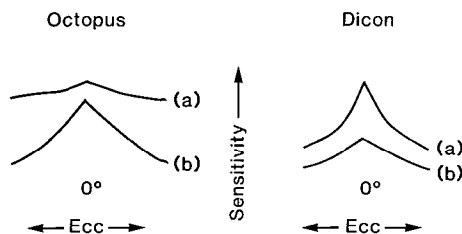
Figure 4 Schematic representation of the influence of intraocular light scatter (b) on the flat sensitivity profile of Octopus program 31 for target size 3 (a) (left) and on the relatively steep profile of the Dicon at 10 asb bowl luminance (a) (right)
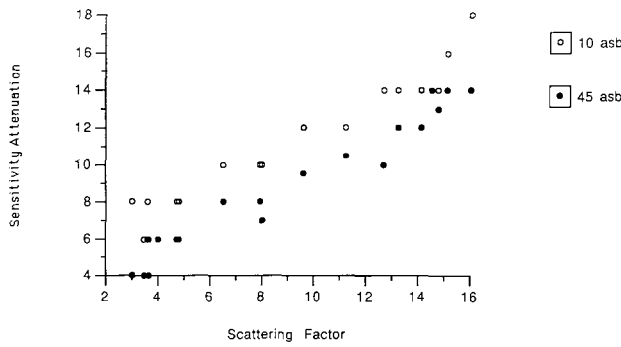
Figure 5 Scattergram illustration attenuation of sensitivity (dB) at fixation for the Dicon against narrow angle light scattering factor as a function of background luminance for the normal subjects in combination with the varying concentrations of latex beads
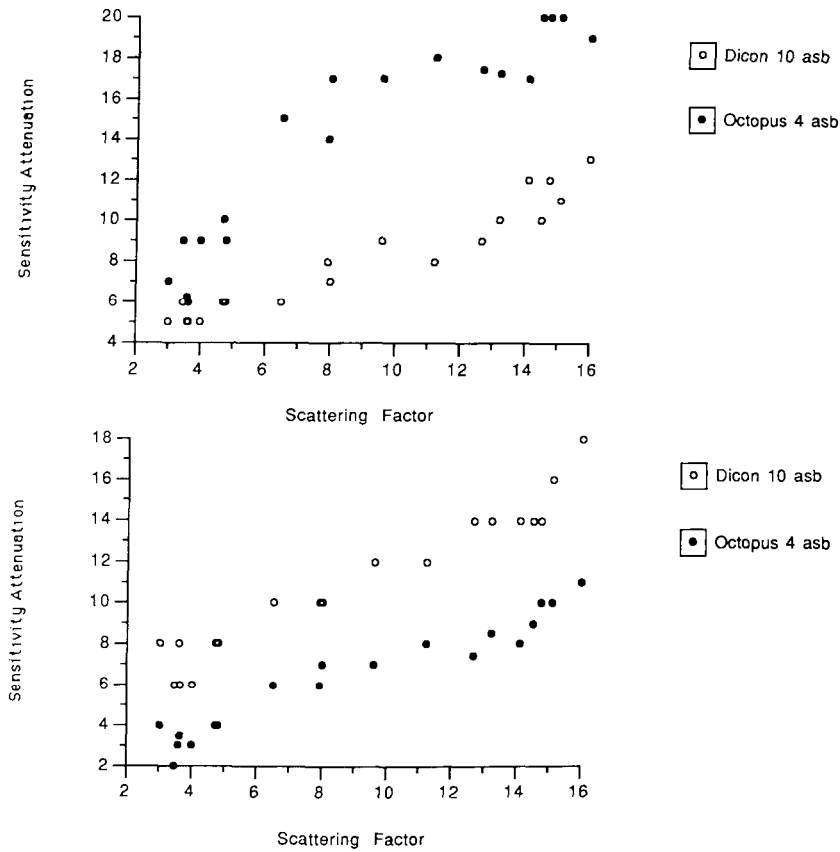
Figure 6 Scattergram illustrating attenuation of sensitivity for the Dicon (10 asb) and Octopus as a function of eccentricity (top) 27 5° (Dicon) and 30° (Octopus) and fixation (bottom)
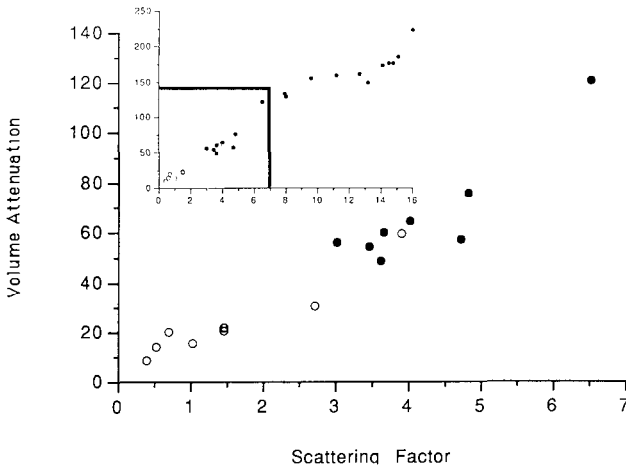
Figure 7 Scattergram illustrating increase in volumetric attenuation (dB rad^2) against light scattering factor for cataractous patients with low scattering factors (open circles) and for the normal subjects in combination with the varying concentrations of latex beads (filled circles) The inset shows the relationship of the cataractous data to the corresponding scattergram shown in Fig 2

the small LED target configuration because of the relative sensitivity of the central areas to small changes in light intensity (Fig. 4) This has the effect of flattening the Dicon sensitivity gradient and is in agreement with the classical belief that cataract reduces central sensitivity more than peripheral sensitivity thus resulting in a flattening of the sensitivity gradient The use of visual field data in this manner, however, is always subject to the short and the long term
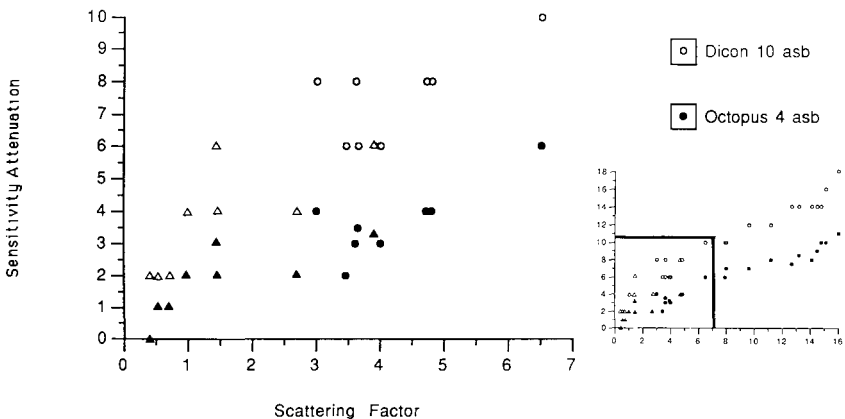
Figure 8 Scattergram illustrating the attenuation of sensitivity at fixation for the cataractous patients with low light scattering factors (open triangles Dicon (10 asb); closed triangles Octopus) The inset shows the relationship of the data to the corresponding scattergram in Fig 6

fluctuations inherent in this type of threshold psychophysical investigation.

The results for the unilateral cataractous patients with low scattering factors (Figs 7 and 8) follow the general relationship between intraocular light scatter and perimetric attenuation described in the first part of the study. The effects of intermediate scattering factors are currently under investigation. Patients with hand movements or less were unable to resolve the grating at the maximum contrast or appreciate the visual field targets. The use of the contralateral eye as a control to determine the perimetric attenuation of the cataractous eye depends upon the assumption that the visual fields of the two eyes are symmetrical. This would seem to be valid since it has been reported for the Humphrey Field Analyser that asymmetry exceeding 6 dB between the two eyes of a given patient at corresponding locations will occur at less than 1% of the test locations [3].

Conclusions

A high correlation is found between perimetric attenuation and the intraocular light scattering function in both normal subjects with the simulated intraocular light scatter and in patients with uniocular media opacities exhibiting low scattering factors. It is proposed that the degree of perimetric attenuation of a patient with media opacities can be predicted from a measure of the light scattering function. Further work will, however, be necessary to investigate the format of such a relationship in subjects with field loss.

References

1 Abrahamsson M, Sjostrand J: Impairment of contrast sensitivity function (CSF) as a measure of disability glare Invest Ophthalmol Vis Sci 27: 1131–1136 (1986)
2 Bettelheim FA, Siew EL: Biological and physical basis of lens transparency In: McDevitt D (ed) Cel biology of the eye, pp 243–297 Academic Press, New York, 1982
3 Brenton RS, Phelps CD, Rojas P, Woolson RF: Interocular differences of the visual field in normal subjects Invest Ophthalmol Vis Sci 27: 799–805 (1986)
4 Bigger JF, Becker B: Cataracts and open-angle glaucoma Am J Ophthalmol 71: 335–340 (1971)
5 Campbell FW, Green DG: Optical and retinal factors affecting visual resolution J Physiol (Lond) 181: 576–593 (1965)
6 Delaye M, Clark JI, Benedek GB: identification of the scattering elements responsible for lens opacification in cold cataracts Biophys J 37: 647–656 (1982)
7 Essock EA, Williams RA, Enoch JM, Raphael S: The effects of image degradation by cataract on vernier acuity Invest Ophthalmol Vis Sci 25: 1043–1050 (1984)
8 Greve EL: Single and multiple stimulus static perimetry in glaucoma; the two phases of visual field examination Docum Ophthalmol 36: 1–355 (1973)
9 Greve EL: Visual fields, glaucoma and cataract Docum Ophthalmol Proc Series 19: 79–88 (1979)
10 Griffiths SN, Barnes DA, Drasdo N: Psychophysical aspects of contrast sensitivity attenuation (Abstract) Ophthalmic Physiol Opt 4: 189 (1984)
11 Hess R, Woo G: Vision through cataracts Invest Ophthalmol Vis Sci 17: 428–435 (1978)

12 Heuer DK, Anderson DR, Knighton RW, Gressel MG: The influence of simulated glare on Octopus 201 and Humphrey field analyser threshold measurements (Abstract) Invest Ophthalmol Vis Sci 27: 158 (1986)
13 Jaffe GJ, Alvarado JA, Juster RP: Age-related changes of the normal visual field Arch Ophthalmol 104: 1021–1025 (1986)
14 Klewin KM, Radius RL: Background illumination and automated perimetry Arch Ophthalmol 104: 395–397 (1986)
15 Kolker AE, Hetherington J: Becker and Shaffer's diagnosis and therapy of the glaucomas, p 163 CV Mosby Co, St Louis, 1976
16 LeClaire J, Nadler P, Weiss S, Miller D: A new glare tester for clinical testing Arch Ophthalmol 100: 153–158 (1982)
17 Lyne AJ, Phillips CI: Visual field defects due to opacities in the optical media Br J Ophthalmol 53: 119–122 (1969)
18 Paulsson LE, Sjostrand J: Contrast sensitivity in the presence of glare light Invest Ophthalmol Vis Sci 19: 401–406 (1980)
19 Radius RL: Perimetry in cataract patients Arch Ophthalmol 96: 1574–1579 (1978)
20 Wood JM, Wild JM, Drasdo N, Crews SJ: Perimetric profiles and cortical representation Ophthalmic Res 18: 301–308 (1986)
21 Wild JM, Wood JM, Hussey MK, Crews SJ: The quantification of computer assisted threshold perimetry Doc Ophthalmol Proc Series (in press)
22 Zuckerman JL, Miller D, Dyes W, Keller M: Degradation of vision through a simulated cataract Invest Ophthalmol is Sci 12:213–224 (1973)

Authors' addresses:
J M Wood, J M Wild,
Department of Vision Sciences,
Aston University,
Aston Triangle,
Birmingham B4 7ET, U K

D L Smerdon, S J Crews,
Retina Department,
Birmingham and Midland Eye Hospital,
Church Street, Birmingham B3 2NS, U K

I.9 Computer perimetry in patients with corneal dystrophies

C. FASCHINGER
Graz, Austria

Abstract

We investigated six eyes of three patients with lattice corneal dystrophy, one with granular corneal dystrophy and one with a recurrence in the graft. We used the Automated Perimeter Octopus and employed the programs 31 and a user-defined program of the software Sargon for the center.

In lattice degeneration all visual fields showed a decrease of local thresholds between 5 and 12 dB. Maybe because of higher glare and scatter in granular dystrophy and possibly because of the recurrence the individual thresholds showed a greater variety.

Introduction

Media opacities may partly lead to an absorption, partly to scattering and reflection of the light. The results can be either metamorphosia or blurred vision with reduction of visual acuity, or discomfort glare, or decrease of visual field sensitivity.

We examined four patients with corneal clouding caused by hereditary stromal dystrophies.

We used the standard program number 31 of the Octopus Automated Perimeter (Type 201) as well as a user-defined program Sargon for the central visual field to determine a change of the thresholds.

Materials and methods

We investigated three patients of a family with lattice corneal dystrophy, who had not yet had a penetrating keratoplasty [2] Their age was 38, 42 and 46 years. The diagnosis was confirmed by ultrastructural examinations of grafts obtained at
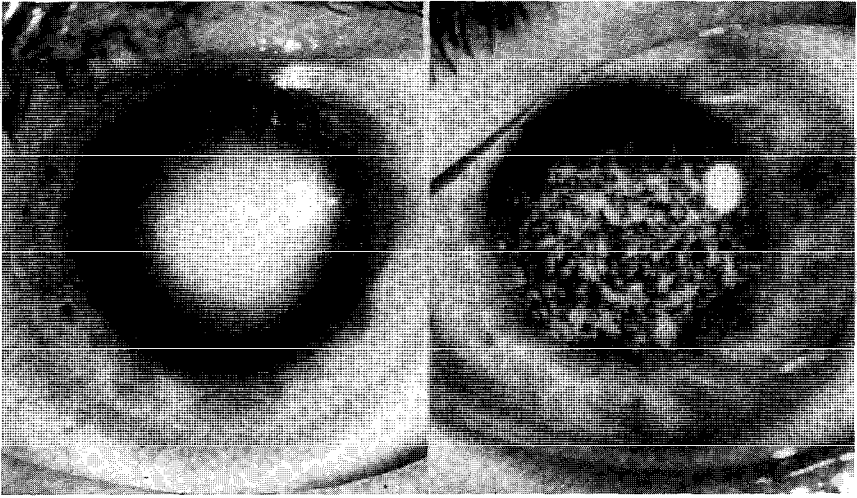
Figure 1 Central homogenous clouding in lattice corneal dystrophy and granular corneal dystrophy

penetrating keratoplasties of other members of the family.

At the point of time of the slitlamp- and visual field examinations all eyes were uninflamed, the epithelium of the cornea closed, the lens and the vitreous clear and the fundus normal. The six corneas showed disciform, relatively homogenous whitish stromal cloudiness in the central third. The periphery was opacified by multiple fine lattice-like lines, which showed a rectangular or irregular crossing in different depth of the stroma The visual acuity was between 0.3 and 0.5.

In addition we investigated a 55-year-old female patient with granular corneal dystrophy. Five years after penetrating keratoplasty the right eye developed a recurrence in the graft, which looked white and radial like a flower. The left eye showed partly seperate well-defined, partly confluent granules in the center of the corneal stroma. The peripheral cornea of both eyes was clear. The visual acuity of the right eye was 0.25 and of the left 0.1 (Fig. 1).

All patients complained of decrease of vision and different discomfort glare sensitivity

After dilation of the pupils we made photographs including retro-illumination and started the visual field investigations with the standard program number 31 to check the area from zero to 30 degrees excentricity. This program consists of a rectangular grid of 6 degrees with 73 targets.

Then we used a special program from the software Sargon. For any area a grid of a maximum of 66 points can be measured using x/y coordinates. We plotted 61 targets in a hexagonal area centered on the fovea with a rhombic grid of 2 and 4 degrees diagonal length. For further control of the fixation and reliability 4 targets were arranged in the blind spot. Thresholds are determined by a repetitive bracketing process.

Profiles (Program 31)
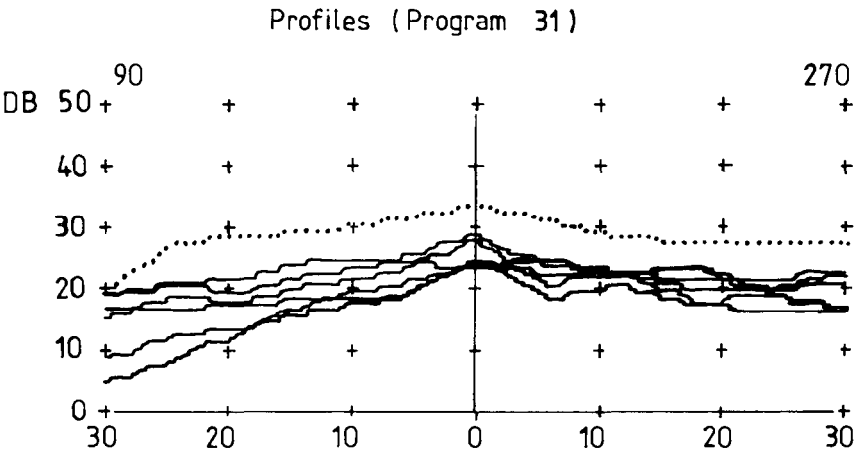
Figure 2 Profiles from 90 to 270 degrees (program 31) Lines: six eyes with lattice corneal dystrophy
Dotted line: 44-years-old patient with clear media

Fixationring:
Program numbers: A1

327 0 Date of printout: 25.02.1986
0(0/ 8) 0(0/ 8)

USER-DEFINED PROGRAM. LABEL: CSR DATE OF PROGRAM: 25.10.1981
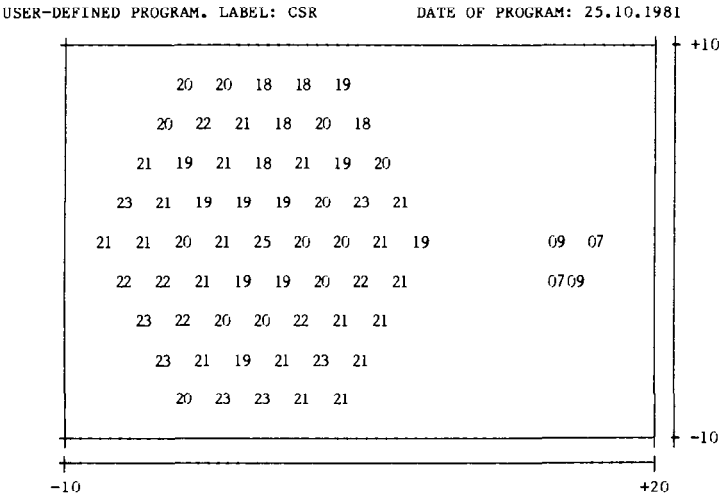
Figure 3 Program Sargon of patient with lattice corneal dystrophy: uniform loss of the thresholds
between 5 and 12 decibels in comparison to the normal values

64

Results

All six eyes with lattice dystrophy showed in the visual field as determined by the program 31 a gentle slope of the central sensitivity. The examination with the program Sargon revealed a uniform loss of the thresholds between 5 and 12 decibels in comparison to the normal values. Neither isolated scotomas nor absolute defects could be found The mean fluctuations were 1.13 ± 0.18 (Figs 2 and 3).

In the patient with the granular dystrophy and the recurrence in the graft the decrease of the thresholds was rather irregularly shaped. In the program Sargon the individual thresholds showed a great variety of values: beside normal values there were some very low ones. Furthermore, one-third of the catch-trials showed either a false positive or a form negative response. The high threshold values in the area of the blind spot demonstrate the poor fixation.

Discussion

Media opacities, e.g. cataract or vitreous hemorrhages, may lead to a severe decrease or restriction of the visual field sensitivity [1, 3].

Patients with opacities caused by stromal corneal dystrophies will usually come early to a penetrating keratoplasty because of reduction of visual acuity, recurrent erosions, glare and not because of the changes of the visual field alone. Despite the limited number of eyes we can conclude that homogenous opacities of the cornea like in lattice degeneration will produce a general reduction of sensitivity to approximately one-third of the normal sensitivity.

Inhomogenous opacities like in granular dystrophy with increase of glare and scatter will lead to a great variety of the individual thresholds.

References

1 Guthauser U, Flammer J, Lotmar W, Niesel P: Einfluß der Katarakt auf das Gesichtsfeld Klin Mbl Augenheik 188: 409–411 (1986)
2 Hesse W, Haller EM: Sechs Generationen gittrige Hornhautdystrophie (Die Grazer Familie) Klin Mbl Augenheilk 183: 372–374 (1983)
3 Lauber H: Der Einfluß von Medientrübungen auf das Gesichtsfeld Graefe's Arch klin exp Ophthal 140: 687–690 (1939)

Author's address:
Christoph Faschinger,
Department of Ophthalmology,
University Eye Clinic Graz,
Auenbruggerplatz 4,
A-8036 Graz,
Austria

I.10 Does higher background illumination lessen the effect of media opacities on visual fields?

L.B. BALDWIN and T.J. SMITH

Lexington, U.S.A

Abstract

Visual field function of the right eyes of five normal subjects was evaluated on the Digilab 350 automated perimeter at background illuminances of 3.15 asb and 31.5 asb. Serial visual field evaluations were repeated under four conditions of retinal illumination at each of the two backgrounds. Threshold sensitivities significantly decreased with increasing neutral density effect at both backgrounds and the effect was greater at 3.15 asb. The choice of background illuminance may be important in obtaining accurate visual fields in patients with decreased retinal illumination, however, the difference in threshold sensitivities obtained at the two backgrounds may be unmeasurable on currently available automated perimeters.

Introduction

The perception of a perimetric stimulus is a complex phenomenon dependent on the relationship of target intensity, background illumination, and the state of retinal adaptation. Under photopic conditions, the Weber relationship states that the ratio of stimulus intensity to background illumination ($\triangle I/I$) is relatively constant. The Rose-deVries relationship ($\triangle I/\sqrt{I}$) more closely applies in the mesopic range.

Although the use of automated perimetry has become widespread, the optimal background luminance has never been established. While Goldmann selected the 31 asb figure because it allowed a greater definition of isopters, and Fankhauser chose 4 asb because of increased dynamic range, the choice of background luminance in perimetry has been based on very little empirical data.

Despite Fankhauser's conclusion that the difference in the effect of miotic pupils on threshold sensitivity at 4 asb and 40 asb backgrounds was not clinically significant [3], the accuracy of visual fields at the lower background has been

questioned in patients with decreased retinal illumination. In a recent article, Klewin and Radius suggest that in subjects with defective light transmission, statistically significant diminutions in test scores may be seen earlier with a 4 asb background (Octopus) than would be seen at 31.5 asb (Goldmann) [4]. In this study we compare the effects of decreased light transmission on automated visual fields measured at high mesopic (31 5 asb) and low mesopic (3.15 asb) background luminances.

Subjects and methods

The central visual field function of the right eye was evaluated in 5 normal volunteers ranging from 25 to 30 years of age. No ocular disease was present and all subjects were corrected to 20/20 visual acuity for each examination.

For each participant, central threshold examinations were performed on a Digilab 350 perimeter using a triple crossing, staircase thresholding technique [5]. Eight fields were obtained per subject, testing four conditions of retinal illumination at each of the two background luminances (3.15 asb and 31.5 asb). Before each examination the subject's left eye was covered with a translucent shield and a standard black scuba mask with the left half of the glass blackened with opaque black plastic was placed over the face. One of three neutral density filters (0.5 log unit, 1.0 log unit, 2.0 log unit), or no filter was placed before the right eye and the patient was appropriately dark adapted. Fifteen minutes of dark adaptation was performed before all fields obtained at the lower background, and for those performed with 1.0 log unit and 2 0 log unit neutral density filters at 31.5 asb.

All field results were inspected for pattern defects and the mean threshold performance value was recorded for each of the eight filter density/background illumination combinations.

Results

The results of these examinations are shown in Table 1. As expected, no pattern

Table 1 Mean threshold sensitivity

Neutral density filter (Log unit)	Performance 3 15 asb	Value/field 31 5 asb	dB/test point	
			3 15 asb	31 5 asb
0 0	636 0	440 6	26 5	18 4
0 5	593 8	405 2	24 7	16 9
1 0	505 0	366 0	21 0	15 3
2 0	418 2	294 0	17 4	12 3
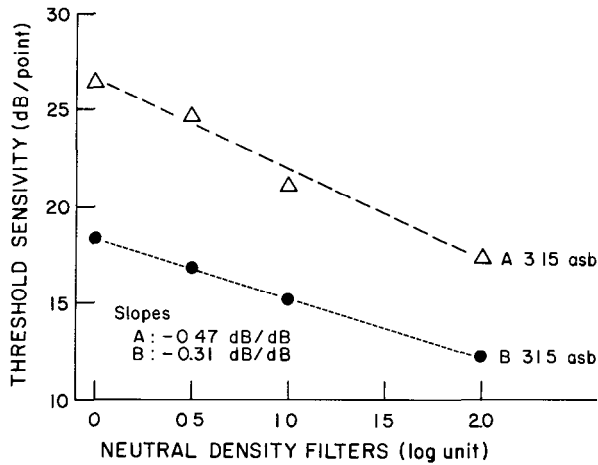
Figure 1 Variations in threshold sensitivity as a result of increasing neutral density effect

defects were found. The data were subjected to an analysis of variance procedure for a repeated measures experiment. A linear trend was found for the measurements at each background and these linear trends varied significantly with the background ($P<0.0001$) (Fig. 1). An estimated generalized least squares procedure was used to obtain the slopes of the two lines with results shown in Table 2. The rate of loss of threshold sensitivity (dB) per unit (dB) decrease in light transmission was calculated with values of -0 47 dB/dB for the 3.15 asb background and -0.31 dB/dB for 31.5 asb.

Discussion

Decreased retinal illumination produced by neutral density filters has a statistically significant effect on threshold sensitivity at both 3.15 asb and 31.5 asb backgrounds. This effect is more marked at the lower luminance. While the change in threshold sensitivity per unit filter is statistically less at 31.5 asb than 3.15 asb, the clinical significance of this remains to be seen.

Table 2 Slope values

Background intensity	For 72 point visual field		For individual test points	
	PV/log unit	dB/dB	PV/log unit	dB/dB
3 15 asb	−112 3	−33 69	−1 56	−0 47
31 5 asb	− 73 6	−22 08	−1 02	−0 31

Neutral density filters probably do not approximate clinical media opacities. Recent work has shown that an afferent pupillary defect may be seen with as little as a 0.3 log unit neutral density filter [2]; media opacities do not produce measurable afferent pupillary defects [1]. Therefore, any neutral density effect is unlikely to be greater than 0.3 log unit (3 dB).

At this level of decreased light transmission there would be a drop of 1.41 dB/point from baseline values for the 3.15 asb background and 0 93 dB/point for 31.5 asb. The difference between these values, 0.48 dB, is not meausurable on any available automated perimeter as used in clinical practice.

It remains an open question whether there is an optimal background illumination for patients with media opacities or decreased retinal illumination secondary to miosis.

References

1 Argus WA, Brenton RS: Background illumination and automated perimetry Arch Ophthalmol 104: 1124 (1986)
2 Cox TA: Pupillogaphy of a relative afferent pupillary defect Am J Ophthalmol 101: 320–324 (1986)
3 Fankhauser F: Problems related to design of automated perimeters Doc Ophthalmol 47: 89–138 (1979)
4 Klewin KM, Radius RL: Background illumination and automated perimetry Arch Ophthalmol 104: 395–397 (1986)
5 Krakau CET: Aspects on the design of an automated perimeter Acta Ophthalmol (KGH) 56 (3): 389–405 (1978)

Author's address:
Department of Ophthalmology,
University of Kentucky,
800 Rose Street, Lexington, KY 40536-0084, U S A

Section II
Normal and pathological variability

II.1 Short-term and long-term fluctuation of thresholds in automated perimetry in normals, ocular hypertensives and glaucoma patients

C.T. LANGERHORST, T J.T.P VAN DEN BERG, H. BOERSMA
and E.L. GREVE
Amsterdam, The Netherlands

Abstract

We analysed the results of visual field examinations, measured repeatedly over time. In 40 eyes of 11 normal subjects, 8 patients with ocular hypertension and 21 glaucoma patients the measurements were performed with the Scoperimeter. In 35 eyes of 18 glaucoma patients the measurements were performed with the Friedmann Visual Field Analyser. We studied the Long-term Fluctuation (based on the standard deviation of differences between sessions) of three visual field parameters· Mean Threshold, Individual General Sensitivity and Mean Defect. We found that the long-term fluctuation of the Mean Threshold was around 1.5 dB (sd). We broke the Mean Threshold down in two components: the Individual General Sensitivity and the Mean Defect. The Mean Defect proved to be the most stable parameter over time. Thus, for assessment of the pathological state of the visual field the Mean Defect seems to be the better choice.

Introduction

It is well known that visual fields can fluctuate considerably [5]. In glaucoma, where one is interested to detect deterioration of the visual field, this phenomenon of fluctuation may make it difficult to judge if there is true progression or large scatter. It is therefore desirable to know more about fluctuation behavior. Much work in this area has been done by Flammer et al. [2] An extensive overview can be found in our chapter in 'Glaucoma' [6]. The aim of this study was to investigate the magnitude of long-term fluctuation (LF) in different groups of subjects, to compare the results of two different instruments, and to evaluate computerized techniques of analyzing long-term fluctuation

Material and methods

We analyzed the results of two entirely separate populations of subjects, tested with different instruments:
- Population I consisted of 40 subjects divided over 5 different groups and tested with the 'Scoperimeter' automated perimeter.
- Population II consisted of 18 subjects (35 eyes) in one group tested with the Friedman Visual Field Analyzer.

Population I. Scoperimeter population

40 Subjects were investigated, falling in one of the following groups:
- *NORMAL* normal controls with visual acuity >0.6, clear media or incipient cataract, normal optic disc, intraocular pressure (IOP) ≤22 mm Hg and without known eye disease.
- *OHT·* ocular hypertensives, with visual acuity >0.6, clear media or incipient cataract, either a normal or a suspect disc, IOP >22 mm Hg, and no visual field defects as measured with our methods.
- *POAG:* patients with primary open angle glaucoma, visual acuity >0.3, with glaucomatous disc excavation and glaucomatous visual fields (relative defects or small maximal defects, stage I–III) [3].
- *HTG:* high tension glaucoma patients, as POAG but with IOP without therapy at least once >40 mm Hg in a diurnal curve.
- *LTG:* Low tension glaucoma patients, as POAG but with IOP without therapy generally <22; an isolated higher IOP with a maximum of 26 mm Hg was accepted

The number of subjects per group and their mean age are given in Table 1. With the Scoperimeter research-perimeter [1] we conducted a full threshold test in 60 locations in the 25° visual field. This was done twice without intermission for each of the subjects. The total test duration was 12 minutes on average. This double threshold test was repeated 2 to 10 times over a period of weeks to 2 years, rendering several sessions per subject.

Table 1 Number of patients and mean age in the 5 groups of the Scoperimeter population

Group	Number of patients	Mean age (years)
Normal controls (NORMAL)	11	67 2 ± 9 8
Ocular hypertension (OHT)	8	54 0 ± 11 3
Primary Open Angle Glaucoma (POAG)	12	63 5 ± 7 5
POAG – High Tension Glaucoma (HTG)	5	49 2 ± 14 1
POAG – Low Tension Glaucoma (LTG)	4	74 5 ± 4 5

Computer analysis of the double thresholds provided us with many parameters, of which three will be considered in this study: the Individual General Sensitivity (IGS), the corrected Mean Threshold (MT cor.) and the Mean Defect (MD). The analysis starts by correcting all threshold values for the eccentricity of the visual field. For this study we used a correction of 0.3 dB per degree of eccentricity, and did not use an additional individual gradient adaptation. The mean of the thus corrected thresholds is called MT-corrected. All further computations are done with the corrected thresholds Subsequently for every test the Individual General Sensitivity is computed, which we use as an individual reference value rather than using population means for normal reference. To compute a reliable IGS, certainly normal positions are selected for which a randomly chosen element of the two thresholds had a high sensitivity. Subsequently the IGS was calculated as the mean value of the second thresholds. This way bias is avoided [7] The Mean Defect MD is the difference between IGS and MT corrected (MD = MT corrected − IGS) Also for every test the Short-term Fluctuation (SF) was computed based on the difference between the two measurements in each location (standard deviation). We looked at the long-term Fluctuation (LF) of IGS, MT cor and MD per individual, defined as the standard deviation based on the differences between sessions We also averaged these LF results per group. In addition we computed the mean values of MD, MT cor and IGS per group, based on the average values of all examinations of every patient.

Population II Friedmann population

In 1971 Greve et al. [4] started a prospective 10-year follow-up study of glaucoma patients (POAG and HTG) who underwent a filtering procedure. We used this material available in our clinic to look retrospectively at long-term fluctuation. Repeated static threshold fields measured with the Friedmann Visual Field Analyzer were available for 35 eyes of 18 patients. The mean age of this patient group was 73.4 ± 10.3 years. We looked at the LF (as standard deviation of differences between sessions) of the Foveal value, Mean Threshold value, and the difference between those two: MD = Fovea − MT.

Results

Figure 1 shows the IGS, MT cor and MD of 4 examples of the Scoperimeter population. It is evident that the MD has the least scatter.

The mean values for the different groups of subjects are shown in Table 2, as well as the standard deviation per group, indicating the mean long-term fluctuation per group. The glaucoma patient groups show a lower mean IGS and mean MT than the normal subjects or ocular hypertensives. In our normals we found a
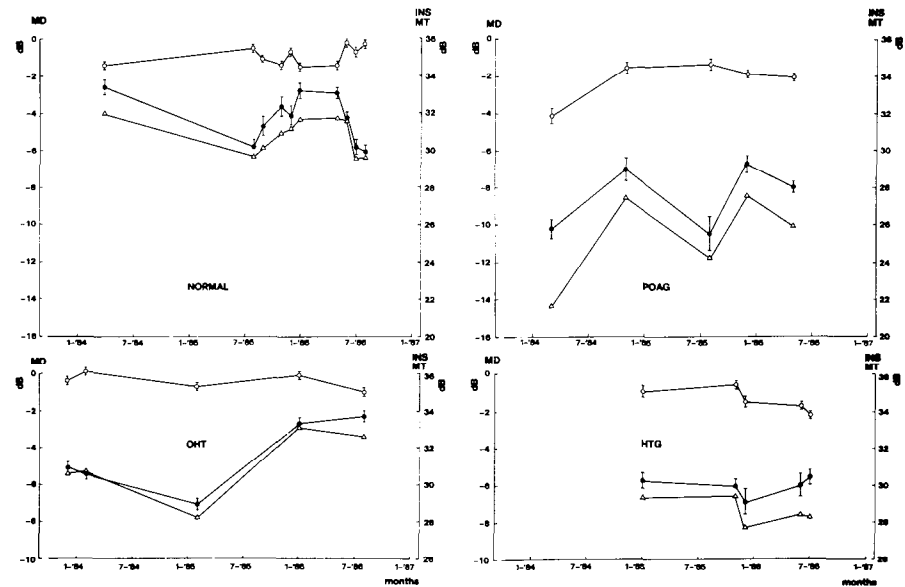
Figure 1 Four examples of long-term behavior of visual field parameters measured with the Sco-perimeter ○ = MD; ● = IGS; △ = MTcor The horizontal axis shows the dates (month) of examination

MD of 1 1 dB. The long-term fluctuation of the MD is less than the LF of the IGS or MT-corrected for all groups in the Scoperimeter population. For the Fried-mann population the LF of MT corresponds with that of the other groups. The LF of fovea and MD are not readily comparable (see Discussion).

Table 2 Mean values and standard deviation (= LF) of three visual field parameters for all groups tested

	Mean values per group (in dB)			Standard deviation per group (LF) (in dB)		
	IGS	MT cor	MD	IGS	MT	MD
Normal	29 6	28 7	−1 1	1 2	1 1	0 5
OHT	30 9	30 3	−0 8	0 8	0 7	0 4
POAG	27 0	23 3	−3 7	1 9	2 6	1 5
HTG	28 5	26 7	−2 1	1 3	1 5	0 8
LTG	26 0	18 6	−7 6	1 8	1 7	1 2
				FOVEA	MT	MD
POAG + HTG (Friedmann population)				3 3	1 7	2 9

Discussion

Several interesting points emerge from this study. First, not only MT but also IGS values are lower in the mean for the patients (POAG, HTG, LTG) than for the normals and ocular hypertensives. This could be evidence for a general reduction of sensitivity of the visual field due to glaucoma, since there was no media disturbance in these patient groups.

Secondly, the LF of the IGS is higher in the combined patient groups. This also points to an influence of pathology on IGS. Whether there is any difference in IGS behavior between the subgroups of the glaucoma patients, e.g. on the basis of differences in age or stage of the visual field defects, cannot be determined with this limited number of subjects. We are presently testing more subjects in each group.

The normal group has an average MD of 1 1dB, which is rather large. A small MD in normals would be unavoidable when using IGS as reference. The large MD in this study is probably due to our present algorithm, which has been corrected. Most interesting is the finding that the LF of the MD is considerably less than the LF of the other two important visual field parameters, IGS and MT cor. When comparing visual fields over time, the results would be most reliable for the parameter(s) which scatter(s) least with long-term follow-up. Our results show that splitting the Mean Threshold into an IGS-part and a Mean Defect part increases the accuracy of long-term comparison by diminishing scatter. This holds true irrespective of the height of IGS. When comparing these Scoperimeter-method results with those of the Friedmann Analyzer, it can be seen that the Mean Threshold, which is the most directly comparable value, has approximately the same LF. This is encouraging in view of the fact that two quite different instruments are concerned here.

The foveal value of the Friedmann group showed a larger LF than the IGS determined with the Scoperimeter. This might be due to the fact that the IGS is based on much more measurements than the foveal value. The same lack of accuracy in LF might be assumed for the MD of the Friedmann group, since MD = Foveal value − MT.

In *conclusion* our results seem to indicate that:
- separating Mean Threshold into IGS and Mean Defect is useful, because the MD gives the most accurate (least scattering) estimate of visual field behavior over time.
- The LF of MT as measured with two different instruments were comparable in our study.

References

1 De Boer RJ, Van den Berg TJTP, Greve EL, De Waal B: Concepts for automatic perimetry, as applied to the Scoperimeter, an experimental automatic perimeter Int Ophthalmol 5: 181–191 (1982)
2 Flammer J, Drance SM, Zulauf M: Short- and long-term fluctuation in patients with glaucoma, normal controls and patients with suspected glaucoma Arch Ophthalmol 102: 704–706 (1984)
3 Greve EL: Performance of computer assisted perimeters Doc Ophthalmol 53: 343–380 (1982)
4 Greve EL, Dake CL, Klaver H, Mutsaerts EMG: Ten year prospective follow-up of a glaucoma operation The Double Flap Scheie in primary open angle glaucoma Int Ophthalmol 8: 139–146 (1985)
5 Greve EL, Furuno F, Verduin WM: The clinical significance of reversibility of glaucomatous visual field defects Doc Ophthal Proc Series 19: 197–203 (1979)
6 Greve EL, Langerhorst CT, Van den Berg TJTP: Examination of visual function in glaucoma In: McAllister J, Wilson R (eds) Ophthalmology Review Series: Glaucoma, pp 54–87 Butterworths Scientific, 1986
7 Langerhorst CT, Van den Berg TJTP, Van Spronsen R, Greve EL: Results of a fluctuation analysis and defect volume program for automated static threshold perimetry with the Scoperimeter Doc Ophthalmol Proc Series 42: 1–6 (1985)

Author's address:
Eye Clinic of the University of Amsterdam,
Academic Medical Center,
Meibergdreef 9, 1105 AZ Amsterdam, The Netherlands

II.2 Visual field variability in stable glaucoma patients

E.B. WERNER, K.I. BISHOP, P. DAVIS, T KRUPIN, B. PETRIG
and C. SHERMAN
Philadelphia, U.S.A.

Abstract

The total long-term fluctuation of the visual field was measured in 22 patients
with open-angle glaucoma who appeared to be clinically stable and well control-
led on medical therapy. All patients had at least three visual fields performed on
the Octopus 201 perimeter with at least 12 months follow-up since their first visual
field. The three most recently performed visual fields were analyzed.

The average total long-term fluctuation per test location was 2.0 db with 95%
of the sample being between 1 and 6.4 db. Fluctuation seemed generally greater in
patients with more extensive visual field defects.

In order to detect true progressive glaucomatous visual field change in the
presence of this amount of fluctuation, the change in any area of the visual field
would have to be greater than approximately 6.4 db per test location.

Introduction

It has been recognized since the inception of automated quantitative perimetry
that the visual field of an individual appears to fluctuate on repeat testing.
Techniques for measuring the fluctuation of the visual field over time have been
developed by several workers [3, 6, 8, 12, 16–19, 24]. It has now been established
that larger amounts of variability are found in the visual fields of glaucoma
suspects and patients than in normal subjects [4, 5, 7, 9, 10, 11, 17, 19, 22, 23].

Clinicians are primarily interested in learning whether or not their patients are
getting worse so that appropriate glaucoma therapy may be applied. In the
presence of large amounts of variability, the separation of true change in the
visual field from fluctuation becomes an important problem. Various statistical
techniques have been applied to the visual field in an effort to define progressive
visual field loss by detecting statistically significant change [1, 2, 14, 15, 21].

The purpose of this study is to determine the total amount of visual field

fluctuation which may be expected over a long period of time in a sample of clinically stable glaucoma patients. Using this information we can develop criteria for the amount of alteration in the visual field which must occur to be interpreted as a significant change when measured by automated perimetry.

Materials and methods

The charts of all patients followed in the glaucoma service of the Scheie Eye Institute were reviewed. All subjects who met the following criteria were included in the study:
1. diagnosis of primary open-angle glaucoma, pigmentary glaucoma or pseudo-exfoliation with glaucoma;
2. at least three available automated visual field examinations with at least 12 months follow-up since the first visual field;
3. Presence of a definitive nerve fiber bundle visual field defect on manual (Goldmann) perimetry;
4. visual acuity of 20/40 or better with no change in visual acuity greater that one Snellen line during the follow-up period;
5. no intraocular pressure greater than 19 mm Hg at any time since the initiation of the patient's present medical therapy;
6. no clinically detectable change in the appearance of the optic nerve head during the follow-up period;
7. no change in medical therapy for glaucoma during the follow-up period;
8. no laser or surgical treatment for glaucoma during the follow-up period and the 12 preceding months.

All subjects were phakic and had no other known ocular, neurologic or systemic disease likely to affect the visual field or other visual functions. All visual fields were performed on the Octopus 201 perimeter using program 32.

A mean and standard deviation was calculated for each test location for each subject using the three most recently available visual field examinations.

Total long-term fluctuation for each test location was defined as the standard deviation of the mean sensitivity for that location. The total long-term fluctuation for each subject was defined as the mean of the standard deviations for each of that subject's test locations, excluding test locations for which the threshold was always 0 decibels (db). Total long-term fluctuation for the entire sample was the mean of the standard deviations for each test location for all subjects, excluding test locations for which the threshold was always 0 db.

FREQ   DIST   MEAN   SENSITIVITY
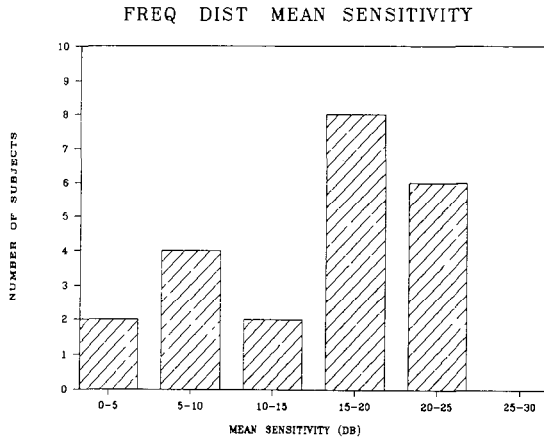
Figure 1 Frequency distribution for the mean sensitivity in decibels of the whole visual field for each of the 22 subjects

Results

Twenty-two subjects were found who satisfied the inclusion criteria If both eyes of a subject qualified for the study, one eye was selected at random. The mean sensitivity of the whole visual field per subject was 15.5 db with a range of 1.2 db to 24.9 db. The study, thus, includes a sample of glaucoma patients ranging from minimal to severe damage (Figure 1). Of the 1628 test locations in the sample, there were 216 whose sensitivity was always 0 db. These points were excluded from further calculations of fluctuation

The mean total long-term fluctuation per subject was 2 0 db with a range of

FREQ   DIST   AVERAGE   LTF   PER   SUBJECT
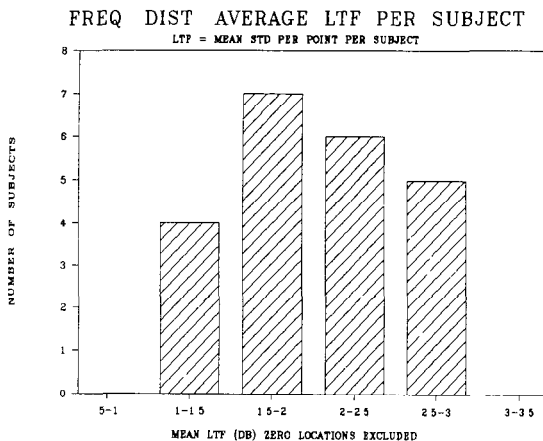
Figure 2 Frequency distribution of the total long-term fluctuation for each subject

AVERAGE LTF VS MEAN SENSITIVITY
ZERO LOCATIONS EXCLUDED
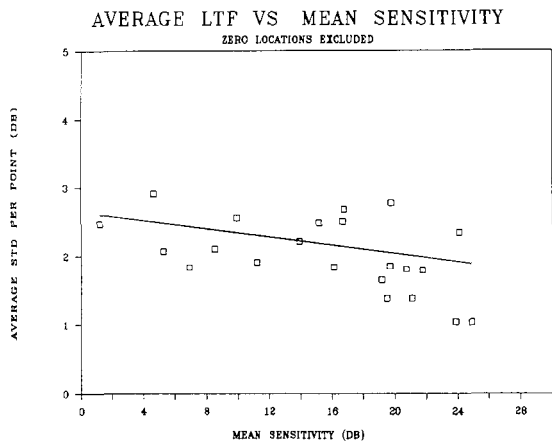
Figure 3 Plot of the total long-term fluctuation for each subject (Y axis) against the mean sensitivity of the whole visual field (X axis) Each point on the graph represents a subject There is a tendency for the absolute value of the total long-term fluctuation to increase as visual field sensitivity decreases. Equation for the regression line is $Y = -0.03X + 2.64$ $R = 0.50$ $p < 0.02$ indicating a significant inverse correlation between sensitivity and fluctuation when test locations with a constant sensitivity of 0 db are excluded from the calculation of long-term fluctuation

1.0 db to 2.9 db (Figure 2) When expressed as a coefficient of variation, the mean total long-term fluctuation per subject was 26.6% with a range of 4.7% to 96.4%. There was a definite relationship between the overall mean sensitivity of the visual field and fluctuation. Fluctuation was greater in fields with a lower overall mean sensitivity (Figures 3 and 4).

COEFF OF VAR VS MEAN SENSITIVITY
ZERO LOCATIONS EXCLUDED
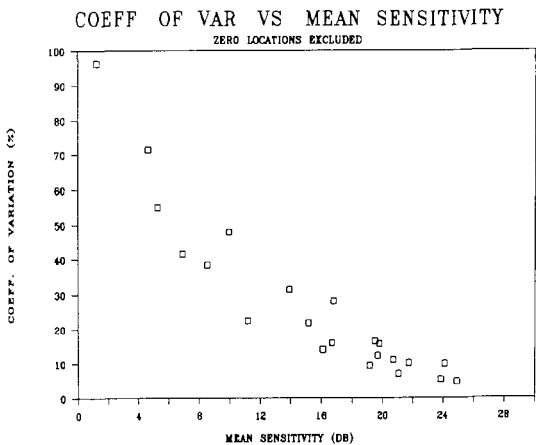
Figure 4 The same plot as in Figure 3 except that total long-term fluctuation is expressed as a per cent coefficient of variation This shows that variability relative to the mean is markedly increased in patients with more extensive visual field defects
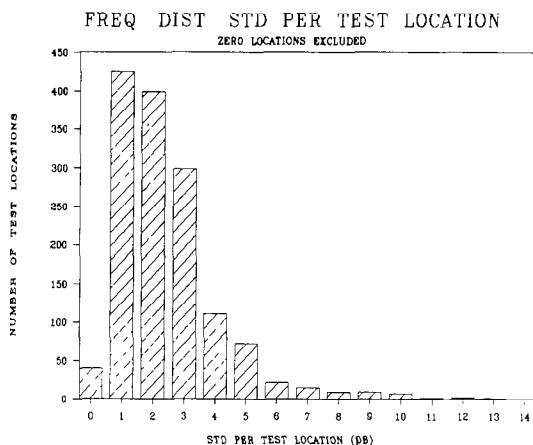
Figure 5 Frequency distribution of the total long-term fluctuation per test location for the entire sample Total number of test locations is 1412 Test locations where all sensitivity determinations were 0 db have been excluded

The mean total long-term fluctuation per test location for the entire sample was 2.0 db with a standard deviation of 1.6 db and a range of 0 db to 12.8 db (Figure 5).

Discussion

The ability of any measuring device to detect a true difference among several measurements depends on the precision of the device, that is the reproducibility of its results. In the case of perimetry, precision is confounded by the fact that the object being measured, the visual field, is apparently constantly changing Furthermore, the magnitude of this change varies among individuals. This constant changing of the visual field has been termed fluctuation. The fluctuation which occurs over periods greater than one day is called long-term fluctuation A true change between two examinations must be greater than the physiologic long-term fluctuation to be recognized as a genuine alteration [1, 12] Thus, any technique which is designed to detect either improvement or progressive detrioration of the visual field in glaucoma must take into account the magnitude of the expected long-term fluctuation in glaucoma patients, not in normal subjects.

With one exception [12] previous studies of long-term fluctuation of glaucoma patients have generally evaluated multiple visual fields performed over a relatively short period of time [10, 20]. Our study reproduces the usual clinical situation in which a patient is examined and perimetry performed at intervals of several months over a period of one or more years. The magnitude of long-term fluctuation in such circumstances should provide useful guidance in developing criteria to evaluate true change in the visual field.

In any sample of patients with chronic glaucoma followed for a long period of time, there will be some who are getting progressively worse. In order to evaluate true long-term fluctuation, these patients would have to be excluded. The patients included in this study were all clinically stable as far as we could determine. There was nothing about them that would have led any reasonable clinician to conclude otherwise. The sample should, therefore, provide the best available approximation of the expected total long-term fluctuation in patients with chronic glaucoma who are receiving medical treatment.

The mean total long-term fluctuation per test location was 2.0 db with a standard deviation of 1.6 db. As can be seen from Figure 5, however, the distribution of total long-term fluctuation per test location is not Gaussian. Table 1 shows the cumulative frequency of the total long term fluctuation per test location for the entire sample. The upper limit of the range which includes 95% of the test locations is 6.4 db. This means that true change for better or worse at any single test location in the visual field would have to be greater than 5 to 7db in order to be detectable 95% of the time by automated perimetry.

Detection of true change as distinguished from fluctuation is complicated by the fact that fluctuation tends to increase in visual fields which are more severely damaged. Criteria for true change will, therefore, have to take into account the baseline sensitivity of the field. Simple statistical techniques which make judgements about progression solely on the basis of tests for statistical significance may not be adequate because fluctuation clearly may be large enough to produce

Table 1 Cumulative frequency of total long-term fluctuation per test location The mean total long-term fluctuation per test location is 2 0 db The range which includes 95% of the test locations is 1 to 6 4 db See Figure 5

Total long-term fluctuation per test location (decibels)	Number of test locations	Cumulative total	Cumulative per cent
0	40	40	2 8
1	425	465	32 9
2	399	864	61 2
3	298	1162	82 3
4	111	1273	90 2
5	72	1345	95 3
6	22	1367	96 8
7	15	1382	97 9
8	9	1391	98 5
9	9	1400	99 2
10	7	1407	99 6
11	2	1409	99 8
12	2	1411	99 9
13	1	1412	100 0

statistically significant differences in the visual field over time

Statistical tests for visual field change should probably take into account what is learned about the expected magnitude of long and short term fluctuation and the tendency of adjacent test locations to show sensitivity changes as a group.

Any technique which analyzes automated visual fields will also have to treat groups of test locations, probably based on the anatomy of the nerve fiber layer of the retina and optic nerve head.

Acknowledgement

References

1 Bebie H: Computerized techniques of visual field analysis In: Drance SM, Anderson DA (eds) Automatic perimetry in glaucoma, pp 147–160 Grune & Stratton, New York (1985)
2 Bebie H, Fankhauser F: Statistical program for the analysis of perimetric data Doc Ophthalmol Proc Ser 26: 9–10 (1981)
3 Bebie H, Fankhauser F, Spahr J: Static perimetry: accuracy and fluctuations Acta Ophthalmol 54: 339–348 (1976)
4 Crick RP, Crick JCP, Ripley LG: Some aspects of perimetry in glaucoma Glaucoma 7: 27–34 (1985)
5 Donovan HC, Weale RA, Wheeler C: The perimeter as a monitor of glaucomatous changes Br J Ophthalmol 62: 705–708 (1978)
6 Fankhauser F, Bebie H: Threshold fluctuations, interpolations and spatial resolution in perimetry Doc Ophthalmol Proc Ser 19: 295–309 (1979)
7 Flammer J, Drance SM, Fankhauser F, Augistiny L: Differential light threshold in automatic static perimetry: factors influencing short-term fluctuation Arch Ophthalmol 102: 876–879 (1984)
8 Flammer J, Drance SM, Schulzer M: The estimation and testing of the components of long-term fluctuation of the differential light threshold Doc Ophthalmol Proc Ser 35: 383–389 (1983)
9 Flammer J, Drance SM, Schulzer M: Covariates of the long-term fluctuation of the differential light threshold Arch Ophthalmol 102: 880–882 (1984)
10 Flammer J, Drance SM, Zulauf M: Differential light threshold short and long-term fluctuation in patients with glaucoma, normal controls and patients with suspected glaucoma Arch Ophthalmol 102: 704–706 (1984)
11 Flammer J, Zulauf M: The frequency distribution of the deviations in static perimetry Doc Ophthalmol Proc Ser 42: 17–23 (1985)
12 Gloor BP, Vokt BA: Long-term fluctuations versus actual field loss in glaucoma patients Dev Ophthalmol 12: 48–69 (1985)
13 Heijl A: A simple routine for demonstrating increased threshold scatter by comparing stored computer fields Doc Ophthalmol Proc Ser 42: 35–38 (1985)
14 Hirsch J: Statistical analysis in computerized perimetry In: Whalen WR, Spaeth GL (eds) Computerized visual fields, pp 307–344 Slack, Thorofare, NJ, 1985
15 Holmin C, Krakau CET: Regression analysis of the central visual field in chronic glaucoma cases Acta Ophthalmol 60: 267–274 (1982)

16   Koerner F, Fankhauser F, Bebie H, Spahr J: Threshold noise and variability of field defects in determinations by manual and automatic perimetry Doc Ophthalmol Proc Ser 14: 53–59 (1977)
17   Langerhorst CT, Van den Berg TJTP, Van Spronsen R, Greve EL: Results of a fluctuation analysis and defect volume program for automated static threshold perimetry with the scoperimeter Doc Ophthalmol Proc Ser 42: 1–6 (1984)
18   Lewis RA, Johnson CA, Keltner JL, Labermeier PK: Variability of quantitative automated perimetry in normal observers Ophthalmology 93: 878–881 (1986)
19   Lynn JR, Batson EP, Fellman RL: Internal inconsistencies vs root mean square as measures of threshold variability Doc Ophthalmol Proc Ser 42: 7–15 (1985)
20   Piltz JR, Starita RJ, Fechtner RD, Twersky YD: Fluctuation of serial automated visual fields in glaucomatous and normal eyes (Abstract) Invest Ophthalmol Vis Sci Suppl 27: 159 (1986)
21   Silverstone DE, Hirsch J: Automated visual field testing, pp 107–122 Appleton-Century-Crofts, Norwalk CT (1986)
22   Werner EB, Drance SM: Early visual field disturbances in glaucoma Arch Ophthalmol 95: 1173–1175 (1977)
23   Werner EB, Saheb N, Thomas D: Variability of static visual threshold responses in patients with elevated IOP's Arch Ophthalmol 100: 1627–1631 (1982)
24   Wilensky JT, Joondeph BC: Variation in visual field measurements with an automatic perimeter Am J Ophthalmol 97: 328–331 (1984)

Author's address:
Elliot B Werner, M D ,
Scheie Eye Institute,
51 North 39th Street,
Philadelphia, PA 19104, U S A

II.3 Total variance of serial Octopus visual fields in glaucomatous eyes

R.J. STARITA, J. PILTZ, J.R. LYNN and R.L. FELLMAN
Dallas, U.S A.

Abstract

Using Octopus program 32, we studied ten eyes of five patients with well controlled primary open angle glaucoma and known visual field disturbances attributed to this disease. A series of eight static threshold fields were performed on each eye over a one month period. For each series, two-way analysis of variance (ANOVA) employing a random-effects model was applied [8, 10] The components of variance were estimated from the ten duplicate thresholds provided routinely on normal bracketing programs. Estimated values for the compo-nents of variance attributed to test location, short-term fluctuation (SF), and homogenous long-term fluctuations [HO (LF)] were equivalent to published values using program JO [2, 6]. Heterogeneous long-term fluctuation [HE (LF)] for this group were larger than previously reported [1, 6] and accounted for a significant proportion of total variance (V_r). This study demonstrates that useful information concerning long-term fluctuation is available free of additional perimetric time penalty using standard programs. The recognition of progressive trends in serial fields would be enhanced if the components which determine fluctuations were profiled individually

Introduction

Computerized perimetry is rapidly becoming the state of the art for visual field analysis. Standardized interactions between patient and machine have led to a more quantitative representation of visual threshold By definition, variability is inherent in the measurement of differential light sensitivity [2, 6] Knowledge of the reproducibility of a measurement is as critical as the precision in which it is determined. Clinical decisions are based on change in the visual field yet what constitutes the earliest significant change in a computerized field is not known. Fluctuations may help distinguish early defects [1, 3] or hinder the recognition of

progressive ones [7, 9]. Repeated examinations over time have been suggested to resolve these discrepancies [6, 7, 9]. Familiarity with expected variability will facilitate interpretation [1–9]. The purpose of this study was to examine the variance of serial automated visual fields in well controlled glaucomatous eyes with known field defects using a standard threshold program.

Material and methods

Prospectively, we studied ten eyes of five patients with primary open angle glaucoma. Glaucomatous eyes had previously documented increased intraocular pressure (IOP), acquired optic nerve cupping, and corresponding visual field loss. Well controlled glaucoma was defined as IOP of less than 20, with stability of nerve and field for at least one year prior to study. Visual fields were obtained on the same Octopus 2000R perimeter using program 32. All patients had prior Octopus experience. On entering the study, the patients were refracted and medication schedules established. Stimulus size, fixation target, and near add were selected and kept constant. Examinations were performed at similar times in the morning (AM) and afternoon (PM) on the same day weekly for four consecutive weeks. For each session a data base was established. Each visual field printout provided the eye studied, pupil size, date, time of day, fluctuation value, false positive response rate, and false negative response rate. Following the visual field, blood pressure, pulse, and IOP by applanation were taken. Medication schedule was recorded.

Program 32 determines threshold at 76 test locations, ten of which are doubly determined. For each visual field the whole field mean senitivity was calculated over 74 locations excluding the blind spot. The location of double determinations are preset by the program and correspond for right and left eyes [8]. These ten locations are used to calculate a fluctuation value using a root mean square (RMS) type of analysis which reflects intratest variability [8]. The ten doubly determined locations per field over eight examination sessions were submitted to two-way ANOVA resulting in location × session data matrix. This factorial design allows one to determine the contribution to V_T accounted for by threshold variation due to location (L), session (S), L-S interaction, and measurement error (E). Each source of threshold variation is tested for significance against that due to (E) only [8]. The output of this analysis provides the sum of squares, degrees of freedom, and mean square for each component of variance [8, 10]. A random-effects model was used in the computation of the F ratio. This requires the denominator for the mean square effect of either L or S to be mean square L-S interaction. When the mean square L-S interaction is equal to or less than the mean square E, a pooled mean square error is substituted for mean square L-S interaction in the denominator of the F-ratio. This is unlike the fixed-effects model where the apropriate denominator in the F ratio is always the mean square

E. Once the values from ANOVA become available, point estimations of variance components can be accomplished and the proportion of variance (POV) accounted for by individual components estimated [10]

Results

The components of variance were estimated in well controlled glaucoma patients with known visual field deficits. The components of variance represent the contributions due to L, S, L-S interaction, and E. Clinically, these components are referred to as test location, homogeneous long-term fluctuation [LF (HO)], heterogeneous long-term fluctuation [LF (HE)], and short-term fluctuation (SF) respectively [4]. Their sum is equal to V_I. The POV can be thought of as a percentage of V_T accounted for by that factor if you move the decimal two places to the right. Results from eight visual fields performed in the AM and PM over a one month period are summarized in Table 1. These values were generated from duplicate threshold locations set by Octopus and used to determine intratest variability.

Clinically, cases 1 and 5 represent moderate to advanced visual field loss associated with marked cupping of the optic nerves estimated at over 90%. The average whole field mean sensitivity for case 5, OS, was 5 4 dB and for the three remaining eyes 8 to 10 dB. Early to moderate visual field loss was found in cases 2 and 3 with glaucomatous cupping estimated in the 50% to 70% range The average whole field mean sensitivity was between 24 and 25 dB. Case 4 represents asymmetrical disease with the right eye having an early field defect, moderate cupping, and a mean sensitivity of 22 dB. The left eye showed advanced field loss and cupping with an average mean sensitivity of 9.8 dB

Of the parameters listed on the visual field printouts, the fluctuation value (RMS) and the false negative response rate were correlated positively to each other and V_T, and negatively to whole field mean sensitivity. As expected in well controlled trained subjects, no correlations were found with IOP, pupil diameter, false positive response rate, blood pressure, and pulse

Discussion

Fluctuation when applied to visual threshold is usually meant as an estimation of the variability that will be encountered if the measurement is repeated. The variability in repeated measurements in the same testing session is referred to as short-term fluctuation (SF) and during different testing sessions as long-term fluctuation (LF) [1, 2]. Total fluctuation is related to SF and LF by their variance. ($V_T = SF^2 + LF^2$). Clinically, SF and V_T can be estimated by repeating measurements in each session and over time. LF is usually not estimated directly but

Table 1. Estimated values for components of variance and proportions of total variance accounted for by each component.

Components (db²) Proportion of variance	1		2		3		4		5		mean ± SD	√mean
	OD	OS	OD	OS	OD	OS	OD	OS	OD	OS		
Location	68*	77*	6.9*	16*	48*	25*	8.6*	27*	51*	8.8*	33.7 ± 24.2	5.8
POV	0.79	0.86	0.52	0.66	0.81	0.68	0.48	0.48	0.70	0.35	0.63 ± 0.19	
LF (HO)	0.7*	0.8	1.9*	1.6*	0.0	0.62	0.45	2.7*	1.5	0.0	1.3 ± 0.7	1.1
POV	0.01	0.01	0.14	0.07	0.00	0.02	0.03	0.05	0.02	0.00	0.03 ± 0.04	
LF (HE)	11.0*	3.1ᵀ	1.1ᵀ	0.0	6.4*	4.4*	4.0*	7.8*	7.6*	13*	5.9 ± 3.7	2.4
POV	0.13	0.03	0.08	0.00	0.11	0.12	0.22	0.14	0.10	0.53	0.15 ± 0.17	
SF	7.0	8.9	3.6	6.7	5.2	6.8	4.8	19	13	3.0	7.9 ± 6.6	2.8
POV	0.08	0.10	0.27	0.28	0.09	0.18	0.27	0.34	0.18	0.12	0.19 ± 0.09	
$\sum$ Components =												
Total variance (V_T)	86.7	89.9	13.4	24.3	59.2	36.9	17.9	57.0	74.0	25.1	48.4 ± 28.8	7.0
$\sqrt{V_T}$	9.3	9.5	3.7	4.9	7 7	6.1	4.2	7.6	8.6	5.0		

* $p < 0.01$: significance of F-test against SF
ᵀ $p < 0.05$: significance of F-test against SF

calculated by factoring out SF from V_T. When ANOVA is applied to individuals, the contribution to V_T is broken down into four components:

1. the proportion due to test location which is a measure of the variability of each point within a session over time,
2. the proportion due to LF (HO) which is a measure of variability of all points within a session over time,
3. the proportion due to LF (HE) which is the measure of variability of interaction between the previous components, and
4. the proportion due to SF which is applied to all three to test for significance [4, 8].

This study was designed as a preliminary investigation of fluctuation patterns in pathologically disturbed fields of well controlled glaucoma patients. Using a random-effects ANOVA, total fluctuation represented by the square root of V_1 varied from 5 to 9.5 dB (Table 1). Larger values tended to be associated with increased pathology but there were clear exceptions (Case 3, OD) The square root of the mean variance components gave values of 5.8 dB for test location, 1.1 dB for LF (HO), and 2.8 dB for SF These values are within 0.1 dB of published values for glaucomatous patients using program JO [2, 6] and a fixed-effects ANOVA [5]. The difference is that LF (HE) is estimated here at 2.4 dB compared to 0.5 dB for program JO being larger than LF (HO) in eight out of ten eyes. This is in closer agreement with the higher value for uncorrelated (heterogeneous) component of LF previously reported in pathologic fields [1]. The higher LF (HE) reflects to a large degree the extent of field damage present, and is an expected rather than contradictory finding. A region of decreased retinal sensitivity will show greater variability over time than normal areas as demonstrated by the high correlation of LF (HE) with the component of test location [5] Clinically, this information is useful in interpreting serial visual fields and draws attention to possible problem areas. A statistically significant value for LF (HE) associated with a high POV suggests that a large percentage of variance over time is due to a non-uniform change in location thresholds (Case 5, OS). On the other hand, a statistically significant value for LF (HE) associated with low POV may represent expected variability for a disturbed field (Case 1, OS) This study agrees with previous work that an increase in fluctuation value (RMS) and false negative response rate correlates with a decrease in mean sensitivity and may indicate field pathology rather than patient's poor cooperation [3].

Further investigation is needed to determine the usefulness of variance component analysis using a random-effects model. Unlike a fixed-effects model, double determinations are not required at each location to make inferences about the entire visual field. The advantages of reducing parametric testing time and statistically profiling fluctuations warrant continued study.

Conclusions

An understanding of fluctuation in glaucomatous visual fields has not been achieved but rather complexity highlighted. The clinical problem of what constitutes a significant change in a series of visual fields still remains. It is clear from this study that fluctuations in glaucomatous fields are common with some components such as LF (HE) larger than anticipated. Patterns of fluctuations in individual patients are difficult to predict but can be estimated using available double determined points. An analysis that can be applied to standard programs to break down serial visual fields into their components of variance seems to offer definite advantages in detecting alterations with time.

Acknowledgements

References

1 Bebie H, Fankhauser F, Spahr J: Static perimetry: Accuracy and fluctuations Acta Ophthalmol 54: 339–348 (1976)

2 Flammer J: Fluctuations in the visual field In: Drance SM, Anderson D (eds) Automatic perimetry in glaucoma: A practical guide, pp 161–174 Grune & Stratton, New York, 1985

3 Flammer J, Drance SM, Fankhauser F, Augustiny L: Differential light threshold in automated static perimetry: Factors influencing short-term fluctuation Arch Ophthalmol 102: 876–879 (1984)

4 Flammer J, Drance SM, Schulzer M: The estimation and testing of the components of long-term fluctuation of differential light threshold Doc Ophthalmol Proc Series 35: 383–389 (1983)

5 Flammer J, Drance SM, Schulzer M: Covariates of the long-term fluctuation of the differential light threshold Arch Ophthalmol 102: 880–882 (1984)

6 Flammer J, Drance SM, Zulauf M: Differential light threshold: Short- and long-term fluctuation in patients with glaucoma, normal controls, and patients with suspected glaucoma Arch Ophthalmol 102: 704–706 (1984)

7 Gloor B: Changes of glaucomatous field defects: Analysis of Octopus fields with programme delta Doc Ophthalmol Proc Series 26: 11–15 (1981)

8 Hirsch J: Statistical analysis in computerized perimetry In: Whalen WR, Spaeth GL (eds) Computerized visual fields: What they are and how to use them, pp 307–344 SLACK, Thorofare, NJ, 1985

9 Piltz JR, Starita RJ, Fechtner RD, Twersky YD: Fluctuation of serial automated visual fields in glaucomatous and normal eyes (Abstract) Invest Ophthalmol Vis Sci 27 (Suppl 3): 159 (1986)

10 Sokal RR, Rohlf FJ: Biometry: The principles and practice of statistics in biological research (2nd ed), pp 321–371 WH Freeman and Co, New York, 1981

Authors' addresses:
R J Starita, J R Lynn, R L Fellman,
Glaucoma Associates of Texas,
7150 Greenville Avenue # 300,
Dallas, TX 75231, U S A

J Piltz,
Montefiore Medical Center,
III East 210th Street,
New York, NY 10467, U S A

II.4 Variability of computerized threshold measurements across the central field in a normal population

A. HEIJL, G. LINDGREN and J. OLSSON
Malmö and Lund, Sweden

Two hundred and ten individuals between 20 and 80 years of age were randomly selected from the population of Malmö and invited for a complete eye health examination. One hundred and forty came for examination and were subjected to a thorough eye examination including computerized threshold perimetry of the central 30° field in both eyes using the 30-2 programme of the Humphrey Field Analyzer. A majority of the subjects accepted repeated perimetry two and four months after the first examination. Abnormal subjects were excluded according to predetermined criteria. Analysis of the results in the remaining normal subjects showed:

1. The normal mean threshold decreases linearily with age, although somewhat faster in the midperiphery than more centrally
2. The inter-individual threshold variability is *not* constant across the central visual field, but increases with eccentricity and is considerably larger in the midperiphery than more centrally
3. The normal deviations among individuals from the normal age-corrected threshold do *not* follow Gaussian distributions, but show significant negative skewness and positive kurtosis. The degree of skewness increases with the distance to the point of fixation.
4. Also the intra-subject inter-test variability is eccentricity-dependent. It is much larger in the midperiphery than more centrally in the visual field.
5. Short-term fluctuation, i.e. the intra-test variation, varies across the central visual field.

This increase of inter-individual, inter-test and short-term variability with eccentricity and the non-Gaussian distributions are of crucial importance in the interpretation of visual fields. They are particularly important when confidence limits for normal computer-measured threshold values are determined and when the significance of measured threshold depressions are established.

The complete paper will be published elsewhere.

II.5 Estimates of variance in visual field data

R.P. MILLS, M. SCHULZER, R.H HOPP and S.M. DRANCE
Seattle, U.S.A. and Vancouver, Canada

Abstract

Local or generalized increases in variance of multiple threshold determinations may indicate abnormality If variance could be reliably estimated from a visual field in which threshold was determined only once, consderable test time could be‑ saved. Meridional threshold data from 40 patients and 18 normals was used to test empirically various methods of estimating variance

A variety of time-series analyses, including combinations of moving average methods, differencing, autoregression models, and forecasting techniques were applied. A modification of the Holt-Winters forecasting algorithm was developed which produced variance estimates which correlated well with standard mean square calculations. Increases in variance attributed to subject fatigue were observed at the end of a 60 minutes test session in normal subjects.

Introduction

Multiple determinations of threshold at a single point in the visual field will yield a set of values distributed about a mean While the mean represents a reasonable estimate of the true threshold at that point, the degree to which the multiple determinations differ from the mean is expressed as a variance. In perimetry, the variance is dependent upon many factors, including the probability of seeing the stimulus, the strategy used to arrive at a threshold value, various patient factors including cooperation and attentiveness, and whether the tested point is abnormal or not [6]. If the multiple determinations are made in different test sessions, the variance increases further.

The variance for many tested points can be pooled to provide a variance estimate for the field as a whole. The square root of the variance of a single visual field test is referred to as the root mean square (RMS) and has been called the short-term fluctuation (SF) by Bebie, Fankhauser and Spahr [1]. SF is a useful

statistic since it provides information about the visual field which is not readily available by perusal of the numeric or graphic charts. Low values of SF, under 2 dB, indicate excellent patient cooperation and make determinations of visual field change over time more reliable. High values of SF, on the other hand, may occur in abnormal fields and confound determinations of progression. SF has also been used by Flammer and his co-workers [5] in the calculation of the corrected loss variance (CLV) visual field index.

Of course, the true SF of a visual field can only be estimated. Fortunately, many threshold determinations at each point are not required to obtain meaningful estimates of SF. Double determinations are performed at each point in the full Octopus program, or at 10 points in the standard Octopus 31 and 32 programs. As Bebie, Fankhauser, and Spahr showed, the estimated SF has a probability of 0.68 of lying within ± 22% of the true SF, and probability of 0.95 of lying within ± 44% of the true SF [1] For coarse uses such as allocations of subject reliability into three classes, ten double determinations are enough, but for more sophisticated uses such as calculation of CLV, a more accurate estimate requiring significant extra testing time is necessary. If SF could be estimated reliably without determining threshold twice at each point, significant time savings could be realized. The attempt to obtain a good SF estimate through mathematical manipulations of single threshold determinations forms the basis for this report. Our calculations were performed on estimates of variance (which is the square of S.F.)

However, the task is made difficult by the fact that there is a definite interrelationship among the threshold determinations of the various points in an individual visual field test. This relationship prevents their use as replicated independent observations in calculations of variance. It is therefore necessary to remove the intercorrelation by data manipulation.

Differential light sensitivity decreases with increasing distance from fixation. While the trend is obvious when plotted graphically, the average curve seems to have many changes of slope. In addition, changes in stimulus size, background intensity, and direction of the meridian tested change the shape of the curve [4]. It is difficult to describe this curve mathematically since it varies a great deal among individuals. Accordingly, it is necessary first to remove the trend from the data by empirical methods in order to produce a stationary series, i.e a series of observations with a constant mean and covariance structure. A method must then be found to estimate the variance from the stationary series. Several techniques of detrending and of variance estimation were tried on data from patients and normal volunteers

Materials and methods

Meridional perimetry was performed with two separate threshold determinations in each test location using the F-series program on the Octopus 201 [3]. In 40 abnormal patients with mild to moderate glaucomatous defects previously discovered with manual Tubingen perimetry, the four oblique meridians of one eye were tested at one degree intervals from 0 to 30 degrees eccentricity with the F2 program. In each meridian, all thresholds were determined once before the second threshold was determined, so the two runs were immediately consecutive. The meridians were tested in the sequence 45°, 135°, 225°, and 315°, and required about 60 minutes total test time.

In 18 normal subjects recruited for the study, a different protocol was followed. In an effort to improve the accuracy of the RMS estimate of SF, three threshold determinations were made at each point in three oblique meridians of one eye at one degree intervals from 0 to 30 degrees eccentricity Software constraints prevented running an 'F3' program Consequently, an F2 program was run in the 45°, 225°, and 315° meridians, followed by an F1 program in the 45°–225° and 315° meridians. Thus, the third run for each meridian was not immediately consecutive to the first two, occurring instead toward the end of testing. Total test time was about 60 minutes.

RMS calculations were applied to the 31 doubly or trebly determined data points from each meridian to obtain an estimate of the variance. This variance estimate was used as a standard against which other methods of estimating the variance were compared (Fig. 1)

RMS was calculated both by omitting and including visual field points with a maximum luminosity scotoma (zero dB threshold). The standard method, as used by the Octopus perimeter, omits them because it is not possible for an absolute scotoma to fluctuate, and the resulting variance estimate would be artificially low. However, some of our detrending techniques required that zeros be included, so they were included also in the RMS calculations to which they were compared.

After detrending the data in various ways, autocorrelation tests were applied to examine the covariance structure of the series.

Single and double difference series were calculated. In the single series, the threshold x at point t + 1 was subtracted from that at point t, $d_t = (x_t - x_{t+1})$, from $t = 0°$ through 29° eccentricity. In the double series, the successive differences were subtracted from one another, producing $s_t = (d_t - d_{t+1})$ from $t = 0°$ through 28°. Calculations were made by excluding and by including zeros. In another series, the normal threshold values stored by the Octopus were subtracted from the observed values in each of the two runs from 0° to 30° eccentricity.

Moving average techniques of various window widths were tried. In the simplest case with a window width of 3 the 'window' includes the points on either side of the test point. The mean of the thresholds at the two neighboring points

NN	V1	V2	Variance estimates		NN	V1	V2
0	28	26	Mean square $(SF)^2$				
1	28	26	= 28 1		16	20	10
2	30	26			17	16	4
3	25	21	Holt-Winters run 1		18	20	10
4	31	29	= 21 0		19	22	0
5	27	21			20	17	17
6	25	27	Holt-Winters run 2		21	13	17
7	25	21	= 25.2		22	8	12
8	25	19			23	2	18
9	21	17			24	16	1
10	13	25			25	14	2
11	17	19			26	4	4
12	23	13			27	12	22
13	23	19			28	2	0
14	13	23			29	4	7
15	11	11			30	6	4
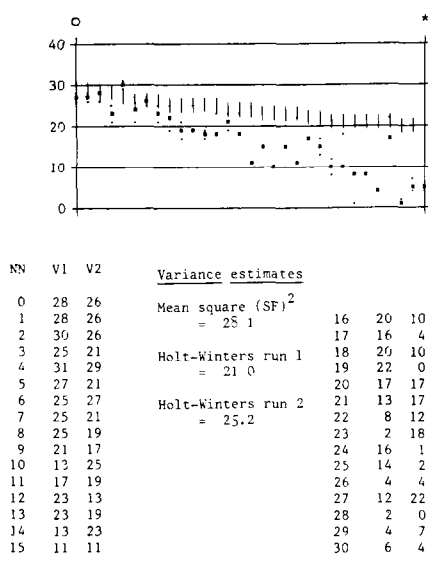
Figure 1 Octopus F2 program, meridian 45°, 0° to 30° eccentricity at 1° intervals Top: Graphic profile representation Short lines are normal values, squares are mean values from 2 threshold determinations each denoted by dots Left and right: numeric representation of two threshold determinations (V_1, V_2) at each eccentricity (NN) from 0° to 30° Center: variance estimates calculated by standard mean square method on double determinations and by modified Holt-Winters method on each of the single determinations

was determined, $M_t = (x_{t-1} + x_{t+1})/2$, or the mean of all three points was used, $M_t = (x_{t-1} + x_t + x_{t+1})/3$. In addition, with larger window widths weighting of the values depending on proximity to point t were used, such as the Spencer moving average method [2]. Following each of the above detrending manipulations, a number of different methods were used to estimate the variance of the series, such as autoregressive techniques, exponential smoothing and forecasting techniques, and others.

Finally, a modification of the Holt-Winters forecasting technique for time series [2] was developed for the spatial visual field data. Since seasonal variations common in time-series were not present in our data the forecasting algorithm was modified accordingly

Results

Correlograms based on the single difference series $d_t = (x_t - x_{t+1})$, the double difference series $s_t = (d_t - d_{t+1})$, and the series obtained by subtraction of normal values varied a great deal among individuals and did not show a stationary behavior. Moving average techniques of various window widths performed some-
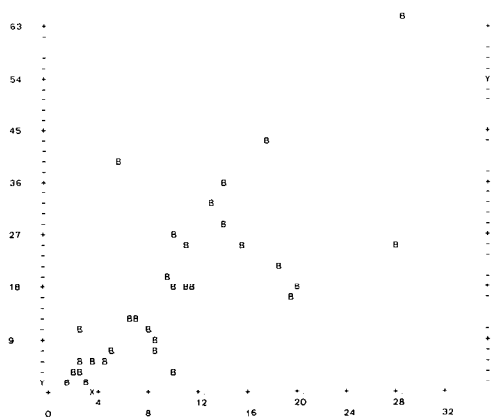
Figure 2 Good correlation is scatterplot of variance estimates from Holt-Winters forecast on second threshold determinations (ordinate) and mean square method on double determinations (abscissa) Data points (B) from 35 135° meridians in glaucoma patients

what better but offered poor prediction of the true variances.

The best variance estimates on our abnormal glaucoma patients were obtained from a modified Holt-Winters forecasting algorithm. The best modification proved to be a forecast based on 8 initial points, working from periphery to fixation, and omitting all zeros except initial ones needed to set the mean level. After exclusion from analysis the 14 meridians containing over 50% zero decibel thresholds, 146 meridians were analyzed. Scatterplots were prepared to display the relationship of the variances estimated by one standard mean square on double determinations to those estimated by the modified Holt-Winters approach on single determinations (figs 2 and 3). Correlation coefficients were

Table 1 Correlation* between log variance estimates from Holt-Winters and standard mean square methods applied to meridional threshold data from 40 glaucoma patients

	Meridian				
	45°	135°	225°	315°	all
H-W I[a] and M S [c]	0 72	0 73	0 75	0 56	0 68
H-W II[b] and M S [c]	0 80	0 83	0 69	0 54	0 73

* Pearson's 'R' coefficient

[a] Variance estimate from modified Holt-Winters algorithm on first threshold determinations

[b] Variance estimate from modified Holt-Winters algorithm on second threshold determinations

[c] Variance estimate from mean square calculation on double threshold determinations from the F2 program
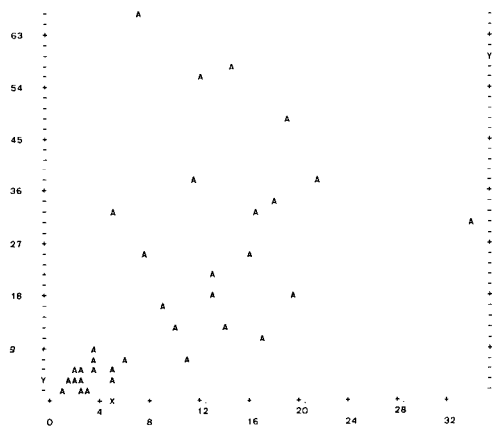
Figure 3 Fair correlation in scatterplot of variance estimates from Holt-Winters forecast on second threshold determinations (ordinate) and mean square method on double determinations (abscissa) Data points (A) from 38 45° meridians in glaucoma patients

calculated after variances had been logged, to approximate a normal distribution (Table 1). The overall correlation of the Holt-Winters and standard mean square log variances were 0.68 and 0.73, respectively, on each of the two repetitions of the F2 program on the glaucoma patients.

The same modification of the Holt-Winters algorithm was then applied to the data from the normal volunteers. A representative scatterplot (Fig. 4) shows overall good correlation, but for a single extreme outlier. Correlation coefficients of the log variances from Holt-Winters and standard mean square methods were 0.59 and 0.84, respectively, on each of the two repetitions of the F2 program though there was considerable variability among the subgroups (table 2).

Data from the third threshold determination (F1 programs) obtained at the end

Table 2 Correlation* between log variance estimates from Holt-Winters and standard mean square methods applied to meridonial threshold data from 18 normal volunteers

	Meridian			
	45°	225°	315°	all
H-W I[a] and M S [c]	0 37	0 33	0 18	0 59
H-W II[b] and M S [c]	0 68	0 68	0 57	0 84

* Pearson's 'R' coefficient

[a] Variance estimate from modified Holt-Winters algorithm on first threshold determinations

[b] Variance estimate from modified Holt-Winters algorithm on second threshold determinations

[c] Variance estimate from mean square calculation on double threshold determinations from the F2 program
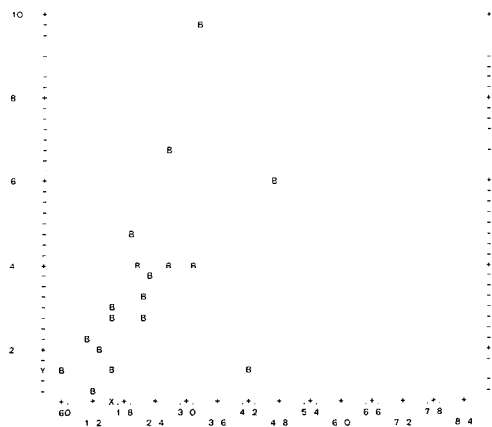
Figure 4 Good correlation in scatterplot of variance estimates from Holt-Winters forecast on second threshold determinations (ordinate) and mean square method on double determinations (abscissa) Data points (B) from 18 225° meridians in normal volunteers

of testing was not used in the variance estimation analysis because the results were markedly different from the first two determinations (F2 programs). Table 3 shows the means and variance estimates obtained from each of the three runs, and from pairings of the runs. The third repetition shows much greater variability but a similar mean threshold than the first two repetitions However, there was no significant overall tendency toward increase in variance or decrease in mean threshold in the meridians tested later over those tested earlier in the session in either the abnormal glaucoma patients or the normal volunteers. Also, the variance estimates from the immediately consecutive first and second runs on the F2 program did not show higher variances for the second threshold determinations.

Table 3 Characteristics of the three repetitions of threshold determination in 18 normal volunteers All data pooled

	Mean threshold	Estimated variance (Holt-Winters)	Estimated variance (mean square)
First determination	28 6	3 8	
Second determination	28 1	3 8	
Third determination	28 2	4 1	
First-second pair			2 8
First-third pair			3 1
Second-third pair			3 2

Discussion

Our attempts to forecast the variance from the single threshold determinations met with excellent success in the glaucoma patients and with moderate success in the normal volunteers when we used a modification of the Holt-Winters exponential smoothing algorithm. Good correlations of estimated log variances of each run with those using standard methods on double threshold determinations were obtained.

Several factors were probably operating to reduce the correlation between the Holt-Winters log variance estimate and the standard double determination estimate. First, the accuracy of variance estimates with 31 points each measured twice in relatively crude. There is a probability of 0.95 that the double determination estimate is within ± 25% of the true variance. Second, variances of visual fields with wide absolute scotomas were difficult to forecast reliably because of too few remaining data points. Third, the wide inter-individual variation in the profile of the visual field affects the accuracy of any autoregressive model.

Correlations were better using our abnormal patient data than the data from the normal volunteers. This may be explained by the fact that exponential smoothing methods work well in data with relatively smooth trends but large 'holes'. In addition, the range of variances among the normals was much narrower, causing smaller differences in variance estimates to reduce the correlation levels. Finally, single point scotomas, such as might be produced by retinal blood vessels, may cause large fluctuations in the estimates of variance resulting in extreme outliers.

The tendency for the estimated variances to increase toward the end of a one hour test session was especially noticeable in our normal volunteers. In retrospect, a protocol design which consecutively measured the first, second, and third thresholds in each meridian would have been preferable from the standpoint of stable variance estimates. However, all third threshold determinations were done in the last 20 minutes of a 60 minute session. The variances estimated by the Holt-Winters method based on the third determination or by pairing the third with either the first or second determinations were quite large. We attributed this observation to subject fatigue.

During test sessions of 30 minutes, deterioration of threshold sensitivity with increase in threshold variation has been described in eyes with pathological visual fields [7, 8]. Our test sessions were about 60 minutes in length, though broken into five segments by Octopus data entry requirements. Presumably normal subjects begin to tire in a measurable way by the end of a prolonged test session.

Acknowledgements

References

1 Bebie H, Fankhauser F, Spahr J: Static perimetry: Accuracy and fluctuations Acta Ophthalmol 54: 339–348 (1976)
2 Chatfield C: The analysis of time series: an introduction, pp 88, 212 Chaplin and Hall, London, 1984
3 Fankhauser F, Haberlin H, Jenni A: Octopus programs SAPRO and F Albrecht v Graefes Arch klin exp Ophthal 216: 155–165 (1981)
4 Fankhauser F, Koch P, Roulier A: On automation of perimetry Albrecht v Graefes Arch klin exp Ophthal 184: 126–150 (1972)
5 Flammer J, Drance SM, Augustiny L, Funkhouser A: Quantification of glaucomatous visual field defects with automated perimetry Invest Ophthal Vis Sci 26: 176–181 (1985)
6 Flammer J, Drance SM, Fankhauser F, Augustiny L: Differential light threshold in automated static perimetry Factors influencing short-term fluctuation Arch Ophthalmol 102: 876–879 (1984)
7 Heijl A: Time changes of contrast thresholds during automatic perimetry Acta Ophthalmol 55: 696–708 (1977)
8 Holmin C, Krakau CET: Variability of glaucomatous visual field defects in computerized perimetry Albrecht v Graefes Arch klin exp Ophthal 210: 235–250 (1979)

Authors' addresses:
R P Mills, R H Hopp,
Department of Ophthalmology,
University of Washington,
Seattle, Washington U S A , 98195

M Schulzer,
Department of Medicine,
University of British Columbia,
Vancouver, Canada

S M Drance,
Department of Ophthalmology,
University of British Columbia,
Vancouver, Canada

II.6 Fluctuation and population differences in automated perimetry and the influence on defect volume estimation

T J.T.P. VAN DEN BERG, R.J. NOOTEBOOM, C T. LANGERHORST
and E L. GREVE
Amsterdam, The Netherlands

Abstract

The shape of the normal visual field and the distribution of threshold values was examined in a normal population and a population of glaucoma patients. Our goal was to optimize the determination of the reference field used in our evaluation program for visual fields. We found true interindividual differences in the gradient of sensitivity of the normal visual field These findings emphasize the importance of individual determination of the reference field. For our normal as well as our glaucoma population the standard deviation of this variation was estimated to be 0.09 dB/degree.

Introduction

It is by now well established that for critical evaluation of an individual visual field the choice of the reference field is of utmost importance. A population mean with age correction is often used A first refinement is a correction for the individual's general level of absolute sensitivity. It has been stressed that the individual general sensitivity should be estimated in an unbiased way [2]. In order to do so optimally we have been studying some aspects of population behaviour (see below). A second refinement is a correction for the individuals normal shape of the island of vision. This shape may well be different from the mean normal shape causing inaccuracy in evaluation of the visual field. This study concerns shape differences and especially differences in the gradient of sensitivity when the visual field is approximated by a linear descent.

Methods

We investigated visual fields with our double threshold determination program

[3]. Threshold values are measured twice at 60 locations within 25 degrees. Seven positions around the blind spot are excluded from the analysis. The normal population consisted of 40 eyes of normal subjects of which 18 eyes were measured 2 to 4 times. The mean age was 57 ± 16 years. The glaucoma population consisted of 71 eyes of patients with primary open angle glaucoma of which 20 eyes were measured more than once. For the histograms only the first measurement was used. The radial gradient is defined on the basis of linear regression analysis of all 53 thresholds as a function of eccentricity.

Results

Figure 1a is a histogram of the radial gradients found in our normal population. The mean gradient is -0.30 dB/degree with a standard deviation of 0.11 dB/ degree. The regression analysis showed measurement uncertainty in individually determined fields to be on the average 0.04 dB/degree. Thus long-term fluctuation and/or true interindividual differences have to account for the spreading of this distribution. In order to further evaluate these possibilities we have plotted the gradients of more than once measured eyes in figure 2a. Points belonging to the same eye are connected. It can be seen that the *intra*individual spreading is considerably smaller than the *inter*individual spreading. Variance analysis gives a F-value corresponding with a p-value smaller than 0.01. Estimates of intra- and interindividual dispersion are 0.04 dB/degree and 0.09 dB/degree respectively.
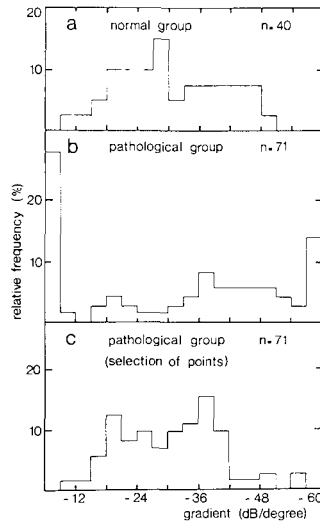
Figure 1 Histograms of radial gradients in (a) the normal group, (b) the glaucoma group, (c) the same glaucoma group using only a selection of (healthy) points
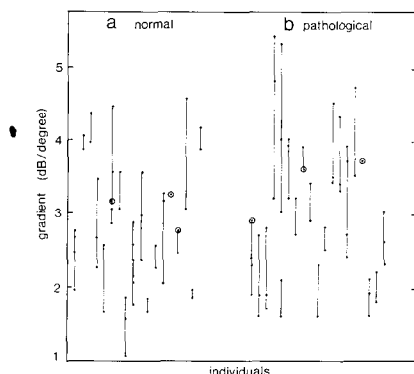
Figure 2 Gradients of more than once measured eyes in: (a) the normal group, (b) the glaucoma group using only a selection of (healthy) points Apart from intraindividual variation, significant interindividual differences are found

We conclude therefore that the gradient of sensitivity is an individual dependent quality (see also [1]).

In figure 1b the distribution of radial gradients found in the glaucoma population is shown. The distribution of gradients of the pathological group is considerably wider than in the normal group because of the pathological areas in the field. Pathologically decreased sensitivity near the center decreases the gradient and pathologically decreased sensitivity located more peripherally increases the gradient. Figure 1c shows the histogram for the pathological group after correction using the normal position criterion as described by Van den Berg et al in these proceedings. We see that this distribution resembles the one of the normal group. The mean is -0.31 dB/degree and the standard deviation 0.10 dB/degree. Variance analysis was also performed on the eyes measured more than once in the pathological group. Here too a significant interindividual difference in gradient was found ($p<0.01$). The intra- and interindividual dispersion were similar as in the normal population 0.04 dB/degree and 0.09 dB/degree respectively These results led to the concept of a gradient adaptive algorithm.

For the estimation of the individual's absolute level of normal sensitivity we need some insight in the shape of the threshold-distribution-function. Since our algorithm evaluates the visual field as a whole we wanted the average distribution over the whole visual field. To obtain this function we first corrected for the island of vision to eliminate the shape effect on the distribution Secondly, since there are appreciable differences between individuals in spreading we normalized the individual distribution function. Thus we looked at the distribution of standardized deviations from the mean value. Figure 3 shows that this distributon averaged over our normal population is asymmetric. The skewness is 0.87 (skewness of a normal distribution = 0).

This distribution can be used to determine a normal position criterion so that
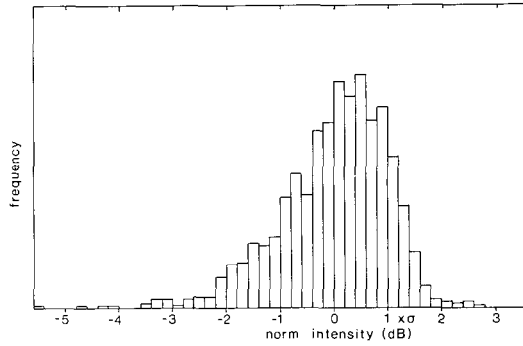
Figure 3 Distribution of normalized deviations from the mean, showing skewness of the distribution of threshold intensities

for example at most 5% of the threshold values are wrongly classified as pathological. Thus the skewness of this distribution has consequences for the boundary between healthy and pathological areas. In fact for a normal distribution the one sided 5% level is at 1 65 × s.d whereas for this distribution it lies at 2.2 × s.d.

It is important to have an unbiased estimate of the height of the normal visual field (individual general sensitivity, IGS). In our IGS determination (see [2]) we take the mean of those threshold values of series 2 of the double threshold program whose corresponding series 1 values lie above a certain limit. This limit could be derived from the lowest thresholds found assuming that these thresholds are representative for normal areas. In figure 4 the spreading of the tresholds is given as a function of their order in the individual distribution. We see that the lowest thresholds scatter more than the second lowest (no 2) etc. Therefore the limits for normal thresholds should not be derived from number 1 but some lower number. We have chosen this number to be 3 since in late stage pathological visual fields only a few normal positions may remain after this choice.
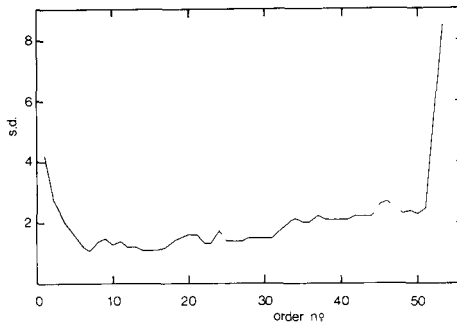
Figure 4 Spreading of threshold values as a function of their order in the individual distribution, showing high scattering of the lowest (and highest) thresholds

Conclusions

There are significant intra- and interindividual gradient differences in the visual fields of normal subjects and of glaucoma patients.

The average distribution of threshold values for a normal visual field is not normal but significantly skewed. For an unbiased height estimate of the visual field the lowest threshold values (best sensitivity) should be ignored since they scatter significantly more. These effects should be used to optimize visual field evaluation

Acknowledgements

References

1 Katz J, Sommer A: Asymmetry and variation in the normal hill of vision Arch Ophthalmol 104: 66–68 (1986)
2 Van den Berg TJTP, Van Spronsen R, Van Veenendaal WG, Bakker D: Psychophysics of intensity discrimination in relation to defect volume examination on the scoperimeter Doc Ophthalmol Proc Series 42: 147–151 (1985)
3 Van Veenendaal WG, Langerhorst CT, Van den Berg TJTP, Greve EL: New programs of the scoperimeter Doc Ophthalmol Proc Series 35: 323–329 (1983)

Author's address:
Laboratory of Medical Physics of the University of Amsterdam
and the Netherlands Ophthalmic Research Institute,
Academic Medical Center,
Meibergdreef 9, 1105 AZ Amsterdam-Zuidoost, The Netherlands

II.7 The distribution of visual field scores in a normal population

B.C. CHAUHAN and D.B. HENSON
Cardiff, United Kingdom

Abstract

The central visual fields of 1161 subjects were measured using a quantitative threshold related suprathreshold strategy. A weighted scoring technique which considers the spatial location of a defect, defect depth and clustering properties is described. The field score distribution is skewed with a long positive tail corresponding to higher scores.

Introduction

Over recent years, considerable research has been conducted in the numerical representation of the visual field. Most of this research has centered on glaucomatous eyes, with very little work undertaken on normal eyes. As the vast majority of patients in a clinical situation will be non-glaucomatous, our understanding of the behaviour and properties of normal visual field are of paramount importance.

Due to the relatively low prevalence of chronic open angle glaucoma (COAG), any quantification of glaucomatous visual fields will be subject to larger sampling errors than normal visual fields. Unless visual fields are recorded from patients with a strict definition of the disease process, then the analysis will also be subject to noise introduced by the inclusion of data from eyes with varying severity of COAG. The need for this selectivity will reduce the COAG sample further.

This paper describes a visual field scoring method and reports on the results from a large sample in addition to a smaller COAG sample. We feel it is important to study the distribution of visual field scores and quantify the probability of a certain score occurring in a population. We can then place confidence limits to isolate patients falling outside these limits for further investigation.

Material and method

A total of 1161 subjects were enrolled from two centres, a large government office and a general medical practice. There were 547 males and 614 females in the sample whose mean age was 55.70, median 58 and range 23 to 79. The visual fields in 45 cases (3.9%) could not be recorded bilaterally, either because the subjects were monocular or because the best corrected visual acuity of one eye was poorer than 6/24.

Those subjects with visual field defects due to retinal factors such as detachment, choroiditis, maculopathy etc., as well as those with frank glaucomatous visual field damage were excluded from the analysis requiring normal data In addition, those eyes with field defects with a neuropathic origin such as stroke were also removed from the normal databank. In all, 112 eyes of 56 subjects were removed

We are aware that by applying these loose criteria for exclusion, we may be including in the normal sample those eyes which may clinically be regarded as suspicious on the basis of their first visit visual field performance. The error incurred by the inclusion of these subjects in the analysis theoretically requiring 'normal' data will be minimal due to the large sample size. The approach taken here aims to be representative of a normal clinical population without known pathology afflicting the visual field.

In addition to the large normal sample visual field data was also collected from a sample of patients with diagnosed COAG. Only those eyes with early field disturbances were used for the analysis requiring defective data. Eyes which had a combined defect area of greater than one quadrant and fellow normal eyes of COAG eyes of COAG subjects were removed from the analysis. This sample contained 106 eyes of 87 subjects.

The instrument used to record the visual fields in this study was a Friedmann Visual Field Analyser (FVFA) mk. 2. The fields were recorded by initially estimating the threshold to 0.1 log unit (l.u.) accuracy. The stimuli were then presented at 0.4 l.u above threshold with any defects measured in increasing steps of 0.2 l.u. The results were then digitised for computer analysis. The four stimuli falling within the charted blind spot were removed from the analysis.

The scoring method

The visual field scoring method utilised informational analysis. This form of analysis has previously been described [2, 4]. The basic logic in the method is the optimisation of sensitivity (the ability of a test to isolate defectives) and specificity (the ability of a test to isolate normals) by looking at the probabilities of certain test events occurring in normal and defective fields This is the foundation for a weighted system which can then be used for scoring.
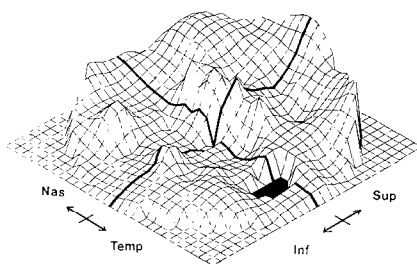
Figure 1 The topograpic information weighting of the right eye The blind spot is removed from the analysis and grounded The index t_x is represented by the z-axis (vertically up)

We have used informational analysis to look at three visual field aspects: spatial location of a defect, defect depth and cluster properties.

1. Spatial location of defect

We have previously shown [4] that the testing of certain locations in the visual field is more pertinent, or gives more information, in the detection of early glaucomatous visual field loss. For this aspect of the analysis, all left eye data were converted to right eye data. Figure 1 shows a topographic representation of relative information of the central 25 degrees of the visual field. The estimates of the informational values for each stimulus location, t_x, are based on the frequency distribution of defects in normal eyes and defective eyes.

2. Defect depth

It is important that a scoring system includes a weighting for the depth of defect. It is possible to look at defect depths in normals and defectives and derive the information provided by each level of defect depth. This has been achieved by a previous smaller study [3] with 114 defective eyes and 240 normal eyes The range of defect depths recorded were from 0.21 u. to absolute.

Figure 2a shows relative information plotted as a function of defect depth A 0.2 l.u. defect gives little information as both normals and defectives have a large percentage of these defects, probably due to the short term fluctuations affecting both groups at this level. Similarly, very deep defects, i.e. 1 2 and 1.4 l u give little information as these defects are obviously abnormal. The maximum information occurs at a depth of 0.6 l.u. If a one-level suprathreshold screening strategy were adopted, this level would be the optimum level above threshold to screen at since it has the best trade-off between specificity and sensitivity.

These information values can now be cumulated to provide indices for scoring defect depths. Figure 2b shows cumulative information as a function of defect depth. The ogive rises sharply to about 0.8 l.u. and after 1.0 l.u. it attenuates quite abruptly. Hence in practice, a defect deeper than 1 0 l.u. provides little information in understanding if it is normal or abnormal. The cumulated information
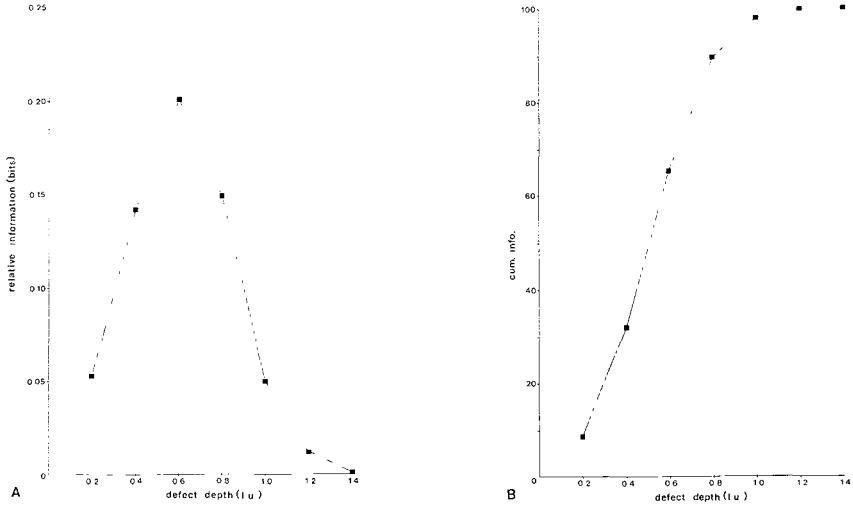
Figure 2 a Relative information as a function of defect depth Maximum information occurs at 0 61 u b: Cumulative information function of defect depth

values are normalised by dividing each value by the minimum value to provide the index t_d for each defect depth

3. Cluster properties

Recently authors [1, 5] have noted the importance of clustered defects, i.e. adjacent stimuli with decreased sensitivity. A patient having three shallow and isolated defects could conceivably be normal, but if these defects were clustered, the probability of such a response being normal is minute. Clearly then, it is valuable to include a cluster analysis in any field quantification.

The cluster analysis in this study is a two-stage procedure. First, we must quantify the information provided by having a given number of clusters and second, by the size of the cluster, i.e the number of stimuli in a cluster.

Figure 3a shows cumulative information function of the number of clusters. The ogive attenuates sharply after 3 clusters with over 95% information attained. As previously, these values are normalised to produce an index, t_n. Figure 3b shows the ogive for cluster size, obviously on the condition that a cluster exists. This is a much gentler function as normals without clusters (approximately 90%) do not contribute towards its derivation. The normalised index here is t_{cs}.

The scoring algorithm

The scoring algorithm has two components, the individual stimulus component and the cluster component. It is described by·
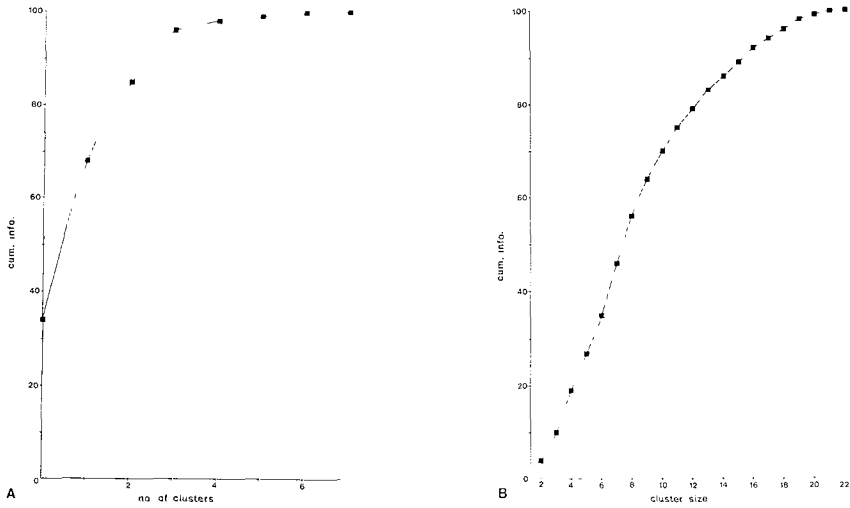
Figure 3 a: Cumulative information function of the number of clusters b: Cumulative information function of cluster size

$$\sum_{i=1}^{z} [t_{s(i)} \cdot t_{d(i)}] + t_{n(c)} \cdot \sum_{j=1}^{c} t_{cs(j)}$$

where
$t_{s(i)}$ is the informational value of the stimulus location i,
$t_{d(i)}$ is the normalised index for the defect depth at i,
$t_{n(c)}$ is the normalised index for a field with c clusters, and
$t_{cs(j)}$ is the normalised index for the cluster size of cluster j.

Results

Each visual field was scored using the algorithm described above. Figure 4 shows the scores histogram of the sample. The distribution is positively skewed (skewness = 6.78, kurtosis = 58.43). Of the 2277 eyes, 5.5% have scores greater than 25. This histogram includes those subjects with field defects described in an earlier section of the paper. If these subjects are removed and cumulative frequency is plotted as a function of score, it will be seen that 95 of the sample have a score of 13 or less points and 98% a score of 24 or less 1.5% have a score of greater than 25.

Figure 6 shows a histogram of the glaucomatous sample. The distribution has a slightly positive skewness (skewness = 0.92, kurtosis = 0.53) The score class intervals are different from Figure 4, nevertheless, it is clear that the distributions are dissimilar.
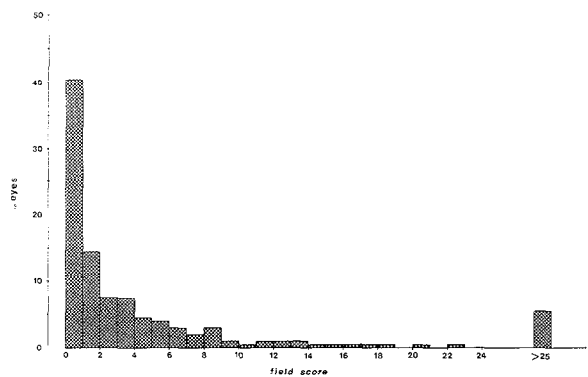
Figure 4 Histogram of visual field score for entire databank (2277 eyes of 1161 subjects)
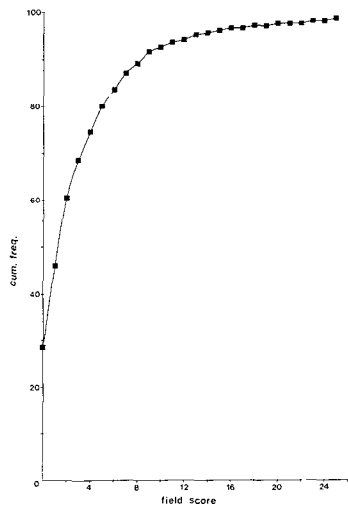
Figure 5 Ogive of field score with eyes with defects (see text) removed (2165 eyes of 1105 subjects)
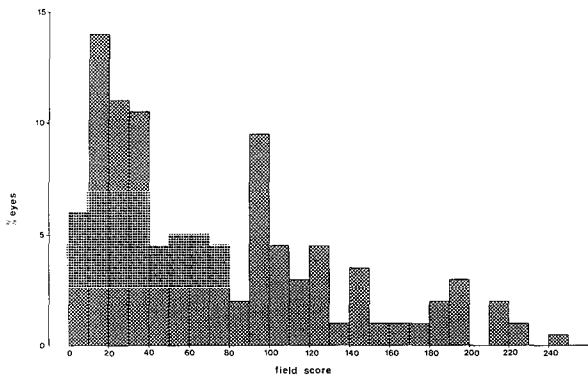
Figure 6 Histogram of visual field score for glaucoma sample (106 eyes of 87 subjects)

Discussion

With the analysis used in this study it is possible to obtain a statistically derived cut-off point based on the ogive in Figure 5. The confidence with which a score can be predicted in a true 'normal' population is probably an underestimate since the sample contains individuals who clinically may be regarded as suspicious or those who have artifactual defects due to poor compliance However, the ogive attenuates after the 95th percentile and those individuals with scores beyond this limit can be isolated for monitoring.

In practice it is difficult to predict confidence limits of field scores in a normal population as this assumes there is no transition zone between normal and defective. This study has shown that there is a long positive tail in the score distribution which may point to such a transition zone or to normals who have higher scores. In either case, it is important to identify these individuals.

Further work examining the longitudinal fluctuations in field scores is being planned. We have described an overview of this study in this paper but a more rigorous explanation of the scoring technique and the derivation of the scoring algorithm is being written.

The scoring system is devised for and is specific to the FVFA mk.2, but it can easily be modified to encompass both threshold and suprathreshold strategies on automated perimeters. This will, of course, enable detailed on-line analysis of a visual field performance.

References

1 Bebie H: Computerized techniques of visual field analysis In: Drance SM, Anderson DR (eds) Automatic perimetry in glaucoma, pp 147–160 Grune and Stratton, Orlando, 1985
2 Chauhan BC, Block MT: City tests and information theory Ophthal Physiol Opt 6: 157–163 (1986)
3 Chauhan BC: Unpublished results
4 Henson DB, Chauhan BC: Informational content of visual field location in glaucoma Doc Ophthalmol 59: 341–352 (1985)
5 Henson DB, Hobley AJ, Chauhan BC, Sponsel WE, Dallas NL: The importance of visual field asymmetry in the detection of glaucoma Am J Optom Physiol Opt 63: 714–723 (1986)

Author's address:
Department of Optometry,
University of Wales,
Colum Drive, Cardiff CF1 3EU, United Kingdom

II.8 Kinetic short-term fluctuation in patients with glaucoma and suspected glaucoma

P. CAPRIS, E. GANDOLFO, M. ZINGIRIAN, M ORCIUOLO
and S ROVIDA
Genova, Italy

Abstract

Threshold fluctuations have already been studied in static perimetry by many authors. In a previous study the static threshold fluctuations have been compared with kinetic ones.

In order to evaluate the possibility of detecting the early signs predicting future visual field defects in ocular hypertension, the short-term threshold fluctuations were studied in normal subjects and subjects with glaucoma and suspect glaucoma, by means of automatic kinetic perimetry (Perikon).

Significant differences were found in the three groups of patients, showing a wider threshold fluctuation in glaucomatous and suspected glaucomatous patients

These results, obtained by repeated threshold measurements during normal automatic screening at different eccentricities, confirm the value of a short-term kinetic fluctuation increase in predicting glaucomatous visual field damage in the peripheral as well as in the central visual field.

Introduction

An increased short-term threshold fluctuation (SF), i.e. an increased scattering of the differential light threshold in the various test locations during a perimetric examination, is today considered an early functional sign of the glaucomatous damage, which precedes the perimetric defects [1, 9]. The sequence of initial glaucomatous perimetric disturbances, is presently considered as follows [7]:
1. a localized SF increase with a normal threshold;
2. a localized SF increase with an increased threshold;
3 a relative scotoma with undefined margins
The attention of researches has been recently focused on the threshold variations in the central visual field [2, 4, 5, 8, 10]

An early increase of threshold fluctuation in this area has been demonstrated in suspected glaucomatous patients. Werner et al [10] found a significant difference in short-term fluctuation between normal and glaucomatous subjects only at 5° eccentricity using the Goldmann perimeter and static stimuli. Flammer et al. [2, 4, 6] studied the threshold fluctuations in normal, glaucomatous and suspected glaucomatous subjects, analyzing the SF and the two components of long term fluctuation (LF): the homogeneous component (HO) being the uniform fluctuation and the heterogeneous component (HE) being the different fluctuation in the various test locations. In this study the SF appeared to be increased in the glaucomatous and suspected glaucomatous subjects and a statistical significant correlation was found between overall and local sensitivity and SF. The false response rate was significantly related with SF.

All these recent studies have been performed using automatic static procedures and examination programs of routine as well as special types (for example the Octopus 'JO' program [3])

In our opinion, kinetic perimetry can also be utilized for the clinical analysis of threshold fluctuations. However, some requirements must be fulfilled: rigorous fixation control, precise recording of responses and uniform test conditions. Presently, only automatic perimetry can guarantee this.

In a previous study we compared threshold fluctuation tested with kinetic and static perimetry, using an automatic Goldmann perimeter (Perikon, Optikon). No significant differences were found in the results obtained with the two methods in the same retinal locations [11] In a more recent preliminary study (1986) we compared kinetic short-term fluctuation in normal and glaucomatous patients, testing numerous points arranged in the whole visual field and in localized critical areas. A significant increase of both the global and the localized SF in glaucoma patients with respect to normals was found [12].

In the present study, kinetic short term fluctuation has been investigated in the paracentral and peripheral visual field during standard kinetic examinations in normal, glaucomatous and suspected glaucomatous subjects.

Materials and methods

One hundred and five eyes of 105 patients (35 normal, 35 with suspected glaucoma and 35 with chronic open-angle glaucoma) were studied. All eyes with suspected glaucoma had IOP >22 mm Hg and a normal visual field in previous examinations The eyes with chronic open-angle glaucoma presented slight visual field defects and IOP well-controlled (<20 mm Hg) by local treatment The patients' age ranged from 21 to 73 years.

The visual field examination was carried out using the 'Standard Kinetic Program' of the Perikon automatic perimeter (Fig. 1). This program performs consecutive kinetic threshold determinations on 16 meridians (87°, 60°, 30°, 5°,
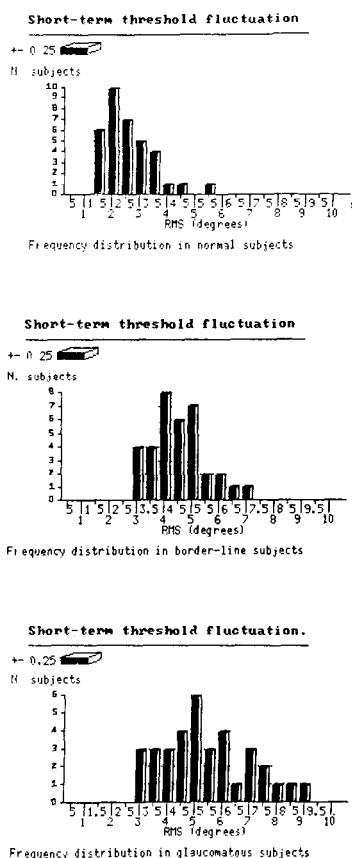
Figure 1 Distribution of SF in normal subjects and subjects with glaucoma and suspect glaucoma

355°, 330°, 300°, 273°, 267°, 240°, 210°, 185°, 175°, 150°, 120°, 93°) with four different stimuli, automatically preselected according to the individual sensitivity. The presentation at each successive meridian began 10° more peripherally than where the stimulus had been perceived on the preceding meridian. The target was moved 5° per second outside 30°, and 3° per second inside 30°. When two different stimuli were perceived on the same meridian with an interval <5°, the two presentations were automatically repeated. In this study the blind spot examination was excluded.

At the end of this examination, 64 kinetic threshold measurements were obtained (examination time about 12'). After a 5' break, the whole examination was repeated in the same eye with the same procedure. In such a way, 64 pairs of threshold values were available for each patient The short term fluctuation (SF) was calculated as the root mean square (RMS) of the 64 twice-tested threshold values for each eye.

Results

The means RMS (square root of the means of the variances) in the three groups is shown in Table 1.

The overall comparison among the three groups, calculated by the nonparametric Kruskal-Wallis range variance analysis demonstrated a highly significant difference (P<0.001)

The comparison by the parametric F-Test confirmed the significance of that difference. The internal comparison between couples of samples, tested with the Sheffe's F-Test and the Tukey's test showed a highly significant difference (Table 2).

The comparison between the RMS values of the points tested inside and outside 30° in normal and suspected glaucomatous subjects revealed no significant difference

The analysis of frequency distribution in the three groups (Fig 1) indicated, for a theoretical error of 14%, the RMS discriminating value of 3.47° between normal and suspected glaucomatous subjects.

The correlation between SF and the patient's age, calculated by the Pearson's coefficient was significant ($r = 0.49$) ($P = 0\ 002$) and confirmed by the Spearman's rank/test. The regression line is represented by equation:

$$y = 1.54 + 0.056^* \ x.$$

Table 1 Square root means of variance

	Mean RMS
Normal eyes	2 525°
Suspected glaucomatous eyes	4 490°
Glaucomatous eyes	5 403°

Table 2 Internal comparison of groups

	Sheffe's test		Tukey's test	
	F	P	Q	P
Normals				
Glaucomatous	48 03	0 000	13 86	0 05
Normals				
Susp glaucom	22 40	0 000	9 46	0 05
Glaucomatous				
Susp glaucom	4 83	0 01	4 40	0 05

Conclusion

On the basis of our results it was possible to establish that in both kinetic and static perimetry SF is significantly increased in subjects with glaucoma and suspect glaucoma.

Kinetic perimetry revealed an increased SF also outside 30° in patients with glaucoma without visual field defects.

Kinetic SF was related to age.

In our sample a RMS value greater than 3.47° in kinetic perimetry was 86% likely to be a sign of suspected or true glaucomatous SF, while a RMS value smaller than 3.00 was 71% likely to be normal.

References

1   Flammer J: Psychophysics in glaucoma A modified concept of the disease Doc Ophthalmol Proc 43: 11–17 (1984)
2   Flammer J, Drance SM, Fankhauser F, Augustiny L: Differential light threshold in automated static perimetry Factors influencing short-term fluctuation Arch Ophthalmol 102: 876–879 (1984)
3   Flammer J, Drance SM, Jenni A, Bebie H: JO and STATJO: programs for investigating the visual field with the OCTOPUS automatic perimeter Can J Ophthalmol 18: 115–118 (1983)
4   Flammer J, Drance SM, Schulzer M: The estimation and testing of the components of long term fluctuation of the differential light threshold Doc Ophthalmol Proc 35: 383–389 (1983)
5   Flammer J, Drance SM, Schulzer M: Covariates of long-term fluctuation of the differential light threshold Arch Ophthalmol 102: 880–882 (1984)
6   Flammer J, Drance SM, Zulauf M: Differential light threshold Short- and long-term fluctuation in patients with glaucoma, normal controls, and patients with suspected glaucoma Arch Ophthalmol 102: 704–706 (1984)
7   Gloor B, Stürmer J, Vökt B: Was hat die automatisierte Perimetrie mit dem Octopus für neue Kenntnisse über glaukomatöse Gesichtsfeldveränderungen gebracht? Klin Mbl Augenheilk 184: 249–253 (1984)
8   Heijl A, Drance SM: Change in differential threshold in patients with glaucoma during prolonged perimetry Br J Ophthalmol 67: 512–516 (1983)
9   Werner EB, Drance SM: Early visual disturbance in glaucoma Arch Ophthalmol 95: 1173–1175 (1977)
10 Werner EB, Saheb N, Thomas D: Viariability of static visual threshold responses in patients with elevated IOP Arch Ophthalmol 100: 1627–1631 (1982)
11 Zingirian M, Gandolfo E, Capris P, Corallo G: Comparison between static and kinetic threshold fluctuations determined by automated perimetry Doc Ophthalmol Proc 42: 49–54 (1985)
12 Zingirian M, Gandolfo E, Capris P: Threshold fluctuation tested by automatic kinetic perimetry: preliminary results Ital J Ophthalmol 1: 47–49 (1986)

II.9 Artefacts of computerized perimetry may simulate glaucomatous defects

E.L. GREVE, A.N. ZEILSTRA, M.A.C. RAAKMAN and D BAKKER
Amsterdam, The Netherlands

Abstract only

Computerized perimetry has improved the quality and standardization of perim-rety. There is however a certain percentage of patients that does not interact with computerized strategies as we would desire. The incomprehension of the task that the computerized examination expects them to perform, may lead to artefac-tual visual field defects. It may also lead to excessive long-term fluctuation. We have collected twenty examples of such artefacts or pseudo-defects, after examin-ing the patients both with fully-automated and with semi-automated perimetry (Peritest-Rodenstock). Clearly these pseudodefects have to be differentiated from glaucomatous defects and in many cases this is possible because: the pseudo-defects are bilateral, they have typical features, there is an optic disc-visual field discrepancy.

These pseudo-defects:
- are usually more outspoken in the upper half than in the lower half,
- usually spare the central 10°-visual field,
- can be found in both eyes though not exactly symmetrical,
- may simulate a central island,
- can be differentiated from a glaucomatous central island because of the equal distance to the center in the nasal and temporal field and because of the absence of a nasal step.

To recognize these defects it is useful to have the result of a complete central and peripheral visual field and to have possibilities of semi-automated and fully-automated perimetry on the same instrument.

The pseudo-defects will be illustrated by 5 examples. It is stressed that the artefacts may occur in all sorts of sizes. The smaller sizes may be difficult to recognize. The beautifull printouts of computerized perimetry should not be accepted at face-value in all cases. Be aware of artefacts. There are more patients who have difficulties in understanding computerized perimetry than we would like to admit.

124

Figure 1 Case 1

Female of 76 years

This patient had a visual field examination because of a suspect excavation The visual acuity was 0 6 in both eyes because of an incipient cataract The IOP was normal

In 1985 the visual field of the right eye showed various scattered defects on *fully*-automated perimetry The left eye showed a defect resembling a nerve fiber bundle defect with nasal extension (Fig 1) In 1986 both visual fields were completely normal on *semi*-automated perimetry

Figure 2 Case 2

   Female of 39 years

   A visual field examination was done because of asthenopic complaints

   The visual acuity was 1 0, clear media, normal IOP, normal optic discs In January 1986 the visual field showed defects in both eyes on *fully*-automated perimetry In May 1986 the examination was repeated The visual field of the right eye was almost normal, while the left eye showed only some scattered defects on *semi*-automated perimetry On this occasion fully-automated perimetry with the Humphrey Field Analyzer and the Scoperimeter showed abnormal results

126

2 c

Figure 3 Case 3

Female of 60 years

Visual field examination was done because of suspicion of glaucoma (positive family history)

The visual acuity in both eyes was 1 0, normal IOP, clear media, normal disc In 1985 defects outside 15 degrees of eccentricity were shown in fully-automated perimetry In 1986 the visual fields were normal on *semi*-automated perimetry

128
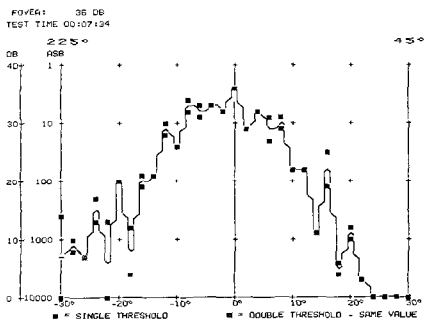
Figure 4 Case 4

Male of 83 years

A visual field examination was done because of a suspect excavation

The visual acuity was 0 5 because of incipient cataract The IOP was normal In 1984 extensive visual field defects were demonstrated in both eyes on *fully*-automated perimetry

In 1986 the visual fields were normal with the exception of a few relative defects on *semi*-automated perimetry

Figure 5 Case 5

Female of 80 years

The visual field was examined because of ocular hypertension The visual acuity ODS was reduced to 0 3 and 0 5 respectively because of cataract

In 1975 the visual fields ODS only showed a general reduction of sensitivity In 1984 and 1985 a progressive central island was found in both eyes on *fully*-automated perimetry

In 1986, a *semi*-automated perimetry, no local defects were found Only the general reduction of sensitivity remained

II.10 A longitudinal study of scotoma variation in glaucoma

V.J. MARMION and G. CHAUVET
Bristol, United Kingdom

Abstract

Numerical classification of the visual field to permit accurate statistical evaluation of the changes taking place in glaucoma is an important development. Variation in the intensity of scotomata may be observed in glaucomatous subjects at different examinations. The differentiation between spontaneous variation and the onset of glaucomatous defects is a clinical judgment which can be assisted by micro-computer analysis of the data. A method for achieving this is presented and the results from 56 eyes followed up over a five year period are presented and analysed.

Introduction

The mode by which a scotoma develops in time in glaucomatous subjects is of importance in relation to the clarification of the natural history of the disorder and patient management. Quantification of visual fields was proposed by Holmin and Krakau [4] using a Competer perimeter and they followed up visual fields in glaucomatous subjects for a period of four years. Mikelberg and Drance [8] used a method of planimetry on the central 30° fields charted with static perimetry and reported a period of follow up between two and fifteen years with a mean of eight, plus or minus 3.5 years. Hart and Becker [2] in a large quantative study over a ten year period noted that static threshold perimetry detected the earliest subtle development of scotomata. Multiple stimulus static perimetry is a technique which is particularly applicable in the clinical situation for the long term surveillance of glaucomatous subjects. Computer analysis of Friedmann Field data, as proposed by Henson [3] is a system for quantification founded on normative data and provides a basis upon which retrospective analysis of glaucoma patients may be readily undertaken.

 The combination of a standard acceptable form of perimetry performed by one

observer over a period of five years should provide data on the extent and type of progressive field loss occuring in open angle glaucoma. A study was therefore instituted to computerise data from visual fields examined by the technique of multiple stimulus static perimetry.

Materials and methods

Thirty-four patients with a mean age of 65 years and a male/female ratio of 18/16 were examined over a five year period with a mean of four years eight months interval between the first and last examination These were all undertaken by the

Table 1 Computer sub-programmes

MENU SELECT

1 New patient
2 Existing patient
3 List patients on disk
4 Exit

Select menu item with prefix key
EDIT ADMIN
Patient: E   E 18

Patient No   E   E 18
Name   E   E
Sex   F
Birth date   12-09-1908
Address
Phone
Consultant   VJM

Press <space> to continue
MENU SELECT
Patient E   E 18

1 Edit admin
2 List visits
3 Enter visit editor
4 Delete visit
5 Display latest
6 Display history
7 Print summary
8 Exit

Select menu item with prefix key
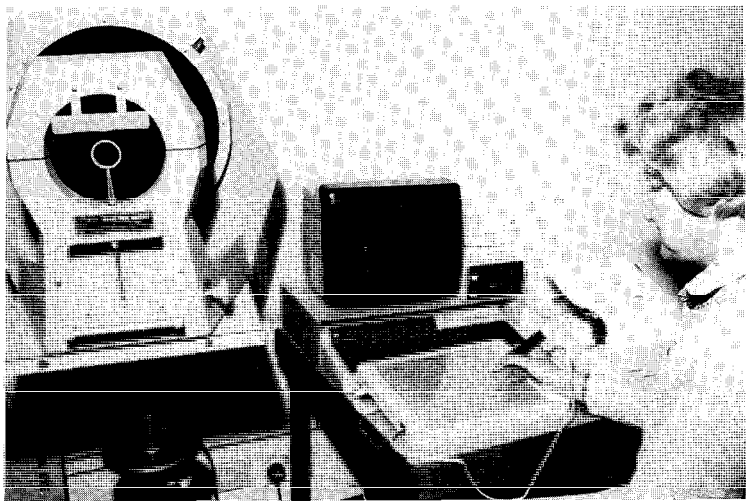
Figure 1 Automated system of analysis

same perimetrist. Severe visual field defects in an eye, amblyopia, cataract surgery on one eye during the period, or high myopia, led to the exclusion of an eye from the assessment in twelve subjects. During the five year period, at any visit, all subjects were examined by either the Friedmann or Goldmann perimetry. The Friedmann examinations closest to the commencement and end of the five year period were chosen for the analysis.

The visual field examination was by maximum threshold technique using the Mark II Analyser. The Henson System (Programme) was adapted for a BBC
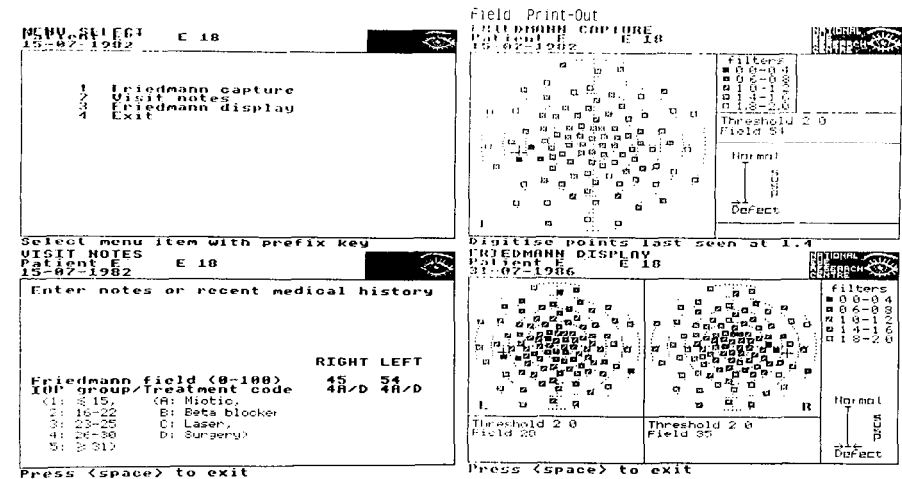
Figure 2 Example of results of one patient at beginning and end of period

Micro computer. The use of assembler routines in the programme has considerably accelerated retrieval and analysis. Figure 1 demonstrates the system, Table 1 shows the computer sub-programme. A specimen of the results from one patient is demonstrated in Fig. 2. A minor modification in the programme has permitted the inclusion of data on intraocular pressure and type of therapy. This can now be recorded on the printed field chart. A further extension of the programme permits the reading of 'at risk' areas and the identification of potential defects. A new scotoma was regarded as one which arose in either the opposite hemifield or in the same field in an area separate from the initial scotoma at an area that could not have been designated as suspect on Henson's criteria. A field change was graded as 'altered' if it differed in overall score by more than plus or minus 5% from the first examination.

Results

During the period of observation some 24 eyes, 42.8% showed evidence of progression. In 7, 12.5% of the total, new scotomata developed. In 21, 37.5% of the eyes the visual fields were unchanged and there were 11, 19/6% where better scores were produced at the end of the period The scores are summarised in Table 2.

In the 7 subjects (ten eyes) who had a pressure of less than 15 mm Hg at the end of the period, half had shown progression and the remainder were the same. None of these had shown any improvement.

No association was noted in this particular group of eyes between deterioration in visual fields and the incidence of optic disc haemorrhages the incidence being particularly low (two eyes). It will be seen from Table 2 that the percentage visual field in subjects who suffer the greatest deterioration was not significantly different from the overall group and no particular identifying feature from the fields emerged by which a prediction could be made of likely deterioration.

Table 2 Results of 34 patients; 56 eyes

56 eyes	Mean % field scores	
	1st year	5th year
	66 5 SD 25	61 6 SD 27
Deteriorated 24 eyes	62 1 SD 24	43 2 SD 20
Unchanged 21 eyes	72 0 SD 27	73 5 SD 29
Improved 11 eyes	57 3 SD 21	73 0 SD 17

Discussion

The facility to express a visual field in percentage terms opens up a prospect of statistical analysis and direct comparison between different reports. The system proposed by Henson in the analysis of multiple stimulus static perimetry has proved to be an efficient clinical tool [9]. The system has also been used in clinic trials [1] and has proved adaptable and has the potential for upgrading. Its principal disadvantage lies with the duplication of effort in relation to recruitment of data and subsequent transferance to the micro-computer base

The incidence of deterioration over the five year period is somewhat lower at 42.8% than that observed by Hart and Becker [2] or Mikelberg and Drance [8]. It is difficult to compare the data presented by Holmin and Krakau [4] as this is for a shorter period. A surprising finding of better scores in 11 eyes at the end of the period could, perhaps, in these, be in part attributable to changing therapy such as the greater use of laser trabeculoplasty and withdrawal of myotics These procedures were used generally in the whole group. In some patients individual eyes showed a significant improvement while the opposite eye had deteriorated. This type of observation also tends to reduce the possibility that there was a conditioning or learning element in relation to the visual field response. The most likely explanation lies with spontaneous variation as occurs in phase two and reported, for example, by Hart and Becker [2] What has not been possible in this initial review of the data, is an annual evaluation of change particularly in relation to eyes which have deteriorated or improved. It is anticipated that this information should become available once storage of the data has become fully implemented. General agreement on the preponderance of early field defects (albeit in stage 3) in one hemifield, is somewhat at variance with changes noted in other aspects of visual function such as diminished contrast sensitivity function [10], loss of colour vision [7] or altered dark adaptation [5]. Progression in field loss in the other hemifield in 12.5% as observed in this series, supports the presence of uniform damage as does general progression in an existing scotoma as observed in 42.8% of our cases These changes stress the urgency to bring diagnosis forward into phase two and the incorporation of several parameters of visual function producing an alternative form of risk factor.

The prevention of extension in existing scotomata might be facilitated by the use of more detailed computer analysis of the 'at risk' areas in the visual field. The potential exists within the system as developed and should permit this facility to be of practical clinical value.

A significant feature of this study has been the quite marked progression in half of the eyes in which the intraocular pressure was in the low range of normal and the total absence in this group of any improvement. This supports the findings of others [6] in relation to the controlled intraocular pressure and highlights the need for identification of alternative risk factors. The low frequency of optic disc haemorrhages in this group prevented a correlation with visual field alterations.

There was also a low incidence of clinical or pre-clinical diabetes. In the main, patients with a family history of glaucoma tend to be detected early and have a slightly better prognosis. There is only one subject (2 eyes) in this group in whom there is a positive family history of glaucoma. The majority of early referrals arose from the practice of non-contact tonometery by optometrists, a practice which results in a high false positive rate and which should be controlled by accurate perimetry.

References

1 Dallas NL: A comparative evaluation of timolol and pilocarpine in the treatment of chronic open angle glaucoma Trans OSUK (in press)
2 Hart WM, Becker B: The onset and evolution of glaucomatous visual field defects Ophthalmology 268–279 (1982)
3 Henson DB, Dix SM, Oborne AC: Evaluation of the Friedmann Visual Field Analyser Mark II, Par 1 Results from normal population Br J Ophthal 68: 458–462 (1984)
4 Holmin C, Krakau CET: Regression analysis of the central visual field in chronic glaucoma cases – a follow-up study using automatic perimetry Acta Ophthalmologica 6O: 267–274 (1982)
5 Isfahani AG: The visual function changes in primary open angle glaucoma before and after medical treatment M Sc thesis, University of Bristol, M 402 (1980)
6 Kidd MN, O'Connor M: Progression of field loss after trabeculectomy: A five year follow-up Br J Ophthal 69: 827–831 (1985)
7 Marmion VJ: The colour vision deficiency in open angle glaucoma – A comparison of tests Mod Probl Ophthal 19: 305–307 (1978)
8 Mikelberg FS, Drance SM: The mode of progression of visual field defects in glaucoma: Documenta Ophthal Proc Series 42: 387–390 (1985)
9 Sponsel WE: Visual field quantification in the diagnosis and assessment of chronic open angle glaucoma M D thesis, University of Bristol (1986)
10 Ross JE, Bron AJ, Reeves BC, Emmerson PG: Detection of optic nerve damage in ocular hypertension Br J Ophthal 69: 897–903 (1985)

Author's address:
Bristol Eye Hospital,
Lower Maudlin Street, Bristol, United Kingdom

II.11 The macular threshold: determination of population normal values

N A. JACOBS, I H. PATTERSON and I J BROOME
Manchester, England

Abstract

While it is accepted that the macula represents a peak of sensitivity, normal population values and ranges are poorly defined. Now that the assessment of macular sensitivity with automated perimetry is being performed clinically to monitor conditions such as senile macular degeneration and cystoid macular oedema following cataract surgery, a better definition is desirable.

The horizontal macular threshold was measured on the Dicon AP2000 perimeter for 160 normal subjects All cases were autorefracted using the Nidek 3000 model, and corrected fully taking presbyopia into account. Threshold values were measured at seven points spanning the central eight degrees of field. Determination was made by a semibracketing technique employed by the Dicon

Our results demonstrate a significant relationship between peak sensitivity and age group. The degree of fall in sensitivity taken at two degrees' eccentricity is firmly governed by the height of the peak

Introduction

Because computerisation is able to offer a wide menu of special field examinations, gone is the need to adhere to 'a field for all reasons' Thus when a suprathreshold screening test confirms a glaucoma suspect, follow up may be performed by a quantitative thresholding of a meridional cut through a known defect. Although the role of the perimetrist may have changed from performer to supervisor, the real responsibility lies in selecting the most appropriate field examination.

One selection on many of these perimeters is a 'macula' program. Detailed central field data beyond earlier expectations is therefore available. Its use has been advocated in monitoring senile macular degeneration and cystoid macular oedema. Other indications might include diabetic maculopathy and optic neu-

138

ritis. Such a test covers a larger area than is evaluated by measuring visual acuity. In the case of the Dicon which uses light emitting diodes inclusion of existing oblique meridional points in addition to the horizontal and vertical ones tested would augment the clinical usefulness of this program. In view of these developments, an improved definition of population normal values is desirable.

Materials and methods

The horizontal macular threshold was measured on the Dicon AP2000 automated perimeter with a background illumination of 31.5 apostilbs (Asb) and a $2\,mm^2$ spot size. Threshold was determined at seven points while the subject fixated the apparent centre of four red light emitting diodes in the 'blind spot' area of the bowl. Tested points were located at 1°, 2°, and 4° either side of fixation (0°) which itself was included.

A semibracketing technique was used where alternate stimulation above and below threshold in decreasing steps is concluded by a double confirmation to a resolution of 0.2 log units (L.U.).

Our 146 subjects were drawn from normal volunteers accompanying patients attending the Manchester Royal Eye Hospital and grouped according to age. The better or preferred eye was used in each case, and the minimum visual acuity was 6/9. In each case autorefraction with the Nidek AR3000 was carried out and full correction taking presbyopia into account was given for the test.

Results

The horizontal macular threshold (Fig. 1) was analysed with regard to two parameters. Firstly the peak value at fixation, and secondly the sharpness of the peak; defined as the average sensitivity drop at 2° eccentricity on either side of the peak.

Table 1 Definition of age groups and correlation of peak sensitivity

Decade group	Group number	Peak sensitivity (Asb)	Standard deviation (L U)
2	15	10 9	0 14
3	20	7 5	0 20
4	22	10 9	0 18
5	22	12 5	0 24
6	21	11 9	0 26
7	28	15 7	0 25
8	18	22 7	0 30
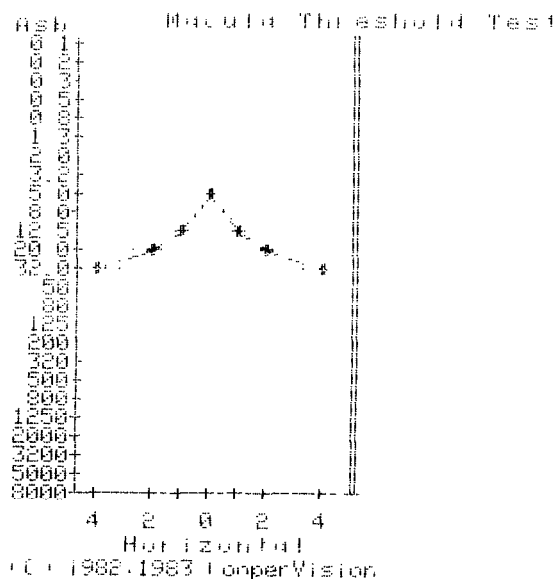
Figure 1 A typical horizontal macular threshold

To assess the influence of age, subjects were assigned to seven decade groups numbering between 15 and 28 (Table 1). Peak sensitivity decreased significantly with age (p = 0.01 – chi squared test – Table 1, Fig. 2) Over six decades this decrease amounted to 0.32 L.U., or in the order of 0 5 decibel per decade. However, the average sensitivity drop did not correlate with age.

Grouping the subjects according to peak sensitivity (Table 2), two further observations could be made. That the distribution of peak sensitivity followed a normal outline (Fig. 3). Ranging from 5 Asb to 50 Asb (1 L.U.) apart from two
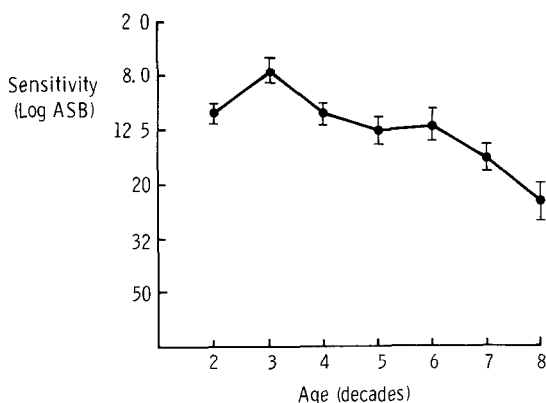
Figure 2 Correlation of peak sensitivity with age
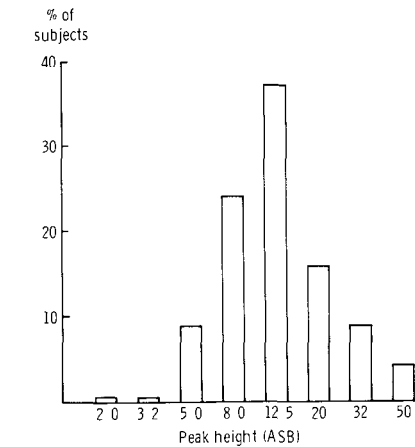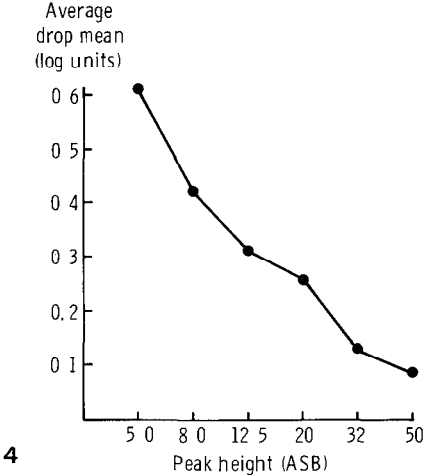
Figure 3 Distribution of peak sensitivity values

Figure 4 Relation of sensitivity drop to peak height

individuals, the largest group of 37% showed a value of 12.5 Asb. Also the average sensitivity drop, ranging from 0.1 to 0.6 L.U apart from two instances, decreased highly significantly with decreasing peak sensitivity (p = 0.001 – chi squared test – Table 2, Fig 4).

Discussion

In defining the macular threshold population normal values, the influence of age is seen to be significant (Fig 2). If any aspect of retinal sensitivity were most likely to be age dependent, it would be the macular peak. Some controversy attends the

Table 2 Distribution of peak sensitivity and associated sensitivity drop

Peak sensitivity (Asb)	Group number	Average sensitivity drop (L U)	Standard deviation (L U)
2 0	1	0 80	–
3 2	1	0 90	–
5 0	13	0 61	0 13
8 0	35	0 42	0 14
12 5	54	0 31	0 12
20 0	23	0 26	0 12
32 0	13	0 13	0 09
50 0	6	0 08	0 15

importance of age to normal findings in perimetry. Haas, Flammer, and Schneider [3] recently examined this question for the central 27° of field on the Octopus They described an overall rate of decrease in sensitivity comparable to our 0 5 decibel per decade for the macula. Previous work on the Dicon carried out by Jacobs and Patterson [5] concerning variability of the normal hill of vision from 2.5° to 60° eccentricity failed to exhibit any effect of age on sensitivity Substantiating these results is the very significant correlation in the present study between sharpness (rate of sensitivity drop) and height of the macular peak (Fig. 4) This implies that a high age related peak will fall rapidly to a non age related paramacular level, whereas a low peak will fall more gradually to achieve a similar status.

Differences in background illumination levels may go some way towards explaining discrepancies between the photopic Dicon (31.5 Asb) and the mesopic Octopus (4 Asb). Using neutral density filters on the Octopus, Klewin and Radius [6] deduced that patients on miotic therapy or with mild opacification of the media would probably show false positive field defects. This suggestion was also made in an intercomparison of fields performed on the Dicon and Octopus [4]. Therefore senile miosis could account for the progressive overall decrease in sensitivity noted by Haas et al. [3], and their finding of uneven change within the field may have been secondary to an uneven bowl illumination. Reaction time is a further factor requiring consideration. Aulhorn and Harms [1] described that a 0.5 second interval is required to reach full temporal summation Perhaps the difference between the 0 4 sec stimulus of the Dicon and that of 0 1 sec on the Octopus becomes more relevant with age. Drance et al [2] reported a steady decrease in isopter area with age on the Goldmann perimeter However kinetic perimetry, which obscures temporal and spatial summation effects [8], would exaggerate any reaction deficit

Normal data gleaned on the Dicon to date reveals that the macular peak sensitivity is influenced by age, although the remainder of the hill of vision is not [5]. Similarly, Ross et al. [7] noted that only certain components of contrast sensitivity function were affected by age For clinical purposes, such data is relevant uniquely to the type of perimeter on which it was obtained.

References

1 Aulhorn E, Harms H: Visual perimetry In: Jameson D, Hurvich LM (eds) Visual psychophysics; Handbook of sensory physiology, Vol II/4, pp 29–55 Springer Verlag, Berlin, 1972

2 Drance SM, Berry V, Hughes A: Studies on the effects of age on the central and peripheral isopters of the visual field in normal subjects Am J Ophthalmol 63: 1667–1672 (1967)

3 Haas A, Flammer J, Schneider U: Influence of age on the visual fields of normal subjects Am J Ophthalmol 101: 199–203 (1986)

4 Jacobs NA: Modern perimetry Seminars in Ophthalmol 1: 14–34 (1986)

5 Jacobs NA, Patterson IH: Variability of the hill of vision and its significance in automated perimetry Br J Ophthalmol 69: 824–826 (1985)

6 Klewin KM, Radius RL: Background illumination and automated perimetry Arch Ophthalmol 104: 395–397 (1986)

7 Ross JE, Clarke DD, Bron AJ: Effect of age on contrast sensitivity function: uniocular and binocular findings Br J Ophthalmol 69: 51–56 (1985)

8 Tate GW, Jr: The physiological basis for perimetry In: Drance SM, Anderson D (eds) Automatic perimetry in glaucoma – a practical guide, pp 1–28 Grune and Stratton, New York, 1985

Author's address:
N A Jacobs,
Dept of Ophthalmology,
Charing Cross Hospital,
Fulham Palace Road, London W6 8RF, United Kingdom

Section III
Computerized visual field analysis

III.1 A system for the analysis of automated visual fields using the Humphrey Visual Field Analyzer

H.D. HOSKINS, S.D. MAGEE, M.V DRAKE and M N KIDD
San Francisco, U S.A

Introduction

Analyzing visual field progression is an important component of glaucoma management. Unfortunately, detecting progression reliably may be difficult Factors such as short-term (intratest) and long-term (intertest) fluctuation, patient fatigue, patient learning curve, etc , can cause transient visual field changes which may mimic improvement or deterioration of the overall visual field [1–4] Over a series of tests, these factors should cancel themselves out, i.e , errors in the positive direction and errors in the negative direction should be approximately equal and overall mean sensitivity should stay roughly the same In practice, one must often repeat a visual field test several times before one can determine whether or not a given degree of depression is due to transient fluctuation or actual pathologic deterioration. However, multiple visual field examinations require a significant expenditure of patient time and effort and may unnecessarily delay diagnosis.

In an effort to improve our ability to recognize significant visual field deterioration, we analyzed a series of three visual fields to assess the predictive value of the second field in determining the likelihood of an overall decrease in sensitivity between the first and third field.

Patients and methods

We analyzed the fields of 136 eyes (86 patients), each of whom had a series of at least three central 30° full threshold fields performed on the Humphrey Visual Field Analyzer with program 30-2 The patients were between 21 and 79 years of age (mean 54.7 ± 14.6 SD) All patients had a corrected visual acuity of 6/12 (20/40) or better at the time of each test. Patients were diagnosed as having glaucoma with at least minimal visual field damage present The fields comprising each series were separated by as little as 4.6 months and as much as 30.5 months For
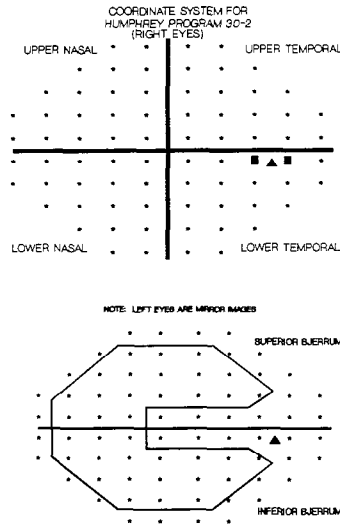
Figure 1 Coordinate system for the Humphrey Visual Field Analyzer program 30-2 Each spot represents a threshold sensitivity measured in dB The two spots marked with a solid box in the lower temporal quadrant were removed from the statistical analysis The diamond represents the approximate location of the blindspot Points selected for the upper and lower Bjerrum regions are shown in the lower part of the figure

90% of the patients, the interval between the first and third field was between 11 and 23 months (mean $16.5 \pm 5\ 4\,SD$)

For each individual field test, the data were analyzed by quadrant, superior and inferior Bjerrum regions, and for the total field. Figure 1 displays the regions analyzed. The mean sensitivity (MS) in each region was determined by adding the individual threshold values in dB and dividing by the number of values. The two points closest to the blindspot in the lower temporal region were eliminated from the analysis. The standard deviation (STD) of each region was also calculated.

To determine the predictive value of the second field in the series, the difference between the MS of the first and second fields was calculated. Also, the difference in MS between the first and third field and the slope of the best fit line through points representing the MS at the first, second, and third fields was calculated for each region. Additionally, we calculated the mean difference in STD between the first and the second fields for each region.

Each series of fields was coded for each region as to possible relationships between fields 1 through 3. Figure 2 shows the possible arrangements of field scores For the analysis, we only considered series where the second field was depressed relative to the first field.

Regression models were constructed to determine what change between the first and second field was required to predict that the third field would show a depression relative to the first field defined in one of 2 ways:
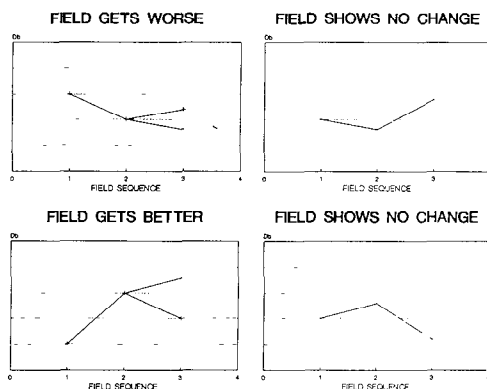
Figure 2 Possible patterns of response for each patient's series of three consecutive fields. A series was considered worse if the third field was at least 1 dB below the first field, or the slope of the best fit line through the 3 fields was negative

1. a negative slope between fields 1 through 3 or
2. the MS of field 3 being 1 dB below field 1.

The data were stratified based on degree of field damage at the first field. Eyes with a MS of greater than 25 dB were placed in one group labeled 'minimal field damage' and eyes with a MS of less than or equal to 25 dB were placed in another group labeled 'moderate field damage'.

Results

Table 1 displays the mean sensitivities and standard deviations for each of the regions studied for fields 1 through 3. These data include only series of eyes where the second field was depressed relative to the first.

Tables 2 through 5 report the results for each of the regression models studied. We determined the amount of change required between the first and second fields to predict a downward trend in the series as confirmed by the third field. The regression equations were solved for the dependent variable using either the slope of line through fields 1–3 or the change in MS between field 1 and field 3 as the independent variable. This value plus the product of the standard error of the model and the t-statistic, adjusted for degrees of freedom and desired confidence interval, yields the upper confidence level for the point where the patient's field is confirmed as getting worse. Table 6 reports the amount of change in MS required between fields 1 and 2 to predict that field 3 will be below field 1 by at least 1 dB for each of the regions studied.

Figure 3 graphically displays the 95% confidence level for change from field 1 to field 3 required to predict that field 3 will be depressed by at least 1 dB relative to field 1 in the upper temporal region of moderately damaged fields.

Table 1 Summary of 3 fields for each region

Region	First		Second		Third	
	Mean	Std	Mean	Std	Mean	Std
UN	21 1	4 1	18 7	4 5	19 2	4 8
UT	22 3	5 2	19 8	5 9	20 7	5 7
LN	24 2	4 0	21 8	4 9	22 2	4 9
LT*	26 0	3 2	23 9	4 1	24 6	4 0
Total	22 6	4 9	20 6	5 4	20 9	5 4
SB	21 4	3 9	19 1	3 8	19 6	4 2
IB	24 5	3 6	22 5	4 0	23 1	4 2

* with blind spot points removed

UN = Upper Nasal, UT = Upper Temporal, LN = Lower Nasal, LT = Lower Temporal, SB = Superior Bjerrum, IB = Inferior Bjerrum

Table 2 Model: drop MS field 1 to 2 vs change MS field 1 to 3

Region	RSQ	Slope	I	P
UN	0 17	0 25	1 66	0 0002
UT	0 18	0 29	1 89	0 0003
LN	0 09	0 17	1 99	0 0150
LT*	0 01	0 05	1 90	0 4312
Total	0 09	0 17	1 61	0 0105
SB	0 20	0 30	1 75	0 0001
IB	0 15	0 25	1 65	0 0004

* with blind spot points removed

Table 3 Model: change in STD field 1 to 2 vs change in MS field 1 to 3

Region	RSQ	Slope	I	P
UN	0 07	− 0 13	0 08	0 03
UT	0 06	− 0 18	− 0 26	0 04
LN	0 03	− 0 09	− 0 90	0 16
LT*	0 02	− 0 06	− 0 83	0 31
Total	0 05	− 0 90	− 0 30	0 06
SB	0 05	− 0 12	0 35	0 06
IB	0 06	− 0 14	0 25	0 03

* with blind spot points removed

Table 4 Model: change STD field 1 to 2 vs change in slope field 1 through 3

Region	RSQ	Slope	I	P
UN	0 07	0 25	0 05	0 03
UT	0 06	0 36	− 0 26	0 04
LN	0 02	0 16	− 0 89	0 20
LT*	0 02	− 0 14	− 0 83	0 23
Total	0 02	0 12	− 0 36	0 21
SB	0 01	0 07	0 94	0 47
IB	0 00	− 0 02	0 84	0 77

* with blind spot points removed

Table 5 Model: drop MS field 1 to 2 vs change in slope fields 1 through 3

Region	RSQ	Slope	I	P
UN	0 15	− 0 48	1 73	0 0007
UT	0 17	− 0 57	1 88	0 0003
LN	0 14	− 0 45	1 95	0 0016
LT*	0 01	0 12	1 90	0 3071
Total	0 09	− 0 34	1 61	0 0092
SB	0 20	− 0 60	1 75	0 0001
IB	0 15	− 0 49	1 65	0 0004

* with blind spot points removed

Table 6 Required change field 1 to 2

Region	Degree of field damage	
	Minimal	Moderate
Upper nasal	5 50	6 50
Upper temporal	4 74	6 91
Lower nasal	5 22	7 20
Lower temporal	*	*
Total	*	5 49
Superior Bjerrum	*	5 76
Inferior Bjerrum	7 85	5 55

* No significant regression model found for these regions
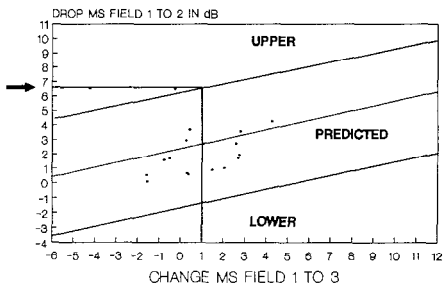
Figure 3 Graphical representation of the method used to determine the 95% confidence level for the amount of change required between the first two fields which would predict that the third field would confirm a downward trend in the series

Figures 4 and 5 demonstrate plots of required change from fields 1 to 2 vs varying confidence intervals for confirming change in field 3 in minimally and moderately damaged fields

Discussion

The visual field examination is but one of a series of tests and evaluations that ophthalmologists use in determining whether or not a patient's glaucoma is progressing Our data indicated that regardless of other factors, i.e., intraocular pressure, family history, cup to disc ratio, etc , if the visual field decreases by an average sensitivity of between about 4 and 7 dB (depending on the region analyzed) then one can predict with great reliability a downward overall trend in sensitivity. The converse is also true· as the change from field 1 to 2 becomes smaller, the probability of a downward trend is less. An average loss of 3.2 dB in moderately to severely damaged fields corresponds to the 50% confidence inter-
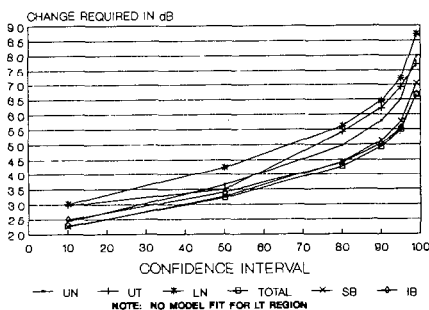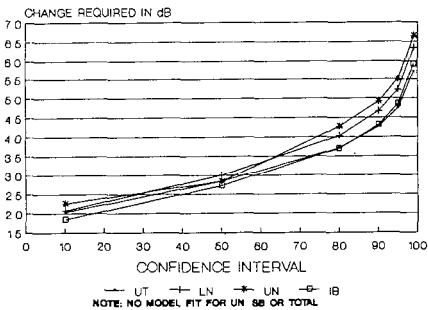
Figures 4 and 5 Plots of drop in MS required to predict a downward trend in the series as confirmed by the third field vs confidence intervals for this confirmation Figure 4 shows required change in minimally damaged fields Figure 5 shows required change for moderate to severely damaged fields

val. This predicts that when the average loss per point between the first two fields is 3.2 dB, 50% of the time the third field will confirm a downward trend and 50% of the time the third field will show an upward trend.

It should be noted that no statistically significant regression model could be constructed for the lower temporal region, even when the two points closest to the blind spot were removed from the analysis This is due to the fact that there was very little deterioration between the successive fields in this region. In this series of eyes, no amount of change in the lower temporal region accurately predicted later field deterioration.

What is perhaps most striking about our findings is that the degree of depression between the first and second field must be quite extensive before the confidence level is high enough for the third field to confirm depression. Substantial loss, on the order of 2 to 2–1/2 dB per point in a given region, can occur and have little or no predictive value Thus, caution is advised in determining visual field deterioration based on only two examinations

In practice, one analyzes multiple factors when making therapeutic decisions about glaucoma patients. The most prominent of these factors include the patient's intraocular pressure, the cup to disc ratio, the presence or absence of optic disc hemorrhage, and visual field deterioration. Unfortunately, incomplete data exist about the predictive validity of these factors

Our results indicate that a relationship exists between the change of mean sensitivity of the first two fields in a series and the likelihood that the third field in a series will also indicate progressive deterioration. However, the model predicted by our data suggests that a large degree of change is required in order to assure high confidence in our ability to confirm actual change

By using this information with other physical findings and test results, one is able to make a more rational therapeutic decision and a more accurate prediction of the patient's short-term outcome.

References

1 Flammer J, Drance SM, Augustiny L, Funkhauser A: Quantification of glaucomatous visual field defects with automated perimetry Invest Ophthalmol Vis Sci 26 (2): 176–181 (1985)
2 Flammer J, Drance SM, Zulauf M: Differential light threshold: short- and long-term fluctuations in patients with glaucoma, normal controls, and patients with suspected glaucoma Arch Ophthalmol 102: 704–706 (1984)
3 Flammer J, Zulauf M: The frequency distributions of the deviations in static perimetry In: Heijl A, Greve EL (eds) Proceedings 6th Int Visual Field Symposium 1984 Dr W Junk Publishers, Dordrect, The Netherlands, 1985
4 Rabineau PA, Gloor BD, Tobler HJ: Fluctuations in threshold and effects of fatigue in automated static perimetry In: Heijl A, Greve EL (eds) Proceedings 6th Int Visual Field Symposium 1984 Dr W Junk Publishers, Dordrect, The Netherlands, 1985

Authors' address:
Foundation for Glaucoma Research and
University of California,
San Francisco (CA), U S A

III.2 A package for the statistical analysis of visual fields

A. HEIJL, G. LINDGREN and J. OLSSON
Malmö and Lund, Sweden

Abstract

We have devised a package for the statistical analysis of computerized visual fields. It is based on a new mathematical model of the normal visual field and intended to facilitate interpretation of single fields and to illustrate changes over time in consecutive threshold fields. Single field analyses include maps showing pointwise total and pattern deviations from the age-corrected normal reference field. These maps are displayed both numerically, in dB, and as noninterpolated greyscaled probability maps illustrating the statistical significance of measured deviations. These probability maps help emphasize shallow, but significant, depressions in the paracentral field while frequently occurring false positive deviations occurring in the midperiphery are de-emphasized. Visual field indices, summarizing the deviations of height (Mean Deviation) and shape (Pattern Standard Deviation and Corrected Pattern Standard Deviation) of the measured field are weighted according to the normal variance among healthy individuals and printed out together with level of statistical significance For follow-up the programme contains several different options. These range from an Overview format where threshold printouts and probability maps from several tests are printed in reduced size, but without any reduction of data, on a single sheet of paper, to a box plot format where the development of the field is shown with an intermediate degree of data reduction and a format employing a high degree of data reduction: graphs over visual field indices over time. If five or more tests are available a linear regression analysis of Mean Deviation is automatically performed. The programme will become available in the Humphrey Field Analyzer.

Introduction

Computerized perimeters produce results in digital format and contain computers capable of performing mathematical calculations. It is quite obvious that one

may use the on-board computer of the perimeter not only to govern the test process itself, but also to help analyse the results of the visual field test by performing statistical analyses or by plotting the results in new ways intended to facilitate interpretation Several such methods and programmes have been devised or suggested [1, 4, 5, 10, 11, 12]

We have developed a package of such statistical and graphical methods intended to facilitate the interpretation of computerized threshold perimetry, single fields as well as sequences of fields from the same eye. The methods are based on a new mathematical model of the normal visual field and will be made available in the Humphrey Field Analyzer under the name Statpac. The aim of the current paper is to describe the model of the field and the methods used in the programme, to show examples and to discuss the concepts involved.

Mathematical visual field model

Naturally statistical judgements on the normality of observations require knowledge of normal results. Data on the normal island of vision, as measured by manual, kinetic perimetry is readily available, including information on the normal decrease of sensitivity with age [2, 3, 13]. In computerized perimetry the most commonly used model of the normal visual field has been the Octopus age-corrected normal threshold values [1]. This model implies that the *shape* of the normal island of vision remains unchanged with age, the sensitivity decreasing 0.1 log unit (= 1 dB) per decade, and that the normal inter-individual variation is constant across the visual field.

Since the mathematical visual field model is so crucial we decided to perform and analyse a large number of visual field examinations in normals as a first step in the development of the statistical package. This was done not only to establish average normal threshold values for different ages, but also in order to study normal visual field variability from a more fundamental point of view.

In a material of randomly selected normals the 30-2 programme of the Humphrey perimeter [6] was used to test both eyes up to three times. In order to get better appreciation of the influence of perimetric training another group of ten volunteers underwent testing of each eye ten times.

The result of these studies [7, 8, 9] made us construct a model of the normal reference field with the following properties:

a) The expected sensitivity at each point decreases continuously and linearily with age. The rate of change (loss of sensitivity) differs between different points in the visual field. Thus the normal reference field is allowed to change both height and shape with age

b) The normal inter-individual variability of the age-corrected threshold, and also the intra-individual inter-test variability is not assumed to be constant across the visual field but is allowed to vary with location.

c) Individual deviations from the normal reference values are not assumed to follow Gaussian distributions. Instead the model is based on actual empirical data. Empirically, skewness and kurtosis are both significantly non-Gaussian, and the shape of the distributions varies across the visual field [7].
d) The model is constructed for patients with some previous perimetric experience. Perimetric experience influences the results of computerized threshold perimetry The mean sensitivity in a group of perimetrically inexperienced subjects increases with experience, more in midperipheral areas than centrally. Inter-individual variation decreases with perimetric training. A mathematical model constructed on the basis of results from totally inexperienced subjects would have very wide limits of normality [9].
e) The model is based on test results fulfilling certain minimum reliability criteria (<20% fixation losses *and* <33% false negative answers *and* <33% false positive answers). This helps keep normal threshold limits reasonably narrow. The variation between normal visual fields is reduced when only fields meeting certain reliability criteria are taken into account [8] The Statpac programme will therefore check whether analysed fields meet these criteria and alert the user if they do not.

Determination of normal values

The empirical data base of the normal visual field model consists of 487 tests of 239 normal individuals. The total number of field tests was considerably larger, but the numbers were reduced when abnormal subjects, fields from inexperienced subjects and tests not meeting the minimum reliability criteria (cf above) were excluded. The data were collected in four different centres.

In the available data base of tests from normals the number of tests per individual differed among, and sometimes within, centres. Thus observations were weighted when estimating pointwise normal threshold values: age slopes, intercepts and variances. Weights were calculated from an ANOVA separating the variance into components depending on individual, eye, session, test point and their interactions.

It seems reasonable to assume that normal age slopes, intercepts and variances of the threshold are continuous functions of the x and y coordinates of the visual field. Polynomials were therefore fitted to the grid of pointwise estimates. In this way new, better estimates of normal threshold values, variances and age slopes were computed both at and between actually measured points.

Normal deviations from this new normal reference field were computed One test was randomly selected among all tests of an individual subject, thus creating a sample of independent observations where each subject was represented only once.

Percentiles of pointwise deviations and indices were computed giving unbiased

estimates of the prediction limits of normality at various level of significance. The random drawing of tests was repeated 50 times and means of the 50 estimates were calculated In this way practically all information was used.

It is reasonable to assume that also percentiles of pointwise deviations are continuous functions of the coordinates. Thus, new estimates of these deviations were computed after fitting to functions of the coordinates as described above.

The programme package

The statistical package is intended for threshold fields within the central 30° field (programmes 30-2, 24-2, 30-1 and 24-1 of the Humphrey perimeter) All analyses are carried out by the onboard computer and the results printed out by the standard printer of the perimeter. The current first version of the programme will analyse single fields in a number of ways and display and analyse series of fields from the same eye with various degrees of data reduction

Single fields

Single visual fields are analysed in three ways
1. as numerical deviation maps,
2. as probability maps,
3. as visual field indices
The perimeter calculates a normal reference field based on the patient's age. The reference field consists of a matrix of floating point dB-values The reference field is subtracted from the measured field and the resulting differences (rounded to the nearest dB) displayed as the *total deviation maps* (Fig. 1d and f). The pattern deviation maps are different displays where the pattern, i.e. the shape, of the deviations from the age-corrected normal shape of the visual field is emphasized (Fig. 1e and g) The measured field is elevated or depressed towards the level of the normal reference field. Through this procedure general changes of height of the measured field are eliminated or diminished while localized field loss remains clearly visible or enhanced.

The total deviation and the pattern deviation are displayed in the traditional way, as *numerical maps* in dBs (Fig 1d and e), but also as *probability maps* (Fig 1f and g). In the probability maps the deviation of the measured threshold from the age-corrected normal threshold at each point is compared with the prediction limits for normality (intervals wherein *new* observations will fall at a certain significance level). The resulting point-wise significancies are displayed as a non-interpolated greyscaled probability maps. A darker tone means that the threshold is less commonly seen among normal subjects. The total deviation and the pattern deviation maps are printed out both in the probability format and numerically

Figure 1 Printout of one single field. The upper part of the form contains all traditional information including reliability parameters (a), and numerical (b) and greyscale threshold printouts (c). The numerical total (d) and pattern (e) deviation maps are printed in smaller size like the corresponding probability plots (f) and (g). Visual field indices are provided together with significance levels (h).

The programme calculates four global visual field indices

1. the mean deviation (MD),
2. the pattern standard deviation (PSD),
3. the short-term fluctuation (SF),
4. the corrected pattern standard deviation (CPSD).

MD is a weighted average deviation from the normal reference field. MD estimates the *uniform* part of the deviation, and may be interpreted as a measure of deviation of height.

$$MD = \left\{ \frac{1}{n} \sum_{i=1}^{n} \frac{(x_i - N_i)}{s_{1i}^2} \right\} \Big/ \left\{ \frac{1}{n} \sum_{i=1}^{n} \frac{1}{s_{1i}^2} \right\}$$

where x_i is the measured threshold and N_i the normal reference threshold at point i and s_{1i}^2 the variance of normal field measurements at point i. The number of test points (excluding the blind spot) is denoted by n. MD will become more negative when visual field defects progress or e g when a progressive cataract causes increasing generalized depression of sensitivity

PSD is a weighted standard deviation of the point-wise differences between the measured and the normal reference fields. PSD estimates the *non-uniform* part of the deviation and may be interpreted as the standard deviation of deviation of the threshold pattern (shape of the hill of vision) from normal. A small values for PSD indicates close agreement in shape between the patient's field and the normal reference field. An irregular field, e.g. one with localized field defects will result in a large PSD.

$$PSD^2 = \left\{ \frac{1}{n} \sum_{i=1}^{n} s_{1i}^2 \right\} * \left\{ \frac{1}{n-1} \sum_{i=1}^{n} \frac{(x_i - N_i - MD)^2}{s_{1i}^2} \right\}$$

Weighting with $1/s_{1i}^2$ minimizes PSD^2 in normals

SF is a weighted mean of the standard deviations at ten test points where the threshold is determined twice SF may be interpreted as an estimate of the measurement error.

$$SF^2 = \left\{ \frac{1}{10} \sum_{i=1}^{10} s_{2i}^2 \right\} * \left\{ \frac{1}{10} \sum_{i=1}^{10} \frac{(x_{i1} - x_{i2})^2}{2*s_{2i}^2} \right\}$$

where x_{i1} is the first and x_{i2} the second threshold value. The normal intra-test variance in point i is denoted by s_{2i}^2. Weighting with $1/s_{2i}^2$ minimizes SF^2 in normals.

CPSD estimates that part of the non-uniform deviation which is not caused by SF It may be interpreted as the 'true' deviation of the threshold pattern (shape of the hill of vision) from the normal. To adjust for the non-uniform fluctuation pattern we let k be a constant >1 and define

$$CPSD^2 = PSD^2 - k*SF^2.$$

If $CPSD^2 < 0$ it is set to 0, since variances never are negative, although their estimates may be

Thus the deviations of the measured field from the reference field are divided into a uniform change of height, estimated by MD, and a deviation of shape, estimated by PSD. PSD consists of the true differences of shape, estimated by CPSD, and the measurement error, estimated by SF. Prediction limits for normality have been calculated for all four visual field indices. If the value of any visual field index falls outside the prediction intervals the level of significance of the deviation is given (Fig. 1k). The printout shown in Fig. 1 replaces the standard printout, thereby providing threshold data plus the results of all statistical analyses on one sheet of paper

Series of fields

The Statpac programme facilitates interpretation of series of follow-up fields in
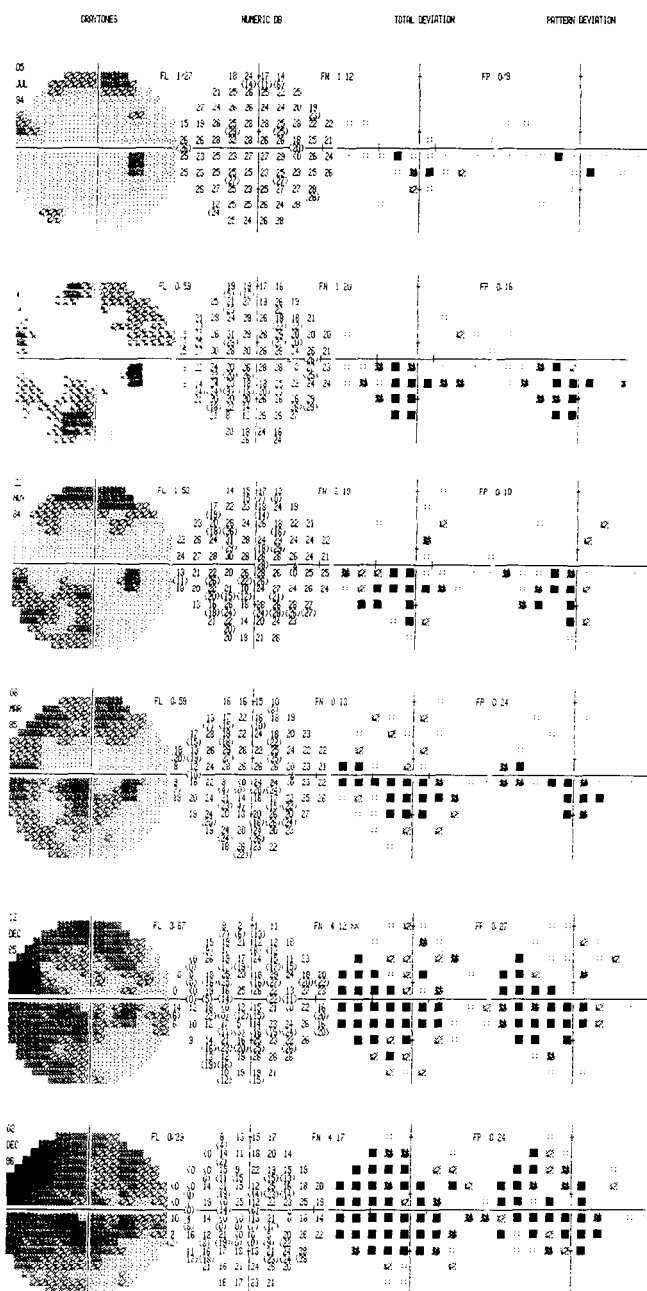
Figure 2 Example of printout using the Overview format Almost all information is provided, although in small format Each row represents one test; greyscale and numerical threshold charts and probability plots It is interesting to see that the field defects in this case of rapidly progressing glaucomatous field loss are visible in the probability maps of the first test, when the threshold printouts still look normal
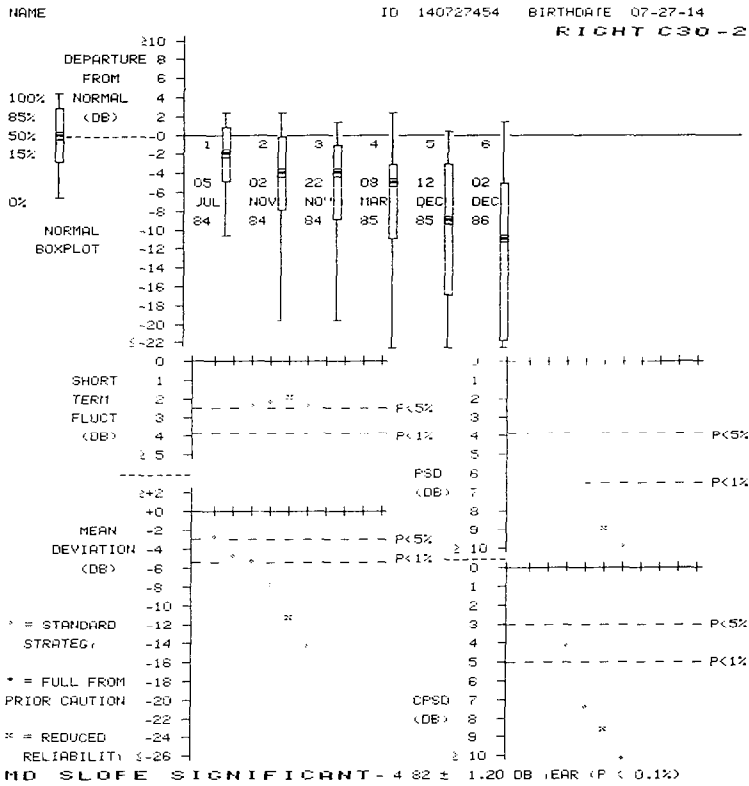
Figure 3 Change Analysis of the same case as that in Fig 2 The series of box plots are printed in the upper part of the form, the graphs over visual field indices in the lower part The rapid deterioration is clear from the box plots and the graphs of MD, PSD and CPSD versus time The change of MD is large and statistically significant (bottom)

various ways. Three different degrees of data reduction are available ranging from none, (presentation of raw results) through intermediate to maximum (presentation of indices). The usage of follow-up data requires almost no extra work. If, after a test, the Change Analysis and/or Overview pads are chosen on the print menu the programme will automatically find all records from the tested eye, sort them in chronological order and print out results in one or both follow-up formats

In the Overview format (Fig. 2) the results of up to ten tests are printed on one sheet of paper without any reduction of data For each test diminished greyscale and numerical representations are printed together with total and pattern deviation probability maps The intention of this format is simply to provide easy overview of as much of the original data as possible.

On the other hand a very high degree of data reduction is used in those graphs where the results of consecutive tests are shown as visual field indices plotted over
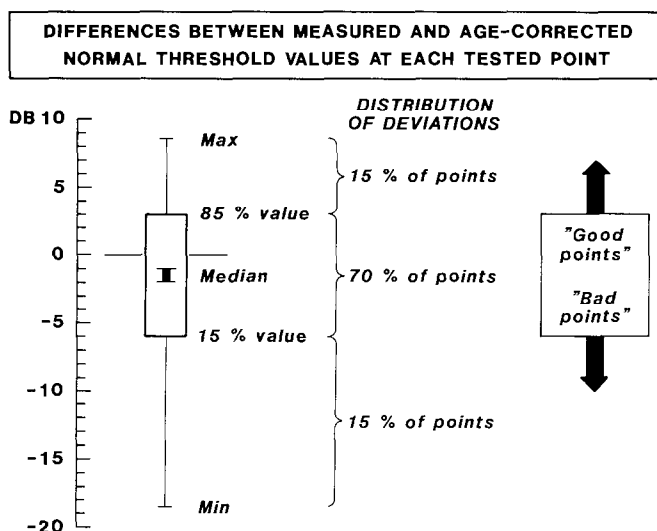
Figure 4 Schematic box plot

time. (Fig. 3). These graphs are straight-forward and require no explanations except that different symbols are used for tests not meeting the minimum reliability criteria (crosses) and 'reliable' fields (diamonds) To facilitate interpretation the p<5% and p<1% lines for the normal population are shown as reference lines.

If five or more fields are available (using the same strategy) a linear regression analysis of MD is automatically performed and the resulting slope printed out including level of significance (Fig. 3, bottom).

The box plot representation (Fig. 3, top) offers the opportunity to judge a series of fields with an intermediate degree of data reduction. A box plot is a modified histogram, giving a five number summary of a sample distribution (Fig. 4). Here the sample is made up of the pointwise differences between the measured field and the normal reference field. Out of these differences the extreme values (minimum and maximum) of the sample, the median, the 15th and 85th percentiles are plotted. Thus 70% of all pointwise differences fall between the upper and lower limits of the box, i e. between the 15th and 85th percentiles. A 'normal' box is presented for comparison. This normal box plot is the mean of the boxes from the normal data base.

Some practical examples may be given A visual field with a small and deep scotoma will have a box plot with a long negative tail, while the position of the lower limit of the box will be fairly normal. If the scotoma deepens over time the length of the tail will increase. If the disturbed area enlarges, involving more points, the lower limit of the box will be depressed. If the only change in a measured field is a general depression of sensitivity, e.g. due to cataract, the

shape of the box plot will be fairly normal, but the whole symbol will be depressed as compared with the normal box.

Discussion

The most important features of the current statistical package are the usage of a new, fairly advanced model of the normal visual field and the fact that the design and choice of analyses have been based on empirical results obtained from a large number of normal subjects, partly a random selection from the population. The statistical analyses of field data necessitates computations of prediction intervals. The characteristics of the normal distributions of deviations from the age normal reference field are not known. In the current programmes therefore the percentiles of empirically determined distributions are used to define probability levels. Incorrect assumptions about these distributions (which are likely to result in completely erroneous prediction limits) are therefore avoided.

The inexperienced user of a computerized perimeter may expect computerized analyses to tell with certainty whether the measured field is normal or not, and whether the field of a followed eye deteriorates, improves or remains the same. It must be emphasized, however, that no visual field index [4], t-test [11] or other statistical analyses can give absolutely reliable judgements on any single field or series of fields. The spatial information available in a visual field chart is not yet fully used by any statistical method of analysis. The statistical approach will therefore sometimes miss in cases where an experienced observer would be correct.

This does *not* mean that computer-assisted analyses generally should be inferior to interpretations performed by trained observers Computerized analyses can be most useful, but the computer and the human observer complement each other. The excellent memory of the computer and its ability to correctly and rapidly perform complicated mathematical tasks makes it extremely suitable e.g. for calculation of threshold prediction limits or regression analyses. At the same time the superiority of the trained human eye as an image analyzer must still be acknowledged. If the computer is programmed to present data in new ways facilitating interpretation by a human observer the result may represent a clear step forward. This approach may be called *computer-assisted interpretation.* Statpac is meant to provide the user with such computer assistance, not to exclude him from the interpretative process

The numerical total deviation map is a simple example. It shows the pointwise deviations of the actually measured threshold values and from those of the age-corrected normal reference field (Fig. 1d). This is certainly helpful but the user must still make a subjective interpretation, now of the total difference map instead of the measured threshold data. He must see if the whole or part of the deviation is due to a general change of sensitivity, judge whether the measured

depression at each point is clinically significant while also considering the location of the depressed point. He must then determine whether the depressed points form a logical or diagnostic pattern.

The computer analyses can provide further help. In the numerical *pattern* deviation map (Fig. 1e) the deviations of the measured threshold values are shown after normalizing the height of the measured field. The deviation of the *shape* of the normal reference field is displayed. In this way it becomes easier to determine whether there is any *localized* field loss in a subnormal field Fig 5 shows a field chart from an eye with cataract. The whole greyscaled threshold chart is dark. The numerical total deviation map shows that the sensitivities generally are depressed as compared with the normal age-corrected reference field. However, the pattern deviation maps clearly show that the *shape* of the field is essentially normal – there are no localized field defects.

By providing probability plots the package takes the analysis one step further. Normal deviations from the age-corrected reference field are not constant across the central 30° field, but varies with the test point location generally being larger further away from the point of fixation, particularly in the most peripheral ring of test points superiorly. Furthermore the distribution of these normal deviations are considerably non-Gaussian, with location-dependent negative skewness and positive kurtosis [7]. This makes it quite difficult to intuitively estimate the significance of measured depressions of sensitivity The normal data base contains information on normal variability and makes it possible to transform threshold deviations in dB to significance levels. The pointwise greyscaled significancies form probability maps. Such maps are clinically quite useful, not seldom remarkably so. Depressions of the measured sensitivities are of course very common in the superior midperiphery also in normal individuals Experienced users of automatic perimeters know this and disregard depressions if they occur only in this area. The analysis package with its normal data base has the same knowledge. Thus depressions occuring in areas which often show depressions also in normal subjects are de-emphasized (Fig 6) effectively decreasing the number of false positive field defects. In the paracentral field, on the other hand, normal variability is much smaller and quite moderate depressions can reach high levels of significance. It is therefore not uncommon to find paracentral areas or points which are significantly depressed in the probability plots while the same areas in the conventional greyscale/numeric threshold printouts look non-conspicuous (Fig. 7). In this way the probability plots often pinpoint perimetric problem areas paracentrally, at an early stage of damage where traditional field charts, and also numerical comparisons with age-corrected normal field data, fail to elicit suspicion. Over time such problem areas often develop into clear-cut field defects, visible also in the conventional printouts (Figs 2 and 7).

The reason that the probability maps funtion in the described way, highlighting paracentral significant changes even if they are fairly shallow while disregarding

164

CENTRAL 30 - 2 THRESHOLD TEST

NAME   BIRTHDATE   12-06-08 DATE   09-09-85
STIMULUS III, WHITE, BACKGND 31.5 ASB BLIND SPOT CHECK SIZE III   FIXATION TARGET CENTRAL   ID u81208458   TIME 12:26:52 PM
STRATEGY FULL THRESHOLD   RX USED   OS   D?   LEG   PUPIL DIAMETER 3 MM VA

LEFT
AGE   77
QUESTIONS ASKED 529
FIXATION LOSSES 0/50
FALSE POS ERRORS 1 17
FALSE NEG ERRORS 3 15
TEST TIME 00:16:33
FOVEA: 28 DB

TOTAL
DEVIATION

PATTERN
DEVIATION

PROBABILITY SYMBOLS
:: P < 5%
:: P < 2%
:: P < 1%
■ P < 0.5%

SIGNIFICANCE
MD - 9.01 DB P < 0 5%
PSD   2 43 DB
SF   1 61 DB
CPSD 1 58 DB

Figure 5 The greyscale threshold representation of this field from an eye with cataract, visual acuity of 0 2 but no other ocular pathology is dark The general depression is clear from the total deviation plots and a highly significant MD The lack of localized field loss is clear from the pattern deviation maps, where the probability plot shows no significant deviations from normality, and from the normal PSD and CPSD values

similar depressions of the measured threshold in more peripheral less reliable areas, is the normal data base of the package and the fact that empirical distributions were used to determine levels of significance If probability plots were based on (incorrect) assumptions of constant variability and Gaussian distributions of normal measured thresholds across the central 30° field [12] they would offer no extra help as compared with the numerical deviation maps. In fact they would even be rather misleading.

The probability maps are excellent examples of computer-assisted analyses. They help the human interpreter by presenting the data in a new way highlighting statistical significance, but they do *not* prevent the human input, e.g. judging whether disturbed points are grouped in a way forming recognizable or perhaps even diagnostic patterns.

The visual field indices summarize important aspects of the measured field in a few numbers achieving considerable reduction of the amount of data. This is practical, especially in follow-up where the amount of field data easily becomes

overwhelming. The development of these field indices over time is displayed in graphs. MD will become a larger negative number when sensitivity decreases, whether this reduction is due to progressing localized scotomata, e.g in glaucoma, or to an increased general reduction of sensitivity, e.g. due to a progressive cataract. PSD and CPSD on the other hand are not influenced by general changes of sensitivity but by an increased roughness of the visual field due to localized field loss. When field defects develop both PSD and CPSD will increase. However, when field defects progress in an already seriously disturbed field, roughness might in fact diminish and PSD and CPSD start decreasing again. The field indices of the current package, being quite obvious and simple statistical concepts (means and standard deviations of the deviations of measured sensitivities from the age-corrected normal reference field), are similar to the indices described by Flammer [4]. In the current package, however, they are weighted according to normal variability. Theoretically this increases the capability of the indices to separate between normal and abnormal fields.

At least for single field analysis visual field indices have obvious shortcomings. Normal variation is quite large and the limits of normality of the indices therefore not particularly narrow. The indices do not take into account any spatial correlation of points with low sensitivity. Quite clear early visual field defects may be

166

TOTAL
DEVIATION

PATTERN
DEVIATION

PROBABILITY SYMBOLS

:: P < 5%

▩ P < 2%

▨ P < 1%

■ P < 0.5%

TOTAL
DEVIATION

PATTERN
DEVIATION

PROBABILITY SYMBOLS

:: P < 5%

▩ P < 2%

▨ P < 1%

■ P < 0.5%
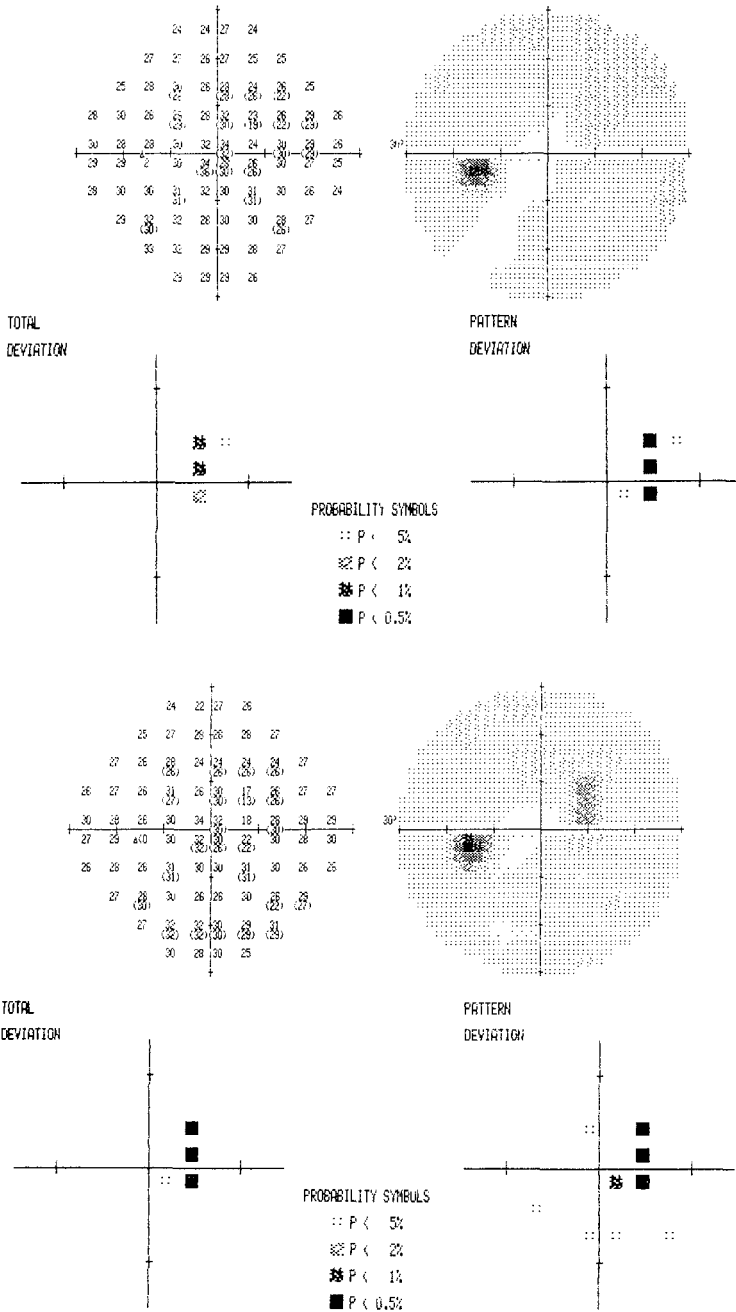
Figure 7 Two consecutive visual field charts from an eye with a clear-cut paracentral scotoma The first test (top), when taken, was interpreted as normal The greyscale representation is rather non-conspicuous despite the fact that some thresholds are quite low A later Statpac analysis show that some points fall outside the normal distributions This is confirmed a few months later (bottom) when the paracentral defect is clearly visible, both in the probability plots and in the threshold maps

seen both in conventional threshold printouts and in probability maps while indices still fall within normal limits. Deviation maps, and particularly probability maps, provide more information and should be preferred in borderline cases, especially when single or few charts are interpreted. The main value of the visual field indices are in follow-up where a reduction of data may be necessary.

On the Change Analysis page (Fig. 3) the four indices are plotted over time providing information on the visual field with a very high degree of data reduction With increasing pathology MD will become more negative and the series of data points will have a negative slope. Since MD is calculated using continuously age-corrected threshold values this series of points would not be expected to drop with age in tests from healthy eyes. The automatic linear regression analysis helps the user determine whether the MD of the measured fields changes in a statistically significant way. Unfortunately MD is subject to disturbing influence from irrelevant factors causing a general depression of the visual field, e.g. media opacities or drug-induced miosis. Localized field loss has higher diagnostic value.

The development and (early) progression of localized visual field loss can be followed in the graphs of PSD and CPSD over time In seriously disturbed fields judgments on progression should not be based on PSD and CPSD (cf above). A progressively deteriorating visual field will sooner or later come to a stage where PSD and CPSD diminish despite further loss of visual function.

The box plot representation is unfamiliar at first and may be hard to use initially. With experience one quickly learns to appreciate its ability to summarize the visual field development in one single chart The learning process may be shortened by regarding each box plot as a reduced histogram of measured threshold deviations.

Computer-assisted visual field interpretation is still in the beginning of its development. Further development is taking place in our laboratory and those of other groups. New versions of this statistical package and new methods from other centres may be expected, e.g. analyses which use the spatial correlation of depressed test points in a more efficient way

Acknowledgement

References

1   Bebie H: Computerized techniques of visual field analysis In: Drance SM, Anderson D (eds) Automatic perimetry in glaucoma A practical guide, p 148 Grune & Stratton, Orlando, 1985

2 Drance SM, Berry V, Hughes A: Studies on the effects of age on the central and peripheral isopters of the visual field in normal subjects Am J Ophthalmol 63: 1667–1672 (1967)

3 Egge K: The visual field in normal subjects Acta Ophthalmol Suppl 169 (1984)

4 Flammer J, Drance SM, Augustiny L, Funkhouser A: Quantification of glaucomatous visual field defects with automated perimetry Invest Ophthalmol Vis Sci 26: 176–181 (1985)

5 Heijl A: A simple routine for demonstrating increased threshold scatter by comparing stored computer fields Docum Ophthal Proc Series 42: 35–38 (1985)

6 Heijl A: The Humphrey Field Analyzer; concepts and clinical results Docum Ophthal Proc Series 43: 55–64 (1985)

7 Heijl A, Lindgren G, Olsson J: Variability of computerized threshold measurements across the central visual field in a normal population Docum Ophthal Proc Series 00: 000–000 (1987) (this volume)

8 Heijl A, Lindgren G, Olsson J: Reliability parameters in computerized perimetry Docum Ophthal Proc Series 00: 000–000 (1987) (this volume)

9 Heijl A, Lindgren G, Olsson J: The effect of perimetric experience on the results of computerized threshold perimetry (in manuscript)

10 Holmin C, Krakau CET: Regression analysis of the central visual field in chronic glaucoma cases; a follow-up study using automatic perimetry Acta Ophthalmol 60: 267–274 (1982)

11 Jenni A, Fankhauser F, Bebie H: New programs for the Octopus automatic perimeter Klin Mbl Augenheilk 176: 536–544 (1980)

12 Schwartz B, Nagin P: Probability maps for evaluating automated visual fields Docum Ophthal Proc Series 42: 39–48 (1985)

13 Zehnder-Albrecht S: Zur Standardisierung der Perimetrie Ophthalmologica 120: 255–270 (1950)

Authors' addresses:
Anders Heijl,
Department of Ophthalmology,
Malmö General Hospital,
S-214 01 Malmö, Sweden

Georg Lindgren, Jonny Olsson,
Department of Mathematical Statistics,
Box 118,
S-221 00 Lund, Sweden

III.3 Artificial intelligence in computerized perimetry

C.E.T. KRAKAU
Malmö, Sweden

Abstract

The computer controlling the visual field testing is also capable of interpreting the test results. An expert system is constructed which analyses the fields for defects, recognizes their pattern and examines the development if a sequence of VF is available Conclusions are drawn and advice given for further investigations. The data base contains so far only glaucoma cases but inclusion of neuro cases are planned

AI is a fuzzily delimited discipline, very much 'en vogue' among datologists. There are numerous definitions of AI, nearly as many as there are workers in that field One of the better claims is that AI is the discipline that aims to understand the nature of human intelligence through the construction of computer programmes that imitate intelligent behaviour Our aspiration is more modest, but that part of our project which aims at an analysis of the rules and formulation of the algorithms we should use to interpret the outcome of a visual field testing bears some relationship to the high ideals of the definition above AI includes two topics with relevance to computerized perimetry, viz. expert systems and – to some extent – pattern recognition.

An expert system incorporates expert knowledge in specific narrow fields and aims at facilitating complicated decisions [3] The programme CASNET is an example of an expert system used in ophthalmology [6]. It was devised for the purpose of assisting the diagnostic of glaucoma in its various forms and to suggest a 'lege artis' treatment. The application of this programme may have advantages in applying its rules of diagnostic and therapy with great rigour It is probably also useful to doctors not so expertly informed. The system, however, involves a drawback inherent in the use of fixed expert rules: it might happen that the expert is mistaken at some points and then the system goes on, unsensitive to new paradigms In other word, we need a feedback system which makes it possible to

make use of the outcome of our treatment, so as to rectify, if necessary, the rules according to experience.

An expert system is being constructed in order to take care of the evaluation of perimetry results to the greatest possible extent.

A computer programme might answer the following questions at least as well as a human interpreter:

a) Is the VF recording reliable or not?
b) Is the visual field normal or not?
   If pathological, are there defect areas and/or a general reduction of sensitivity?
c) Does the localization of defects correspond to a glaucomatous atrophy or/and a neurological disease, or to something else?
d) If a series of VF recording is available, is there a progression of defects or general level?

a The reliability of a test is estimated by means of the blind spot control. A reliable patient who keeps his fixation should not detect light stimuli falling in the blind spot area. A programme, optionally applied, for a systematic plotting of the blind spot area finds a central blind area initially and then continues to use this as fixation check. Somewhat arbitrarily, a fraction of stimuli of more than 30 per cent seen of the blind spot trials makes the denoted testing unreliable. In a group of about 1500 people in a population survey not accustomed to the test method, about 4 per cent perceived the blind spot more often than in 30 per cent of the trials and were denoted unreliable [1]. At a second testing, preceded by forceful instructions on the importance of constant fixation, reliable tests were produced (except in a few cases that refused taking part in the repeated test).

b. The sum of threshold values (the performance value, P) is a simple and often informative measure, but it does not discriminate between localized defects and a generally reduced sensitivity [4].

The conditions for detecting localized defects was guided by the experiences made in a study of a 'normal' population of about 3000 eyes. A supra-threshold programme called 'screening' was used [1]. At the first test session about 10 per cent of the cases showed at least one defect point. At a second screening test the defects were confirmed in 2.5 per cent of the eyes. 16 false positive cases were also detected, all of which could be explained by simple and natural causes.

In this study rigorous rules for defect detection were applied with satisfying results With similar rules introduced in a computer programme the evaluation of defects might be completely entrusted to the computer. The programme designed for the analysis of fields obtained at threshold testing runs through the following sequence of orders:

1. Print number of defect points in 5, 10 and 15 degree circle. A defect point is defined by a sensitivity ≥ 2 steps lower than the highest or next highest level of the circle.
2. Print the number of 'clusters' (≥ 2 defect points adjacent) and the number of defect points in the clusters.

THR   18 December 1979   THR   18 December 1980

Q = 10   Q = 10

P = 611   P = 590

```
                -1                                                        0
      0    -1      -20                                        -20  -20       -300
                -1      -1                                 -20          -300
 -1        -1    0 -20       -1      -1        -1     -1         0 -6000          -300      -20
                0      -20                                -1            -6000
       -20        0          -1      0              -20  -1                        -1   -300
  0         0      0      0     1         0   -1   -1   -1      0     0   1     0       -1         -20
       -20            0     0   1                        -20              -1            -20
          0        1   1       1     1                        0      1            -1   -20
     -10000      0      0           1       2      0              0      0        1      2      -20
          0        1   1   1                           -1                  1
  0         0      1   1    1       0       1     0    0  -10000    0   1   1   1    1     2    1      0
       -1        -1           1     1                        -1    -1
  0        -1       -1     0   0    1       0      0        0     -1      0   0   1    0         0
                                                                0       0   1
       0      -1        0   0   -1                             0         0          0
          0      -1         0                                        -1
```

E A , born 1911, Left eye

Figure 1 Defect point analysis

1			5	10	15	circle	2		5	10	15
	No of def points		0	2	2				0	3	9
				2 clusters						3 clusters	

1 + 2   4 common points, 2 overlappings, 3 clusters
               Verified defects Likely type: glaucoma

If previous fields are available:

3 Compare with other field: steps 1 and 2 repeated.

4. Print number of defect points, number of clusters and of overlappings of the
   two fields combined. An overlapping occurs when a cluster from one testing
   has points in common with the second one or if one of the two clusters contains
   points adjacent to the other.

Fig. 1 illustrates the outcome of a search for defect points.

The glaucoma material from Lund was analyzed using this programme. The
number of eyes with relatively small or moderate defects (less than 20 def points)
subjected to perimetry more than once was 175. At the second testing of this
group the number of eyes with defects was 169. The number of eyes without
defect points in the second test was 6. Common points and overlappings in 147.
No common points in 44. No overlappings (i.e. no confirmed defects) in 28.

The proportion of confirmed defects was higher in this group than in the survey
material. This is not surprising since the glaucoma group consists of patients well
acquainted with the testing programme.

c. The characteristic location of the defect points is important heuristic knowl-
edge. In the population survey of Dalby 75 visual field defects were found (apart
from the 16 false positives), of which nearly one third were expected. They were
mostly caused by peripapillar atrophy in myopics. The perimetry finding was an
enlarged blind spot.
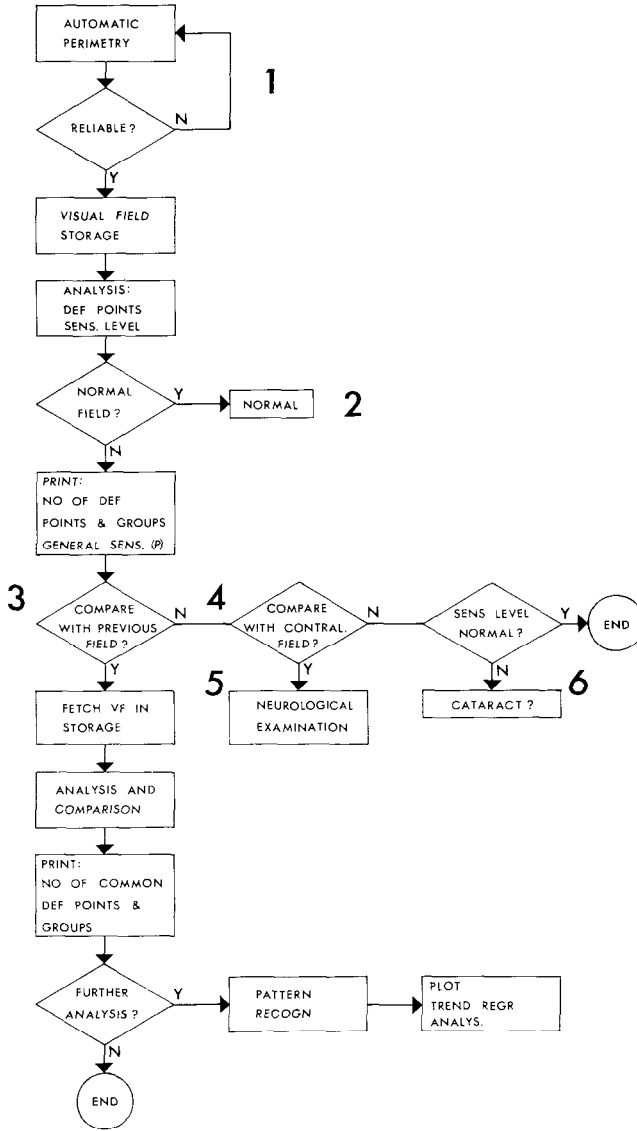
Figure 2 Flow diagram Numbers refer to the *conclusion-advice* table

Likewise more or less characteristic localizations had a few hemianopias and the glaucoma cases In all we conclude that in two thirds of the cases the localization of the defect gave a hint to its cause The rest of the defects and most of those mentioned had changes detectable at the ophthalmoscopic examination. No doubt the detection was facilitated by the knowledge of the field defects.

In the early stages of glaucoma the pattern of defects characteristically starts in

the outer circle (15 degr.) – as far as the central field is concerned [2]. In the material from Lund few defect points were found in the inner circles at the beginning, but as the defect grows these circles also become involved. When 10 defect points or less are detected only 5 per cent of them are found in the inner circles. (By the way, the pattern showed no differences between cases with a high IOP (>25 mm Hg) and those with a low IOP ($\leqslant 21$ mm Hg).)

Consequently, a small defect limited to the inner circles is not typical of glaucoma. A more differentiated analysis of pattern recognition type was attempted with the aim of correlating the visual field pattern with the interpretation of morphological disc changes [5]. The salient features of the field, such as localization and depth of defects, are expressed in a condensed form by a small number of parameters.

The efficiency of the system is assessed by making it carry out a comparison between glaucomatous disc changes and the visual field analysis. 'Saucerization' was associated with a general reduction of sensitivity, whereas 'notch' meant a characteristic pattern with local sensitivity reduction.

Whenever more than one disorder coincide, the analysis becomes complicated. A case of glaucoma may for instance be the victim also of some neurological disorder with field defects. An *a priori* knowledge of the probable location in field defects of various causes may improve the chance of solving the mixture Comparison with the outcome of the contralateral testing eye may be of use.

d. Provided the patient has been followed for a considerable time with field testing, using the same technique every time, an estimate based on the calculation of the linear regression coefficients may be useful in discriminating stationary from non-stationary processes At least five performance values have been found necessary to motivate this calculation. The coefficient is tested for significance against zero by means of a t-test.

Synthesis and outcome. After the initial analysis for defect points, the programme should be able to draw conclusions and give advice. The flow diagram (Fig. 2) shows how the analysis proceeds.

Conclusion	Advice
1. Unreliable VF test	Repeat test, instruct patient
2. Reliable VF, no defect normal sensitivity	On special indications· provocation, inspect earlier fields
3. Reliable VF, with defect points (cf. example)	Compare with previous fields Plot P-values/time Plot quadrant profiles Trend analysis
4. Defect location – not typical for glaucoma	Compare with contralateral VF Ophthalmoscopy, pattern recognition Neurological examination

5. Large blind spot	Myopia? Ophthalmoscopy
	Neurological examination
6. Low sensitivity	Cataract? Provocation test
7. Dispersed defect points	Repeat test

Feed back. Many of the decisions made as to both analysis and advice are based on tentative conditional probabilities. It is a great advantage if the system is not static but permits to educate itself by experience. This is achieved by introducing a verified diagnosis when this is available. This principle was applied with promising results in the pattern analysis of visual field defects [5] In this way the system became selfeducating since it starts from complete ignorance and becomes an expert system by analysing and memorizing a great number of fields.

The present material comprises only glaucoma cases and a diagnosis is therefore not interesting but according to plans also neuro-ophthalmological cases will be introduced in the data base.

Acknowledgement

References

1 Bengtsson B, Krakau CET: Automatic perimetry in a population survey Acta Ophthalmol (Copenh) 57: 929–937 (1979)
2 Heijl A, Lundqvist C: The frequency distribution of earliest glaucomatous visual field defects documented by automatic perimetry Acta Ophthalmol (Copenh) 62: 658–664 (1984)
3 Krakau CET: A feasible development of computerized perimetry Acta Ophthalmol (Copenh) 59: 485–494 (1981)
4 Krakau CET: Visual field decay in chronic glaucoma Glaucoma Update II: 123–128 (1983)
5 Krakau CET, Holmin C: Computerized analysis of visual fields Doc Ophthalmol Proc Ser 43: 35–40 (1985)
6 Weiss SM, Kulikowski CA, Amaral S, Safir A: A model-based method for computer-aided medical decision-making Artificial Intelligence, 11, North-Holland Publishing Co , 1978

Author's address:
Prof C E T Krakau,
Department of Experimental Ophthalmology,
S-214 01 Malmö, Sweden

III.4 Trend analyses of automated visual fields

D.-C. WU, B. SCHWARTZ and PAUL NAGIN
Boston, U.S.A

Abstract

The accumulation of data from automated visual fields presents a problem for the clinician in determining whether there is a significant change in visual fields with time. We have developed a software package with appropriate graphic displays for determining the trends of mean visual field thresholds with time

We have created and actively maintained a database of Octopus 31 program fields. In addition to the threshold measurements for program 31 data, several other variables are entered, including visual acuity for near, pupil size, RMS error, and diagnostic code. Whenever five or more visual fields are available, our software performs trend analyses
1. on the mean threshold values of visual fields versus time,
2. on each of the 73 test locations versus time, and
3. on the mean threshold values of seven selected regions in the visual field versus time.

This approach obviates the problems of evaluating the effect of short and long term fluctuations The trends are analyzed statistically and provide an easily interpretable presentation for clinical diagnosis and management of glaucoma patients.

The usefulness of this approach is shown for several clinical situations: first, for detection of significant trends in the visual field that could not be determined by visual inspection of grey scales or comparison of difference modes; second, for following ocular hypertensive and glaucoma patients to detect the earliest loss of visual field, and third, for determining the effect of a change in treatment on the trend of the visual field

Introduction

Automated perimetry [1] produces quantitative threshold measurements of visual

fields. However, its merits are hampered by the vast amount of output of data. As visual field data are accumulated on patients with glaucoma, the clinician is overwhelmed by the number of grey scales and difference modes to evaluate. Furthermore, the evaluation of a significant change of a visual field with time is difficult due to variability of thresholds with each examination and the biases of the clinical observer In chronic diseases such as glaucoma, quantitative methods are needed to determine statistically significant trends of disease with time.

We have created and actively maintain a data base of program 31 (P31) data generated from the Octopus 2000R (Interzeag. Schlieren, Switzerland). A software package was written to perform statistical analyses, to study the trend of visual fields with time, and to create data files to be used in other analyses which are not covered by our software The purpose of this paper is to present our initial experience with this system, which is being routinely used on an every day clinical basis.

Methods

Hardware

The computer system that we use for transmission and displaying the visual field data has been described in detail elsewhere [7], [8]. Briefly, it consists of an Octopus 2000R automated perimeter with peripherals such as a floppy disk drive, terminals and a printer. Two RS232 interfaces and two modems are used in transmitting and receiving the data to a host VAX 11/780 computer (Digital Equipment Corp., Maynard, MA). A terminal connected to the VAX 11/780 computer is used in the outpatient facility to provide easy and fast access to the results, which can be displayed on the screen or obtained as a hard copy.

Transmission/receiver software

In the Octopus 2000R automated perimeter, a transmission diskette supplied by the Interzeag Co. is put into the floppy disk drive to transmit all data of the visual fields. We wrote a program to receive the transmitted data to the host VAX 11/780 computer. All of our patients undergo initial testing with the Octopus perimeter with programs 7 and 33 to obtain experience with the visual field examination. We presently use only P31 data and convert the data to a suitable format for the data base. The ten duplicate measurements for determination of the RMS error in program P31 are averaged to provide one data point. The transmitted data and other variables are edited regularly to ensure that the patient's name, code of diagnosis, visual acuity for near, pupil size and RMS error are correct before these entries are put into the data base.

The data base

The data base is a direct access file built into the VAX environment as an indexed file which can search and retrieve patient's information and data faster than a sequential file. The main menu of our software package allows the selection of a particular patient or a group of patients with a given number of visual fields.

Statistical software

If we wish to study the visual fields of a particular patient, the program asks for the patient's name and the eye (right/left). Next, it displays the dates of examinations and all other information stored in the database. Since a file which contains all P31 data has been created, the data are ready for the statistical analyses available in our software package or in other statistical packages (e.g. SAS, BMDP, etc).

For patients who have 5 or more visual fields, the software performs trend analyses on the mean threshold values of visual fields versus time; on each of the 73 test locations versus time; and on the mean threshold values of 7 selected regions in visual field versus time. For patients with fewer than 5 field examinations, a paired-t test can be performed. The program can also provide scatterplots of 3 indices (mean defect, short term fluctuation, corrected loss variance) versus time [2].

Results

Trend analyses of visual fields following filtration surgery

In our glaucoma service, we routinely use the trend analyses for all patients with at least 5 visual fields. We first generate a report on all visual fields for a particular eye listing date of visual field, diagnosis code, corrected visual acuity for near (Jaeger type -J) for the Octopus perimeter testing distance, pupil diameter, RMS error, number of false positives and negatives and stimulus size (Table 1). This is the output on a 47-year-old female (B D.) with open-angle glaucoma who is being followed after previous filtration surgery for her glaucoma in 1981. Her initial visual field (P31) is shown in Figure 1. There was no significant variation in her visual acuity for near during the course of visual field testing with a range of visual acuities from J_1 to J_3 (average, visual acuity – $J_{1.6}$), with no significant trend in pupil size (Table 1).

Figure 2 shows the scatterplot of the mean threshold values of the 73 tested points versus time from January 18, 1983 to August 5, 1985. It also displays the
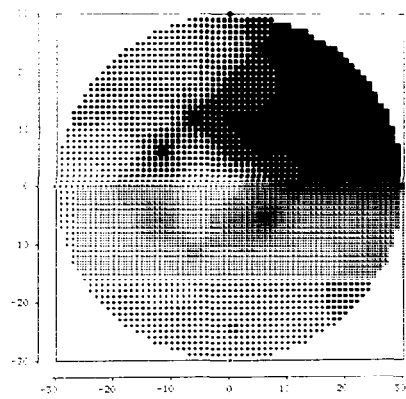
Figure 1 Grey scale for program 31 of initial visual field for left eye (patient B D)

following. at the top of the graph the non-parametric Spearman correlation value and the corresponding p value, the parametric Pearson correlation value and the corresponding p value, and the slope of the regression line. At the bottom of the graph is a listing of dates of visual field examinations, number of months for each visual field in relation to baseline (zero), mean threshold value for each field and percent difference of mean threshold value of each field in relation to baseline. The percent difference is calculated as (last mean threshold value minus first mean threshold value) × 100/first mean threshold value. The program also has the

Table 1

Name: BD – Eye: OS

No	Exam date	Diag	Vision	Pupil Diam	RMS error	False posi	False nega	Stimu size
1	01/18/83	1401	J2	4 0	3 5	00/16	02/17	3
2	02/16/83	1401	J2	3 0	3 5	00/16	02/16	3
3	07/05/83	1401	J2	3 0	0 5	00/15	00/15	3
4	09/27/83	1401	J1	2 0	3 8	00/16	01/16	3
5	01/09/84	1401	J1	4 0	2 2	00/15	00/16	3
6	04/18/84	1401	J1	3 0	1 6	00/14	00/15	3
7	05/30/84	1401	J2	1 0	3 1	00/14	00/15	3
8	09/11/84	1401	J1	2 0	1 5	00/15	01/15	3
9	02/18/85	1401	J1	4 0	1 4	00/15	02/16	3
10	04/30/85	1401	J1–	2 0	1 3	00/14	01/15	3
11	06/11/85	1401	J3–	2 0	1 1	00/14	02/15	3
12	08/05/85	1401	J2–	2 5	2 2	00/16	04/16	3

```
NAME: BD                    EYE: OS

SCATTERPLOT OF MEAN THRESHOLD VALUE VS. TIME, SESSION  1 TO SESSION 12

                                  SPEARMAN R = -0.73, SPEARMAN P =  0.02
                      EYE: OS, SLOPE = -0.11, PEARSON  R = -0.75, PEARSON  P =  0.00


                    I
                  16I
                    I
                    I                    *
                    I
                    I
                  14I*  *
       MEAN         I
     THRESHOLD      I              *
       VALUE        I       *
      (UNIT db)     I                   *
                  12I
                    I                                                  *
                    I
                    I                        *       *      *
                    I                                        *
                  10I                             *
                    ----------------------------------------------------------------
                    I           I            I          I            I
                    0           7           14         21           28
                                    TIME (UNIT MONTH)


    NUMBER  DATE OF EXAM  TIME(UNIT MONTH)  MEAN TH. VALUE  PER CENT DIFF.(%)
       1      01/18/83         0.00            14.18           0.00%
       2      02/16/83         0.93            13.81          -2.61%
       3      07/05/83         5.57            13.01          -8.25%
       4      09/27/83         8.30            15.01           5.85%
       5      11/29/84        11.70            13.43          -5.29%
       6      04/18/84        15.00            12.84          -9.45%
       7      05/30/84        16.40            10.38         -26.80%
       8      09/11/84        19.77            11.00         -22.43%
       9      02/18/85        25.00            11.15         -21.37%
      10      04/30/85        27.40            10.90         -23.13%
      11      06/11/85        28.77            11.10         -21.72%
      12      08/05/85        30.57            12.21         -13.89%

    (c) 1986 TMCA
```
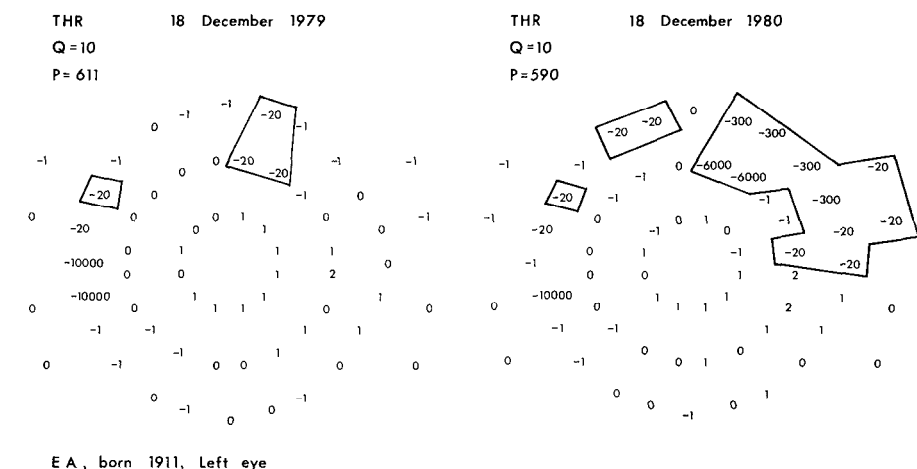
Figure 2 Scatter plot of mean threshold values of whole field of left eye versus time (patient B D)

ability to study the trend for any given period, not necessarily from the first field to the last field.

Similar analyses can be done for each of the 73 tested locations The output is shown as a probability map of the visual field [8] (Figure 3) The analyses are grouped by degree of slope or rate of change of threshold values (large, medium or small), sign of slope (− or +) and the probability values for the Spearman correlations of the trend of each test location with time (≤0.02 and 0 02–0 10) The area of the visual field where significant changes in the slope and its degree occur (eg. −0 02M or −0 02S) can be easily visualized In this instance the temporal area is showing the most change. The nasal area has severe visual field loss and does not change any further (Figure 1)

Figure 4 is a frequency histogram of the 73 slopes obtained from the regression results and provides the proportion of negative to positive slopes, e.g. 63 to 10.

Each of seven selected regions of the visual field can also be analyzed [8]. A similar regression analysis is done for each region as for the whole visual field (Figure 2). Peripheral values for the visual fields are excluded from the regions since these values often show artifactual abnormalities [6] Figures 5a and 5b show the seven regions for the right and left eye respectively, which are routinely presented or displayed for reference with each regional analysis at the top of the plot. A number has been chosen for each region and the number of points analyzed in each region is shown in brackets. The points marked X are the

```
NAME: BD                    EYE: OS

          SLOPE MAP WITH SIGNIFICANT SPEARMAN P VALUE MAP

.02 IS SIGNIFICANT LEVEL FOR ALL SPEARMAN P VALUES <= .02
.10 IS SIGNIFICANT LEVEL FOR ALL SPEARMAN P VALUES BETWEEN .02 AND .10
PLUS(MINUS) SIGN INDICATES A POSITIVE (NEGATIVE) SLOPE
L(LARGE) : ABSOLUTE SLOPE VALUE >= .5
M(MEDIUM): ABSOLUTE SLOPE VALUE IS BETWEEN .25 AND .5
S(SMALL) : ABSOLUTE SLOPE VALUE <= .25
N/A(NOT APPLICABLE) : TH  VALUES ARE ESSENTIALLY THE SAME FOR ALL VISUAL FIELDS


                                      - S

                       -0.10S -0.02M    - S     + S     + S

                -0.02S -0.02S -0.10S    - S     - S     - S     - S

        - S  -0.10S    - S    N/A     N/A     N/A     N/A    N/A    N/A

       -0.02S -0.02S    + S    - L     + S     N/A     N/A    N/A    N/A

-0.02S -0 02S    + S  -0.10M -0 02S -0.10S    + S     + S     - S     - S    N/A

        - S  -0.02S    - M     + S   0.10M   N/A     - M     - M     - S

       -0.10S -0.02S -0.10S    - S  -0.10M -0.10S    - S  -0.10M     - S

            - S  -0.10S    - S  -0.10S    - S     - S     - S

           -0 10S -0.02S    + S  -0.10S    - S

                             -0.10S

(c) 1986 TMCA
```

Figure 3 Probability and slope map of left eye (Patient B D) The points marked N/A are zero values for threshold

peripheral test locations excluded from the analysis Figure 6 shows region 7 for the left eye, which is the inferior nasal area. For each regional analysis below the plot, as for the whole visual field, a similar listing is provided of dates of visual field examinations, mean threshold values and percent differences. However, this information has been deleted in Figure 6 as well as for all subsequent figures in this paper (Figures 7–14).

```
        NAME: BD                    EYE: OS

        HISTOGRAM OF SLOPES(FROM REGRESSION RESULT)
                (ONE * IS ONE COUNT)
        (# OF POS  SLOPES: 10; # OF NEG  SLOPES: 63)


           I *
-0 500I-
           I ***
-0 375I-
           I ****
-0 250I-
           I ************************
-0 125I-
           I *******************************
0 000I-
           I *******
0 125I-
           I **
0 250I-
           I *
0 375I-
           I
0 500I-
           I

        (c) 1986 TMCA
```
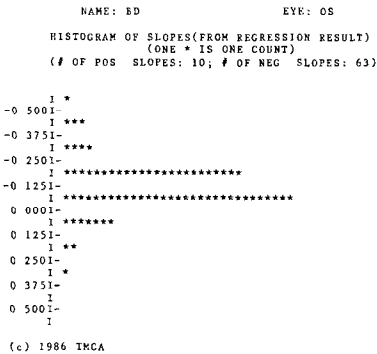
Figure 4 Frequency histogram of 73 slopes of regression lines for visual field of left eye (patient B D)
The points marked N/A in Figure 3 are included in the categorization of negative slopes

EYE: OD

"X" IS THE POINT (LOCATION) TESTED BY THE OCTOPUS PERIMETER
NUMBERS INSIDE THE PARENTHESIS ARE THE NUMBER OF POINTS TESTED
BY THE PERIMETER

```
                        X
              X   X   X   X   X
              -------------------
          _X_I        I          I X
       _X_I___  2 (7)I  1 (9)  I_X__  X
     __I_____I_____I_____I___I_X_
   I___  5 (8) I___4_(4)____I___3 (5)___I X
     I_____I_____I_____I____I X
     X I___I 7 (6)I  6 (9)  I X   X
       X I_____I_____I X
              X   X   X   X   X
                        X
```
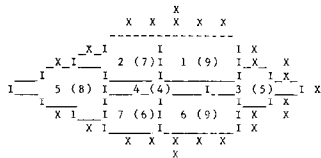
A

(c) 1986 TMCA

EYE: OS

"X" IS THE POINT (LOCATION) TESTED BY THE OCTOPUS PERIMETER
NUMBERS INSIDE THE PARENTHESIS ARE THE NUMBER OF POINTS TESTED
BY THE PERIMETER

```
                        X
              X   X   X   X   X
              -------------------
          X I        I        I_X_
       X  _X_I  1 (9)  I 2 (7)___I_X_
       _X_I___I_____I_____I___I
     X I___3 (5)___I__4_(4)_____I 5 (8)___I
       X I__I        I        I____I
     X   X I  6 (9)  I 7 (6)I___I X
       X I_____I_____I X
              X   X   X   X   X
                        X
```
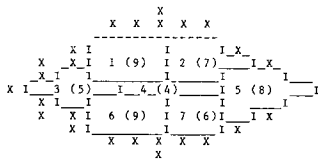
B

(c) 1986 TMCA

Figure 5 Position of regions for each visual field a) right eye b) left eye

NAME: BD   EYE: OS

SCATTERPLOT OF MEAN TH VALUE OF REGION 7 VS. TIME, SESSION 1 TO SESSION 12

SPEARMAN R = -0.80, SPEARMAN P = 0 02
EYE: OS, SLOPE = -0.14, PEARSON R = -0 80, PEARSON P = 0 00

```
           20I
             I
             I*
             I
           18I
             I  *
             I
    MEAN     I
 THRESHOLD 16I          *
   VALUE     I                *
 (UNIT db)   I      *              *              *
             I
           14I
             I                 *         *
             I              *                   *
             I                              *
           12I
             ----------------------------------------------------
             I        I        I        I        I
             0        7       14       21       28
                       TIME (UNIT MONTH)
```
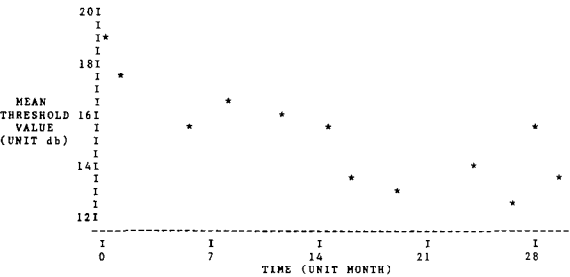
(c) 1986 TMCA

Figure 6 Trend analysis for region 7 – left eye – inferior nasal region (patient B D)
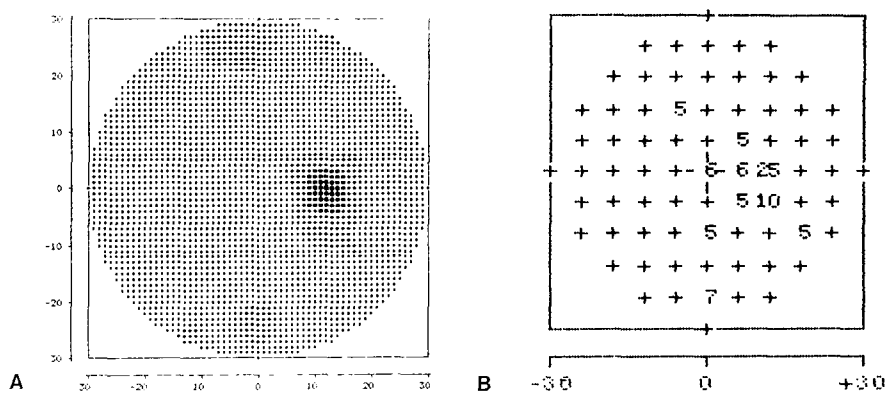
Figure 7 Visual field of right eye of patient K B just prior to starting timolol drops a) grey scale, b) difference mode

Detection of visual field loss not apparent on inspection of visual fields or optic disc

Patient K B is at present a 17-year-old female with juvenile rheumatoid arthritis who had repeated episodes of iritis treated with topical steroid therapy She has secondary open-angle glaucoma of the left eye which had been treated surgically. The right eye demonstrated elevated ocular pressures in the past, but these have decreased to normal values when the topical steroid therapy was discontinued. The patient's ocular pressures for the right eye ranged from 10 to 23 mm Hg. Most of the ocular pressures were in the high teens (mean ± standard deviation (S.D.) (no) – 18 0 ± 3 3 (28)). The optic disc appeared normal and repeated examinations of the visual fields, using program 31, appeared normal, both for the grey scale and for the difference mode. (Figures 7a and b) Her corrected visual acuity for near ranged from J_1 to J_2 with an average of $J_{1.3}$ with no significant trend in pupil size. Trend analysis for the whole visual field (Figure 8) showed a significant decrease in the mean threshold, beginning 11.5 months following the initial visual field for program 31. The maximum decrease from the initial mean threshold value was 13.6%, 26.4 months following the initial visual field (P31). Timolol drops (0 25%) twice a day were started about 30 months after the initial visual field (P31) It appears that the decrease in mean threshold values was halted and perhaps even reversed, following initiation of the therapy.

Detection of a change of visual field in a region of the field, not apparent in the whole field

Patient R B. is a 63-year-old female with open-angle glaucoma who has been followed with medical therapy and had a laser trabeculoplasty 20.9 months after

NAME: KB   EYE: OD

SCATTERPLOT OF MEAN THRESHOLD VALUE VS TIME, SESSION 1 TO SESSION 18

SPEARMAN R = -0 69, SPEARMAN P = 0.02
EYE: OD, SLOPE = -0 11, PEARSON R = -0 83, PEARSON P = 0 00

```
              I
           31 I
              I                 *
              I         *   *
              I*
              I
           29 I                  *
   MEAN        I                        *
THRESHOLD     I
   VALUE      I
 (UNIT db)    I              *       *              *        *
           27 I                *          *
              I                      *    *   *
              I
              I                   *
              I
           25 I
              --------------------------------------------------------
              I            I              I            I            I
              0           10             20           30           40
                             TIME (UNIT MONTH)
```

(c) 1986 TMCA
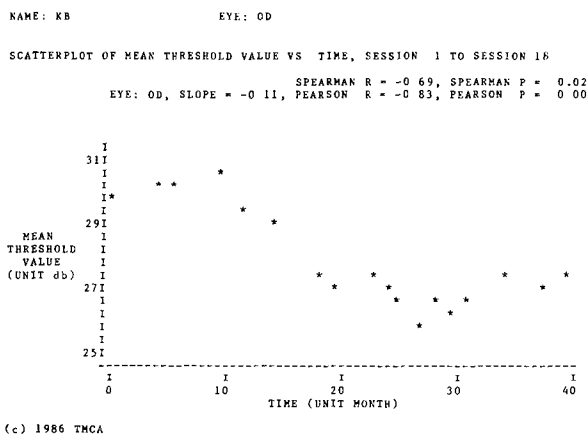
Figure 8 Trend analysis of whole field – right eye (Patient K B)

her initial P31 visual field Her corrected visual acuity for near ranged from J_1 to J_2 with an average of J_{17}, with no significant trend in pupil size. Inspection of the mean threshold value plot with time for the whole visual field shows no significant trend for the right eye (Figure 9). However, region 7, the inferior nasal area, (Figure 10) shows a significant trend that indicates an improvement of the inferior nasal field for a maximum increase of 43.2% of the peak threshold from the initial mean threshold value.

NAME: RB   EYE: OD

SCATTERPLOT OF MEAN THRESHOLD VALUE VS TIME, SESSION 1 TO SESSION 10

SPEARMAN R = 0 02, SPEARMAN P > 0 10
EYE: OD, SLOPE = 0 00, PEARSON R = -0 03, PEARSON P = 0 94

```
              I
           16 I
              I                         *
              I
              I             *
              I                 *                    *
           14 I*      *
   MEAN        I                                          *
THRESHOLD     I
   VALUE      I           *
 (UNIT db)    I       *
           12 I
              I
              I                      *
              I
           10 I
              --------------------------------------------------------
              I            I              I            I            I
              0            9             18           27           36
                             TIME (UNIT MONTH)
```

(c) 1986 TMCA
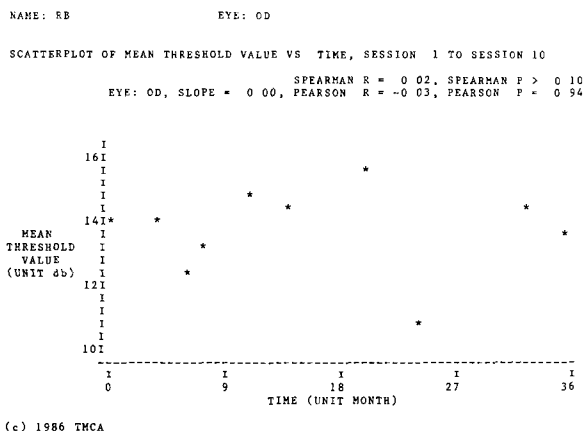
Figure 9 Trend analysis for whole visual field – right eye (patient R B)

```
NAME: R B                     EYE: OD

SCATTERPLOT OF MEAN TH. VALUE OF REGION 7 VS  TIME, SESSION  1 TO SESSION 10

                               SPEARMAN R =  0.80, SPEARMAN P =  0.02
                EYE: OD, SLOPE =  0 17, PEARSON  R =  0.79, PEARSON  P =  0.01


            24 I
               I
               I
               I                                               *
               I
            22 I
               I
               I                          *
               I                                                      *
    MEAN       I
THRESHOLD  20 I                     *
    VALUE      I                                      *
  (UNIT db)    I
               I
            18 I
               I          * *
               I
               I *
               I *    *
            16 I
               ---------------------------------------------------------
               I          I          I          I          I
               0          9          18         27         36
                              TIME (UNIT MONTH)

    (c) 1986 TMCA
```
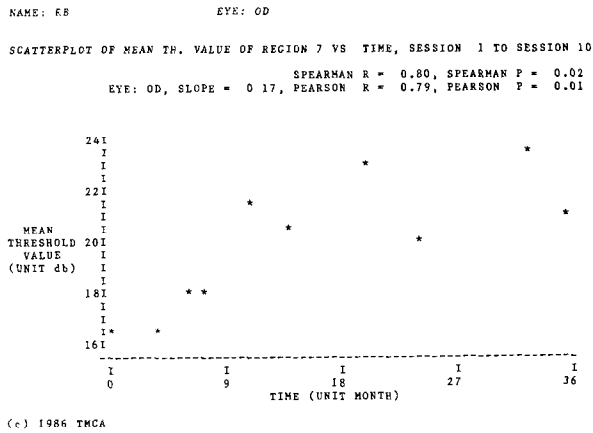
Figure 10 Trend analysis for region 7 – inferior nasal area – right eye showing improvement in visual field not apparent in trend analysis for whole visual field (Figure 9) (patient R B)

Reversibility of trend in the visual field following surgery with subsequent decrease in visual field threshold

Patient J.D is a 63-year-old male with a diagnosis of open-angle glaucoma. He had filtering surgery (trabeculectomy) of his left eye for progressive visual field loss 6.4 months after his initial P31 visual field The corrected visual acuity for near ranged from J_1 to J_2 with an average of $J_{1\ 7}$ with no significant trend in pupil size. Following surgery there was reversibility of the visual field as indicated by the increase of threshold values (Figure 11). Until the time of surgery, there was a 20.8% decrease in mean threshold values from baseline. However, following

```
    NAME: J D                     EYE: OS

SCATTERPLOT OF MEAN THRESHOLD VALUE VS  TIME, SESSION  1 TO SESSION 17

                               SPEARMAN R =  0 03, SPEARMAN P >  0 10
                EYE: OS, SLOPE =  0.00, PEARSON  R =  0 00, PEARSON  P =  0 99


            21 I
               I
               I                       *    *
               I                   *    *        *   *
            19 I                 *
               I
               I
    MEAN       I
THRESHOLD  17 I*                                                        *
    VALUE      I*                                *    *
  (UNIT db)    I                                             *
               I    *    *                        *
            15 I                                                  *    *
               I
               I
               I
            13 I           *
               -----------------------------------------------------
               I          I          I          I          I
               0          9          18         27         36
                              TIME (UNIT MONTH)

    (c) 1986 TMCA
```
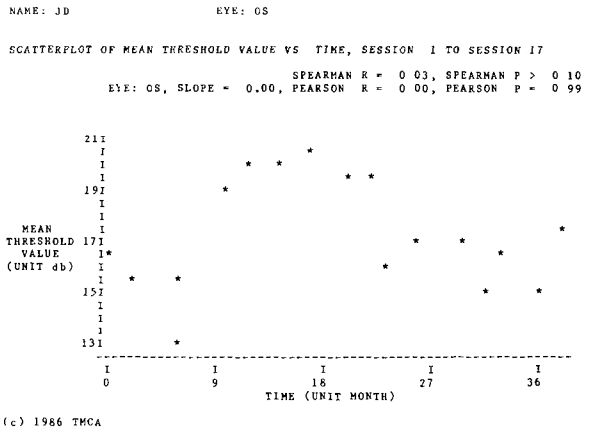
Figure 11 Trend analysis for whole visual field – left eye (patient J D)
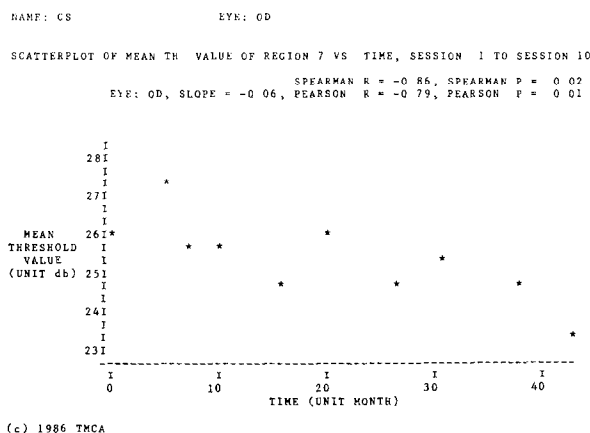
Figure 12 Trend analysis of inferior nasal region of visual field – right eye (Patient C S)

surgery, there was an increase of 47.7% in mean threshold values from the time just prior to surgery. Subsequently, there has been a steady decrease of 33.9% in mean thresholds, so that the mean threshold is close to baseline. This case illustrates how the graphic display of mean threshold values for the whole visual field can be used to follow changes of the visual field, especially for determining trends with treatment.

Detection of trends in visual field thresholds, for presumably adequately controlled ocular hypertension and open-angle glaucoma

C.S. is a 60-year-old male with ocular hypertension in the right eye and secondary open-angle glaucoma in the left eye due to trauma The left eye is being treated medically, including methazolamide (neptazane) 25 mg once to twice a day The range of ocular pressures of the right eye was from 14 to 26 mm Hg (mean ± S.D. (no) – 18.8 ± 2.9 (12)). The corrected visual acuity for near ranged from J_1 to J_2 with an average of J_1. with no significant trend in pupil size The trend analysis of the right eye shows a significant decreasing trend in the visual field in the inferior nasal region (Figure 12) with a decrease of 15.7% of mean threshold values from the peak value or 10.6% from initial mean threshold. Only a trend of borderline significance was detected in the whole visual field.

E.B. is an 80-year-old female with open-angle glaucoma who is being treated medically and had a laster trabeculoplasty 16.3 months following her initial P31 visual field. Her ocular pressures ranged from 12 to 23 mm Hg on treatment (mean ± S.D. (no) – 16.8 ± 2.9 (20)). The corrected visual acuities ranged from J_1 to J_3 with an average of $J_{2.2}$ with no significant trend in pupil size. The trend analyses of the whole visual field for the left eye, which was not significant,

```
NAME: EB              EYE: OS

SCATTERPLOT OF MEAN TH. VALUE OF REGION 7 VS  TIME, SESSION  I TO SESSION 11

                              SPEARMAN R = -0 95, SPEARMAN P =  0 02
                   EYE: OS, SLOPE = -0.20, PEARSON  R = -0.90, PEARSON  P =  0.00


              8 I
                I
                I         *
                I *                      *
              6 I
                I
                I
   MEAN         I
THRESHOLD     4 I
   VALUE        I              *         *
 (UNIT db)      I                            *
                I                              *
              2 I
                I                       *
                I                                  *
                I
              0 I- - - - - - - - - - - - - - - - - - - - - - - - - *- - - - *- -
                I         I         I         I         I
                0         9         18        27        36
                              TIME (UNIT MONTH)

   (c) 1986 TMCA
```
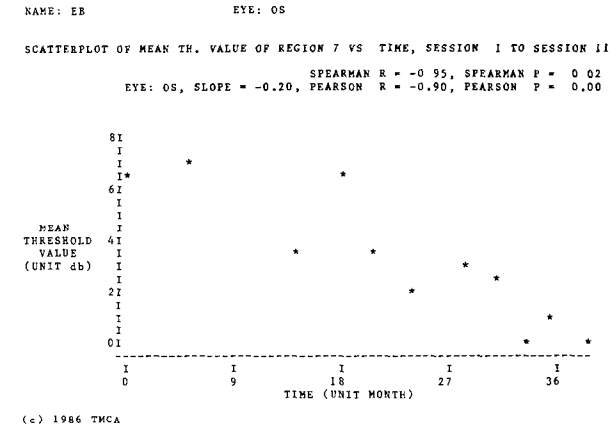
Figure 13 Trend analysis of inferior nasal region visual field – left eye (Patient E B)

showed decreasing thresholds. However, analysis of the inferior nasal region showed a significant decrease in thresholds to a mean value of zero (Figure 13).

C H. is a 79-year-old female with a diagnosis of low tension glaucoma. She is being treated medically and had a laser trabeculoplasty 38.8 months following her initial P31 visual field. Her ocular pressures ranged from 10 to 19 mm Hg (Mean ± S.D. (no) – 14.3 ± 2.7 (29)) The corrected visual acuities for near ranged from J_1 to J_3 with an average of $J_{1.8}$ with no significant trend in pupil size. For the right eye, Figure 14 shows a significant trend of decrease of mean thresholds with time of 42.25% from the initial mean threshold.

From inspection of the visual fields and from the measurement of ocular pressures, it appeared that, clinically, these patients were under adequate control. However, these three examples illustrate that the control was inadequate

```
NAME: CH              EYE: OD

SCATTERPLOT OF MEAN THRESHOLD VALUE VS  TIME, SESSION  1 TO SESSION 14

                              SPEARMAN R = -0 76, SPEARMAN P =  0 02
                   EYE: OD, SLOPE = -0 21, PEARSON  R = -0 77, PEARSON  P =  0 00


                I
             20 I          *
                I
                I *      *                          *
                I            *
                I
             16 I              * *
   MEAN         I
THRESHOLD       I                  *
   VALUE        I
 (UNIT db)      I              *      *    *
             12 I                              *
                I
                I                                  *
                I
                I                              *
              8 I- - - - - - - - - - - - - - - - - - - - - - - - - - - - - - -
                I         I         I         I         I
                0         10        20        30        40
                              TIME (UNIT MONTH)

   (c) 1986 TMCA
```
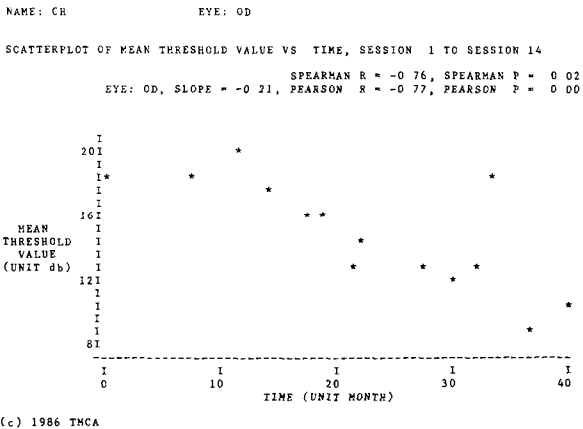
Figure 14 Trend analysis of whole visual field – right eye (patient C H)

since trend analysis indicated significant trends of the mean visual field thresholds with time.

Discussion

The detection of a significant change in the course of disease is an important attribute and has clinical usefulness especially in following patients with chronic disease. With glaucoma, the development of a significant change in the visual field, either deterioration or improvement, is important to the clinician in establishing a diagnosis and determining the adequacy of therapy. The regression analysis of visual field thresholds with time is an approach that can be useful in the management of patients with glaucoma. A continuing decrease in thresholds would suggest a change of therapy. An increase in thresholds would suggest that therapy is adequate and is reversing previous visual field loss. Krakau [4] first documented the use of regression analysis and recently Gloor [3] has also presented data using regression analysis.

A fundamental assumption in the use of regression analysis is that linear regression is the model which can adequately fit the change of the data with time. As shown in the examples above, the changes of the mean visual field thresholds with time appear to be linear. However, for analysis, a conservative approach was taken, and the non-parametric Spearman correlation was calculated, which involves no assumption of normality or Gaussian distribution. This is in contrast to the Pearson correlation coefficient that assumes normal frequency distribution of the data.

Another advantage of the regression analysis is that both long-term and short-term fluctuations [2] are obviated in the interpretation and determination of any trends. Both short-term and long-term fluctuation can provide significant 'noise' so that the trend of visual fields can be easily misinterpreted. The disadvantage of regression analysis is that an adequate number of visual fields is required for a significant determination of a trend. In our studies, we have chosen a minimum of 5 visual fields and believe that an even larger number would be more satisfactory. Krakau [5] has shown the changes in the frequency distribution of the slopes of regression lines for the sum of thresholds of visual fields when they are estimated on small sample sizes and then estimated on larger sample sizes.

We used the mean of the thresholds for the whole visual field, rather than the sum of the values as used by Krakau [4] and Gloor [3] The mean allows for an easier determination of trends, especially on inspection of the scatter plots of mean thresholds versus time. Also, we determined trends in seven regions of the visual field, rather than the whole visual field. As indicated in the examples above, significant changes can occur especially in the nasal areas, which were not found in the whole field.

To definitively use trend analysis, any significant trend in visual field thresholds

in ocular hypertensive and glaucomatous eyes has to be compared with trends in normal eyes over time [4] Such data for normal eyes are not presently available, but are being gathered by us in a separate study.

To adequately utilize trend analysis, it is important that an edited data base be obtained and maintained for the visual field data. The transmission of the visual field data, as well as the analysis by our software programs are fairly routine. However, human errors that occur when entering the data, such as the misspelling of a patient's name, are the most important aspects leading to difficulties in trend analysis. Furthermore, the data base system should be set up so that the accuracy of all transmissions is checked. Subsequent editing should be done to correct errors.

In *conclusion,* we have established a workable system for determining significant trends of visual field thresholds This system requires setting up and maintenance of a data base. Future developments will compare subjective evaluation of changes of the visual field versus this system, will determine the trends of threshold values with age in normal eyes, and will also evaluate which other variables besides the disease process may contribute to a significant trend in the visual field thresholds, such as the root mean square error, pupil size and visual acuity.

References

1 Fankhauser F, Koch P, Roulier A: On automation of perimetry Albrecht v Graefes Arch Klin Ophthalmol 184: 126–150 (1972)
2 Flammer J, Drance SM, Augustiny L, Funkhouser A: Quantification of glaucomatous visual field defects with automated perimetry Invest Ophthalmol Vis Sci 26: 176–181 (1985)
3 Glooi BP, Vokt BA: Long-term fluctuations versus actual field loss in glaucoma patients Dev Ophthal 12: 48–69 (1985)
4 Krakau CET: Visual field decay in chronic glaucoma In: Krieglstein GK, Leydhecker W (eds) Glaucoma update II, pp 123–128 Springer Verlag, New York, 1983
5 Krakau CET: A statistical trap in the evaluation of visual field decay Acta Ophthalmol 63 (Suppl) 173: 19–21 (1985)
6 LeBlanc RP: Abnormal values in computerized perimetry In: Whalen WR, Spaeth GL (eds) Computerized visual fields: what they are – how to use them, pp 165–193 Thorofare, NJ, 1985
7 Nagin P, Schwartz B: Data transmission and management In: Whalen WR, Spaeth GL (eds)

Computerized visual fields: what they are – how to use them, pp 140–144 Slack Thorofare, NJ, 1985

8 Schwartz B, Nagin P: Probability maps for evaluating automated visual fields In: Heijl A, Greve EL (eds) Proceedings of the 6th International Visual Field Symposium Dr W Junk Publishers, Dordrecht, The Netherlands, Doc Ophthalmol Proc 42: 39–48, 1985

Author's address:
Dr Bernard Schwartz,
Dept of Ophthalmology,
New England Medical Center, Inc ,
171 Harrison Avenue,
Boston, MA 02111, U S A

III.5 The quantification of the visual field in computer-assisted threshold perimetry

J.M. WILD, J.M. WOOD, M.K. HUSSEY and S.J. CREWS
Birmingham, United Kingdom

Abstract

Computer simulations were carried out to investigate the suitability of the Monte Carlo technique as a means for deriving the integral of sensitivity as measured over the three-dimensional surface area and thus providing a quantitative expression of the visual field. The simulations were based upon the standard normal data of Octopus programs 21 and 31 and upon age matched data for the central 30° threshold program of the Dicon AP3000. In addition, the sensitivity values at each eccentricity derived by the Octopus were also weighted for the product of retinal ganglion cell receptive field density and spatial summation and a further integration carried out. The indices for various types of field loss are illustrated.

Introduction

A single index to express the extent and depth of the visual field has been sought for many years. The demand for such an index arises in particular from the need to enhance diagnostic capability, to simplify analysis of serial visual field examinations and to describe the functional visual field in disability assessment.

Previous studies have generally derived a quantitative expression by applying various arbitrary transformations of the data which in some cases have also emphasized the different regions of the field. Some authors have adopted this approach merely for statistical handling of the data [2, 8, 14] whilst others have utilized the process to formulate a measure of the field based upon functional performance [18, 1, 7]. The relative crudity of many of these previous attempts stems largely from the complexity of the necessary mathematical computations and from the lack of electronic data processing techniques. Indeed, the representation of kinetic information has been particularly retarded by these limitations although more recently techniques to handle this type of data have been reported [11, 15]. In addition, the various functional assessments have adopted criteria

which have been based in general upon empirical clinical judgement rather than the underlying visual anatomy and physiology. Nevertheless, an assessment of the field based upon neural representation has been proposed [6]. Furthermore, the use of a volume calculation for the three-dimensional representation of kinetic sensitivity has been reported [19] and a similar analysis weighted for retinal ganglion cell receptive field density has been described [12].

The aim of the present study was threefold: to investigate the suitability of a procedure by which the volume of the three-dimensional representation of sensitivity could be determined; to develop and apply a weighting factor for each examined eccentricity based upon the underlying visual physiology and to derive indices for varying types of field loss.

Method

Sensitivity plots were utilised from two computer assisted perimeters the Octopus 201 and the Dicon AP3000. These perimeters were chosen as they provide widely different approaches to visual field investigation e.g. the type and size of the target; and the thresholding strategy.

Computer simulations and analysis using a VAX series 11/750 computer were undertaken on the normative data corresponding to the under 25 age group catagory of Octopus programs 21 and 31 (target size 3) and on normal age matched values obtained for the Dicon 70 point threshold central 30° field (10 asb background luminance; presentation time 400 msec; inter-stimulus duration 1 sec).

The Monte Carlo technique was applied to derive an integration of the sensitivity measure over the three dimensional surface area. This technique is discussed in detail [17] and estimates the integral by a statistical sampling process which has proved very useful in areas such as the evaluation of multiple integrals which do not lend themselves to classical mathematical methods. It has, for example, been recently applied to problems in visibility [3]

Two Monte Carlo methods were utilised, the expected value method and the hit and miss method, to evaluate the integral V where

$$V = r^2 \int_A F(\varnothing, \Omega) \, d\varnothing \, d\Omega$$

over the irregular surface area A on the perimeter bowl, for the bowl radius r and the polar angles $\varnothing$ and Ω defining the respective stimulus points.

The volume V_1 corresponding to the weighted data was determined similarly where

$$V_1 = r^2 \int_A F(\varnothing, \Omega) \, W(\varnothing, \Omega) \, d\varnothing \, d\Omega$$

and $W(\varnothing, \Omega)$ is the appropriate weighting function.

Because of the irregular shape of the surface area of the field on the bowl a pseudo area A_1, which was regular, was defined and points were selected at random within the pseudo area. The required random distribution of points was obtained by defining $F(\varnothing, \Omega)$ as zero within the region R, where $A_1 = A + R$. In the case of the Octopus programs the technique assumed orthogonal axes for the integration as opposed to the actual curvilinear lines. Since the integral is used for comparative purposes, the error arising from this assumption can be discounted One hundred thousand replications were used for each integral This sample size was selected to provide an optimum compromise between minimum error and the length of the pseudo random number cycle generated by the computer.

The point at 15° eccentricity temporally corresponding to the blind spot was assigned a value of zero in the integration of the sensitivity data derived by program 21. In the case of program 31, however, the measured values of the 12° and 18° points temporally lying within the blind spot region were included in the calculation. The index for the Dicon, however, was derived without reference to the blind spot region as the Dicon system does not permit thresholding of the points in this area.

The Octopus sensitivity values at each eccentricity were weighted for the physiological coverage factor defined as the product of retinal ganglion cell receptive field density and ganglion cell receptive field size. Ths was selected as it is thought to represent the number of ganglion cells which sample a given point on the retina and may be a more appropriate index of cortical representation than ganglion cell receptive field density alone [16]. An estimate of receptive field density was obtained using the equations of Drasdo [5] which are corrected for the effects of optical magnification with increasing eccentricity. The receptive field size was estimated from spatial summation data which is considered to be an index of receptive field size [9, 20]. The summation values at each eccentricity for programs 21 and 31 of the Octopus were calculated using Gougnard's equation [10] from the sensitivity data obtained for an age-matched sample of 10 emmetropic obsevers using the six standard Goldmann stimuli [21].

Results and discussion

The volume of the unweighted normal sensitivity values of the under 25 age group for the full-field Octopus program 21 and for the central 30° program 31 are shown in Fig. 1 together with the corresponding values for the Dicon 70 point central 30° program. The units of these integrals are linearly related to the true units which are dB.Rads². The Monte Carlo technique is based upon the principals of random sampling and the evaluation of each integral therefore has an associated precision error. It can usually be assumed that the exact value of the integral will lie within plus or minus three standard deviations of the estimate. The index is not comparable mathematically between instruments possessing different bowl radii and, in

	EXPECTED VALUE METHOD	HIT AND MISS METHOD
Octopus program 21		
unweighted	1248 1 ± 3 23	1236 28 ± 5 4
weighted	106171 0 ± 1930 01	
Octopus program 31		
unweighted	278 79 ± 0 76	279 04 ± 1 02
weighted	83796 5 ± 674 22	
Dicon (10asb) central 30°		
unweighted	446 48 ± 0 19	447 07 ± 0 93
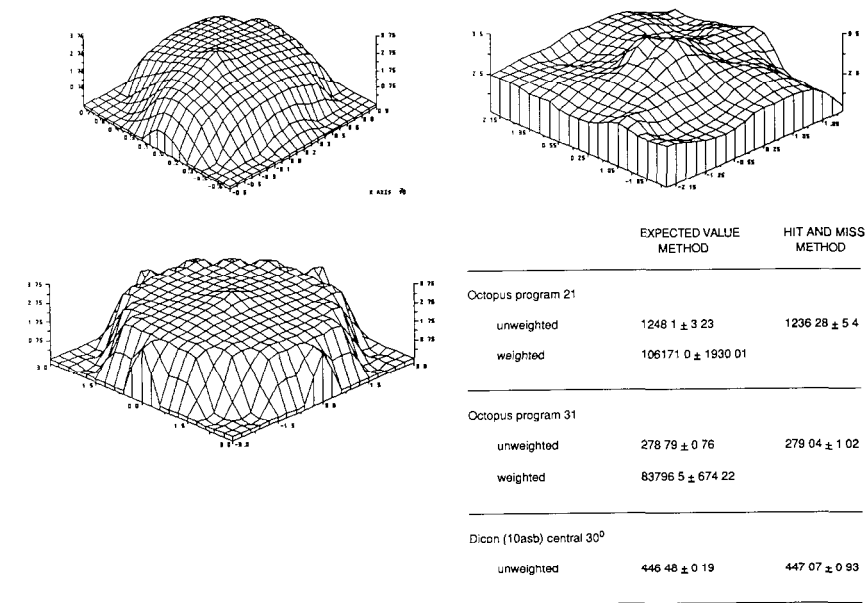
Figure 1 The unweighted and weighted volumes for the right eye under 25 age group normal values of Octopus programs 21 and 31 and the age matched normal unweighted volume for the Dicon (10 asb) central 30° threshold program derived by the Expected Value and Hit and Miss Monte Carlo methods (table) The three dimensional representations of snsitivity are shown for comparison (x and y axes eccentricity [° × 10^{-1}]; z axis sensitivity [dBs × 10^{-1}]: program 21 (top left) program 31 (bottom left) and central 30° program (top right) It should be noted that the volumetric indices are not derived from these graphical representations The blind spot has been omitted from the program 21 plot to avoid artificial enlargement arising from the computer interpolation

addition, is not comparable clinically between instruments with different stimulus and dynamic ranges

The normalised volumetric indices for programs 21 and 31 respectively for five different forms of simulated field loss as a function of perimetric attenuation are shown in Figs 2 and 3. The volumes corresponding to the simulated fields with the Dicon are shown in Fig. 4. The effect on the volume of reduction in sensitivity at a single point is insignificant and is independent of eccentricity; an attenuation of 35 dB at fixation with the Octopus, for example, accounts for approximately 2% of the unweighted volume The technique could, however, be applied on a more local basis with an increased resolution to provide a measure of the reduced sensitivity less identifiable on the global integral. Similarly, the influence of the short term fluctuation inherent in the visual field examination has little effect on the magnitude of the index. The volumetric indices for programs 21 and 31 normalised with respect to the corresponding age-matched values for six patients exhibiting various types of field loss are illustrated in Fig. 5.

The effect of the weighting function (Figs 1, 2, 3 and 5) is to enhance the contribution arising from the central field and reduce that from the peripheral
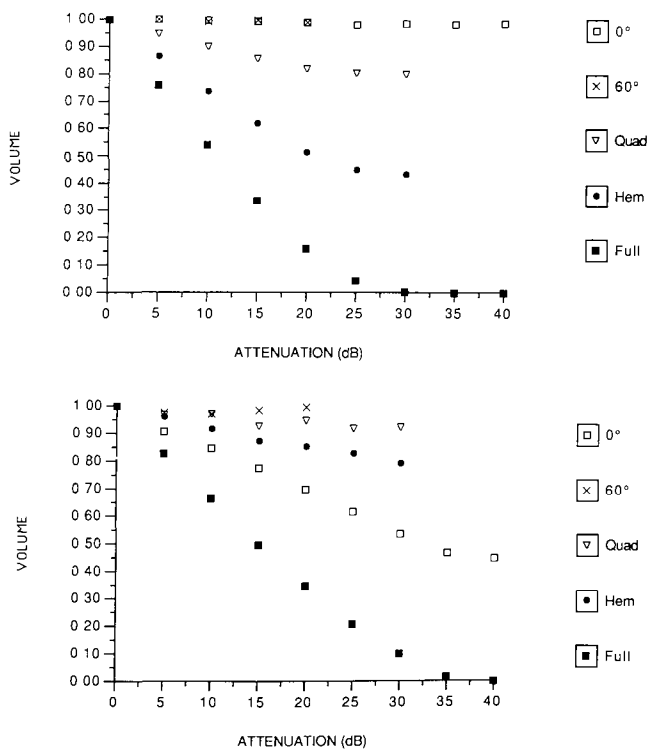
Figure 2 Normalised unweighted (top) and weighted (bottom) volumes against attenuation for Octopus program 21 for various types of simulated field loss The quadrantic defect is arbitrarily defined as an upper temporal loss bounded by, but not including, points on the horizontal and vertical midlines The temporal hemianopia is defined similarly whilst the full field indicates attenuation at all points

field and is in accord with those advocating a parabolic projection of the visual field chart [2, 4]. The units corresponding to the weighted integral are directly related to the true units which are dB. radians.[2] receptive fields per solid degree. coefficient of spatial summation. The error term of the weighted integral is larger than that for the unweighted volume and arises from the inclusion of the extra dimension in the calculation. Intuitive clinical assessment of functional perform-ance would suggest that the weighting underestimates the importance of pe-ripheral vision. The spatial summation values in the weighting function currently represents the best correlate of receptive field size available in human while the cell counts are also the most accurate available. In addition, the weighting function does not allow, by any further weighting, for the increased diagnostic significance of clusters of adjacent points of reduced sensitivity [13]. The derived index could however, be further transformed to reflect the relative topographical functional importance of the visual field while, clearly, the Monte Carlo tech-nique could accommodate any more suitable weighting function which may arise.
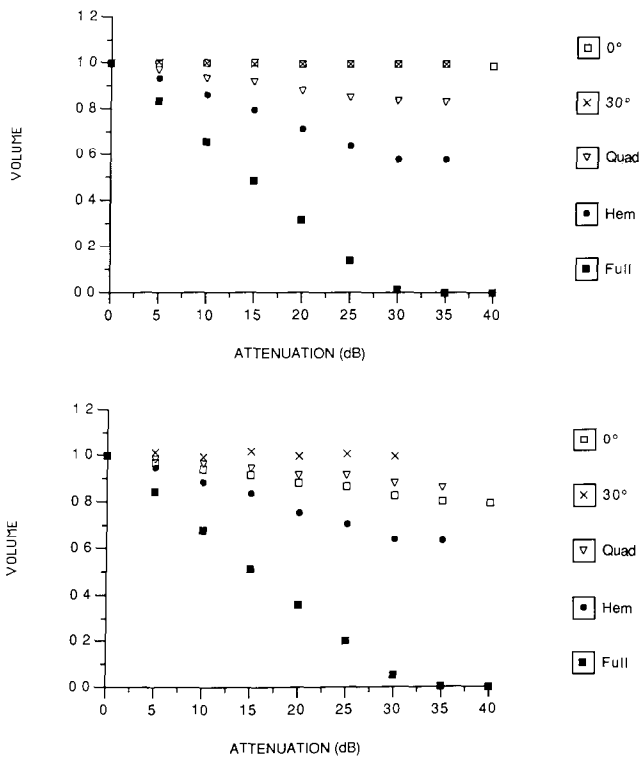
Figure 3 Normalised unweighted (top) and weighted (bottom) volumes against attenuation for Octopus program 31 for various types of simulated field loss The criteria for field loss is that described for program 21 in Fig 2
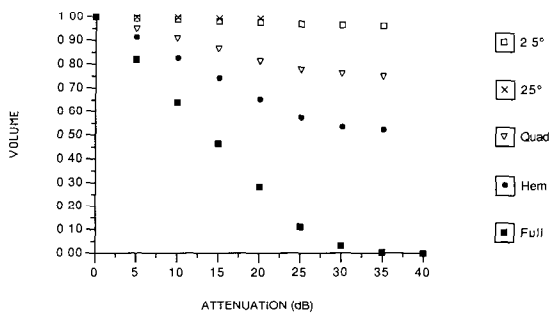
Figure 4 Schematic representation of the influence of intraocular light scatter (b) on the flat sensitivity profile of Octopus program 31 for target size 3 (a) (left) and on the relatively steep profile of the Dicon at 10 asb bowl luminance (a) (right)

Figure 5 Unweighted and weighted volumes normalised with respect to the corresponding normal age matched values for six patients exhibiting various types of field loss with either Octopus program 21 (left) or program 31 (right)
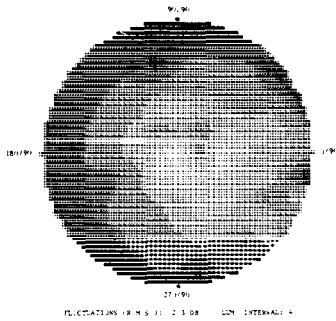
VOLUME 0.789

WEIGHTED VOLUME 0.878
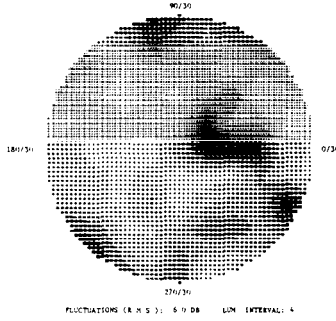
VOLUME 0.712

WEIGHTED VOLUME 0.622
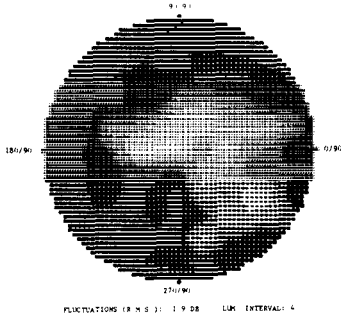
VOLUME 0.460

WEIGHTED VOLUME 0.765
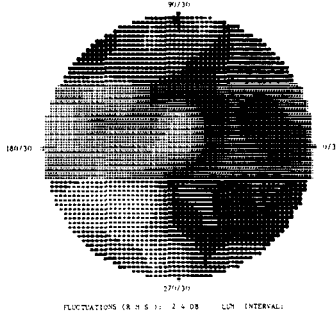
VOLUME 0.304

WEIGHTED VOLUME 0.330
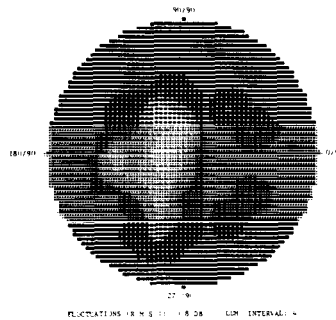
VOLUME 0.193

WEIGHTED VOLUME 0.362
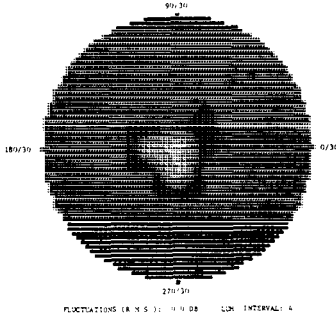
VOLUME 0.006

WEIGHTED VOLUME 0.138

Symb	:::	:::	:::	:::	:::	:::	▦	▦	■
dB	51–36	35–31	30–26	25–21	20–16	15–11	10–6	5–1	0
asb	0.008–0.25	0.31–0.8	1–2.5	3.1–8	10–25	31–80	100–250	315–800	1000

1 asb = 0.318 cd/m²

Conclusions

The Monte Carlo technique has been found to be theoretically suitable for the multi dimensional analysis of threshold static visual field data. Indeed, the technique would appear to be equally suitable for the analysis of any form of suprathreshold static data e g., gradient adapted; two or three zone methods and for kinetic information and could be utilized to provide a measure of function based upon the binocular field. The method in this context requires the use of a minicomputer in order to generate a sufficiently large random number cycle. Nevertheless, this could easily be facilitated by interfacing the computer assisted perimeter with the clinic or hospital minicomputer.

Acknowledgements

References

1   Colenbrander MC: Visual acuity, visual field and physical ability Ophthalmologica 171: 100–108 (1975)
2   Crick RP, Crick JCP, Ripley L: The representation of the visual field Doc Ophthalmol Proc Series 35: 193–203 (1983)
3   Davis JM, McKee TB, Cox SK: Application of the Monte Carlo method to problems in visibility using a local estimate: an investigation Appl Optics 24: 3193–3204 (1985)
4   Dannheim F: Non-linear projection in visual field charting Doc Ophthalmol Proc Series 35: 217–220 (1983)
5   Drasdo N: The neural representation of visual space Nature 266: 544–546 (1977)
6   Drasdo N, Peaston WC: Sampling systems for visual field assessment and computerised perimetry Br J Ophthalmol 64: 705–712 (1980)
7   Estermann B: Functional scoring of the binocular visual field Doc Ophthalmol Proc Series 35: 187–192 (1983)
8   Flammer J, Drance SM, Augustiny L, Funkhouser A: Quantification of glaucomatous visual field defects with automated perimetry Invest Ophthalmol Vis Sci 26: 176–181 (1985)
9   Glezer VD: The receptive fields of the retina Vision Res 5: 497–525 (1965)
10 Gougnard L: Etude des sommations spatiales chez le sujet normal par la périmetrie statique Ophthalmologica 142: 469–486 (1961)
11 Hart WM, Hartz RK: Computer processing of visual field data Arch Ophthalmol 99: 128–132 (1981)
12 Haruta R, Kani K, Inui T: A new numerical representation of the visual field in regard to the retinal ganglion cell density Doc Ophthalmol Proc Series 42: 131–136 (1985)
13 Henson DB, Chauhan BC: Informational content of the visual field location in glaucoma Doc Ophthalmol 59: 341–352 (1985)
14 Katz J, Sommer A: Asymmetry and variation in the normal hill of vision Arch Ophthalmol 104: 65–68 (1986)

15 Pe'er J, Zajicek G, Barzel I: Computerised evaluation of visual fields Br J Ophthalmol 67: 50–53 (1983)
16 Perry VH, Cowey A: The ganglion cell and cone distributions in the monkeys retina: implications for central magnification factors Vision Res 25: 1795–1810 (1985)
17 Rubinstein RY: Simulation and the Monte Carlo method Wiley, New York, 1981
18 Spaeth EB, Fralick FB, Hughes WF: Estimation of loss of visual efficiency Arch Ophthalmol 54: 462–468 (1955)
19 Suzumara H, Furuno F, Matsuo H: Volume of the three-dimensional visual field and its objective evaluation by shape coefficient: normal values by age and abnormal visual field Doc Ophthalmol Proc Series 42: 533–537 (1985)
20 Wilson ME: Invarient features of spatial summation with changing locus in the visual field J Physiol (London) 207: 611–622 (1970)
21 Wood JM, Wild JM, Drasdo N, Crews SJ: Perimetric profiles and cortical representation Ophthalmic Res 18: 301–308 (1986)

Authors' addresses:
J M Wild, J M Wood,
Department of Vision Sciences, Aston University,
Aston Triangle, Birmingham B4 7ET, UK

M K Hussey,
Information Management Division, Management Centre, Aston University,
Aston Triangle, Birmingham B4 7ET, UK

S J Crews,
Retina Department, Birmingham and Midland Eye Hospital,
Church Street, Birmingham B3 2NS, UK

III.6 Behaviour of visual field indices with a gradient adaptive method

T.J.T.P. VAN DEN BERG and R.J NOOTEBOOM
Amsterdam, The Netherlands

Abstract

We developed an algorithm that determines the reference field from the field under investigation itself. After subtraction of the population mean an individually determined cone is used as a reference field. To test the algorithm and the behaviour of different statistical indices we used visual fields simulated by the computer. Computer simulations were also used to study the behaviour of spatial autocorrelation coefficients for different defects

Introduction

We investigated visual fields with our double threshold determination program [5]. Threshold values were measured twice at 60 locations within 25 degrees. On the basis of a linear cone approximation for the normal visual field significant interindividual differences in gradient of sensitivity from center towards 25 degrees eccentricity were found (Van den Berg et al., in this book). Are these interindividual gradient differences important for the evaluation of the visual field? In order to study this question we used as a more accurate approximation the population mean plus a linear cone with individually estimated gradient.

In order to determine how accurately the model describes the actual visual field we have plotted in Figure 1 the residual error of a cone approximation after subtraction of the population mean (RMSW) against the short term fluctuation (SFM).

For an ideal model all points should be lying near the 45 degree line. We see that the model is a rather good description. A simpler alternative would be fitting the population mean. The resulting residual error of this approximation (RMSP) is depicted on the right of Figure 1 and is slightly worse then the model including the individual difference in gradient
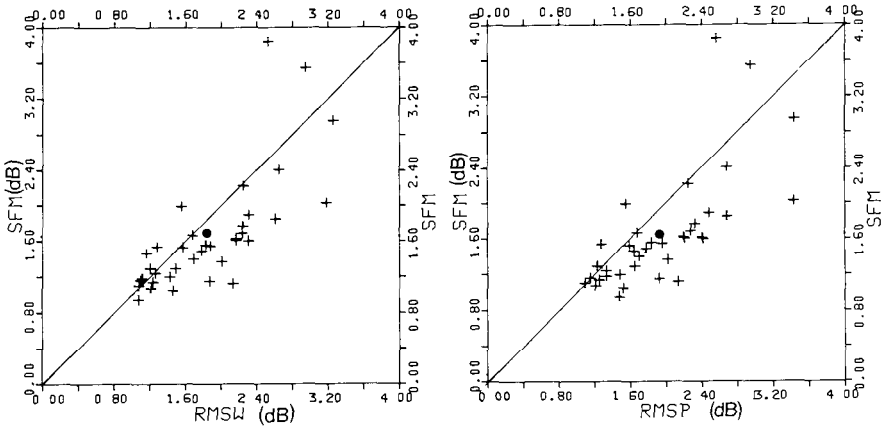
Figure 1 Horizontally residual errors for two approximations for the visual field are plotted against the short term fluctuation RMSW (left) refers to fitting the population mean plus individual cone RMSP (right) refers to fitting only the population mean

Methods

The basic idea of the computer analysis is to extract information on the normal part of a visual field and then to derive from this selection of normal positions the reference field. The word normal is used for positions where no localized reduction of sensitivity is found; there may be a generalized reduction in this position. This is indicated separately. As model for the reference field the sum of the population mean and an individual cone is used. After subtraction of the population mean from an actual pathological field a selection of positions is made to extract the normal positons in the field. By linear regression of the normal positions the cone shaped reference field is then found. The first step in the selection of normal positions is the calculation of an unbiased estimate of the height of the visual field called the IGS (individual general sensitivity; see Van den Berg et al. in this volume and [4]). Positions with a sensitivity not too far below the IGS are supposed to be normal and are used to calculate the reference field The boundary was made to depend on the short term fluctuation (boundary = IGS − k × SFHP).

We based the choice of this boundary on the frequency distribution of standardized deviations of the threshold values in our normal control group (van den Berg et al., in this book). This distribution is skew (see also Heijl et al. in this book) and to stay in the 5% level we had to choose 2 2 for k.

SIMULATED VISUAL-FIELD

expected relation

RGRA (dB / degree)

GRAD (dB / degree)

STVAL	0.15
INCR	0.03
TI	3.00
BAND	3.00
FI	2.20
FG	1.90
SLOP	0.30
DIF	6.00
DEPT	8.00
SFGH	2.20
SFGP	3.00
GRAD	0.48
CVAL	30.00
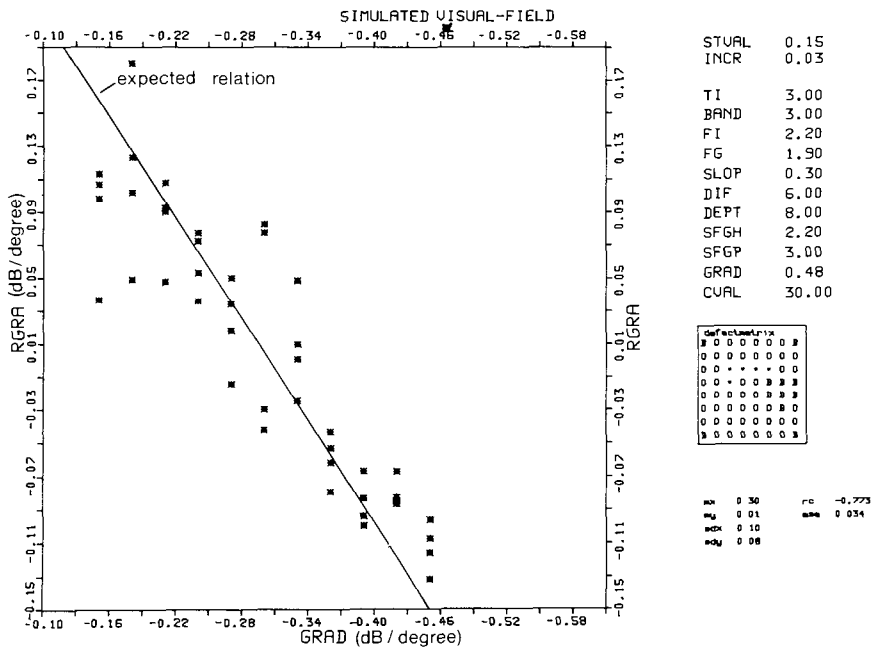
Figure 2 This figure shows that there is a correct computer estimation of the corrected gradient (RGRA) as a function of the gradient of the simulated visual field

Results

In order to evaluate whether the algorithm correctly extracts the normal part of the visual field in a pathogical case a priori knowledge about the visual field would be needed. Such a priori knowledge is not available for actual visual fields Therefore we decided to perform a simulation experiment. A realistic simulation of visual fields is possible because the model approximation for a normal visual field is based on sufficient grounds:
1. population mean + linear cone;
2. actual threshold values are more or less normally distributed around the individual's local mean [2].
The simulated visual field has the following parameters. a central value (CVAL), the gradient (GRAD) in dB/degree, the short-term fluctuation of healthy points (SFHP), the short-term fluctuation of pathological points (SFGP) and an array containing the defect depth of all locations. SFGP was chosen larger than SFHP because actual fields also show such a difference.

First we used the simulations to evaluate how well the method estimates the normal visual field parameters. Figure 2 shows the result for the gradient determination after correction for the average normal gradient of sensitivity of -0.30 dB/degree. The resulting gradient is called RGRA. We generated cone shaped

204
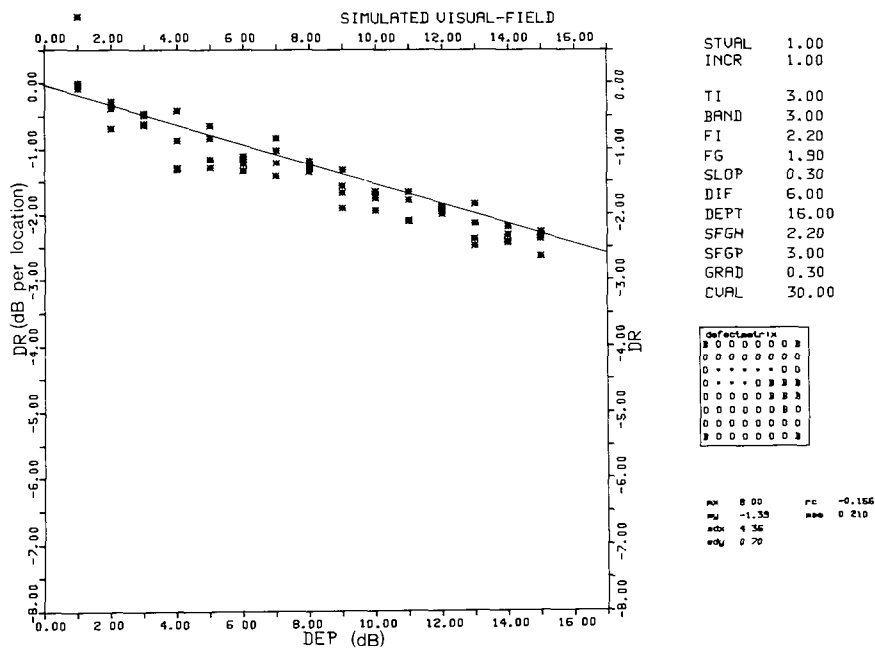
Figure 3 Mean defect (DR) as calculated by our program as a function of the defect depth of a relative scotoma consisting of 8 points (see rectangle on the right) The drawn line is the expected relation

fields and varied the gradient from -0.15 dB/degree to -0.45 dB/degree. A defect consisting of 5 adjacent positions was placed in the upperhalf. Inspection of figure 2 shows that RGRA is estimated quite well (rmse again about 0.04 dB/degree).

Simulations were performed also for other defects and furthermore for the evaluation of the quality of estimation of the CVAL and SFHP parameters of the normal visual field. The algorithm resulted in all tested cases in an unbiased and adequately accurate estimation.

The next step was to test whether the algorithm also estimates the pathological part correctly In Figure 3 we see the mean defect determined with our method (DR) as a function of the defect depth. A uniform defect consisting of 8 adjacent points was placed in the upperhalf. We did the same for the mean defect using IGS directly as the reference level (MD). The measurement error for MD was however about two times larger than the measurement error of DR. The improved accuracy is due to the fact that with our method the reference field is estimated on the basis of as many positions as possible.

The analysis up till now refers only to a reduction of sensitivity below the reference field. For evaluation of a visual field however the way positions with a reduced sensitivity cluster is also of importance To judge clustering separate statistics are needed. We tested several cluster parameters with our simulation
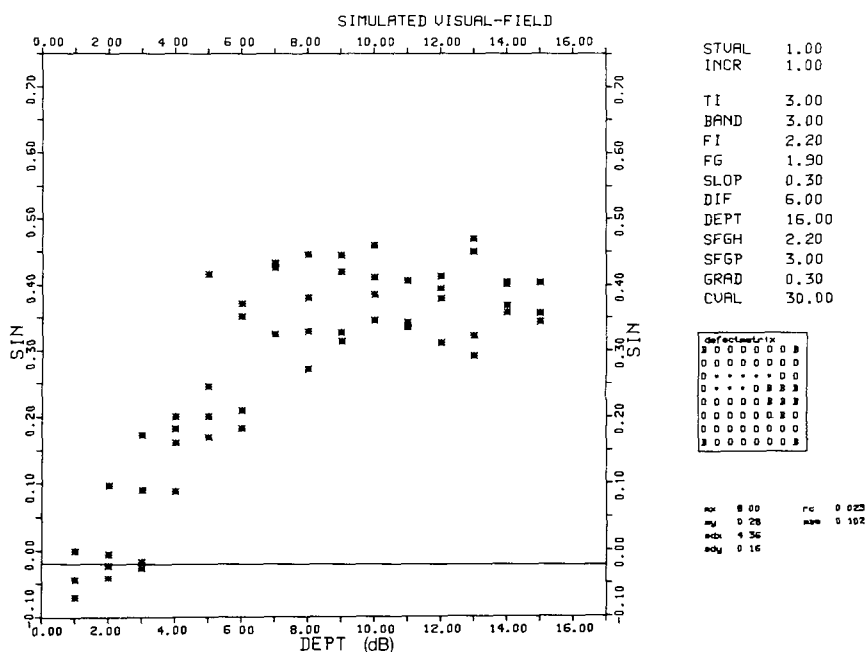
Figure 4 SIN-statistic as a function of the defect depth The drawn line indicates the theoretical expectation value for a completely uncorrelated field

technique. The Moran statistic and the Geary coefficient were used both for a neighbours interaction model and for an inverse distance model [1]. We tested when the statistics reached significant difference with the base value for a series of more or less realistic visual field defects while varying the defect depth.

The inverse distance model gave the worst results for both statistics. The Moran statistic with the nearest neighbours interaction mode (SIN) was the most sensitive one. For a uniform defect of 8 adjacent positions in the upper half SIN became already significant with a defect depth of 4 dB (Figure 4). Notice that the pathological positions were generated with a short term fluctuation of 3 dB.

Conclusions

From these simulation studies we conclude that with our method an accurate estimation of visual field parameters including gradient and defect depth is possible. There are significant differences in visual field gradients between subjects. Correction for the individual gradient is however not necessary for an unbiased estimation of defects [3].

Accuracy can be improved by making the collection of positions used to estimate the reference field as large as possible Finally for evaluation of clustering of pathological positions the SIN statistic seems to be promising.

References

1 Cliff AD, Ord JK: Spatial autocorrelation Pion, London, 1973
2 Flammer J, Zulauf M: The frequency distribution of the deviations in static perimetry Doc Ophthalmol Proc Series 42: 17–24 (1985)
3 Langerhorst CT, Van den Berg TJTP, Van Spronsen R, Greve EL: Results of a fluctuation analysis and defect volume program for automated static threshold perimetry with the scoperimeter Doc Ophthalmol Proc Series 42: 1–6 (1985)
4 Van den Berg TJTP, Van Spronsen R, Van Veenendaal WG, Bakker D: Psychophysics of intensity discrimination in relation to defect volume examination on the scoperimeter Doc Ophthalmol Proc Series 42: 147–151 (1985)
5 Van Veenendaal WG, Langerhorst CT, Van den Berg TJTP, Greve EL: New programs of the scoperimeter Doc Ophthalmol Proc Series 35: 323–329 (1983)

Author's address:
Laboratory of Medical Physics of the University of Amsterdam
and The Netherlands Ophthalmic Research Institute,
Academic Medical Center,
Meibergdreef 9, 1105 AZ Amsterdam-Zuidoost, The Netherlands

III.7 Computer-assisted visual field assessment: quantification, three- and four-dimensional representations

G.N. LAMBROU, Ph. SCHALK, R.V. RECHENMANN and A. BRONNER
Strasbourg, France

Abstract

Due to recent technological advances in perimetry, the display of visual field data tends to become overloaded with (often numerical) information, certainly useful but hard to assess rapidly. This problem can be partly solved through a convenient, perimeter-independent, three- or four-dimensional representation of the hill of vision.

As far as quantitative assessment is concerned, an adequate weighting factor can be used to infer from the perimetric data such information as the functional value of the field to the patient or the extent of optic nerve fiber damage

Introduction

It is commonplace to state that perimetry has undergone a revolution during the last fifteen years Due to (a) an almost universal adoption of static testing techniques and (b) an ever-increasing sophistication of perimeters, what used to be an essentially qualitative examination has become a highly quantitative one This transformation, although undoubtedly beneficial both to patient and examiner, has a number of problems. Some of them concern the display of perimetric results and can be enunciated as follows·

1. Simultaneous unprocessed display of all data collected through static testing, although very rich in information, is hard to assess, compelling the examiner to a great amount of abstraction Computer-processed display of the same data, only partially solves the problem, since it either still necessitates a certain amount of abstraction (e g 'depth of defect' display) or has lost its quantitative aspects, reverting to a qualitative character (e.g 'interpolated greyscale' display).
2. Diversity of testing techniques, multiplication of chart-projection systems [1, 2, 7] and profusion of commercialized perimeters have resulted in the loss of

the *de facto* standardization provided by Goldmann perimetry. Comparison of visual fields obtained through different perimeters is difficult and, anyhow, can only be qualitative

We believe that a first step toward the solution of these problems would be the systematic adoption of a perimeter-independent, twin display of perimetric results associating:

- a high-quality, easy-to-interpret, topographic representation, aimed at qualitative assessment;
- a purpose-oriented, numerical evaluation of either the surviving visual field or of its disturbances, aimed at quantitative assessment.

Visual field representation

The fact that there exist almost as many different forms of perimetric data display as there are perimeter manufacturers, results from a lack of agreed-upon guidelines regarding the aim of the display. Starting from the postulate that *representation* of visual fields aims at *overall, single-glance, qualitative* assessment, we established the criteria of an 'ideal' graphic representation, which should, as far as possible:

1. *Use a standard cartographic projection* In spite of well-founded recent criticism [1, 2], the isometric projection used for the Goldmann chart is an acceptable compromise. Other projection types, although very interesting from a conceptual point of view, are much too distorting to be used as standards (with the possible exception of the 'equivalent' projection, which could profitably substitute for the isometric one).
2. *Favor qualitative assessment.* Provided a quantitative assessment is simultaneously displayed, the purpose of visual field representation is not to show how much damage has occurred, but where it has occurred.
3. *Use familiar concepts.* For assessment to be straightforward to all ophthalmologists and until new standards emerge, visual field representations should use such familiar concepts as isopters or hill of vision.
4. *Display an overall view of visual field,* or of the part of visual field being studied (most do).
5. *Allow good DLT-level* discrimination*, lack of which results in 'haziness' of scotomatous zones and hence in inaccurate assessment.
6. *Clearly display distribution and morphology of defects*, first clue to diagnosis and basis of follow-up.
7. *Conserve maximum perimetric data*

This list may seem redundant and some of its items obvious, yet we thought its enunciation useful as a first guideline for the development of standardized representations.

* DLT: Differential Light Threshold

Visual field quantification

Unlike visual field (V.F.) representation, which has been merely transformed by recent advances in perimetry, V F. quantification was born with them. A brand new and promising subject, it has excited much interest among authors [4, 5, 6, 11, 12] as well as among manufacturers, with the result that almost every quantification method proposed today is perimeter-dependent, and quantitative comparison between visual fields recorded through different devices is extremely difficult. It is therefore urgent that a new generation of perimeter-independent quantification methods be developed.

A closer look at such existing methods reveals another common feature, i e. their descriptive character. Indeed, most of them aim at summarizing the overall state of the visual field through one or a small number of indices, in other words at mere data reduction

It is however possible to deduce much more information from the visual field by supplying additional data through the quantification method Scoring with the Esterman grid, for instance, supplies 'functional value of each location' data and yields the information 'functional value of V.F. to patient' [4] Such quantification methods imply the use of a weighting factor (introducing the additional data) and, as opposed to descriptive ones, can be called *deductive* or *inferential.*

The Esterman grid example raises an important point. any data reduction method extracts from a mass of data only the information it has been built to seek. (In this, it is similar, to a signal-processing system built to extract a certain information considered as most relevant). One say it is *purpose-oriented*

But what information *is* relevant in the case of the visual field? This depends entirely on the purpose of the examination, which guides the choice of an adequate weighting factor. If, for example, functional assessment is required, the weighting factor could be directly derived from the Esterman grid. If, on the other hand, evaluation of optic nerve fiber damage is the major concern, the weighting factor should be related to the retinal receptive field distribution. In the same way, cortical magnification could be used as a weighting factor to assess occipital lobe damage.

These are only examples of various weighting methods possible The important point to note is that several such methods must be available, offering the examiner the choice of a purpose-oriented quantification of the visual field.

A new approach to computerized assessment of visual fields

We are trying to develop an integrated assessment system, founded on the forementioned principles [8, 10] We obtained our data either through a Goldmann perimeter fitted for static testing, or through such devices as the Tübinger Automatic Perimeter or the Humphrey 630 Visual Field Analyzer In routine

cases we thresholded around 100 points in the central 30° area, while the precise limits of the blind spot were tested kinetically. We processed the data through software we developed on an IBM 3081 computer. Plotting was carried out on a Tektronix 4691 ink-jet plotter. The results obtained up to now can be outlined as follows

1. '3-D' representation

Figures 1 to 8 show examples of perspective visualisation of 'hills of vision'. Any viewpoint can be chosen, according to the morphology of the hill. All visual fields represented are from left eyes.

Figures 1 and 2 show whole and half visual fields, plotted over a ± 90°square. All other figures display only central visual fields, plotted over a ± 30°square. Note blind spot 'pit' and nasal relief imprint on far wall of figure 2.

Figures 1, 2 and 3 represent normal visual fields, figure 4 shows a superior arcuate glaucomatous defect with nasal step, figure 5 superior and inferior arcuate as well as peripheral defects, figure 6 advanced glaucomatous loss of superior visual field communicating with blind spot. Figures 7 and 8 display visual fields taken at a 20-day interval in a patient suffering from multiple sclerosis optic neuropathy.

2. The 'fourth' dimension

In all previous 3-D representations, the third dimension (DLT value) is displayed both as height and as color, so as to facilitate single-glance qualitative assessment. This extra feature, colour, can be used to convey further information about every point of the visual field, thus adding a 'fourth dimension' to the representation. This can be of particular interest, since it allows us to superimpose upon the DLT the distribution of any parameter we may wish to study, such as:
– deviation from normal values of DLT,
– evolution since previous examination,
– short-term fluctuation,
– colour, pattern or contrast sensitivity,
– optic nerve fiber loss,
– probability of DLT being disturbed [11]
– . . or any other.
Figure 9 is such a '4-D' representation, displaying the same 'hill of vision' as figure 8 and, through the color scale, the evolution since the previous examination (figure 7).

Figs 1–6 Perspective 3-D representations of 'hills of vision' of a normal (Figs 1 to 3) and three glaucomatous eyes, all left Color scale is the same as in Figs 7 and 8 Temporal, nasal, superior and inferior directions are indicated on the axes by T, N, S and I respectively See text for detailed description

212

DECIBELS

FIG 7

DECIBELS

FIG 8

VARIATION (dB)

FIG 9

Figs 7–9 Principle of 4-D representation: Figures 7 and 8 display 3-D representations of visual fields of an eye suffering from optic neuropathy, examined twice at a 20-day interval Figure 9 displays same hill of vision as Fig 8 (2nd examination) but colour scale displays evolution since previous examination Yellow areas have undergone no change while green-blue areas have undergone improvement (whose importance is expressed through colour scale) Orange-red areas normally indicative of deterioration, probably correspond here to fluctuations

Figs 1–6 Perspective 3-D representations of 'hills of vision' of a normal (Figs 1 to 3) and three glaucomatous eyes, all left Color scale is the same as in Figs 7 and 8 Temporal, nasal, superior and inferior directions are indicated on the axes by T, N, S and I respectively See text for detailed description

Figs 7–9 Principle of 4-D representation: Figures 7 and 8 display 3-D representations of visual fields of an eye suffering from optic neuropathy, examined twice at a 20-day interval Figure 9 displays same hill of vision as Fig 8 (2nd examination) but colour scale displays evolution since previous examination Yellow areas have undergone no change while green-blue areas have undergone improvement (whose importance is expressed through colour scale) Orange-red areas normally indicative of deterioration, probably correspond here to fluctuations

3. Quantification

Quantification can be performed through various scoring systems tailored for different purposes, as explained above We quantified each of the three glaucomatous fields represented using three such systems:
- *no weighting:* quantification is equivalent to measuring the volume of the hill of vision;
- *functional weighting,* through an Esterman-grid-derived weighting factor;
- *'extent of damage' estimate* based on the receptive field density [3] we developed a model permitting one to estimate, from the DLT distribution, the amount of unharmed optic nerve fibers. Our model is still crude (hence the question-marks in the table) but we are working to improve its accuracy.

The results are shown in Table 1, where column I displays unweighted volume of hills of vision, column II functional value of field to patient and column III estimate of unharmed optic nerve fibers, all percentual (normal = 100).

Discussion

Three particular points need to be discussed.

1. The interpolation dilemma

The discrete data set obtained through a perimetric examination is a sample of the continuous distribution of DLT over all or part of the visual field. Interpolation processes the sampled data to yield an estimate of the continuous distribution, i.e. an estimated value of DLT in every location of the field

The use of an interpolation is a delicate and dangerous choice. Indeed, as pointed out by various authors, computing DLT values at points where no data are available can be a source of errors. However, powerful interpolation algorithms can give a fairly acceptable estimate Of course no interpolation algorithm will be able to 'guess' a focal defect situated between normal points: subsequent data processing will simply ignore it, if it exists, for representation as well as for scoring.

Table 1 Effect of weighting factor on scoring (see text for comments)

	I	II	III
Figure 4	60	65	30 (?)
Figure 5	40	40	25 (?)
Figure 6	35	35	20 (?)

But, interpolation or not, if such a defect has been missed it will not be taken into account in scoring, whatever the scoring technique, thus giving an inaccurate score. Besides, even if no graphic representation is made, the results are displayed in one form or another (numerical display, for instance) and the spaces between the tested points are assumed, during interpretation, to be of intermediate value – which is, after all, an inaccurate form of interpolation

On the other hand, interpolation offers various advantages (provided one keeps in mind it is an estimation one has to deal with): first of all, it permits a continuous detailed representation of the hill of vision, much easier to interpret than the usual gross mental reconstruction of the visual field. Second, and most important, interpolation can be performed on any balanced grid of sufficient tested points, with very similar results. The advantage of this is to produce a comparable score whatever the location of the points tested, unlike many scoring systems which require fixed point locations This may be the first step towards standardization of visual field quantification, independent of the device used for testing.

2. What use is there for 3-D representations?

It may be objected that 3-D representation displays no more data than a 'classic' interpolated 2-D greyscale or color display and that, for the time being, 3-D processing is very time-consuming and expensive This could lead to the argument that, apart from teaching purposes, 3-D representations are useless, even if they facilitate qualitative assessment

It is obvious, however, that progressive software sophistication will lower costs and accelerate processing. Moreover, the main interest of such representations is to display simultaneously the distribution of more than one parameter and it is in this direction that future developments ought to be sought

3. Estimation of unharmed optic nerve fibers

Our actual model, based on a logarithmic relationship between the amount of unharmed optic nerve fibers and DLT is only tentative We therefore give our results with the utmost reserve. Although the figures seen surprisingly small, they are consistent with those found in the literature [9]. We hope, in the near future, both to refine our model and demonstrate its validity.

Finally, before any clinical use can be made of this or any similar model, pre-retinal factors affecting DLT (refractive errors, impaired media, etc) must be studied and taken into account in scoring.

References

1 Crick RP, Crick JCP, Ripley L: The representation of the visual field Doc Ophthal Proc Series 35: 193–203 (1982)
2 Dannheim F: Non-linear projection in visual field charting Doc Ophthal Proc Series 35: 217–220 (1982)
3 Drasdo N: The neural representation of visual space Nature 266: 554–556 (1977)
4 Esterman B: Grids for functional scoring of visual fields Doc Ophthal Proc Series 26: 373–380 (1980)
5 Flammer J, Drance SM, Augustiny L, Funkhouser A: Quantification of glaucomatous visual field defects with automated perimetry Invest Ophthal Vis Sci 26: 176–181 (1985)
6 Flanagan JG, Wild JM, Barnes DA, Gilmartin BA, Good PA, Crews SJ: The qualitative comparative analysis of the visual field using computer-assisted, semi-automated and manual instrumentation: I Scoring system Doc Ophthal 58: 319–324 (1984)
7 Frisén L: The cartographic deformation of the visual field Ophthalmologica 161: 38–54 (1970)
8 Lambrou GN, Schalk Ph, Bronner A: High resolution 3-D analysis and representation of visual fields Acta XXV International Congress of Ophthalmology, Roma 1986 (in press)
9 Quigley HA, Addicks EM, Green WR: Optic nerve damage in human glaucoma Arch Ophthal 100: 135–146 (1982)
10 Schalk Ph, Lambrou GN, Bronner A: Representation en 3 ou 4 dimensions et quantification du champ visuel Bull Mem SFO (in press)
11 Schwartz B, Nagin P: Probability maps for evaluating automated visual fields Doc Ophthal Proc Series 42: 39–48 (1985)
12 Sponsel WE, Dallas NL, Burbridge L: Visual field survival; the response to Timolol therapy in open angle glaucoma Br J Ophthal 67: 220–227 (1983)

Author's addresses:
ULP; LBRM-INSERM U220, 11 rue Humann, 67085 Strasbourg Cedex, France
and
Clinique Ophthalmologique C H U , Hospices Civils, 67000 Strasbourg, France

III.8 Quantitative supra-threshold static perimetry; the value of field score and asymmetry analysis in the early detection of chronic open angle glaucoma

W.E. SPONSEL, A HOBLEY, D.B. HENSON, B.C CHAUHAN
and N.L. DALLAS
Bristol and Cardiff, United Kingdom

Abstract

Visual fields and intraocular pressures of 107 glaucoma suspects were compared with those of 115 healthy volunteers of comparable age. Of the 107 referral patients, 50 were deemed glaucomatous on routine clinical grounds. Using field scoring algorithms designed to recognise early glaucomatous defects, the diagnosis of glaucoma in 43 (86%) of these patients was readily confirmed. The remaining 7 showed little evidence of field deficiencies but had high intraocular pressures.

Of the 57 referral patients for whom no clinical diagnosis of glaucoma had been made, 27 (47%) showed evidence of highly significant glaucomatous defects when perimetric data was analysed by microcomputer. On follow-up 1-2 years later a representative subgroup of these untreated individuals showed an increase in their visual field defect scores by a factor of 3 (p<0.003).

Intraocular pressures showed no useful correlation with the visual prognosis of these untreated patients; indeed, IOP levels were significantly lower at follow-up in the most progressively afflicted eyes (p<0.05). In contrast to the IOP findings, the computerised field score-asymmetry analysis achieved a wide bimodal separation of normal from glaucomatous subjects. The diagnostic false-positive rate of this technique was 3%. These findings suggest that novel visual field scoring techniques can detect glaucomatous pathology at a subclinical level.

Introduction

It has been suggested that the difference in visual field response between the two paired eyes in individuals with subclinical glaucoma might be of a larger order than that observed in age-matched normal individuals [5]. If this were true, then an eye with a statistically normal field score when considered in isolation might still be shown to diverge from its fellow eye beyond acceptable limits of visual asymmetry.

This elementary concept is appealing, since many pathological processes in paired organs tend toward asymmetric function, even in bilateral disease states. Multitudinous evidence exists to confirm that this is indeed the case in established COAG. If such a fundamental principle could be exploited at a much earlier stage of the disease process, the diagnosis of glaucoma in some individuals might be considerably expedited.

Aside from increasing the potential sensitivity of diagnostic perimetry, asymmetry analysis might also help reduce the 'false positive' rate. For example, 'random misses' during visual testing, which can result from angioscotomata or inattentiveness, tend to create a nonspecific 'background noise level' in quantitative assessments of suprathreshold static perimetry. Such anomalies would be expected to occur in a symmetrical manner with any given individual under examination.

In order to determine whether quantification of visual field asymmetry might indeed assist in glaucoma detection, a large database of normal central fields is required as a standard for comparison with those of glaucoma suspects. An appropriate control-group study has been performed and is reported elsewhere in this volume [1]; the normative data in the present study is derived from the first 115 age-related volunteers so assessed.

Statistically, the foundations for discriminating visually normal suspects from pathological suspects on the basis of static perimetry scores and/or bilateral field score asymmetry are already highly encouraging [2]. Nevertheless, it remains to be shown whether any advancement of visual defect scores and/or increases in field score asymmetry occur in those individuals amongst whom these analytical methods suggest the presence of subclinical glaucoma. A preliminary follow-up of such a group of untreated subclinical cases has now been completed and is presented below.

Methods and normative data

The visual fields and intraocular pressures of 115 volunteers with no ocular pathology were compared to those of 107 patients of comparable age referred to the Bristol Eye Hospital with suspected early glaucoma. Of these 107 referral patients, 90 (84%) had intraocular pressure levels at or above 21 mm Hg. All individuals under assessment had open anterior chamber angles. Referrals with evidence of cataract or corrected visual acuity levels below 6/12 were excluded, as were those with concurrent ocular or cardiovascular therapy and/or a history of previous ophthalmic surgery or diabetes. Friedmann Mark II suprathreshold static perimetry was carried out by the same perimetrist on all clinical subjects, and trial entry was progressive over two years. Strobe bulb testing was carried out periodically to ensure consistency of test point intensities Efforts to detect a learning effect amongst patients in this trial by repeat testing proved negative,
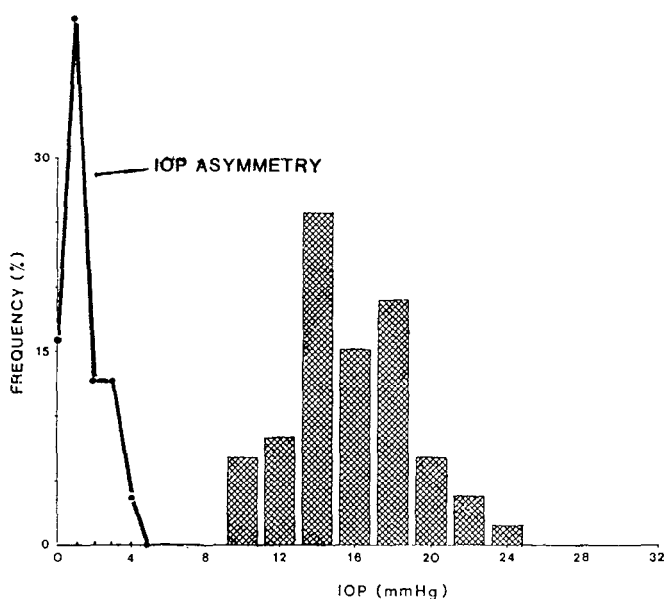
Figure 1 Relationship between the higher IOP and bilateral IOP asymmetry in 105 age-related nonglaucomatous control subjects

and the extent of field score variability upon retesting amongst both referral subjects and volunteers was trivial (approximately 3% and 1%, respectively) [3]. The referral population included individuals with and without cupping of the optic disc and/or other fundal anomalies related to glaucomatous disease, and correlation of these physical parameters to visual function is not considered here.

Four techniques were employed in an attempt to determine with maximal sensitivity and specificity which of the referral patients were in fact glaucomatous;
1. the higher of the IOP readings from their two eyes,
2. the higher of the Friedmann field defect scores from their two eyes,
3. the difference (asymmetry) between their right and left IOP readings, and
4. the difference between their right and left Friedmann field scores
Applanation tonometry was carried out by a consultant ophthalmologist in each case.

The mean values for intraocular pressure and IOP asymmetry (right minus left) in the control population were 15.19 (SD 3.11) and −0.24 (SD 1 82) mm Hg, respectively. Hence, the probability of a worse eye IOP of 23 mm Hg in the normal population was <0.01; of 25 mm Hg <0.001; and of 27 mm Hg <0.0001. Skewing of the IOP distribution was observed in this random sample, so the statistical probability levels cited are approximate guidelines only.

Similarly, given the normal distribution for IOP asymmetries observed, a difference of 4 mm Hg would correspond to p<0.01; probability values of <0 001
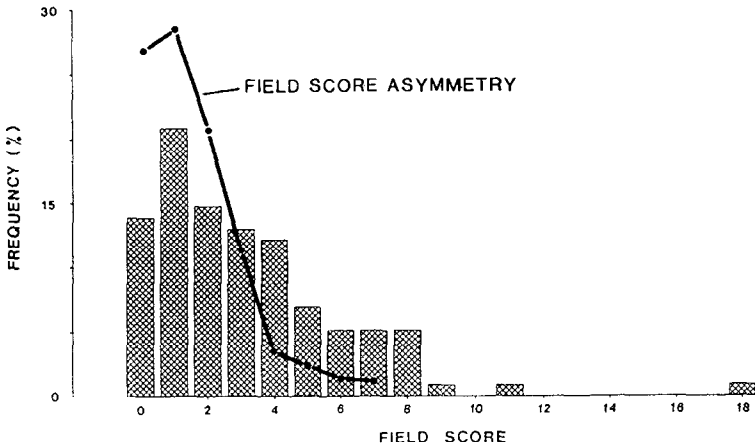
Figure 2 Relationship between the higher visual field defect score and bilateral field score asymmetry in age-related nonglaucomatous control subjects

and <0.0001 apply for IOP asymmetries of 6 and 7 mm Hg, respectively. A comparative display of the distributions for IOP and IOP asymmetry in the normative group is shown in Figure 1.

Field scores were calculated according to the method of Henson et al [4], which compiles the sums of F1 and F2 (for point misses and clustering) without the inbuilt truncation at 100 as is used in field survival assessment. Thus, here a higher score infers a greater degree of field defect. The normal distribution of field scores in the control population had a mean value of 2.2 and a standard deviation of 3.1. On this basis, a score of 10 has a p value of 0.01, and scores of 12 and 14 have probabilities of <0 001 and <0.0001, respectively

The mean value for field score asymmetry was −0.01 in normal individuals (R minus L), with an SD of 2.70. Thus, probabilities of <0.01, <0.001, and <0.0001 correspond to field score asymmetry values of 7, 9 and 11, respectively. The narrower distribution of field score asymmetry as opposed to unilateral field score measures alone is shown graphically in Figure 2.

It is clear from the foregoing account that, given equivocal findings for IOP or field score in a glaucoma suspect, asymmetry analysis might still yield evidence of pathology. For example, a patient presenting with a worse eye field score of 8 might be deemed normal on that basis alone, but if the fellow eye of that patient had a field defect score of zero, the asymmetry observed would exceed acceptable limits and hence be labelled as suspect. A similar argument on pressure grounds could be made for a patient presenting with IOP values of say 22 and 16, neither of which is grossly abnormal in its own right, but which deviate from one another to an abnormal extent.

Certain individuals will nevertheless undoubtedly present with symmetrically defective field or IOP scores. A simple algorithm has therefore been applied to
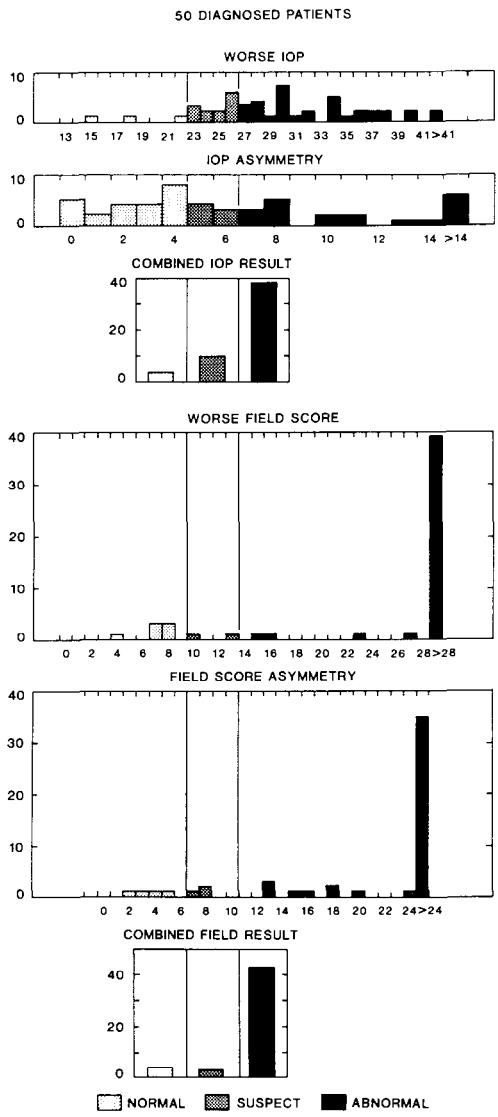
Figure 3 Colinear probability distributions for higher IOP, IOP asymmetry, combined IOP/asymmetry result, worse eye field defect score, bilateral field score asymmetry, and combined field score/asymmetry result for 50 clinically diagnosed glaucoma referrals at the time of their initial assessment

the assessment of the referral patients in both the treated (COAG diagnosed) and untreated (clinical diagnosis deferred or denied) groups. This formula immediately adopts any patient with a worse eye field score probability of <0 0001 as being 'abnormal', but refers all remaining 'normal' and 'suspect' patients to asymmetry analysis. Patients for whom asymmetry assessment gives a p value of
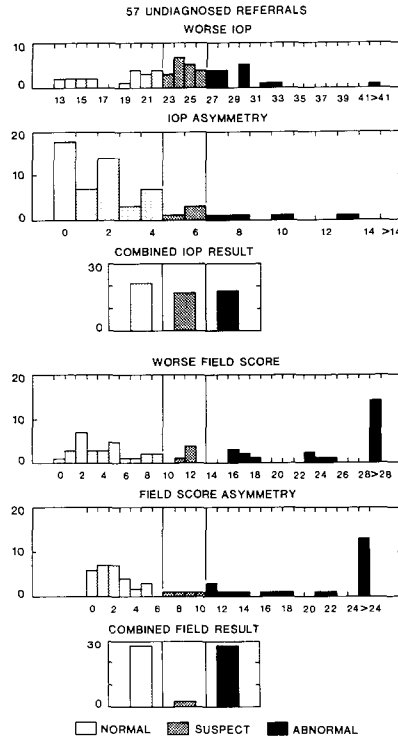
Figure 4 Colinear probability distributions for higher IOP, IOP asymmetry, combined IOP/asymmetry result, worse eye field defect score, bilateral field score asymmetry, and combined field score/asymmetry result for 57 patients deferred from diagnosis or therapy at the time of their initial assessment

<0.0001 are then similarly labelled as 'abnormal', while those who have results in the 0 01–0 0001 range by either worse eye or asymmetry assessment are labelled as 'suspect' Patients for whom both methods of assessment yield results with >0.01 probability are labelled as 'normal'. These designations are referred to below as the 'combined field result'. An equivilent logical process is employed in deriving a 'combined IOP result'.

Figures 3 and 4 show the colinear probability distributions obtained, using the six evaluative methods just described, in assessing the 107 referral patients. Figure 3 summarises findings for the 50 referrals in whom glaucoma was diagnosed and subsequently treated, and Figure 4, those of the referrals for whom no definitive diagnosis, nor treatment, were established. In each case the senior ophthalmologist reviewing the patients had access to the IOP and raw (unquantified) perimetry data in reaching his diagnostic decision

The most striking feature of Figure 3 is the very high correlation of defective field scores with the clinical diagnosis of glaucoma. Contrasted with this is the indeterminate scatter of IOP and IOP asymmetry values within or around the

DIAGNOSED   NOT DIAGNOSED

DEFECTIVE   NORMAL
FIELD   FIELD

HIGH
IOP

SUSPICIOUS
IOP

NORMAL
IOP

HIGH SUSPICIOUS NORMAL
FIELD SCORES
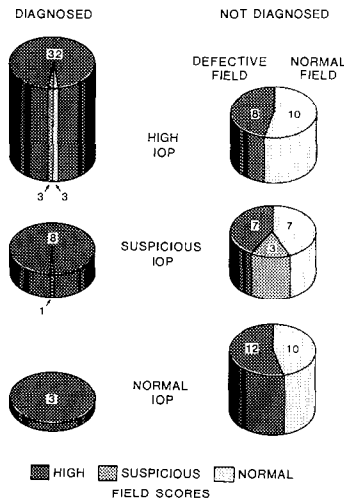
Figure 5 Left: Relationship between IOP probability levels and field score probability levels amongst the 50 clinically diagnosed glaucoma referrals Right: Relationship between IOP probability levels and field score probability levels amongst the 57 patients for whom diagnosis and therapy were deferred

suspect probability region Such a distribution, even assuming some direct clinical relevance of IOP, illustrates the very limited practical diagnostic utility of IOP measures amongst this referral group Nevertheless, since high IOP values appear to have been a virtual prerequisite for selection into this clinically-diagnosed group, there is at first sight an apparent correlation between IOP excess and field loss.

More careful examination reveals the associations seen in Figure 5a which shows correlations between the field score findings and the IOP findings, using the combined algorithms. Eleven of the twelve patients in this group whose IOP levels were not statistically abnormal exhibited highly abnormal field results. Thus, of the 43 abnormal fields observed, only 32 (84%) were associated with abnormal IOP values, roughly the same extent of IOP abnormality initially observed in the 107 patient referral group as a whole. Hence, no statistical correlation can be assumed between the IOPs in this referral population and the prevalence of field defects therein.

Figure 4 shows the frequency distributions for IOP and field score findings from the 57 referral patients in whom no diagnosis was made. Note the high yield (47%) of field scores which are statistically incompatible with normality Only 5% gave 'suspect' field score results, the remaining 47% falling well within normal limits. Field scoring techniques thus appear potentially able to produce the hitherto elusive bimodal distribution we require for confident COAG diagnoses to be made. Note as well the striking potential for field score asymmetry analysis to contribute in the diagnostic process.
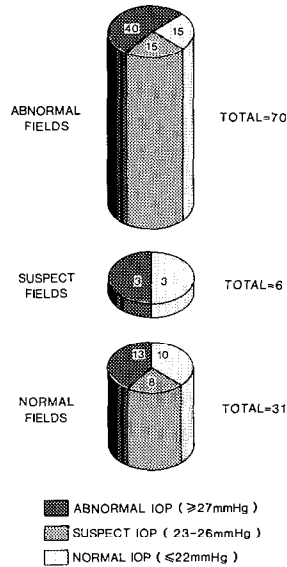
Figure 6 Distribution of IOP probability levels amongst the visual field score categories in the referral population as a whole

In contrast, the IOP findings amongst this group were merely a 'downshifted' version of those seen in the clinically-diagnosed group, with a somewhat higher degree of IOP symmetry amongst those with the higher IOP levels. These distributions were again unimodal, and a high proportion (>68%) of the IOP readings were either entirely normal or indeterminate, even when considered by combined analysis. Now, however, with a wider range of IOP values available for correlation with field scores, it is abundantly clear that no useful satistical association existed between the IOP levels of these clinically undiagnosed individuals and their presenting visual field status (Figure 5b).

Figure 6 shows the outcome of visual field scoring for the entire referral population without regard to clinical diagnosis. Highly abnormal fields were observed in 70 (65 4%) of the referral population, compared with the clinical yield of 50 (46.7%). The distribution of IOP values in each field score category were comparable, and overlapped each other extensively.

Comment

These results would appear to confirm a high degree of competence in the referral of glaucoma suspects to the eye clinic. Unfortunately, despite the availability of field traces and full clinical assessment (but without the direct aid of computer analysis), only 61% (43/70) of the apparently pathological suspects were diag-

nosed and treated for glaucoma by their consultant ophthalmologist. Not all of the remainder were even scheduled for a routine reassessment of their visual function. The IOP values appeared to hold an influential and dominant determinant role in the diagnosis of glaucoma amongst these suspects.

With the added dimension of asymmetry analysis, the computer scoring system for Friedmann fields appears to have the potential to detect visual pathology with a very high degree of statistical accuracy. The finding of a diagnostic cutoff gap of many statistical orders of magnitude such as that found between the normal and abnormal field asymmetry suspect subgroups is unprecedented amongst glaucoma detection methods

Over 5% of suspects designated as abnormal on field analysis had independent worse-eye Friedmann scores which fell within the normal or suspect range. In these cases asymmetry analysis enabled the detection of levels of ocular pathology too subtle to be detected by the unocular field scoring program alone. Such fine levels of differentiation could never be realistically achieved by clinicians working without the advantages of a computer assessment system and a large normative database

A tremendous clinical burden would be lifted if such an assessment system could be made routinely available. The first priority, however must be to determine whether those eyes deemed to be pathological by this method actually progress if untreated, and if eyes deemed normal retain their high degree of symmetry over a period of time. The remainder of this paper is devoted to a clinical follow-up study of the untreated referral population described above, to ascertain whether field score/asymmetry analysis might really fulfill its compelling statistical promise on a practical clinical level.

Field score asymmetry follow-up assessment of untreated referral patients

Patients and methods

The 35 patients studied in this follow-up trial formed a representative sample of the 57 untreated individuals. Their mean age was 60.49 (SD 11.5). Their normal: suspect: defect ratios on the basis of combined field scoring at presentation was 16:2:17, proportionally almost identical to that of the full group of 57 described earlier.

In many cases, patients had been followed-up two or more times before the reassessment used in this analysis. The follow-up visit chosen for evaluation was the most recent one, and only one review visit per patient was considered. The IOP values considered were recorded by applanation within one hour of perimetric assessment. The patients included here represent all those for whom the necessary records were available at the time of writing

The mean follow-up time for these patients was 17.94 (SD 4.9) months. All

226
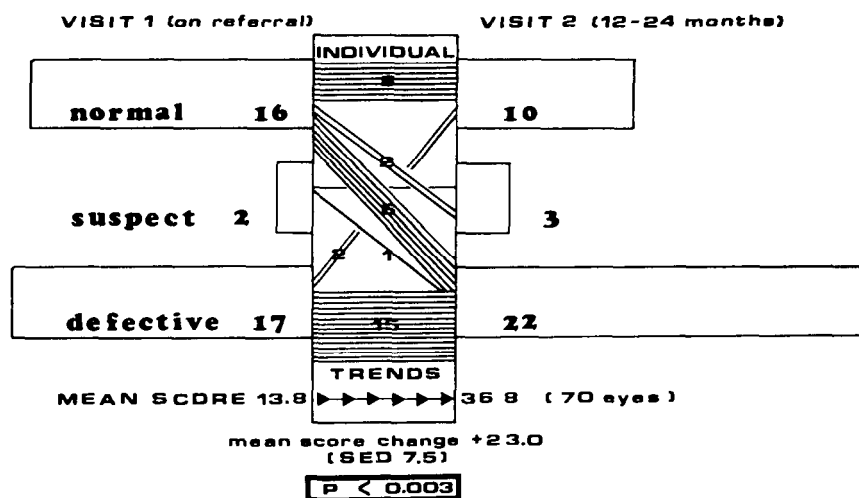
Figure 7 Progression of visual field defects according to probability groups between initial referral assessment and follow-up visit at 1–2 years amongst clinically undiagnosed and untreated individuals

were followed up at least one year after their initial presentation to clinic. The perimetric methods and scoring techniques used were those described previously.

Results

Raw data for the referral and follow-up Friedmann analyses and intraocular pressures are presented elsewhere [4]. Figure 7 illustrates the progression of Friedmann scores between presentation and follow-up on the basis of three probability groups. As previously, the 'defective' designation implies a combined worse eye/asymmetry score probability <0.0001 (and 'suspect' a 0.01–0.0001 probability) of falling within the score distribution of the normal control population.

It can be readily seen from Figure 7 that a substantial shift in field scores has occurred, from a mean defect score of 13.8 at presentation to 36.8 on follow-up. This change is highly significant, as shown (p<0.003).

The majority of patients (24; 69%) remained within their presenting probability group on follow-up including 8 of the 16 'normals' and 15 of the 17 'defectives'. One 'suspect' patient progressed to 'defective' status. Half [8] of the patients presenting with statistically normal field scores progressed into either the 'suspect' [2] or 'defective' [6] group on follow-up. Only two 'defective' patients actually reverted to 'normal' status at follow-up Hence, over 94% [33] of the untreated patients assessed by Friedmann analysis had either retained their presenting status or progressed into a more advanced subclinical (or frank clinical) state of field loss
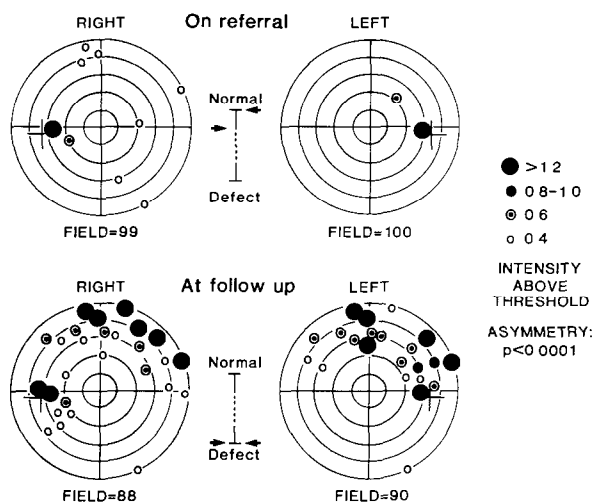
Figure 8 Presentation and follow-up fields of 60 year old male statistically abnormal on the basis of field score asymmetry despite having a worse eye field score within the normal range upon initial assessment

A resumé of the IOP findings for these patients reveals some fascinating correlations. The overall mean IOP for the 70 eyes at presentation was 21.9 mm Hg (SD 4 88), and at follow-up 19.94 (SD 4.78). This 1.96 mm Hg difference is 2.4 × the SED of 0.82, which means that the overall mean IOP for the total group of patients on follow-up was significantly lower than at presentation (p<0.05). This is of considerable interest, given the virtual trebling of defect scores (from 13.8 to 36.8; p<0.003) observed on follow-up.

A breakdown of the IOP findings for specific patient subgroups is clearly called for. Of primary interest are the 9 patients (26%) who progressed to a more pathological statistical status on follow-up; the mean IOP for their 18 eyes was 23.4 (SD 3.65) at presentation and 20.7 (SD 4.19) on follow-up. The 2.7 mm Hg difference observed is more than twice the SED (1.30) Thus, even this hand-picked subgroup of progressively deteriorating eyes exhibited a significant decrease in IOP (p<0.05) at follow-up

The 'fine servo' function of asymmetry analysis was only called into action on one occasion in this particular group of 35 suspects. In a male patient aged 60 the worst-eye score at presentation was 12, earning only a 'suspect' designation. However, the fellow eye score was virtually perfect [1], giving an overall asymmetry value [11] transcending the 0.0001 probability level. As can be seen from Figure 8, at his follow-up visit one year later, both of this patients' eyes exhibited substantial glaucomatous defects.

As a guide to pathology on its own terms, the field score-asymmetry technique exhibited an 89% specificity and a 70% sensitivity when comparing first to second visits. The sensitivity figure was compromised largely by the actual progression of

field defects into more pathological probability groups on follow up. This would seem to indicate even further the veracity of the referral criteria employed by those who initially requested ophthalmological assessment for these patients.

The above figures should be viewed in the context of results from the 50 positively-diagnosed glaucoma suspects referred to clinic during the same period as these 35 untreated suspects. It will be recalled from the previous section that field score/asymmetry analysis would have detected virtually all those submitted to subsequent therapy. The 35 patients here form a representative sample of the 57 untreated (clinically equivocal) referral patients who presented concurrently with that clinically-diagnosed group. Given the advanced status of the vast majority of defects in the former group, overall diagnostic specificity and sensitivity values approaching 90% may be reasonably anticipated using this method of bilateral perimetric field scoring.

Discussion

The potential for field scoring methods to expeditite and simplify glaucoma diagnosis appears considerable. The wide bimodal distribution of field score/asymmetry assessments contrasts sharply with the eccentric unimodal distribution of intraocular pressures observed in the referral population The latter measures gave no indication of the likely progress of untreated patients, and indeed pressures were reduced on review in those patients who had suffered the most severe field loss.

Acknowledgements

References

1 Chauhan BC, Henson DB: The distribution of visual field scores in a normal population Doc Ophthalmol Proc (7th Int Vis Field Symp, Amsterdam), 1986
2 Henson DB, Hobley AJ, Chauhan BC, Sponsel WE, Dallas NL: The importance of visual field score and asymmetry in the detection of glaucoma Am J Opt Physiol Optics 63: 714–723 (1986)
3 Hobley AJ: The quantification of visual fields in the detection of chronic open angle glaucoma M Sc thesis, University of Wales Institute of Science and Technology, Cardiff, Wales, 1985
4 Sponsel WE: Visual field quantification in the diagnosis and assessment of chronic open angle glaucoma M D Thesis, University of Bristol, Bristol, England, 1985
5 Sponsel WE, Williams AH, Dallas NL, Henson DB: A microcomputer-based glaucoma assessment system designed for clinical ophthalmologists Res Clin Forums 5(5): 25–36 (1983) and J Biomed Info Data 5(1): 1–11 (1984)

Authors' addresses:
W E Sponsel,
University Department of Ophthalmology, F4 Clinical Science Center, 600 Highland
Avenue, Madison, Wisconsin, U S A

A Hobley, D B Henson, B C Chauhan, N L Dallas,
University Department of Ophthalmology, Bristol, England
and
Department of Experimental Optometry, UWIST, Cardiff, Wales

Section IV
New instruments, test programmes and displays

IV.1 Clinical results with the Henson-Hamblin CFS2000

D.B. HENSON and H. BRYSON
Cardiff, United Kingdom

Abstract

Ninety-four eyes from patients suspected of having glaucoma were examined with a new computerised visual field analyser, the Henson-Hamblin CFS2000. The screening program, which tests 26 retinal locations was found to have a sensitivity of 90% and a specificity of 88%. The results from the 2 quantification systems, programmed into this instruments software, are discussed.

Introduction

A new computerised central visual field analyser, the Henson-Hamblin CFS2000, has recently been introduced into the market place (see Figure 1). This instrument contains a screening program which tests 26 retinal locations and a full program which test 132 simulus locations. It also contains 2 quantification systems, the first gives an estimate of the likelihood that a given response is normal while the second gives a measure of the visual field survival (100-percent field loss) [1]. It is the purpose of this paper to evaluate the screening program and the quantification techniques.

Materials and method

The Henson-Hamblin CFS2000 uses a multiple stimulus supra threshold static technique to examine the visual field. The stimulus intensity is gradient adapted. It increases, by 0.8 log units, from the centre of the visual field to an eccentricity of 25 degrees. Its stimuli are matched solid state LEDs which have a flat diffusing front surface of diameter 3.4 mm. The LEDs are inserted into holes in a tangent screen positioned 33 cms from the patients eye and inclined at 15 degrees to the vertical. This inclination is designed to give a more comfortable viewing angle for
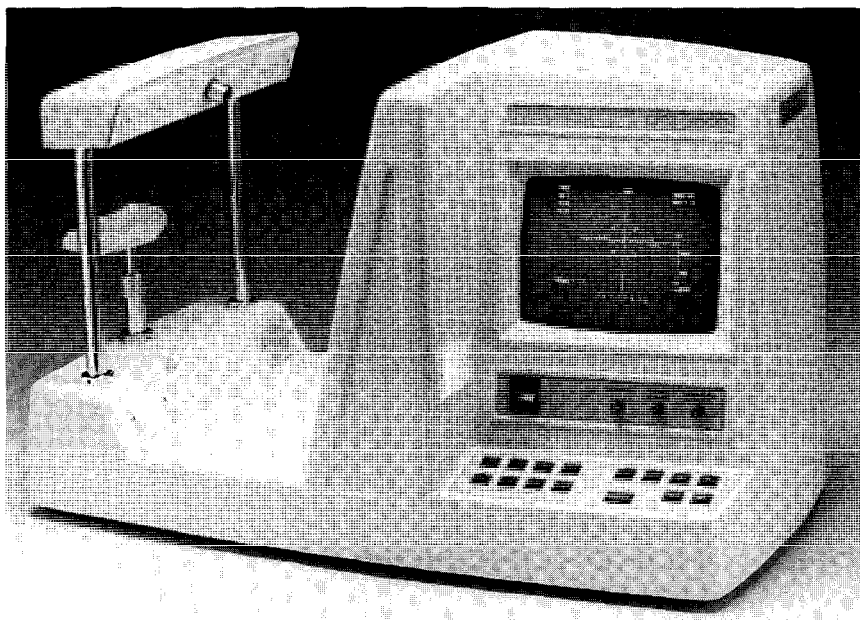
Figure 1 The Henson-Hamblin CFS2000

the patient The background luminance of the screen is 0 25 cd/m^2, a value which is set by the perimetrist with the aid of an internal light meter. On the side of the instrument there is a monitor which presents to the perimetrist all the relavant information about the test, such as the number and position of any missed stimuli. Underneath the monitor there is a small keyboard with which the perimetrist controls the test The results can be printed out on a separate dot matrix printer and stored on magnetic disc for later recall/analysis.

Ninety-four eyes of patients attending the outpatients clinics of 2 local hospitals were examined with the CFS2000. The patients were all referred to the hospitals with suspected glaucoma.

The threshold of each patient was established at the beginning of the examination with the screener in the threshold determination mode. In this mode different multiple stimulus patterns were presented at different intensities (0.1 log unit steps) until an intensity was found at which the patient missed approximately 50% of the stimuli Once the threshold had been established the instrument was put into the testing mode In this mode the intensity is automatically incremented by 0.5 log units above the threshold value All 132 stimuli were then presented at this intensity value. Any missed stimuli were initially retested at the same intensity and if missed on both occasions were entered into the computer as a 0.5 log unit miss. These stimuli were later retested at 0.8 and 1 2 log units above the threshold intensity. The CFS2000 quantifies visual field loss by testing at these 3 suprathreshold intensities.
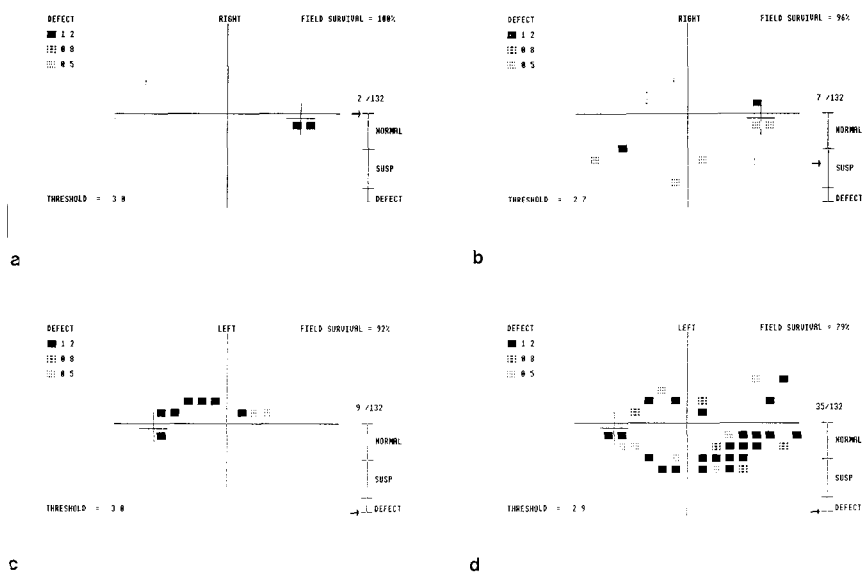
Figure 2 Typical results from the Henson-Hamblin CFS2000

The 26 retinal locations tested in the screening program are included in the full program which tests 132 locations. By testing all 132 stimulus locations we therefore have information on the screening program.

The two quantification systems both operate automatically throughout the examination. The first, that which evaluates the probability that the results come from a patient with a normal visual field, displays its results, on the monitor, in the form of an arrow and a scale (see Figure 2). The second, that which calculates the visual field survival, prints out its result at the end of a full examination

The visual field quantification systems operate in the following way For each pattern of misses a score is derived which takes into account the number of missed stimuli, the intensity at which the missed stimuli were, if at all, seen and whether the missed stimuli are clustered together. The formula for the derivation of the score is as follows:

$$\text{Score} = a \cdot \sum_{i=1}^{n} D + 2 \cdot b \cdot C$$

where
a   is a constant,
n   is the number of missed points,
D   represents the depth of any misses and is given a value of
1   for a stimulus missed at 0.5 log units above threshold,
2   for a stimulus missed at 0.8 log units above threshold, and
3   for a stimulus missed at 1.2 log units above threshold,

b   is a constant/function,
C   is the number of clusters; a cluster being defined as 2 missed points falling within 8.5 degrees of each other.

For the quantification system which evaluates the probability that a given result comes from a patient with a normal visual field both the constants 'a' and 'b' are 1. The position of the arrow corresponds to the score. The borders of normal/suspicious and suspicious/defect are based upon the results from a normal population.

For the quantification system which measures field survival the constant a = 100/396 and b is a function based upon the Gausian distribution

$$\frac{1}{\sigma\sqrt{2\pi}} \exp\left[-\frac{(X-\mu)^2}{2\sigma^2}\right]$$

These two values ensure
- that the field survival score goes from 100 to 0,
- that the measure of field survival is sensitive to clusters in the early stages of any defect,
- that as the defect enlarges the contribution of the cluster component reduces.

Missed stimuli that fall within the blind spot region are not included in either of the quantification systems.

Results

The quantification system of the CFS2000 classed 21 of the 94 eyes examined as having a defective visual field, 4 as having a suspicious visual field and 69 as having a normal visual field.

Figure 2 gives the visual field results from 4 of the eyes. The first, Figure 2a, has been classed as normal by the quantification system. Two stimuli have been missed at 1.2 log units above the patients threshold The field survival score remains at 100% because both of the missed stimuli fell within the blind spot region. The result shown in Figure 2b has been classed as suspect. The patient

Table 1 Comparison of the results from the screening program, which tests 26 retinal locations, and the full program, which tests 132 retinal locations

Full program	N	Screening program	
		Pass	Fail
Defective	21	2	19
Suspect	4	0	4
Normals	69	61	8
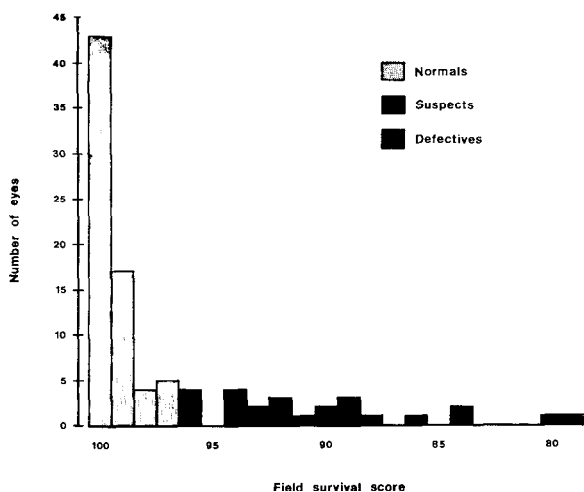
Figure 3 Distribution of visual field survival scores from 94 eyes of patients suspected as having glaucoma Patients visual fields have been classed normal, suspicious or defective on the basis of the CFS2000's quantification system

missed 4 non blind spot stimuli all in the inferior arcuate region. One of these stimuli was missed at 1 2 log units above the patients threshold while the other 3 were missed at 0.5 log units above the threshold. These 4 misses are arranged in 2 clusters. This increased the visual field score and therefore contributed to the suspect classification. The third and forth visual field examples have been classed as defective by the quantification system. Figure 2c is the result from a patient with an early defect and a visual field survival score of 92% while Figure 2d is from a patient with a more advanced defect and a field survival score of 79%. Figure 2d is the most advanced visual field defect included in our sample.

The distribution of field survival scores is given in Figure 3. All of the patients classed as having a normal visual field had survival scores ranging from 97 to 100. The eyes classed as suspect had survival scores ranging from 94 to 96 and those classed as defective had scores ranging from 79 to 96.

The criteria for a patient failing the visual field screening test is them missing one or more non blind spot stimuli at 0 5 or more log units above their threshold. Table 1 gives the number of patients that would pass and fail the screening test using these criteria. The patients visual fields have been classified as defective, suspect and normal with the full 132 stimulus program. On the basis of this data, the sensitivity of the screening test is 90.5% and the specificity 88 4%.

Discussion

It is very important, when designing a visual field screening test, to develop a strategy that is both sensitive and specific to early glaucomatous visual field defects The results from this evaluation indicate that the sensitivity of the CFS2000's screening program is 90.5% and the specificity 88 4%. These results have been obtained from a sample of suspected early glaucoma cases in which the visual field defects were often very subtle and in which no advanced visual field defects existed

Of the 8 eyes which failed the visual field screening program and which later were shown by the full program to have a normal visual field, 4 had displaced blind spots. If these 4 are removed from the fail catagory then the specificity of the screening program increases to 95 2%.

The visual fields of the patients examined in this evaluation were classified as normal, suspect or defective on the basis of the quantification system included in the CFS2000 Obviously this quantification system will have its own sensitivity and specificity with the result that some cases classified as normal with this instrument may have been classed as defective if tested in some other way. The program used to classify the patients tested 132 retinal locations all of which fell within the central 30 degrees of the visual field This program is more extensive than most of the programs incorporated in visual field instruments. The sensitivity obtained with this program is likely to be close to the maximum that can be realistically obtained in a clinical environment.

All of the patients examined in this study were referred to the hospitals with suspect glaucoma in either one or both eyes Of the 94 eyes examined only 4% were placed within the suspect catagory by the CFS2000's quantification system This type of quantification system clearly differentiates the majority of eyes from suspect patients into those that have a normal visual field and those that have a defective visual field.

References

1 Sponsel WE, Dallas NL, Burbridge L: Visual field survival; the response to Timolol therapy in open angle glaucoma Br J Ophthalmol 67: 220–227 (1983)

Author's addresses:
Department of Optometry,
University of Wales,
Colum Drive, Cardiff CF1 3EU, UK

IV.2 Visual field screening using two symmetrical stimuli – prototype of a new automatic perimeter

H KOSAKI and H. NAKATANI
Osaka City, Japan

Abstract

We have devised a method of screening glaucoma and hemianopsia patients using two symmetrical stimuli, and developed a new automatic screening perimeter which incorporates this method, with 8 programs available.

We have obtained satisfactory results in detecting the early stage glaucoma and hemianopsia. However, we obtained a false-positive reaction with normal eyes, and learned that interpretation of results from normal eyes needs further improvement.

Introduction

The majority of patients needing visual field screening are those suffering from glaucoma and hemianopsia which cannot be found by a funduscope For visual field screening for these two diseases, we have designed a diagnostic method using the difference in two symmetrical thresholds For glaucoma, we use one point above and one point below the horizontal meridian on the nasal side, and one point above and one point below the horizontal meridian on the 15^c circle. For hemianopsia, two points, one on the right and one on the left of the vertical meridian are measured. We present here a prototype of an automatic screening perimeter which incorporates this symmetrical method, and we would welcome comments.

Description of perimeter (Fig. 1)

Dimensions: 580 mm (w) × 560 mm (d) × 650 mm (h), weight 43 kg
Specification: 60 cm rear diameter, 30° central visual field, 31.5 asb.
Stimulus· Luminance range 1.3–1,000 asb Visual anglc 10′ (0 9 mm in diameter).
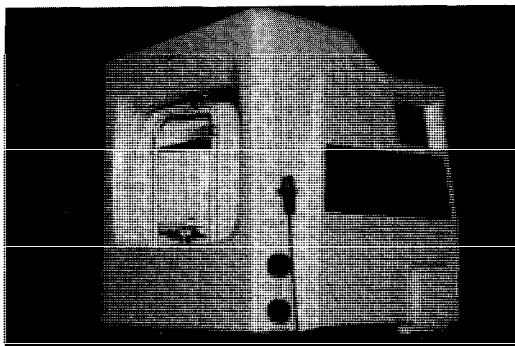
Figure 1 Demonstration of the perimeter (KP-132)

Red (660 nm), LED, single stimulus, 132 points in total
Stimulus duration: 0.8 sec , 1.0 sec., 1.2 sec.
Stimulus interval: 0.8 sec , 1 0 sec., 1.2 sec.
Fixation. Single fixation. Central visual angle 2° (10.5 mm in diameter) (flashes when eyes not fixed, 2 brightness levels).
Fixation monitor: Fixation checked by an automatic infrared light with a TV monitor.
Programs: 8 programs. No 1 DEMO, No. 2 CENT TH, No. 3 STANDARD 1, No. 4 GL-NASAL, No. 5 GL/15 CIRCLE, No. 6 HEMI, No. 7 STANDARD 2, No. 8 CIRCLE

Main programs

Program No. 3: STANDARD 1 (for general screening) (Fig. 2). The stimuli are presented randomly (total: 99 points), and the luminance levels are fixed (3 levels· 100, 315, 1000 asb).
Program No 7: STANDARD 2 (for general screening) (Fig. 2). The stimuli are presented randomly (total of 99 points), and the luminance levels are selected
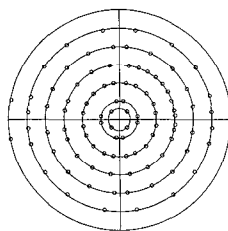
Figure 2 STANDARD (R)
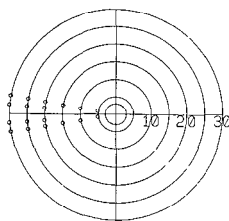
Figure 3 GL-NASAL (R)

based on the individual's normal sensitivity curve (I.N S C). Abnormal positions are detected by the presence or absence of reaction.

Program No. 4: GL-NASAL (for screening glaucomatous nasal step) (Fig. 3)

Stimulation by pairing two symmetrical stimuli, one above and one below the horizontal meridian (total of 9 pairs), the stimuli are presented alternately, and measurements are taken from each pair in turn, from the nasal side towards the center.

Judgment. when a threshold difference between the upper and lower points of a pair shows more than 4 dB, it is regarded as an abnormal response.

Program No. 5: GL-15 CIRCLE (program for screening glaucomatous Bjerrum scotoma) (Fig. 4).

Stimulation two symmetrical stimuli, one above and one below the horizontal the horizontal meridian on the 15° circle are paired (total of 17 pairs), and the stimuli are presented alternately Each pair is measured in turn from the temporal side moving towards the center. When the measurement of a pair finishes on the vertical meridian, the measurement is then taken from the pairs on the nasal side moving towards the center.

Judgment: When a threshold difference between the upper and lower points of a pair shows more than 4 dB, it is regarded as an abnormal response.

Program No. 6: HEMI (program for screening hemianopsia) (Fig. 5).

Stimulation: stimuli are set symmetrically right and left of the vertical meridian, and to avoid inaccurate fixation, stimulation is in a random order.

Judgment. by pairing the two symmetrical stimuli right and left of the vertical meridian, if a threshold difference between the points of each pair indicates more than 4 dB, it is regarded as an abnormal response

Figure 4 GL-15 CIRCLE
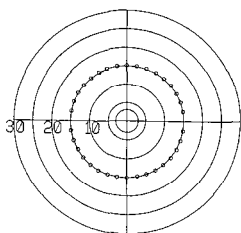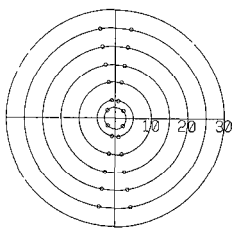
Figure 5 HEMI

Results

The results of the two symmetrical stimuli method for glaucoma

The result from programs GL-NASAL and GL-15 CIRCLE for detecting early stage primary glaucoma (Kosaki's classification [4] IIa, IIb) and middle stage primary glaucoma (Kosaki's classification [4] IIIa) are shown in Table 1.

With primary glaucoma patients there were 58 eyes from 35 patients (14 eyes from 9 males and 44 eyes from 26 females), and their ages ranged from 17–80 years with a mean age of 60.8 years. According to Kosaki's classification of chronic glaucoma; IIa is the stage at which abnormality is found in the area inside the isopter I_3 by Goldman kinetic topography, IIb is the stage at which abnormality is found in the area inside the isopter I_4, and IIIa is the stage at which abnormality is found in isopter V_4 but the visual defect is limited to within one quadrant.

Table 1 Results of two symmetrical stimuli method (for glaucoma) Number of cases: 58 eyes

Program No 4 (GL-NASAL)	(+)	(−)	Total
Kosaki's classification Stage IIa	34	0	34
Kosaki's classification Stage IIb	8	0	8
Kosaki's classification Stage IIIa	16	0	16
Total	58 (100%)	0	58
Program No 5 (GL-15 CIRCLE)	(+)	(−)	Total
Kosaki's classification Stage IIa	34	0	34
Kosaki's classification Stage IIb	8	0	8
Kosaki's classification Stage IIIa	16	0	16
Total	58 (100%)	0	58

(+) Abnormality detected by programs GL-NASAL or GL-15 CIRCLE
(−) Abnormality not detected by these two programs

Patient Name ___ E.M. ___ 52 yrs Glaucoma L
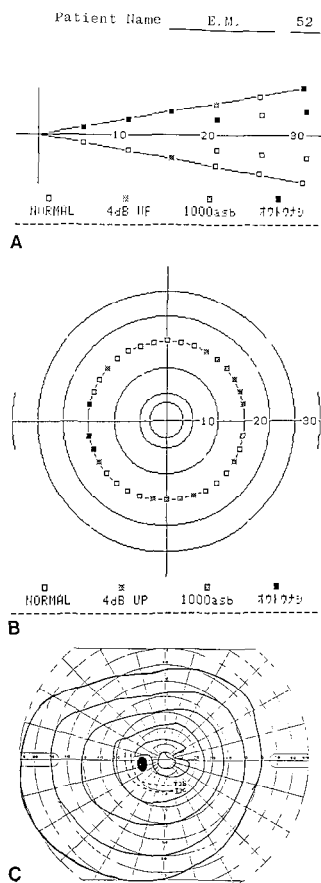
Figure 6 a Result with GL-NASAL b Result with GL-15 CIRCLE c GP visual field topograph

The results were positive for all 58 eyes, and the screening record for one of the cases is shown in Fig. 6.

The results of the symmetrical method for hemianopsia

In screening for hemianopsia, we used program HEMI, and the results were positive in all cases One of the cases is shown in Fig. 7

The results of the symmetrical method for normal eyes

Table 2 shows the results of screening normal eyes by using programs GL-NASAL, GL-15 CIRCLE, and HEMI

Patient Name   M B   67 yrs Hemi R

A

B
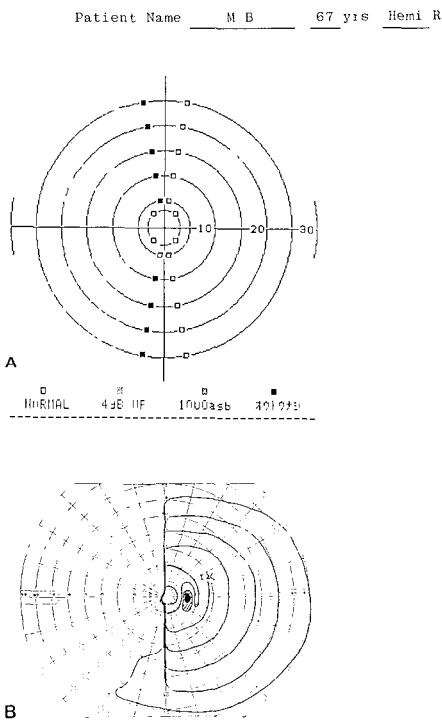
Figure 7 a Result with HEMI b GP visual field topograph

The breakdown of the normal eyes was 36 eyes from 18 patients (12 eyes from 6 males and 24 eyes from 12 females), and their ages were from 19–56 years with a mean age of 31.6 years These had normal eyesight, the refraction abnormality was within ± 2.0 D, with no abnormality in the cornea, lens, vitreous body, or fundus, with normal ocular pressure, and no abnormality in Goldman's kinetic topography

The results using these programs on the 36 eyes gave false-positive readings of 4, 7, and 3 respectively. The rate of these false positives was 11 1%, 19.45%, and 8.3%

Table 2 Results of the two symmetrical stimuli method (for normal eyes) Number of cases: 36 eyes

	(+)	(−)	Total
GL-NASAL	4 (11 1%)	32	36
GL-15 CIRCLE	7 (19 4%)	29	36
HEMI	3 (8 3%)	33	36

(+) Abnormality detected by these programs
(−) Abnormality not detected by these programs

Discussion

In our busy daily clinical work, it is not desirable from the point of the time taken or the physical burden on patients to perform either extensive kinetic or static perimetry in all patients. Under these circumstances, visual field screening tests become necessary. However, if we want to find all the visual field abnormalities in screening, we have to carry out complicated tests. It becomes time consuming, and the purpose of the screening will be lost. Therefore, screening should focus on the diseases which can be easily detected by the field test, and not by the other tests. Diseases related to the fundus are easily found by a funduscope, so it becomes limited to the diseases line glaucoma and hemianopsia When the screening is focused on these two diseases, the number of stimuli can be limited, testing becomes simple, and so the screening becomes meaningful.

It is well-known that the visual patterns of glaucoma progression take specific courses (8 types). These patterns involve a scotoma in the Bjerrum area (mostly in the upper temporal part), an arcuate scotoma (mostly in the upper part), a horseshoe scotoma, a nasal step (mostly in the upper part), a break-through (linking of an arcuate scotoma and a nasal step), an upper hemianopsia (as non-specific type, lower hemianopsia), a field separation (separation of fixation area and peripheral area), and a field remaining in the temporal periphery. Visual field defects usually start in the Bjerrum area and the nasal area on each side of the horizontal meridian, and then spread.

This means that for detecting glaucoma, we have only to test two areas, that is, the Bjerrum area and the area aromol the horizontal meridian area.

For these reasons, we have made two programs GL-15 CIRCLE and GL-NASAL. For GL-15 CIRCLE, the stimuli are located above and below the horizontal meridian on the 15° circle. For GL-NASAL, they are above and below the nasal side of horizontal meridian These programs measure the threshold difference between the upper and lower symmetrical points.

For hemianopsia, we developed the program named HEMI. For this program, we located the stimuli on both the right and the left of the vertical meridian, and the threshold difference between these two symmetrical points is measured In actual use of these three programs (although the number of cases are not enough), we have obtained a satisfactory result, and could establish that our two symmetrical stimulus method is correct in its basic concept.

However, we have obtained a fair proportion of false-positive reactions (average 13%) in normal eyes. 'The flicker triple circle method', which was published at 4th IPS. Symposium in 1980, also showed 13% false-positive reactions. Considering these two results, we assume that some normal eyes have a reduced sensitivity in the upper temporal part of the Bjerrum area We will study and improve the interpretation of results from normal eyes

When considering the problems of screening perimeters of glaucoma patients, firstly there is the position for checking As mentioned before, the visual defect in

glaucoma always occurs in the Bjerrum area, and also around the nasal side of horizontal meridian. However, at a very early stage the defect may be seen in other areas, but only rarely. At this stage, even if glaucoma is not found, the visual defect is easily restored with treatment If we have to screen the patient for very early stage glaucoma, many points must be checked, so we cannot screen quickly.

Secondly, when we seek speedy screening, our two symmetrical stimuli method is very good Under the static visual field methods, suprathreshold screening is common In this screening, even if no abnormality is found, we cannot classify a patient as 'no abnormality' without repeated examinations using several levels of low stimulus luminance. In the threshold screening, if the value is different from normal, it is said to be abnormal. However, the normal value differs greatly depending on age, and strictly speaking, it also differs depending on the perimeter Therefore, in diagnosing abnormality, it is really necessary to define the normal value using many data. In the two symmetrical stimuli method, screening is done by detecting the difference between the upper and lower readings in the Bjerrum area and on the nasal side of the horizontal meridian, so it is not necessary to set a normal value The visual field screening is done under the presumption that a further standard visual examination is subsequently done in positive cases

Thirdly, when we compare perimeters, there is the historically famous Armaly method [1] This Armaly method is very good (using Goldman's perimeter), but skill is needed since the kinetic and static methods must be combined manually.

With the Armaly method, there is a risk of not detecting defects in the lower temporal area, so Drance et al. modified this method [2]. However, since their analysis involves a very complicated operation, the examination by standard kinetic perimeters is quicker if operated manually. So, from a screening point of view, Drance's method is less valuable

The automatic perimeters with proper stimulus positions for both glaucoma and hemianopsia screening, are limited to the very recent ones like that produced by Dicon, or by Humphrey. From a technical point of view, as mentioned above, we think that our two symmetrical stimuli method gives better screening.

References

1 Armaly MF: Ocular pressure and visual fields – a ten year follow-up study Arch Ophthal 81: 25–40 (1969)
2 Rock WJ, Drance SM, Mogan RW: Modification of the Armaly visual field screening technique for glaucoma Can J Ophthal 6: 283–292 (1971)
3 Drance SM, Anderson DR: Automatic perimetry in glaucoma – A practical guide Grune & Stratton, USA, 1985
4 Kosaki H, Nakatani H, Tsukamoto H, Nakauchi M: Topographical studies of field defects in various stages of primary chronic glaucoma Doc Ophthal Proc Series 14: 121–129 (1977)

5 Kosaki H: The earliest visual field defect (IIa stage) in glaucoma by kinetic perimetry Doc Ophthal Proc Series 19: 255–259 (1979)
6 Kosaki H: A new screening method for the detection of glaucomatous field changes – the flicker triple circle method Doc Ophthal Proc Series 26: 253–258 (1981)
7 Kosaki H, Nakatani H: Computer analysis of kinetic field data determined with a Goldman perimeter 5th International Visual Field Symposium, pp 473–477 Dr W Junk Publishers, Dordrecht, 1983
8 Kosaki H, Nakatani H, Azuma I, Sakaguchi K: Practical use of area computation for assessment of visual field: Analysis of the result of mecobalamin therapy for visual field defects in chronic glaucoma 6th International Visual Field Symposium, pp 435–442 Dr W Junk Publishers, Dordrecht, 1985

Editorial comment

The concept of comparing the sensitivity of a position with its mirror-image position in the other visual field half (whether around the horizontal or vertical axis) has been used both for glaucoma and for hemianopsias These authors propose to use this comparison for a screening method In present-day automated perimetry the threshold values of a given position are compared with a normal value, either derived from a normal population or computed from the individuals own normal positions in the visual field A method as proposed by the authors should be compared with one of the above mentioned methods.

The authors state that all glaucomatous defects begin in the Bjerrum area or in the nasal area. This statement does not take in account the work by Aulhorn, Heyl and others that has presented the frequency distribution of early glaucomatous defects. Furthermore early nasal defects outside 30°-eccentricity may occur in 10% of cases (Werner, Caprioli and others). If a general reduction of sensitivity exists in early glaucoma the 'symmetrical stimuli' will not detect it

Finally the sensitivity of a new screening method should be compared with the results of repeated carefull threshold measurements using a high resolution It should be indicated what size and depth of defect will go undetected A 100% succes-rate as reported by the authors will depend on the selection of the defects to be detected by the method

IV.3 A new computerized perimeter ('Competer 750') for examination of neuro-ophthalmic patients

H. BYNKE, C.E.T KRAKAU, R ÖHMAN and A. AITTALA
Lund and Malmö, Sweden

Abstract

Computerized perimeters provided with suitable threshold programmes, e.g. the 'Competer', can test the visual field more accurately than is feasible with manual routine methods However, a problem in neuro-ophthalmology is that hemianopic field defects may be hard to characterize and may even be missed if the examination is confined to the central area, as was the case with the first 'Competer' models. Although the test point pattern was enlarged to cover the area inside 35°, further experience showed that manual perimetry still had to be added in too many cases. Therefore, a new model, 'Competer 750', was constructed. In contrast to earlier models this is a bowl perimeter, which can test the field out to 45° nasally and 75° temporally This instrument can replace manual perimetry in almost all cooperative neuro-ophthalmic patients with a visual acuity of 0.1 or more and is superior to manual perimetry for detecting and following up neurological field defects.

Introduction

Automated perimeters provided with suitable threshold programmes are capable of testing the visual field more accurately than is feasible with manual routine methods, not only in glaucoma (5–8) but also in neuro-ophthalmology [1, 2, 4, 9, 10]. The computerized perimeter 'Competer' has this capacity [1, 2, 4–7). However, although the test point pattern of the first models, which covered the central field area between 5° and 20°–25°, was enlarged in order to explore the area between 2.5° and 35° [4], further experience showed that many neurological field defects were hard to characterize, rendering topical diagnosis difficult In addition, it was demonstrated that the depth of most incomplete bitemporal and homonymous defects increases towards the periphery [2]. As a matter of fact, it is not very rare for hemianopic defects to be restricted to peripheral parts of the
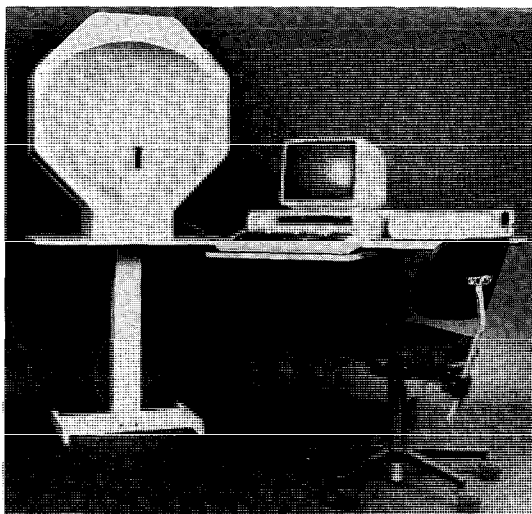
Figure 1 'Competer 750' Bowl perimeter and personal computer with printer and monitor

field, the central area being spared. Such defects may be missed if the examination is confined to the central 20° area, and are often hard to evaluate even though the area between 20° and 35° is explored. For these reasons, manual perimetry must still be added in too many cases, particularly at the first visit of the patient. This is certainly not very practical.

In order to make the 'Competer' capable of replacing manual perimetry in as many cases as possible, further enlargement of the test point pattern had to be accomplished without prolonging the test session too much. This article deals with a new model, 'Competer 750', which can test the visual field out to 45° in the nasal hemifield and out to 75° in the temporal hemifield.

Instrument

Major components of the equipment are a bowl perimeter and a personal computer with printer and monitor (Fig. 1)

In order to make exploration of the peripheral field possible, the flat board of earlier 'Competer' models was replaced by a bowl.

As in previous models the stimuli are produced by light-emitting diodes (LEDs) These are mounted on the spherical surface and covered by a white, translucent film, making them invisible when unlit. They are exposed one after another in a randomized sequence and the patient responds by pressing a button when they are seen. The exposure time of the LEDs can be varied between 0.25 and 1.0 sec, but is routinely kept at 0.5 sec. If the button is not pressed within

2.0 sec after the start of the exposure, the response is recorded as negative by the computer. Depending on the answers of the patient the intensity of the LEDs is decreased or increased by the computer until the threshold has been measured at all points. The LEDs can be lit at 16 intensity levels, the ratio between two adjacent levels being 1:2. A monitor was introduced for watching the procedure, but in most cases the method requires attendance only during the first few minutes of the test session Since the original projection system for checking the fixation was afflicted with practical problems, it was replaced by a new system, comprising an automatic search for a reliable test point (LED) inside the blind spot area, which is then used for checking the fixation.

At the end of the examination the results are charted by the printer The print-out was described previously [4] The results can be stored on discettes.

The test points are located in concentric circles, but their number and distribution differ from those of earlier models (Figs 2–4) The *central part* comprises 60 test points located symmetrically at 2.5°, 5°, 10°, 15°, and 20° of eccentricity. The *peripheral part* comprises another 42 tests points. Eigtheen of them are located in the nasal hemifield at 20°, 30° and 45° and 24 in the temporal hemifield at 20°, 30°, 45°, 60° and 75° On each of the last two circles there are only 3 test points, since preliminary examinations showed that false positive responses were common, particularly in the superior peripheral area

As an option chosen at the start of the test, even the size of the blind spot can be evaluated using a set of 15 additional test points reserved for this purpose (Fig 5).

Attaching a personal computer to the perimeter involves great advantages. Besides its capacity of storing the test programmes and guiding the test procedure, it stores the test results which can later be drawn It is further possible to apply programmes for an analysis of the trend in a series of test results similar to those used in the system for a glaucoma care unit [6]. An automatic system for interpretation of the outcome belongs to projects at work.

Testing procedure

A very accurate examination of the *central field area* can be performed using a threshold programme. The test logic of this programme was described previously [4]. The duration of the test is about 6 min if the central area is normal but may be longer if there are defects. For a less detailed examination, a 'suprathreshold' screening programme can be used. Points seen at the suprathreshold intensity level are not tested any further, but points not seen are tested until the threshold is found, using stepwise higher intensities Screening of the center takes only 3–4 min and may be the best choice e.g. in sick patients and in children. When needed, correction lenses are applied.

The *peripheral area* can be tested as a second step, or in unbroken succession. The threshold values obtained at the 15°–20° points of the central field are spread

Modal value = 10
Performance = 392

Modal value = 10
Performance = 579

L.S, age 53
Right eye
June 13, 1986

Modal value = 10
Performance = 474

Modal value = 10
Performance = 692

L.S., age 53
Left eye
June 13, 1986
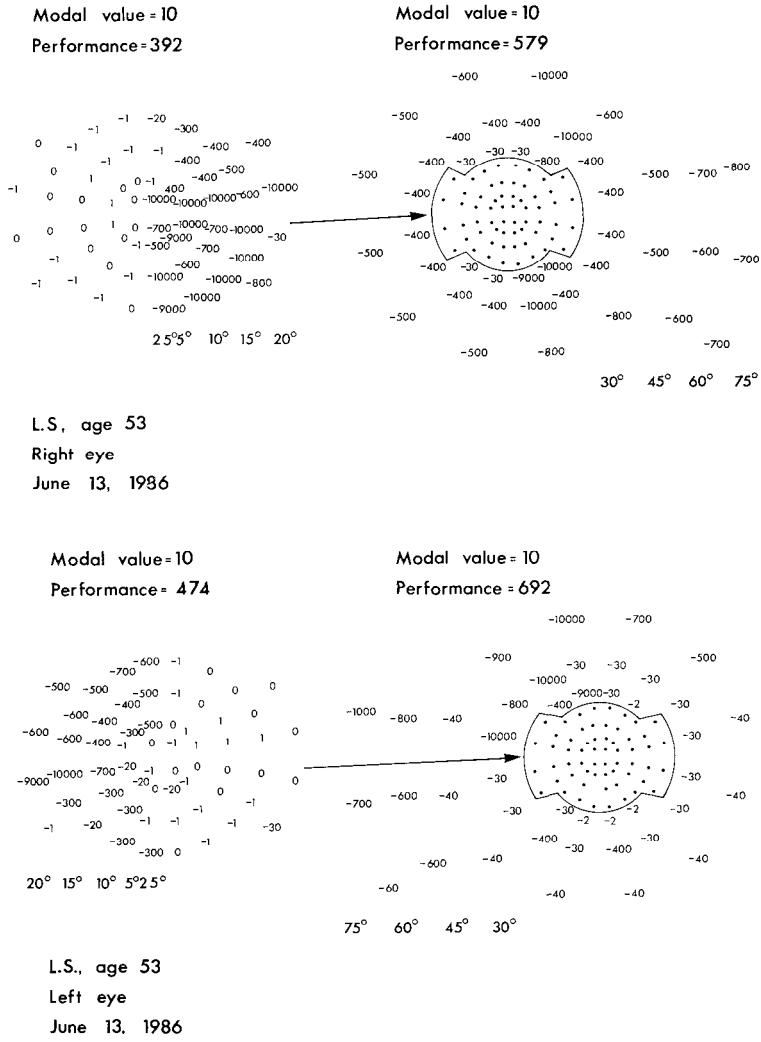
Figure 2 Bitemporal hemianopia (see text) In both charts the central part was extracted and placed to the left

radially to the peripheral points and these values are increased in intensity by one or two steps and are used as the starting levels in testing the periphery. The threshold is determined by the first 'change of sign' met with, i.e. the faintest level seen followed or preceded by the strongest level not seen. The duration is 3–4 min. Since the depth of hemianopic defects is usually larger in the periphery than in the center [2], it is likely that very few peripheral defects are missed although this programme is relatively simple.

After completing the peripheral test the total field is chartered (Fig. 4).

Modal value = 10
Performance = 580

Modal value = 10
Performance = 851
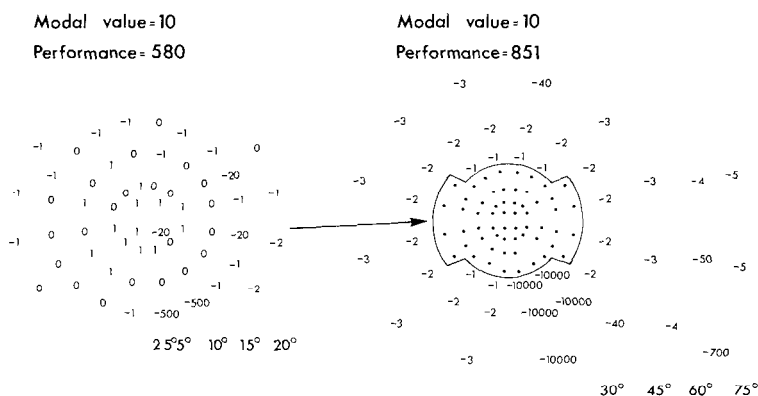
KO, age 38
Right eye
June 19, 1986

25°5° 10° 15° 20°

30° 45° 60° 75°

Modal value = 10
Performance = 584

Modal value = 10
Performance = 852

20° 15° 10° 5°25°

75° 60° 45° 30°
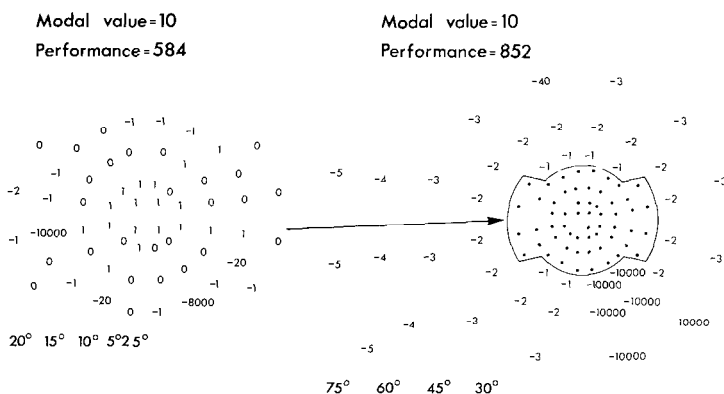
KO, age 38
Left eye
June 19, 1986

Figure 3 Homonymous defects in right inferior quadrants (see text)

Statistical analysis of results

Since the results are numerical, virtually all kinds of calculations can be made by the computer. The detection and follow-up of visual field defects are facilitated by particular statistical parameters, which are printed on the charts [1, 4] (Figs 2–4). For 'Competer 750' the elaboration of these parameters is not yet finished. The 'performance' is the sum of all test point values. Most important is this parameter in the central area when the threshold programme is used. The normal value is 500–600.

```
MODAL VALUE= 10   PERFORMANCE= 845
PERF.C MAS        PERF C TEMP    ZEROES PERIPHERY
295               278            0
```
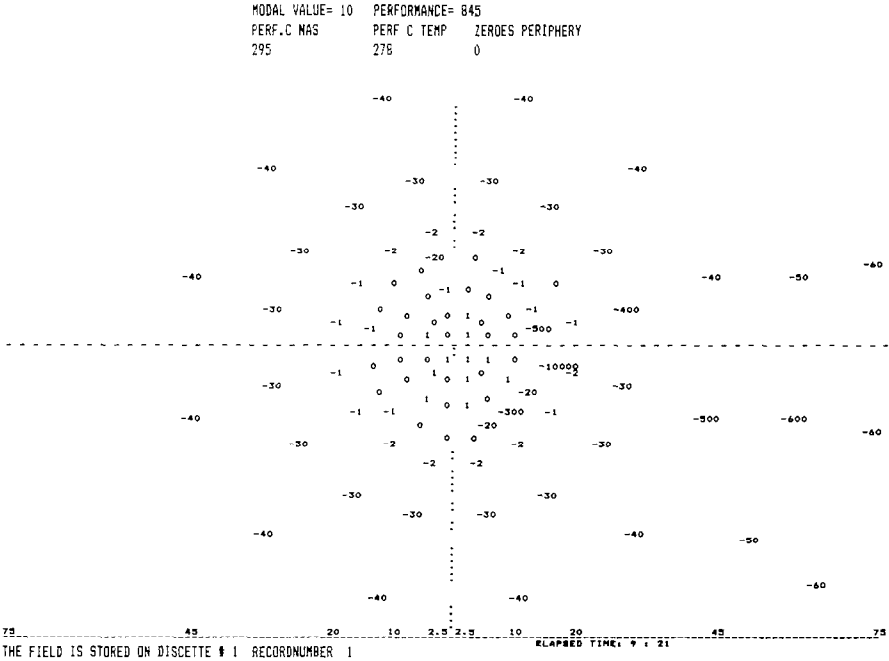
Figure 4 Central and peripheral field as plotted by the printer

Programmes for analysis of sequences of fields include regression analysis, plotting of 'performance' values and of successive quadrant profiles.

Clinical applications

The instrument has been used in the Department of Neuro-Ophthalmology, University Eye Clinic, Lund, for about two years. The test point pattern was modified in several steps on the basis of increasing clinical experience with the

20°   15°   10°   5° 2 5°
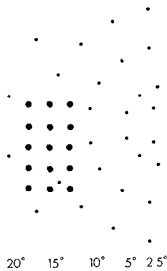
Figure 5 Additional test points for plotting the blind spot

instrument. About 500 patients with neuro-ophthalmic problems were examined using the optimized test point pattern described It was found that the instrument can replace manual perimetry in almost all cooperative patients with a visual acuity of 0 1 or more. In addition, it was confirmed that this instrument, like earlier models of the 'Competer', may be superior to manual perimetry (Goldmann's kinetic perimeter), particularly for detecting and following up small and shallow neurological field defects, e.g central and paracentral scotomas in demyelinating disorders, homonymous hemianopic scotomas in occipital lesions and bitemporal defects before and after treatment of suprasellar tumours The instrument facilitated the detection of very small bitemporal defects, a common finding in patients with pituitary adenoma treated during the last years [3]

The visual field charts of two cases were selected for illustration. The first case was a 53-year-old man with bitemporal hemianopia before the removal of a large pituitary adenoma (Fig. 2). The hemianopia was partly absolute in the right field and relative in the left. It should be noticed that the sensitivity was reduced also in the nasal periphery. This is common in chiasmal compression but may be hard to reveal with manual perimetry [1, 2]

The second case was a 38-year-old woman with homonymous defects in the right inferior quadrants (Fig. 3). Computed tomography and angiography were negative, but the history, visual fields and other clinical findings indicated that the lesion was vascular and situated in the superior part of the left occipital lobe It should be noticed that the central area was almost spared, although there were absolute congruous defects in the periphery, demonstrating the importance of testing that part of the field.

Acknowledgement

References

1 Bynke H: A statistical analysis of normal visual fields and hemianopsias recorded by the computerized perimeter 'Competer' Neuro-ophthalmology 3: 129–137 (1983)
2 Bynke H: A study of the depth of hemianopic field defects for optimizing computerized perimetry Neuro-ophthalmology 4: 237–247 (1984)
3 Bynke H: Pituitary adenomas with ocular manifestations Incidence of cases and clinical findings 1946–1984 Neuro-ophthalmology 6: 303–311 (1986)
4 Bynke H, Krakau CET: A modified computerized perimeter and its use in neuro-ophthalmic patients Neuro-ophthalmology 2: 105–115 (1981)
5 Heijl A: Computerised perimetry Trans Ophthalmol Soc UK 104: 76–87 (1984)
6 Holmin C, Krakau CET: Regression analysis of the central visual field in chronic glaucoma cases A follow-up study using automatic perimetry Acta Ophthalmol 60: 267–274 (1982)

7 Krakau CET: Aspects of the design of an automatic perimeter Acta Ophthalmol 56: 389–405 (1978).

8 Leydhecker W: Perimetry update Ann Ophthalmol 15: 511–543 (1983)

9 Wildberger H: Zum Nachweis der zentralen Empfindlichkeitsverminderung bei Optikus-Neuropathien mit der Computer-perimetrie (Octopus) und mit den visuell evorzierten Potentialen (VEP) Klin Monatsbl Augenheilk 184: 377–381 (1984)

10 Younge BR: Computer-assisted perimetry in visual pathway disease: Neuro-ophthalmic applications Trans Am Ophthalmol Soc 82: 899–942 (1984)

Author's address:
Dr Hans Bynke,
University Eye Clinic, S-221 85 Lund, Sweden

IV.4 Sappar: an auxiliary program for SAPRO

A.T. FUNKHOUSER and H P. HIRSBRUNNER
Berne, Switzerland

Abstract

The SAPRO spatially-adaptive program for the Octopus automated perimeter uses various parameters in order to specify its operating environment. Collections of 22 such parameters, which comprise the so-called subprograms, control program functions such as intergrid relationships as well as upper and lower limits of grid measurement activity. With the new SAPRO parameter program SAPPAR, the user is enabled to modify one (or more) of the ten subprograms and thus customize it for his or her own requirements. SAPPAR usage and operation is described.

SAPPAR stands for SAPRO PARameter manager. For its operation, SAPRO utilizes many parameters. Some of these are set up by the operator in the SAPRO dialogue phase while others (22 in all) are taken over as a predetermined set known as a 'subprogram'. There are 10 such subprograms designated HO to H9. Five of these are currently defined and available for use, while the other five can be modified for specific applications Using SAPPAR, the SAPRO user is able to alter one of the predefined subprograms, or configure one of the not-yet defined subprograms for his or her own use.

A subprogram can be protected from inadvertant changes or blocked from listing and use. With the ALTER STATUS option, a protected subprogram can have its protected status changed so that alterations can be made and then re-protected. Similarly, a blocked subprogram can be unblocked so that it can be modified, listed, and used.

After calling up SAPPAR, the user can:
- Print a DIRECTORY of the unblocked subprograms and their labels (a typical example is shown in Table 1).
- LIST a particular unblocked subprogram (see Table 2).
- CHANGE an unblocked subprogram label and/or a particular pair of subprogram parameters.
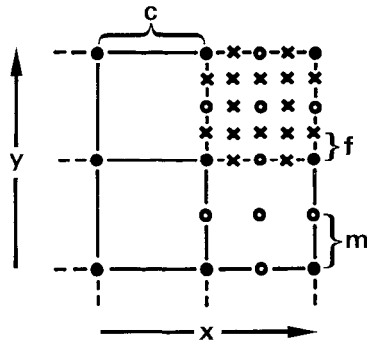
Figure 1 The three grids and their spacing relationships

- Change an unblocked subprogram label and/or SOME or all of the subprogram parameter pairs
- EXIT from SAPPAR and save a revised set of subprograms.
- QUIT SAPPAR, retaining the previous set of subprograms.
- RESTORE the previous set of subprograms without leaving SAPPAR.
- ALTER protected/blocked status of a subprogram

The 22 parameters affect SAPRO operation in the following ways:

a) Four *scaling factors* (x and y directions) set the spacings of the coarse and medium grids with respect to the fine grid spacing, thereby determining their spatial resolution.

That is, if f = fine grid spacing, m_x, m_y = medium grid spacings (x, y directions), and c_x, c_y = coarse grid spacings (x, y directions), then $m_x = S_{mx} \cdot f$, $m_y = S_{my} \cdot f$, $c_x = S_{cx} \cdot m_x$, and $c_y = S_{cy} \cdot m_y$.

S_{mx}, S_{my}, S_{cx} and S_{cy} are the scaling factors. Normally, $S_{mx} = S_{my} = S_{cx} = S_{cy} = 2$, as in Figure 1.

b) The *minimum luminance interval* sets the finest luminance step (usually 2 dB) used in the examination (shown schematically in Figure 2).

c) The *reference niveau* sets the value with respect to the age-corrected normal value where measurement begins (see Figure 2). If zero (the usual case) initial

Table 1 A typical SAPPAR directory (subprograms H6, H8–H9 are blocked)

Program number		Program label	
H0	*	NON-ADAPTIVE	
H1	*	PERCENT LIMITS: 30/0	
H2	*	PERCENT LIMITS: 25/5	protected
H3	*	PERCENT LIMITS: 25/10	
H4	*	NO FINE GRID	
H5		USER LABEL 2	
II7		USER LABEL 2	unprotected
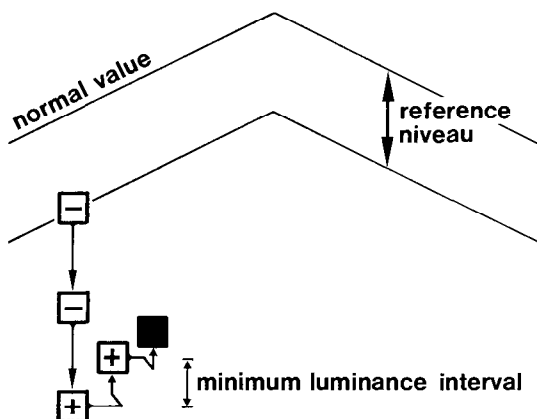
Figure 2 A schematic hill of vision' showing SAPRO bracketing, beginning at the reference niveau
The minimum luminance interval is also depicted

measurement starts with the normal value. If greater than zero, initial measurement begins above the normal value If negative, initial measurement begins below the normal value.

d) Six upper and lower *loss limits* for the coarse, medium, and fine grids determine the loss ranges where measurement takes place or ceases. (Loss is defined as the difference between the measured value and the age-corrected normal value for the location examined.) In addition, the coarse grid limits control activation of the medium grid, while the medium grid limits set boundaries for the activation of the fine grid Three upper loss limits are shown in Figure 3.

e) Six upper and lower *differential light sensitivity (d l.s) limits* for the coarse, medium, and fine grids are similar to the loss limits described in d, but are d.l.s limits. Three lower d.l.s. limits are also shown in Figure 3

Table 2 A typical SAPPAR subprogram listing

THIS IS A LABEL		
1	X, Y MEDIUM GRID SCALING FACTORS:	2/2
2	X, Y COARSE GRID SCALING FACTORS:	2/2
3	MIN LUMINANCE INTERVAL, REFERENCE NIVEAU:	2/0
4	UPPER, LOWER COARSE GRID LOSS LIMITS:	50/−50
5	UPPER, LOWER COARSE GRID SENS LIMITS:	51/0
6	UPPER, LOWER MEDIUM GRID PERCENTAGES:	30%/0%
7	UPPER, LOWER MEDIUM GRID LOSS LIMITS:	− 6/−50
8	UPPER, LOWER MEDIUM GRID SENS LIMITS:	51/4
9	UPPER, LOWER FINE GRID PERCENTAGES:	20%/0%
10	UPPER, LOWER FINE GRID LOSS LIMITS:	− 10/−50
11	UPPER, LOWER FINE GRID SENS LIMITS:	51/6
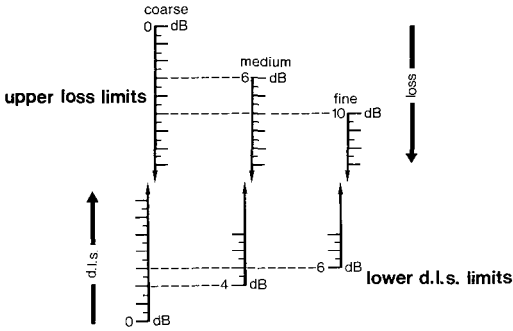
Figure 3 Typical upper loss limits and lower d l s limits for the coarse, medium and fine grids

f) Four upper and lower *percentage limits* control medium and fine grid activation If negative, the fixed loss and d.l s limits, described in d and e, are used to limit grid activation and activity during a measurement. If positive, the percentage limits, based on the loss distribution encountered (histogram adaption) are used. Figure 4 shows two histograms, one from a slightly damaged visual field and one from a more disturbed one. The shaded portion in each histogram shows the corresponding part of the loss distribution that would be further examined if an upper percentage limit of 20% were to be employed (For a more detailed explanation of histogram adaption, see [1, 2].)
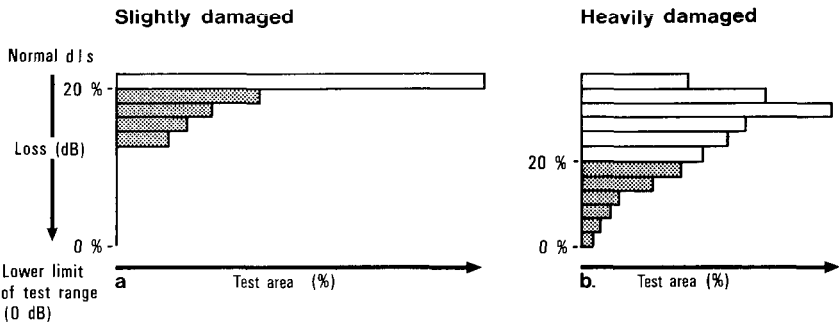
Figure 4 Two (simulated) histograms for a slightly damaged and a more severely disturbed visual field showing the portion of the loss distribution (shaded) which would be further investigated with higher resolution if a 20% percentage limit were to be employed

Acknowledgements

The authors are indebted to P Schneider and CH. Langenegger for help with the figures and C. Rutishauser for her assistance with the poster. They would also like to thank Prof. F. Fankhauser and M. Zulauf for guidance and helpful criticism

References

1 Fankhauser F, Haeberlin H, Funkhouser A: SAPRO operating manual INTERZEAG AG, 1986
2 Funkhouser AT, Fankhauser F: Spatially adaptive programs In: Whalen WR, Spaeth GL (eds) Computerized visual fields, pp 117–139 SLACK Thorofare, NJ, 1985

Author's addresses:
University Eye Clinic,
Insel Hospital, Bern, Switzerland

IV.5 Dynamic representation of the visual field

J.R. CHARLIER, J SACHY, F VERNIER and J.-C HACHE
Lille and Paris, France

Abstract

Computerized perimetry has not eliminated the need for operator's intervention throughout the examination This article describes a new technique for the representation of the visual field which provides the information necessary for a precise follow-up of the examination

It includes a graphic display of the estimated map of sensitivity thresholds which is updated according to the patient's response after each stimulus presentation Other graphic informations indicate the status of each testing point and its evolution along the examination.

Introduction

The dependance of the visual field examination results upon the communication between the patient and the operator has already been stressed. 'One principal psychological defect of computer perimetry is the disconnection of patient and operator. This disconnection is not desirable and means have to be provided to reestablish it' There are reasons to conceive stability of threshold as a function of time as a communicatory problem between perimetrist and patient [5]

The presently available automated perimeters are not suitable for such purpose as the operator has very little means of understanding the examination process.

Interactivity is also needed in order to cope with situations not expected in the examination protocol [2] Most experienced visual field technicians feel extremely frustrated when operating a computerized system They are often left with a supervision task when the computer system spends lengthy periods of time analysing areas presenting little or no interest without any consideration about the patient's exhaustion or distress.

The purpose of the present work is to develop new graphic, real time display techniques suitable for an interactive control of the examination and compatible
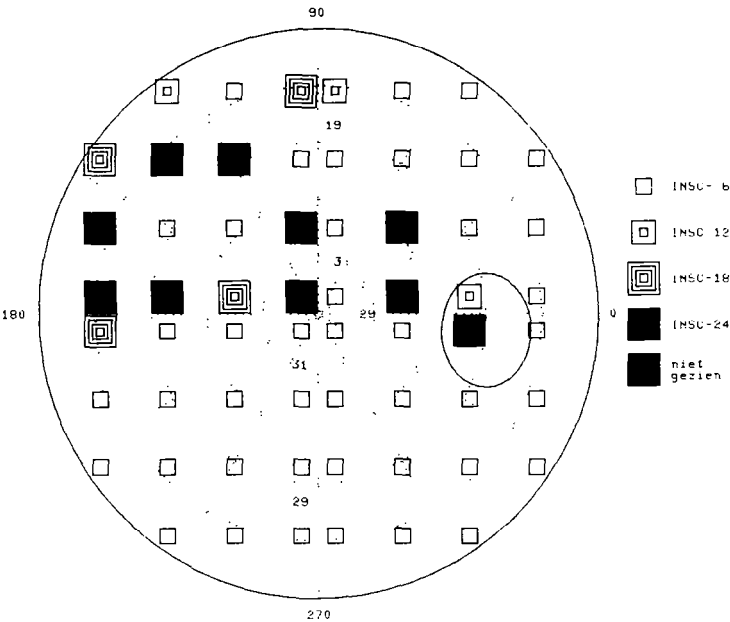
Figure 1 Representation of visual field data with a map of symbols (from Greve et al [6])

with the amount of information and real time constraints involved in a clinical situation

Background

In manual perimetry, most representations are bidimensional, due to the fact that only one parameter of the stimulus is changed at a given time: eccentricity versus the meridian angle in kinetic perimetry, luminance versus the eccentricity in profile static perimetry, or sensitivity versus the meridian angle in static perimetry along a given parallel [10].

Computers have introduced examination protocols which implicate the simultaneous variation of several parameters. For instance, visual stimuli are displayed at random, in order to avoid patient's anticipation and local photoadaptation effects

Several methods have already been proposed for the representation of visual field 3 dimensional data. First of all, maps of numbers of symbols (Figure 1) indicate the sensitivity threshold values in each test location. These maps do not provide a rapid understanding of the visual field as the evaluation of the shape and location of scotomas from a large array of numbers is rather difficult and time consuming.
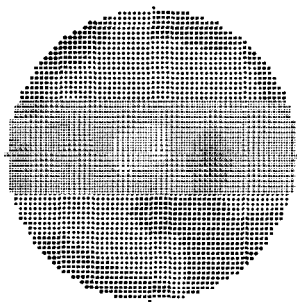
Figure 2 Representation of the visual field with an interpolated map (from Jay and Yavitz, [8])

Another solution is the use of a map interpolated between the measuring points (Figure 2) as initially proposed by [4] By means of a half tone display, the perception of the visual field topography is greatly improved However, it should be emphasised that these interpolated maps have to be used very cautiously. Most often, less than 100 of the 2000 or so displayed points are really measured. A scotoma located in between the measuring points does not show up and values different from the real threshold are displayed in the exact same location
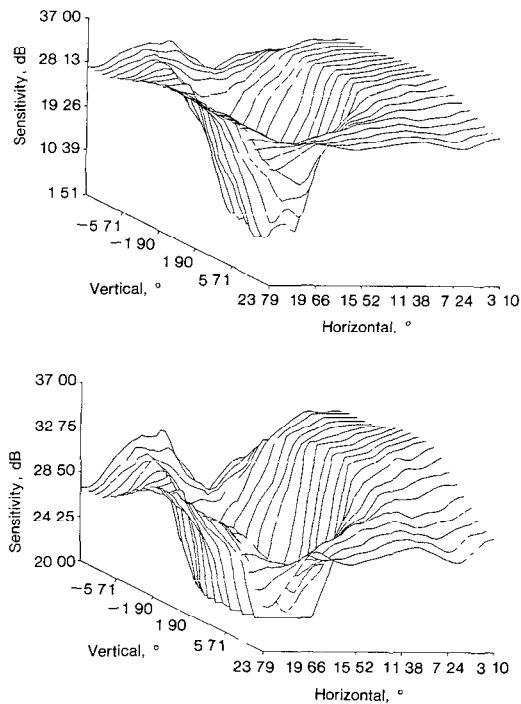
Figure 3 Three-dimensional representation of the visual field (from Hart and Hartz [7])
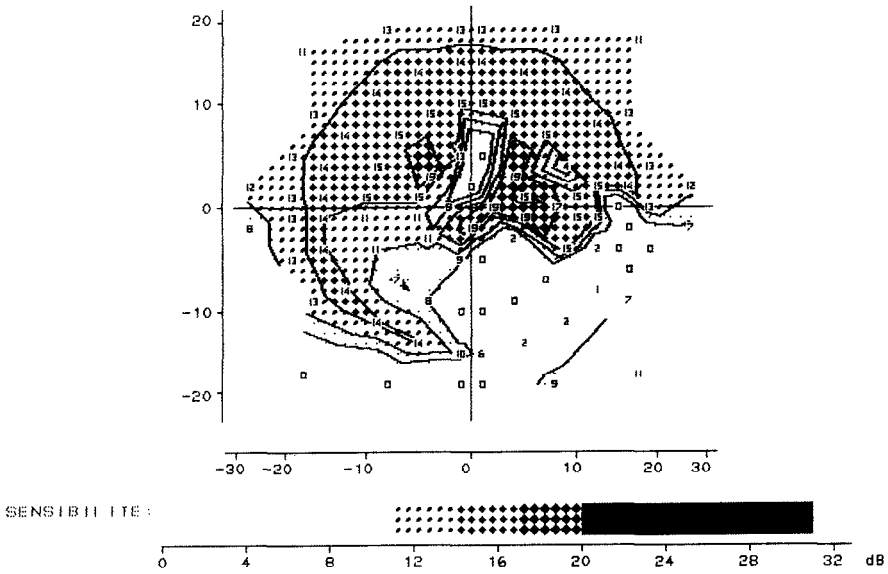
Figure 4 New representation of the visual field sensitivity

Furthermore, these maps provide an erroneous feeling of precision about the definition of the scotoma shape and location

Several authors have also proposed the use of 3-dimensional representations [7] and even 4-dimensional representations [9] (Figure 3). These representations are quite attractive. However, their clinical applicability is limited by the deformations resulting from the perspective view which impede a direct quantitative evalution of deficits.

Static representation of the visual field

The problem of the static representation of the static visual field (i.e. after completion of the examination session) will first be assessed as a simplification of the problem of the dynamic representation (i e. throughout the examination).

The two maps which have been described previously appear to be complementary, one indicating the location of the testing points and their estimated threshold values, the other providing the information necessary for the evaluation of scotomas location and shape. It is therefore quite rational to superimpose both maps on the same graphic representation. The readability of this new representation was greatly improved by the use of several colors and by outlining the seperation between areas of different sensitivity. The resulting graph offers the familiar aspect of the isopter representation used in manual perimetry and is well accepted by most ophthalmologists (Figure 4)
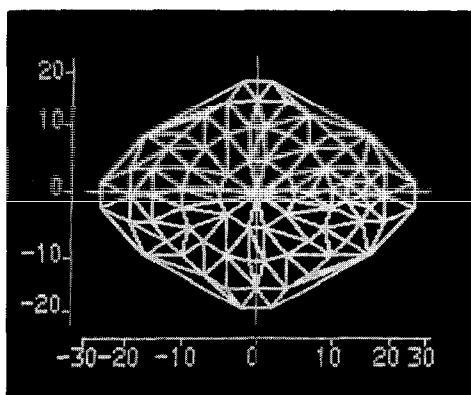
Figure 5 Dissection of the visual field into triangles

Another problem is the determination of the interpolated map. In most methods, the surface is defined from a set of data regularly located over the domain to be represented. This is clearly not acceptable for visual field maps where some areas yield significantly more information than others. A suitable method should be capable of handling non equispaced data and also of representing with an acceptable accuracy the magnitudes and gradients of sensitivity. Polynomial methods were rejected for they can produce anomalies and require lengthy calculations. Weighing methods were found improper as the effect of a local change in threshold extends in an isotropic way upon a large area of the visual field. For instance, they produce undesirable anomalies in the neighbourhood of steep, elongated scotomas. A method initially proposed by Bengtsson and Nordbeck [1] was finally selected. The explored domain is dissected into triangles, using the measuring points as vertices (Figure 5). The intermediate values used in the half tone display and the contours are calculated by linear interpolation between the 3 vertices of each triangle Real time constraints lead to the selection of a local iterative interpolation method [11]

This method presents several interesting features First of all, the information brought by measuring points affects only the triangles which share these points as a summits. Second, its effects can easily be understood without an extended background in mathematics, hence by most ophthalmologists.

This map is diplayed in one of three modes, which ever is found the most suitable for the interpretation of the acquired data:

– the sensitivity mode (Figure 4) is found to be most informative with large deficits, when the remaining areas of sensitivity are best emphasised,
– the deficit mode (Figure 6) is obtained by substracting measured values from 'normal' ones obtained from a reference map built into the computer memory. It is ideal for small deficits as it eliminates the masking effect over small deficits of the sensitivity gradient with excentricity;
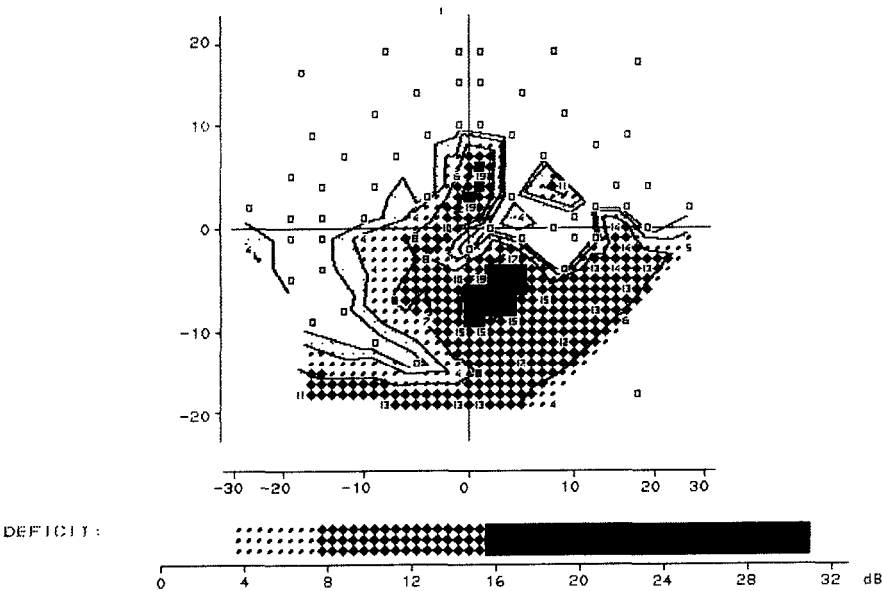
Figure 6 New representation of the visual field deficits
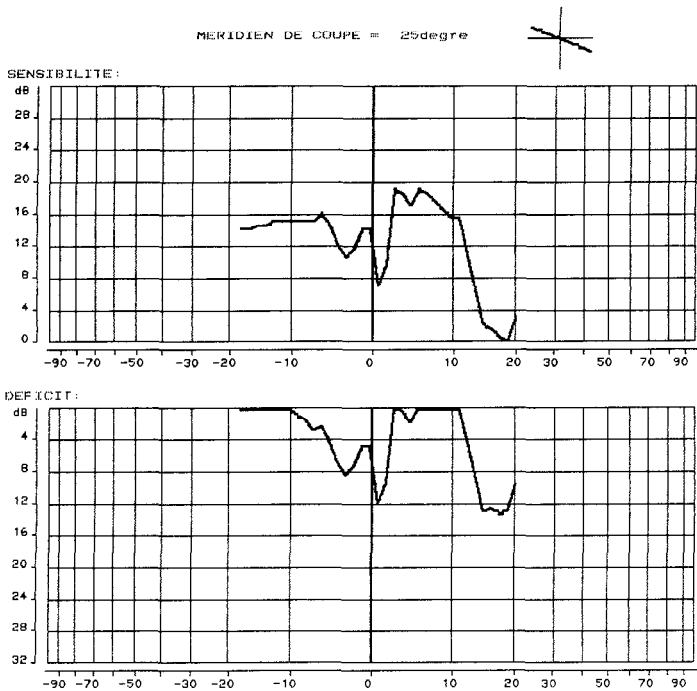
Figure 7 New representation of the visual field profile

– the profile mode (Figure 7) allows a more precise, quantitative evaluation of sensitivity or deficit values along a given meridian.

Dynamic representation of the visual field

It is important to understand that the information visualised at any time during the examination, or even after its completion, is not the true patient's map of sensitivity. It is an estimated map which is more or less accurate, depending upon many parameters such as the threshold evaluation strategy, the patient's cooperation, etc. Therefore, what is relevant for clinical purpose is not only the topography of the visual field but also the amount of confidence given to its determination. The dynamic representation is derived from the static one. Additional color marks characterise the reliability of the threshold evaluation in each testing point. At the beginning of an examination, the best, a priori, estimation of the visual field is displayed with reliability indicators at their minimum value. The initial threshold values are selected from the 'normal' visual field if the patient's own visual field is unknown, or from a prior visual field if one is available. The visual display is updated after each measurement, with a local correction of the interpolated and isopter maps as well as of the corresponding reliability indicators.

Conclusion

The present method has been tested for several months in four different medical centers in Lille, Paris, Reims and Tours More than 4000 visual fields have been completed. The dynamic representation is rapidly accepted by most ophthalmologists and technicians. The major reason is the improved understanding of the examination protocol as well as of the final results. The availability of a dynamic visual field representation throughout the examination is one step toward the implementation of semi-automated examination strategies. For instance, the examination protocol can be stopped at any time and changed for a new protocol more adapted to the patient's fatigue or sudden lack of cooperation.

References

1   Bengtsson BE, Nordbeck S: Construction of isarithmic maps by computer BIT 4: 87 (1964)
2   Charlier J, Moussu L, Hache JC: Optimization of computer-assisted perimetry Fifth international visual field symposium, pp 359–364 Dr W Junk Publ, Dordrecht, 1983
3   Charlier J: L'examen du champ visuel assisté par ordinateur Bull Soc Ophthalmol Fr Numéro spécial, 61–82 (1984)
4   Fankhauser F, Koch P, Roulier A: On automation of perimetry Albrecht v Graefes Arch klin exp Ophthal 184: 126–150 (1972)

5 Fankhauser F: Problems related to the design of automated perimeters Doc Ophthalmol 47: 113–121 (1979)
6 Greve EL, De Boer RW, Bakker D, Moed I: Clinical evaluation of the Scotoperimeter, an experimental automatic perimeter Int Ophthalmol 5: 193–200 (1982)
7 Hart WM, Hartz RK: Computer generated display for three-dimensional static perimetry Arch Ophthalmol 100: 312–318 (1982)
8 Jay WM, Yavitz EQ: Improved viewing of half-tone display of Octopus perimeter Annals Ophthalmol 1 (12): 1369–1371 (1981)
9 Lambrou GN, Schalk P, Rechenman RV, Bronner A: Computer assisted visual field assessment: quantification, three and four dimensional representations 7th international visual field symposium (in press)
10 Ourgaud AG, Etienne R: L'exploration fonctionnelle de l'oeil glaucomateux Rapport Soc Fr Ophthalmol, 1961
11 Sachy J, Vernier F, Charlier J, Hache JC: Méthodes de représentation du champ visuel statique Innov Techn Biol Med 7: 177–188 (1986)

Authors' addresses:
Jacques R Charlier,
U279 INSERM, 1 rue Calmette, 59800 Lille, France and Essilor
International, 6 rue Pastourelle, 75003 Paris, France

Joel Sachy,
U279 INSERM, Lille, France

Françoise Vernier,
Essilor International, Paris, France

Jean-Claude Hache,
Centre Hospitalier Place de Verdun, 59000 Lille, France

IV.6 Comparative evaluation of the Humphrey Field Analyser, Peritest and Scoperimeter

E.L. GREVE, D. BAKKER and A N ZEILSTRA
Amsterdam, The Netherlands

Abstract only

Table 1 Comparative data on the Humphrey Field Analysei Peritest and Scopeimeter

	Humphrey Field Analyzer	Peritest	Scopeimeter
type of perimeter	hemisphere	hemisphere	cathode Ray tube
lightsource	incandescent light	LED	cathodc Ray tubc
dynamic range 0°	3 5 log u (35 dB)	2 8 log u (28 dB)	2 5 log u (25 dB)
operation	automatic	automatic and semi-aut	automatic
	lightpen + scieen	push button	keyboard
	single stimulus	single and multiple stimulus	single stimulus
detection strategies	threshold-related supra threshold	thieshold-related supra threshold	thieshold-related supra threshold
assessment	0 2 threshold	0 6 thieshold and 0 2 threshold	0 2 thieshold
fluctuation	minimal 10 random (10 fixed) double measuiements	--	+ all double
fix control	Heijl-Kiakau + monitor	optical	Heijl-Krakau method
reliability measurements	+	+	+
fatigue measurements	–	–	–
peiformance (?) measurements	–	–	–
zero-feai provision	--	+	+
computer	Intel 8088	Siemens	Noith Star Horizon
statistics separation GRS-LRS, IGS*	+	+	+

Table 1 Continued

	Humphrey Field Analyzer	Peritest	Scoperimeter
significant defect	+	−	+
SF	+	−	−
SF normal/path	−	−	+
mean defect	+	−	+
defect volume	+	−	+
change analysis	+?	−	+
trend analysis	+?	−	+
print out			
interpolated greyscale	+	−	−
non-interpol greyscale	−	+	+
defect intensity	+	+	+
numbers	+	+	+
meridians	+	−	+
central + periph field	+ for supra-threshold strategies − for threshold	+	only central

* GRS = general reduction of sensitivity
  LRS = local reduction of sensitivity
  IGS = individual general sensitivity

Meridional static threshold perimetry

Humphrey FA vs Scoperimeter:
– results show excellent comparability,
– defects Scoperimeter somewhat deeper.
Causa:
– stimulus size probable,
– stimulus duration probable,
– stimulus colour unlikely,
– background level unlikely.
Duration of examination:
– HFA· 7'26"/2 merid. = 30 positions,
– Scope: 4'30"/2 merid. = 24 positions

Threshold-related programme

Table 2 Central and peripheral field; Humphrey FA vs Peritest

	HFA	P' test
# positions	121	131
dynamic range	3 5	2 8
stepsize	large	0 6
IGS range*	1 0	2 8
duration of examination	9'22"	7'14"

* IGS range: level of general reduction of sensitivity above which the general reduction is no longer indicated seperately

Conclusions:
- Detection rate similar, as expected in two instruments with comparable strategies and stimulus positions.
- Graphical representation of central *and* peripheral field on one chart is advantage.
- Symbols give less clear pictures than greyscale blocks.
- The use of non-interpolated greyscales is only advisable if sufficient number of positions have been examined (i.e. more than the present 121 and 131 respectively).
- The configuration is much better demonstrated for maximal defects than for relative defects.
- The reproducibility is variable for relative defects due to intrinsic fluctuation of pathological thresholds in relative defects
- An examination as done with the Peritest (threshold-related, 216 positions, full field) stands between so-called screening strategies and grid-threshold examinations à la Octopus The cost-benefit ratio is high.
- The differences between the mean defect in the first and in the second examination is the same in the two perimeters.
- The mean defect *differences* range from 0 1 to 6 0 for the Humphrey F.A. and from 0 to 6.8 for the Peritest.

Table 3 Humphrey Field Analyser and Peritest

Case	DV1	DV2	△DV	MD1	MD2	△MD	
1	243	324	81	16 2	18 0	1 8	HFA
	144	186	42	18 0	15 5	2 5	Peritest
2	429	339	90	15 5	15 4	0 1	HFA
	330	312	18	16 5	17 6	1 1	Peritest
3	558	576	18	18 6	17 4	1 2	HFA
	342	468	126	17 1	18 0	0 9	Peritest
4	486	516	30	18 0	19 8	1 8	HFA
	504	1170	666	16 8	17 7	0 9	Peritest
5	1941	2154	213	22 0	22 6	0 6	HFA
	1692	954	378	19 4	18 3	1 1	Peritest
6	39	30	9	19 5	15 0	4 5	HFA
	72	72	0	24 0	24 0	0	Peritest
7	1269	1629	360	20 1	20 9	0 8	HFA
	1554	1152	402	19 2	16 9	2 3	Peritest
8	1953	2136	183	21 7	22 2	0 5	HFA
	1200	906	294	17 6	20 1	2 5	Peritest
9	951	1011	60	19 4	21 0	1 6	HFA
	870	846	24	20 7	21 1	0 4	Peritest
10	552	495	57	21 2	20 6	0 6	HFA
	318	372	54	15 1	21 9	6 8	Peritest
11	498	168	330	17 7	16 8	0 3	HFA
	150	156	6	12 5	12 0	0 5	Peritest
12	114	129	15	16 3	16 1	0 2	HFA
	300	384	84	14 2	12 8	1 4	Peritest
13	1440	1512	72	27 1	22 9	4 2	HFA
	960	1302	342	20 4	21 0	0 6	Peritest
14	996	1041	75	26 1	21 2	4 9	HFA
	852	828	24	19 4	17 6	1 8	Peritest
15	378	312	66	18 0	19 5	1 5	HFA
	450	396	54	19 6	18 9	0 7	Peritest
16	481	885	404	14 1	20 1	6 0	HFA
	480	270	210	17 1	15 0	2 1	Peritest
17	291	312	21	20 7	19 5	1 2	HFA
	360	246	114	22 5	17 6	4 9	Peritest
18	504	324	180	18 7	18 0	0 7	HFA
	186	306	120	18 6	17 0	1 6	Peritest
19	387	339	48	18 4	21 1	2 7	HFA
	486	300	186	17 4	20 0	2 6	Peritest
20	1689	1719	30	23 1	22 9	0 2	HFA
	1368	1488	120	20 7	21 3	0 6	Peritest
	Mean △DV 41 H F A				Mean △MD 0 1 H F A		
	Mean △DV 14 Peritest				Mean △MD 0 1 Peritest		

DV = Defect Volume; MD = Mean Defect

Threshold perimetry 60-grid

Table 4 Humphrey FA vs Scoperimeter Number of stimuli: HFA (H) 76; Scoperimeter (S) 60

case	DV1	DV2	△DV	MD1	MD2	△MD	rms norm	rms path rel	rms HFA	rms HFA total
1H	86	259	173	20 4	15 6	4 8	2 1	4 7	2 5/2 1	3 9
S	176	314	138	17 7	17 7	0	1 9	4 1		
2H	112	184	72	17 7	16 6	1 1	1 6	3 1	2 1/1 9	2 5
S	177	144	33	17 4	17 1	0 3	1 4	2 7		
3H	302	632	330	22 1	15 1	7 0	1 9	4 5	2 1/2 0	4 6
S	209	157	52	19 9	23 7	3 8	1 4	3 9		
4H	290	285	5	16 9	14 9	2 0	1 8	4 3	1 9/1 7	2 9
S	331	305	26	19 7	18 9	8 0	1 8	2 2		
5H	1074	1375	301	15 0	11 9	3 1	1 5	7 1	4 7/2 3	6 1
S	1053	796	257	14 9	15 1	0 2	1 4	3 6		
6H	31	31	0	23 0	21 6	2 2	1 8	1 9	2 4/1 6	2 0
S	48	56	8	21 0	20 0	1 0	1 3	3 4		
7H	568	610	42	13 5	13 1	0 4	1 7	3 3	1 7/3 6	3 0
S	614	704	90	13 7	14 8	1 1	1 3	4 8		
8H	733	1007	274	12 1	13 0	0 9	1 3	4 0	- -/3 0	3 7
S	403	269	134	12 8	13 4	0 6	3 0	4 7		
9H	443	429	14	15 1	16 7	1 6	2 8	3 2	- -/3 4	3 1
S	544	531	13	16 3	16 4	0 1	2 7	4 0		
10H	348	357	9	13 8	11 5	2 3	1 4	3 2	1 0/2 7	1 7
S	262	321	59	19 1	20 6	1 5	2 5	3 1		
11H	117	347	230	23 2	20 7	2 5	1 7	3 8	2 8/3 8	3 5
S	195	135	60	20 7	21 1	0 4	1 4	2 6		
12H	105	157	52	22 9	23 2	0 3	1 6	4 0	2 4/- -	2 8
S	70	67	3	25 2	24 9	0 3	1 4	1 8		
13H	763	966	203	13 6	12 9	0 7	2 4	5 3	4 5/3 1	5 0
S	935	855	80	13 7	13 4	0 3	1 5	4 1		
14H	944	719	225	14 4	14 1	0 3	2 5	4 8	2 4/2 3	4 2
S	461	283	178	17 5	19 2	1 7	2 1	4 3		
15H	271	267	4	17 9	19 5	1 6	1 5	3 2	2 9/2 3	2 7
S	446	265	201	16 8	17 5	0 7	2 0	4 6		
16H	354	423	69	12 1	12 4	0 3	1 6	4 3	2 9/2 1	3 6
S	339	182	157	13 4	14 0	0 6	2 4	5 3		
17H	209	273	64	18 1	17 5	0 6	1 6	3 8	2 7/2 8	2 5
S	150	236	86	20 3	19 4	0 9	1 7	2 8		
18H	372	179	193	30 7	31 3	0 4	2 3	3 5	2 3/- -	3 3
S	93	90	3	20 5	20 0	0 5	1 5	3 1		
19H	145	118	27	17 2	15 6	1 6	1 9	3 5	4 2/0 6	2 4
S	52	108	56	18 7	18 0	0 7	1 5	3 5		
20H	994	1022	28	13 6	13 7	0 4	1 8	4 4	4 0/2 6	4 1
S	757	678	79	14 5	16 0	1 5	1 8	2 8		
H	Mean		116			1 7	1 8	4 0		
S	Mean		85			1 5	1 8	3 6		

Conclusions:
– The mean difference between the mean defect of the first and second examination is 1 7 for the HFA and 1.5 for the Scoperimeter.
– The differences between the mean defect of the first and second examination ranges from 0.3 to 7 0 for the HFA and from 0 0 to 8.0 for the Scoperimeter. This indicates that considerable differences in MD are possible between two examinations on the same day.
– The rms in normal areas of the visual field is 1.8 for both perimeters.
– The rms in relative defects is 4.0 for the HFA and 3.6 for the Scoperimeter.
– No rms as measured by the HFA at 10 positions may show considerable differences between two examinations.
– The rms measured at 10 positions is not an attractive substitute for the rms of the whole visual field.
– The rms HFA should preferably be separated in an rms normal and rms pathological.
– The rms should be measured at *all* relative pathological positions.

Authors' addresses:
Eye Clinic of the University of Amsterdam,
Academic Medical Center,
Meibergdreef 9, 1105 AZ Amsterdam-Zuidoost, The Netherlands
and
Eye Department of the St Lucas Hospital,
Jan Tooropstraat 164, 1061 AE Amsterdam-West, The Netherlands

IV.7 Computer-aided analysis in automated dark-adapted static perimetry

P.P. APÁTHY, S.G. JACOBSON, L. NGHIEM-PHU, R.W. KNIGHTON
and J.-M. PAREL
Miami, U.S.A.

Abstract

Dark-adapted two-color static perimetry is useful for evaluating and subtyping
patients with retinitis pigmentosa Perimetric data were acquired from the entire
visual field with a modified automated perimeter and then transmitted to a
microcomputer for further analyses. Programs were developed to determine
whether rods, cones, or both photoreceptor systems mediated function at all test
loci; calculate sensitivity loss at these loci; and display any loss in gray scale,
contour, and perspective form.

Introduction

Two-color dark-adapted static perimetry is a useful technique for evaluating
patients with retinitis pigmentosa (RP) (1–6) With this technique, it is possible to
determine whether rods, cones, or both mediate function in different regions of
the visual field and to what degree the function of each photoreceptor system may
be impaired The patterns of rod and/or cone dysfunction in RP patients have
been used to define subtypes of the disease [1, 2, 4, 6].

   We modified an automated perimeter to perform two-color dark-adapted static
perimetry in RP patients [2]. The specialized analyses necessary to interpret the
results, however, could not be accomplished on the automated perimeter used to
collect the data. Data were therefore transferred to an external microcomputer
and software was developed to perform the analyses. The present report details
the methods for transfer, decoding, analysis, and display of results of two-color
dark-adapted static perimetry in RP patients.
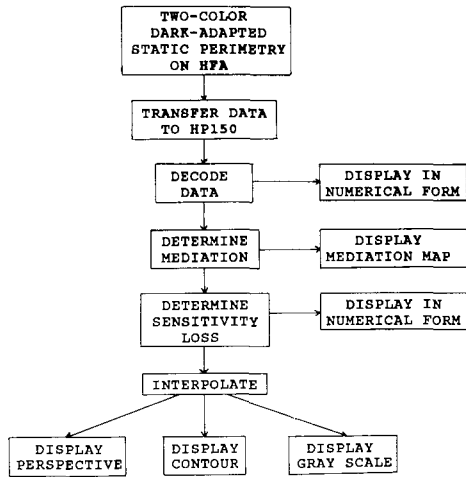
Figure 1 Steps in the analysis and display of results from two-color-dark-adapted perimetry

Methods and results

A modified Humphrey Field Analyzer (HFA) is used to measure dark-adapted sensitivity to monochromatic red (650 nm) and blue-green (500 nm) targets (Goldmann size V) At maximum intensity, the energy of the blue-green stimulus is 2.3 μW and the red stimulus is 88 μW in the beam incident on the perimeter Measurements are made at 75 loci across the visual field using a test strategy termed the 'RP Threshold Test' [2] Further details of the principles and technique of two-color dark-adapted static perimetry are given elsewhere [1, 2, 5]

Data from RP Threshold Tests are stored on floppy disk. Subsequent analyses and display of these data are performed on an external microcomputer, a Hewlett-Packard 150B (HP150). Fig. 1 lists the necessary steps in these procedures. Each step is described in detail below.

Data transfer

The HFA has a provision for transmitting files to another computer via a serial port (RS232). The HFA's 'transmit files' option and a communications program (DSN/LINK) are used to transfer data to the HP150. Files are sent one at a time and stored on floppy disk for further processing

DARK-ADAPTED, red target V:

```
                  |                                              |
A     19  19   7   6   0   4   3          C      28  32  34  33  33  32  30      + 36
                  |                                              |
   27  27   0   0   0   0   0   0  15         32  35  36  37  36  35  35  33  31    |
                  |                                              |                | S
28  27  11   0   4   0   8   2   0  15  16    32  35  38  38  38  38  37  36  35  32  28 |
              14  13                                  37  38                      |
27--29-- 0-- 7--32-- X-- 2-- 0-- 0-- 0-- 9   33--37--38--39--39-- X--37--37--36--35--31 + 0
              12  11                                  39  39                      |
32  26   0   0   3   0   0   0   0   4  20    33  37  38  39  40  39  37  38  37  34  31 |
                  |                                              |                |
   28   0   0   0   0   0   0  14  23         34  37  37  39  38  38  37  36  34    | I
                  |                                              |                |
      23   6   1   2   0   0  21  21             34  35  37  37  37  36  35  32     |
                  |                                              |                |
         26  24   0   0  21  26                     34  35  36  35  33  33        + 48
                  |                                              |

+-----------------+-------------------+     +-----------------+-------------------+
48      N     0        T         72     48      N     0        T         72
```
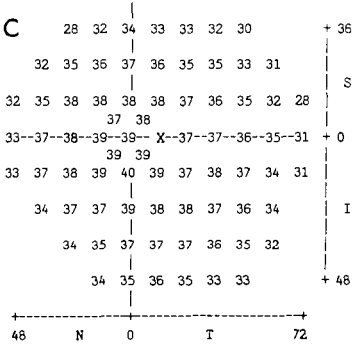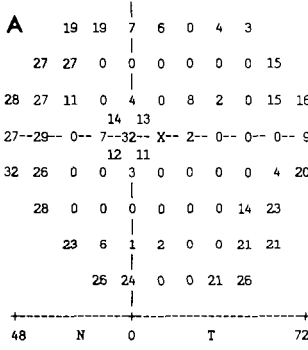
DARK-ADAPTED, blue-green target V:

```
                  |                                              |
B     40  29  28  16   0  32  23          D      45  49  49  49  48  47  46      + 36
                  |                                              |
   46  41   0   0   0   0  24  31  30         48  50  52  53  52  51  51  49  47    |
                  |                                              |                | S
40  38  17   0   9   0   0   0   0  30  33    47  51  53  53  53  53  53  52  51  49  46 |
              14  15                                  52  52                      |
44--42-- 0--17--25-- X-- 2-- 0-- 0-- 9--22   48--52--53--55--44-- X--53--53--52--50--48 + 0
              13   9                                  54  53                      |
48  41   0   6   0   0   0   0   0  17  34    50  53  54  54  54  54  53  53  52  51  47 |
                  |                                              |                |
   43   6   0   0   0   0   0  20  34         50  52  54  55  54  54  53  52  50    | I
                  |                                              |                |
      42  20   6   0   0   4  40  42             50  51  53  53  52  52  50  48     |
                  |                                              |                |
         38  40  21  18  36  39                     49  51  52  51  50  48        + 48
                  |                                              |

+-----------------+-------------------+     +-----------------+-------------------+
48      N     0        T         72     48      N     0        T         72
```
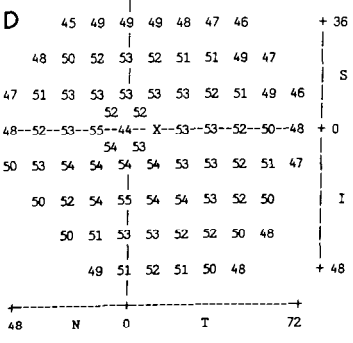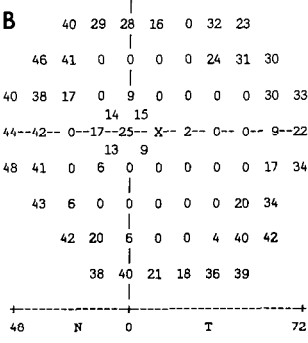
Figure 2 Dark-adapted sensitivity measurements to red and blue-green stimuli throughout the visual field of the right eye of a 10 year old female RP patient (A, B) Mean results from 16 normal subjects are shown (C, D) The blind spot is denoted by an X

Data decoding

The files consist of encoded data divided into two sections: miscellaneous data (e.g. patient information and test parameters), and sensitivity levels for the test loci A FORTRAN program decodes both the miscellaneous data and the sensitivity levels. A mean sensitivity is determined at any locus at which more than one measurement was made. Results from the entire field of the patient are then printed out along with those from a normal population

Fig. 2 shows numerical displays of results from RP Threshold Tests in the right eye of a 10 year old girl with simplex RP (Figs 2A, B); normal results (mean, n = 16) are also shown (Figs 2C, D). This RP patient did not detect either red or blue-green stimuli in the midperipheral field There was some detection, albeit impaired, centrally and in the far periphery. Sensitivity at some loci in the far nasal field approach normal levels for both colors.

Determination of photoreceptor mediation

The difference in sensitivity for red and blue-green stimuli at each test locus determines which photoreceptor system mediates detection. When the red and blue-green stimuli are equal in energy, the rod photoreceptor system is 32 dB more sensitive to blue-green than to red, while the cone photoreceptor system is 8 dB more sensitive [7]. A difference between 8 and 32 dB indicates cone detection of the red stimulus and rod detection of the blue-green stimulus, i.e. mixed mediation

Variability in the sensitivity difference expected for rod mediation was examined in normal subjects (n = 16; ages 15 to 57) by measuring dark-adapted sensitivities to red and blue-green stimuli at 47 of the 75 loci in the RP Threshold Test (excluding foveal, parafoveal and far peripheral loci). The mean sensitivity difference was 31.6 dB (s.d., 0.9), compared to the expected value of 32 dB. A criterion difference below which loci would be classified as mixed in mediation rather than rod-mediated was then determined. A cutoff was considered satisfactory if, for any subject, no more than 5% of the total points expected to be rod-mediated would be considered as mixed The mean sensitivity difference for which this condition was met was 28.1 dB; 95% confidence limits were 28.6 and 27.5. With a lower limit of 28 dB, 14 of 16 normal subjects had less than 5% of points misclassified as mixed; the remaining two subjects had 6 4% classified

Table 1 Criteria for determining photoreceptor mediation and sensitivity loss

Red sensitivity (dB)	Blue-green sensitivity (dB)	Sensitivity difference* (dB)	Symbol	Rod sensitivity loss[+] (dB)	Cone sensitivity loss[++] (dB)
Both colors detected:					
> 0	> 0	≥ 28	R	N-P	$\geq$ N-P
		≤ 12	C	$\geq$ N-P	N-P
		12<DIFF<28	M	N-P	N-P
One color detected:					
≥ 4	0	≤ 12	?C	$\geq$ N	N-P
< 4	0	< 16	?MC	$\geq$ N	N-P
0	≥ 12	≥ 28	?R	N-P	$\geq$ N
0	< 12	> 16	?MR	N-P	$\geq$ N
Neither color detected:					
0	0	**	??	+ + +	+ + +

* Blue-green minus red plus 16 dB
** difference is indeterminate
[+] N-P (normal minus patient); N (normal); blue-green stimuli
[++] N-P (normal minus patient); N (normal); red stimuli
[+++] rod and cone losses indeterminate and not displayed

```
A   R  M  R  M  ??  R  R        B    5 20 21 33     15 23      C   >0  0 >13 13     >14 >13    + 36

    R  R  ?? ?? ?? ?? ?R ?R  R       2  9           27 18 17       >0 >0              >21 >18 >2           S

R  M  M  ?? M  ?? ?C ?MC ?? R  R    7 13 36   44   >53 >52  19 13   >0  0 10    21    15 19   >4 >0
         M  M                                38  37                        16  17
R- R- ??- M- C- X- M- ??- ??-?MR- R  4- 10-  - 38->19- X- 51-  -  - 41- 25   >0- >0-  - 21- 2- X- 26-  - ->20->7 + 0
         M  M                                41  44                        20  19
R  R  ?? ?MR ?MC ?? ?? ?? ?? R  R   2 12   48 >54          34 13   >0 >0   >27 24          >16 >0

    R ?MR ?? ?? ?? ?? ?? M  M       7 46           32 16       >0 >19              7   0       I

    R  R  M ?MC ?? ?MR  R  R        8 31 47 >53    48 10  6      >0 >12 18 18    >21 >0 >0

       R  R ?R ?R  R  R            11 11 31 33 14  9        >0 >0 >17 >18 >0 >0   + 48

48     N     0      T     72      48    N     0      T     72    48     N     0      T     72
```
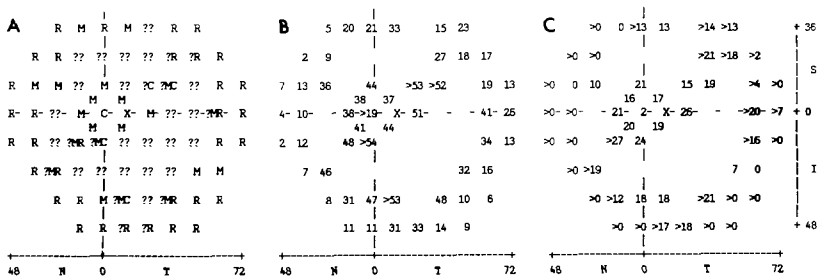
Figure 3 Photoreceptor mediation (A), rod sensitivity loss (B), and cone sensitivity loss (C) at all tested loci in the visual field of the same patient shown in Figure 2 Sensitivity loss is not displayed for loci at which neither red nor blue-green stimuli were detected (symbol ?? in A)

incorrectly. The cutoff above which cone-mediated loci would be misclassified as mixed was taken as 12 dB, 4 dB higher than the expected value of 8 dB. This is consistent with the 4 dB difference between expected and cutoff in the rod data

Table 1 lists the criteria used for classifying test loci as rod, cone, or mixed in mediation. Based on these criteria, 'mediation maps' can be generated (see Fig. 3A). Under actual test conditions, both red and blue-green, only one color, or neither color may be detected When both are detected, a sensitivity difference greater than or equal to 28 dB indicates rod mediation (R, Fig 3A, far peripheral field); less than or equal to 12 dB indicates cone mediation (C; Fig. 3A, fovea), and between 12 and 28 dB indicates mixed mediation (M; Fig. 3A, parafoveal loci). It should be noted that a factor of 16 dB is added to all blue-green sensitivity measurements prior to determining sensitivity differences; this equates the energies of the red and blue-green stimuli in our instrument [2].

When only one color is detected the symbol for mediation is preceded by a question mark (?). These responses are divided into four categories and examples can be found in Fig. 3A. If the blue-green stimulus is not detected and the red sensitivity is greater than or equal to 4, the difference cannot be greater than 12 dB and cones must mediate vision (?C). If the blue-green stimulus is not detected and the sensitivity to red is less than 4 dB, the difference must be less than 16 dB and mediation could be provided either by cones or by a mixed photoreceptor population (?MC). For an undetected red stimulus and a sensitivity to blue-green greater than or equal to 12 dB, the difference must be at least 28 dB and the point must be rod-mediated (?R). A sensitivity to blue-green of less than 12 dB and no measurable sensitivity to red results in a difference that must be greater than 16 dB, indicating mixed or rod mediation (?MR)

When neither stimulus color is detected, mediation is impossible to determine. These loci are shown with two question marks (??) on the mediation map (Fig. 3A, midperipheral ring).

Determination of sensitivity loss

Once the mediations at all loci in the RP Threshold Test have been determined, the sensitivity of the rod and cone systems in the patient data are compared to the mean sensitivity in normals Normal rod sensitivity was determined in fully dark-adapted normal subjects (n = 16, ages 15 to 57). Normal cone sensitivity was measured during the cone plateau (n = 4, ages 22 to 41). Sensitivity losses are calculated as shown in Table 1.

Rod sensitivity loss at rod or mixed-mediated loci (R, M, ?R, ?MR; Fig. 3B, periphery) is equal to the difference between blue-green sensitivity in the patient and that in the normal Loss could be greater than this difference at cone-mediated loci (C; Fig. 3B, fovea). At other loci not mediated by rods (?C, ?MC), rod sensitivity loss is greater than or equal to normal sensitivity. Cone sensitivity loss is equal to the difference between normal and patient responses to the red stimuli at mixed or cone-mediated loci (C, M, ?C, and ?MC; Fig. 3C, foveal and parafoveal loci). At rod-mediated loci (R), losses may be even greater than the difference between patient and normal responses (Fig. 3C, periphery). Cone sensitivity loss at other loci not cone-mediated (?R, ?MR) is greater than or equal to normal sensitivity.

Interpolation

Although rod and cone sensitivity losses across the visual field can be shown in numerical form (Figs 3B, C), these data also lend themselves for display as gray scales, contours, and perspective plots. The computer programs used to generate these plots (from the National Center for Atmospheric Research, Boulder, CO) require regularly spaced input data. All loci in the RP Threshold Test are equally spaced except for the four parafoveal test loci. To provide suitable input data for the programs, results are fit to a multidimensional cubic spline for arbitrarily located data using a 9 × 8 matrix with 12 degree spacing as the basis for interpolation, minimizing the squared error between the spline and the data points. Sensitivity losses at a 21 × 15 matrix of points with 6 degree spacing are computed from this spline and used as a basis for the three types of displays.

Additional processing of the data is required for contour and perspective displays. The contouring program performs further interpolation of the sensitivity loss data to produce smoothed contour lines This interpolation is also based on a spline interpolating technique and is thus consistent with our initial interpolation processing. The perspective algorithm eliminates hidden lines but does not modify the input data in any way
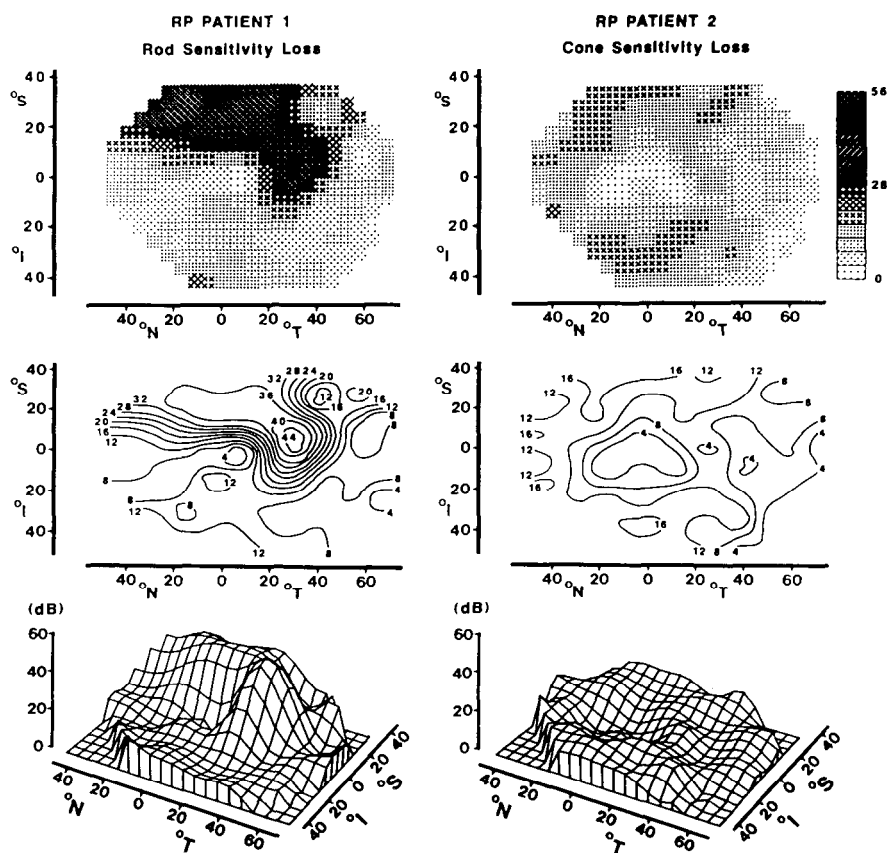
Figure 4 Gray scale (upper), contour (middle), and perspective (lower) displays of rod and cone sensitivity loss in the right eyes of two RP patients Gray scale representations employ 14 levels of gray, each covering a 4 dB range in sensitivity loss Darker areas indicate regions of greater loss in function In the contour displays, lines of constant sensitivity loss are drawn at 4 dB intervals Elevated areas in the perspective plots show regions of greater sensitivity loss

Displays

Figure 4 shows gray scale, contour, and perspective plots of rod sensitivity loss across the visual field of one RP patient (left column) and cone sensitivity loss in another (right column). Patient 1, a 49 year old man with simplex RP, typifies the 'regionalized' (or Type 2) functional subcategory of RP [1, 2, 4]. The rod sensitivity loss in this patient is greatest in the superior field with maximum loss occurring at about 30° in the temporal field. Near the fovea, rod sensitivity loss is at a minimum.

Patient 2, a 26 year old man with dominant RP, exemplifies the 'diffuse' (or Type 1) functional subcategory; only cone function is measurable throughout his

visual field. The various displays of the data indicate that cone sensitivity is minimally affected centrally and in the far periphery, but there is decreased sensitivity in a midperipheral ring.

Conclusions

Dark-adapted static thresholds to red and blue-green stimuli are measured throughout the visual field of RP patients using a commercially-available auto-mated perimeter modified for this purpose [2] The test results are analyzed on an external microcomputer. Displays of the analyzed data permit the identification of different functional subclasses of RP and provide a means to view variations in rod and cone function across the visual field of RP patients.

Acknowledgements

References

1 Ernst W, Faulkner DJ, Hogg CR, Powell DJ, Arden GB, Vaegan: An automated static perimeter/adaptometer using light emitting diodes Br J Ophthalmol 67: 431–442 (1983)
2 Jacobson SG, Voigt WJ, Parel J-M, Apáthy PP, Nghiem-Phu L, Myers SW, Patella VM: Auto-mated light- and dark-adapted perimetry for evaluating retinitis pigmentosa Ophthalmology 93: 1604–1611 (1986)
3 Marmor MF et al: Retinitis pigmentosa: a symposium on terminology and methods of examination Ophthalmology 90: 126–131 (1983)
4 Massof RW: Psychophysical subclassifications of retinitis pigmentosa In: LaVail M, Hollyfield JG, Anderson RE (eds) Retinal degeneration: experimental and clinical studies, pp 91–107 Alan R Liss, New York, 1985
5 Massof RW, Finkelstein D: Rod sensitivity relative to cone sensitivity in retinitis pigmentosa Invest Ophthalmol Vis Sci 18: 263–272 (1979)
6 Massof RW, Finkelstein D: Two forms of autosomal dominant primary retinitis pigmentosa Doc Ophthalmol 51: 289–346 (1981)
7 Wyszecki G, Stiles WS: Color science: concepts and methods, quantitative data and formulae (2nd ed) John Wiley & Son, New York, 1982

Author's address:
Peter P Apáthy,
Bascom Palmer Eye Institute,
P O Box 016880, Miami, FL 33101, U S A

Section V
Glaucoma

V.1 Visual field and neuroretinal rim area changes with time

P.J AIRAKSINEN, P A. JUVALA, A. TUULONEN, H I ALANKO,
R. VALKONEN and A. TUOHINO
Oulu, Finland

Abstract

We measured the change of neuroretinal rim area of the optic disc in 143 eyes of 143 patients including 38 patients with glaucoma, 85 patients with ocular hypertension and 20 normal controls The average follow-up time was 9 years. A statistically significant decrease of rim area was found in all clinical groups. The change was greatest in the 35 ocular hypertensives who developed clinically detectable glaucomatous changes during the follow-up. An unexpectedly high yearly rate of rim area decrease was found in the group of patients who had glaucomatous abnormalities already in the initial examination and were on treatment. Regression of neuroretinal rim area change to the change of mean defect of the visual fields examined with a Friedmann analyzer showed a statistically significant correlation only in patients who entered the study as ocular hypertensives and developed glaucomatous abnormalities during the follow-up

Introduction

Neuroretinal rim area is a measure of the optic nerve head reflecting the amount of nerve fibers in the eye. It was shown recently that neuroretinal rim area corrected for the individual magnification of the patient's eye is a useful tool in identifying normal and abnormal optic discs. Rim area was better in separating normals and patients with glaucoma than cup/disc ratio [4]. In our recent studies [1] we found that rim area was highly correlated with semi-quantitative retinal nerve fiber layer scores, another expression of the structural integrity of the nerve. We further found that rim area was highly correlated with visual field indices of the Octopus J0 program [2]. The J0 program is a predecessor of the currently available G1 program [5]. There are, however, no long-term follow-up studies to show what happens to the neuroretinal rim area over time and how the change of rim area correlates with visual field abnormalities.

Material and methods

In this retrospective follow-up study we examined 143 eyes of 143 patients (95 women, 48 men) including 38 patients with chronic open angle glaucoma, 85 ocular hypertensives and 20 normal controls. The glaucoma patients had glaucomatous optic disc and visual field abnormalities. The ocular hypertensives had an IOP more than 21 mm Hg repeatedly and they had clinically normal disc appearance and normal visual fields. The normal controls were individuals whose IOP was always less than 21 mm Hg and who had normal optic discs and normal visual fields.

The mean ages of the clinical groups were statistically significantly different from each other (Table 1). We included only patients whose optic discs had been photographed at least three times during a minimum follow-up of 5 years (Table 2). Optic disc stereophotographs were taken on black-and-white film with a Zeiss fundus camera using an Allen stereoseparator and a green Wratten No. 58 filter. Neuroretinal rim area was measured from enlarged black-and-white photographs using a previously described technique [3]. The area measurements were corrected for the individual magnification of the patient's eye with the technique described by Littmann [6] taking account of the axial length of the eye.

Visual fields were examined on the day of photography with a Friedmann visual field analyzer We calculated the mean defect of the visual fields by taking an average of the differences between measured thresholds and normal values suggested by the manufacturer.

Table 1 Mean age of the patients in the clinical groups

Patient group	Mean age (yrs) +/− SD
Glaucoma patients	63 3 +/− 8 5
Ocular hypertensives	57 1 +/− 8 8
Normals	43 9 +/− 13 7

Table 2 Period of follow-up and number of occasions of photography

Patient group	Period of follow-up		Number of occasions of photography	
	yrs	range	yrs	range
Glaucoma patients	8 5	5–14	3 7	3–6
Ocular hypertensives	9 2	5–15	4 3	3–8
Normal controls	8 5	4–16	3 1	2–4

Results

Change of neuroretinal rim area

The base line neuroretinal rim areas were not different among the normals and ocular hypertensives, but the initial value of the glaucoma patients was statistically significantly lower than in the other two clinical groups (Table 3).

Rim area change on each occasion of photography as compared to the initial value was regressed to time. A statistically highly significant R^2 of 32% was found among the glaucomas and 26.7% among the ocular hypertensives (p = 0.000). Among the normal controls the correlation of neuroretinal rim change to time among the normal controls was weaker with an R^2 or 12.1% (p<0.01).

The ocular hypertensive patients could be divided into two subgroups: patients who developed clinically detectable glaucomatous optic disc and visual field changes during the follow-up (n = 35) and patients in whom no such changes could be observed and who remained clinically ocular hypertensive throughout the study (n = 50). The R^2 of rim area change to time was statistically highly significant but markedly different between the two groups with an R^2 of 56.1% among the patients who developed glaucoma and 16.6% among the patients who remained ocular hypertensives.

We also calculated the average change of rim area per year of follow-up in different clinical groups (Table 4). Analysis of variance showed that the yearly rim area change of the glaucoma patients was statistically highly significantly different both from that of the two ocular hypertensive groups and of the normals. The two ocular hypertensive groups differed statistically significantly from each other and also from the normals.

Table 3 Mean initial neuroretinal rim area of the patients

Patient group	Mean +/− SD (mm²)
Glaucoma patients	0 94 +/− 0 41
Ocular hypertensives	1 32 +/− 0 29
Normal controls	1 47 +/− 0 41

Table 4 Average change of neuroretinal rim area per year of follow-up

Patient group	mm²/yr +/− SD
1 Ocular hypertensives → Glaucoma	−0 036 +/− 0 012
2 Glaucoma patients	−0 024 +/− 0 024
3 Ocular hypertensives → Ocular hypertensives	−0 012 +/− 0 012
4 Normal controls	−0 006 +/− 0 001

Change of visual fields

We calculated the regression coefficients of mean defect changes to time (mean defect change was calculated by subtracting the mean defect value of the initial visual field from the mean defect of each subsequent visual field). A statistically significant correlation was found only in the group of ocular hypertensives who developed clinically detectable glaucoma during the follow-up. The R^2 was 12.7% (p = 0.000).

Correlation of rim area changes to visual field changes

Neuroretinal rim area decreased in 67% of glaucoma patients and 24% of them showed no change of visual field. On the other hand, 16% of glaucoma patients showed an increase of mean defect without a corresponding change of neuroretinal rim area. Among the ocular hypertensive patients who developed glaucoma during the follow-up a neuroretinal rim area decrease was found in 94%. 40% of them showed no change of visual fields. In the ocular hypertensive group of patients in whom no clinically detectable glaucomatous changes were observed during the follow-up neither rim area nor visual field changes were recorded in 63% of cases. There was a rim area decrease in 30% of patients in this group and 25% of them also showed an increse of the mean defect of the visual fields. Regression of the visual field changes to neuroretinal rim area changes over time showed a statistically significant correlation only in the group of patients who entered the study as ocular hypertensives and developed glaucoma during the follow-up. The R^2 was 13.7% (p = 0.02).

Discussion

Results of the present study show a decrease of neuroretinal rim area with time in all clinical groups including the normal controls The average yearly change was largest in the ocular hypertensive patients who developed clinically detectable glaucoma during the average follow-up of 9 years. Their yearly rate of change was 0.036 mm^2 of rim area which is a large number and will lead from a normal disc with a rim area of e.g. 1.4 mm^2 to the lower limits of the normal controls and to clinically noticeable glaucomatous optic disc in approximately 10 years.

It is remarkable that in the ocular hypertensive patients in whom no clinically detectable glaucoma was observed during the follow-up the rate of change, although much lower than in the other group, was still 0.012 mm^2 per year of follow-up. Closer observation of this group showed that there are a number of patients whose rate of change is closer to that of the normal controls and there are other patients in whom the rate of yearly change is closer to that of the ocular

hypertensives who developed glaucoma. This means that within the next 5 years or so also the latter patients will show manifest glaucomatous abnormalities.

It was unexpected to find a high rate of rim area decrease also in the patients who were glaucomatous already at the first examination All of these patients were reasonably well controlled either with medical treatment, with laser trabeculoplasty or with filtering surgery or combination of these

The low rate of rim area decrease of 0.006 mm^2 per year in the normal controls may be an expression of the loss of axons by aging alone.

The correlation of neuroretinal rim area changes with the changes of mean defect of the visual fields was not very good and was found to be statistically significant only in the group of ocular hypertensives who developed glaucomatous abnormalities. In this group rim area decrease was associated with increase of the mean defect of the visual fields in 60% of the cases This seems to stress the importance of optic disc observation and quantitation in the management of glaucoma. A good visual field and rim area correlation can, however, be found when highly sophisticated and sensitive automated perimetry programs are available [2].

References

1 Airaksinen PJ, Drance SM: Neuroretinal rim area and retinal nerve fiber layer in glaucoma Arch Opthalmol 103: 203–204 (1985)
2 Airaksinen PJ, Drance SM, Douglas GR, Schulzer M: Neuroretinal rim area and visual field indices in glaucoma Am J Ophthalmol 99: 107–110 (1985)
3 Airaksinen PJ, Drance SM, Schulzer M: Neuroretinal rim area in early glaucoma Am J Ophthalmol 99: 1–4 (1985)
4 Balazsi AG, Drance SM, Schulzer M, Douglas GR: Neuroretinal rim area in suspected glaucoma and early chronic open angle glaucoma Correlation with parameters of visual function Arch Ophthalmol 102: 1011–1014 (1984)
5 Flammer J, Drance SM, Augustiny L, Funkhauser A: Quantification of glaucomatous visual field defects with automated perimetry Inv Ophthalmol Vis Sci 26: 176–181 (1985)
6 Littmann H: Zur Bestimmung der wahren Grösse eines Objektes auf dem Hintergrund des lebenden Auges Klin Monatsbl Augenheilkd 180: 286–289 (1982)

Author's address:
Dr P Juhani Airaksinen, M D ,
Department of Ophthalmology,
University of Oulu, SF-90220 Oulu, Finland

V.2 Comparison of the changes in the area of optic disc pallor and visual fields: a 9-year follow-up study

A. TUULONEN, P.A JUVALA, D.-C. WU, H.I ALANKO,
P.J. AIRAKSINEN and B. SCHWARTZ
Oulu, Finland and Boston, U.S.A

Abstract

The changes in the optic disc pallor and Friedmann visual fields were compared in 38 glaucomatous, 85 ocular hypertensive and 20 normal eyes during a mean follow-up of 8.9 years. The highest rate of change of both visual field mean defect and pallor area occurred in 35 initially ocular hypertensive patients who developed glaucoma during the follow-up. The changes were second largest in the glaucoma group. Ocular hypertensives who were regarded clinically stable were placed between normals and glaucomas. The measurement of pallor seems to be a more sensitive indicator of glaucoma damage in early glaucoma than in further advanced glaucoma in which visual field examination may be more useful to quantitate progression. The changes of pallor showed good correlation to the changes of neuroretinal rim area.

Introduction

The optic disc can be evaluated using two characteristics, structure and color. The importance of distinguishing cupping and pallor as different signs of glaucomatous optic disc damage has been emphasized in the literature [5]. The area of pallor is defined as the region of maximal color contrast in the optic disc [5]. The brigthness of the neuroretinal rim represents another aspect in evaluating the color of the optic disc in glaucomatous patients in whom the relative brightness of the neuroretinal rim has been reported to be greater than in normals [4] The present study concentrates only in measuring the area of pallor

The area of optic disc pallor has been established to be an important indicator of optic nerve damage in glaucoma [5] with good correlation to glaucomatous visual field changes [6]. In ocular hypertensives the increase in the percent area of pallor, that is the ratio of pallor area to disc area, has been found to be greater than in normal subjects [3].

However, there are no reports in which the changes of optic disc pallor have been studied in a large number of patients over a long period of time. The purpose of this retrospective study was to evaluate the changes of pallor area over time and correlate them to the visual field changes.

Material and methods

Hundred fourty-three eyes of 143 patients (95 women and 48 men) were followed for a mean of 8.9 years. 38 patients had open angle glaucoma (13 simple glaucoma, 13 capsular glaucoma and 12 low tension glaucoma) and 85 patients were diagnosed as ocular hypertensives (intraocular pressure was more than 21 mm Hg repeatedly with clinically normal disc appearance and visual fields) in the beginning of the study. Twenty subjects were normal. All patients were photographed at least 3 (up to 8) times during a minimum follow up of 5 (up to 16) years (Table 1). The mean follow-up periods did not differ statistically significantly in the three groups. The mean ages of the glaucomas, ocular hypertensives and normals were statistically significantly different between all groups (Table 1).

Black-and-white disc stereophotographs were taken using a Zeiss fundus camera and an Allen stereoseparator [1] The negatives of the photographs were digitized into the computer and measured using the technique of computerized image analysis [3] with the aid of manually applied plan points (AT). The intraphotographic error was 5 3% and the interphotographic one 3.8% (coefficient of variation). All computerized images of each patient were measured at one session and they were masked for the date of the photograph, patient's clinical data and name. The area of pallor is expressed as a ratio to the disc area × 100%.

The central visual fields were examined with a Friedmann analyzer on the day of photography. A mean defect of each visual field was calculated by comparing it with the screening values of different age groups of the Friedmann analyzer

For each eye the pallor measurements and mean defects of visual fields were plotted against time and the changes in them over time were calculated by using a

Table 1 The mean ages, mean follow-up periods and mean number of occasions of photography in glaucomas (OAG), ocular hypertensives (OH) and normals (NOR)

	Mean age (yrs +/− SD)	Mean follow-up (yrs +/− SD)	Mean number of occasions of photography (+/− SD)
OAG	63 3 +/− 8 5	8 5 +/− 2 3	3 7 +/− 0 9
OH	57 1 +/− 8 8	9 2 +/− 2 6	4 3 +/− 1 1
NOR	43 9 +/− 13 7	8 5 +/− 2 9	3 1 +/− 1 2

simple regression with the method of least mean squares (the rate of change = regression coefficient). The means between groups were analyzed by the analysis of variance

Results

The mean initial areas of pallor and the mean defects of visual fields (Table 2) were statistically significantly larger in glaucomatous eyes than in ocular hypertensive and normal eyes (p<0 001).

The mean yearly changes of visual field mean defect and pallor in different diagnostic groups are presented in Table 3. When the patients with an initial diagnosis of ocular hypertension were divided into ones who were regarded clinically stable during the follow-up (n = 50) and into ones who developed glaucoma by the end of the study period (n = 35), the yearly rate of change of pallor in ocular hypertensive patients developing glaucoma was 3 times higher than in glaucoma patients (p<0.01) and 47 times higher than in normals (p<0.001) (Table 3) The rate of change of pallor was statistically significantly

Table 2 The mean initial area of pallor and initial mean defect of the visual field in glaucomas (OAG), ocular hypertensives (OH) and normals (NOR)

	Initial pallor area (% +/− SD)	Initial mean defect of visual field (dB +/− SD)
OAG	58 8 +/− 11 5	3 11 +/− 3 65
OH	33 6 +/− 15 1	0 06 +/− 0 21
NOR	36 0 +/− 18 8	0 01 +/− 0 04

Table 3 The mean yearly changes of pallor and mean defect of the visual field in glaucomas (OAG), ocular hypertensives (OH) and normals (NOR) OH patients were divided into ones who clinically developed glaucoma (OH → GLA) and into ones who remained ocular hypertensives (OH → OH)

	n	Mean change of pallor per year (% +/− SD)	Mean change of mean visual field defect per year (dB +/− SD)
OAG	38	0 528 +/− 0 732	0 192 +/− 0 432
OH	85	0 792 +/− 1 368	0 132 +/− 0 360
NOR	20	0 036 +/− 0 084	0 000 +/− 0 012
OH → GLA	35	1 692 +/− 1 764	0 204 +/− 0 336
OH → OH	50	0 156 +/− 0 216	0 072 +/− 0 372

lower in normals than in glaucoma patients (p<0.01) and in clinically stable ocular hypertensive patients (p<0.001).

The mean visual field defect increased in 68% (26 eyes) of the glaucoma patients. Half of these 26 eyes also showed an increase in the area of pallor. An increase of pallor area without a visual field defect was detected in 11% of the glaucoma patients. 11% of the glaucoma cases showed neither visual field nor pallor changes.

The rate of change of mean defect was statistically significantly higher in ocular hypertensive patients developing glaucoma than in normal subjects (p<0.01). The mean visual field defect increased in 54% (19 out of 35 eyes) of the ocular hypertensive patients who became glaucomatous during the follow-up and the area of pallor increased in all of these 19 eyes. The increase of pallor area without field loss was detected in 26% of ocular hypertensive patients who developed glaucoma and 18% of them had neither visual field nor pallor changes.

An increase of pallor area was measured in 28% (14 out of 50 eyes) of the ocular hypertensives who were regarded clinically stable. 21% of these 14 eyes showed also an increase of mean defect of the visual field.

The neuroretinal rim area was measured in the same material [2]. Regression of yearly changes of pallor area to neuroretinal rim area showed an R^2 of 32.5% (p = 0.000) in glaucoma group and an R^2 of 19.0% (p = 0 006) in ocular hypertensive group which developed glaucoma during the follow-up.

Discussion

The results of the present study indicate that changes in the area of pallor correlate with progression of glaucoma However, in only half of the glaucoma cases with visual field progression also an increase in pallor area was detected. In all initially ocular hypertensive patients who became glaucomatous during the follow-up, development and progression of field changes was accompanied by pallor increase. Pallor increased without visual field deterioration in 11% of glaucomas and 26% of initially ocular hypertensives who developed glaucoma later on. These findings may indicate that in early stages of glaucoma measurement of pallor changes may be more beneficial indicating the progression of the disease than in more advanced cases In further advanced glaucomatous eyes with large areas of pallor, pallor changes may no longer be as sensitive and reliable indicator of disease progression as visual field examination.

The rate of change of pallor correlated with the rate of change of neuroretinal rim area. However, the R^2 was only 32.5%. Hence, in some cases the change in structure while in others the change in color of the disc indicated the progression of the disease. For accurate and reliable finding of all the progressing glaucoma cases, measurement of both pallor area (in completion with measuring the color of the rim) and neuroretinal rim area are necessary in addition to visual field

examination. Further studies are needed to show whether the correlation of visual field and pallor changes improve when patients are examined with threshold measurements of automated perimeter in far more test locations than the 46 points of Friedmann analyzer.

Acknowledgements

References

1 Airaksinen PJ, Nieminen H: Retinal nerve layer photography in glaucoma Ophthalmology 92: 877–879 (1985)
2 Airaksinen PJ, Juvala PA, Tuulonen A, Alanko HI, Valkonen R, Tuohino A: Visual field and neuroretinal rim changes with time Doc Ophthalmol Proc Ser 287–291 (1987)
3 Nagin P, Schwartz B: Detection of increased pallor over time Computerized image analysis in untreated ocular hypertension Ophthalmology 92: 252–260 (1985)
4 Robert Y, Hendrickson P: Color appearance of the papilla in normal and glaucomatous eyes A photopapillometric study Arch Ophthalmol 102: 1772–1775 (1984)
5 Schwartz B: Cupping and pallor of the optic disc Arch Ophthalmol 89: 272–277 (1973)
6 Schwartz B: Correlation of pallor of optic disc with asymmetrical visual field loss in glaucoma XXII Concilium Ophthalmologicum, Paris 1974 Paris, Mousson Publishers, 632–638 (1976)

Author's address:
Anja Tuulonen, M D ,
Department of Ophthalmology, University of Oulu, SF-90220 Oulu, Finland

V.3 The changes of visual field sensitivity accompanied by enlargement of the glaucomatous optic cup

N KATSUMORI, K. OKUBO and K. MIZOKAMI
Kobe, Japan

Abstract

The correlation between visual field damage and enlargement of the optic disc was evaluated by means of cup to disc area ratio (C/D A) and visual field sensitivity measured with Octopus program 31 (% S).

Optic disc and visual field were divided into 12 sectors according to the distributional patterns of the nerve fiber bundles of the retina. To evaluate the correlation, we paid specific attention to the inferotemporal and superotemporal sectors. A highly significant correlation between C/D.A and % S was obtained. Visual field damage was divided into 3 stages.

In the early stage, the change of C/D.A. was more prominent than that of % S and some cases showed marked increase of C/D.A without change of % S. We conclude that progression of cupping may precede visual field defects. However, in the late stage, % S decreased remarkably, accompanied by only slight increase of C/D.A.

Introduction

The correlation between visual field damage and enlargement of the optic cup is not defined yet especially in the early glaucomatous stage.

Previously [4], we evaluated this correlation by means of cup to disc area ratio (C/D.A) and visual field sensitivity (% S) measured with Octopus automatic perimeter. In analysing correlation between C/D.A and % S, the optic disc was divided into 12 sectors according to the distributional patterns of nerve fiber bundles of the retina. Especially for the inferotemporal sectors and superotemporal sectors, a highly significant correlation was obtained. A 13–17% decrease in % S was found prior to detectable visual field defects by the Goldmann perimetry.

In the present study, the correlation between change of the optic disc and the visual field was evaluated in patients who had been followed up for about 5 years.
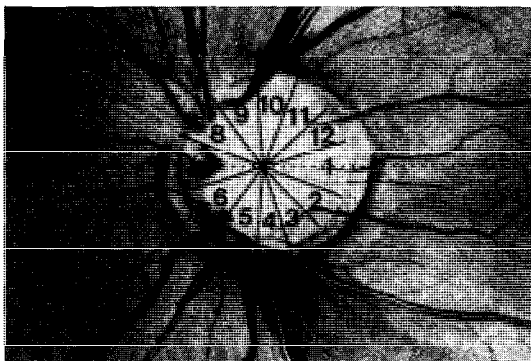
Figure 1 Dividing of the disc

Materials and methods

Thirty eyes of 19 patients (11 male, 8 female) with early glaucomatous visual field defects were followed up for about 3 to 6 years (average 5.1 years). The initial age range was 21–70 years with a median age of 44 years. Stereoscopic disc photographs and red-free fundus photographs were taken several times during the period of follow-up. Visual fields were examined with Octopus automatic perimeter at or near the time of disc photographs.

The disc photographs were projected with 20 times magnification and disc and cup margins were traced on paper while comparing with stereoscopic photographs. The optic disc was divided into 12 sectors according to the distributional patterns of nerve fiber bundles of the retina (Fig. 1). The papillomacular fiber area (sector 1) was defined as a sector with an angle of 35 degrees. The arcuate fiber bundle areas were divided into 3 sectors with an angle of 25 degrees (sectors 2 to 4 and 10 to 12) The nasal area was divided into 5 sectors (5 to 9). With the use of a digitizer operated by a microcomputer, the area of the disc and the cup were determined and the cup to disc area ratio at each sector was calculated. The variation of measurements in our method was within ± 0.9% [4].

The central visual field within 30 degrees of fixation was examined with Octopus using program 31. The 73 test points were divided into 12 parts according to the course of the nerve fibers of the retina corresponding to the disc sectors (Fig. 2). The normal blind spot and the nasal 5 points on the horizontal meridian were excluded because they could not be divided according to the nerve fiber disribution. For each sector, the ratio of the average sensitivity of the glaucomatous eye to that of an age-matched normal eye was calculated (% S).

In this study we employed the inferotemporal sectors, sectors 3 and 4, and the superotemporal sectors, sectors 10 and 11 for the evaluation of the change of C/D.A and % S. Based on the previous results, visual field damage was divided

```
                        4
                5   4   4   4   4
            5   4   4   4   3   3   3
        6   5   4   3   3   3   3   3   3
        6   5   3   2   2   2   2   3   3
    7   7   X   1   1   1   X   X   X   X   X
        8   9  11  12  12  12  12  11  11
        8   9  10  11  11  11  11  11  11
            9  10  10  10  11  11  11
                9  10  10  10  10
                       10
```

Figure 2 Dividing of the visual field measured by Octopus program 31

into 3 stages, i.e. early stage (% S > 83%), middle stage (83% > % S > 50%), late stage (50% > % S).

Results

Changes of C/D A (final C/D.A − initial C/D.A) vary from 0.1% to 25% Changes of % S (initial % S − final % S) vary from −11% to 35.8%. Fig. 3 shows changes of C/D A and % S The closed circles represent early stage visual field defects and the open circles the late stage defects. In the early stages there is only a slight change of % S; some cases show a marked increase of C/D.A without change of % S. However, in the late stages, the change of % S is more prominent.

The ratios of the change of % S to that of C/D A are shown in Table 1. A statistical significant difference is found for each stage (p<0 01).

Fig. 4 shows the eyes with visual field damage in the early to middle and middle to late stages. Enlargement of cupping in the early to middle group is greater. The ratio of % S to C/D.A is 0.97 ± 0.47 in the early to middle group and 5 05 ± 4.77 in the middle to late group. There is a significant difference between the two groups (p<0.01).

Table 1 Ratios of the change of % S to that of C/D A Difference statistically significant (p<0 01)

Stage	% S / C/D A
Early	− 0 26 ± 1 17
Middle	0 68 ± 1 84
Late	3 68 ± 3 46

Figure 3 Changes of C/D A and % S
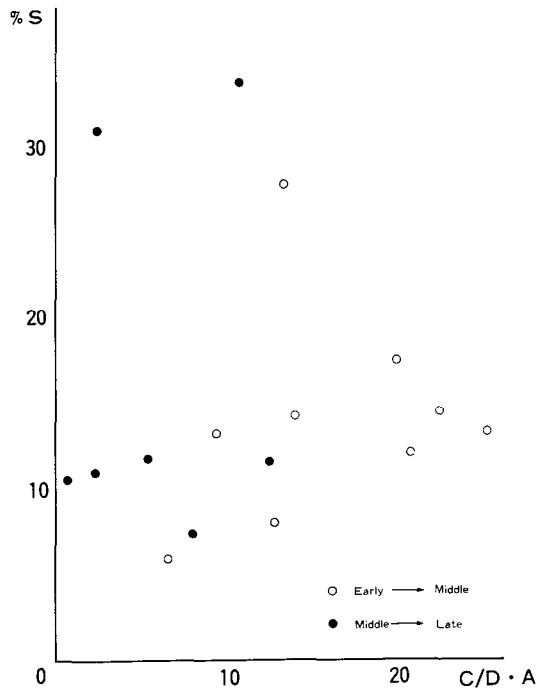
Figure 4 Changes of C/D A and % S

Sector No.	%S	C/D.A
3	31.2 (M-L)	13.6
4	8.4 (M-M)	12.4
10	6.6 (E-E)	11.7
11	2.5 (E-E)	21.2
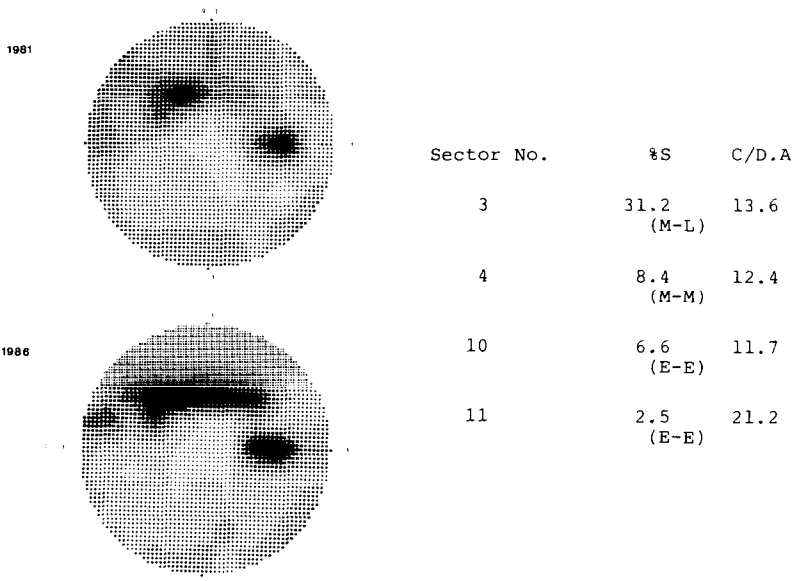
Figure 5 Changes of C/D A and % S with Octopus visual field (case 1) E: early stage, M: middle stage, L: late stage

Case presentation

Case 1· 26-year-old male

The change of C/D.A and % S is shown in Fig. 5. In the nasal upper area, the visual field defect has progressed during 5 years In sectors 3 and 4, the % S decrease corresponds to the increase of C/D.A But in sectors 10 and 11, the C/D.A increases without change of % S. This case shows that in the early stage, progression of cupping occured prior to a detectable visual field defect

Case 2· 51-year-old male

Fig. 6 shows the results of case 2. Both in the nasal upper and lower areas, the visual field defect has progressed. Comparing sector 4 (early stage) with sector 11 (late stage), the change of % S is almost equal, but the increase of C/D.A is greater in sector 4. This shows that in the late stage, the visual field defect may progress with only a slight increase of C/D.A

Sector No.	%S	C/D.A
3	18.9 (M-M)	23.4
4	13.5 (E-M)	25.0
10	3.1 (M-M)	6.7
11	12.0 (L-L)	4.4
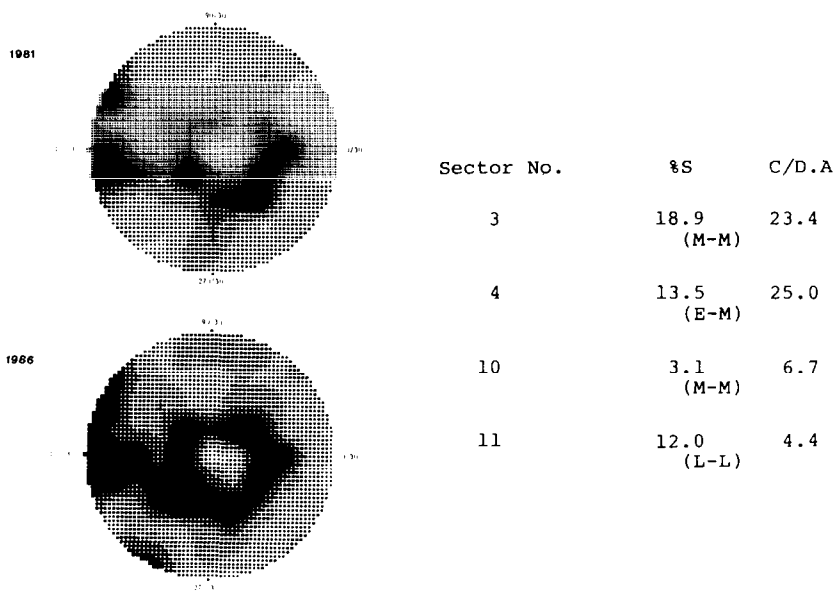
Figure 6 Changes of C/D A and % S with Octopus visual field (case 2) E: early stage, M: middle stage, L: late stage

Discussion

To evaluate the correlation between visual field damage and enlargement of the optic cup, one of the major problems is the quantification of the visual field. We solved this by measuring the sensitivity with the Octopus automatic perimeter which provides numerical values that allow quantification of the visual field defect.

In this study, most of the early stage cases showed negative changes in % S, that is, recovery of visual function. It suggests that there may be about 10% variation in the glaucomatous visual field sensitivity and in our modified method for the calculation. But it has also been reported that reversibility of glaucomatous visual field damage is seen after intraocular pressure normalization, especially in early stage visual field damage [2]. Thus, it may also be considered that most of these cases show possible functional recovery in the early stage.

Pederson et al. [5] reported that progression of disc cupping often preceded visual field progression from elevated IOP. Okubo et al. [3] reported that a 20% increase in C/D A seemed to be necessary before detection of a visual field defect with manual perimetry using the Goldmann-perimeter was possible. In our study, a change of C/D.A was more prominent than a change of % S in the early stage of visual field damage. Some cases showed a marked increase of C/D.A without a change of % S. We conclude that progression of cupping precedes visual field defects

Several explanations were presented for the progression of cupping in this stage, for example, selective glial loss from the disc substance [1] and enlargement of scleral opening without loss of disc tissue following the backward stretching of the lamina cribrosa [7] Recently Quigley et al. [6] demonstrated that histologically definite diffuse loss of axons occured prior to reproducible visual field defect in glaucoma suspect patients. In our patients with early stage visual field defects, it seemed that the cup enlarged due to nerve fiber loss even if a visual field defect could not be detected clinically.

In the late stage, the % S decreased remarkably although the increase of C/D.A was only slight. In this stage, many nerve fibers of the disc have already been lost.

Acknowledgements

References

1 Anderson DR: Pathogenesis of glaucomatous cupping: A new hypothesis In: Symposium on glaucoma, pp 81–94 CV Mosby, St Louis, 1975
2 Mizokami K, Tagami Y, Isayama Y: The reversibility of visual field defects in the juvenile glaucoma cases Docum Ophthal Proc Series 19: 241–246 (1979)
3 Okubo K, Mizokami K: Correlation between glaucomatous optic disc and visual field defects I Early glaucomatous stage Jpn J Clin Ophthalmol 37: 607–612 (1983)
4 Okubo K, Katsumori N, Mizokami K: Correlation between glaucomatous optic disc and visual field defects II Quantitative evaluation Acta Soc Ophthalmol Jpn 88: 332–337 (1984)
5 Pederson JE, Anderson DR: The mode of progressive disc cupping in ocular hypertension and glaucoma Arch Ophthalmol 98: 490–495 (1980)
6 Quigley HA, Addicks EM, Green WR: Optic nerve damage in glaucoma III Quantitative correlation of nerve fiber loss and visual field defect in glaucoma, ischemic neuropathy, papilledema and toxic neuropathy Arch Ophthalmol 100: 135–146 (1982)
7 Robin AL, Quigley HA, Pollack IP, Maumenee AE, Maumenee IH: An analysis of visual acuity, visual fields and disc cupping in childhood glaucoma Am J Ophthalmol 88: 847–858 (1979)

Author's address:
Dept of Ophthalmology,
School of Medecine,
Kobe University, 7-chome,
Kusunoki-cho, Chuo-Ku, Kobe, 650, Japan

Editorial comment

These authors report a change of cup over disc area varying from 0.1% to 25%. It is well known that measurements of cup-disc parameters are subject to considerable intra-observer variation. Even with computerized methods of optic nerve head analysis the variation of measurements may be up to 10%. A change of 0.1% must be in the range of measurement errors.

Similarly the authors report changes in the so-called percentage-sensitivity of the visual field ranging from −11 to +35.8%. A large part of these changes is to be expected because of long-term fluctuation.

If one assumes that a 10% change in disc-or field parameters is within intraobserver error or caused by long-term fluctuation, then about 6 points in figure 3 show a greater change in both visual field and cup/disc parameters. All these points represent early defects.

V.4 Patterns of early visual field loss in open angle glaucoma

J. CAPRIOLI and M SEARS
New Haven, U.S.A.

Abstract

The pattern of visual field loss in patients with low tension glaucoma may be different from that of patients with high tension glaucoma, suggesting two separate mechanisms for glaucomatous optic nerve damage However, intraocular pressure criteria may not adequately segregate groups of patients with different causes of glaucomatous optic nerve damage. We identified two groups of open angle glaucoma patients with distinctly different patterns of early visual field loss. The first group showed diffuse depression of the differential light sensitivity throughout the entire visual field. The second group manifested localized, dense scotomata without depression of the remaining field Patients in each visual field group were identified in a masked fashion using only visual field criteria, and were matched for total field loss. Significant differences in intraocular pressure levels and optic disc rim width were found between the two groups. Patients with diffuse loss had higher intraocular pressure and wider temporal optic disc rims than patients with localized loss.

Introduction

Patterns of visual field defects in low tension glaucoma and in high tension glaucoma have been investigated [1, 2, 6–11]. Some authors have reported significant differences in patterns of field loss between the two groups, while others have found no differences. Variations in the criteria used for patient selection make direct comparisons between different studies difficult Stages of the disease may frequently not be comparable. More importantly, the single criterion of intraocular pressure probably does not adequately separate subpopulations of glaucoma patients. The terms 'low tension' and 'high tension' imply that intraocular pressure differences alone may adequately separate these two 'entities' [3–4], but the semantics are not reassuring. Functional and, ultimately, pathophysiological definitions are required.

To supply additional useful information in this area, we have taken a new approach. We examined a number of ocular characteristics of patients with open angle glaucoma differentiated on the basis of visual field findings alone. The criteria for visual field abnormalities were designed to separate patients whose eyes showed diffuse depression of the visual field from from patients whose eyes showed dense, localized scotomas.

Methods

The screening criteria for initial patient selection are given in Table 1. These criteria were designed to reduce the possibility of including eyes with diffuse depression due to non-specific causes such as uncorrected refractive error, cataract, and miosis. Patients were selected from the records of the Yale Glaucoma Service, and carried a diagnosis of primary open angle glaucoma or low tension glaucoma and had serial automated static threshold visual fields (Octopus) during the last five years. The screening of records was performed by the technical staff of the Yale Glaucoma Service. The investigators remained masked as to the identity of patients selected. Sixty-three eyes of fifty-nine patients met the initial screening criteria. Of patients who qualified bilaterally, one eye was chosen for inclusion into the study by the toss of a coin. The most recent visual fields of each eye were used for the study.

Visual field indices introduced by Flammer et al. [5] were used to select eyes with a relatively pure form of diffuse visual field loss and those with a relatively pure form of localized dense loss. Mean defect (MD) is the average sensitivity loss compared to age-matched normals of all points tested. While its value may be affected by any visual field abnormality, it is increased relatively little by localized

Table 1

Criteria for selection	
Diagnosis	primary open angle glaucoma or low tension glaucoma
History	no eye surgery
	no other eye disease
	no other reason for visual field loss
Age	50–80 years
Refractive error	≤3 diopters ammetropia
	≤2 diopters astigmatism
Visual acuity	≥0 67
Visual field	total loss 100–300 decibels
	root mean square ≤3 0 decibels
	rate of false (+) and false (−) ≤10%
	pupil size ≥3 0 mm
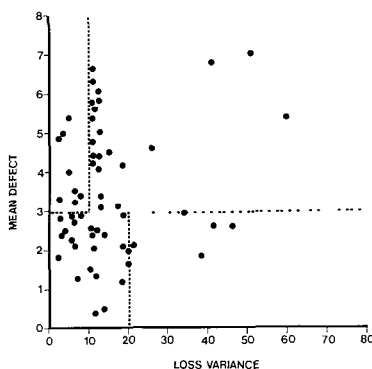
Figure 1 Mean defect (decibels) versus loss variance (decibels²) in fifty-nine eyes meeting the selection criteria The dotted lines represent criteria for mean defect and loss variance designed to identify two groups of patients with relatively pure types of visual field loss

scotomas but increased greatly by diffuse depression of sensitivity The statistical variance of sensitivity loss compared to normal values for all points tested is termed loss variance (LV), and includes a component of variance over time (short term fluctuation). Corrected loss variance (CLV) is calculated from LV by subtracting out short term fluctuation (SF). SF can be estimated by measuring the threshold of the same test location multiple times over the course of the test. CLV (and to a lesser extent, LV) is a measure of scatter or local non-uniformity of visual field thresholds. It is not affected by uniform diffuse depression of sensitivity, but is increased by localized defects. Thus, MD and CLV are visual field indices which are sensitive to different types of loss: MD is sensitive to diffuse depression, while CLV is sensitive to localized defects.

MD and LV were calculated from each visual field (Program 32) after eliminating the most peripheral loci of test locations and the three loci usually containing the blind spot. LV was used rather than CLV, since an estimate of scatter over time (SF) is limited with Progam 32, which tests only ten locations twice. However, selection criteria demanded that the root mean square fluctuation (a measure of short term fluctuation) be ≤ 3 decibels. Correction of LV for short term fluctution (i.e., the use of CLV) would not have altered the selection of patients for study. Values for MD and LV for all fifty-nine eyes in the study population were plotted on a scattergram (see Figure 1). Arbitrary definitions were made to select patients with predominantly diffuse loss (MD > 3 decibels, LV < 10 decibels) and localized scotomas (MD ≤ 3 decibels, LV ≥ 20 decibels). These definitions identified eight eyes with diffuse field loss, and seven eyes with localized scotomas.

Information regarding each of the patients whose eyes were selected for final analysis was obtained from our patient records, and from referring physicians where appropriate. This included medical history, surgical history, ocular his-

tory, ocular medications, blood pressure, intraocular pressure (IOP), and visual field data. This information was complied without the investigators' knowledge of the patient's identity, or to which visual field group the patient belonged.

It is impossible to derive a single number which adequately summarizes an eye's intraocular pressure history. Therefore, we took several approaches The mean, median, high, and low values of all recorded pressures were identified for each eye, on or off medication. In addition, eyes were assigned to IOP categories in a masked fashion as follows: eyes with recorded pressures frequently above 25 mm Hg were included in a 'high' IOP group; eyes with pressures frequently above 20 mm Hg but infrequently above 25 mm Hg were assigned to an 'intermediate' IOP group; eyes with IOP infrequently above 20 mm Hg were assigned to a 'low' IOP group The optic disc of each patient was analyzed from stereoscopic color photographs taken on the same day the visual field was obtained. While viewing a photographic pair stereoscopically, the disc rim and cup rim were traced on a projected image for each eye using contour clues only, and measurements of rim width normalized to the disc diameter were made along eight meridians

Data were analyzed with the help of Student's t-test and chi-square testing, with a significance level of $p < 0.05$.

Results

The diffuse loss group included four males and four female patients, and the localized loss group included two males and five females. Two patients in the

Table 2

	Clinical data (mean ± SEM)	
	Diffuse (n = 8)	Localized (n = 7)
Age (years)	68 0 ± 3 3	65 4 ± 3 3
Visual acuity	0 81 ± 0 05	0 89 ± 0 05
Refractive error (spherical equiv , diopters)	0 9 ± 0 6	0 9 ± 0 4
Pupil size (mm)	3 5 ± 0 3	4 0 ± 0 5
Eye medications	2 0 ± 0 3	1 5 ± 0 3
Visual field (decibels)		
Mean defect	4 0 ± 0 3	2 1 ± 0 2
Loss variance	5 5 ± 0 8	29 5 ± 4 0
Root mean square	2 0 ± 0 2	1 9 ± 0 2
Total loss	211 ± 15	166 ± 24

diffuse group and three patients in the localized group had been treated for systemic hypertension. One patient in the diffuse group was receiving systemic beta blockers, while three patients in the localized group were similarly treated One patient had a history of significant systemic hypotension and belonged to the localized group. All patients in the diffuse group carried a clinical diagnosis of primary open angle glaucoma, while four of the seven patients in the localized group carried the diagnosis of low tension glaucoma Three patients in the diffuse group had a family history of glaucoma, while two patients in the localized group had such a history.

Data regarding age, visual acuity, refractive error, pupil size, number of eye medications, and visual field are given in Table 2. There were statistically significant differences beteen visual field MD and LV due to patient selection criteria. There was no difference in the RMS value between the two groups, nor was there a statistically significant difference in total loss

IOP data are given in Tables 3 and 4. The diffuse group manifested significantly higher pressures than the localized group regardless of the statistic used That is, the diffuse group had higher mean pressures, had higher median pressures, and had higher extremes of IOP than did the localized group The difference in IOP values between the two groups ranged from 3 to 5 mm Hg. Table 4 summarizes the IOP categories assigned to eyes of the two groups. The diffuse group was

Table 3

	Intraocular pressure (mm Hg, mean ± SEM)	
	Diffuse (n = 8)	Localized (n = 7)
Mean	21 9 ± 0 9	17 6 ± 0 8 (p<0 01)
Median	22 0 ± 0 9	17 7 ± 0 6 (p<0 01)
High	27 6 ± 1 2	22 4 ± 1 4 (p<0 02)
Low	17 0 ± 1 0	13 3 ± 0 8 (p<0 05)

Table 4

	Intraocular pressure categories*	
	Diffuse	Localized
High	3	0
Intermediate	5	2
Low	0	5
		(p<0 01)

* See text for criteria
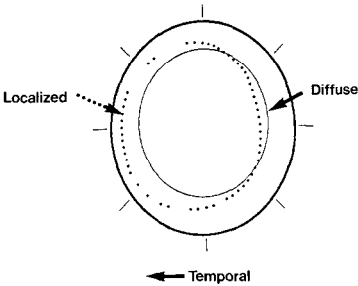
Figure 2 Diagramatic representation of the mean optic nerve rim width in patients with diffuse visual field loss, and in patients with localized visual field loss There are significant differences in the rim width temporally (see Table 5)

skewed toward the high range of pressure while the localized group was skewed toward the low range of pressure. However, overlap between the two groups is apparent.

Analysis of stereoscopic photographs of the optic nerve head revealed the disc rim to be_significantly thinner in the localized group compared to the diffuse group. The largest differences were noted in the temporal area of the rim (see Table 5). The mean position of the cup edge in each of the two groups is demonstrated graphically in Figure 2. The cup is larger and shifted eccentrically towards the temporal and inferotemporal disc rim in the localized group compared to the diffuse group.

Table 5

Position*	Rim/Disc ratio (mean ± SEM)		
	Diffuse (n = 8)	Localized (n = 7)	
12:00	0 13 ± 0 03	0 10 ± 0 02	
10:30	0 18 ± 0 02	0 07 ± 0 02	(p<0 01)
9:00	0 15 ± 0 02	0 06 ± 0 03	(p<0 05)
7:30	0 16 ± 0 01	0 05 ± 0 03	(p<0 01)
6:00	0 20 ± 0 01	0 12 ± 0 08	
4:30	0 22 ± 0 02	0 16 + 0 01	(p<0 02)
3:00	0 22 ± 0 02	0 18 ± 0 02	
1:30	0 20 ± 0 01	0 19 ± 0 02	
Mean	0 19 ± 0 01	0 11 ± 0 02	(p<0 05)

* The clock-hour position is standardized to the right eye (i e , 9 o'clock is temporal)

Discussion

Several investigators have searched for differences in patterns of visual field loss in patients with low tension glaucoma compared with high tension glaucoma [1, 2, 6–11]. While some have found no differences in types of visual field loss between the two groups [7, 9, 10], others have found significant differences [1, 2, 6, 8, 11]. Varying patient selection criteria may account for the apparent differences in these results. Clearly, intraocular pressure criteria alone do not adequately subdivide groups of patients, unless perhaps extremes of intraocular pressure are used to divide patients. Then clear patterns may emerge [2, 3].

Utilizing differences in measured intraocular pressures is probably not the best way to subdivide potential subgroups of patients with open angle glaucoma Because of the controversy in this area, we took a new approach to examine the problem. Eyes were assigned solely on the basis of visual field criteria in an effort to study eyes with a relatively pure type of diffuse visual field loss contrasted to those with a relatively pure type of localized loss. Pure examples are difficult to find so that the numbers of subjects in this initial study are small. Nevertheless, different patterns appear to emerge between these groups with respect to intraocular pressure and optic nerve cupping. The selection criteria were designed to minimize the problem created by eyes included in the diffuse loss group because of non-glaucomatous reasons such as cataract, miosis or refractive error. Selection criteria also included standards for patient reliability and placed a limit on the magnitude of short term fluctuation, further reducing the number of eyes included.

Although considerable overlap was evident between the groups regarding intraocular presure levels, the pressures were consistently higher in the diffuse group compared to the localized group whether analyzed by IOP mean, median, high values, or low values. A better way of summarizing IOP history may be to place eyes into intraocular pressure categories in a masked fashion. The diffuse group contained more eyes in the high IOP category, while the localized group contained more eyes in the low IOP category. Still, there was some overlap in the intermediate pressure category.

We emphasize that all eyes included in this study were in an early phase of glaucomatous optic nerve damage and were matched for equal amounts of total visual field loss. We believe it is rational to match patients for stage of the disease by using visual field criteria rather than using disc cupping. There are no 'normal' values for optic disc cupping, but there are 'normal' values for visual field thresholds. In eyes matched by visual field criteria, it is evident that the pattern of optic disc cupping in patients with localized loss is different from that of patients with diffuse loss. The diffuse loss eyes have round optic nerve cups which are central, and have a disc rim which is intact and uniform in thickness. By contrast, eyes in the localized loss group have optic discs with significantly more cupping occurring eccentrically with shallow thinning of the disc rim temporally and inferotemporally.

We hypothesize, based on this preliminary information and pending further work, that diffuse loss of visual field sensitivity from glaucoma is largely pressure dependent, and may be secondary to diffuse axonal dysfunction (and later death) leading to progressive concentric enlargement of the optic nerve cup. In the localized loss group, visual field loss seems less pressure dependent. Here loss may occur at low pressures as well as high pressures. The damage to the optic nerve head tends to be less generalized, leading to focalized loss of the disc rim temporally. It is tempting to speculate that pressure-dependent gradual diffuse loss may involve a prolonged phase of ganglion cell dysfunction without death, leading to visual abnormalities with relatively small amounts of progressive cupping. This could explain the presence of psychophysical disturbances preceding detectable morphologic change. On the other hand, the localized loss group may be associated with accelerated ganglion cell death leading to thinning of the disc rim and dense scotomas in a relatively 'early' phase of the disease.

The eyes selected for this study represent examples of relatively pure types of visual field loss. It is apparent that the majority of patients with glaucomatous optic nerve damage have a mixed type of visual field loss; with both diffuse depression and scotomas occuring in the same field. Diffuse loss may precede scotomas in many patients, and at an advanced stage of the disease, patterns of visual field loss may become indistinguishable. This study represents a beginning to identify possible subsets of patients with glaucoma and to quantify the abnormalities within these subsets.

Acknowledgement

References

1 Anderton S, Hitchings RA: A comparative study of visual fields of patients with low-tension glaucoma and those with chronic simple glaucoma In: Greve EL, Heijl A (eds) Fifth international visual field symposium, pp 97–99 Dr W Junk Publishers, Dordrecht, 1983
2 Caprioli J, Spaeth GL: Comparison of visual field defects in the low-tension glaucomas with those in the high-tension glaucomas Am J Ophthalmol 97: 730–737 (1984)
3 Caprioli J, Spaeth GL: Comparison of the optic nerve head in high- and low-tension glaucoma Arch Ophthalmol 103: 1145–1149 (1985)
4 Drance SM: Low-tension glaucoma Arch Ophthalmol 103: 1131–1133 (1985)
5 Flammer J, Drance SM, Augustiny L, Funkhouser A: Quantification of glaucomatous visual field defects with automated perimetry Invest Ophthalmol Vis Sci 26: 176–181 (1985)
6 Greve EL, Geijssen C: Comparison of glaucomatous visual field defects in patients with high and with low intraocular pressures In: Greve EL, Heijl A (eds) Fifth international visual field

symposium, pp 101–105 Dr W Junk Publishers, Dordrecht, 1983

7 King D, Drance SM, Douglas G, Schulzer M, Wijsman K: Comparison of visual field defects in normal-tension glaucoma and high-tension glaucoma Am J Ophthalmol 101: 204–207 (1986)

8 Levene RZ: Low-tension glaucoma A critical review and new material Surv Ophthalmol 24: 621 (1980)

9 Motolko M, Drance SM, Douglas GR: The visual field defects of low-tension glaucoma A comparison of the visual defects in low-tension glaucoma with chronic open-angle glaucoma In: Greve EL, Heijl A (eds) Fifth international visual field symposium, pp 107–112 Dr W Junk Publishers, Dordrecht, 1983

10 Phelps CD, Hayreh SS, Montague PR: Visual fields in low-tension glaucoma, primary open angle glaucoma, and anterior ischemic optic neuropathy In: Greve EL, Heijl A (eds) Fifth international visual field symposium, pp 113–124 Dr W Junk Publishers, Dordrecht, 1983

11 Primrose J: Clinical review of glaucomatous discs In: Cant JS (ed) The optic nerve, p 314 CV Mosby, St Louis, 1972

Author's address:
Department of Ophthalmology and Visual Science,
Yale University School of Medicine,
P O Box 3333, New Haven, CT 06510-8061, U S A

V.5 Is there a difference between glaucoma patients with rather localized visual field damage and patients with more diffuse visual field damage?

A. GLOWAZKI and J. FLAMMER
Berne, Switzerland

Abstract

Fifty-four patients with diffuse visual field damage were compared with the same number of patients with localized visual field damage. The visual fields were measured with the Octopus program G1. Patients with predominantly diffuse visual field damage were significantly younger and tended to have higher IOP than patients with localized visual field damage.

Introduction

Glaucoma is known to produce characteristic visual field defects. Besides these typical scotomas, diffuse damage is also thought to be related to glaucoma [1, 2]. It is, however, not well known how far diffuse damage is caused by increased intraocular pressure [3]. If we consider localized as well as diffuse visual field damage as glaucomatous damage, which patients are going to develop localized and which ones diffuse visual field defects?

The purpose of this study was to evaluate whether patients with predominantly diffuse damage are in some respect different from the patients developing localized damage. We compared therefore a group with localized visual field defects with a group with diffuse visual field defects.

Material and methods

The visual fields were performed with the OCTOPUS automated perimeter using the program G1 [4]. This program calculates automatically the visual field indices MD, CLV and others [5]. MD (mean damage) is a parameter representing the total visual field damage, whereas CLV (corrected loss variance) represents the localized visual field damage. Some hundreds of patients with glaucoma or

glaucoma suspects were measured with this program over the last two years For this retrospective study we selected visual fields with MD between 2 and 10 dB from this pool of data The analysis was based on the left eyes only. 188 patients had an MD between 2 and 10 dB in their left eye measurement. We divided these patients into two groups: One having low and the other having high CLV. In other words: into a group with more diffuse and a group with more localized visual field damage

CLV was defined as being high when it was larger than twice the corresponding MD The grouping was made pairwise, matched by MD. This pairwise matching resulted in 108 patients or 54 pairs.

Excluded were patients with ocular or systemic diseases, and patients with a rate of false responses in the catch-trials higher than 15%.

In a first step of this still ongoing study we compared the age of the patients and the highest pressure ever recorded in their history. This pressure will be referred to as the peak pressure The statistical comparison between the two groups was performed by a Wilcoxon-Mann-Whitney-test.

Results

Figure 1 represents the frequency distributions of the age of the two groups. The group with predominantly diffuse damage was on the average younger than the group with localized damage This difference was statistically significant $(p = 0.008)$

The analysis of the peak pressures revealed a slight tendency for higher pressure in the group with diffuse damage The difference between the two groups did, however, not reach the level of statistical significance $(p = 0.1)$. The mean values of the age and the mean of the peak pressures of the two groups are summarized in Tab. 1

Discussion

From our results we can conclude that patients with predominantly diffuse damage are on the average younger and have the same of even higher intraocular

Table 1 Type of visual field damage (mean $\pm$ SD)

	Diffuse	Localized
Ages (years)	57 8 $\pm$ 15 2	64 2 $\pm$ 13 8
Peak pressure (mm Hg)	34 2 $\pm$ 10 6	30 9 $\pm$ 9 2
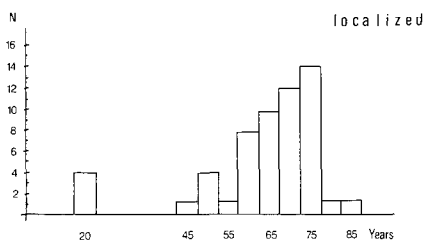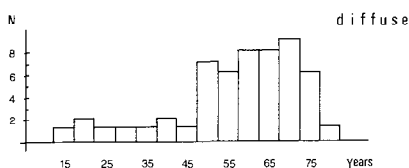
Figure 1 Frequency distribution with age Top: Patients with predominantly localized visual field damage Bottom: Patients with predominantly diffuse visual field defects

pressure than patients with localized damage Diffuse damage in glaucoma is as important therefore as localized damage. The fact that it occurs more often in young patients and that these patients have the same or even higher IOP emphasizes that this type of damage is also pressure related and not or not only due to cataract. These observations correspond with the concept that diffuse damage may represent a mechanical damage of the optic nerve head by the IOP, whereas localized defects may represent vascular insufficiency [6]. The insufficiency of the circulation may be caused by too increased IOP as well as by other factors.

Acknowledgement

References

1 Airaksinen PJ, Drance SM, Douglas GR, Schultzer M: Neuroretinal rim areas and visual field indices in glaucoma Am J Ophthalmol 99: 107–110 (1985)
2 Flammer J: Diffuse visual field damage in glaucoma In: Ticho U, David R (eds) Recent advances in glaucoma Excerpta Medica International Congress Series 636: 9–12 (1984)
3 Flammer J, Eppler E, Niesel P: Die quantitative Perimetrie beim Glaukompatienten ohne lokale Gesichtsfelddefekte Graefe's Arch Clin Exp Ophthalmol 219: 92–94 (1982)
4 Flammer J, Jenni A, Keller B, Bebie H: The Octopus glaucoma program G1, Glaucoma (in print) 1986

5 Flammer J: The concept of visual field indices Graefe's Arch Clin Exp Ophthalmol 224: 389–392 (1986)
6 Flammer J: Psychophysics in glaucoma A modified concept of the disease In: Greve EL, Leydhecker W, Raitta C (eds) Proceedings of the European Glaucoma Society, Second Eropean Glaucoma Symposium, Helsinki, 1984, pp 11–17 Dr W Junk Publishers, Dordrecht, 1985

Author's address:
PD Dr J Flammer,
Dept of Ophthalmology,
University Eye Clinic, CH-3010 Berne, Switzerland

V.6 First experiences with the new Octopus G1-program in chronic simple glaucoma

F. DANNHEIM
Hamburg, F R G.

Abstract

The new G1-program of the Octopus Computer Perimeter was applied to 112 eyes of healthy subjects, glaucoma suspects, eyes with suspicious looking disks and chronic glaucoma. It compared favourably to a single normal program in providing a higher spatial resolution and some information from the peripheral field. A data reduction results in a number of 'visual field indices', which are printed with each field plot. These indices showed some correlation with topometric values of the Rodenstock Optic Nervehead Analyzer. A diffuse reduction of sensitivity occurs not only in glaucoma or glaucoma suspects, but also in normal subjects, especially with myopia.

Introduction

The Octopus G1-program provides a strategy designed for glaucoma [3]. It turned out, however, to be well applicable to many other conditions. In this study the preliminary version of the G1-program was used in a group of patients who are regularly seen for probable or manifest glaucoma, and in healthy subjects. The findings were compared with previous Octopus fields, if available, and with topometric data from the Rodenstock Optic Nervehead Analyzer.

Material and methods

In 112 eyes of 64 individuals both the visual field and the optic disk had been evaluated. In about one half of the eyes the examination had been repeated after 6 months. All pairs of measurements were used separately resulting in a total number of 185. The eyes were grouped according to the following criteria: 17 normal eyes (24 examinations) had no abnormalities and full visual acuity with

	MS	MD	LV	CLV	Q	XM3	SF	RF
NORMAL		|-3....2| 0...5	0...2			0...2	
PHASE 1	24.2	2.6	20.3	⬇	1.3	6.1		4.0
PHASE 2	23.6	3.1	24.7		1.4	6.9		0.0
MEAN	23.9	2.8		20.4	1.4	6.4	1.5	3.0
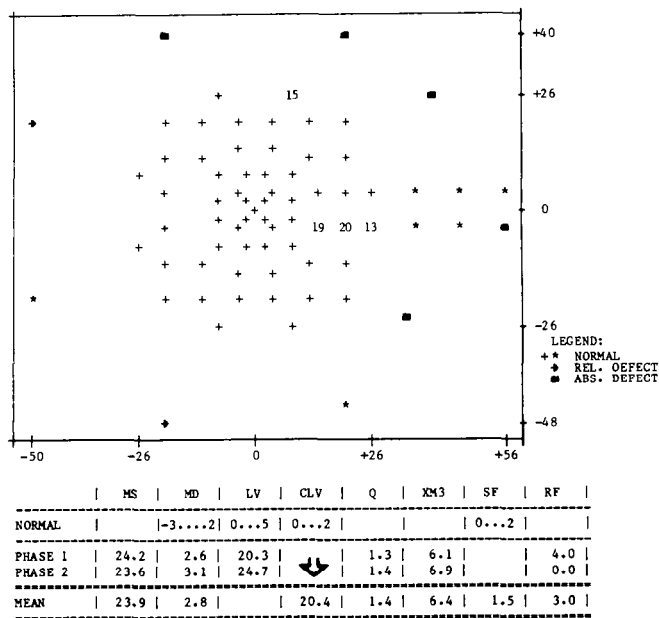
Figure 1 Comparison printout (above) of Octopus Gl-program, preliminary version, of a left visual field with isolated glaucomatous nerve fibre defect Numbers represent loss of sensitivity in decibels, compared to age corrected normal values Visual field indices (below) with normal and actual values (normal values changed in final version) Abnormal CLV-value (arrow) with borderline MD-value Description of indices in the text

proper correction. 40 eyes (74 examinations) from glaucoma suspects had intraocular presssures at times above 22 mm Hg, normal visual fields previously, and an optic cup not larger than 0.7. 20 eyes (30 examinations) had suspicious looking disks with a c/d-ratio of more than 0,7, normal previous fields and diurnal pressures below 22 mm Hg without therapy. 28 eyes (45 examinations) were classified as glaucoma having pressures above 22 mm Hg with or without treatment, and either abnormal visual fields, or abnormal disks, or both in previous examinations. 7 eyes (12 examinations) with low tension glaucoma presented with abnormal disks and fields, and their pressures lied always below 22 mm Hg without treatment Cupping had been judged as vertical c/d-ratio with the aid of color stereo photographs.

All subjects were familiar with visual field testing, had a visual acuity of at least 0,6, and no media opacities. The Octopus Gl-program [3] performs a thorough bracketing threshold evaluation in 59 positions within 30° The spatial resolution is increasing towards the center, maximally 2° in the macular region (Fig. 1). The targets are placed symmetrically as to facilitate detection of nasal steps and hemiopic abnormalities. This first phase is followed by a more superficial screening procedure in 14 peripheral positions with some predominance for the nasal step area. A second threshold examination of all 59 paracentral positions may be

added. It allows a calculation of the fluctuation. The whole procedure takes about 13 to 18 minutes.

A number of 'visual field indices' are printed together with their normal range underneath the topographical field plot Four of them are of special clinical interest·

- The 'Mean Defect' (MD) is a calculation of the loss of sensitivity per test location and is abnormal either in cases of uniform depression or when localized defects of considerable size or depth are present
- The 'Corrected Loss Variance' (CLV) indicates the non-uniformity of the sensitivity, corrected for the effects of the short term fluctuation. It is specifically abnormal in localized defective fields.
- The 'Short Term Fluctuation' (SF) is the scatter of sensitivity within one examination. It is calculated as root mean square of the deviation of measurements between the two phases.
- The 'Rate of False Replies' (RF) indicates the false-positive and false-negative responses to catch trials in percent. It reflects the consistency of the patient's cooperation.

The Rodenstock Optic Neverhead Analyzer provides a set of optic disk parameters, calculated from depth measurements using a stereo-videocamera device [2]. From the c/d-ratios of the 4 quadrants the mean value for the upper and lower one was used, comparable to vertical c/d-values recorded in the patients files.

Results

In 33 eyes the visual fields of the regular programs were available for comparison with those of the Gl-program. In 22 of them both program 31 and 32 had been applied. By and large the results were in accordance. The finer grid of the Gl-program as compared to a single regular program yielded a higher detection rate, however: In 2 of 22 eyes the isolated defect was found only by program 31, whereas the field of program 32 appeared unaffected.

The screening procedure in 14 peripheral positions gave additional information. In 4 eyes the field could thus be interpreted more clearly. In another 4 eyes only the peripheral test allowed a decision in favour of a superior nerve fibre defect due to a peripheral nasal step. This interpretation was supported by a regular examination from 30 to 60° excentricity (program 42).

The calculated visual field indices gave further hints. The values for CLV and MD have been sampled for the different diagnostic groups and correlated with the vertical c/d-ratio as printed by the Optic Nervehead Analyzer (Figs 2–5). The c/d-ratio is given as the abscissa, the CLV- as the ordinate superiorly, and the MD-value as the ordinate inferiorly All corresponding values for CLV and MD are connected to show their relationship The borderline for the normal range (MD 2,0, CLV 4,0) is indicated by two horizontal broken lines
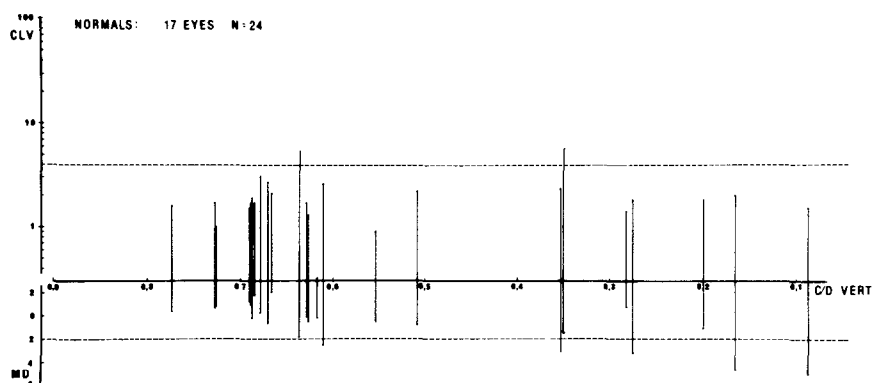
Figure 2 Scattergram of Corrected Loss Variance (superior ordinate) and Mean Defect (inferior ordinate) versus vertical cup/disk-ratio (abscissa) for normal subjects Corresponding values of CLV and MD connected by vertical lines Normal range for CLV and MD marked with horizontal broken line

In the 24 examinations of *normal sujects* (Fig. 2) nearly all values lie within the normal range. Only two CLV-values exceed the limit of 4,0 slightly. The 5 eyes with abnormal MD-values and normal CLV-values are separately given in Fig. 6. Regarding the c/d-ratio, 3 times its value exceeded 0,7 due to an overrestimation of the Optic Nervehead Analyzer.

In $^1/_3$ of the 74 examinations of *glaucoma suspects* (Fig. 3) the values for CLV and/or for MD exceeded the normal range moderately. 5 times the c/d-ratio was over 0,7.

From 30 examinations in *suspicious disks* (Fig. 4), CLV and/or MD-values were only a few times slightly abnormal. The two highest and 2 more abnormal CLV-values correspond to two eyes of one subject with only a relatively large blind spot resulting in one abnormal threshold value. In the final version of the Gl-program this target has been placed more away from the blind spot to avoid those effects. The c/d-ratio was in $^1/_3$ of the measurements smaller than 0,6 indicating relatively small estimates of the Optic Nervehead Analyzer.

From 45 examinations of *chronic glaucoma* and 12 of *low tension glaucoma* (Fig. 5) most CLV-values and nearly all MD-values exceeded the normal range. C/D-ratio was around and above 0,6 in most cases A few smaller values were due to either underestimation of the Optic Nervehead Analyzer or to focal cupping at only one pole of the optic disk

Abnormal MD-values in cases with normal values for CLV are being discussed as indicative of early glaucomatous damage [3]. All measurements, in which CLV did not exceed 4,4, but MD was greater than 2,2 were separately analyzed (Fig. 6). The lower half of the ordinate, as in Fig. 2 to 5, reflects the MD-values. The abscissa gives the vertical c/d-ratio.

In *normal subject* this situation was present in 5 examinations of 3 eyes, all of
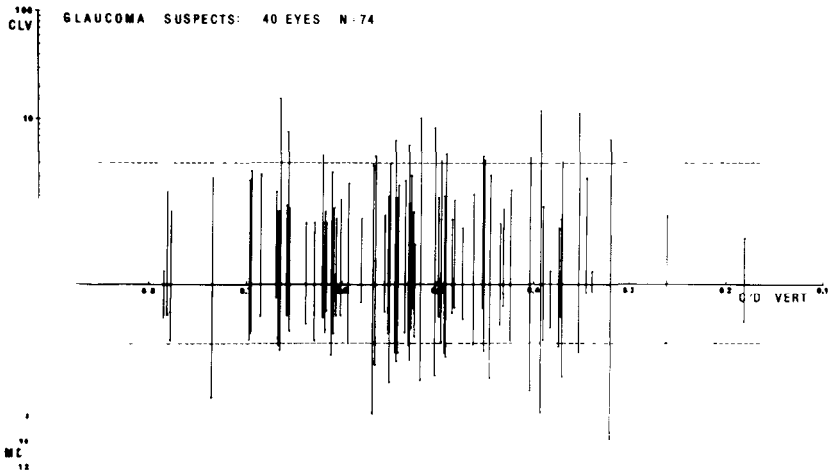
Figure 3 Scattergram of CLV and MD versus vertical c/d-ratio for glaucoma suspects, given as in Fig 2

which had a myopia of —7 to —10 dpt. In *glaucoma suspects* 14 examinations of 9 eyes presented with this feature. 8 times the MD-value exceeded 3,0 From these 8 a myopia of −3 to −7 was recorded in 5 and a wide cup of just 0,7 in one, who was labelled with a c/d-ratio of 0,735 by the Optic Nervehead Analyzer The remaining 2 eyes had fellow eyes with definite glaucomatous visual fiel defects and disk damage. In eyes with *suspicious disks* only marginal elevations were twice observed for MD with normal CLV-values. In eyes with *chronic glaucoma* 3 from 5 examinations corresponded to a myopia of −1 to −6,5 dpt.

A diffuse reduction of sensitivity could also be due to lens opacities or miosis
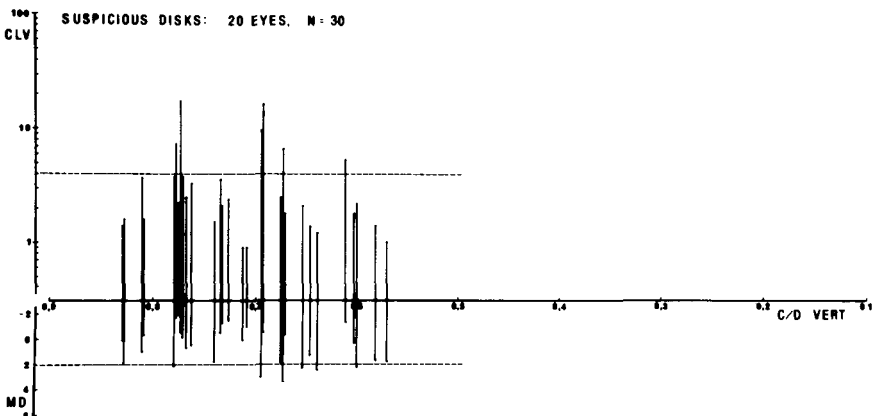
Figure 4 Scattergram of CLV and MD versus vertical c/d-ratio for suspicious disks, given as in Fig 2

326
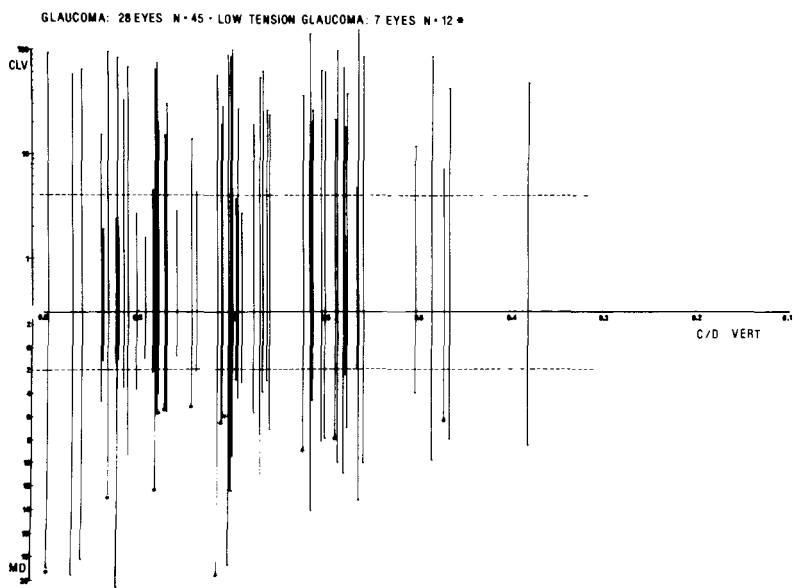
Figure 5 Scattergram of CLV and MD versus vertical c/d-ratio for glaucoma and for low tension glaucoma (asterix), given as in Fig 2
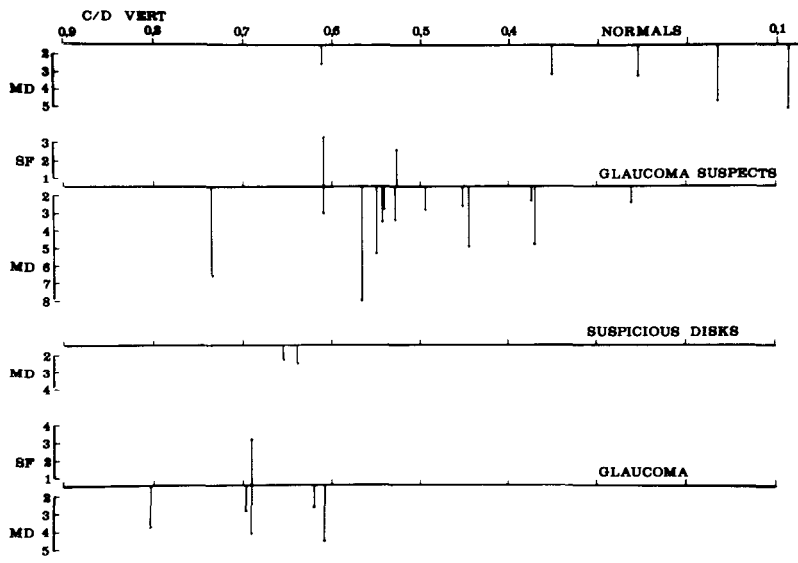
Figure 6 Scattergram of *S*hort te1m *F*luctuation (superior ordinate) and *M*ean *D*efect (inferior ordinate) ve1sus c/d-ratio for measurcments with values of CLV within 4,4 and MD exceeding 2,2, sampled for normal subjects, glaucoma suspects, suspicious disks and chronic glaucoma Abnormal values of SF under this condition only present in glaucoma suspects and glaucoma patients

Eyes with cataracts had been excluded from this study, however The pupil size of the eyes of Fig. 6 did not differ significantly from the remaining eyes.

An increased Short Term Fluctuation (SF) in cases with a normal Corrected Loss Variance and normal false reply rates (RF) was also attributed to possible early glaucomatous damage [3]. This feature is given in Fig. 6 in the upper half of the ordinate. It occurred only in 3 examinations of the glaucomas and glaucoma suspect, however. One in each group had also an enlarged MD-value.

Comment

The values both for 'Mean Defect' and 'Corrected Loss Variance' show some correlation with the appearance of the optic cup, as already discribed for a manual topometric study [1]. A somewhat similar result was obtained in our material by using values of an automated topometric device. In figs 2–6 the cup is chacterized by vertical c/d-ratio and not by rim area We thus avoided conversion of 'units' into absolute values, and we were able to directly compare the digital measurements with clinial observations in the patients files Repeated measurements of single eyes after 6 months had been used like separate eyes, since the measurement errors of both the field test and the disk analysis are to some extent independently present again. Changes of field – or disk parameters in time were neglected in this preliminary report. A consideration of only one examination per eye did not change the overall result

It should be noted, however, that the perimetric indices correlate well with the different diagnostic groups. The correlation with c/d-values is much less obvious, especially in the groups of glaucoma suspects and in that of high- and low-tesion glaucoma. Some field indices are perfectly normal widely cupped disks, whereas small c/d-ratios may correspond to definite field damage. Those discrepancies are not only due to over- or underestimations of the Optic Nervehead Analyzer. They are much more induced by our definition of these clinical entities and by individual features of some glaucomatous eyes A statistical calculation of an overall correlation [1] did not seem appropriate for our still limited number of paired measurements with this amount of fluctuation.

A homogeneously depressed sensitivity as the only perimetric sign could be glaucomatous in origin [3]. It actually occured in a number of eyes with true or questionable glaucomatous damage. It was also present in normal eyes, however, especially the ones with a myopia. An increased short term fluctuation was too rare to be readily ascribed to decent glaucomatous damage

The clinical value of the new GI-program does not only lie in the introduction of visual field indices. Its merits are also due to the higher detection rate thanks to the better spatial resolution [4], and to a screening procedure of the peripheral field.

Acknowledgement

References

1 Airaksinen PJ, Drance SM, Douglas GR, Schulzer M: Neuroretinal rim areas and visual field indices in glaucoma Amer J Ophthalmol 99: 107–110 (1985)
2 Dannheim F, Klingbeil U: Die Bestimmung räumlicher Papillendaten mit dem 'Fundusanalysator' Fortschr Ophthalmol 83: 527–529 (1986).
3 Flammer J, Drance SM, Augustiny L, Funkhouser A: Quantification of glaucomatous visual field defects with automated perimetry Invest Ophthalmol 26: 176–181 (1985)
4 Weber J, Dobek K: What is the most suitable grid for computer perimetry in glaucoma patients? Ophthalmologica, Basel 192: 88–96 (1986)

Author's address:
Prof Dr F Dannheim,
Universitäts-Augenklinik,
Martinistr 52, D-2000 Hamburg 20, F R G

V.7 Cup/disk ratio, excavation volume, neuro-retinal rim area of the optic disk in correlation to computer-perimetric quantification of visual field defects in glaucoma with and without pressure

A clinical study with the Rodenstock Optic Nerve Head Analyzer and program Delta of the Octopus Perimeter 201

E. GRAMER, M. BASSLER and W. LEYDHECKER
Würzburg, F.R.G.

Abstract

Investigating the correlation between optic disk and visual field measurements we found that for a given amount of rim area and cup/disk ratio in eyes with low IOP smaller field defects appeared than in eyes with high IOP The transition from ocular hypertension to glaucoma, or from suspected low tension glaucoma to manifest low tension glaucoma can be observed to occur at a mean cup/disk ratio alteration of less than 10%, so that the borderlines are arbitrary, since depending on the sensitivity of the perimetric method. In eyes with low IOP the evaluation of rim area values may allow better differentiation of healthy and affected eyes than field examination.

The first visual field defects occur in glaucoma with low IOP at a stage of a greater rim area loss ($1.0\,mm^2$) and higher cup/disk ratio than in eyes with high IOP, which show first field defects for mean rim areas of $1.45\,mm^2$. Thus, in LTG there must be more intact nerve fibers per mm^2 rim area than in POAG The smaller rim area in LTG may result from loss of other than neuroretinal substance. It may be concluded that in LTG there is either less glial tissue present or that a loss of glial tissue precedes the loss of nerve fibers. In eyes with high IOP the neuroretinal substance must be damaged first, since we found the visual field defects at a stage of minor alteration of rim area and CDR. This suggests different pathomechanisms in the initial stages of LTG and POAG, and shows the genetic impact of high intraocular pressure.

Introduction

The purpose of the present study is to reevaluate (24, 25) the correlation between visual field loss and the morphology of the optic nerve head by means of quantitative data from measurements with the Optic Nerve Head Analyzer

(ONHA) of Rodenstock and the program Delta of the Octopus Perimeter 201, under controlled and quantifying conditions. Using a multivariate analysis we investigated which of the four parameters, i.e. cup/disk ratio, excavation volume, neuroretinal rim area, and maximum intraocular pressure, showed the best correlation to the total loss in visual field. For eyes with different IOP levels, we investigated at which mean value of rim area and mean cup/disk ratio the first visual field defects occur. This was examined for different types of glaucoma. If there are differences between these eyes with different IOP levels, this can be a sign of the influence of the damaging effect of high intraocular pressure.

Methods

Seventy-nine eyes in 79 patients were examined with the Octopus Perimeter 201 (program 31) and tested on the same day or a few days later with the Optic Nerve Head Analyzer (ONHA) 58 eyes had glaucomatous visual field defects: 18 eyes had low tension glaucoma (LTG); 15 eyes primary open-angle glaucoma (POAG) with a maximum IOP of 22–29 mm Hg; 16 eyes POAG with a maximum IOP of 30 mm Hg and more; 9 eyes had pigmentary glaucoma (see Table 1, column 7). The control group comprised 21 eyes without visual field defects: 8 eyes with ocular hypertension; 7 eyes had a pathologic CDR of 60–80% without field defects, while the fellow eyes of the patients showed LTG with visual field defects; this is the group with suspicion of LTG: and 6 eyes were healthy (see Table 2, column 7)

All eyes had a visual acuity of 0.8 or better, no opacities of the optic media. The eyes with field defects had no other pathology of the anterior segment than glaucoma. To exclude errors in the examination with the OHNA (axial bulbus length correction), or refractive scotomas in perimetry, only eyes with a maximum ametropia of ± 3 dpt were included in this study. There was no significant difference in pupil size and refraction (only the pigmentary glaucoma group had significantly more myopic eyes) in the groups compared Diurnal tension curves without medication were established for all eyes. In addition, the maximum height of IOP was explored by the eye doctors sending the patients to our Clinic.

All patients were controlled by the author over a time of up to 8 years and were examined with standardized examination pattern and evaluated with standardized documentation The peripheral visual fields (Goldmann Perimetry) done maximally 14 months before showed no defects in the peripheral isopters at the initial stages. At the advanced stages, the rate of peripheral defects was similar in all groups. Additional quantifying measurements with Octopus program 41 could not be performed on the same day, because this would have been too exacting for these out-patients. For the comparison of the different glaucoma groups, the maximum IOP was calculated from these data and from the diurnal tension curves without medication. The highest value of the diurnal curve describes in our

3331

Table 1. Comparison of visual field and disk parameters in glaucoma.

Type of glaucoma	Visual field parameters	Optic disk parameters of ONHA						
	1	2	3	4	5	6	7	8
	m-total loss ± SD (dB)	m-rim area ± SD (mm²)	m-cup/disk ratio ± SD (?)	m-disk diameter ± SD horiz./vertic. (mm)	m-excav volume ± SD (mm³)	m-IOP$_{max}$ ± SD (mm Hg)	n	m-age ± SD (yrs)
Glaucoma without pressure LTG	733 ± 124.5	0.799 ± 0.053	0.800 ± 0.017	1.920 ± 0.056/ 1.753 ± 0.058	1.223 ± 0.136	17.5 ± 0.6	18	60.3 ± 12.7
Glaucoma simplex IOP 22–30 mm Hg	943 ± 120.0	0.836 ± 0.058	0.763 ± 0.030	1.905 ± 0.067/ 1.768 ± 0.060	1.189 ± 0.134	25.1 ± 0.6	15	63.7 ± 8.9
Glaucoma simplex IOP >30 mm Hg	678 ± 137.0	1.123 ± 0.120	0.731 ± 0.027	1.953 ± 0.066/ 1.787 ± 0.070	1.134 ± 0.115	35.8 ± 1.4	16	62.8 ± 9.9
Pigmentary glaucoma	474 ± 153.0	1.118 ± 0.144	0.678 ± 0.089	1.755 ± 0.048/ 1.602 ± 0.049	0.693 ± 0.090	36.7 ± 3.5	9	52.6 ± 21.9

Table 2. Comparison of normal field and disk parameters in ocular hypertension, suspected LTG and healthy eyes.

	Visual field parameters	Optic disk parameters of ONHA						
	1	2	3	4	5	6	7	8
Control group	m-total loss ± SD (dB)	m-rim area ± SD (mm^2)	m-cup/disk ratio ± SD (?)	m-disk diameter ± SD horiz./vertic. (mm)	m-excav volume ± SD (mm^3)	m-IOP_{max} ± SD (mmHg)	n	m-age ± SD (yrs)
Ocular hypertension (excavat. 45–80%)	0	1.369 ± 0.042	0.687 ± 0.034	2.047 ± 0.088/ 1.912 ± 0.069	0.977 ± 0.157	28.1 ± 1.48	8	57.1 ± 9.6
Suspect LTG (excavat. 60–80%) IOP_{max} <21 mmHg	0	1.209 ± 0.077	0.728 ± 0.026	2.070 ± 0.061/ 1.933 ± 0.062	1.060 ± 0.164	17.0 ± 0.84	7	49.2 ± 14.6
Healthy eyes	0	1.785 ± 0.179	0.473 ± 0.065	1.987 ± 0.045/ 1.825 ± 0.056	0.481 ± 0.097	15.8 ± 1.49	6	53.8 ± 6.8
	Visual field parameters	Optic disk parameters of ONHA				IOP	n	Age

opinion the damaging influence of IOP better than the mean of all IOP values. The height of the untreated pressures was known from diurnal tension curves and additional measurements. In all eyes the CDR was evaluated for the vertical diameter with direct ophthalmoscopy. Polaroid photography of the optic disk was done in all eyes.

Diagnosis of LTG was obtained through many diurnal tension curves without medication, through examination of the optic disk and of the glaucomatous visual field. The patients with LTG were also examined neurologically to exclude neurologic diseases. Diagnosis of pigmentary glaucoma was established by defects in the pigmentary cell layer of the iris, by pigment in the chamber angle, or by Krukenberg's Spindle of the cornea. All eyes had wide open chamber angles.

Examination of the optic disk

With regard to technical details we may refer to a former study [29].

The following calculated disk parameters were evaluated for this study: cup/disk ratio, rim area, excavation volume, disk diameter. The CDR value is not identical to the value obtained by estimating the cup ophthalmoscopically, but shows good correlation with clinical measurements [41, 42]. There is an upper, lower, nasal and temporal quadrant, bounded by oblique diameters, in contrast to the visual field [35]. The parameters are given in cubic and square mm. These values are for the dimensions of a Gullstrand normal eye [29]. During measurement, when the disk is focused a value is recorded for refraction. Thus, the different disk parameters are transposed to the dimensions of the eye under examination, assuming that there is axial ametropia. As in this study the refractional deviation for all eyes examined is defined and as the square units for the single groups serve only as basis for comparison, the deviations of the measured values from the actual values is of no importance. The measurement of the rim area in square mm is retained and can also be taken as relative square units [30]. A study on the reproducibility of ONHA measurements resulted, for example, in neuroretinal rim area values which differed up to 5.6% in normal eyes and up to 7.5% in glaucomatous eyes [5].

If the pupils of glaucomatous eyes could not be dilated properly to 5 mm, although miotics had been discontinued in all cases 2 days before, these eyes were excluded. Double measurements with the ONHA were performed. After the second measurement, eyes were excluded if the photographic results showed stripes, or if the two results were not reproducible. If we had reproducible results for both eyes, the eye to be evaluated was chosen at random.

Examination of the visual field

The visual field was checked with Octopus Perimeter 201, program 31 (73 test-

points, 6°-grid, central 30°). We used stimulus size III [14]. The detection probability for scotomas is determined by the 6°-grid of program 31 [31] and the test field size, as proved in our former studies [19, 31]. Limitations of the rate of detection are discussed there in detail For the quantifying correlation between disk parameters and total loss only the central 30° visual field was considered in our study. According to the topography of early gluacomatous field defects [17–19, 26, 43], which are mainly found in the central field, this limitation is justified for the initial stages of the disease; as in our study it concerns all glaucoma groups examined, it is less relevant for comparison. In this visual field test, a static threshold measurement is done in each testpoint with the staircase-up-and-down method. We used this method since it is superior to other computer-perimetric methods [15, 20–22, 27, 28, 32, 38, 39) with regard to sensitivity and specifity [16, 23]. Using program Delta (mode series) the absolute and relative scotomas in the single testpoints are summarized in one number which gives the total loss. This number indicates the functional loss in the visual field summarizing depth and size of the scotomas in the central field [8–11, 30, 33–35].

For the comparison of the groups the mean values of the parameters obtained for the optic disk and the visual field were tested with the Mann-Whitney-U-Test and the T-Test for normally scattered values to find out significant differences. The statistical calculations were done at the Mathematical Institute of the University of Würzburg

According to the restrictive inclusion criteria, 58 eyes with visual field defects and 21 eyes without field defects and correct measurement results remained for our evaluation. We divided these 79 eyes of 79 patients into 7 groups (see Tables 1 and 2). The eyes with field defects were subgrouped, as in our former study [24] according to the maximum IOP measured in diurnal pressure curves without medication.

Results

Cup/disk ratio in correlation to total loss

The correlation between CDR and total loss in the visual field for the 7 groups is shown in Table 1 (columns 1 and 3). In eyes with LTG we find a mean CDR of 0.8 and a corresponding total loss of 733 dB (Table 1). In eyes with POAG we find a somewhat smaller mean CDR of 0.76 and 0.73 respectively, but compared to eyes with LTG, a greater total loss of 943 and 678 dB, respectively. In pigmentary glaucoma, we have a mean CDR of 0.67, with a total loss of 474 dB (Table 1).

Although in LTG (see Table 1, column 6) with a mean IOP of 17.5 mm Hg the lowest IOP value is found, we observe then the largest excavations of the optic disk.

Comparing the identical single value ranges of CDR for all groups (Fig. 1) the
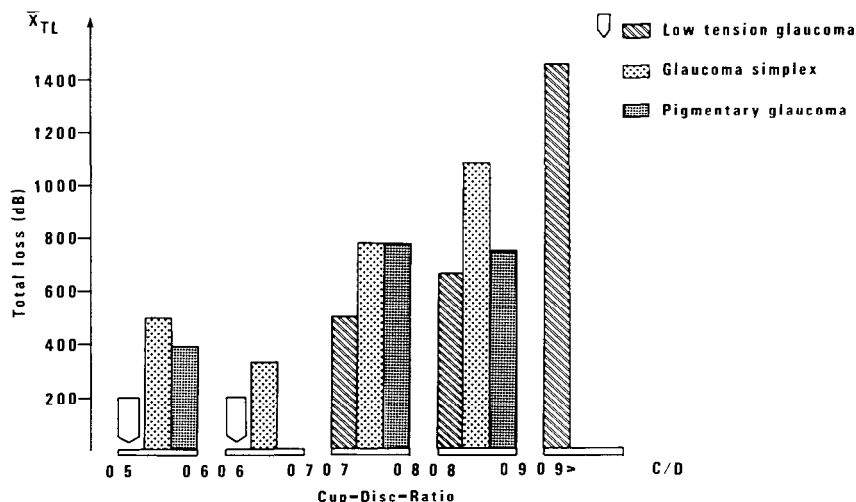
Figure 1 Mean total loss (ordinate) in correlation to equal ratios of CDR, as calculated by the ONHA, for eyes with LTG (hatched columns), POAG of all IOP levels (dotted columns) and pigmentary glaucoma (black columns) For CDR values from 0 5 to 0 7 LTG does not yet show visual field defects (white arrows), whereas there are already scotomas found for these CDR values in glaucomas with elevated IOP

differences become even more significant. For LTG, field defects are not yet observed in a CDR range between 0.5 and 0.7 (arrows in Fig. 1) For POAG of all IOP levels and for pigmentary glaucoma, we find for a calculated CDR range from 0.5 to 0.6, already field defects of 500 and 386 dB, respectively, that is, for CDR values which are just a little higher than the CDR value of 0.473 in healthy eyes (see Table 1, column 3) In ocular hypertension (see Table 2, column 3) the mean CDR is 0.68, in eyes with suspected LTG 0.72. The transition from ocular hypertension to POAG occurs with an increase of the mean CDR from 0.68 to 0.76 and 0.73, respectively In glaucoma without pressure elevation an increase of the mean CDR from 0.72 to 0.80 leads to manifest visual field defects with a mean total loss of 733 dB.

Since the mean values presented here (Table 1, column 1) also describe advanced field defects, as they are found with a CDR change by 10%, it may be assumed that, before the first scotomas are detected, a CDR change by approximately 5% within the crucial range may be needed until the nerve fiber loss can be verified with program 31. In LTG this transition from an apparently normal visual field to a pathologically altered field occurs at a stage of optic disk excavation which is on the whole by 10% higher, in the same limited narrow range. An optic disk alteration by 5% cannot be estimated ophthalmoscopically, and also falls within the data scatter of the ONHA measurements. This shows that subdivision of glaucomatous diseases into 'Ocular Hypertension' and 'Glaucoma' is rather arbitrary, and dependent upon the sensitivity of the perimetric method.
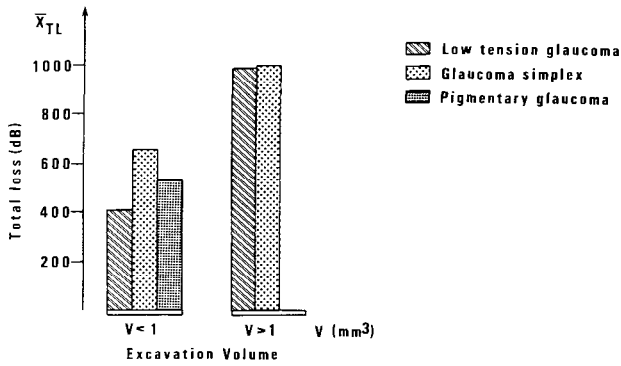
Figure 2 Mean total loss (ordinate) in correlation to ONHA-calculated excavation volumes of below and above 1mm^3 in eyes with LTG, POAG and pigmentary glaucoma

In LTG visual field defects occur first at a CDR range from 0.7 to 0.8, with total loss values of 500 dB, whereas in glaucoma with elevated IOP at this CDR range already mean total loss values of 780 dB are observed.

At the same stage of CDR we find for glaucomas with elevated pressure significantly larger visual field defects (p = 0.03) (Fig. 1). The CDR values of the 7 groups can be compared, since in the calculated mean disk diameters (horizontal and vertical) there are no significant differences to be seen within the groups (Table 1, column 4). This disk diameters are not distributed normally and do not show significant differences within the groups (p between 0.20 and 0.80).

Excavation volume in correlation to total loss

The mean excavation volume (see Table 1, column 5) in glaucomatous eyes as compared to the normal value of 0.48 is significantly higher: It amounts in eyes with LTG and a total loss of 733 dB to 1.22mm^3 (p = 0.006); in eyes with POAG to 1.18mm^3 (p = 0.005) and 1.13mm^3 (p = 0.008), respectively. The mean values appear to be relatively broad-scattered.

When considering the mean total loss values for optic disks with excavation volumes of above and below 1mm^3, we find for large excavations in POAG and LTG a mean total loss of 1000 dB, which shows that there are no differences in the later stages (p = 0.01) (Fig 2). The values for LTG, however, are scattered between 141 dB and a maximum of 1556 dB, and for POAG between 134 dB and 1597 dB at a range of excavation volume above 1mm^3. For excavation volumes of less than 1mm^3 a similar scattering of the single measurement data can be seen. Therefore, the single measurements of the excavation volume do not permit conclusions as to the size of the scotomas.
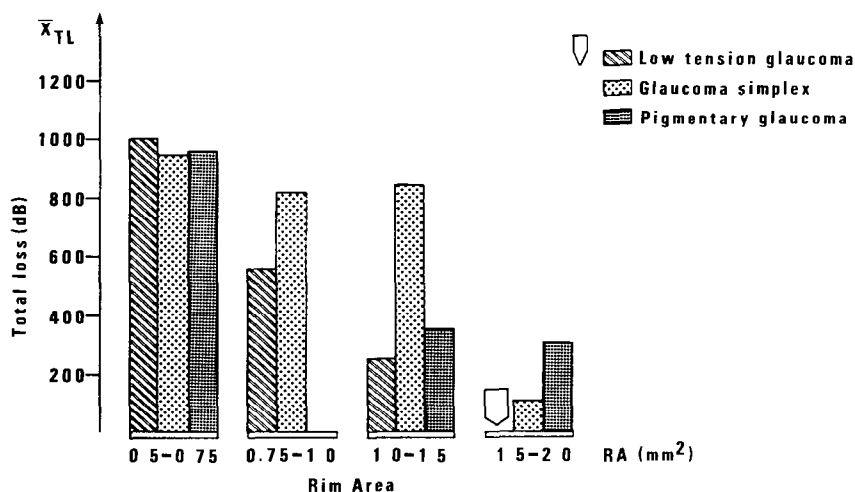
Figure 3 Mean total loss (ordinate) in correlation to equal amounts of neuroretinal rim area in eyes with LTG, POAG and pigmentary glaucoma

In advanced stages of the disease (rim area loss between 0 5 and 0 75 mm²) no differences are found between the glaucoma types, in contrast to the initial stages: For large rim areas from 1 5 to 2 0 mm² scotomas are not yet found in LTG For rim areas between 1 0 and 1 5 mm² first visual field defects appear in LTG For rim areas between 0 75 and 1 5 mm² smaller visual field defects are found in LTG than in glaucomas with elevated IOP

Rim area in correlation to total loss

In LTG with a mean rim area of 0.79 mm² a mean total loss of only 733 dB is found. in POAG, however, with markedly larger rim areas (0.83 and 1 12) (p = 0.01) we have far more advanced field defects (943 dB and 678 dB). In pigmentary glaucoma, with also larger rim area of 1.11 mm², there is a mean field defect of 474 dB (see Table 1, columns 1 and 2). In healthy eyes the rim area amounts up to 1.785 mm², and in ocular hypertension to 1 36 mm², that is, the latter value is somewhat less reduced in comparison to suspected LTG with a rim area of 1.2 mm² (see Table 2, column 2). For elevated IOPs with less reduced rim areas the overall functional field loss is found to be larger than in LTG (p = 0.01) (see Table 1, columns 1 and 2)

The comparison of equal sizes of neuroretinal rim area with the total field loss can be seen for the 3 types of glaucoma in Figure 3. The visual field defects in POAG are much more pronounced than in LTG (p = 0 01) in the initial stages Per square unit of rim area there is obviously a larger number of intact nerve fibers in eyes with LTG than in those with POAG So, a pressure-dependent, direct damage of neurons is probable, whereas the pressure effect on the astroglial cells will appear later.

Eyes in the final stage of the disease with a neuroretinal rim area reduced to
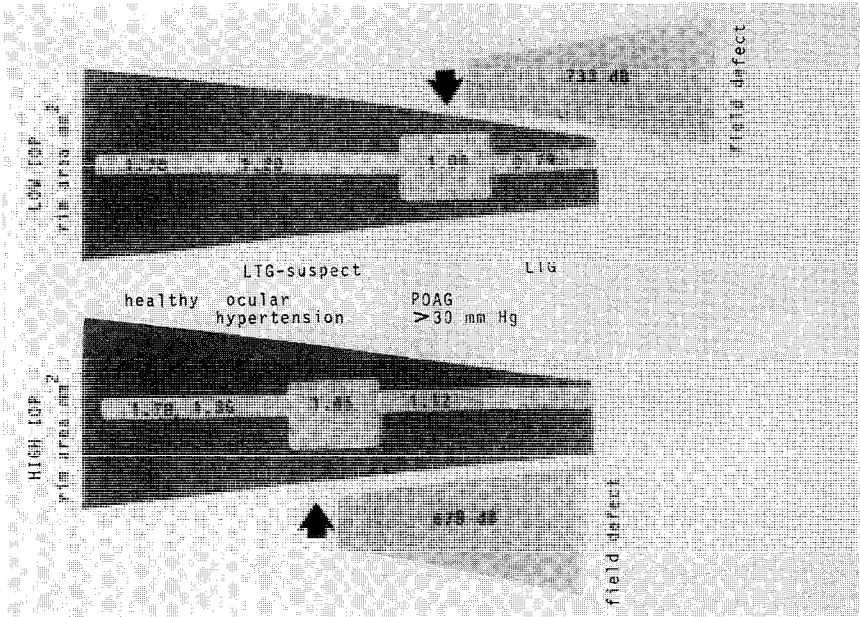
Figure 4 Upper part: Alteration of mean rim area in healthy eyes via glaucoma suspicion to LTG, with a mean total loss (TL) of 733 dB The first visual field defects up to 200 dB occur at a mean rim area of 1 0 mm²

Lower part: Alteration of mean rim area from healthy eyes via ocular hypertension to POAG, with a mean TL of 678 dB The first visual field defects up to 200 dB occur at a mean rim area of 1 45 mm²

0.5–0 75 mm² show a total loss of 1005 dB for LTG, of 942 dB for POAG, and of 996 dB for pigmentary glaucoma in the central visual field, but show no difference between LTG and glaucoma with high IOP (p = 0.8) (see Fig. 3). Significantly different results (p<5%) for LTG and POAG are found when the rim area covers 0.75 to 1.0 mm² and 1.0 to 1.5 mm². For a rim area of 0.75 –1.0 mm² we find in LTG a mean total loss of 563.5 dB, and in POAG of 824 dB, that is, a mean difference in functional loss of 261 dB. This difference is even higher in the range from 1.0 to 1 5 mm² of rim area, amounting then to 389 dB. In LTG there are only small scotomas up to a total loss of 257 dB, while in POAG the mean visual field loss is 846.2 dB and 359 dB, respectively (Fig. 3).

It can be seen that for the range from 1.5 to 2.0 mm² of rim area in LTG there are no visual field defects in contrast to POAG (see Fig. 3), and that, as shown in Table 2 (column 2),in suspected LTG a mean rim area reduction to 1.20 is found. This is 30% less than in normal eyes. For rim area values in the normal range, we can see socotomas of 111.3 and 406.0 dB, respectively; these are eyes with a maximum IOP of 40–48 mm Hg High intraocular pressures can cause a direct nerve fiber damage and thus corresponding visual field defects, while the optic

	NERVE FIBERS PER MM²/RIM AREA	VISUAL FIELD	M-TOTAL LOSS (DB)	M-RIM AREA (MM²)
LOW TENSION GLAUCOMA IOP MAX 21 MMHG			733	0.799
GLAUCOMA SIMPLEX IOP MAX 22-29 MMHG			943	0.836
GLAUCOMA SIMPLEX IOP MAX > 30 MMHG			678	1.123
PIGMENTARY GLAUCOMA			474	1.118
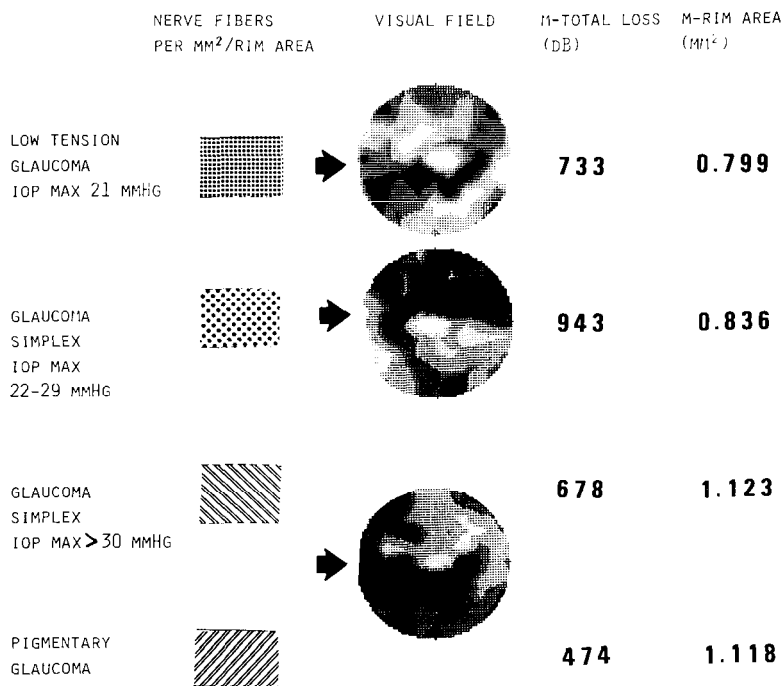
Figure 5 Right: Mean total loss and mean rim area for eyes with LTG, POAG with an IOP maximum of 22–29 mm Hg, POAG with an IOP maximum of ≥30 mm Hg, as well as pigmentary glaucoma Despite smaller mean rim areas, in LTG larger mean total losses of visual field occur Therefore, in LTG there must be more intact nerve fibers per mm² rim area (left: dark) than in glaucomas with high IOP (hatched)

The number of intact nerve fibers in correlation to the mean total loss is found in between these two ranges in POAG with IOP_{max} from 22–29 mm Hg

It can be concluded that especially in this group both vascular and pressure-dependent factors are contributing to the visual field damage

disks are still found morphologically 'normal' with regard to CDR and rim area. Eyes with suspected LTG in comparison to healthy eyes with a mean rim area of 1.20 mm² show significant changes (p = 0.009) of the rim area values while the visual field is still normal.

Figure 4 shows the mean values of rim area in eyes with and without elevated pressure at which first visual field defects up to 200 dB occur. In LTG the rim area values may allow a more exact differentiation of healthy and affected eyes than the visual field. For eyes with POAG, however, it is the field examination that yields the more exact definition of healthy and affected conditions.

Discussion

Cup/disk ratio in correlation to total loss

For LTG we find larger optic disk excavations than for the glaucomas with pressure, and at the same time smaller socotomas. In LTG visual field defects begin to occur only at excavations of 0.7 of CDR (see Fig. 1), whereas in POAG and pigmentary glaucoma the scotomas may occur already for a 20% smaller CDR, i e. for 0.5 of CDR. The smaller mean excavation value in pigmentary glaucoma (see Table 1, column 3) can be explained by the lower average age of patients, since the increase in optic disk excavation is age-dependent. The shorter duration of pressure effects may also be causative of this result.

The size of the CDR and rim area depends on the optic disk diameter. With a large disk diameter we find a CDR which may show the same amount of rim area as a small optic disk with a small CDR. As shown in Tables 1 and 2, the optic disk diameters in the 7 groups are not essentially different, because the maximum ametropia was ± 3 dpt.

These findings on CDR-differences in LTG and POAG with the same visual field defects confirm by the now quantifying examination of optic disk and visual field the results of a former study [24], and they support our hypothesis [25] with regard to the pathogenesis of low tension glaucoma. In LTG the increase of excavation precedes to a considerably larger degree the visual field defects than in purely pressure-caused damage of the optic nerve. Therefore, we may assume that in LTG, due to reduced perfusion pressures and often in relation to low blood pressure [24, 25], it is probably the glial tissue of the optic nerve which is reduced first Caused by increasing loss of glial cells the capillaries lose their support and thus tend to collapse even with normal IOPs; therefore, by way of chronic ischemia, a secondary vascular atrophy of optic nerve fibers may develop.

In glaucoma with high IOP, however, we must assume a different or an additional damaging factor, consisting in a direct damaging effect of elevated IOP Thus it may be explained why eyes with high IOP show in spite of smaller excavations and larger rim areas a markedly higher functional field loss than, for instance, glaucomas without pressure. Therefore, in glaucoma with high IOP there must have perished a greater amount of nerve fibers per square unit of neuroretinal rim area

These results in combination with the findings in our further studies on quantitative differences between glaucomas with and without pressure [17, 24, 25, 30, 33, 34, 35] represent an indirect confirmation of the damaging effect of elevated IOP, which even in more recent publications [3, 36] is still described as a hypothetical effect. The new quantifying measurement methods show that despite smaller mean cup/disk ratios and larger mean rim areas the visual field defects found in POAG are greater than those in LTG. This may provide new aspects for the discussion whether the disk findings or the perimetric findings

represent the more reliable examination method. Until now, it has been accepted that the cup/disk ratio (CDR) indicates the presence of visual field defects. This question may be further elucidated by our studies, which for the first time aim at a comparison of optic disk features and visual field findings, according to the height of maximum IOP and considering separately the different types of glaucoma.

If pressure-dependent differences of disk morphology (CDR, rim area, excavation volume) in correlation to visual field defects are found, the height of IOP must be taken into account. According to the above described results, the comparison of the different glaucoma groups with different IOP levels at the same stage of the disease should no longer be based on CDR evaluation alone, but should be carried out on the basis of the new quantifying visual field examination.

Since even with the 6°-grid used in our examinations the differences for the three glaucoma groups can be seen clearly, the great impact of IOP as damaging factor in glaucoma becomes evident.

Excavation volume in correlation to total loss

The excavation volume alone can only describe very roughly the degree of functional visual field loss. In all 3 groups of IOP level, the excavation volumes between 1 and 2 mm^3 were associated with large visual field defects. Smaller excavations up to 1 mm^3 did not allow any conclusion as to the size of scotomas in the single measurements, because there was a high variation. In this group, small or large field defects up to 1005 dB can occur in excavation volumes below 1 mm^3

Neuroretinal rim area in correlation to total loss

The decrease of rim area is combined with an increase of visual loss (see Table 1, columns 1 and 2). In the initial stages of the disease, however, quantitative differences between the glaucomas with and without IOP elevation are noticed (see Fig. 4). It is a striking observation that in POAG and in pigmentary glaucoma with a larger rim area than in LTG we find more larger scotomas than in LTG (see Figures 3 and 4). The tendency towards larger field defects with a larger rim area is also confirmed, if eyes with POAG in correspondence to the height of IOP are subdivided into two groups: eyes with maximum IOP above and below 30 mm Hg (Fig. 3).

In POAG with IOP values above 30 mm Hg and a mean IOP of 35.8 mm Hg, and in pigmentary glaucoma with a mean maximum IOP of 36.7 mm Hg the comparatively high rim area values of 1.12 and 1.11 mm^2, respectively, are rather conspicuous. It seems interesting that for pigmentary glaucoma and glaucoma with high IOP there is a great similarity of the correlation between disk findings

and visual field loss; this may indicate the same underlying damaging factor for both glaucomas, i.e. the high intraocular pressure

POAG with low IOP tends in its correlation of optic disk findings to field findings already more towards the measurement data found for LTG; thus it may be assumed that in this group the vascular and the pressure-related damaging factors are overlapping. In LTG, however, as compared to POAG and pigmentary glaucoma, there are smaller field defects for smaller rim area values. This could be explained by the predominance of the vascular pathomechanism in combination with low blood pressure, which in this group of our study was 110 : 80 mm Hg on the average. The average patient age is similar in both the LTG and the POAG groups, while patients with pigmentary glaucoma are younger by 8 years on the average. In the control group of eyes without field defects (see Table 2) the mean age is also above 50 years. Thus, we have on the whole good age comparability in all groups

On the assumption that the functional visual field loss results from a loss of axons, there must be more intact axons per square mm rim area in LTG than in POAG. Thus, the smaller rim area can only result from loss of other than neuroretinal susbstance. It may be concluded that in LTG there is either primarily less glial tissue ('weakness of connective tissue') present, or that a loss of glial tissue precedes the loss of nerve fibers [25, 26, 30].

In the comparative analysis of systemic risk factors we found for LTG markedly low blood pressures (hypotony) [24, 25]. Whether a resulting chronic perfusion decrease can explain the primary atrophy of glial tissue, will not be discussed here. In any case, a primary loss of glial tissue in LTG would offer an explanation for the reduced tension tolerance of the optic nerve head, which also with normal IOP values may lead to localized ischemia in the optic disk tissue [30]. With regard to acute pressure elevations, the glial substance is far more resistant than the neurogenctic substance [2, 25]. This might account for the large rim areas with simultaneous great functional field loss in eyes with high IOP.

From these results and from the differences in location and depth of scotomas, as shown in former studies on LTG, POAG and pigmentary glaucoma, as well as from the differences in field damage progression in the 3 glaucoma types [17, 24 25, 30, 34] it may be concluded that between glaucomas with and without pressure elevation there exist differences in the initial stages. So we have in LTG, for example in the early stages deep localized scotomas which indicate a vascular pathomechanism [30, 34]. The glaucomatous disease is a multifactorial disease [6, 7, 25, 30, 34] inwhich in the early stages the optic disk appears to be affected to different degrees by pressure-dependent and by vascular damaging factors. In POAG with high IOPs, for instance, may occur visual field defects when the rim area is not yet altered markedly and the disk excavation is still small, i.e. when the disk still appears to be normal. In LTG, minor visual field defects can be seen despite great CDR values and relatively small rim area values, as we found in the present study.

It may be concluded that an overall assessment of disk parameters without considering the IOP levels can hardly provide reliable data on the extent of the functional loss of visual field. From this follows with regard to diagnosis that in LTG and in POAG with lower IOP a deterioration of the disease may be detected earlier by investigation of the optic disk parameters, whereas in glaucoma with very high IOP computerized perimetry may be the more sensitive examination method in the early stage of the disease.

Conclusions

1. The degree of visual field loss at a given amount of CDR is smaller in LTG than in POAG or in pigmentary glaucoma.
2. In POAG the first visual field defects occur at a mean CDR values smaller by 20% in comparison to LTG.
3. The transition from ocular hypertension to POAG (or from suspected LTG to manifest LTG) can be observed on the basis of a mean CDR with a mean increase of CDR of still less than 10%, if the field examination is done wit program 31 in a 6°-grid.
4. The alteration of the mean rim area via ocular hypertension towards glau-comatous damage shows that visual field defects are measured only when already a remarkable loss of rim area has occurred. The borderline between ocular hypertension and glaucoma is, therefore, determined by the sensitivity of the perimetric method.
5. The optic disk excavation volume allows no conclusions as to the degree of visual field defects
6. In eyes with elevated IOP there must be less intact nerve fibers per square unit of rim area than in eyes with LTG, since in LTG as compared to POAG smaller field defects can be found despite smaller rim areas
7. In eyes with very high IOP, beginning visual field defects may already occur when the rim area damage appears not yet advanced considerably
8. In all types of glaucoma the neuroretinal rim area correlates best with the degree of visual field defects, together with the height of IOP.
9. Since in LTG the field defects occur only when the disk parameters already show great alteration, disk analysis may be the more sensitive method in LTG to detect early progression of the disease. In eyes with high IOP, however, a threshold measurement of the visual field may be the more sensitive examin-ation.
10. The quantitative differences in disk morphology (CDR and rim area) and location and depth of visual field defects [30, 34] in correlation to total loss suggest different pathomechanisms in eyes with and without IOP elevation, at least in the initial stages.
11. These differences may provide indirect information on the extent of the

damaging effect of IOP as well as vascular factors.

12. It seems probable that there are at least two different factors (vascular and mechanical) involved in causing disk alterations and visual field defects: one which is predominant in LTG, and another which is predominant in glaucoma with high IOP. In glaucoma with IOP values from 22 to 30 mm Hg both factors appear to be overlapping.

Acknowledgement

Remark

The preliminary results of this study were presented at the Workshop on the Optic Nerve Head Analyzer (June 27–29, 1985, in Würzburg).

Editorial comment

These authors compare several disc parameters as measured with the Rodenstock Optic Nerve Head Analyser with the visual field in four groups of patients with glaucoma: low-tension glaucoma (LTG), medium-tension glaucoma ($IOP_{max} =$ 22–30 mm Hg) (POAG 22), high tension glaucoma (IOP >30 mm) (POAG 30) and pigmentary glaucoma (PIGM). In their tables I and II they present the following data for the cup/disk ratio and total loss:

	Cup/Disk	Total	Total loss/ Cup/Disk
LTG	0.80	733	916
POAG 22	0.76	943	1240
POAG 30	0.73	678	928
PIGM	0.68	474	707
OH	0.69	0	–
Normals	0.47	0	–

In the third column I have given the ratio of total loss divided by cup/disk. I conclude that there is no significant difference between the low-tension glaucomas and the high-tension glaucomas (POAG 30). Furthermore the medium tension glaucomas show a relatively greater total loss in comparison with the cup/

disk ratio, while the pigmentary glaucoma patients show a small total loss with a relatively large excavation.

Thus, in this series I cannot find evidence for a striking difference between the high-tension and low-tension glaucomas.

There may be a problem in any selection of low-tension glaucoma cases. A low-tension glaucoma patient will usually be detected because of a suspect excavation. In the series of Gramer et al. the six normal eyes have a cup/disk ratio of 0.473 ± 0.065. A patient with a cup/disk ratio of 0.6 would still fall within the $2 \times$ standard deviation limit. On the basis of the cup/disk ratio one would expect suspicion to begin at cup/disk ratios over 0.6. It is therefore possible that low-tension glaucoma patients with smaller cup/disk ratios did not participate in the study for simple selection reasons. It should furthermore be realised that there are considerable differences in the shape and size of excavations in different types of low-tension glaucoma. Patients with focal ischaemic glaucoma may have a small cup/disk ratio (Greve and Geijssen, Docum. Ophthalmol. Proc. Series 35: 35–42, 1983):

	Cup/Volume	Total	Total loss/ Cup/Volume
LTG	1.223	733	599
POAG 20	1.189	943	793
POAG 30	1.134	678	597
PIGM.	0.693	474	683

The comparison of cup volume and total loss shows that the ratio of excavation volume and total loss in high tension glaucoma is similar to that in low tension glaucoma.

At a given cup volume the medium-tension glaucomas have a larger visual field defect than both the low-tension and the high-tension glaucomas.

In these Proceedings Caprioli and Sears present evidence that patients with a diffuse type of visual field loss have higher intraocular pressures and different type of excavation than patients with more localized defects. Such differences are not expressed by the notion of total loss. The authors point out that there is no significant difference in the disk-diameter in the groups with low-tension glaucoma, medium-tension glaucoma and high-tension glaucoma.

The authors found that the rim-area in low tension glaucoma is smaller than in high tension glaucomas for a certain size of field defect.

I find it difficult to explain how a difference in rim-area can exist without differences in cup/disk ratio or in cup/volume. A possible explanation may be found in differences in shape of the excavation and the method of measurements by the Optic Nerve Head Analyser.

The authors have presented a number of interesting data on quantitative measurements of the excavation and the visual field. Their conclusions provide food for further thought and discussion.

The differences in excavation and visual field in low-tension glaucoma and high-tension glaucoma deserve our continued attention (see also Caprioli and Sears, and Glowazki and Flammer in this volume).

References

1 Airaksinen PJ, Drance SM, Schulzer M: Neuroretinal rim area in early glaucoma Am J Ophthalmol 99: 1–4 (1985)

2 Anderson DR: Pathogenesis of glaucomatous cupping: a new hypothesis In: Symposium on Glaucoma, pp 81–94 Trans Orleans Acad Ophthalmol, CV Mosby, St Louis, 1975

3 Bengtsson B: Aspects of the epidemiology of chronic glaucoma Acta Ophthalmol 146: 1–48 (1981)

4 Caprioli J, Spaeth GL: Comparison of the optic nerve head in high and low tension glaucoma Arch Ophthalmol 103: 1145–1149 (1985)

5 Caprioli J, Klingbeil U, Sears M, Pope B: Reproducibility of optic disk measurements with computerized analysis of stereoscopic video images Arch Ophthalmol 104: 1035–1039 (1986)

6 Drance SM, Balazsi G: Die neuroretinale Randzone beim frühen Glaukom Klin Monatsbl Augenheilk 184: 271–273 (1984)

7 Drance SM: Low tension glaucoma Editorial Arch Ophthalmol 103: 1131–1133 (1985)

8 Gloor B, Schmied U, Fässler A: Glaukomgesichtsfelder – Analyse von Octopus-Verlaufsbeobachtungen mit einem statistischen Programm Klin Monatsbl Augenheilk 177: 423–436 (1980)

9 Gloor B, Schmied U, Fässler A: Changes of glaucomatous field defects Analysis of Octopus fields with program Delta Doc Ophthal Proc Ser 26: 11 (1981)

10 Gloor B: Die Computerperimetrie in der langfristigen Beurteilung des Glaukoms In: Krieglstein GK, Leydhecker M (eds) Medikamentöse Glaukomtherapie, pp 59–72 Bergmann, München, 1982

11 Gloor B, Stürmer J, Vökt B: Was hat die automatisierte Perimetrie mit dem Octopus für neue Kenntnisse Über glaukomatöse Gesichtsfeldveränderungen gebracht? Klin Monatsbl Augenheilk 184: 249–253 (1984)

12 Gramer E, Pröll M, Krieglstein GK: Die Perimetrie des blinden Fleckes Ein Vergleich zwischen kinetischer und computergesteuerter statischer Perimetrie Ophthalmologica 179: 201–208 (1979)

13 Gramer E, Pröll M, Krieglstein GK: Die Reproduzierbarkeit zentraler Gesichtsfeldbefunde bei der kinetischen und der computergesteuerten statischen Perimetrie Klin Monatsbl Augenheilk 176: 374–384 (1980)

14 Gramer E, Kontic D, Krieglstein GK: Die computer-perimetrische Darstellung glaukomatöser Gesichtsfelddefekte in Abhängigkeit von der Stimulusgröße Ophthalmologica 183: 162–167 (1981)

15 Gramer E: Der Informationsgehalt der computergesteuerten Perimetrie für die Diagnostik und Verlaufskontrolle von Augenkrankheiten Habil -Schrift, Würzburg, 1982

16 Gramer E, Steinhauser B, Krieglstein GK: The specifity of the automated suprathreshold perimeter Fieldmaster 200 A v Graefe's Arch Clin Exp Ophthalmol 218: 253–255 (1982)

17 Gramer E, Mohamed J, Krieglstein GK: Der Ort von Gesichtsfeldausfällen bei Glaucoma simplex, Glaukom ohne Hochdruck und ischämischer Neuropathie Indikationen zur vaso-

aktiven Therapie In: Krieglstein GK, Leydhecker W (eds) Medikamentöse Glaukomtherapie, pp 59–72 Bergmann, München, 1982

18 Gramer E, Gerlach R, Krieglstein GK, Leydhecker W: Zur Topographie früher glaukomatöser Gesichtsfeldausfälle bei der Computerperimetrie Klin Monatsbl Augenheilk 180: 515–523 (1982)

19 Gramer E, Gerlach R, Krieglstein GK: Zur Sensitivität des Computerperimeters Competer bei frühen glaukomatösen Gesichtsfeldausfällen Eine kontrollierte klinische Studie Klin Monatsbl Augenheilk 180: 203–209 (1982)

20 Gramer E: Computerperimetrie bei Glaukom, pp 99–120 In: Krieglstein GK, Leydhecker W (eds) Kaden, Heidelberg, 1982

21 Gramer E, Krieglstein GK: The role of computerized perimetry in the management of optic nerve disease Chibret Int J Ophthalmol 1: 41 (1983)

22 Gramer E, Leydhecker W: Zum gegenwärtigen Stand der Perimeterentwicklung (Teil II) Z prakt Augenheilk 5: 221–236 (1984)

23 Gramer E, De Natale R, Krieglstein GK: Zur Spezifität überschwelliger Prüfmethoden bei der automatischen Perimetrie Klin Monatsbl Augenheilk 186: 110–113 (1985)

24 Gramer E, Leydhecker W: Glaukom ohne Hochdruck Eine klinische Studie Klin Monatsbl Augenheilk 186: 262–267 (1985)

25 Gramer E, Leydhecker W: Zur Pathogenese des Glaukoms ohne Hochdruck Z prakt Augenheilk 6: 329–333 (1985)

26 Gramer E, Leydhecker W: Papillendiagnostik bei Glaukom Z prakt Augenheilk 6: 294–302 (1985)

27 Gramer E: Gegenwärtiger Stand der Perimeterentwicklung (III) Z prakt Augenheilk 6: 334–346 (1985)

28 Gramer E: Lesen von Gesichtsfeldbefunden bei der automatischen Perimetrie Z prakt Augenheilk 6: 353–364 (1985)

29 Gramer E, Klingbeil U: Quantitative Papillenanalyse mit dem Optic Nerve Head Analyzer Z prakt Augenheilk 7: 30–36 (1986)

30 Gramer E, Althaus G, Leydhecker W: Lage und Tiefe glaukomatöser Gesichtsfeldausfälle in Abhängigkeit von der Fläche der neuroretinalen Randzone der Papille bei Glaukom ohne Hochdruck, Glaucoma simplex, Pigmentglaukom Eine klinische Studie mit dem Octopus-Perimeter 201 und dem Optic Nerve Head Analyzer Klin Monatsbl Augenheilk 189: 190–198 (1986)

31 Gramer E, Althaus G, Leydhecker W: Die Bedeutung der Rasterdichte bei der computergesteuerten Perimetrie Eine klinische Studie Z prakt Augenheilk 7: 197–202 (1986)

32 Gramer E, De Natale R, Leydhecker W: Training effect and fluctuations in long-term follow-up of glaucomatous visual field defects calculated with program Delta of the Octopus Perimeter 201 Glaucoma Society Meeting, Turin 1986, Proceedings, Part 1 New Trends in Ophthalmology, Vol I, Nr 1, 219–228 (1986)

33 Gramer E, Althaus G: Quantifizierung und Progredienz des Gesichtsfeldschadens bei Glaukom ohne Hochdruck, Glaucoma simplex und Pigmentglaukom Eine klinische Studie mit dem Programm Delta des Octopus-Perimeters 210 Klin Monatsbl Augenheilk (in press) (1987)

34 Gramer E, Althaus G, Leydhecker W: Topography and progression of visual field damage in open-angle glaucoma, low tension glaucoma, and pigmentary glaucoma with program Delta of the Octopus Perimeter 201 IPS Amsterdam, 1986 pp 349–363 in this volume

35 Gramer E: Gesichtsfeldveränderungen bei Glaukom In: Das chronische Glaukom – zeitgemäße Diagnostik und Therapie Symposiumsband der Glaukom-Tagung, Rom, 05/05/86 (in press)

36 Krakau CET: Intraocular pressure elevation – cause or effect in chronic glaucoma? Ophthalmologica 182: 141–147 (1981)

37 King D, Drance SM, Douglas G, Schulzer M, Wijsman K: Comparison of visual field defects in normal-tension glaucoma and high-tension glaucoma Am J Ophthalmol 101: 204–207 (1986)

38 Krieglstein GK, Schrems W, Gramer E, Leydhecker W: Detectability of early glaucomatous field defects A controlled comparison of Goldmann versus Octopus perimetry Doc Ophthalmol Proc Ser 26: 19–24 (1981)

39 Krieglstein GK, Rüdiger E, Gramer E: Der Informationsgehalt einfacher, halbautomatischer Screening-Perimeter in der Glaukomdiagnostik Eine kontrollierte klinische Studie Z prakt Augenheilk 3: 123–128 (1982)

40 Leydhecker W: Eine neue Definition der okulären Hypertension In: Leydhecker W, Krieglstein GK (eds) Medikamentöse Glaukomtherapie, pp 41–48 Bergmann, München, 1982

41 Mikelberg FS, Airaksinen PJ, Douglas GR, Schulzer M, Wijsman K: The correlation between optic disk topography measured by the Video-Ophthalmograph (Rodenstock Analyzer) and clinical measurement Am J Ophthalmol 100: 417–419 (1985)

42 Mikelberg FS, Douglas GR, Schulzer M, Airaksinen PJ, Wijsman K, Manson D: The correlation between cup/disk ratio, neuroretinal rim area, and optic disk area measured by the Video-Ophthalmograph (Rodenstock Analyzer) and clinical measurement Am J Ophthalmol 101: 7–12 (1986)

43 Phelps CD, Hayreh SS, Montague PR: Visual fields in low-tension glaucoma, primary open-angle glaucoma, and anterior ischemic optic neuropathy In: Greve EL, Heijl A (eds) 5th Int Visual Field Symposium, pp 113–124 Junk, Dordrecht, 1983

44 Quigley HA, Addicks EM, Green R: Optic nerve damage in human glaucoma III Quantitative correlation of nerve fiber loss and visual field defect in glaucoma, ischemic neuropathy, papilledema, and toxic neuropathy Arch Ophthalmol 100: 135–145 (1982)

Author's address:
Privat-Dozent Eugen Gramer, M D , L L D ,
University Eye Hospital,
Josef-Schneider-Str 11, D-8700 Würzburg, F R G

V.8 Topography and progression of visual field damage in low tension glaucoma, open angle glaucoma and pigmentary glaucoma with the program Delta of the Octopus Perimeter 201

A clinical stud /

E. GRAMER, G. ALTHAUS and W. LEYDHECKER
Würzburg, F.R.G.

Abstract

451 eyes of 451 glaucoma patients were examined under controlled conditions with the programs 31 or 33 of the Octopus Perimeter 201: 83 patients with low tension glaucoma (LTG), 316 patients with primary open-angle glaucoma (POAG), and 52 patients with pigmentary glaucoma (PG).

Location, depth and progression of the field defects were investigated with the quantitative method of program Delta in order to search for significant quantitative differences between LTG, POAG and PG.

For definition and comparison of visual fields in the three types of glaucoma at identical stages (as defined according to the amount of total loss = TL) we subdivided the 3 patient groups into 4 stages of sensitivity loss: stage 1: TL ≤ 100 dB; stage 2: TL = 101–400 dB; stage 3: TL = 401–800 dB; stage 4: TL = 801–1600 dB.

With respect to course and kind of the visual defects in the 3 types of glaucoma we found differences which can be explained by the different influence of IOP rises and/or vascular damaging factors. The comparison of eyes with LTG, POAG and PG at identical stages showed the following results.
Location of scotomas·
1. Defects more frequent in the lower field in LTG as compared to POAG, especially in stage 2.
2. Defects more frequent in the upper than in the lower field in POAG.
3. A most equal number of defects in upper and lower field halves in PG.
4. In LTG as compared with POAG and PG the defects are more frequent in the nasal than in the temporal half of the field. In all 3 glaucomas, however, the nasal quadrants are affected more frequently than the temporal field.
5. Both in LTG and POAG the defects occur most frequently in the upper nasal quadrant, and most seldom in the lower temporal quadrant.
Depth of scotomas:
1. LTG shows the deepest scotomas; in POAG they are less deep; the least deep are found in PG.

2. Quantitative differences of scotoma depth are mainly found in the initial stages of the diseases.

Progression of field damage: the mean visual fields in the different stages, calculated from a great number of single fields with comparatively similar amount of of total loss, allow conclusions as to the progression of glaucomatous field loss in the 3 types of glaucoma:

1. Initially the field defects in POAG and PG increase mainly in size; only later, in the advanced stages of the disease, the increase in scotoma depth gains weight.
2. LTG presents from the very beginning deep localized scotomas. The increase in scotoma depth and the increase in scotoma size remain in a constant proportion throughout the further course. The increase in size, however, is predominant.

Introduction

The aim of the study was a quantitative comparison of the visual field defects in low tension glaucoma (LTG), primary open-angle glaucoma (POAG), and pigmentary glaucoma (PG) by using the statistical program Delta of the Octopus Perimeter 201 as a new method. The comparison is based on identical stages [1–4] of the 3 glaucoma types. Quantitative differences at the same stage of disease may allow conclusions as to the importance of pressure-dependent damaging factors as well as the vascular and systemic causes of field loss, which are difficult to quantify.

Method

451 eyes of 451 glaucoma patients with visual field defects of the stages 1–4 were examined with Octopus 201: 83 patients had LTG, 316 had POAG, and 52 had PG. We used program 31 or 33 with an eccentricity range up to 30°, 73 testpoints, and a 6°-grid. The examinations were done over a period of 8 years. The mean total field loss (TL) as well as the mean loss per testpoint (TL/TP) in the 30°-field and in the field quadrants were calculated for each patient with program Delta [4, 8, 9, 12, 17–19, 25, 26]. In addition, for each field the quotient of total loss and of the number of disturbed testpoints (TL/PP) was calculated; it provides a measure for the mean depth of field defects [8, 9].

For definition and comparison of the visual fields in the different glaucomas at identical stages of disease according to the amount of TL, we subdivided the 3 groups also according to the 4 stages of sensitivity loss: stage 1: TL $\leq$100 dB; stage 2: TL = 401–400 dB; stage 3: 401–800 dB; stage 4: 801–1600 dB. All eyes had a visual acuity of 0.8 or better, with a maximum ametropia of $\pm$ 3 dpt and no other

Table 1. Cols 1, 6, 11: *Mean scotoma depth* (total loss per pathologic testpoint = TL/PP) + mean standard deviation. Cols 2, 7, 12: *Relative increase of TL/PP* in stages 1–4. Cols 3, 8, 13: *Mean total loss per testpoint* (= TL/TP) + mean standard deviation. Cols 4, 9, 14: *Relative increase of TL/TP* in stages 1–4. Cols 5, 10, 15: *Mean age* + mean standard deviation. These data are shown for LTG in columns 1–5, for POAG in columns 6–10, and for PG in columns 11–15.

	Low tension glaucoma					Glaucoma simplex					Pigmentary glaucoma				
	TL/PP ±SD (dB)	Relative increase of TL/PP	TL/TP ±SD (dB)	Relative increase of TL/TP	Mean age ±SD (yrs)	TL/PP ±SD (dB)	Relative increase of TL/PP	TL/TP ±SD (dB)	Relative increase of TL/TP	Mean age ±SD (yrs)	TL/PP ±SD (dB)	Relative increase of TL/PP	TL/TP ±SD (dB)	Relative increase of TL/TP	Mean age ±SD (yrs)
	1	2	3	4	5	6	7	8	9	10	11	12	13	14	15
Stage I (TL <100 dB)	7.2± 0.5	–	● 0.9± 0.1 ●	–	48.0± 23.7	** 7.2± 0.3	–	0.7± 0.3 •••	–	62.3± 13.0	** 6.0± 0.2	–	● 0.4± 0.1 •••	–	48.3± 12.8
Stage II (TL = 101–400 dB)	*** 12.2± 0.6 ***	+69%	3.7± 0.3	+311%	50.3± 13.9	*** 9.1± 0.2	+26%	3.5± 0.1	+400%	64.7± 13.4	8.1± 0.4 ***	+35%	3.5± 0.5	+775%	51.1± 14.5
Stage III (TL = 401–800 dB)	*** 16.2± 0.7	+34%	9.3± 0.3	+151%	69.3± 9.2	*** 12.7± 0.4 *	+40%	● 8.6± 0.2	+146%	68.4± 10.3	14.6± 0.6 *	+80%	● 10.0± 0.5	+186%	50.5± 13.1
Stage IV (TL = 801–1600 dB)	19.6± 0.6	+21%	16.2± 0.9	+74%	60.7± 12.8	18.5± 0.3	+46%	● 16.5± 0.4	+92%	64.6± 13.5	19.9± 0.8	+36%	● 18.7± 0.9	+87%	54.5± 15.9

* Significant differences in scotoma depth for the 3 types of glaucoma in stages 1–4 are marked by asterisks.

● Significant differences in total loss for the 3 types of glaucoma in stages 1–4 are marked by dots.

Two significantly different values are marked by the chosen symbols above or below the compared values: *depth* (TL/PP) $p<5.0\%$ = *, $p<1.0$ = **, $p<0.1\%$ = ***; *total loss* (TL/TP) $p<5.0\%$ = ●, $p<1.0\%$ = ●●, $p<0.1\%$ = ●●●

pathology of the anterior segments than glaucoma. All patients were examined and recorded by the author during 8 years according to standardized examination and anamnestic patterns.

For comparing the 3 groups of glaucoma the mean maximum IOPs were calculated from diurnal tension curves without medication and additional measurements, also without medication. The eye to be evaluated in a patient was chosen at random, if both eyes showed field defects. Diagnosis of LTG (IOP maximum 21 mm Hg) was established through many diurnal tension curves, after exclusion of neurological diseases [20, 21]. Diagnosis of PG was established if there were pigmentary iris defects, Krukenberg's Spindle, or pigmentation of the chamber angle. All eyes had wide, open chamber angles.

The mean total loss per testpoint in the field quadrants and in the field halves were checked as to significance of differences between the 3 glaucoma types with the Mann-Whitney-U-Test (cf. Table 1, Fig. 2).

$\longrightarrow$

Figure 1 The *differences* of mean total loss per testpoint (= TL/TP) in the *quadrants* of the central visual field (circles with quadrants) are shown for LTG, POAG and PG in the stages 1–4, and also for all stages together Significant differences (p<5%) of TL/TP between more than two quadrants are marked either white, light grey, dark grey, or black; and marked by asterisks if only between two quadrants *Example* POAG of stage 3 (68 eyes) has a larger mean total loss per testpoint (TL/TP = 11 3 dB) in the upper nasal quadrant than in the other 3 quadrants This is a significant difference Therefore, the upper nasal quadrant shows the darkest colour in this visual field The difference between mean losses is not significant between upper temporal and lower nasal quadrants, which therefore show the same colour The mean total loss per testpoint in the lower temporal quadrant (TL/TP = 5,6 dB) is significantly smaller than in the other three, so this quadrant has the lightest shade of grey Thus, the more colour differences are seen in the field quadrants, the more significant differences are found between the single quadrants The *differences* between TL/TP in the *upper quadrants* and TL/TP in the *lower quadrants* are calculated separately for each single examination; the mean value of the single results is given as quotient at the right side of the circles. TL/TP in the upper field is identified as 1 The denominator of the fraction thus gives the TL/TP in the lower field in percents of the damage in the upper field *In our example* for POAG of stage 3 the proportion between TL/TP in *the upper and lower field is 1 : 0 66, i e the field loss is less in the lower half, amounting to only 66% of* the loss in the upper half This difference is significant (p<0 1%) and is marked by 3 asterisks In the same way, the *difference* of mean loss per testpoint for the *nasal and temporal half* of the visual field is calculated and given as quotient below the circles *In our example* for POAG of stage 3 the proportion between TL/TP in the nasal and temporal half is 1 : 0 78, i e the temporal field is less affected than the nasal field TL/TP in the temporal half amounts to 78% of that in the nasal half, again a significant differences in the range of p<0 1% (= * * *) The asterisks mark significant differences either between only 2 field quadrants, or between two halves of the visual field (p<5% = *; p<1% = * *; p<0 1% = * * *) The number of visual fields evaluated for the single examination groups is given in the right upper corner The group of stages 1–4 also includes 4 patients with LTG and 10 patients with POAG, who show a total loss of 1600 dB, but still have an intact central visual field

Results

Location of scotomas

Comparison of upper and lower half of visual field at the 4 stages (quotients beside fields in Fig. 1). In LTG the visual field defects, except those of stage 2 (TL 101–400 dB), are found more often in the upper half than in the lower; the differences, however, are not significant (Fig. 1, left). In POAG the visual field defects are

	LOW TENSION GLAUCOMA	GLAUCOMA SIMPLEX	PIGMENTARY GLAUCOMA
STAGE I (TOTAL LOSS ≤ 101 DB)	n=8; 0 8 / 1 2, 0 7 / 0 5; 1/0.60; 1/1.06	n=58; 0 8 / 0 9, 0 7 / 0 4; 1**/0.59; 1/0.93	n=19; 0 3 / 0 5, 0 2 / 0 3; 1/0.75; 1/1.60
STAGE II (TOTAL LOSS = 101–400 DB)	n=23; 2 6 / 3 2, 7 5 / 1 9; 1/1.62; 1/0.50**	n=106; 4 0 / 3 5, 3 5 / 2 6; 1**/0.82; 1/0.82**	n=13; 3 1 / 4 5, 3 1 / 3 3; 1/0.85; 1/1.26
STAGE III (TOTAL LOSS = 401–800 DB)	n=27; 12 9 / 8 3, 10 0 / 4 7; 1/0.69; 1/0.57***	n=68; 11 3 / 9 3, 7 9 / 5 6; 1***/0.66; 1/0.78***	n=10; 11 4 / 6 1, 14 6 / 8 2; 1/1.30; 1/0.55**
STAGE IV (TOTAL LOSS = 801–1600 DB)	n=21; 19 3 / 15 8, 17 9 / 12 3; 1/0.86; 1/0.76***	n=74; 19 3 / 16 3, 16 6 / 14 0; 1*/0.86; 1/0.84***	n=10; 20 9 / 17 0, 18 5 / 18 8; 1/0.98; 1/0.91
STAGE I–IV (TOTAL LOSS ≤ 101–1600 DB)	n=83; 11 0 / 8 9, 11 1 / 6 4; 1/0.89; 1/0.68***	n=316; 9 2 / 7 9, 7 7 / 6 2; 1***/0.82; 1/0.84***	n=52; 7 1 / 5 7, 7 2 / 6 1; 1/1.04; 1/0.83

CENTRAL 30% FIELD
QUADRANTS
UPPER NASAL | UPPER TEMPORAL
LOWER NASAL | LOWER TEMPORAL

SIGNIFICANT DIFFERENCES ($p <$ 5%) OF MEAN LOSS PER TESTPOINT (L/TP) IN THE FIELD QUADRANTS

INCREASING LOSS PER TESTPOINT (L/TP)

SIGNIFICANCE
$p < 5\%$ *
$p < 1\%$ **
$p < 0.1\%$ ***
FOR DIFFERENCES OF MEAN LOSS PER TESTPOINT (L/TP)
a) IN TWO FIELD QUADRANTS
b) IN THE UPPER AND LOWER HALF OF THE FIELD
c) IN THE NASAL AND TEMPORAL HALF OF THE FIELD

significantly more frequent in the upper half at all stages (Fig. 1, middle). In PG the field defects are distributed almost equally in the upper and lower half of the field (Fig. 1, right).

Comparison of nasal and temporal half of visual field (quotients below fields in Fig. 1). In all glaucoma types the field defects are found more frequently in the nasal half than in the temporal half of the visual field. In LTG as compared to the glaucomas with high IOP the nasal field half is affected more strongly in all eyes at stages 2–4 than the temporal half.

Comparison of quadrants In stage 1(TL ≤100 dB) the field defects are most frequently found in the upper temporal quadrants in all types of glaucoma (Fig. 1). In stage 2 (TL 101-400 dB) there are differences, which grow even more significant in the following stages with a greater total loss. In POAG, for instance, the upper nasal quadrant is affected most. In LTG at stage 2 the lower nasal quadrant is affected most, while at stages 3 and 4 the upper nasal and the lower nasal quadrants show the same amount of defects. For stages 2–4 with approximtely equal amount of mean total loss we find for LTG, as compared with POAG (Table 1), a greater TL/TP in the lower nasal quadrant. In both LTG and POAG, the lower temporal quadrants show the significantly smallest amount of scotomas per testpoint In PG, there is no accumulation at all of scotomas in certain quadrants

Mean depth of scotomas

Compared to POAG and PG the eyes with LTG at the stages 2–4 show the greatest values of scotoma depth (Table 1, col. 1), both absolutely and in relation to the mean total loss (TL/TP) (Table 1, col. 3). In POAG, with a mean total loss (Table 1, col. 8) comparable to that in LTG (Table 1) the defects at stages 2–4 are less deep (Table 1, col. 6) and slightly larger in size in POAG than in LTG. At stage 1 (TL ≤100 dB) the eyes with PG and a significantly smaller total loss (0.4 dB/TP) than eyes with POAG (0.7 dB/TP) and eyes with LTG (0.9 dB/TP) show, nevertheless, the relatively largest amount of total loss per testpoint (TL/PP = 0.6 dB), i.e. the relatively greatest scotoma depth. The initial field defects in eyes with PG, therefore, seem to be smaller in size, but relatively deep. In the stages 2–4, however, the eyes with PG show the smallest sensitivity loss per disturbed testpoint (Table 1, col. 11) of all glaucoma types. The defects in PG are on the whole spread more diffusely across the visual field than in LTG and POAG.

Comparing the 3 glaucoma groups we find that the scotomas in LTG are the deepest, and those in PG the least deep. The visual field defects in POAG and in PG, which occur together with elevated IOP, show with respect to depth greater similarity than those in POAG and in LTG.
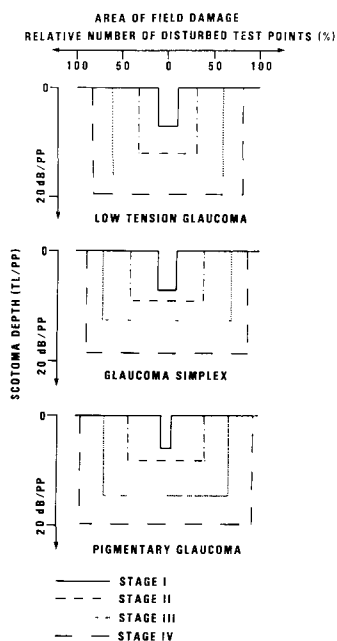
Figure 2 Differences of increase in mean scotoma size (number of distuibed testpoints in %) and of mean defect depth (TL/PP) for LTG, POAG, and PG at identical stages of disease *Mean scotoma size* calculated from the relative number of disturbed testpoints If all 69 testpoints (blind spot excepted) show a pathologic sensitivity loss (printed out by program Delta), the mean scotoma size (%) is 69/69 = 100% In this way, the mean scotoma size is calculated for the 3 groups in stages 1–4 *Mean scotoma depth* calculated for all single examinations from the total loss in the central visual field and the number of disturbed testpoints The mean scotoma depth for the 3 types of glaucoma in the 4 stages (cf Table 1, cols 1, 6, 11) is shown in the ordinate Stage 1: PG shows the deepest scotomas in relation to scotoma size Stages 2 + 3: LTG shows significantly deeper defects than POAG and PG Stage 4: There are significant differences of scotoma depth in the 3 groups In LTG, the inciease of scotoma depth and the increase of scotoma size are found to differ duiing all stages in constant proportions The field defects in LTG and PG are increasing mainly in size in the early stages In the later stages it is the increase in scotoma depth wich is predominant

Differences in progression of field loss

The course of progression in LTG, POAG, and PG is elucidated by comparing the mean values which are obtained from a great number of field examinations at identical stages, successively through the 4 stages. In LTG, the mean total loss (TL/TP) increases from stage 1 to stage 2 by 311% from 0.9 to 3 7 dB/TP (Table 1, col. 4). From stage 2 to stage 3 there is an increase by 151%, and from stage 3 to stage 4 by 74%. The mean total loss in scotoma depth (TL/PP) increases by 69% from 7.2 (stage 1) to 12.2 dB (stage 2), and in the further stages by 34% and by 21% (Table 1, col. 2). Therefore, the increase in scotoma depth and the increase in total field loss are found to be in relatively constant proportions, as shown by

the quotients of 0.22, 0.23, and 0.28. Since in LTG the scotomas are initially deeper than in POAG and PG, we may conclude that they are increasing more in size than in depth during all 4 stages. This proportion remains constant right through the course of scotoma development (cf. Fig. 2, above). In POAG, the increase in scotoma depth and the increase in total loss are found in proportions which yield the quotients of 0.07, 0.27 and 0.50. The defects in POAG, therefore, are increasing mainly in size from stage 1 to stage 2, which means that field sections not yet damaged before become included into the damaged area gradually, whereas the increase in scotoma depth is comparatively less important. Only at the later stages, there is a more obvious increase in depth of the field defects (Fig. 2, middle). In PG, the proportions between increase of scotoma depth and increase of total loss result in the quotients 0.05, 0.43 and 0.41%. The development in PG is therefore quite similar to the course of increase of depth and size in POAG.

Discussion

Location of scotomas

Comparison of upper and lower half of visual field. The differences in TL/TP (size and depth of scotomas) between upper and lower half of the visual field in LTG of all stages, and also with respect to all eyes together, are always smaller than in POAG and are of the same amount only at stage 4. The differences in TL/TP between the upper field half (more often affected) and the lower field half (more rarely affected) are, however, in LTG never statistically significant. In POAG, however, the upper field half is more frequently affected to a significant degree. At stage 2 in LTG the defects occur more often in the lower than in the upper half, as shown in former studies [15] (Fig. 3, middle).

In ischemic neuropathy as well as in Apoplexia papillae (Fig. 3, right) the defects are also found in the majority of cases in the lower field half, as agreed upon in several studies [3, 15, 16, 38]. In comparison with these diseases, in which the damage of the optic disk is caused by vascular factors, the upper field half is on the whole still relatively often affected in LTG (Fig. 1, left) [15, 25, 26, 38]. In the initial stage, LTG appears to range in the middle between POAG and ischemic neuropathy, where the topography of the defects is concerned. At the advanced stage 4, however, the defects are spread almost equally in the upper and lower half, so that there is much greater similarity to POAG than to ischemic neuropathy in this respect. This may suggest predominance of vascular pathomechanisms in the early stage of field damage in LTG [15, 25, 26].

In PG, the field defects are spread with almost the same frequency across upper and lower half of the field [25, 26]. The damaging effect of IOP seems therefore to affect the upper and lower part of the optic disk to the same degree. As for the
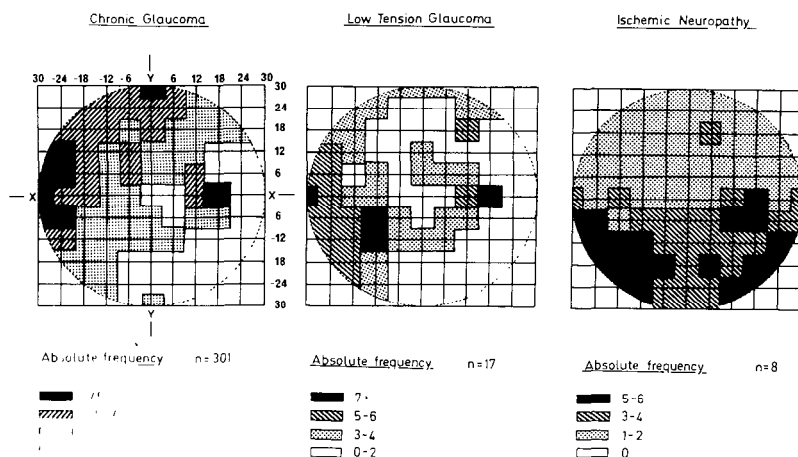
Figure 3 *Left* frequency distribution of absolute glaucomatous field defects up to stage II in the 73 testpoints of program 31 of Octopus Perimeter 201, investigated in 301 eyes [11, 14] Absolute scotomas in the single testpoints of the difference table were transferred according to their location into an evaluation pattern [11, 14] The testpoints are placed in the intersections of the given lines Those testpoints in the black areas show the greatest amount of absolute scotomas, the testpoints in the hatched areas show the second-greatest amount of absolute scotomas For POAG of stage II the evaluation of all single testpoints led to the following results: 1 Absolute scotomas are found more frequently in the upper half of the field 2 The upper field half, especially the upper nasal quadrant, shows frequently absolute scotomas, whereas they are seldom in the lower temporal quadrant 3 In the upper field absolute scotomas are nearer to the fixation point and the blind spot, while the area between optic disk and macula remains largely free of defects The axon bundle related to the lower portion of the disk seems therefore to be of increased vulnerability towards glaucomatous damage, due to a pathomechanism as yet unknown [11, 12, 14, 16] *Middle* frequency distribution of absolute scotomas in LTG up to stage II It is similar to that in POAG The scotomas are somewhat more frequent in the lower temporal quadrant [15] *Right* frequency distribution for AION, with the defects mainly in the lower field half [15] The shift of defect frequency towards the lower field in LTG might indicate that here the amount of vascular factors in visual field damage is predominant [15]

lack of such regular distribution of the defects in the upper and lower half in LTG and POAG, one may assume an additional damaging impact as the reason for the more frequent incidence of the defects above the 0°-meridian. In PG of stage 3 (Fig. 1, right) we observed the defects more frequently in the lower field half, and thus a distribution of defects similar to that in stage 2 of LTG. In these eyes we found the highest mean IOP peaks of all groups and all stages (36 ± 7 mm Hg). This may indicate that very high IOP can induce acute ischemia, which causes a pattern of damage similar to that in LTG [25]. The visual field defects in POAG and in LTG were investigated in several publications [1, 5, 14, 15, 27, 29, 35–38], which are, however, difficult to compare, since they are based on different perimetric methods and on different definitions of the stages of glaucoma Motolko and Drance [35, 36] compared mainly qualitative differences. The basis for their comparison were visual fields in eyes with the same cup/disk ratio. The

cup/disk ratio, however, according to more recent studies [20], which have been confirmed in the meantime [6, 23, 26], is no longer considered a suitable parameter for comparing POAG and LTG, because in LTG there occur large disk excavations than in POAG for the same size of visual field damage [20, 21, 23, 26]. The studies of Motolko and Drance [35, 36] do not reveal either how often the examined fields showed advanced defects. Their results do not state differences between LTG and POAG with respect to scotoma topography and are therefore not necessarily in contradiction to our results, which show such differences between the 3 glaucomas, particularly in the initial stages (Fig. 1) [25, 26]. Greve [27] observed in his study on eyes with field defects at all stages in LTG also a greater incidence of defects in the upper field half, and in eyes with very high IOP (more than 40 mm Hg) an approximately equal distribution of scotomas for the upper and the lower halves of the field. His results agree with ours for PG with its doubtless pressure-dependent damaging mechanism. The location of absolute glaucomatous scotomas up to stage 2, without regard of the IOP level, was examined by Aulhorn [2, 3]. The amount of absolute scotomas found in the upper and lower field half was approximately the same. In our own studies [14, 15], the examination of 301 eyes with POAG of all IOP levels with program 31 of Octopus 201 showed that the field defects occurred more frequently in the upper field half in POAG up to stage 2 (Fig 3, left). This topography of early glaucomatous field damage in POAG was confirmed in studies of Phelps [38], Heijl [28] and Nicholas [37]. Phelps [38] investigated the topography of field defects in a frequency distribution of absolute scotomas by means of Goldman's Perimetry. He found for LTG and POAG the incidence of scotomas in the upper field half greater than in the lower, basing his study on at least roughly differentiated stages of field damage. Our studies [25, 26] were the first to attempt with program Delta a quantitative analysis of absolute and relative field defects for comparing LTG and POAG. By applying a testpoint grid (6° grid of programs 31/33) the detection probability of early glaucomatous scotomas was defined [24]. Working with computerized perimetry (staircase-up-and-down method) gives a higher rate of detection probability than the usual perimetric routine methods [10–13, 16, 31].

Comparison of nasal and temporal half of visual field. For all 3 glaucomas we found larger defects in the nasal than in the temporal field. Lynn [33] points out that there must be a direct correlation between the probability of damage to axons from the different retinal areas *and* the length of way the axons pass in the optic disk. Those axons with the longest way through the papilla are the most susceptible to ischemic damage. The temporal areas of the optic disk contain primarily macular fibers [33, 34]. This may be the reason why nerve fibers from the temporal retina, which also have to pass the temporal areas of the optic disk, have a longer way through the disk tissue than the nerve fibers from the nasal periphery. Randomized local ischemia will therefore damage axons from retinal areas, which are located temporally of the optic disk, more than axons from the

nasal periphery This could explain the larger defects in the nasal visual field. This unequal distribution of defects in the vertical halves of the visual field is more pronounced in LTG and less evident in POAG and PG (with exception of stage 3, see above). Therefore, the vascular pathogenesis must have a different degree of influence in the etiology of field defects in glaucomas with and without elevated IOP.

Comparison of field quadrants. The earliest field defects (stage 1. TL ≤100 dB) are found in all 3 glaucomas most frequently in the upper temporal quadrants (Fig. 1, upper part). Our quantifying evaluations confirm similar findings on the detection rate for earliest scotomas [30]. In the more advanced stages of damage, especially in POAG, we find a high incidence of scotomas in the upper nasal quadrants. In LTG the upper nasal quadrants also show the greatest amount of total loss at stages 3 and 4; but there are (with exception of stage 2) never any significant differences in comparison to the lower nasal quadrant.

In a former study we established the frequency distribution for absolute and relative scotomas In 301 eyes with field defects up to stage II the defects in POAG were more frequently in the upper, and above all the upper nasal field [11, 13, 14, 16]. Perhaps, the greater damage found in the upper field for LTG and POAG as compared to PG (equal frequency distribution of defects in upper and lower field) as well as compared to ischemic neuropathy and Apoplexia papillae (damage of mainly the lower field by acute ischemic defects) can be explained by chronic microvascular mechanisms. The latter may lead to chronic ischemia in LTG and POAG and may affect (for reason yet unknown) the axons of the lower retina more than those of the upper, with the result of greater frequency of defects in the upper visual field [11]

The higher frequency of field defects in the upper and upper nasal field correlates with different alterations of the glaucomatous optic disk Studies based on experimental elevations of IOP [30, 40, 45] found a blockade of the axoplasmic transport mainly in the temporal disk quadrants. Quigley [41–43] describes for the upper and lower poles of the Lamina cribrosa, through which the axons from the upper and lower Bjerrum region pass, larger pores and thinner protective connective tissue than for the horizontal poles of the Lamina cribrosa If the bulbus wall tension is increased, those parts of the Lamina cribrosa with the least support by connective tissue would also show the least resistance against structural distortion. So, it would be these parts in which the first mechanical damage of axons or the capillary compression may occur. Fluorescein angiography of the optic disk [7] proved that eyes with POAG show particularly often local filling defects with resultant ischemic areas in the region of the lower pole of the optic nerve head; this would correlate with the field defects in the upper field. Disk hemorrhages are found in 70% of the cases in the lower temporal disk quadrant. Furthermore, it was proved that such disk hemorrhages go hand in hand with notches in the neuroretinal rim area at the site of bleeding and with corresponding

further loss of visual field function [46]. The frequent occurrence of disk hemorrhages in the lower temporal area and of disk pallor and rim notching also in the lower temporal area of the disk agrees well with the high frequency of visual field defects in the nasal and upper quadrants [22].

Depth of scotomas

LTG shows the deepest scotomas, both absolutely and in relation to total loss (Table 1). Deep and less diffuse scotomas indicate isolated damage of nerve fiber bundles [25].

In PG with its primarily pressure-related damaging process we find the least deep scotomas in relation to total loss (Table 1, right). From this we can conclude that elevated IOP seems to affect in equal distribution all parts of the optic disk. The mean value for depth of absolute and relative scotomas describes the amount of field loss better than the profiles of single scotomas [1, 5, 29] next to the central field. This is discussed elsewhere [25].

Here we can present only partial aspects of the whole study [25]. Some results for the 451 eyes may be summarized as follows: for the 52 eyes with PG the correlation between IOP (maximum IOP of 33 ± 8 mm Hg) and the depth of scotomas (TL/PP) (Table 1) showed a significant dependence of scotoma depth upon IOP (p <5%) [25]. For the 316 eyes with POAG (maximum IOP of 31 ± 8 mm Hg), however, there was no dependence found between scotoma depth and IOP as damaging factor [25]. This may suggest on the one hand that there are other than pressure-related damaging factors involved in POAG. On the other hand, it underlines in general the damaging effect of elevated IOP.

Progression of field damage

The comparison of mean visual fields, whose basic comparability is statistically ensured [25], at consecutive stages of the glaucomatous diseases results in the observation of different dynamics of visual field loss in eyes with and without elevated IOP (Table 1, Fig. 2). While in LTG the increase of scotoma depth and the increase of total loss are found in a constant proportion to each other (Fig. 2), the defects in POAG and PG increase mainly in size in the initial stages. In the later stages (3 and 4) of POAG and PG, however, in relation to the increase of total loss, there is a much more pronounced increase of depth of the visual field defects [25].

Conclusion

These differences in the dynamics of visual field loss, as well as the differences in location and depth of defects and the different correlations between scotoma depth and IOP levels in POAG and PG, may be caused by different amounts of influence of vascular damaging factors. Therefore, in glaucoma the presence of at least two etiologic mechanisms may be assumed.

Acknowledgement

References

1 Anderton S, Hitchings RA: A comparative study of visual fields of patients with low tension glaucoma and those with chronic simple glaucoma In: Greve EL, Heijl A (eds) 5th international visual field symposium, pp 90–97 Dr W Junk Publ, Dordrecht, 1983
2 Aulhorn E, Karmeyer H: Frequency distribution in early glaucomatous visual field defects Doc Ophthalmol Proc Ser 14: 75–83 (1977)
3 Aulhorn E, Tanzil M, Litricin V: Vergleich der Gesichtsfeldausfälle bei der Apoplexia papillae und beim Glaukom Ber Dtsch Ophthalmol Ges 76: 663–640 (1979)
4 Bebie H, Fankhauser F: Delta manual Interzeag AG, Schlieren, Switzerland, 1982
5 Caprioli J, Spaeth GL: Comparison of visual field defects in the low-tension glaucomas with those in the high-tension glaucoma Am J Ophthal 97: 730–737 (1984)
6 Caprioli J, Spaeth GL: Comparison of the optic nerve head in high- and low-tension glaucoma Arch Ophthalmol 103: 1145–1149 (1985)
7 Fishbein SL, Schwartz B: Optic disc in glaucoma Topography and extent of fluorescein filling defects Arch Ophthalmol 95: 1975–1979 (1977)
8 Gloor B, Schmied U, Fässler A: Changes of glaucomatous field defects Analyis of Octopus fields with program Delta Doc Ophthalmol Proc Ser 26: 247–253 (19??)
9 Gloor B, Vökt B, Stürmer J: Was hat die automatisierte Perimetrie mit dem Octopus für neue Erkenntnisse über glaukomatöse Gesichtsfeldveränderungen gebracht? Klin Monatsbl Augenheilk 184: 249–253 (1984)
10 Gramer E, Pröll M, Krieglstein GK: Die Reproduzierbarkeit zentraler Gesichtsfeldbefunde bei der kinetischen und der computer-gesteuerten statischen Perimetrie Klin Monatsbl Augenheilk 176: 374–384 (1980)
11 Gramer E: Der Informationsgehalt der computergesteuerten Perimetrie für die Diagnostik und Verlaufskontrolle von Augenkrankheiten Habil.-Schrift, Würzburg (1982)
12 Gramer E: Computerperimetrie bei Glaukom In: Leydhecker W, Krieglstein GK (eds) Programmgesteuerte Perimetrie, pp 99–120 Kaden Verlag, Heidelberg, 1982
13 Gramer E, Gerlach R, Krieglstein GK: Zur Sensitivität des Computerperimeters Competer® bei frühen glaukomatösen Gesichtsfeldausfällen Eine kontrollierte klinische Studie Klin Monatsbl Augenheilk 180: 203–209 (1982)
14 Gramer E, Gerlach R, Krieglstein GK, Leydhecker W: Zur Topographie früher glaukomatöser Gesichtsfeldausfälle bei der Computerperimetrie Klin Monatsbl Augenheilk 180: 515–523 (1982)

362

15 Gramer E, Mohamed J, Krieglstein GK: Der Ort von Gesichtsfeldausfällen bei Glaucoma simplex, Glaukom ohne Hochdruck und ischämischer Neuropathie Indikationen zur vaso-aktiven Therapie In: Krieglstein GK, Leydhecker W (eds) Medikamentöse Glaukomtherapie, pp 59–72 JF Bergmann Verlag, München, 1982

16 Gramer E, Krieglstein GK: The role of computerized perimetry in the management of optic nerve diseases Chibret Int J Ophthalmol 1: 41 (1983)

17 Gramer E, Leydhecker W: Zum gegenwärtigen Stand der Perimeterentwicklung Teil II Z prakt Augenheilk 5: 221–236 (1984)

18 Gramer E: Gegenwärtiger Stand der Perimeterentwicklung Teil III Z prakt Augenheilk 6: 334–346 (1985)

19 Gramer E: Lesen von Geschichtsfeldbefunden bei der automatischen Perimetrie. Z prakt Augenheilk 6: 353–364 (1985)

20 Gramer E, Leydhecker W: Glaukom ohne Hochdruck Eine klinische Studie Klin Monatsbl Augenheilk 186: 262–267 (1985)

21 Gramer E, Leydhecker W: Zur Pathogenese des Glaukoms ohne Hochdruck Z prakt Augen-heilk 6: 329–333 (1985)

22 Gramer E, Leydhecker W: Papillendiagnostik bei Glaukom Z prakt Augenheilk 6: 294–302 (1985)

23 Gramer E, Bassler M, Leydhecker W: Cup/disk ratio, excavation volume, neuroretinal rim area of the optic disk in correlation to computerperimetric quantification of visual field defects in glaucoma with and without pressure Clinical study with the Rodenstock Optic Nerve Head Analyzer and the program Delta of the Octopus Perimeter 201 IPS Amsterdam, 1986, see pp 329–348 in this volume

24 Gramer E, Althaus G, Leydhecker W: Die Bedeutung der Rasterdichte bei der computer-gesteuerten Perimetrie Eine klinische Studie Z prakt Augenheilk 7: 197–202 (1986)

25 Gramer E, Althaus G: Quantifizierung und Progredienz des Gesichtsfeldschadens bei Glaukom ohne Hochdruck, Glaucoma simplex und Pigmentglaukom Eine klinische Studie mit dem Program Delta des Octopus-Perimeters 201 Klin Monatsbl Augenheilk (in press) (1987)

26 Gramer E, Althaus G, Leydhecker W: Lage und Tiefe glaukomatöser Gesichtsfeldausfälle in Abhängigkeit von der Fläche der neuroretinalen Randzone Eine klinische Studie mit dem Octopus-Perimeter 201 und dem Optic Nerve Head Analyzer Klin Monatsbl Augenheilk 189: 190–198 (1986)

27 Greve EL, Geijssen HC: Comparison of glaucomatous visual field defects in patients with high and low intraocular pressure In: Greve EL, Heijl A (eds) 5th international visual field sym-posium, pp 101–105 Dr W Junk Publ, Dordrecht, 1983

28 Heijl A, Lundquist L: The frequency distribution of earliest glaucomatous visual field defects documented by automatic perimetry Acta Ophthalmol 62: 658–664 (1984)

29 King D, Drance SM, Douglas G, Schulzer M, Wijsman K: Comparison of visual field defects in normal-tension glaucoma and high-tension glaucoma Am J Ophthal 101: 204–207 (1986)

30 Kitazawa Y, Tarahashi O, Ohiwa J: The mode of development and progression of field defects in very early glaucoma A follow-up study In: Greve EL, Heijl A (eds) 3rd international visual field symposium, pp 211–221 Dr W Junk Publ, Dordrecht, 1979

31 Krieglstein GK, Schrems W, Gramer E, Leydhecker W: Detectability of early glaucomatous field defects A controlled comparison of Goldmann versus Octopus perimetry Doc Ophthalmol Proc Ser 26: 19–24 (1981)

32 Levene RA: Low-tension glaucoma A critical review and new material Surv Ophthalmol 24: 621–663 (1980)

33 Lynn JR: Correlation of pathogenesis, anatomy, and pattern of visual field loss in glaucoma In: Symposium on glaucoma, pp 151–189 Trans Orleans Acad Ophthalmol Mosby, St Louis, 1975

34 Mincklers DS, Bunt AH, Johanson GW: Orthograde and retrograde axoplasmic transport during acute ocular hypertension in the monkey Invest Ophthal Vis Sci 16: 32–225 (1977)

35 Motolko M, Drance SM, Douglas GR: Visual field defects in low-tension glaucoma Arch Ophthalmol 100: 1074–1078 (1982)

36 Motolko M, Drance SM, Douglas GR: The visual field defects of low-tension glaucoma In: Greve EL, Heijl A (eds) 5th international visual field symposium, pp 107–111 Dr W Junk Publ, Dordrecht, 1983

37 Nicholas SP, Werner EB: Location of early glaucomatous visual field defects Can J Ophthalmol 15: 131–133 (1980)

38 Phelps CD, Hayreh SS, Montague PR: Visual fields in low-tension glaucoma, primary open-angle glaucoma, and anterior ischemic neuropathy In: Greve EL, Heijl A (eds) 5th international visual field symposium, pp 113–124 Dr W Junk Publ, Dordrecht, 1983

39 Phelps CD, Harry SS, Montague PR: Comparison of visual field defects in low-tension glaucomas with those in the high-tension glaucomas; letter Am J Ophthalmol 98: 823–825 (1984)

40 Quigley HA, Anderson DR: The dynamics and location of axonal transport blockade by acute intraocular pressure elevation in primate optic nerve Invest Ophthal Vis Sci 15: 606–616 (1976)

41 Quigley HA, Addicks EM: Regional differences in the structure of the lamina cribrosa and their relation to glaucomatous optic nerve damage Arch Ophthalmol 99: 137–143 (1981)

42 Quigley HA, Addicks EM, Green WR, Maumenee AE: Optic nerve damage in human glaucoma II The site of injury and susceptibility to damage Arch Ophthalmol 99: 635–649 (1981)

43 Quigley HA: The pathogenesis of optic nerve damage in glaucoma In: Symposium on the laser in ophthalmology and glaucoma update, pp 111–128 Trans Orleans Acad Ophthalmol Mosby, St Louis, 1985

44 Quigley HA: Changes in the appearance of the optic disk Surv Ophthalmol 30: 111–126 (1985)

45 Radius RL: Distribution of pressure-induced fast axonal transport abnormalities in primate optic nerve – an autoradiographic study Arch Ophthalmol 99: 1253–1257 (1981)

46 Shihab HM, Lee PF, Hay P: The significance of disc hemorrhage in open-angle glaucoma Ophthalmology 89: 211–213 (1982)

Author's address:
Privat-Dozent Eugen Gramer, M D , L L D ,
University Eye Hospital,
Josef Schneider Strasse 11, D-8700 Würzburg, F R G

V.9 The comparison of kinetic and static perimetry by means of the Arden test, the glare test, the colour vision test and PERG in patients with glaucoma and ocular hypertension

R. FUSCO, P. GUACCI, A. DI CAPUA and G. AMBROSIO
Naples, Italy

Abstract

Patients affected with glaucoma or ocular hypertension underwent kinetic and static perimetry, Arden test, glare test, Farnsworth 100 hue test, PERG. Our aim was to compare possible perimetric defects with alterations of other functional tests, in order to estimate the diagnostic value of each during the course of the disease.

Introduction

In clinical practice the diagnosis of wide angle glaucoma is defined as follows. ocular hypertension, change of the optic nerve head and the characteristic defects in the visual field. The perimetric examination is also used as a baseline measurement in order to establish the effectiveness of therapy and the evolution of the disease; but it is necessary for a 30% damage of the optic nerve fibres to be present before the smallest perimetric defect appears [17].

This fully justifies the numerous attempts of various authors to utilize other tests in order to obtain diagnosis cures as early as possible Therefore, the adaptometry test [14], the colour vision tests [6] and evaluation of nerve fibre layer atrophy [18] and VEPs [10] have been introduced in the study of glaucoma.

Moreover, in case of ocular hypertension, tests capable to demonstrate the early changes in the function of the optic nerve would indicate those who are destined to develop glaucoma in the future.

The purpose of our study is to compare the perimetric defects and changes revealed by Arden and glare tests, test for chromatic vision and PERG in glaucoma and in ocular hypertension.

Methods

The PERG was recorded using silver chloride cup electrodes. The exploring electrode was placed in the lacrimal fossa, the reference electrode in the inner canthus of the opposite eye, the ground was placed on the forehead and had a resistance of less than 2 kohms. The signals obtained were of similar amplitude to those obtained with bipalpebral postioning.

The subject was placed in front of a television screen. The stimulated eye fixed a point of reference at the centre of the screen while the other eye was prevented from seeing the structured stimulus by a screen placed 5 cm from the apex of the cornea.

The stimulated visual field was 14°, positioned at a distance of 114 cm; vertical sinusoidal wave stimuli were generated on the black and white television screen with pattern-reversal frequency of 12 5 Hz; the contrast used was 50% with mean luminance of 12 cd/m², the spatial frequency varied from 0.2 to 5 cycles/degree The signals were filtered, amplified and averaged after 300 repetitions using a Nicolet CA 1000 with an analysis of 110 msec. The amplifier was triggered so that at each reversal the signal was composed substantially of the second harmonic [1].

The perimetric and the adaptoperimetric test were carried out with the perimeter of Harms. The comparative study of the luminous sensitivity curves at different levels of retinal adaptation or adaptoperimetry was performed with static perimetry from 0 to 30 degrees of eccentricity and along the horizontal meridian from 0 to 180 degrees. Background luminance was maintained at the values recommended by Grignolo A. and Zingirian M [8].

The colour vision was examined with the desaturated test of Lanthony and with the Farnsworth 100 hue test. Using the second method a quantitative valuation of the eventual deficits present is possible.

Contrast sensitivity was studied with Arden printed contrast gratings. The test is composed of six plates numbered 2 to 7. The sinusoidal patterns of grey and white subtend 0.2, 0.4, 0.8, 1.6, 3 2 and 6.4 cycles per degree of visual angle, respectively, when viewed at 57 cm. The test was presented to the patient according to the manner described by Arden [2].

We also used a glare tester to assess the patients' sensitivity to glare. The glare test combines an autoviewer table-top projector with a series of specially made slides Each slide supplies a constant glare source and a variable contrast central target [11].

Material

We examined 32 eyes with wide angle glaucoma and visual field defects, either restricted to the Bjerrum area or represented by nasal peripheral isopter contractions. The intraocular pressures were controlled at the time of the tests. We

also examined 32 eyes affected with ocular hypertension (I O P >21 mm Hg) in which the I.O P. increased ≥6 mm Hg after a water drinking test The visual acuities were ≥20/30, the optic nerve was normal or with slight increase in the physiological excavation and the visual field was normal We also tested 32 eyes of normal controls

Ages of the subjects ranged from 30 to 60 in all groups. All subjects were free from other ophthalmological disease, including amblyopia Both sexes were present in all groups in the same percentage and all eyes examined had 2.5–3.5 mm pupils.

Results

Results of the test in the glaucomatous eyes are shown in Fig 1

In 30 eyes changes of the colour vision of tritan and tetartan types were revealed as previously described both for the Farnsworth 100 hue test as well as for the Lanthony 15 hue test In evaluating the Farnsworth test, we performed – as suggested by Drance [6] – a subdivision of the total score in 3 groups: from 0–100; from 101–200; over 201. The average total score was 174 6.

Adatoperimetry was normal in 28 eyes. The overall drop in retinal sensitivity produced an imbalance in the pattern of 1 logarithmic unit greater than the norm only in 4 eyes, and this was present only in the mesopic and the scotopic adaption

The PERG was altered in 30 eyes, showing a drop around 2 cycles/degree on varying the spatial frequency.

The glare test did not show more glare sensitivity than in normal eyes.

The result of the Arden contrast sensitivity test is obtained by summing the results of the values obtained from each table Arden has established the following norm: ≤62 normal score, 63–78 suspect, ≥79 abnormal The mean score of the glaucomatous eyes was 90 (min. 72 – max 119) Among the 32 glaucomatous eyes 22 had pathologic scores, 10 suspect. None of the examined eyes had a normal score.

The examination of the eyes affected with ocular hypertension is shown in Fig. 2.

In 28 eyes the test for chromatic vision revealed changes along the yellow-blue axis; the average total score for the Farnsworth 100 hue test was 165.4

The perimetric and the adaptoperimetric test results were normal in all eyes examined.

The PERG showed a drop around 2 cycles/degree on varying the spatial frequency,in 24 eyes. In 8 eyes the PERG had a maximum amplitude around 2 cycles/degree as in normal subjects.

The glare test showed normal results

The mean Arden score was 86 (min. 68 – max 95) Among 32 eyes examined 19 gave pathological scores, 13 suspect We also compared the scores of all eyes on
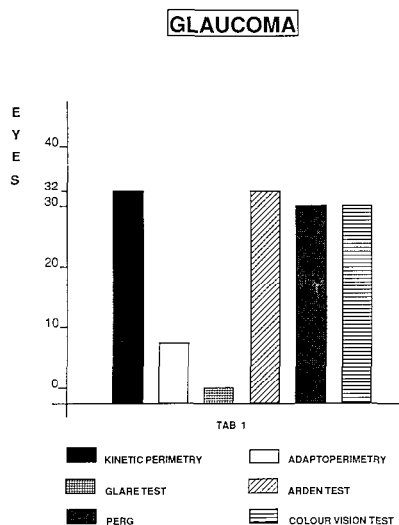
Figure 1 Number of glaucomatous eyes with abnormal test results in the different tests

plates 6 and 7 with the total scores of plates 2 to 7, but we did not obtain significant differences in specificity for glaucoma and ocular hypertension. All eyes affected scored worse than normal on plate 6 and 7 but these results were not more indicative than those from the total score of all plates.

In normal subjects the colour vision results were normal in 30 eyes and the average total score for the Farnsworth 100 hue test was 99.4; the perimetric and the adaptoperimetric results were normal. The PERG showed a maximum amplitude at 2 cycles/degree in 32 eyes. The glare test and the Arden test gave normal results in all eyes examined.

Discussion and conclusion

The purpose of our work is to emphasize differences and similarities in the results of various tests performed in the glaucoma and in the ocular hypertension. This could show which test or set of tests could be considered more suitable to identify those patients with ocular hypertension, who have a higher probability of developing functional damage and consequently require an early therapeutic treatment.

Perimetry is the most specific examination in glaucoma and it cannot now be replaced. However, the tests for chromatic function, the PERG and the Arden test gave interesting results. The Farnsworth 100 hue test and the Lanthony 15 hue test showned the same type of change in the yellow-blue axis in 30 eyes affected by glaucoma and in 24 eyes with ocular hypertension. The PERG results were

OCULAR HYPERTENSION
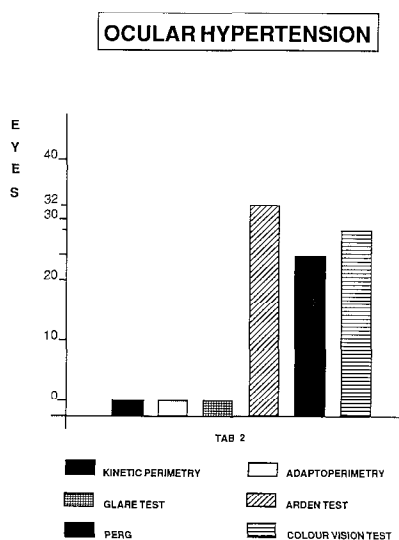
Figure 2 Abnormal results in the group of ocular hypertensives

abnormal in 30 eyes with glaucoma and in 24 eyes with ocular hypertension. The Arden test results were altered both in the 32 eyes affected with glaucoma and in the 32 eyes affected with ocular hypertension.

Some fuctions seem to change more precociously than others, probably because there may be, at least, two or more mechanisms for developing a nerve fiber bundle defect in glaucoma [6]

We emphasize that the data given are preliminary, since our research is actually still taking place with the aim of increasing the number of cases and also with the purpose of identifying those subjects among the ocular hypertensives who with time will develop manifest glaucoma.

References

1 Ambrosio G, Colasanti A: Pattern electroretinograms (PERG): an optimization of the contrast components (submitted for publication)

2 Arden GB: The importance of measuring contrast sensitivity in cases of visual disturbance Br J Ophthalmol 62: 198–209 (1978)

3 Arden GB, Jacobson JJ: A simple grating test for contrast sensitivity: Preliminary results indicate value in screening for glaucoma Invest Ophthalmol Vis Sci 17: 23–32 (1978)

4 Bobak P, Bodis-Wollner I, Harnois C, Maffei L, Mylin L, Podos S, Thornton J: PERG and VEP in glaucoma Am J Ophthalmol 96: 72–83 (1983)

5 Brusini P: Perimetria Statica Mcridiana nel Glaucoma Bollettino di Oculistica 60: 29–38 (1981)

6 Drance SM, Lakowski R, Schulzer M, Douglas G, Arch Ophthalmol 99: 829–831 (1981)

7 Fiorentini A, Maffei L, Pirchio M, Spinelli D, Porciatti V: The PERG in response to alternating gratings in patients with diseases of the peripheral visual pathway Invest Ophthalmol Vis Sci 21: 490–493 (1981)

8   Grignolo A, Zingirian M, Tagliasco V: L'esame del campo visivo: Stato attuale e prospettive Atti SOI, 1975, pp 187–193

9   Hamil TR, Post RB, Jhonson CA, Keltner JL: Correlation of colour vision deficits and observable changes in the optic disc in a population of ocular hypertensives Arch Ophthalmol 102: 1637–1639 (1984)

10 Howe JW, Mitchell KW: Simultaneous recording of pattern electroretinogram and visual evoked cortical potential in a group of patients with chronic glaucoma Doc Ophthalmol Proc Series 40: 101–107 (1984)

11 Le Claire et al: A new glare tester for clinical testing Results comparing normal subjects and variously corrected aphakic patients Arch Ophthalmol 100: 153–158 (1982)

12 Marmion VS: A comparison of contrast sensitivity function and field loss in glaucoma 6th Int Visual Field Symposium, pp 443–451 Dr W Junk Publ, Dordrecht, 1984

13 May JG, Ralston JV, Reed JL, Van Dyk JL: Loss in pattern-elicited electroretinograms in optic nerve dysfunction Am J Ophthalmol 93: 418–422 (1982)

14 Meduri R, Puddu P, Anselmi P: Comportamento del senso luminoso nel glaucoma cronico semplice Rass Ital Oftal 19: 370 (1968)

15 Papst N, Bopp M, Schwudigel OL: The pattern evoked electroretinogram associated with elevated intraocular pressure Graefe's Arch Clin Exp Ophthalmol 222: 34–37 (1984)

16 Porciatti V, Von Berger GP: Pattern electroretinogram and visual evoked potential in optic nerve disease: early diagnosis and prognosis Doc Ophthal Proc Series 40: 117–126 (1984)

17 Quigley HA: Clinical implications of anterior optic nerve and nerve fiber layer anatomy Ophthalmic Reports 6: 1–2 (1981)

18 Quigley HA, Miller NR: Clinical evaluation of nerve fiber layer atrophy as an indicator of glaucomatous optic nerve damage Arch Ophthalmol 98: 1564–1571 (1980)

19 Rabin S, Kolesar P, Podos SM, Wilensky JT: A visual field screening protocol for glaucoma Am J Ophthalmol 92: 530–535 (1981)

20 Stamper RL, Hsu Winges C, Sopher M: Arden contrast sensitivity testing in glaucoma Arch Ophthalmol 100: 947–950 (1982)

21 Wanger P, Persson HE: Pattern reversal electroretinograms in unilateral glaucoma Invest Ophthalmol Vis Sci 24: 749–753 (1983)

22 Zingirian M: L'uso razionale della perimetria nel glaucoma Atti del 7mo corso di aggiornamento APIMO, 1985, pp 89–93.

Author's address:
Rosa Fusco,
II Policlinico – Clin Oculistica 2,
Via Panzini 5, I-80131 Napoli, Italy

V.10 Glaucomatous field changes related to the method and degree of intraocular pressure control

C. MIGDAL, R.A. HITCHINGS and P. CLARK
London, United Kingdom

Abstract

Surgery produced a greater reduction in intraocular pressure than both laser and medicine. There is little difference between laser and medicine. From the graphs, it appears that the reduction in intraocular pressure shows a small general decline in all three groups from 3/12 onwards.

Surgery produced lower intraocular pressure range and peak intraocular pressure than medicine. The result for laser is somewhat between these two.

In general surgery appears to be better than medicine regarding visual fields. The laser result is somewhat in between. This result is statistically significant for 0.4 log units above threshold but not maximum intensity when compared with the readings at the initial visit.

The impression (not statistically analysed) is that there is a gradual increasing trend in the field loss of all three treatment groups over the period of observation.

Introduction

The intraocular pressure (I.O P.) level, visual field changes and alterations in the appearance of the optic disc or retinal nerve fibre layer are the three modalities most commonly used to monitor the progress or otherwise of a patient with chronic simple glaucoma. During the short-term follow-up of a patient undergoing treatment because of fluctuations in the visual fields, the efficacy of therapy is usually judged on the basis of its pressure reducing ability. Successful treatment, however, should result, not only in the lowering of intraocular pressure, but also in the prevention of further damage to the optic nerve.

Patients who, on the basis of intraocular pressure measurements in the clinic, often appear to be 'controlled', may later be shown to have continuing field loss. This may be due to inadequate pressure reduction for a specific eye, or that random intraocular pressure measurements are an unsatisfactory method of

monitoring this disease, and that the pressures are, in fact, elevated at other times of the day.

In a prospective study comparing primary laser, medical or surgical treatment for chronic simple glaucoma, the intraocular pressure measurements in the three treatment groups were compared with the diurnal pressure curves, and these results related to the visual field changes in an attempt to assess whether there was a statistically significant difference between the pressure control and field changes in the three treatment groups.

Materials and methods

168 patients with untreated chronic simple glaucoma presenting to Moorfields Eye Hospital were entered into the trial. There is a minimum follow-up so far of one year and a maximum of $3^{1}/_{2}$ years.

The inclusion criteria and principles of the three types of treatment have been previously described [6].

All patients were seen for regular follow-up and the intraocular pressures were monitored at each clinic visit. At the end of each twelve month period, the patients were admitted for a daytime phasing, when the intraocular pressures were checked at 2 hourly intervals between 9.30 a.m. and 3.30 p.m.

Visual fields were charted at the initial visit, at 3 months and thence every quarter. For the purposes of this report, the fields charted on the Friedmann Field Analyser (Mark I) will be considered. The threshold was calculated and the number of spots missed at steps of 0.4 log units greater than threshold increasing to maximum illumination noted These results were documented numerically for each eye.

Treatment was considered successful if the intraocular pressure was $\leqslant 22$ mm Hg by 3 months. In the event of failure, a second line of treatment was taken, again randomly allocated by computer selection.

Results

This report deals specifically with the successfully treated patients – i.e. those whose intraocular pressures at the clinic visits were found to be controlled at $\leqslant 22$ mm Hg.

There was no significant difference between the numbers of early middle and late stage glaucoma (judged on the degree of field loss) in each of the three groups.

The mean intraocular pressures for the three groups can be seen in Fig. 1. Although the mean pre-treatment intraocular pressures for the three groups were similar, the surgical groups consistently maintained the lowest pressures through-
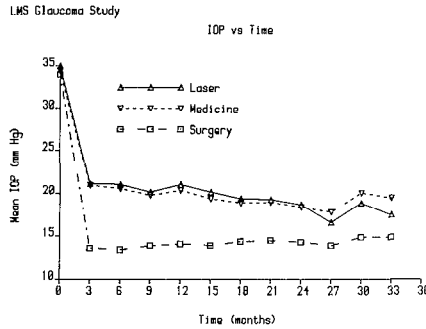
Figure 1 Mean intraocular pressure

out the period of the follow-up. There was little difference between laser and medicine. A small general decline in intraocular pressure reduction was noted in all three groups from 3/12 onwards.

Considering the day-time phasing results, it can be seen that the surgical group fared better than the other two as regards peak pressures (Fig. 2) and intraocular pressure range (Fig. 3). Regarding the latter, at one year, surgery is lowest with the laser and medicine very close to one another (p = 0.04) At year two, surgery is lower than medicine with laser in between (p = 0.0009). The results for peak intraocular pressures are similar to those for intraocular pressure range.

Friedmann fields (Mark I), when analysed numerically for changes in the *relative* defects (using the number of spots missed at intensities between 0 4 log units greater than threshold and maximum) since the initial reading (Fig. 4) showed, in general, significant differences between the treatments.

Surgery performed significantly better than medicine (showing a small decrease as opposed to a small increase) with laser somewhere in between Taking the treatments individually, medicine, at most time points, shows small (but not statistically significant) increases. Surgery shows a significant decrease (p = <0.05).
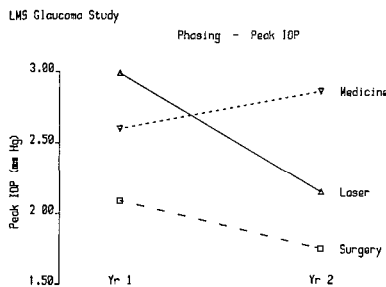
Figure 2 Phasing – peak intraocular pressure
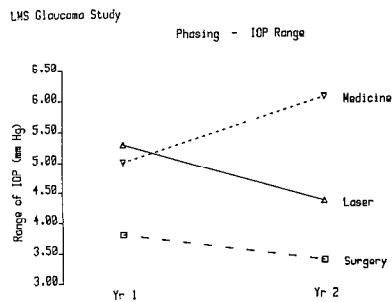
Figure 3 Phasing – intraocular pressure range
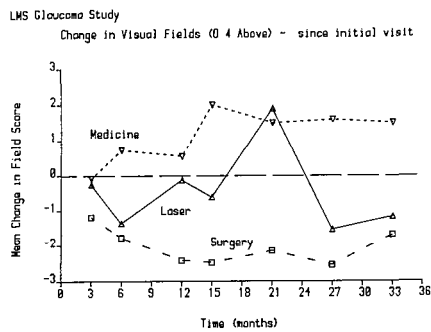
Figure 4 Visual field change – relative defects
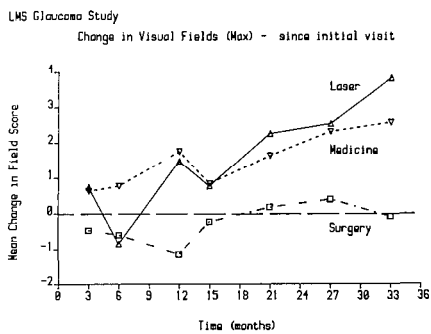
Figure 5 Visual field change – absolute defects

Considering changes in the absolute defects (intensity 0.0 log units) since the initial visit (Fig. 5), although there were no statistically significant differences between the treatments, surgery tended to be marginally lower than laser and medicine, which were very close. Taking each individual treatment, surgery, at any time point shows no real change. Laser and medicine, however, show significant increases at 27 months, implying that laser and medicine could be getting worse (p = <0.05).

Discussion

Our results suggest that, for glaucoma patients whose intraocular pressures appear to have been successfully controlled at levels of 22 mm Hg or less with either laser, medicine or surgery, there is a difference between the rate of field loss for the three groups. These findings are comparable to those of other studies [2, 3, 4]. Our figures point to the patients who had undergone primary surgery losing field slower than medicine or laser

As the composition of the three groups was very similar in terms of starting intraocular pressure, severity of disease, age, etc., there are a number of possibilities that may explain these findings·

1. The concept of 'control' of intraocular pressure based on a pressure reading in the clinic of less than 22 mm Hg may be insufficient.
2. Peak pressures >22 mm Hg which occur as shown in our patients at other times of the day may be causing this further damage. Therefore diurnal pressure curves may be necessary to identify the patient at risk of further visual loss in this way.
3. In the medically-treated group, patients may not be instilling their drops between visits as prescribed [5].
4. It is possible that the progressive field loss in the medically treated group may not be intraocular pressure related at all. Recent studies with β-blockers suggested that they may adversely effect visual function independent of intraocular pressure [1].

It should be remembered that these results are comparatively short term Continued follow-up is required to confirm these results before any definite pronouncements are made.

References

1 Drance SM, Flammer J: Some effect of antiglaucoma drugs on visual function In: Drance SM, Neufeldt AH (eds) Glaucoma Applied pharmacology in medical treatment, pp 569–576 Grune and Stratton, U S A , 1984

2 Heijl A, Bengtsson B: Visual fields after laser trabeculoplasty Acta Ophthalmol 62: 705–714 (1984)

3 Holmin C: Personal communication, 1986
4 Jay J: Earlier trabeculectomy Trans Ophthalmol Soc UK 103: 35–38 (1983)
5 Kass MA, Meltzer DW, Gordon M, Cooper D, Goldberg J: Compliance with topical pilocarpine
   Am J Ophthalmol 101: 515–523 (1986)
6 Migdal C, Hitchings R: Primary therapy for chronic simple glaucoma The role of Argon laser
   trabeculoplasty Trans Ophthalmol Soc UK 104: 62–66 (1985)

Author's address:
Clive Migdal, FRCS ,
Glaucoma Unit,
Moorfields Eye Hospital,
London, WC1V 7AN, United Kingdom

V.11 Correlation of intraocular pressure and visual field following argon laser trabeculoplasty

R.J. STARITA, R.L. FELLMAN and J.R. LYNN
Dallas, U.S.A.

Abstract

Argon laser trabeculoplasty (ALT) was performed on 85 eyes of 70 patients with uncontrolled primary open angle glaucoma (POAG). Clinically, all eyes were considered to have continued glaucomatous damage despite maximum tolerated medical therapy. Minimum requirements for study were reliable Octopus visual fields performed just prior to laser intervention and again on two separate occasions after ALT. A repeated analysis of variance was used to determine the statistical relationship between changes in the mean sensitivity (MS) of each quadrant in the visual field and laser-induced changes in the intraocular pressure (IOP). Following ALT the short-term effects on pressure and field were negligible. Between the first and second visual fields after ALT, related changes in MS and IOP were found. With moderate glaucomatous cupping, there was a negative correlation in the upper and lower nasal quadrants. With advanced glaucomatous cupping, there was a positive correlation in the upper temporal quadrant. In this select group of patients no other statistically significant correlation could be made.

Introduction

The definition of glaucoma is simple. Its etiology, mechanism of injury, and relationship to IOP are complex. This lack of understanding is not new to the physician who regularly faces this potentially blinding disease. The belief is that by lowering the IOP, visual function will stabilize thereby altering the chronic progressive course of the untreated condition. A safe level of IOP is relative and depends on individual susceptibility to injury. Adequate control is determined retrospectively by apparent stability of disc and field over time [12]. The problem is that control may be inadequate despite a reduction of IOP to a normal range. In POAG progressive visual field loss has been reported despite medical [2, 8],

surgical [18], and laser mediated reductions of IOP [5, 6, 7]. Visual field deterioration following ALT is not fully understood. It may result from increased IOP during the immediate post operative period [17], labile IOP over the first months following treatment [11, 14], or inadequate long-term IOP control [10]. Despite the lack of understanding of the mechanism by which ALT works [15], it has become a common and accepted procedure for the management of POAG since its introduction in 1979. Its ability to lower IOP in the majority of cases is well documented [11,14], yet its effect on the visual field is speculative. It seems that ALT can be used as a unique tool for studying the relationship between pressure and field since IOP may be chronically altered without changing optical aspects of the eye. The addition of computerized perimetry provides a more objective numerical representation of data which lends itself to statistical analysis [1]. The short-term effect of ALT on the glaucomatous visual field using computerized perimetry has been previously reported [3, 4, 13, 19]. Pressure reduction was not associated with reversibility of glaucomatous field defects and did not affect the rate of visual field decay. The long-term effect of ALT on computerized perimetry is confusing. Pressure reduction has been associated with stabilization [19], improvement [13, 15], and deterioration [5, 13]. It is the purpose of this study to exam the relationship between a change in the IOP and a change in the MS of the visual field following ALT using serial Octopus visual fields

Material and methods

Patients were selected retrospectively based on the following criteria:
1 ALT performed for uncontrolled POAG,
2. reliable pre-laser Octopus visual field less than one month prior to ALT,
3. post-laser Octopus visual fields using the same program and stimulus size separated by a minimum of two months,
4. pupil size and visual acuity constant between the pre-laser and first post-laser field.
Review of all 232 eyes of 168 patients undergoing ALT over a two year period (1981–1983) at Wills Eye Hospital revealed 85 eyes of 70 patients that met these criteria. For this selected group, an individual patient profile was constructed and consisted of the following: patient's age, eye treated, date and parameters of initial ALT, date and parameters of additional ALT, date and type of further glaucoma surgery, severity of glaucomatous disease, number of pre- and post-laser Octopus fields, and Octopus program number. The severity of glaucomatous disease was estimated based on the appearance of the optic nerve alone. Stage 1 (early damage) was considered cupping of less than 60%, Stage 2 (moderate disease) was 60 to 80%, Stage 3 (advanced disease) was greater than 80% and less than 99%, Stage 4 (far advanced disease) was 99% or greater. All visual fields were performed on an Octopus 201 perimeter using program 31 or 32. For each

individual test, a visual field profile was constructed and consisted of the follow-ing: pre- or post-laser field, time to ALT in weeks, MS of whole field, MS of each of the four quadrants, pupil size, stimulus size, and IOP. IOP was recorded during routine follow-up visits within one week of visual field testing IOP was recorded without knowledge of visual field result and visual fields were reviewed without knowledge of IOP result. Repeated analysis of variance was used to examine the relationship between changes in IOP between visual field examin-ations with changes in the mean sensitivity of the whole field and its quadrants over the same time period. A multiple regression analysis was applied to establish functional relations among the variables listed under patient profile and the variables being studied. For the visual field profile, the estimated linear effect of pupil size and stimulus size was adjusted for by calculating the partial correlation coefficients. This adjustment describes the correlation between the variables (change in IOP and change in MS) holding constant the covariates (pupil size and stimulus size).

Results

ALT was performed on 70 patients with progressive POAG Mean age group was 68 ± 10 years. Of the 85 eyes treated, 56% were right eyes. Initial laser treatment covered all 360° of the angle in 66%. Of the 34% whose initial laser covered only 180°, half went on to a second 180° treatment within three months Glaucoma surgery has been performed in 29% of treated eyes. The distribution of cases was as follows: 4% (3 eyes) in Stage 1, 39% (33 eyes) in Stage 2, 27% (23 eyes) in Stage 3, and 30% (26 eyes) in Stage 4. Of the 70 patients, 81% had previous Octopus visual fields experience. Program 31 was used 82% of the time. Stimulus size 3 was adequate in 74% of the fields. Stimulus size 4 was required in 14% and size 5 in 12%.

Variables from patient and field profiles were analyzed. Examination of the

Table 1 Correlation of IOP and mean sensitivity from first to second field after ALT

	Stage 2 r/r′	Stage 3 r/r′	Stage 4 r/r′
Whole field	−0 27/−0 30	+0 33/+0 40	−0 33/−0 20
Upper nasal	−0 31/−0 34*	+0 32/+0 32	+0 11/+0 12
Lower nasal	−0 34/−0 39*	+0 29/+0 30	−0 24/−0 03
Upper temporal	−0 18/−0 20	+0 44/+0 46*	−0 25/−0 16
Lower temporal	−0 13/−0 15	+0 24/+0 24	−0 36/−0 23

r = correlation coefficient
r′ = r adjusted for stimulus and pupil size
* = p less than 0 05

raw data indicated that the most meaningful relations were between changes in IOP from the first post-laser field to the second post-laser field following ALT and changes in mean sensitivity over this period has a function of stage of glaucomatous disease. The mean sensitivity of the whole field was further broken down into its constituent quadrants: upper temporal, lower temporal, upper nasal, and lower nasal. Three of the 85 eyes tested were classified as Stage 1, 33 as Stage 2, 23 as Stage 3, and 26 as Stage 4. Stage 1, representing early damage, had too few cases to analyze and will not be discussed further. The correlation coefficients and their adjusted values for change in IOP and change in MS from first post-laser to second post-laser visual field are shown in Table 1. The corresponding time in months of the visual field examinations after laser treatment are shown in Table 2 and IOP readings in Table 3. When comparing pre-laser visual field to either first post-laser or second post-laser visual field, no significant correlation could be made between changes in pressure and changes in mean sensitivity. Correlations beyond the second post-laser field could not be made because of decreasing sample size.

Discussion

The ability of ALT to lower IOP in this group was anticipated and did occur (Table 3). The question is: did the visual field change in response to this? The answer can be dependent on the statistical method chosen to demonstrate the effect, for example: Chi-square [15] versus regression analysis [5]. For this study, a regression analysis was used which is weighted toward the mean. The advantage

Table 2 Mean time in months of Octopus visual field examination following ALT

	Stage 2	Stage 3	Stage 4
1st Post-ALT	2 4 ± 1 9	3 0 ± 2 3	2 3 ± 2 2
2nd Post-ALT	8 4 ± 3 7	9 0 ± 4 5	8 0 ± 4 5
Final	21 4 ± 11 3	21 7 ± 11 3	21 6 ± 9 6

Table 3 Mean IOP at time of Octopus visual field examination

	Stage 2	Stage 3	Stage 4
Pre-ALT	22 7 ± 5 2	20 8 ± 5 5	20 6 ± 5 2
1st Post-ALT	18 8 ± 4 6	18 1 ± 5 2	15 7 ± 3 5
2nd Post-ALT	17 1 ± 5 4	16 3 ± 5 1	15 7 ± 3 3
Final	19 9 ± 5 5	17 1 ± 5 8	16 2 ± 3 4

of all IOP and threshold values being analyzed directly and repeatedly without interpretation or exclusion, outweigh the disadvantage of the diluting effects of events occuring at the extremes of what was being measured. This analysis showed a relationship between a change in IOP and a change in visual field only between first and second post-laser examinations following ALT. This relationship could only be found when the field was broken down into quadrants and the eyes into stages reflecting severity of glaucomatous disease. In eyes with moderate damage (Stage 2) a negative correlation occurred in the upper and lower nasal quadrants (Table 1, $p \leq 0.05$). A decrease in IOP was linked to an increase in mean sensitivity and increase in IOP to a decrease in mean sensitivity. In contrast to this, in eyes with advanced damage (Stage 3) a positive correlation occurred in the upper temporal quadrant (Table 1, $p \leq 0.05$). A decrease in IOP was associated with a decrease in mean sensitivity and an increase in IOP with an increase in mean sensitivity. In eyes with far-advanced damage (Stage 4) no correlation was found. In a straight forward fashion, this implies the changes in IOP which occurred from two to three months up until eight to nine months after ALT may reflect changes in the visual field. Whether these changes in IOP are associated with improvement (increased MS) or deterioration (decreased MS) seems to be dependent on the severity of glaucomatous damage. Due to the low-grade significance of the values in Table 1 caution must be exercised in interpreting these results. A key to this analysis is to remember that it is changes in pressure and field and not their absolute values that are being looked at.

No correlation could be found when pre-laser values were used. A short-term beneficial effect of ALT on the visual field could not be found. This is in agreement with other studies [3, 4, 5, 13, 19]. A long-term beneficial effect on the whole visual field considering all stages together could not be found. Again, this is in agreement with other studies [5, 9].

Although the findings of this study can be clearly stated, their meaning cannot be. It is exciting to speculate that in moderately damaged patients retinal sensitivity may improve with the lowering of IOP by ALT. It is disconcerting to imagine that lowering IOP by the same technique has no benefit in advanced disease. Further studies may be enhanced by more controls for severity of disease and by attempting more quantitative approaches to portioning the visual field. Until this is accomplished the clinical significance of the findings presented here is uncertain. It is hoped that others will be stimulated to look more closely at the relationship of a change in pressure and a change in field. Possibly, the development of better methods of quantitating the structural and functional changes in glaucoma will lead to a new definition of glaucomatous control based on improvement in visual function [12]. As of yet, that goal has not been reached.

Conclusions

1. Short-term (1–3 months) there is no detectable correlation between IOP and field
2. Long-term (4–9 months) there is a correlation between IOP and field from the first to the second examination following ALT.

   A. Negative correlation of the upper and lower nasal quadrants of the moderately damaged eyes

   B. Positive correlation noted in the upper temporal quadrant of the advanced damaged eyes.
3. Above correlations were based on changes in pressure and field. No correlation was found using absolute values.
4. Clinical significance of these findings is uncertain.

References

1 Flammer J, Drance SM, Zulauf M: Differential light threshold: Short- and long-term fluctuation in patients with glaucoma, normal controls, and patients with suspected glaucoma Arch Ophthalmol 102: 704–706 (1984)
2 Hart WM Jr, Becker B: The onset and evolution of glaucomatous visual field defects Ophthalmology 89: 268–279 (1982)
3 Heijl A, Bengtsson B: The short-term effect of laser trabeculoplasty on the glaucomatous visual field A prospective study using computerized perimetry Acta Ophthalmol 62: 705–714 (1984)
4 Holmin C, Bauer B: Computerized perimetry before and after trabeculoplasty A study of the short-term effect Doc Ophthalmol Proc Series 43: 153–156 (1985)
5 Holmin C, Krakau CET: The visual field before and after argon laser trabeculoplasty: Regression analysis based on computerized perimetry Doc Ophthalmol Proc Series 42: 371–375 (1984)
6 Hoskins HD Jr, Hetherington J Jr, Minckler DS, Lieberman MF, Schaffer RN: Complications of laser trabeculoplasty Ophthalmology 90: 796–799 (1983)
7 Lieberman MF: Laser trabeculoplasty-complications In: Wilensky JT (ed) Laser therapy in glaucoma, pp 37–42 Appleton-Century-Crofts, Norwalk, 1985
8 Mikelberg FS, Schulzer M, Drance SM, Lau W: The rate of progression of scotomas in glaucoma Am J Ophthalmol 101: 1–6 (1986)
9 Schultz J, Werner EB, Krupin T, Bishop KI: Long-term effect of argon laser trabeculoplasty on glaucomatous visual field loss (Abstract) Invest Ophthalmol Vis Sci 27 (Suppl 3): 252 (1986)
10 Schwartz AL, Love DC, Schwartz MA: Long-term follow-up of argon laser trabeculoplasty for uncontrolled open-angle glaucoma Arch Ophthalmol 103: 1482–1484 (1985)
11 Spaeth GL: Argon laser trabeculoplasty in the treatment of glaucoma In: Schwartz L, Spaeth G, Brown G (eds) Laser therapy of the anterior segment: A practical approach, pp 59–94 Slack, Thorofare, NJ, 1984
12 Spaeth GL: Control of glaucoma: new definition Ophthalmic Surg 14: 303–304 (1983)
13 Starita R, Traverso C, Spaeth G, Fellman R, Poryzees E: Short- and long-term effects of argon laser trabeculoplasty on the relationship between intraocular pressure and visual field (Abstract) Invest Ophthalmol Vis Sci 26 (Suppl 3): 41 (1985)
14 Thomas JV: Laser trabeculoplasty In: Belcher CD, Thomas JV, Simmons RJ (eds) Photocoagulation in glaucoma and anterior segment disease, pp 61–86 Williams & Wilkins, Baltimore, 1984

15 Traverso CE, Spaeth GL, Fellman RL, Starita RJ, Greenidge KC, Poryzees E: The effect of argon laser trabeculoplasty on the visual field of patients with glaucoma Doc Ophthalmol Proc Series 42: 365–369 (1984)
16 Van Buskirk EM, Pond V, Rosenquist RC, Acott TS: Argon laser trabeculoplasty: Studies of mechanism of action Ophthalmology 91: 1005–1010 (1984)
17 Weinreb RN, Ruderman J, Juster R, Zweig K: Immediate intraocular pressure response to argon laser trabeculoplasty Am J Ophthalmol 95: 279–286 (1983)
18 Werner EB, Drance SM: Progression of glaucomatous field defects despite successful filtration Can J Ophthalmol 12: 275–280 (1977)
19 Werner EB, Krupin T, Bishop KI: Visual field behavior following argon laser trabeculoplasty (Abstract) Invest Ophthalmol Vis Sci 26 (Suppl 31): 41 (1985)

Author's address:
Glaucoma Associates of Texas,
7150 Greenville Avenue #300,
Dallas, Texas 75231, U S A

V.12 Perimetric changes induced by artificial hypotension as an attempt towards determination of risk IOP in early open angle glaucoma

M. VIRNO, E.C. CAMPOS, J. PECORI-GIRALDI and G. GAROFALO
Rome and Modena, Italy

Abstract

A system of computerized video-screen perimetry has been used in order to evaluate sensitivity in the central visual field (20 degrees) of 70 eyes (52 patients) whose IOP was higher than 24 mm Hg. With this technique visual field deficits were found even in patients in which no changes were detected with the Goldmann Perimeter. After initial testing and tonometry all patients received oral glycerol (1 g/kg bw). Retesting was performed 30 and 45 minutes after administration of glycerol. In 78.57% of the eyes there was an improvement in the visual field and a concomitant IOP decrease (8 mm Hg as a mean). Timolol maleate used at least for 6 months thereafter maintained visual field improvement in all eyes. These results indicate the existence of reversible visual function changes responding to treatment.

Introduction

A satisfactory way for establishing risk intraocular pressure (IOP) has not yet been found. Differential susceptibility to the same IOP clearly exists, as far as the neuron layer of the retina is concerned. Some attempts have been made towards definition of testing procedures assessing the individual retinal sensitivity to elevated IOP [2, 3, 4].

The aim of this paper is to present evidence of an improvement of the visual field induced by artifical hypotension in some early open angle glaucoma patients and to show that this improvement could be maintained with appropriate medical therapy.

Material and methods

Fifty-two consecutive patients (70 eyes) took part in this study. Their IOP was higher than 24 mm Hg. Twentynine were females and 23 were males. The age of the patients ranged from 12 to 74 years (mean age: 43.01 ± 19 years). The best corrected visual acuity was not worse than 6/7.5. Gonioscopy revealed an open angle in all eyes tested. In all patients a routine Goldmann perimetry was performed and shown normal in 49 eyes. Early glaucomatous field changes were present in 21 eyes. The experimental protocol was the following:
1. determination of IOP with a Mackay-Marg Tonometer;
2. visual field examination with computerized video-screen perimetry;
3. oral administration of 1 g/kg bw of 50% glycerol;
4. tonometry at 15–30 and 45 minutes after glycerol administration;
5. repetition of visual field examination with computerized video-screen perimetry, when IOP was reduced by 6 to 10 mm Hg.

Subsequently, treatment with timolol maleate was started with a concentration of 0.50% twice daily. Follow-up visual field examinations and IOP measurements were performed 2–4 and 6 months thereafter.

Analysis of the visual field was carried out with a computerized video-screen perimeter [1], which detects central visual field abnormalities and blind spot enlargements within 20°. The computer (an Apple II 48K personal with standard peripherals) generates randomly a preset number of dots from a 960-point matrix subtending an angle of 45° and presents a fixation cross at the center of the screen. Each dot grows in six steps at 0.5 s intervals from a diameter of 1 to 10 mm. The surface of the dots is $2\,mm^2$ (level 1), $4\,mm^2$ (level 2), $6\,mm^2$ (level 3), $10\,mm^2$ (level 4), $38\,mm^2$ (level 5) and $80\,mm^2$ (level 6), respectively.

The patient is instructed to press a switch as soon as a spot of light is seen on the screen. Immediately after pressing the switch, the target disappears and its position and step are stored. Soon after, with a random delay from 300 to 800 ms another dot is generated and the cycle is repeated. Two hunderd dots are sufficient to complete the image. The blind spot position at the end of the examination informs on fixation compliance. Relative intensity of the background and target luminance are preset by the TV contrast control, matching the standard mesopic condition of the Goldmann perimeter (background = $1\,cd/m^2$; stimuli = $4\,cd/m^2$).

The computer program allows also special features for enhancing map display, scotoma capturing, filling functions, map quantification and makes archives routine possible.

Testing was performed with all room lighting switched off and the patient seated 50 cm in front of the TV screen at a chin-rest and looking at the fixation cross. The non-tested eye was patched and the tested eye centered with the screen. The examination takes from 5 to 8 minutes

The computer prints out the number of dots having reached the level of

perception and the percent of each level with respect to the total dot population. This allows quantification and statistical processing of the evolution of a visual field deficit.

The computer is furthermore able to calculate the total surface of the perceived dots by multiplying the number of dots perceived at each level for their dimension and summing up the relative values. The total area of perceived dots of an eye can be so obtained numerically. In normals the total area does not exceed 3,500 mm² ($\pm$ 300 mm²). If the area exceeds this value the subject is pathological In fact, larger size stimuli are necessary in order to obtain perception.

As a control visual field testing before artificial hypotension was repeated 3 times in all patients in order to check reliability of responses. A visual field change was considered significant when a decrease or an increase in the total area of perception was greater than 300 mm².

A mean and standard deviation were determined for each parameter examined and the significance of differences in IOP and perimetric data before and after glycerol administration was assessed with Student's t-test.

Results

A significant reduction in the total area of perception was found with computer-assisted perimetry when IOP was decreased by an average of 8 mm Hg after oral osmotic hypotonization in 55 out of 70 eyes tested. This means that sensitivity was increased.

Figure 1 shows the mean value of IOP (A), total area of perceived dots (B) and the number of perceived dots at the six dimension levels (C), respectively prior to and following ocular osmotic hypotonization. No significant differences were observed in three successive visual field examined before hypotonization. This confirms that visual field changes after hypotonization are due to IOP reduction and not to chance. The subsequent topical treatment with timolol maleate maintained retinal sensitivity integrity throughout the entire period considered. An example of this behaviour can be seen in Figure 2 in which visual fields prior to (A) and after (B) hypotonization and at the end of the 1st (C), 2nd (D), 4th (E) and 5th (F) month of treatment with timolol maleate are plotted.

The remaining 15 eyes of the 70 considered in this study showed no changes in the area of perception despite IOP decrease after hypotonization (Figure 3). However, for these eyes timolol maleate has been effective in preserving retinal integrity throughout the entire period considered in 8 eyes (53%).
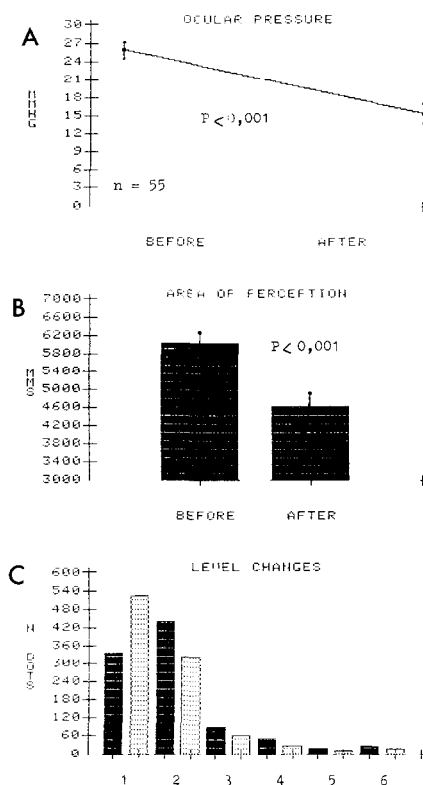
Figure 1 Mean values (55 eyes) of IOP (A), the total area of perception (B) and the number of perceived dots at the six dimension levels (C) prior to and after osmotic hypotonization Visual field improvement is evident and strongly correlated to IOP decrease Each point is a mean of 55 values and bars indicate SEM

Discussion

Oral osmotic hypotonization seems to be a reliable way for ascertaining patients with open angle glaucoma whose visual field deficits are still reversible. This can be determined before starting medical treatment and thus making prognostic judgements possible In essence, by obtaining a reduction in the area of perception and an increase in targets of lower levels (expression of higher retinal sensitivity) together with an abrupt IOP decrease, it is possible to find the individual no-risk IOP. In those patients in which an IOP decrease determined visual field improvements, retinal sensitivity stayed improved with timolol maleate treatment for as long as 6 months.

The test presented in this paper has the advantage of being simple, easy to perform for the patient and of short duration. Noteworthy is also the high number of points in the central visual field which were tested (200), uncommon for other
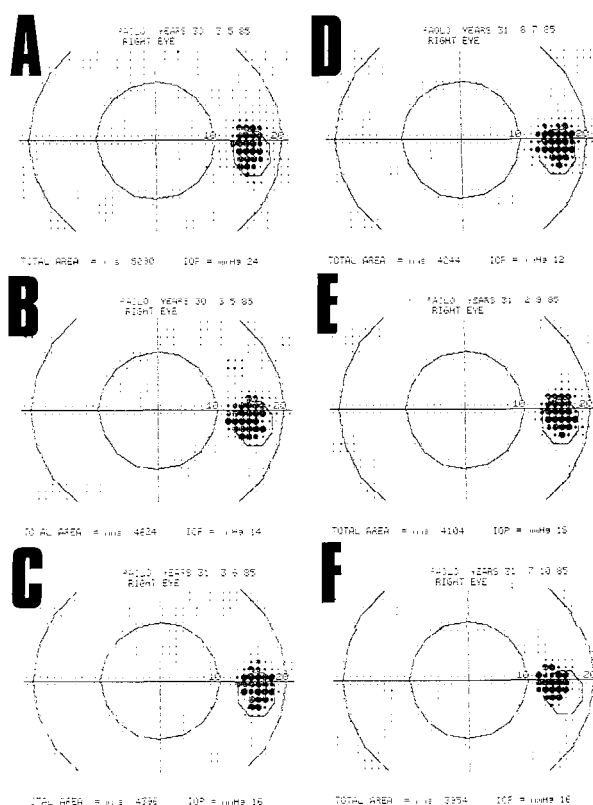
Figure 2 Visual field plots of a patient (V P , male, 34 years) before (A) and after (B) osmotic hypotonization C, D, E, F represent visual fields after 1, 2, 4, 5 months of treatment with timolol maleate respectively
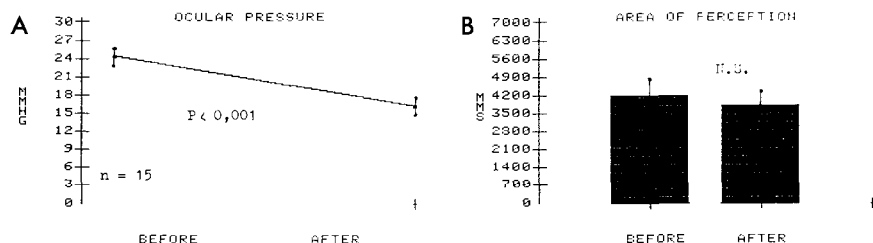
Figure 3 Mean values (15 eyes) of IOP (A) and the total area of perception (B) prior to and after osmotic hypotonization The IOP decrease is evident, whereas no significant visual field changes are present Each point is a mean of 15 values and bars indicate SEM

previously described procedures. Obviously, because of the use of a computer-controlled TV monitor for generating background and stimuli, the test could not be performed at higher luminance levels. Moreover, the target luminance/size ratio could not meet Ricco's law nor could absolute scotomas be detected. We hope to improve the system in a near future in order to match the IPS standards requirements and to be able to use stimuli of fixed size and variable luminance. In conclusion, osmotic hypotonization can inform reliably on the reversibility of visual field changes only if combined with perimetric techniques scanning precisely and accurately the central 20° of the visual field.

References

1 Accornero N, Berardelli A, Cruccu G, Manfredi M: Computerized video-screen perimetry Arch Ophthalmol 102: 40–41 (1984)
2 Pecori-Giraldi J, Ciarnella A, Taverniti L, Costantini MP, Garofalo G: Correlazione tra ipotonizzazione osmotica e riduzione dei deficit campimetrici: rilevamento della pressione di rischio Boll Ocul 64: 1013–1029 (1985)
3 Spaeth GL: The effect of change in intraocular pressure in the natural history of glaucoma Lowering intraocular pressure in glaucoma can result in improvement of visual fields Trans Ophthalmol Soc UK 104: 256–264 (1985)
4 Vodovosov AM, Martemianov F: Kampimetricheski metod izmereniia individualno perenosimovo vnutriglavnovo davleniia pri glaukome Vest Oftal 1: 3–5 (1978)

Authors' addresses:
Emilio C Campos,
Clinica Oculistica dell'Università,
Via del Pozzo 71, 4100 Modena, Italy

M Virno, J Pecori-Giraldi, G Garofalo,
Laboratory of Ocular Physio-pharmacology,
Dept of Ophthalmology,
University of Rome, Rome, Italy

V.13 The usefulness of automated perimetry in detecting early glaucoma

I. AZUMA and S. TOKUOKA
Osaka, Japan

Abstract

We evaluated the screening ability of a central screening program of the Compe-ter 350 in 60 patients (120 eyes) with ocular hypertension (OH) and 40 patients (70 eyes) with primary open angle glaucoma (POAG) in various stages of develop-ment. A control group of 40 normal subjects (80 eyes) was also taken into consideration.

Fourteen percent of eyes with OH and normal Goldmann visual field were found to be abnormal by automated static perimetry. Sensitivity and specificity was found to be 90% and 96% respectively

The frequency distribution of the glaucomatous scotomas in each group was calculated and illustrated graphically.

Introduction

The usefulness of the original Competer for glaucomatous patients is well estab-lished [7, 8]. The Competer 350 is a modified model of the original Competer [4, 10]. We used a central screening program of the Competer 350. The pattern of this program is slightly different from that of the original Competer.

The aim of this report is to compare the performance of this program with Goldmann visual fields obtained by well trained examiners. Another aim is to describe the frequency distribution of defects in normal subjects (false positives), patients with ocular hypertension (OH) and with primary open angle glaucoma (POAG).

Materials and methods

Three groups of patients were studied: 80 eyes of 40 normal subjects, 120 eyes of

60 patients with ocular hypertension and normal Goldmann visual field and 70 eyes of 40 patients with primary open angle glaucoma.

The Goldmann perimeter and the central screening program of the Competer 350 were used for all cases.

The Competer 350 is a modified model of the original Competer [4, 10]. The test points are located in concentric circles from 1° to 35°. The central srceening program on Competer 350 uses 72 test points which are located in concentric circles from 2.5° to 20°. The arrangement of the test points is slightly different from that of the original Competer. Eight points are added at 2.5° eccentricity and test points arrangement at 20° is slightly different from the original Competer

The Competer 350 was used under standard conditions. The stimulus duration was 0.5 sec The background illumination was 1 cd/m². The maximum permissible reaction time was 2.0 sec The strategy of this program has previously been described in detail [2, 3]. The following cases were excluded:
a) Cases with a disease other than glaucoma which affects the visual field.
b) Strong myopia and aphakia.
c) Modal value (most common threshold value) of less than 6 (18 dB in sensitivity).

The interpretation of the results were based on the following criteria:
a) Criteria for scotoma. Degression of 9 dB or more relative to the most common threshold value.
b) Criteria for the classification of a Competer field as either normal or abnormal:
   1. Two or more adjacent defects-positions are considered to be abnormal.
   2 One abnormal position coresponding to an abnormal Goldmann visual field is considered to be abnormal.
   3. Scotomas just temporal to the blind spot are considered to be normal.
   4. Scotomas adjacent to the blind spot are considered to be normal if the blind spot has shifted towards the scotoma in the sensitivity map of the blind spot.

The frequency distribution of scotomas according to their respective stage of development was calculated and represented by symbols. The frequency of scotomas at each point was calculated as follows:

$$\text{Frequency} = \frac{S}{N}$$

where N is number of the eyes in each groups and S is number of scotomas.

The POAG group was devided into the following two subgroups according to the presence of V-4 isopter abnormality [12]:
a) POAG with normal V-4 isopter (stage II in Kosaki's classification).
b) POAG with abnormal V-4 isopter (stage III or more in Kosaki's classification).
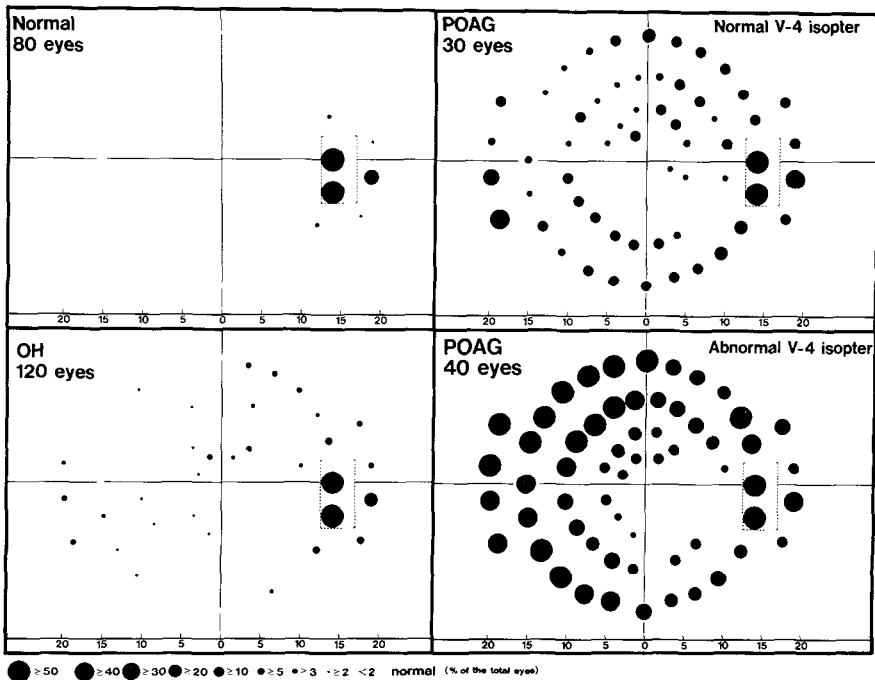
Figure 1 Frequency distribution of scotomas

Results

Age, test time, performance value (e.g. sum of sensitivity of all test points) and number of abnormal eyes of each group are summerized in Table 1. The average test time increases for the later stage of the disease. According to the development of stages. An inverse relationship was found for the Performance value.

Out of 80 normal eyes with normal Goldmann visual fields, the Competer 350 showed a false positive results in three eyes (4%). Out of 120 eyes with OH 17 eyes

Table 1 Age, test time, performance value and number of abnormal eyes in three different clinical groups

	No of subjects	No of eyes	Age	Test time (sec)	Performance value	No of abnormal eyes
Normal	40	80	42 ± 17	162 ± 17	534 ± 34	3 (4%)
OH	60	120	39 ± 15	177 ± 43	529 ± 54	17 (14%)
POAG	40	70	53 ± 14	311 ± 109	343 ± 116	63 (90%)

(14%) were found to be abnormal. These patients should be treated more carefully than the patients with normal Competer fields. Out of 70 eyes with POAG 63 eyes (90%) were found to be abnormal by the Competer 350. Therefore the sensitivity and specificity of the central screening program on Competer 350 was rated as about 90 and 96% respectively.

The frequency distribution of scotomas according to their respective stages of development were represented by symbols (Fig. 1).

Discussion

The high sensitivity and high specificity of this instrument indicate its usefulness for evaluating glaucomatous field change. The time required for examination is very short.

Several authors have reported on the frequency distribution of early glaucomatous field defects. Aulhorn and Karmeyer reported on the frequency-distribution of defects obtained with 400 eyes. They reported that the defects were most frequent in the inferior nasal and the superior paracentral field [1]. Furuno and Matsuo reported a lower frequency of defects in the inferior nasal field and much higher frequency in the superior field, especially in the area superior to blind spot [6]. Coughlan and Friedmann reported that a higher frequency of scotomas was found in the superior field and a low frequency around the fovea and in the inferior temporal quadrants [5]. Heijl and Lundqvist, using an original Competer, reported a high frequency in the superior nasal region rather than the inferior nasal region [9]. Henson reported a high frequency in the superior visual field, especially beyond 20° of eccentricity [11].

Our data from the OH group presented the earliest changes of glaucomatous defects in the absence of Goldmann visual field abnormality (Stage I in Kosaki's clasification).

Our data suggest a high frequency of scotomas adjacent to blind spot, superior-temporal region of 15° eccentricity, inferior-nasal region and superior-paracentral region in order of frequency.

A high frequency of scotomas was found in the regions adjacent to the blind spot even in normal subjects This finding indicates the existence of a high false positive rate in this region and low informational value when it comes to differentiating between a normal condition and glaucoma. Heijl recommended that a large number of missed points around the blind spot should not be taken as a sign of a glaucomatous visual field, because small defects due to angioscotomas are common in this region [9]. However, the frequency distribution of scotomas, after substracting the defects in the normal groups from the defects in the OH group, suggests that a certain number of scotomas should be considered as glaucomatous change.

Our data also suggest that scotomas are more common in the inferior-nasal

field than in the superior-nasal field, similar to the findings of Aulhorn and Karmeyer and contrary to the findings of Hiejl and Lundqvist. The high frequency of defects in the superior-paracentral region at 2 5° eccentricity suggest an improvement of the Competer 350 over the original Competer in detecting early change of glaucoma.

A higher frequency of abnormality in the OH group than in Heijl's data was found [9]. The reason may be found in different standards for selection. Heijl's patients initially had normal Competer visual fields and were shown to have abnormal Competer visual fields with several years follow up and our data was obtained from patients who had normal Goldmann visual fields and elevated IOP.

The results from POAGs with normal V-4 isopter are similar to those of OHs but the frequently of scotomas increased. The results from POAGs with abnormal V-4 isopter are also similar to that of OHs but the frequency of scotomas in the superior-nasal region is higher than in the other qaudrants. Eyes with a modal value of less than 6 were excluded so that advanced glaucoma cases are not included in this group. All eyes of this group were Stage III (middle stage) in Kosaki's clasification. A low frequency of scotomas in all groups was found in the centrocecal area and the infrior paracentral area.

References

1 Aulhorn E, Karmeyer H: Frequency distribution in early glaucomatous visual field defects Doc Ophthalmol Proc Ser 14: 75–83 (1977)
2 Bengtsson B, Krakau CET: Automatic perimetry in secondary prevention of glacoma A preliminary report (Nara symposium 1978) In: Glaucoma update Springei Verlag, Berlin, 1979
3 Bengtsson B, Krakau CET: Automatic perimetry in a population survey Act ophthalmologica 57: 929–937 (1979)
4 Bynke H, Krakau CET: A modified computerized perimeter and its use in neuro-ophthalmic patients Neuro-ophthalmol 2: 105–115 (1981)
5 Coughlan M, Friedmann AI: The frequency distribution of early visual field defect in glaucoma Doc Ophthalmol Proc Ser 26: 345–349 (1981)
6 Furuno F, Matsuo H: Early stage progression in glaucomatous visual field changes Doc Ophthalmol Proc Ser 19: 247–253 (1979)
7 Heijl A, Drance SM, Douglas GR: Automatic perimetiy (Competer) Ability to detect early glaucomatous visual field defects Arch Ophthalmol 98: 1560–1563 (1980)
8 Heijl A, Drance SM: A clinical comparison of three computerized automatic perimeters in the detection of glaucomatous defects Arch Ophthalmol 99: 832–836 (1981)
9 Heijl A, Lundqvist L: The frequency distribution of earliest glaucomatous visual field defects documented by automatic perimetry Acta Ophthalmol 62: 658–664 (1984)
10 Heijl A: The competer In: Drance SM, Anderson DR (eds) Automatic perimeter in glaucoma A practical guide Grune and Stratton, London, 1985
11 Henson DB: Frequency distribution of early glaucomatous visual field defects Am J Optom Physiol Optics 63: 455–461 (1986)
12 Kosaki H, Inoue Y: A new classification of chronic glaucomas Acta Soc Ophthalmol Jpn 76: 1258–1267 (1972)

Author's address:
Ikuo Azuma, M D ,
Department of Ophthalmology,
Osaka Medical College,
Daigaku-cho 2-7, Takatsuki, Osaka 569, Japan

V.14 Do ocular vasospasms help cause low tension glaucoma?

J. FLAMMER, U. GUTHAUSER and F. MAHLER
Berne, Switzerland

Abstract

Ocular vasospasms cause visual field damage which can be aggravated or pro-
voked by cooling one hand in cold water and which often improves with Nifedi-
pine treatment. Ocular vasospasms are very often combined with digital vas-
ospams, as can be diagnosed with a nailfold capillaroscopic local cooling test
Sixteen patients were identified in our department of ophthalmology as having
such a vasospastic syndrome. The visual field defects were very similar to the ones
that occur in glaucoma. The optic nerve heads looked entirely normal in some
patients; but were, however, pale in some other patients. At least six patients had
clearly glaucomatous cupped optic nerve heads. This indicates that the vasospasm
may be an important factor in the genesis of low tension glaucoma.

In 1983 we examined a forty year old lady suffering from low tension glaucoma
with progressive visual field loss According to her history and to her internist,
she was in excellent general health and working as a teacher in a high school. She
once mentioned that she often had cold hands, even in summer. She did not pay
particular attention to this. We referred the lady to an angiologist (F.M.) who
documented by means of a nailfold capillaroscopic cooling test the presence of a
Raynaud's phenomenon [6] without an underlying disease We speculated that
her low tension glaucoma might be related to this Raynaud's phenomenon. After
this, we systematically asked all patients with unexplained visual field defects
whether they often had cold hands or any other symptoms indicating a vasospastic
tendency. Within a few months twenty-five suspicious cases were referred to the
angiologist. Sixteen patients with the combination of marked visual field loss and
primary Raynaud's phenomenon could be identified. Patients with increased IOP
or any other ocular diseases were excluded from this group.
   In thirteen of these patients the capillary blood flow stoppage period provoked
by cooling could be shortened by the application of Nifedipine, a calcium entry

blocker, 10–20 mg per os 30 min prior to subsequent test.

In twelve of the sixteen patients, the visual fields were worse after one hand had been immersed in cold water (4° C) for 15 minutes and fifteen patients improved 30 minutes after treatment with Nifedipine per os [5].

This led us to the assumption that the tendency for vasospastic reaction might occur not only in the hands (Raynaud's phenomenon), or in the coronaries (variant angina), but also in the eyes [3, 4]. The visual field defects of these patients were not homonymous, indicating a pre-chiasmal location of the suspected vasospasm. The retinal artery did not change in a way that could be detected by biomicroscopy even in cases with large absolute scotomas. Furthermore the retinal arteries did not change with provocation or by treatment with Nifedipine. This led us to the assumption that the location of the vasospasm is most probably in the choroid. It is known that the choroid has a sympathetic innervation [1] which is similar to the one of the peripheral vessels.

In this study we investigated whether the ocular damage caused by vasospasm could be classified as low tension glaucoma. For this purpose we re-examined our sixteen patients with vasospastic syndrome with respect to the type of visual field defects and optic nerve head damage.

The visual fields were indeed very similar to those found in chronic open angle glaucoma. We observed the following types of defects: diffuse damage, nerve fiber bundle defects including nasal steps, and small paracentral scotomas [2]. The optic nerve head, however, ranged from entirely normal looking discs to pale discs without cupping to typical glaucomatous, excavated discs. The young patients tended to have normal or pale discs, whereas most of the older patients had cupping of the optic disc that allowed the unequivocal diagnosis of a low tension glaucoma.

In summary the following conclusions may be drawn: at least a part of the patients with Raynaud's phenomenon has vasospastic disorders of the eye. The vasospasm of the eye causes (partially reversible) visual field damage that resembles visual field changes in chronic glaucoma. The optic nerve head can be either normal, pale or excavated. Thus it appears reasonable to assume that functional vasospasms play an important role in the genesis of low tension glaucoma.

Acknowledgement

References

1 Ehinger B: Adrenergic nerves to the eye and to related structures in men and the cynomolgus monkey Invest Ophthalmol Vis Sci 5: 42–52 (1966)

2 Flammer J, Drance SM, Augustiny L, Funkhouser A: Quantification of glaucomatous visual field defects with automated perimetry Invest Ophthalmol Vis Sci 26: 176–181 (1985)
3 Gasser P, Flammer J: Influence of vasospasm on visual function Docum Ophthalmol (in press)
4 Gasser F, Flammer J, Guthauser U et al: Bedeutung des vasospastischen Syndroms in der Augenheilkunde Klin Mbl Augenheilk 188: 393–399 (1986)
5 Guthauser U, Flammer J, Mahler F: The relationship between digital and ocular vasospasm (in preparation)
6 Mahler F, Saner H, Boss C, Annaheim M: Local cold exposure test for capillaroscopic examination of patients with Raynaud's syndrome Microvasc Res (in press)

Author's address:
Prof Dr J. Flammer,
Dept of Ophthalmology,
University Eye Clinic,
CH-3010 Berne, Switzerland

V.15 On the provocation of visual field defects in glaucoma cases

C. HOLMIN, A. AITTALA and C.E.T. KRAKAU
Lund and Malmö, Sweden

Abstract

A group of glaucoma cases were subjected to repeated test sessions with computerized perimetry. The stimulus exposure time was either 0 5 sec or 0.25 sec An effect of the stimulus exp time on the outcome of the visual field was found in all cases. When the shorter exp time was used the Performance value was lower due to
1. reduction of the general sensitivity
2. enlargement and deepening of defects and
3. appearance of new defects.

Introduction

Tiredness or inattention are no doubt of great importance for the outcome of visual field testing, an effect which is less marked in normal fields than in fields with relative scotomas [2]. As a consequence one will understand that more accurate threshold values in defect areas are not obtained by testing of much prolonged duration, since a steady state of the threshold values in any reasonable sense is not obtained. It was further demonstrated that the exposure time at automatic perimetry might be of great importance to the decay and fluctuation of threshold level during a long test session (30 min).

A more far-reaching study of the factors which influence the thresholds in areas of defect is not only of pathophysiological interest It seems likely that knowledge can be obtained which is clinically useful in revealing field defects at an earlier stage than is possible in routine perimetry. Long session investigations are, however, much too time-consuming in clinical work The aim of the present work is to demonstrate examples of how field defects can be provoked or enlarged by changing a relevant parameter other than duration of the test session

Material and methods

From a glaucoma care unit 7 patients (7 eyes) with glaucomatous changes of the visual fields (6 eyes) or/and other signs of glaucoma (Table 1) were selected for repeated test sessions with computerized perimetry (Competer).

All patients were previously well acquainted with this type of perimetry. The threshold programme which requires about 10 min per session was used. The thresholds at 64 points inside 20 degrees are estimated [3]. Background illumination was put at $0.1 \, cd/m^2$. The maximal reaction time was 2 sec. The exposure time for the test light at the trials is optionally preselected. In routine examinations 0.5 sec has been found convenient. In the present study also 0.25 sec was used. As a measure of performance the sum of the sensitivity values from the 64 test points was used in denoted P.

Two 'seances' were carried through, usually on different days. In both of them there were two test sessions with a few minutes' interval. The stimulus exposure time was varied as follows: in 4 patients 0.25 sec was used in the first, and 0.5 sec in the second test session and vice versa. In the remaining three patients one of the seances was made using 0.5 sec in both sessions and one was made with one session of 0.25 sec exposure time, the other with 0.5 sec.

Table 1 L = 0 5 sec exp time, S = 0 25 sec exp time PL = P value when using 0 5 sec exp time $\triangle$P = PS-PL LS = 1st session L, 2nd session S, analogously for SL and LL % = change of PL

	Age		GVFD	DISC	PL		$\triangle$P	%
IS	73	S	+		626	LS	− 87	14
					588	SL	− 89	15
EW	73	D	+		466	LS	−159	34
					455	SL	−125	28
AH	72	D	+		438	LS	−150	34
					417	SL	−122	29
GG	74	S	+		437	LS	−160	37
					297	SL	− 67	23
AL	78	S	−		583	LS	− 72	12
					569	LL	+ 12	2
EN	81	D	+		512	LS	− 99	19
					541	LL	+ 1	0
ALW	69	S	+		394	SL	− 99	25
					370	LL	+ 20	6

SYMBOL CODE

saucerization

narrow rim

incomplete notch

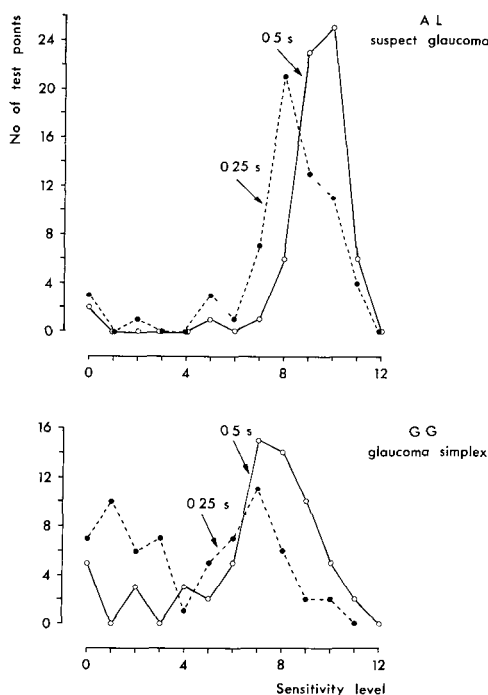excavation reaching the disc margin

haemorrhage

Figure 1 Histograms giving the number of test points (ordinate) versus sensitivity level (abscissa)

Results

In all cases the *Performance* value was lower when the shorter (0.25) than when the longer exposure time was used (Table 1). This difference varied between 12 to 37% and the smallest differences were found in eyes with high performance values (i.e. those with none or small defects). In three (of four) cases the P difference was somewhat larger when 0.25 sec was used in the second session than when it was used in the first. However, when 0.5 sec exposure time was used in the two consecutive test sessions there was no reduction of the performance value (Table 1).

The histogram (Fig. 1, top) for the number of tested points falling on the various sensitivity levels shows that a *general decrease in sensitivity* at shorter exposure time by a dislocation of the peak of (most common) threshold values to the left has taken place. Besides this general depression the defects usually became larger and deeper and *new defects* appeared in places where the papillary examination indicated suspect areas (Figs 2 and 3). In five of the tested eyes disc haemorrhages (hh) were previously observed. In one of these, defects in the corresponding half of the visual field were seen only when 0.25 sec exposure time was used. In the remaining four eyes defects – though smaller – were observed
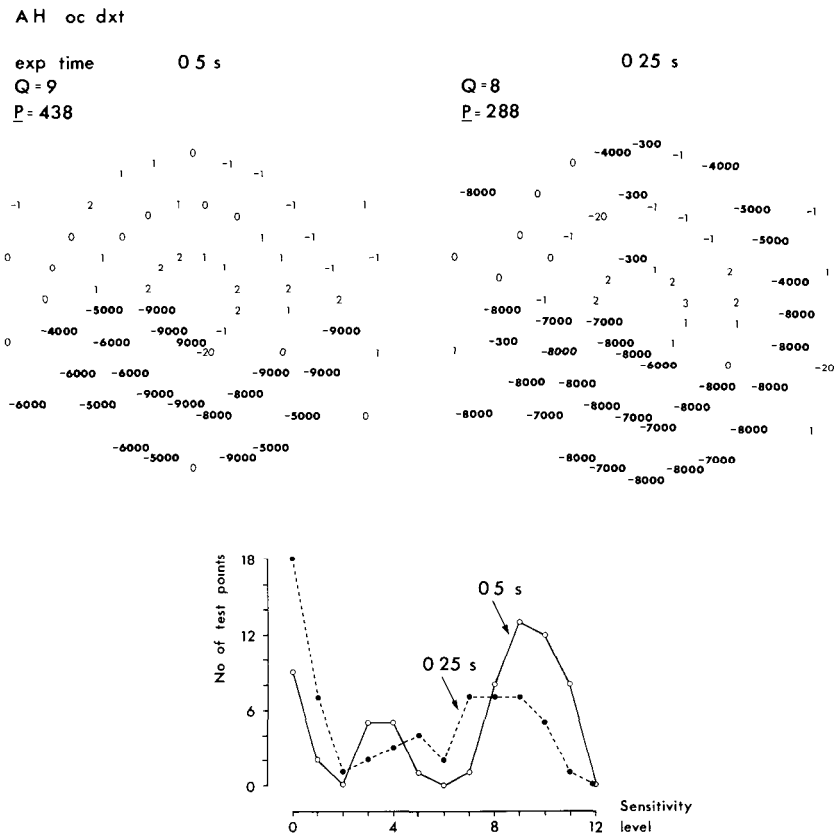
A H   oc dxt

exp time   0 5 s   0 25 s
Q = 9   Q = 8
P = 438   P = 288

```
                0                              -300
         1    1    -1   -1                -4000      -1
 -1    2    1  0    0    -1    1      0              -4000
         0        0                        -300
    0    0         1   -1        -8000   0      -1      -5000   -1
 0    1    2  2  1    1    -1   -1              -20
    0         2         1    -1   -1     0    -1         -1   -5000
    0    1    2    2    2    2            0    0    -300
 0                                       0    -1    2    1      2       1
        -5000 -9000  2   1   2                                  2    -4000
   -4000      -9000   -1    -9000  -8000     -1   2         3    2
 0  -6000  9000     0             -7000  -7000           1    1   -8000
         -20                             -300   -8000  -8000   1
   -6000 -6000     -9000 -9000  1        -8000            -6000      -8000
      -9000  -8000                  -8000  -8000                    0      -20
 -6000  -5000  -9000                               -8000  -8000
         -6000         -5000    0  -8000  -7000   -8000 -7000
   -5000  0   -9000                            -7000      -8000   1
                                         -8000      -7000
                                            -7000  -8000  -8000
                                               -8000
```


Figure 2 A new defec appears in the upper half when testing with 0 25 sec exposure time The defect is also revealed in the histogram

even with the longer exposure time The histogram (Fig. 1, bottom) illustrates the appearance of new defect points in the displacement to very low sensitivity levels apart from the moderate general sensitivity decrease.

Discussion

Defect areas correspond to a rarification of normally functioning neuronal elements. It is obvious that a malfunction is to a certain extent hidden by some spare capacity, which makes it possible to compensate deficient performance by a longer exposure time. At these early stages of incapacity a morphological correlate may be hard to detect. On the other hand a discrepancy is sometimes found between the pathological appearance of the optic nerve head and the outcome of visual field testing. To the trained ophthalmologist the disc may appear truly
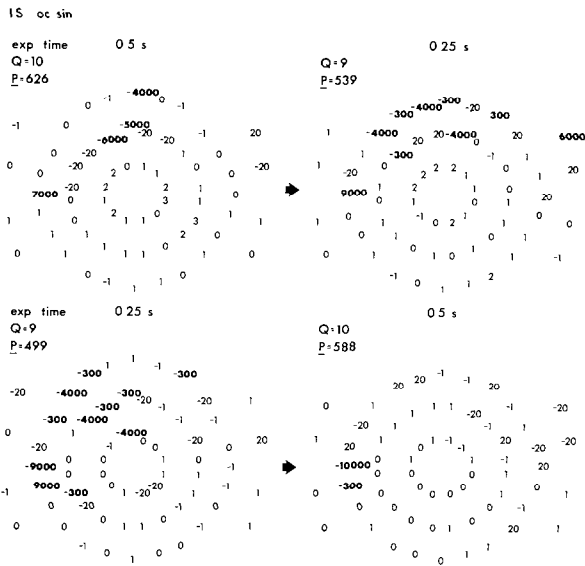
Figure 3 0 5 sec exp time: no or small defect 0 25 sec exp time: new or larger defect

pathological with signs of tissue destruction, whereas the routine automatic perimetry test may be practically normal

The use of the short exposure time obviously may reveal this relative incapacity, whereas tiredness plays a minor role, since the relation between the performances when 0.5 or when 0.25 sec session is tested first changes but slightly.

For routine investigation we cannot at present tell how long exposure time should be preferred. Short exposures may be highly sensitive in detecting defects but perhaps also give more unstable results.

We find it highly interesting that defects areas, which might correspond to previously observed disc haemorrhages, were provoked by using a short exposure time. As we have noted [1] the early hh appear without functional disturbances but indicate the spots where defects may develop, a process which may require several years. We have now an indication that defects can be made visible at an earlier stage using provocation as described. The role of hh as specific precursors, intimately connected with the glaucoma disease, thus becomes even more probable.

According to Bunsen-Roscoe's law the product of exposure time (t) and light intensity for a stimulus to be percieved is constant if t is ≤ 0.1 sec. The quantity of light integrated inside this period determines the threshold sensitivity. Longer exposure times should improve the threshold level but slightly. No great influence on the threshold level or the P values should be expected if the exposure time is

changed from 0.5 to 0.25 sec in normals. However the P reduction noted among the glaucomas is not limited to this group, but may also be found among normals. Work is in progress on the importance of age and other factors.

Acknowledgement

References

1 Bengtsson B, Holmin C, Krakau CET: Disc haemorrhage and glaucoma Acta Ophthalmol (Copenh) 59: 1–14 (1981)
2 Holmin C, Krakau CET: Variability of glaucomatous visual field defects in computerized perimetry Albrecht v Graefes Arch Klin Exp Ophthalmol 210: 235–250 (1979)
3 Holmin C, Krakau CET: Regression analysis of the central visual field in chronic glaucoma cases A follow-up study using automatic perimetry Acta Ophthalmol 60: 267–274 (1982)

Author's address:
Prof C E T Krakau,
Department of Experimental Ophthalmology,
S-214 01 Malmö, Sweden

V.16 Glaucoma follow-up by means of central differential threshold measurements

M. ROLANDO, G. CORALLO, E. GANDOLFO and M. ZINGIRIAN
Genova, Italy

Abstract

By mean of the Perikon and Peritest Computerized Perimeters, Central (10°) Differential Threshold (CDT) and Global Differential Threshold (GDT) variations at different IOPs have been studied, to evaluate the sensitivity of the macular area to IOP changes in glaucoma.

A statistically significant difference (p<0.01) of the mean sensitivity of 21 points in the 10° area was found by measuring the CDT of the same eye at differential IOP values.

Linear regression showed a statistically significant (p<0.01) correlation between CDT changes and IOP variations.

The macular area because of its anatomic and physiologic properties could be used as a highly sensitive area for the detection of subtle light threshold variations in glaucoma.

Introduction

The direct and indirect effect of intraocular pressure (IOP) on optic nerve fibers has been identified as the main cause of visual field damage in glaucoma.

A diffuse threshold increase has been described ad the first sign of glaucomatous damage [1]. More recently, some macular functions as color discrimination and contrast sensitivity, thought to be related to a diffuse neural fiber loss, have been reported to be impaired early in this disease [2, 7].

Because of the high sensitivity of the area, the study of the central differential threshold could provide a quick method to detect early glaucomatous damage.

This paper deals with the relations occurring between IOP and central differential threshold.

Material and methods

Twenty-four subjects aged 18 to 64 classified as glaucoma patients at the Glaucoma Service of the Department of Ophthalmology of the University of Genoa have been considered.

Criteria for the inclusion in the study were:
- visual acuity higher than 20/30,
- characteristic visual field defects at initial stage not involving the central area,
- no other ocular pathology,
- no known metabolic or systemic disease.

For each eye a 'Global' Differential Threshold GT (GDT) at the Peritest perimeter and a 'Central' (10°) Differential Threshold (CDT) at the Perikon perimeter were studied at different intraocular pressures.

While for the GDT the existing threshold program of the Peritest was used, for CDT a specially designed program able to study the threshold of 21 points inside 10° was implemented on the Perikon perimeter.

The program specifications for the CDT determination were:
- target size: $1/4$ mm^2;
- five threshold determinations at each point, the first two were discarded, the average value of the remaining was taken into consideration;
- points explored: fixation and 2°, 4°, 6°, 8°, 10° in emimeridians 0°, 90°, 180° and 270°.

The mean sensitivity of the area was then calculated.

Each eye was tested for the first time one week after cessation of any antiglaucoma therapy and was then closely followed without any therapy. When a significant change in IOP was detected, the eye was immediately retested for the second time. This happened in 27 eyes of 24 subjects. This procedure was designed to avoid the influence of antiglaucoma therapy on differential threshold [4]

No significant variation of IOP was detected in the fellow eye of 21 subjects at the time of the second differential threshold determination. The values of GDT and CDT of these eyes were used as controls.

The correlation between the IOP changes and the variation of GDT and CDT were then studied and evaluated statistically by mean of regression curves.

Results

IOP changes between the two examinations ranged between 2 and 11 mm Hg (4.85 ± 2.8 SD).

Considering as separate groups the CDT recorded at the higher level of IOP (25.67 ± 10.67) and the CDT recorded at the lower IOP (17.56 ± 8.25) the difference was statistically significant (p<0.01, Fisher 't' test).

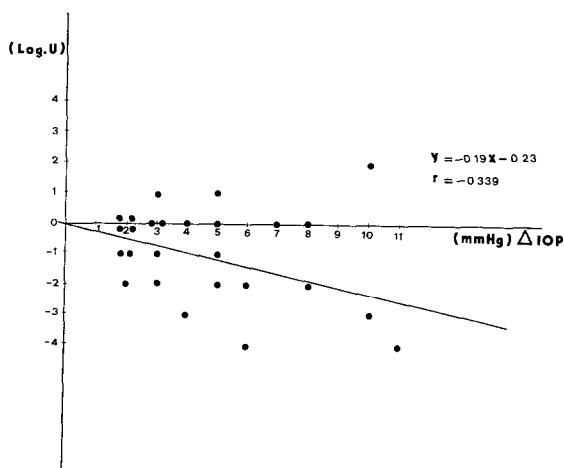*Figure 1* Results Linear regression showing the correlation between IOP changes (△IOP) and Global Differential Threshold (GDT)

There was no statistically significant difference of the GDT between the same groups.

There was also no statistically significant difference between GDT and CDT recorded at the time of the two determinations in the control eyes.

Linear regression analysis showed a low statistically significant correlation between IOP changes and GDT (p<0.02) while a highly significant correlation was found between IOP changes and CDT inside 10° (0.01< p <0 001)

Figures 1 and 2 show the details of our results and their correlations.

Discussion

Our results suggest that in glaucoma even small IOP variations can induce immediate variations of differential threshold and that IOP variation and Central Differential Threshold are correlated in a statistically significant way.

This seems to corroborate the data by Werner and coworkers [8] who found a significantly increased scatter of threshold values at 5° of eccentricity in ocular hypertensives if compared to normal control eyes. On the other hand these authors were not able to find any significant difference from normals in the mean sensitivity of the central visual field in the same group of eyes.

Even if the long term fluctuation can justify some of the threshold variations we have found [4], the consistency and the statistic significance of the correlation between IOP changes and CDT variations seems to lessen the influence of fluctuation in the interpretation of our results.

All the eyes included in our study showed initial visual fields defects which
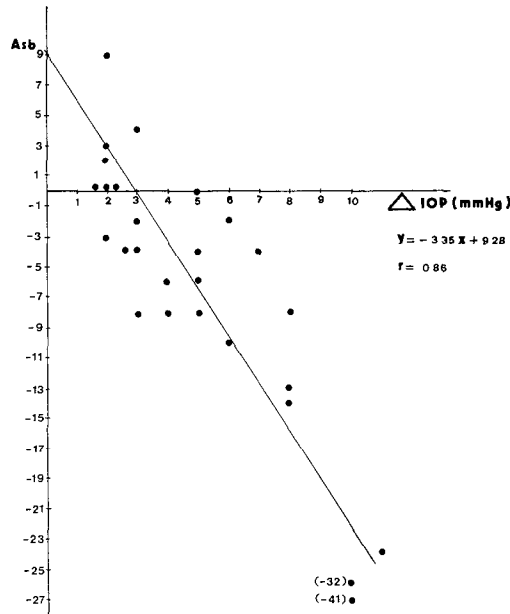
Figure 2 Results Linear regression showing the correlation between IOP changes ($\triangle$IOP) and Central Differential Threshold (CDT) The correlation is statistically highly significant (0 01< p<0 001)

suggest that a quite large number of optic nerve fibres had already been lost [6]. Such a diffuse damage, because of the loss of redundance, could have made the remaining fibers particularly sensitive to any IOP damage.

Furthermore the macular area shows some anatomic and physiologic properties such as the great sensitivity and small receptive fields which can make it more sensitive than other areas for the detection of subtle differences.

As the macular involvement in glaucoma is thought to be the expression of diffuse damage, this could suggest that a diffuse fibre loss often comes together with a fibre bundle defect.

Complete procedures of static threshold perimetry are time-consuming, can induce visual fatigue [5] and cannot be easily repeated at close intervals in a busy clinic. By means of the Perikon Computerized Perimeter 21 points in the 10° area can be analyzed in less than 7 min allowing a rapid detection of the effect of the IOP change on the nerve fibre function.

Further studies are warranted to define the reliability and the limits of this technique to assess the safe IOP level for each eye.

References

1 Drance SM: The early structural and functional disturbances of chronic open angle glaucoma Ophthalmology 92: 853–857 (1985)
2 Drance SM, Lakowski R, Schulzer M et al: Acquired colour vision changes in glaucoma: use of 100 Hue test and Pickford anomaloscope as predictors of glaucomatous field change Arch Ophthalmol 99: 829–831 (1981)
3 Flammer J, Drance SM: The effect of a number of glaucoma medications on the differential light threshold Doc Ophthalmol Proc Series 35: 145–148 (1983)
4 Flammer J, Drance SM, Zulauf M: Differential light threshold Short- and long-term fluctuation in patients with glaucoma, normal controls and patients with suspected glaucoma Arch Ophthalmol 102: 704–706 (1984)
5 Heijl A, Drance SM: Change in differential threshold in patients with glaucoma during prolonged perimetry Br J Ophthalmol 76: 512–516 (1983)
6. Quigley HA, Addiks EA, Green WR: Optic nerve damage in human glaucoma III-Quantitative correlation of nerve fiber loss and visual field defect in glaucoma, ischemic neuropathy, papilledema, and toxic neuropathy Arch Ophthalmol 100: 135–146 (1982)
7 Ross JE: Clinical detection of abnormalities in central vision in chronic simple glaucoma using contrast sensitivity Int Ophthalmol 8: 167–177 (1985)
8 Werner EB, Saheb M, Thomas D: Variability of static visual threshold responses in patients with elevated IOPs Arch Ophthalmol 100: 1627–1631 (1982)

Author's address:
Glaucoma Service,
University Eye Clinic,
Viale Benedetto XV,5,
16132 – Genova, Italy

Section VI
New psycho-physical tests

VI.1 Multi-flash campimetry: the rapid assessment of temporal resolving power

E.M. BRUSSELL, M. DIXON, J. FAUBERT and A.G. BALAZSI
*Montreal, Canada*

Abstract

Multi-flash campimetry is a technique in which temporal resolving power in 120 points of the visual field can be measured in about a half hour. It entails assessing the duty cycle (i.e., the proportion of a cycle that is lit) required to detect 5 Hz flicker. Two- and three-dimensional visual field plots can be created from the data that allow an easy identification of impaired regions. A comparison of multi-flash data and those from a temporal sensitivity experiment suggests that the amplitude of the fundamental Fourier frequency mediates flicker detection in both tasks and may provide a link between different tests that measure temporal aspects of vision. An example of how the amplitude of the fundamental can be used as the basis for quantitatively describing multi-flash data is given.

Introduction

Multi-flash campimetry [2, 19] is a computer implemented, psychophysical technique that uses flicker detection capability to obtain information about visual fields. In a typical test administration, the temporal resolving power in 120 points per eye can be assessed in about a half hour. Since temporal resolving power correlates with sensitivity to light per se, multi-flash campimetry can also be used to detect conventional field loss. The technique has been shown to be sensitive to a variety of pathologies including glaucoma [1, 7], multiple sclerosis [2, 13, 19], macular degeneration [14], and optic neuritis with no other evidence of demyelination [14], among others.

As illustrated in Figure 1, the flat display consists of 6 concentric circles, with each circle containing 20 points. Each point in the display is 6' in diameter. The radius of the innermost circle subtends 0.625°, with each succesive radius doubling in size such that the largest subtends 20°, enabling this standard display to probe a 40° visual field. During a set of trials, the computer randomly selects one
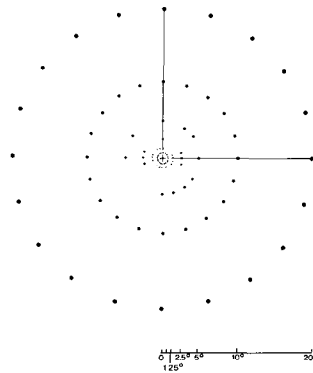
Figure 1 The full display used in multi-flash campimetry, with one quadrant being presented at any given time All points are 6' in diameter, but are shown to be different sizes for the sake of clarity

of four quadrants to be presented, and then tests 30 of the 36 points in this quadrant. The test entails flickering a point at 5 Hz, and systematically decreasing the duty cycle (i.e., the proportion of a flicker cycle that is lit) from 100% in steps of no more than 2%. An observer, who maintains fixation on a cross, is asked to press a response key whenever flicker is detected. The computer stores the duty cycles necessary to detect flicker in all points, and calculates which points are statistically deviant with respect to data from a given circle, or the entire visual field. Points reflecting aberrant data are retested, and the original data is either replaced by the replicated value, averaged with this value, or retained depending upon whether certain predetermined criteria are met.

Once all testing is completed two and/or three dimensional visual field plots can be created. Values for the fields are calculated from the data using an interpolation algorithm that includes inverse weighting by distance. For each plot, eccentricity is expressed on an octave scale which tends to exaggerate the size of the central visual field, corresponding to its functional importance and representation in the visual cortex. The two-dimensional (2D) fields are comprised of severn shades of grey that are equally spaced on a log luminance scale, with darker shades reflecting poorer performance. Data are not categorized in the three-dimensional (3D) fields, thus allowing them to show continuous changes in temporal resolving power; higher mountains reflect poorer performance. (See Figure 5 for examples.)

The importance of assessing temporal sensitivity or resolving power has been reinforced by research findings indicating that temporal loss may precede any attenuation of light sensitivity per se, in pathologies such as multiple sclerosis [10, 17] and glaucoma [1, 7, 15, 18]. However, different methods for assessing temporal sensitivity or resolving power (e.g., multi-flash campimetry, critical fusion frequencies (CFF), double-flash thresholds) are associated with unique ways of expressing the results and do not allow easy, direct comparisons among them.
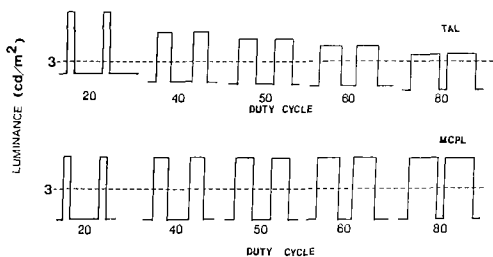
Figure 2 Timing diagrams for the flicker stimuli used in the experiment In the upper half of the figure the time-average luminance (TAL) is held constant, and in the lower half, the pulse luminance (MCPL) is held constant

One possible way of relating data from a variety of temporal tests can be derived from the analysis of temporal waveforms into their sinusoidal harmonic components using Fourier's theorem [5, 11]. The component with the lowest frequency is referred to as the fundamental and has been implicated as the basis of flicker detection in the CFF paradigm (i.e., assessing the highest flicker frequency that can be resolved) regardless of duty cycle [11, 16]. In order to evaluate how well the amplitude of the fundamental can predict temporal sensitivity in general, and multi-flash campimetry data in particular, the following experiment was conducted.

Methods

All displays were generated on an Hewlett Packard 1310A CRT, equipped with a P15 phosphor, that was interfaced through digital-to-analog converters with a PDP11/10 computer (Digital Equipment Corportation). Each display consisted of a fixation cross and a line of six points (6' diameter) that were spaced at retinal eccentricities of 0.625°, 1.25°, 2.5°, 5.0°, 10.0° and 20° relative to the fixation cross. This line of points could be positioned in one of eight orientations: along the vertical, horizontal, or one of the principal oblique axes. As is illustrated in Figure 2, 5 Hz flicker could be presented so that a constant pulse luminance (MCPL) is maintained across all duty cycles. In the MCPL case the *unweighted* average luminance level equaled the steady state luminance of the point (3 cd/m² or 9 asb). Alternatively, the waveform could be manipulated so as to maintain a constant time-average luminance (TAL) across all duty cycles affording a *weighted* average luminance of 3 cd/m² or 9 asb.

A block of trials consisted of measuring depth of modulation thresholds (i.e., the minimum modulation needed to detect flicker) for 7 duty cycles (20, 30, 40, 50, 60, 70, 80%) at each of the six points. This was accomplished through the use of 42 ascending randomized staircases [3]. Each staircase began at a depth of modulation 4% below a threshold estimated during a practice procedure con-
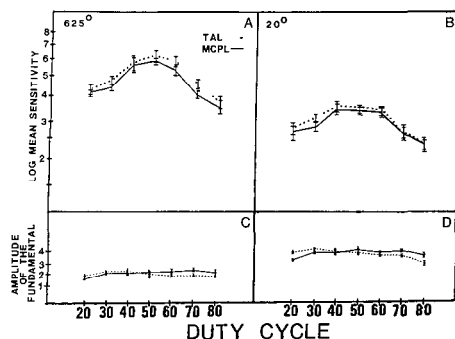
Figure 3 Temporal sensitivity (upper half) and threshold amplitude of the fundamental frequency (lower half) as a function of duty cycle for 0 625° (Panels A & C) and 20° (Panels B & D) eccentricities

ducted before each testing session. The modulation depth was incremented or decremented in steps of 1% within a staircase, and each staircase was considered complete after four reversals. Separate blocks of trials were run for the TAL and MCPL conditions. Thirty-two healthy observers (6/6 or 20/20 corrected or uncorrected far acuity in the eye that was tested) participated in the experiment with each observer being exposed to all conditions for one of the 8 line orientations.

Results

The upper half of Figure 3 presents temporal sensivity, the reciprocal of the depth of modulation required to detect flicker, as a function of the duty cycle of the 5 Hz flickering point. Since there were no significant differences among the data collected from the eight orientations (largest $F_{42,144} = 1.31$, $p>0.05$) each data point in the figure represents the geometric mean across 32 observers. Each graph exhibits functions for the TAL and MCPL conditions, with Panel A reflecting data from points at a 0.625° eccentricity and Panel B from a 20° eccentricity. The principal difference between eccentricities was the expected lower sensitivity found in the periphery ($F_{5,120} = 76.32$, $p<0.01$) given the small points that were presented [4, 9], and the similar, but not identical shapes of the TAL and MCPL functions across eccentricities.

The shapes and relative displacements of the TAL and MCPL functions depend upon what determines temporal sensitivity. If it is the amplitude of the fundamental frequency, then each temporal sensitivity data point should reflect the depth of modulation needed to allow the amplitude of the fundamental to cross a fixed threshold. Given the constant 5 Hz frequency, if all of the temporal sensitivity data is converted into amplitudes of the fundamental, then the TAL and MCPL functions should be flat and overlap within a given eccentricity. Panels C and D of Figure 3 present these functions calculated using the sensitivity data in

the upper half of this figure. A statistical analysis of these data revealed a light-type by duty cycle interaction ($F_{6,186}$ = 19.51, p<0.01) indicating that at least one of the light-type functions is not flat and, therefore, that all of the functions cannot overlap. However, this interaction only accounted for 2.13% of the variance. In other words, the effect was significant, but cannot be considered meaningful [13]. It is therefore concluded that the same amplitudes of the fundamental were required for flicker to be detected within a given eccentricity. This conclusion is consistent with a similar finding reported by de Lange ([5], p. 938).

Discussion

The results of this experiment indicate that the amplitude of the fundamental frequency determined temporal sensitivity to duty cycle. If this conclusion can be extrapolated to the multi-flash campimetry paradigm, then one should be able to predict multi-flash thresholds from knowledge about performance on the sensitivity task used in this experiment. Given that the temporal frequencies, time-average luminance levels, and retinal eccentricities are equated, this means that the same amplitude of the fundamental should be required to detect flicker in both tasks. In order to test this hypothesis, eight observers from the sensitivity experiment were administered the multi-flash test described in the Introduction section. Figure 4 presents the ampltudes of the fundamental needed to detect flicker in both the TAL sensitivity and TAL multi-flash tasks as a function of retinal eccentricity. The results of an analysis of variance revealed that there were neither differences between the two functions ($F_{1,7}$ = 1.72, p>0.05), nor a significant interaction between the task and eccentricity variables ($F_{5,35}$ = 2.17, p>0.05). In other words, for the six retinal eccentricities tested the same amplitudes of the fundamental were required to detect flicker in both the sensitivity and multi-flash paradigms. (It should be noted that reaction time is a consideration in the multi-flash procedure, but not in the sensitivity paradigm. This influence of reaction time was discounted in the following manner. The average reaction times to flicker at threshold level duty cycles were assessed for each observer, for the six eccentricities of the multi-flash quadrant that contained the test display used in the sensitivity experiment. Increases in the muli-flash thresholds due to reaction time were then calculated, and subtracted from the original multi-flash data. This corrected data was then expressed in terms of the amplitude of the fundamental.)

In conjunction with other evidence that the amplitude of the fundamental frequency can account for classical CFF data [5, 11], the results of this study suggest that it can be used as a basis for comparing results either among or within a variety of temporal sensitivity and resolution psychophysical techniques. The key is to express the data in terms of the amplitude of the fundamental. As an
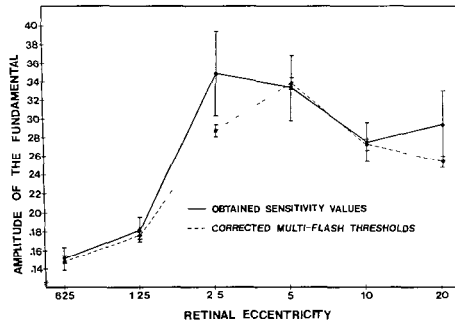
Figure 4 Threshold amplitude of the fundamental frequency as a function of eccentricity for the sensitivity data and corrected multi-flash data

example consider the statistics that can be used to describe multi-flash campimetry data [6]. The first two statistics are similar in principal to those proposed by Flammer and Drance [8] to describe Octopus fields.

The 'Average Deficit' (AD) is defined as:
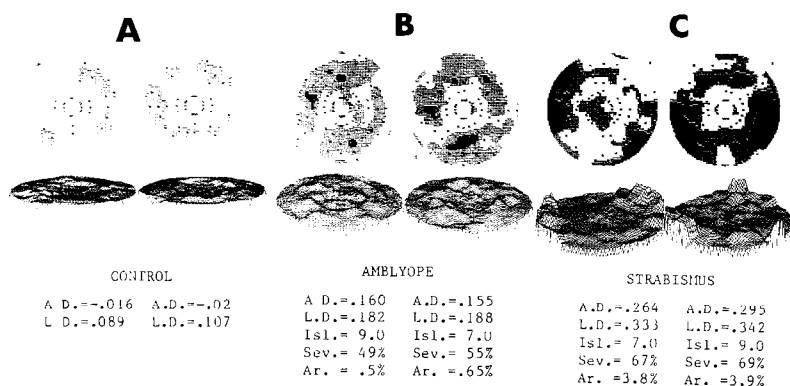
$$\frac{\sum_{i=1}^{m} (P_i - \bar{C}_i)}{M}$$

where P_i refers to the amplitude of the fundamental required by a patient to detect flicker in the i-th point of the visual field, $\bar{C}_i$ refers to the calculated average amplitude required by a group of aged categorized control observers for this same point location, and M equals the number of points tested. The value of AD can vary around zero with larger positive values indicating greater general impairment.

The 'Local Deficit' (LD) is defined as:

$$\sqrt{\frac{\sum_{i=1}^{m} (P_i - \bar{C}_i) - AD)^2}{M-1}}$$

where P_i, $\bar{C}_i$, and M are defined as above, and AD is the Average Deficit value. LD, whose lower limit is zero, reflects the dispersion around the Average Deficit value. Relatively uniform impairment across the visual field would result in low LD values, whereas a tendency towards localized areas of dysfunction would result in higher LD values.

Although AD and LD make use of only the data that was collected, the following three statistics are calculated with the inclusion of the interpolated data used in creating the visual fields plots. The 'Islands' statistic reveals the number of areas within a visual field in which higher amplitudes of the fundamental than

A	B	C

CONTROL	AMBLYOPE	STRABISMUS
A D.=-.016 A.D.=-.02	A D.=.160 A.D.=.155	A.D.=.264 A.D.=.295
L D.=.089 L.D.=.107	L.D.=.182 L.D.=.188	L.D.=.333 L.D.=.342
	Isl.= 9.0 Isl.= 7.0	Isl.= 7.0 Isl.= 9.0
	Sev.= 49% Sev.= 55%	Sev.= 67% Sev.= 69%
	Ar. = .5% Ar. =.65%	Ar. =3.8% Ar. =3.9%

Figure 5 Two and three dimensional multi-flash fields with corresponding statistics for a healthy observer (Panel A), an anisometropic amblyope (Panel B), and a strabismic amblyope (Panel C)

normal are required to detect flicker. Because normal temporal resolving power, assessed with small points, is poorer beyond a 1.25° eccentricity, different criteria for defining Islands of abnormality are used within these two regions of the visual field. The 'Average Severity' statistic indicates the magnitude of a deficiency within a typical Island for a given visual field; an average that is weighted by the areas of the Islands. It is expressed as a percentage of the maximum possible severity that can be presented within a 2D plot. Finally, the 'Average Area' statistic reflects the average size of any Islands of deficit within the tested visual field. It is calculated by adding the number of sampled and interpolated points that are associated with abnormal amplitudes of the fundamental, and dividing by the number of Islands. It is expressed as a percentage of the total visual field plot area in order to provide an upper limit as a point of reference. Figure 5 represents the visual fields and corresponding statistics from a healthy control observer (Panel A), an anisometropic amblyope (Panel B) and a strabismic amblyope (Panel C).

These statistics provide an efficient way of communicating the information contained in the multi-flash fields, and in combination with the raw data and field plots can provide a rather comprehensive picture of human temporal resolving power within a 40° visual field. Further, the relatively short period of time required to obtain all of this information, the correlation between temporal resolving power and light sensitivity, and the ability to quantitatively compare its results with those of other tests, makes multi-flash campimetry a potentially useful perimetric tool.

422

References

1 Brussell EM, White CW, Faubert J, Dixon M: Multi-flash campimetry as an indicator of visual field loss in glaucoma Am J Optom Physiol Optics 63: 32–40 (1986)

2 Brussell EM, White CW, Bross M, Mustillo P, Borenstein M: Multi-flash campimetry in multiple sclerosis Curr Eye Res 1: 671–677 (1981/82)

3 Cornsweet T: The staircase-method in psychophysics Am J Psychol 75: 485–491 (1962).

4 Creed RS, Ruch TC: Regional variations in sensitivity to flicker J Physiol 74: 407–423 (1932)

5 De Lange H: Experiments on flicker and some calculations on an electrical analogue of the foveal systems Physica 18: 935–950 (1952)

6 Dixon M, Brussell EM: Quantifying the magnitude of visual impairment with multi-flash campimetry In: Proceedings of the International Symposium on Low Vision Springer-Verlag, Berlin, in press

7 Faubert J, Brussell EM, Overbury O, Balazsi G, Dixon M: Spatial vs temporal information in suspected and confirmed chronic open angle glaucoma In: Proceedings of the International Symposium on Low Vision Springer-Verlag, Berlin, in press

8 Flammer J, Drance SM, Augustiny L, Funkhouser A: Quantification of glaucomatous visual field defects with automated perimetry Invest Ophthalmol Vis Sci 26: 176–181 (1985)

9 Granit R, Harper P: Comparative studies on the peripheral and central retina: II Synaptic reactions in the eye Am J Physiol 95: 211–227 (1930)

10 Galvin RJ, Regan D, Heron JR: Impaired temporal resolution of vision after acute retrobulbar neuritis Brain 99: 255–268 (1976)

11 Ives HE: A theory of intermittent vision J Opt Soc Am 6: 343–361 (1922)

12 Kirk RE: Experimental design: Procedures for the behavioral sciences Brooks/Cole Publishing Company, Belmont CA, 1982

13 Mustillo P, Brussell EM, White CW, Anderson DP: Monitoring demyelination in multiple sclerosis with multi-flash campimetry Int Ophthalmol 7: 75–86 (1984)

14 Overbury O, Brussell EM, White CW, Jackson WB, Anderson DP: Evaluating visual loss with multi-flash campimetry Can J Ophthalmol 19: 255–260 (1984)

15 Regan D, Neima D: Balance between pattern and flicker sensitivities in the visual fields of ophthalmological patients Br J Ophthalmol 68: 310–315 (1984)

16 Ross RT: The fusion frequency in different areas of the visual field: IV Fusion frequency as a function of the light-dark ratio J Gen Psychol 29: 129–144 (1943)

17 Titcombe AF, Wilson RG: Flicker fusion in multiple sclerosis J Neurol Neurosurg Psychiat 24: 260–265 (1961)

18 Tyler CW: Specific deficits of flicker sensitivity in glaucoma and ocular hypertension Invest Ophthalmol Vis Sci 20: 204–212 (1981)

19 White CW, Brussell EM, Overbury O, Mustillo P: Assessment of temporal resolution in multiple sclerosis by multi-flash campimetry In: Breinin GM, Siegel IM (eds) Advances in diagnostic visual optics, pp 239–246 Springer-Verlag, Berlin, 1983

Authors' addresses:
Edward M Brussell,
Dept of Psychology, Concordia University, 1455 de Masionneuve
Blvd West, Montreal, Quebec H3G 1M8, Canada

Mike Dixon, Jocelyn Faubert,
Dept of Psychology, Concordia University, Montreal, Canada

Gordon A Balazsi,
Dept of Ophthalmology, McGill University, Montreal, Canada

VI.2 Multi-flash campimetry and other psycho-physical tests in chronic open angle glaucoma

J. FAUBERT, A.G. BALAZSI, O. OVERBURY and E.M BRUSSELL
Montreal, Canada

Abstract

Multi-flash campimetry (MFC) is a computer implemented psycho-physical technique which allows sampling of temporal resolution at 120 points of a 40 degree visual field. The technique is rapid (about 20 minutes per eye), reproducible and easy to perform. We compared MFC to Octopus perimetry, colour vision and spatial contrast sensitivity in a series of thirty eyes of 30 observers. Nine were early glaucomatous eyes, 10 were glaucoma suspect eyes and 11 were normal controls.

Analysis of variance show MFC in the early glaucoma and suspect eyes to be significantly different from the control eyes ($p < 0.05$). This was not found for colour vision and contrast sensitivity. All five eyes with abnormal Octopus fields had abnormal MFC. Conversely, nine eyes had abnormal multi-flash fields and normal Octopus fields. MFC is likely sensitive to alterations of both temporal and luminance sensitivity.

Introduction

The aim of psycho-physical testing in the chronic glaucomas is to detect and follow the evolution of optic nerve dysfunction and/or damage. Recent studies have concentrated on the significance of alterations of the differential light threshold as determined by static perimetry (1,14), of spatial contrast sensitivity [2], and of colour vision [11]. A loss of temporal resolving power in glaucomatous eyes was first appreciated by investigators using a flickering stimulus target on the tangent screen [16, 22]. In 1959, Campbell and Rittler found abnormal flicker fields in 19 of 23 chronic simple glaucoma eyes with equivocal or normal tangent screen fields [9]. More recently, abnormality in time-related visual function in glaucoma has been demonstrated with other psycho-physical methods which test a localized area of the visual field: the double-flash test in the central 10 degrees

[15]; 5 degree stimulus fields presenting a flickering, diffusely illuminated target or a counterphase flickering target viewed centrally [3, 4], and in the periphery [18, 20, 21]; and both sustained and transient-like functions as determined by quantitative layer-by-layer perimetry [12, 13].

Multi-flash campimetry is a computerized, reproducible clinical method developed in our laboratory [8]. It allows a rapid assessment of temporal resolving power in 120 points of the central 40 degrees of visual field. Multi-flash campimetry shows definite abnormalities in optic nerve disorders such as multiple sclerosis [8, 17, 23], in which the speed of nerve conduction is known to be impaired. We have studied this technique in control, glaucoma suspect and early glaucoma eyes which were also tested for colour vision, spatial contrast sensitivity, and static perimetry.

Methods

Subjects

The study group consisted of thirty eyes of 30 different observers, separated into three groups: early glaucoma, glaucoma suspect and control of 9, 10 and 11 eyes respectively. These groups had similar distributions with means of 52,49 and 49 years respectively. All of the eyes had a best corrected acuity of 6/7.5 or better, and no other ocular disease. The suspect group was comprised of eyes with intraocular pressure consistently greater than 21 mm Hg, normal optic nerve heads, and reproducible normal Armaly-Drance visual fields on the Goldmann apparatus [10]. The early glaucoma group consisted of eyes with elevated intraocular pressure (>21 mm Hg), early disc changes and/or early reproducible visual field defects such as a nasal step or a paracentral scotoma.

Apparatus

Both mutli-flash campimetry and the spatial sensitivity gratings were implemented on a PDP11/10 computer interfaced with a large screen CRT (Hewlett Packard 1310A equiped with a p15 phosphor). The sine wave gratings were produced by Wavetek function generators under the control of the PDP11/10. Colour testing was performed with the American Optical H-R-R Pseudoisochromatic plates (HRR) and the Farnsworth-Munsell 100-hue test. An Easel Lamp (Macbeth Corporation) was used for the colour tests. Computerized perimetry was performed with either program 38 or G1 on the Octopus 500R perimeter.

Procedure

All 30 eyes were tested for temporal resolution (multi-flash campimetry), spatial contrast sensitivity, and computerized static perimetry. Twenty-six of the 30 eyes were available for the colour tests.

Multi-flash campimetry samples temporal resolution at 120 points of a 40 degree visual field. The visual display consists of 6 concentric circles: the eccentricities subtend 0.625, 1.25, 2.5, 5.0, 10.0 and 20.0 degrees of visual angle. The stimuli points subtend 5 minutes, and are presented simultaneously lit in one randomly chosen quadrant at a time A randomly chosen point is then manipulated to assess the ability to perceive a 5 Hz flicker. In each 200 ms cycle, the duty cycle (period of cycle that is lit) of the stimulus is systematically decreased and the off period increased by 2.8 ms (1.4 percent) until the observer perceives flicker and hits the response key. Prior to the testing session, a display of 15 points with one point located in the blind spot is used for practice This is repeated until the observer feels comfortable with the task and the point in the blind spot is not responded to. The average luminance of the display is 3 cd/m² and the viewing distance 57 cm.

Following the testing period, a complete printout of the multi-flash thresholds (off-period needed to perceive flicker) for the individual points is obtained. Statistically deviant points are replicated immediately to avoid misinterpretation due to momentary lapses of attention or occasional eye movements. A point is considered statistically deviant if the threshold is 7 standard errors greater than the circle mean or 21 standard errors greater than the general mean. Finally 2- and 3-dimensional maps are created which allow for easy interpretation of the results.

The spatial contrast sensitivity functions were generated using the 'Anticipated Threshold Technique' [6]. This allows for a rapid assessment of 5 spatial frequencies. For this study we used spatial frequencies of 1.00, 1.82, 3.31, 6.03 and 10.99 cycles per degree (c/d). Delayed intervals and catch trials were used to avoid habituation responses. The average luminance was 5 cd/m², the viewing distance was 1 meter and the target subtended 8×8 degrees The task is to depress the paddel when the static gratings are just perceived.

Conventional instructions were given for the colour tests except that no time limits were imposed to complete the FM 100-hue test.

Results

An analysis of variance (ANOVA) was performed on the mean multi-flash thresholds across retinal eccentricity. The results show a statistically significant difference between groups ($F(2,27) = 3.718$, $P<0.05$). No statistical difference was found between groups for the spatial contrast sensitivity test or the FM 100-hue test. No errors were made on the HRR colour plates.

Figure 1 demonstrates the mean multi-flash thresholds of the different groups as a function of retinal eccentricity. Average standard error bars for the individual diagnostic categories are given. Post hoc Sheffé tests reveal that the glaucoma suspect group is different from the controls at 5, 10 and 20 degrees of eccentricity. The glaucoma group is different from the controls at all eccentricities.

For a more individualized analysis, the multi-flash data were compared to a 95% confidence interval obtained from the control data. This was done separately for the younger age group (20–49), and the older age group (over 50). If the mean multi-flash threshold of at least 1 concentric circle fell beyond the normal range the multi-flash field was considered abnormal. Similarly, the spatial contrast sensitivity data was considered abnormal if at least one of the five spatial frequencies tested was beyond the 95% confidence level obtained from our controls. The FM 100-hue error score was defined as abnormal using a similar

Table 1 Information of abnormality for each patient across different measures

	MFC*	Octopus	FM-100	Spatial+
20–49 glaucoma				
Patient 1	4	Normal	N	0
Patient 2	6	Generalized depression	N	3
Patient 3	0	Normal	A	0
Patient 4	0	Normal	A	1
20–49 suspects				
Patient 5	5	Superior depression	N	2
Patient 6	6	Normal	–	5
Patient 7	2	Normal	A	1
Patient 8	0	Normal	–	4
Patient 9	4	Normal	N	2
50-over glaucoma				
Patient 10	2	Local paracentral scotoma	N	1
Patient 11	4	Gen & local NFBD	N	0
Patient 12	2	Normal	A	3
Patient 13	3	Sup & inferior NFBD	N	1
Patient 14	6	Normal	N	3
50-over suspects				
Patient 15	0	Normal	N	0
Patient 16	0	Normal	N	1
Patient 17	4	Normal	N	1
Patient 18	4	Normal	N	2
Patient 19	5	Normal	N	1

* Values represent number of abnormal eccentricities (mean MFC score) over a total of 6 eccentricities

¹ Values represent number of abnormal spatial contrast sensitivities over a total of 5 spatial frequencies
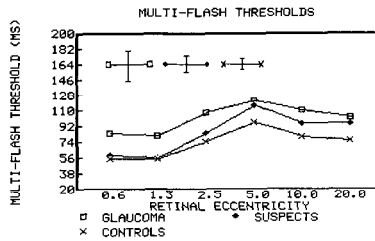
MULTI-FLASH THRESHOLDS

Figure 1 Mean multi-flash threshold (ms) for each diagnostic category as a function of eccentricity Average standard error bars are given for the individual conditions

95% confidence interval. These data are shown in Table 1 along with the Octopus fields as blindly assessed by our clinician (GB).

When Octopus fields were abnormal multi-flash campimetry fields were always abnormal. This is not the case for colour or spatial contrast sensitivity data. Further, multi-flash was abnormal in 9 instances where no abnormality could be measured by Octopus perimetry. The test showing the most frequent abnormality was the spatial contrast sensitivity test. However, this may be biased by our normality criterion: in MFC, we have averaged 20 points for each eccentricity, whereas in the spatial contrast sensitivity, we have averaged 5 measurements for each spatial frequency. Seven of the eyes with spatial contrast sensitivity abnormality had a deficiency for only one spatial frequency. Only 4 of the 17 patient group eyes demonstrated abnormal FM-100 scores, 3 in the glaucoma group and one in the suspect group.

Discussion

Our results are consistent with the notion that temporal resolution is reduced in glaucoma. The possibility that Y or transient cells are damaged early in glaucoma has been suggested by quantitative histopathological and psycho-physical studies [3, 19, 20]. It is expected that the loss of such cells would affect the temporal resolution of the visual system. Of importance is the finding that all 5 abnormal Octopus perimetry fields are reflected by abnormal multi-flash data, and that 9 eyes with normal Octopus fields also had abnormal MFC. The Ferry-Porter law states that the ability to perceive flicker is directly dependent on the luminance of the flickering target [5]. This renders MFC sensitive to alterations of both temporal and light sensitivity.

Multi-flash campimetry has the additional advantage of sampling 120 points across the visual field in about 20 minutes per eye. It also presents the data in two and three-dimensional maps for rapid assessments. Figure 2 shows two- and three-dimensional maps of a multi-flash field from a 27-year-old normal observer. Figure 3 shows two and three-dimensional multi-flash maps and Octopus fields of
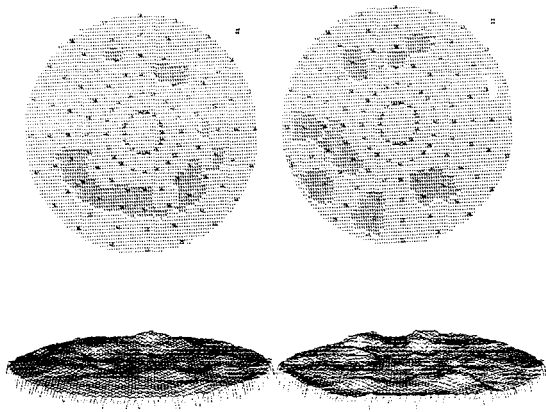
430

Figure 2 Two- and 3-dimensional multi-flash maps of a 27-year-old normal observer Loss of resolution is represented by darker shading and higher mountains respectively Square symbols beside the 2D maps represent the angle of presentation for the 3D maps
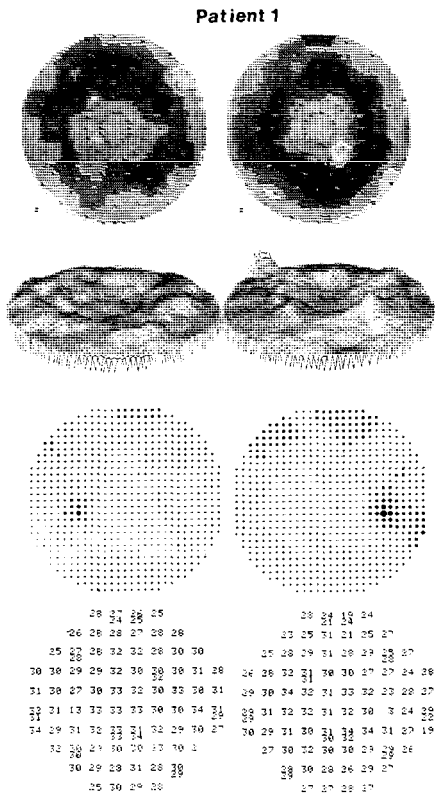
Patient 1

Figure 3 Two- and 3-dimensional multi-flash maps and Octopus field maps (#38) of a 24-year-old patient with an early glaucomatous left eye and a glaucoma suspect right eye

a 24-year-old patient with glaucoma in the left eye (abnormal disc) and suspected glaucoma in the right eye.

The multi-flash data presented in Table 1 limits our interpretation of specific localized defects. We are presently developing numerical measures of variability, and generalized and localized defects of multi-flash fields [7].

A long term follow-up study is being conducted to test whether multi-flash campimetry is predictive of glaucomatous optic nerve damage

References

1 Anctil JL, Anderson DR: Early foveal involvement and generalized depression of the visual field in glaucoma Arch Ophthalmol 102: 363–370 (1984)
2 Arden GB, Jacobson JJ: A simple grating test for contrast sensitivity: preliminary results indicate value in screening for glaucoma Invest Ophthalmol Vis Sci 17: 23–32 (1978)
3 Atkin A, Bodis-Wollner I, Wolkenstein M, Moss A, Podos SM: Abnormalities of central contrast sensitivity in glaucoma Am J Ophthalmol 88: 205–211 (1979)
4 Atkin A, Wolkstein M, Bodis-Wollner I, Anders M, Kels B, Podos SM: Intraocular comparison of contrast sensitivities in glaucoma patients and suspects Br J Ophthal 64: 858–862 (1980)
5 Brown JL: Flicker and intermittent stimulation In: Graham C (ed) Vision and visual perception, pp 251–320 John Wiley & Sons, New York, 1966
6 Brussell EM, Cavanagh P: An anticipated threshold technique for measuring contrast sensitivity Am J Opt Phys Optics 61: 125–126 (1984)
7 Brussell EM, Dixon M, Faubert J, Balazsi GA: Multi-flash campimetry: the rapid assessment of temporal resolving power Doc Ophthal Proc Ser, 7th International Visual Field Symposium, Amsterdam, 1986
8 Brussell EM, White CW, Bross M, Mustillo P, Borenstein M: Multi-flash campimetry in multiple sclerosis Current Eye Res 1: 671–677 (1981/2)
9 Campbell CJ, Rittler MC: The diagnostic value of flicker perimetry in chronic simple glaucoma Tr Am Acad Ophthal 63: 89–98 (1959)
10 Drance SM, Brais P, Fairclough M et al: A screening method for temporal visual field defects in chronic simple glaucoma Can J Ophthalmol 7: 428–429 (1972)
11 Drance SM, Lakowski R, Schulzer M et al: Acquired colour vision changes in glaucoma Use of the 100-hue test and Pickford anomaloscope as predictors of glaucomatous field changes Arch Ophthalmol 99: 829–831 (1981)
12 Enoch J: Quantitative layer-by-layer perimetry Proctor lecture Invest Ophthalmol Vis Sci 17: 208–257 (1978)
13 Enoch J: Quantitative layer-by-layer perimetry: an update Am J Opt Phys Optics 59: 952–953 (1982)
14 Flammer J, Drance SM, Zulauf M: Differential light threshold: short- and long-term fluctuation in patients with glaucoma, normal controls, and patients with suspected glaucoma Arch Ophthalmol 102: 704–706 (1984)
15 Galvin RJ, Regan D, Heron JR: Impaired temporal resolution of vision after acute retrobulbar neuritis Brain 99: 255–268 (1976)
16 Miles PW: Flicker fusion fields Arch Ophthal 43: 661–677 (1950)
17 Mustillo P, Brussell EM, White CW, Anderson DP: Monitoring demyelination in multiple sclerosis with multiflash-campimetry Internat Ophthalmol 7: 75–86 (1984)
18 Neima D, LeBlanc R, Regan D: Visual field defects in ocular hypertension and glaucoma Arch Ophthal 102: 1042–1045 (1984)

19   Quigley HA, Dunkelberger GR, Sanchez RM: Chronic experimental glaucoma causes selectively greater loss of larger optic nerve fibers Invest Ophthalmol Vis Sci (Suppl) 27: 42 (1986)
20   Regan D, Neima D: Balance between pattern and flicker sensitivities in the visual fields of ophthalmological patients Br J Ophthalmol 68: 310–315 (1984)
21   Tyler CW: Specific deficits of flicker sensitivity in glaucoma and ocular hypertension Invest Ophthalmol Vis Sci 20: 204–212 (1981)
22   Weekers R: L'exploration des fonctions visuelles en clinique par la mesure de la frequence critique de fusion Bull Soc Fr D'oph 69: 331–337 (1947)
23   White CW, Brussell EM, Overbury O, Mustillo P: Assessment of temporal resolution in multiple sclerosis by multi-flash campimetry In: Breinin GM, Siegel IM (eds) Advances in diagnostic visual optics, pp 239–246 Springer-Verlag, Berlin, 1983

Authors' addresses:
Jocelyn Faubert,
Dept of Psychology, Concordia University,
7141 Sherbrooke West, Montreal, Quebec, Canada, H4B IR6

A G Balazsi, O Overbury,
Dept of Ophthalmology, Royal Victoria Hospital, McGill University, Montreal, Canada

E M Brussell,
Dept of Psychology, Concordia University, Montreal, Canada

VI.3 Pattern discrimination perimetry: a new concept in visual field testing

B. DRUM, M. BRETON, R. MASSOF, H. QUIGLEY, T. KRUPIN,
J. LEIGHT, J. MANGAT-RAI and D. O'LEARY
Baltimore, U.S.A.

Abstract

The subject's task in conventional perimetry is to detect an incremental spot of light on a uniform background. Recent evidence indicates that, at least in glaucoma, this task can be insensitive to large amounts of neural damage. In an attempt to find more effective ways to detect early glaucomatous damage, we are developing alternative perimetric techniques that are based on pattern discrimination rather than light detection. The subject fixates a small square at the center of a large field of dynamic random dots and tries to detect a patch of non-random, or coherent, dots embedded in the background The stimuli are displayed on a projection CRT, and all test target parameters, including position, size, shape, exposure duration, dot density, dot arrangement and dot dynamics, are under computer control. In particular, spatial and temporal coherence parameters are defined in terms of the spacing and motion of the target dots.

We have obtained preliminary control data and glaucoma patient data for four different static protocols that test different stimulus parameters: size and exposure duration thresholds for fully coherent targets, and spatial coherence and temporal coherence thresholds for large, long-duration targets. Our results suggest that the temporal coherence test may be especially sensitive to early glaucomatous defects.

Introduction

Conventional perimetry is based on detection of an incremental spot of light on a uniform background. It has recently become clear that conventional perimetry cannot detect the earliest stages of glaucomatous nerve damage [5]. This lack of sensitivity is not surprising in hindsight Electrophysiological studies [1, 2] have shown that individual ganglion cells can respond to light intensities that are close to normal psycho-physical thresholds. A significant sensitivity loss may therefore

require a nearly complete gap in ganglion cell receptive field coverage. Because retinal ganglion cell receptive fields are large and extensively overlapping [3], many ganglion cells could be lost before such a gap in visual field coverage occurs.

We hypothesized that ganglion cell loss might disturb the coding of relative position in the visual field well before a sensitivity loss becomes apparent. In other words, ganglion cell loss might tend to randomize the apparent positions of neighboring points in the field. To test this idea, we have built an instrument that we call the pattern discrimination perimeter [4].*

Hardware

A prototype of the pattern discrimination perimeter is shown in Fig. 1. The instrument is a computer-controlled video display with provisions added for maintaining the subject's alignment, monitoring fixation and recording responses We currently are using a 40" diagonal Mitsubishi rear-projection television, controlled with a North Star Horizon microcomputer. The stimulus display is generated with a Matrox graphics board and a custom hardware random-dot generator. The fixation monitor consists of a miniature CCD television camera that sends a magnified image of the subject's eye to a standard TV display, as shown in Fig. 1. A pushbutton is provided for automatically recording patient responses, and a warning beep 0.5 sec before each trial cues the subject to prepare for the next stimulus presentation.

Stimuli

The basic stimulus configuration is a dynamic random-dot background upon which is placed a square target patch of non-random dots. The stimulus patch always has the same average dot density as the background, but a different spatial and/or temporal arrangement. Therefore, the only way to detect the stimulus is to distinguish a difference in texture or motion between the stimulus patch and the surrounding random-dot field. Within this framework, the only additional limitations on the stimulus pattern are hardware limitations of the computer and graphics display.

As a start toward categorizing the potentially vast selection of different stimulus patterns, we have defined two variables, called spatial and temporal coherence, that are essentially measures of the amount of order, or regularity, of the pixels in the stimulus. A fully spatially coherent pattern is defined as one in which the white and black pixels are interspersed as regularly as possible within the

---

* Similar theoretical ideas form the basis of the acuity perimeter developed by Phelps et al [4]
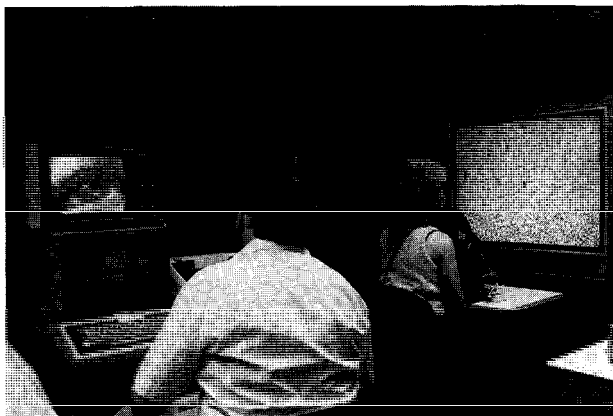
Figure 1 Prototype pattern discrimination perimeter

stimulus area. For a dot density with equal numbers of black and white pixels, this is a checkerboard pattern with one pixel per square, as shown at the far left of Fig. 2. A fully incoherent pattern, on the other hand, is simply a patch of random dots, as shown at the far right of Fig. 2. Between these extremes, a coherence scale can be defined, based on the percentage of randomly selected pixels that are 'scrambled', or moved from their fully coherent position to a position that previously was the opposite color. For a background and test target with equal numbers of black and white pixels and a test target with P_w scrambled white pixels, P_b scrambled black pixels and N total pixels,

$$\% \text{ coherence} = 100 - [200(P_w + P_b)/N]$$

I.e., the coherence falls to 0 when half the pixels of each polarity are reversed. The lower row of stimuli in Fig. 2 shows several different spatial coherences, and also illustrates the concept of a spatial coherence threshold. In practice, a new set of scrambled pixels appears with each frame of the dynamic random-dot background.

A fully temporally coherent pattern can be either motionless (static temporal coherence) or moving as a unit (dynamic temporal coherence). Dynamic temporal coherence does not necessarily imply overall translation; *e.g.*, scrolling and rotation also qualify as temporally coherent motion. A temporal coherence scale can be defined only in the time domain, but is completely analogous to the spatial coherence scale. That is, with each new frame of the background, a new random subset of stimulus pixels is scrambled.

SIZE SERIES

20x20	12x12	8x8	4x4	0x0

SPATIAL COHERENCE SERIES

100%	80%	60%	40%	0%

Figure 2 Top: checkerboard stimuli of different sizes decreasing from left to right, embedded in a random-dot background Checkerboard height and width in pixels is indicated below each stimulus square Bottom: checkerboard stimuli with spatial coherences decreasing from left to right, embedded in a random-dot background Percent spatial coherence is indicated below each stimulus square See text for definition of spatial coherence

Threshold protocols

As a start toward testing the feasibility of the pattern discrimination perimeter, we have designed four threshold tests to evaluate how changing different parameters of the stimulus affect its detectability. The four tests are:

A) Size thresholds for counterphase checkerboards, *i.e.*, spatially coherent but dynamic stimuli. The size threshold is defined as the size (in pixels/side) at which the target square disappears. This type of threshold task is illustrated in the top row of stimuli in Fig. 2.

B) Duration thresholds for counterphase checkerboards, defined as the duration at which the target disappears,

C) Spatial coherence thresholds for counterphase checkerboards, illustrated in the bottom row of stimuli in Fig. 2.

D) Static temporal coherence thresholds for spatially random patches that can be seen only because they are temporarily frozen against the dynamic random background.

The stimulus positions for all threshold tests are the same as the central 24 positions for the Octopus program 32 and the Humphrey program 30-2. The stimuli are arranged in a square array with 6° of visual angle between nearest neighbors, and are offset 3° from the horizontal and vertical meridians. At the testing distance of 2/3 meter, the entire screen subtends about 49° vertically by 62.5° horizontally, and each pixel subtends approximately 15′ of arc.

Thresholds are measured automatically with a brief staircase procedure in which the step size is halved after each reversal, and threshold is defined as the first negative response in the second decreasing sequence. An 'absolute' defect is recorded if two consecutive presentations of the most visible available stimulus elicit negative responses. Threshold staircases for four randomly selected positions are run simultaneously. When threshold for one position is completed, one of the remaining positions is randomly selected to take its place. The 4 diagonal positions 9° from the horizontal and vertical axes are tested twice to estimate within-session variability. When fewer than four positions remain to be completed, dummy positions are tested to keep the subject's spatial uncertainty constant. Approximately 10% of the stimulus trials are 'blanks' inserted to assess the subject's response criterion.

Results and discussion

We have recently begun a large-scale study comparing the abilities of the pattern discrimination perimeter, the Octopus perimeter and the Humphrey Visual Field Analyser to detect early visual field defects in glaucoma and suspected glaucoma. In this section we present some preliminary pattern discrimination data, using the four threshold tests described above

Figure 3 shows averages of data from 16 normal subjects ranging in age from 26 to 70 years, with a mean age of 45.4 years. All subjects had visual acuities $\geq 20/20$, refractive errors ≤ 5 diopters, intraocular pressures <20 mm Hg, normal-appearing optic disks and retinal nerve fiber layers, normal visual fields (Humphrey program 30-2), and no fundus or anterior segment abnormalities detectable from clinical examination.

Figure 3a shows size threshold data expressed in pixels per side of the stimulus. The stimulus was a counterphase checkerboard 0 6 sec in duration. Horizontal eccentricity is plotted on the 'X' axis, vertical eccentricity on the 'Y' axis and threshold on the 'Z' axis. The data are all plotted in a left eye format, so the blind spot is toward the left. Thresholds range from about 4 pixels per side at the 3-degree positions to 7 pixels per side at the 15-degree positions excluding the blind spot.

Figure 3b shows a similar threshold surface of duration thresholds, for a counterphase checkerboard 12 pixels on a side. The threshold durations are quite low except for the blind spot. In many cases, the subjects could reliably see targets presented for only a single background frame (1/15 sec).

Figure 3c shows a spatial coherence threshold surface for a 20×20 pixel counterphase checkerboard of 0.6 sec duration Thresholds range from about 42% coherence at 3° to 67% coherence at 15° eccentricity. There is less threshold elevation at the blind spot than for the size and duration tests, perhaps because the stimulus is larger.
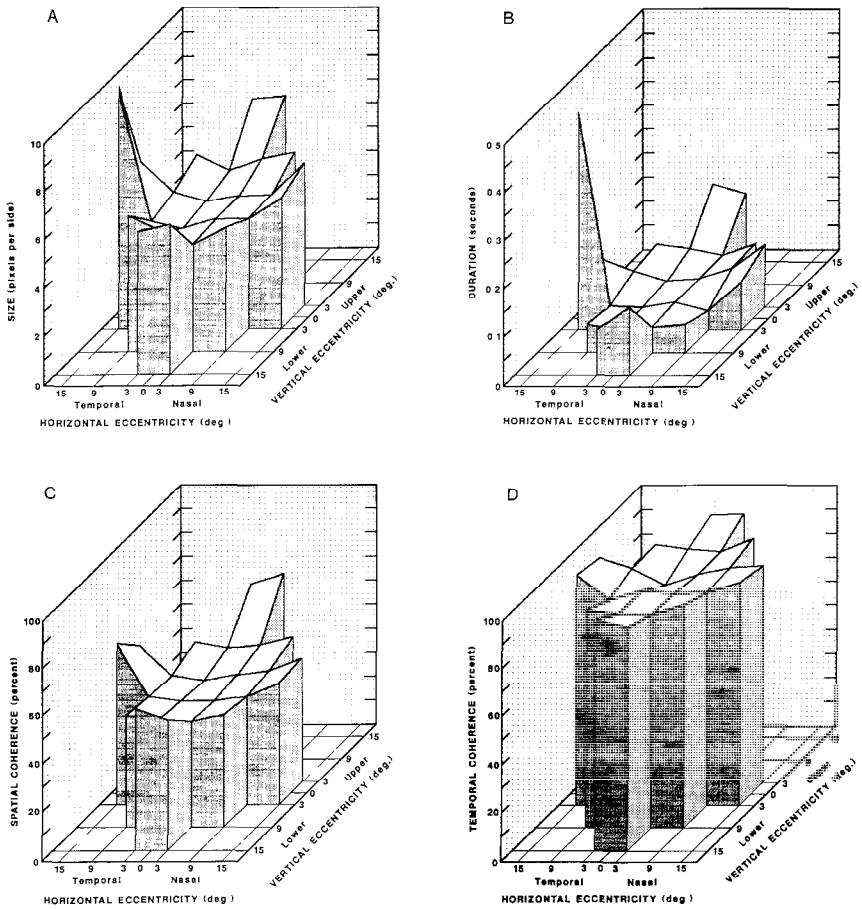
Figure 3 Mean pattern discrimination threshold data for 16 normal subjects Visual field position is plotted on the horizontal plane, and threshold is plotted on the vertical axis Each graph shows thresholds for the central 24 test positions in program 30-2 of the Humphrey Visual Field Analyser and program 32 of the Octopus perimeter Test positions are at the vertices of the squares on the threshold surface All data are plotted in a left eye format The refresh rate for both background and stimuli was 15 Hz for all data, and all backgrounds and stimuli contained equal numbers of black and white pixels A: size thresholds plotted in pixels per side for 0 6 sec duration counterphase checkerboard stimuli B: duration thresholds for 12 pixels per side counterphase checkerboard stimuli C: spatial coherence thresholds for counterphase checkerboard stimuli 20 pixels per side and 0 6 sec in duration See text for definition of spatial coherence D: static temporal coherence thresholds for a spatially random stimulus 20 pixels per side and 1 6 sec in duration See text for definition of static temporal coherence

Table 1 Ranges of means and average S D 's of Fig 3 data (excluding blind spot)

Threshold test	Range of means	S D
Size	4 1 – 6 8 pixels	± 1 65 pixels
Duration	0 04– 0 16 sec	± 0 084 sec
Spatial coherence	41 9 –67 4%	±10 8%
Temporal coherence	81 9 –95 7%	± 7 92%

Figure 3d shows a temporal coherence threshold surface for a static, spatially random patch of dots, 20 pixels per side and 1.6 sec in duration. The long duration was dictated by pilot studies showing temporal integration of sensitivity up to durations well over a second. Nevertheless, this stimulus is much harder to see than a checkerboard pattern, and the thresholds are therefore much higher The lowest average threshold is about 82% coherence.

Table 1 lists the range of means and the average standard deviation (excluding the blind spot) for the four tests. The S D. and the upper end of the range are slightly depressed for the temporal coherence test because a few subjects were unable to see one or more fully coherent targets. Also, the range and S.D. of the duration test are expanded because some subjects consistently saw single target frames, resulting in recorded duration thresholds of zero.

In addition to normals, we have begun to test glaucoma suspects (intraocular pressure >21 mm Hg, on at least three occasions, apparently normal otherwise) and glaucoma patients with confirmed field loss So far, our results for the size, duration and spatial coherence thresholds all appear to be consistent with data from the Octopus and Humphrey perimeters. However, temporal coherence thresholds often are elevated where sensitivity otherwise appears normal, both for confirmed glaucoma patients and glaucoma suspects These temporal coherence results look promising, and we are exploring ways to increase the range of coherence above normal threshold without reducing the test's apparent sensitivity to early glaucomatous defects.

Acknowledgements

References

1 Barlow HB, Levick WR, Yoon M: Responses to single quanta of light in retinal ganglion cells of the cat Vision Res Suppl 3: 87–101 (1971)

440

2 Kaplan E, Shapley RM: The primate retina contains 2 groups of ganglion cells, with high and low contrast sensitivity (Abstract) Invest Ophthalmol Vis Sci Suppl 25: 120 (1984)

3 Perry VH, Oehler R, Cowey A: Retinal ganglion cells that project to the dorsal lateral geniculate nucleus in the macaque monkey Neuroscience 12: 1101–1123 (1984)

4 Phelps CD, Blondeau P, Carney B: Acuity perimetry: a sensitive test for the detection of glaucomatous optic nerve damage Doc Ophthalmol Proc Ser 42: 359–363 (1984)

5 Quigley H, Addicks E, Green RW: Optic nerve damage in human glaucoma III Quantitative correlation of nerve fiber loss and visual field defect in glaucoma, ischemic neuropathy, papilledema, and toxic neuropathy Arch Ophthalmol 100: 135–146 (1982)

Authors' addresses:

Bruce Drum, Robert Massof, David O'Leary,

Laboratory of Physiological Optics, Wilmer Eye Institute, B-27, Johns Hopkins University School of Medicine, 601 North Broadway, Baltimore, MD 21205, U S A

Harry Quigley,

Glaucoma Service, Wilmer Eye Institute, B-110, Johns Hopkins University School of Medicine, 601 North Broadway, Baltimore, MD 21205, U S A

Michael Breton, Theodore Krupin,

Scheie Eye Institute, Presbyterian-University of Pennsylvania Medical Center, Myrin Circle, 51 North 39th Street, Philadelphia, PA 19104, U S A

Jerome Leight, John Mangat-Rai,

LKC Systems, Inc , 2 Professional Drive, Gaithersburg, MD 20879, U S A

VI.4 A computer-graphics visual field screener using high-pass spatial frequency resolution targets and multiple feedback devices

L. FRISÉN
Göteborg, Sweden

Rational testing of visual fields requires a filtering procedure capable of identifying those subjects who need a time-consuming examination in an advanced instrument, and those who do not. Such a procedure must be both quick and trustworthy. The first demand can be realized by reducing the number of tested locations, or by dispensing with exact threshold measurements, or both. Unfortunately, these strategies work directly against the demand of high dependability. A reduction in test locations should be less perilous if the test target is replaced with one that probes function over a larger visual field area than an ordinary perimetric target. Crisper visibility at threshold should also be advantageous, for quicker thresholding. So-called high-pass spatial frequency resolution targets appear promising in these regards [6, 7].

High-pass targets are best generated by computer graphics. This technique also allows the introduction of several modes of feedback for enhancing attention and motivation. A visual field screener devised along these lines will be briefly outlined in the following.

Materials and methods

Hardware

The test is adapted to IBM Personal Computers PC/XT and AT, and exact compatibles. A special graphics card and a 25 kHz black-and-white monitor with low-persistence phosphor are required, in addition to a system display. The latter shows options and test progression. The 17″ test monitor is set to 520 × 400 picture elements in noninterlaced mode, at 60 Hz. It is free from flicker. The modular set-up allows testing of subjects confined to beds or wheelchairs.

442

Software

The program has several phases (Table 1). Some of these terminate with a presentation of options for continuation, while others merge automatically. Optional demonstration and training sections are included, as is a blindspot-searching routine. Testing can be aborted any time, without wasting partial results. Track is kept of legal and illegal responses, reaction time, test duration, and other statistics. Records can easily be reviewed, compared, or printed on a dot-matrix printer.

Stimuli: properties, loci and threshold strategies

High-pass circular rings of 13 different sizes (step factor 1.26) serve as test targets (Fig. 1). Width is 1/5 of the diameter, and ranges over 10 to 160 minutes of arc. Core, border and background luminances are 25, 15 and 20 cd/m², respectively. Rings that are too small to be resolved are invisible because core and borders then blend into the background This makes detection and resolution thresholds closely similar [6]. Targets are shown for 165 ms only, to frustrate refixation.

There are 50 test locations within 30° of eccentricity (Fig. 2). To ensure a uniform distribution of information even upon premature termination of the test,

Table 1 Sequential outline of the new test Sections marked with asterisks can be disabled Test can be stopped for rest or terminated any time without loss of partial results

–	Calibration display
* –	Brief instructions
–	Main selection menu
* –	Demonstration of blindspot test
* –	Automatic blindspot search
* –	Demonstration of test targets
* –	Demonstration of field test
–	*Phase 1* screening for very extensive field defects by means of 20° diameter target in each quadrant center If positive, the corresponding quadrant is excluded from further testing
–	*Phase 2* finding threshold level in center of remaining quadrants Bracketing steps 3-2-1 dB
–	*Phase 3* finding thresholds in 5 strategically spaced points in each quadrant Start level is based on center result, with adjustment for eccentricity, but may be modified by incoming results in other loci Bracketing steps 2-1 dB
–	Interpolation of best start values for remaining loci
* –	Mid-test rest interval
–	*Phase 4* finding thresholds in remaining locations Bracketing step 1 dB
–	*Phase 5* checking results for smooth slopes, and retesting up to 10 locations Step factor 1 dB
–	Statistical analysis, graphic display of results, writing to disk
* –	Printing results
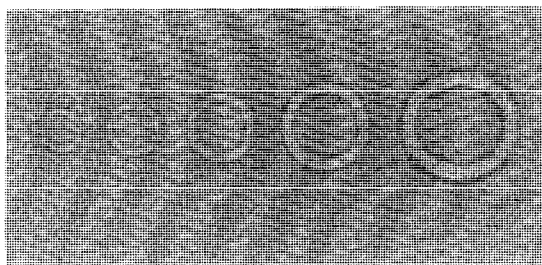
Figure 1 Photograph of part of the test target series Note how the number of visible rings changes with altered viewing distance

loci are distributed among 3 groups. These are tested in sequence, with random order within each group.

Thresholds are bracketed in up-and-down strategies employing unequal step sizes (Table 1), continuously alternating among loci. The start value is based on any information obtained for nearby loci. A single change of sign for a 1 dB step defines the threshold. Final results are checked for a monotonic increment with increasing eccentricity. Up to 10 deviating loci are retested The retest results illuminate reproducibility.

Feedback

Each legal response is acknowledged b a brief display of a contrasting square at the tested locus. This allows the subject to check for coincidence of actual and perceived locations. An erroneous response can be corrected on the fly, by pressing the response button for 1–5 s. Illegal responses are signalled by annoying beeps, and a brief exchange of the fixation mark for an 'error' text. The pace is adapted to the current reaction time, with a random component to discourage 'metronome responses'. Rest can be requested anytime, by keeping the response button depressed for more than 5 s.

Fixation promotion and checking

The fixation mark consists of a high-contrast cross subtending 2° The cross contracts smoothly just before target presentation. The movement is calculated to attract fixation, to cue extra attention, and to counteract after-images. Subjects automatically tend to synchronize blinks with target-free intervals. The fixation mark is occasionally briefly replaced by a 'look here' text.

Any tendency to loose fixation with too long delays between seen targets is counteracted by showing a 'catch' target after 4 non-seen presentations Catch
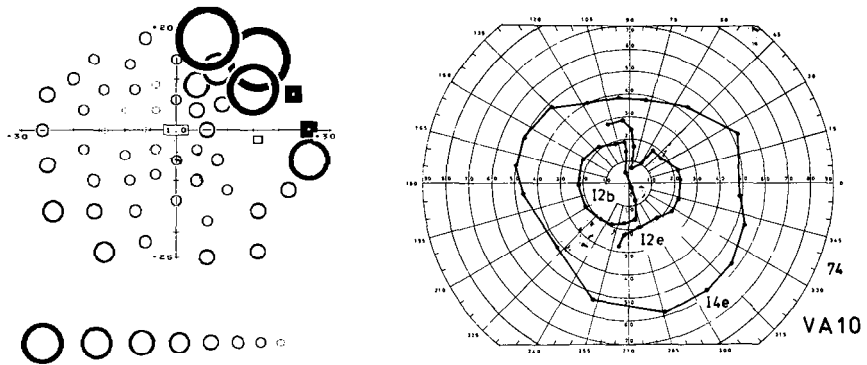
Figure 2 Comparison of results in the new test (left) and in manual perimetry, in the right eye of a subject with a midchiasmal lesion Note the different field coverage In the new test, results are given as size of threshold target in each tested location Only the upper nasal quadrant shows normal thresholds Black squares identify loci were the largest target was not seen Range of target sizes is shown below Inset: visual acuity Test time 6 2 min, retest change 0 5 ± 0 9 dB

targets are shown in different positions until a legal response is obtained. Size is about 2 dB larger than the local threshold.

Fixation is checked by occasionally presenting a high-contrast target in the blindspot area. A response initiates the error routine dscribed above and decreases temporarily the intervals between checks.

Results

Although the new test is fundamentally different from ordinary perimetry, experience from more than 200 examinations of normal and abnormal visual fields indicates that it furnishes qualitatively similar results. Quantitative comparisons are not meaningful because the two methods give radically different views of visual capacity (see Fig. 2 for an example). Comparisons of sensitivity and specificity are possible, however, and are being planned. Although precise normal limits remain to be defined, it seems that subtle abnormalities may be easier to identify in the new test, but this requires confirmation.

Average testing time was 5.0 ± 1.5 (SD) minutes for 50 consecutive eyes. Most had field defects, ranging from barely discernible to very severe. Retest variability (as estimated within each test) had a median value of 0.3 dB, and median SD was 1.2. Median duration of the blindspot search equalled 15 s. The modal number of recorded fixation losses was 0.

While experience with the new test as yet is fairly limited, it appears to meet the demands on an efficient screening procedure. Automatic perimeters typically use 2–4 times more time for a similar task [8]. An accurate assessment of dependability requires a larger case material, but the first impressions are encouraging.

Discussion

Several visual field tests using microcomputers and television displays have been described previously [1–4, 9, 11]. All have mimicked classical perimetric procedures of assessing differential light sensitivity. This approach is not necessarily the best. It has at least one major short-coming in addition to its time-consuming nature, namely the difficulty of understanding how the results reflect the state of the visual system. Resolution measurements are superior in this regard because of the simple relationship that exists between measuring values and the spatial density of functional néural channels [5, 10]. Unfortunately, conventional measurements of resolution in peripheral vision are very demanding: resolution is much more difficult than mere detection. High-pass spatial frequency filtering offers a unique solution to this problem by closing the gap between detection and resolution thresholds [6, 7].

Generating high-pass targets by computer graphics is fairly straightforward although corrections need to be made for screen curvature and glass thickness It is more problematic to define the best compromise between cost and performance. A radically improved resolution, for instance, would allow threshold measurements closer to the fixation point However, it would also raise the cost of equipment very considerably. The present compromise seems adequate for clinical needs.

Disadvantages appear limited to the inability to identify scotomata of smaller diameter than the locally liminal test target, and the inability to measure precise depth within small, circumscribed defects. While theoretically objectionable, these limitations should have little if any significance in clinical practice.

Patient acceptance was nearly universally good. The exceptions generally concerned a too high pace. This is not a reflection of a design fault but of failure to explain how the test adapts to the subject's own tempo. On informal questioning, a very clear majority of subjects preferred the new test over conventional perimetry. Features that were particularly appreciated included the interesting task, the sense of being in command, the feedback, and the intelligible result presentation.

Note

The author has a proprietary interest in the computer program described here, but not in the design principles.

References

1   Accornero N, Beiardelli A, Cruccu U, Manfredi M: Computerized video screen perimetry Arch Ophthalmol 102: 40–41 (1984)

2 Béchetoille A, Dauzat M, Brun Y: Présentation d'un systeme automatisé d'analyse du champ visual central Bull Soc Ophtalmol Franc 82: 491–493 (1982)

3 Chaplin GBB, Edwards JH, Gedye JL, Marlowe S: Automated system for testing visual fields Proc IEE 120: 1321–1327 (1973)

4 De la Rosa MG, Martin PA, Guerra PC, Moreno CM, Cedres DR, Martin SG: The hipocampus: instrument and strategies for screening campimetric lesions in glaucomatous patients Chibret Int J Ophthalmol 2: 42–53 (1984)

5 Frisén L: The neurology of visual acuity Brain 103: 639–670 (1980)

6 Frisén L: Vanishing optotypes A new type of acuity test letters Arch Ophthalmol 104: 1194–1198 (1986)

7 Howland B, Ginsburg A, Campbell F: High-pass spatial frequency letters as clinical optotypes Vision Res 18: 1063–1066 (1978)

8 Keltner JL, Johnson CA, Lewis RA: Quantitative office perimetry Ophthalmology 92: 862–872 (1985)

9 Matsuo H, Kikuchi G, Hamazaki S, Hamazaki J, Suzuki E, Yamada M: Automatic perimeter with graphic display Doc Ophthalmol Proc Ser 26: 1–7 (1980)

10 Phelps CD, Blondeau P, Carney B: Acuity perimetry: a sensitive test for the detection of glaucomatous optic nerve damage Doc Ophthalmol Proc Ser 42: 359–363 (1985)

11 Postaire JG, Hache JC, Diaf M: Fully automated procedure for early detection of visual field defects J Biomed Eng 8: 156–162 (1986)

Author's address:
Lars Frisén,
Department of Ophthalmology,
Sahlgren's University Hospital,
S-413 45 Göteborg, Sweden

VI.5 Peripheral displacement thresholds in normals, ocular hypertensives and glaucoma

F.W. FITZKE, D. POINOOSAWMY, W ERNST and R.A. HITCHINGS
London, United Kingdom

Abstract

Displacement thresholds may depend on processing by ganglion cells and, like contrast sensitivity and colour vision, may therefore be affected in glaucoma. However, unlike contrast sensitivity and colour vision, human sensitivity to motion is relatively retained outside the fovea so that displacement thresholds may provide a sensitive measure of ganglion cell mediated function throughout the visual field. We have investigated displacement thresholds to a 2 minute by 2 degree line generated by computer on a green phosphor video display unit. We found that displacement thresholds are abnormal in ocular hypertension and glaucoma and suggest that this may provide a more sensitive and specific measure of loss of vision in glaucoma and ocular hypertension than conventional perimetric measures.

There has been considerable interest recently in new methods of measuring visual function in glaucoma and ocular hypertension in part because it has been shown that glaucoma can cause the loss of a substantial number of optic nerve fibers and ganglion cells without detectable abnormality in standard perimetry [6]. It has long been known that ophthalmoscopically visible changes in the disc frequently precede detectable field loss [4] and early cup changes are thought to represent nerve fiber loss. This leads to the need for better clinical methods of detecting loss of vision.

A number of psycho-physical techniques have been used with varying success. These include measurements of contrast sensitivity [1] and measurements of colour vision [3]. If a psycho-physical response is heavily dependent on processing by ganglion cells then it may be that this would show greater loss than another response which is less mediated by ganglion cell processing.

The responses of monkey phasic ganglion cells have been measured to displacement of a stimulus and related to human psycho-physical measurements of displacement thresholds [8].

Since displacement thresholds may depend on processing by ganglion cells they, like contrast sensitivity and colour vision, may therefore be affected in glaucoma. However, sensitivity to motion is relatively retained outside the fovea (unlike contrast sensitivity and colour vision) so that displacement thresholds may provide a sensitive measure of ganglion cell mediated function throughout the visual field.

Human displacement thresholds measured psycho-physically depend on retinal eccentricity [7], luminance, line length, and duration of movement [5]. For brisk-sustained ganglion cells in the cat retina response depends on contrast and bar length [2]. These factors suggest that varying the parameters of the stimulus may allow optimization of selectivity to damage of ganglion cells. We have begun our study of displacement thresholds in glaucoma and ocular hypertension by using a single, medium contrast, green line.

We have measured displacement thresholds to a 2 minute by 2 degree vertical line generated by computer on a background on a green phosphor video display unit. The luminance of the background was 7 cd/m^2. and the stimulus was 27 cd/m^2. The background subtended 8 degrees by 10 degrees and was viewed at 1.24 meters. A warning tone was sounded which was followed by 1.5 seconds during which the stimulus was stationary. During the following 2 seconds the stimulus (if it were to move) would undergo displacement (at 2.5 Hz) which would begin at a random time after the start of this stimulus interval. If the patient pressed the response key before movement commenced, then this was counted as a false positive response. Displacement immediately ceased upon response. Reaction time following onset of motion was recorded. This was followed by a post-stimulus interval when the line remained stationary for 1.5 seconds. After a short instruction period measurements commenced. Frequency of seeing curves were constructed by presenting the moving stimulus 10 times (in random order) at 0–18 minutes of arc displacements at 2 minutes of arc intervals and asking the subject to press a response key when movement was seen.

Figure 1 a: the open circles show the fraction of stimuli seen as moving in a normal subject and the dashed lines indicate the 95% confidence limits from the probit analysis. The 50% point is indicated by the arrow at 4 2 minutes of arc b: summary of 50% points in the normal population
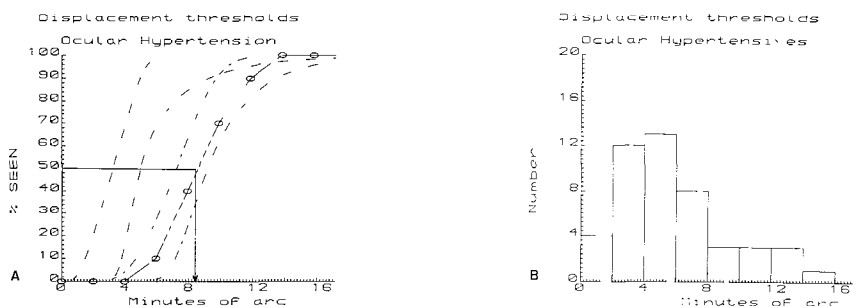
449

Figure 2 a: similar to the previous figure for a patient with ocular hypertension Values from the previous normal subject are also indicated for comparison b: summary of results of the thresholds for ocular hypertension

Measurements were made at 15 degrees in the temporal field just above and just below the blind spot (i.e., on the 30 and 330 degree meridians). The data were fit by probit analysis to provide a 50% point. A group of age matched normals was recruited from the spouses of patients. The mean age of the normals was 58.6 years with a standard deviation of 11.2. The mean age of the patients was 56.8 years with a standard deviation of 12.6. This was not significantly different (p = 0.6). The testing is completely under computer control and entirely automated. A measurement for each eye can be completed within ten minutes and there is no need for lengthy dark adaptation or other time consuming factors. The testing from the patient's point of view is very easy to understand and perform.

Displacement thresholds for a normal eye are shown in Figure 1a. The 50% point determined from a probit fit (using SPSS-X 21 release 2.1 University of London Computer Center) is indicated by the arrow and is 4.2 minutes of arc. The mean displacement threshold for 38 normal eyes (Fig. 1b) was 3.23' with a standard deviation of 1.9 minutes of arc.

Displacement thresholds for an eye with ocular hypertension are shown in Figure 2a. Note that the curve has been shifted to the right with a 50% point at 8.4
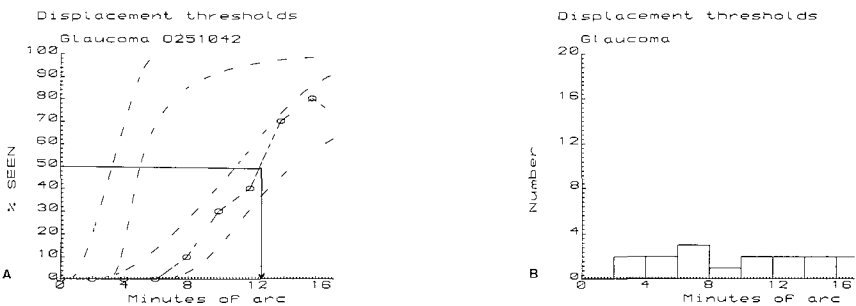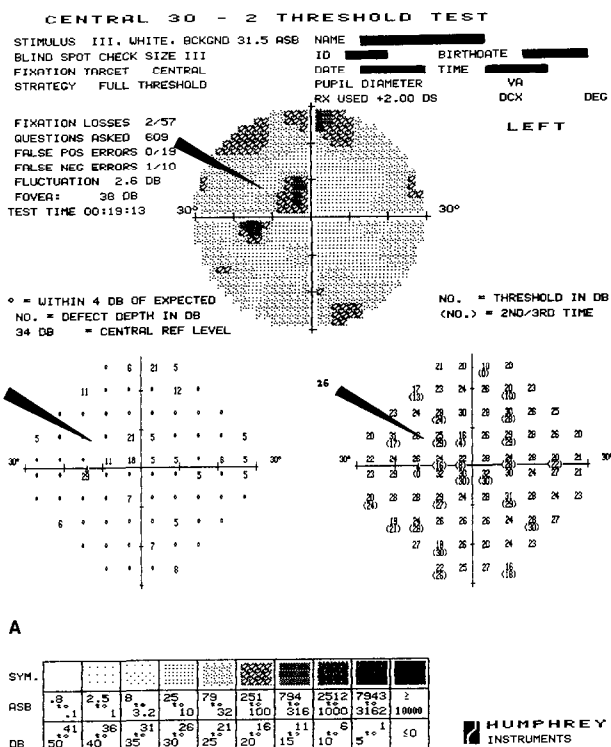

Figure 3 a: similar results for a glaucoma patient b: summary of results in glaucoma

450
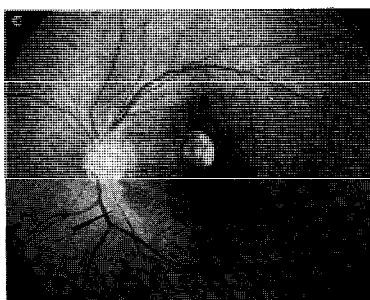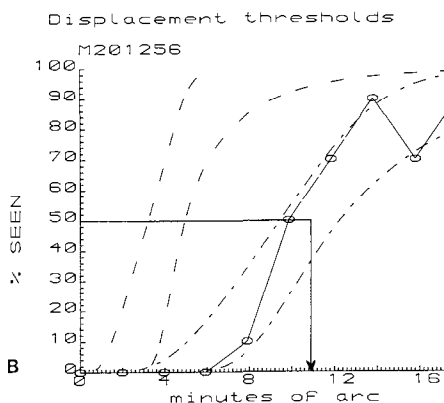
Figure 4 Results in one patient with low tension glaucoma a: Humphrey visual fields with arrow indicating test location b: results of displacement threshold determination This patient showed severely abnormal thresholds of 10 9 minutes of arc in an area where visual fields gave normal values c: retinal nerve fiber layer photograph with the test location indicated by the arrow A diffuse fiber defect was identified in that area

minutes of arc. In Figure 2b are summarized the results of 45 ocular hypertensive eyes which gave values of 5 49′ ± 3 14′.

The results of a measurement in an eye with glaucoma are shown in Figure 3a. Sensitivity to displacement has been severely reduced to 12.6 minutes of arc. 16 eyes with glaucoma gave values of 9.73′ ± 4 93′ (Fig 3b) The Newman-Keuls test showed these three groups to be different from each other at the 0 01 level

Case report: Figures 4a–c show the results in a patient with low tension glaucoma. Humphrey visual fields showed a small upper arcuate scotoma corresponding to the location of a haemorrhagic lesion (Fig 4a). The displacement thresholds were 10.9′ (Fig. 4b), determined in a visual field location (above the blind spot) with normal intensity (Humphrey) thresholds The retinal nerve fiber layer photograph (Fig. 4c) shows diffuse fiber defect in the area where the abnormal displacement thresholds were measured. That is, in this patient, in a location where conventional computer controlled perimetry showed normal sensitivity, displacement thresholds are severely abnormal.

In conclusion, we have found that peripheral displacement thresholds are abnormal in ocular hypertension and glaucoma Because sensitivity to movement is relatively retained in the periphery and because motion detection depends on processing by ganglion cells, perimetric displacement thresholds may provide a more sensitive measure of visual function abnormalities in ocular hypertension and glaucoma.

We are currently investigating the effects of spatial frequency, contrast, colour, and temporal frequency on perimetric displacement thresholds with the goal of finding a more sensitive and specific measure of loss of vision in glaucoma and ocular hypertension than conventional perimetric measures.

References

1 Arden GB, Jacobson JJ: A simple grating test for contrast sensitivity Preliminary results indicate value in screening for glaucoma Invest Ophthalmol Vis Sci 17: 23–32 (1978)
2 Cleland BG, Harding TH, Tulunay-Keesey U: Response to the length of moving visual stimuli of the brisk classes of ganglion cells in the cat retina J Physiol 345: 27–45 (1983)
3 Hamill TR, Post RB, Johnson CA, Keltner JL: Correlation of color vision deficits and observable changes in the optic disc in a population of ocular hypertensives Arch Ophthalmol 102: 1637–1639 (1984)
4 Hitchings RA, Spaeth GL: The optic disc in glaucoma: II Correlation of the appearance of the optic disc with the visual field Br J Ophthamol 61: 107–113 (1977)
5 Johnson CA, Scobey RP: Foveal and peripheral displacement thresholds as a function of stimulus

luminance, line length and duration of movement Vision Res 20: 709–715 (1980)

6 Quigley HA, Addicks EM, Green R: Optic nerve damage in human glaucoma III Quantitative correlation of nerve fiber loss and visual field defect in glaucoma, ischemic neuropathy, papilledema, and toxic neuropathy Arch Ophthalmol 100: 135–146 (1982)

7 Post RB, Scobey RP, Johnson CA: Effects of retinal eccentricity on displacement thresholds for unidirectional and oscillatory stimuli Vision Res 24: 835–839 (1984)

8 Scobey RP, Horowitz JM: Detection of image displacement by phasic cells in peripheral visual fields of the monkey Vision Res 16: 15–24 (1976)

Author's address:
Institute of Ophthalmology,
Judd Street,
London WC1H 9QS, England

VI.6 Application of the Troxler effect in campimetry of glaucoma suspects

I. IINUMA
Wakayama, Japan

Abstract

A trial campimeter with three illuminating systems, one for the target holes (a), a second for the screen (b), and a third for additional screen illumination providing for the off-response (c) is presented. The subject stares at the fixation point in the center of the lighted screen campimeter without blinking; the light (c) is then turned off. If there is any depression in the visual field, the subject may notice some of the target lights have vanished due to the Troxler effect (TE) excited by the off-response. In glaucoma suspects this effect can be detected in the Bjerrum area in the very early stages of the disease.

Introduction

The clinical application of the Troxler effect has been limited to only a small number of works [2, 3, 8, 9] since the effect was first reported in 1804 by Troxler [10].

I used a trial perimeter in which the Troxler effect (TE) excited by off-response is applied. The results obtained for patients with primary open angle glaucoma (POAG) and glaucoma suspects (GS) as well as the results for normal and subnormal subjects are reported in this paper

A trial campimeter

The instrument (Fig. 1)

A trial campimeter consists of a flat screen with a central fixation point and 80 target holes. The target holes are lined up in five concentric rings forming 16 meridians within a 25 degree field; the holes are four mm in diameter on the
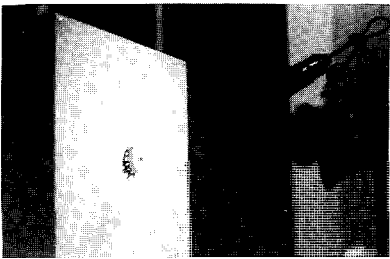
Figure 1 Trial campimeter

innermost circle and five mm on the other four circles. There are three illuminating systems described as follows:
(a) the light for the target holes illuminated from a light box behind the screen,
(b) the main background illumination of the campimeter field from the front which is set constant during the test, and
(c) an additional background field illumination also from the front designed to evoke the off-response [1, 4, 5, 6, 7] in observers. The Troxler effect can be evoked by both on-response and off-response. However, it is easier for the observer to notice the target disappear in the off-response than in the on-response.
The luminance of the (a), (b) and (c) lights are ordinarily 500, 16 and 5 asbs respectively; that of (a) can be lowered to 400, 315, 250 or 200 asbs according to the patient, (for older subjects lower luminance may be better to avoid glare); and that of (c) can be adjusted between 1 to 15 asbs (Table 1).

Method

The campimeter is placed in a dark room, and all three illuminating systems are turned on. For the illumination (c), a luminance of five asbs is normally used as the starting point which is then made darker or brighter according to the case.

The subject sits 30 cm in front of the campimeter, one eye covered, looking at the central fixation point without blinking or moving during the main test period (5–10 seconds).

Table 1 Various light intensities

Target lights		a)	200 ------------------------------ *500* asbs
Field illumination	main	b)	*16*
	additionals	c)	1 ---- 5 -------------------------- 15

c) Used for excitation by the off-response
in italic: used most commonly
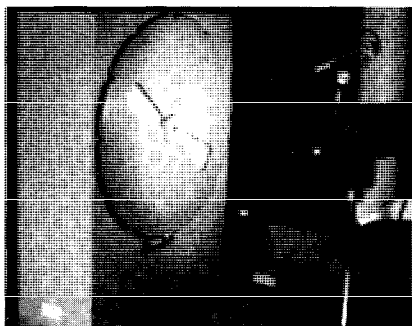
Figure 2 Cover with propeller-shaped windows This cover allows the observer to notice the vanishing of target lights more easily because of a small number of symmetrically placed stimuli

The operator makes a sign for the subject to keep his eye open after one blink At the same time, the operator turns on a time switch which is connected to the off-switch of the (c). After two seconds, the illumination (c) is turned off. If the subject can notice that some target lights in the field have vanished, he reports them. The test is repeated several times, changing the luminance of the illumination (c) to obtain a static quantitative campimetric map.

It is important that the subject understands that the target lights may vanish from his sight in spite of the fact that they are still illuminated. For this reason the subject must be trained several times before the main test Untrained subjects frequently miss the vanishing of several lights because of eye movements induced by many other extra-central target lights in the field In uncertain cases, I use a cover with propeller-shaped windows on the surface of the instrument (Fig. 2) This cover hides the entire field except for two symmetrical areas, each with a meridian of 30 degrees and a field angle of 20 degrees By turning this cover six times the whole area can be easily surveyed

Results

Glaucoma suspects (GS)

Twenty-four cases of GS showing no definite glaucomatous findings except for glaucomatous cuppings of the optic nerve head (C/D>0 4) were examined using the trial campimeter with the excited TE. Vanishing of some target lights in the Bjerrum area was observed in both eyes in all cases (Fig. 3)
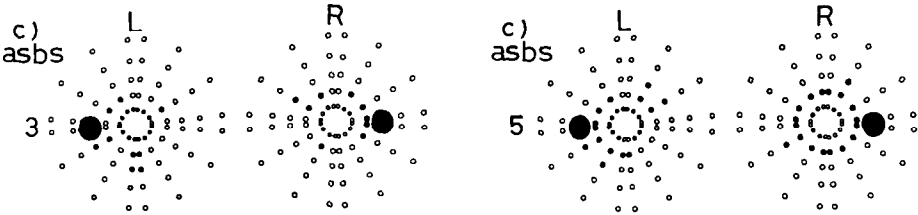
Figure 3 A glaucoma suspect: a ten-year-old boy showing cupping of the optic discs with C/D ratio of 0 7 (R) and 0 65 (L) but with no other glaucomatous findings Vanishing of the target lights is observed in the Bjerrum area from the TE excited by the off-response of 5 asb of the illumination (c) and even of 3 asb (April 5, 1986) The vanished target lights are shown by black dots (●●), as in Figs 4 and 5

Primary open angle glaucoma (POAG)

Ten cases of POAG, with diagnosis based on several glaucomatous signs such as elevated intraocular pressures, enlarged cupping of the optic nerve heads, or glaucomatous field defects were examined with the same instrument. Vanishing of the target lights produced by the excited TE in the Bjerrum area was observed in both eyes in all cases. In the majority of the cases the area with vanished target lights had broked through into periphery of the field (Fig. 4) (Table 2).

Normal or subnormal subjects

There were twenty subjects in this group. All were under 60 years of age. Seven

Table 2 Results in glaucoma

Cases	Sex	Number	Average age	Result
GS	F	17	53 9	Some of the target lights vanished in BA in all cases
	M	7	38 4	
POAG*	F	7	55 1	Most of the target lights vanished in BA in all cases
	M	3	44 7	

GS: glaucoma suspects
POAG: primary open angle glaucoma
* This group includes only patients under 60 years of age
BA: Bjerrum area
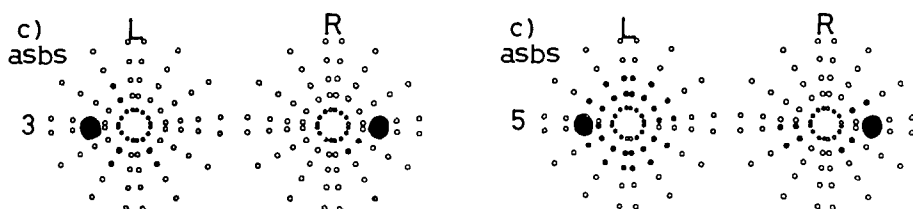
Figure 4 A low-tension glaucoma: a 12-year-old boy with cupping of C/D of 0 6 (R), 0 7 (L), and nasal step in both visual fields Vanishing of the target lights is detected in the Bjerrum area using the TE excited by off-response of 5 asb and even of 3 asb (July 18, 1986)

were considered almost perfectly normal and the others, subnormal. The subnormal subjects included individuals who had good visual acuities, almost normal visual fields by the Goldmann perimeter, no abnormal ocular findings or complaints but who showed slightly blurred margins and/or slight temporal atrophies of the optic nerve heads ophthalmoscopically

With this group, vanishing of the target lights was seen in the para-central area in five cases with the off-response of five asbs, in nine cases with 10 asbs, and in 12 cases with 15 asbs. The rest of the cases showed no vanishing under any given condition.

Fig. 5 shows maps of vanished target lights in one of the cases in this group.

Discussion

I have clinically applied the TE excited by the off-response in the early diagnosis of POAG, especially in GS. I believe the mechanism of this examination to be as
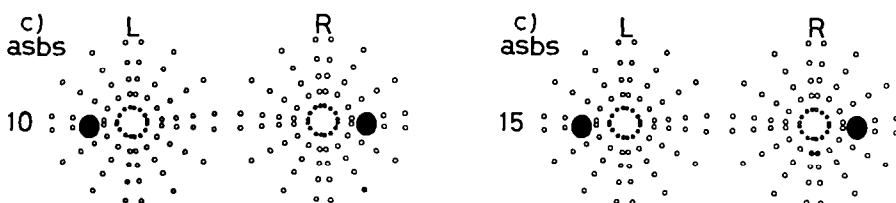
Figure 5 A normal or subnormal case: an 8-year-old boy with an anamnesis of 'Kawasaki disease' (muco-cutaneous lymphadenoma syndrome) 5 years ago Margin of the optic disc is slightly blurred Vanishing of the target lights is detected in the para-central area by the TE excited by the off-response of 10 and 15 asb of illumination (c), but not of 5 asb (April 20, 1986)

follows: under normal condition, when a background illumination is partly extinguished, the subject's eye immediately makes an adaptation to the darker field. If there are target lights in the field, they may be seen as brighter than before. However, under abnormal conditions, the target lights may become too bright for the eye. The eye adjusts to the over-brightness most likely by means of the autonomic nerves [9] The weak part of the retina may quickly respond and produce an inhibitory charge resulting in the vanishing out some of the target lights.

Conclusion

Twenty-four patients regarded as glaucoma suspects with cupping of the optic discs (C/D>0.4) but no elevated intraocular pressure or visual field defect by the Goldmann perimeter were tested with the Troxler effect in the target lights exited by the off-response in the background illumination. All subjects noticed the vanishing of the target lights in the Bjerrum area.

References

1 Crawford BH: Visual adaptation in relation to brief conditioning stimuli Proc Roy Soc B 134: 283–302 (1947)
2 Enoch JM, Sunga RN, Bachmann E: Static perimetric technique believed to test receptive field properties Am J Ophthal 70: 113–126 (1970)
3 Enoch JM, Sunga RN, Bachmann E: Static perimetric technique believed to test receptive field properties II Adaptation of the method to the quantitative perimeter Am J Ophthal 70: 126–137 (1970)
4 Iinuma I: Trial campimetry based on a new idea making use of Troxler phenomenon Folia Ophthl Jap 36: 1154–1158 (1985)
5 Iinuma I: A trial campimeter adopting the vanishing of the target lights A preliminary report Ganka Rinsho Iho 79: 788–792 (1965)
6 Ikeda M, Boynton RM: Negative flashes, and flicker examined by increment threshold technique J Opt Soc Am 55: 560–566 (1965)
7 Pirenne MH: Light adaptation I The Troxler phenomenon In: Davson H (ed) The eye, Vol 2, pp 197–199 Academic Press, New York, 1962
8 Sunga RN, Enoch JM: A static perimetric technique believed to test receptive field properties III Clinical trials Am J Ophthal 70: 244–272 (1970)
9 Sunga RN, Enoch JM: Further perimetric analysis of patients with lesions of the visual pathways Am J Ophthal 70: 403–322 (1970)
10 Troxler IPV: Über das Verschwinden gegebener Gegenstände innerhalb unseres Gesichtskreises In: Himly K, Schmidt JA (eds), Ophthalmol Bibliothek, Vol 2 F Fromann, Jena, 1804

Author's address:
1-18 3-chome Higashi-hagoromo,
Takaishi-shi Osaka-fu 592, Japan

Section VII
Fundus perimetry

VII.1 Visual field in diabetic retinopathy – light sensitivity in retinal lesions

K. YABUKI, T. OGAWA and H. MATSUO
Tokyo, Japan

Abstract

We examined regional retinal sensitivity in diabetic retinopathy by superimposing fluorescein angiograms on Octopus results.

The decrease of retinal sensitivity at the site of each retinal lesion was found to depend on the degree of retinal capillary abnormality. In extensive areas of non-perfusion the retinal sensitivity decreased and frequently showed 0 dB on the Octopus system. Scotomas of various depth were detected on kinetic perimetry using a fundus perimeter, and the margins of the scotomas agreed almost completely with the outline of the non-perfusion area depicted on the fluorescein angiogram.

Introduction

Most former studies of visual fields in diabetic retinopathy have been concerned only with disseminated changes in each stage [5, 9]. Meanwhile, fluorescein angiography studies suggested that diabetic retinopathy was primarily the result of occlusion of retinal capillaries. While a correlation between capillary abnormality as revealed by fluorescein angiography and retinal dysfunction, i.e., visual field abnormality can be expected, this point has not received sufficient attention [1, 2, 6–8].

The authors examined patients using computerized perimetry (Octopus) and fluorescein angiography to study the correlation capillary abnormalities and retinal sensitivity.

Subjects

We examined 67 eyes of 50 patients with different stages of diabetic retinopathy,
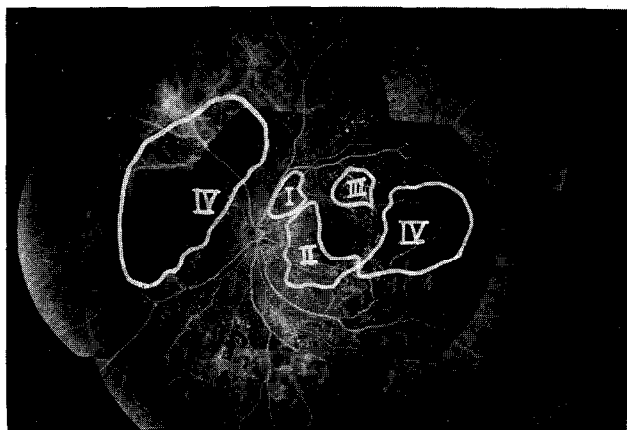
Figure 1 Examples of Type I-IV lesions were outlined on the fluorescein angiogram

consisting of simple retinopathy in 18 eyes, 38 eyes with preproliferative retinopathy and 11 eyes with proliferative retinopathy.

Methods

Composite panoramic views of the fluorescein angiographic findings of the retina were made with a fundus camera (CF 60Z, Canon Co., Tokyo). The retinal capillary lesions in case of diabetic retinopathy were classified into four types, according to the venous mid-phase findings of the fluorescein angiogram, as shown in Table 1. All lesions were outlined on the panoramic photographs as shown in Fig 1 Octopus programs 31 and 41 were performed in each eye. In some cases also kinetic perimetry was performed using the fundus perimeter. The panoramic fluorescein angiograms were inverted and superimposed on the Octopus results. The average loss per test point for each of the four types were calculated and the retinal sensitivity in each of the four types was estimated based on the amount of loss.

Table 1 Definition of the lesions of diabetic retinopathy

Type I	almost normal retinal capillary network
Type II	hyperpeimeability of microaneurysms or capillaries
Type III	small non-perfusion areas either solitary or in combination with surrounding hyperpermeability capillaries
Type IV	extensive non-perfusion areas
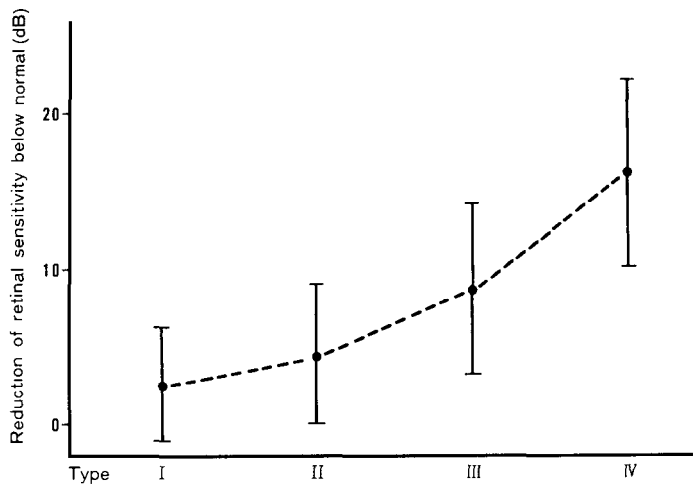
Figure 2 Average value of sensitivity loss from the Octopus normal values in the 4 types of lesion

Results

The average amount of sensitivity loss from the normal Octopus values was 2.6 ± 3.5 dB for type I, 4.4 ± 4.4 dB for type II, 8 6 ± 5.3 dB for type III and 16.1 ± 6.6 dB for type IV retinopathy. As retinal capillary lesions progressively deteriorated, the average amount of sensitivity loss also increased proportionately (Fig. 2).
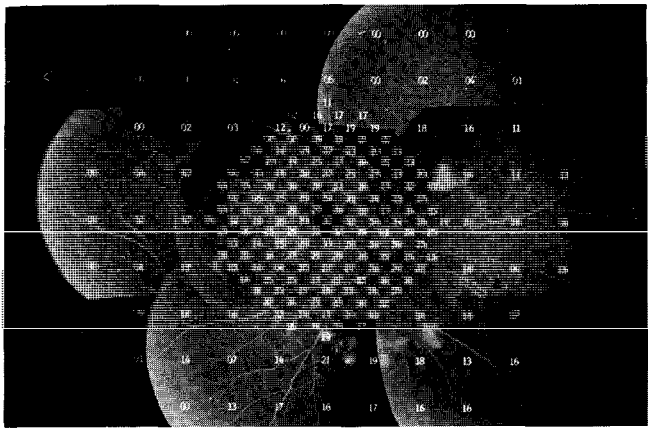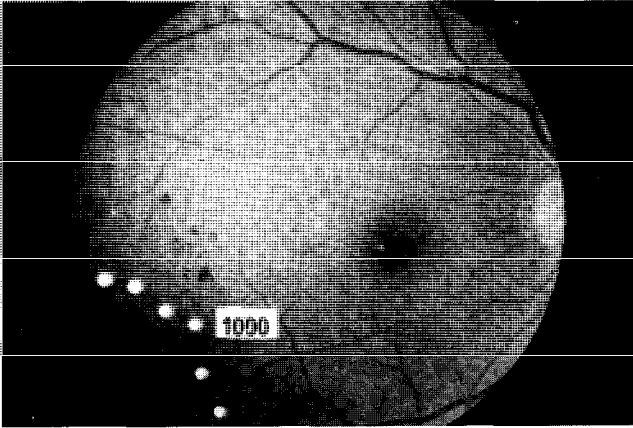
Statistically significant differences were recognized between each type. In

Figure 3 Fluorescein angiogram with superimposed Octopus results Retinal sensitivity in the extensive non-perfusion area of temporal region is markedly reduced

Figure 4 A maximum luminosity scotoma was detected using the fundus photo perimeter The white dots are response points at maximum luminance

extensive areas of non-perfusion the retinal sensitivity decreased frequently being 0 dB in the Octopus charts. However, some points showed approximately normal values. In kinetic fundus perimetry, non-perfusion areas appeared as scotomas of varying depths. These scotomas had steep descending edges, their border corresponding with the outline of the non-perfusion area on the fluorescein angiograms.

A typical type IV case is demonstrated in Figs 3–5. In the fluorescein angiogram with superimposed Octopus results, retinal sensitivity is markedly reduced in the extensive non-perfusion area of the temporal region (Fig. 3). In addition, on kinetic perimetry using the fundus photo perimeter at 1000 asb a scotoma was
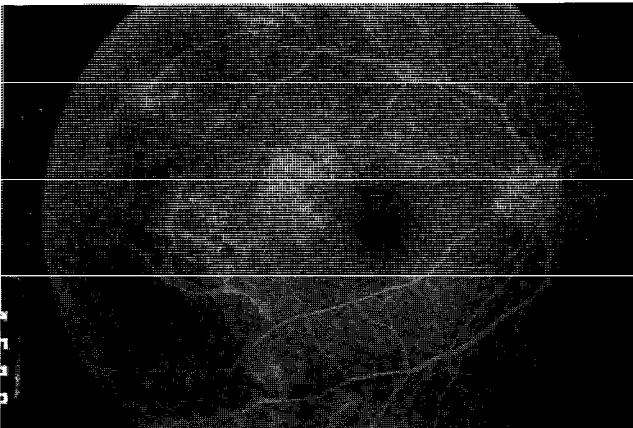
Figure 5 The scotoma border corresponded with the non-perfusion area
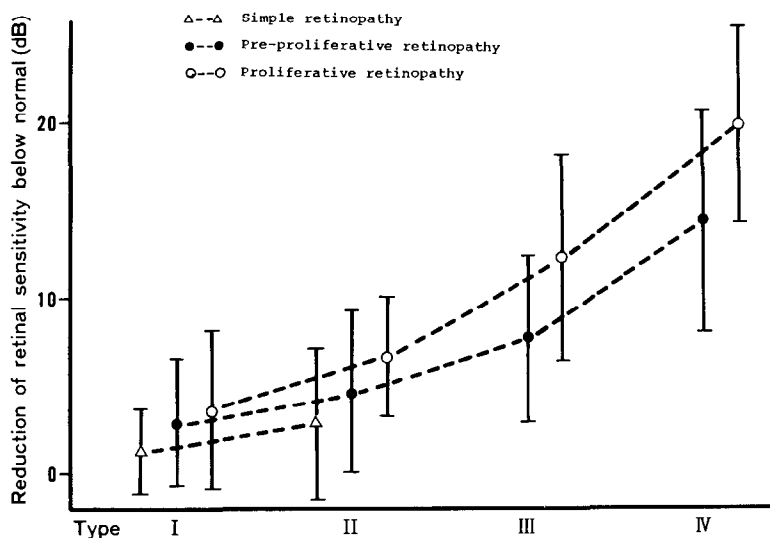
Figure 6 Average value of sensitivity loss from the Octopus normal values in the 4 types of lesion in various stages of diabetic retinopathy

detected (Fig. 4), the border of which agreed with the non-perfusion area on the fluorescein angiogram (Fig. 5).

When cases were divided into the categories of simple retinopathy, pre-proliferative retinopathy and proliferative retinopathy and the average value of sensitivity loss for each of the four types defined in Table 1 was calculated, it became clear that the decrease in retinal sensitivity for each type became more marked as the stage of the disease advanced (Fig. 6).

Discussion

Greite et al. [3] [4] studied changes in visual fields in diabetic retinopathy using the Octopus perimeter and reported that the decrease in retinal sensitivity was more marked in the mid-periphery than in the central area. They pointed out that, since capillary non-perfusion areas tended to occur in the middle peripheral areas, capillary non-perfusion areas were closely correlated with decrease in retinal sensitivity. Their method of comparison of visual field results with fluorescein angiograms remained somewhat vague, however.

Hasunuma et al. [6] compared fluorescein angiograms with Goldmann kinetic visual field results by a superimposition technique to study retinal sensitivity at non-perfusion areas in diabetic retinopathy, and concluded that:
1. The severity of visual field abnormality paralleled the degree of retinal capillary non-perfusion.

2. Visual field results generally did not show a complete defect but only a depression at non-perfusion areas.

3. The isopter contour corresponded to the non-perfusion area.

However, since kinetic perimetry is affected by spatial summation, static perimetry seemed more suitable for accurate evaluation of the loss in sensitivity associated with the retinal lesion.

Bell et al. [1] studied regional retinal sensitivity classified in terms of the state of capillary perfusion in both cases of diabetic retinopathy and retinal branch vein occlusion using the Octopus perimeter, and found that retinal sensitivity in these diseases correlated with the state of capillary perfusion and that there was no difference in sensitivity between the two disease entities above.

This suggests a correspondence between retinal sensitivity and capillary abnormality, which can be demonstrated by fluorescein angiography. The authors therefore examined retinal sensitivity in diabetic retinopathy in relation to four different conditions at sites of almost normal retina, hyperpermeability of microaneurysms or capillaries, relatively small non-perfusion areas and extensive non-perfusion areas. This revealed that the extent of decrease in retinal sensitivity depended on the type of lesion, i.e., it correlated with the severity and extent of retinal capillary abnormality.

In cases with extensive non-perfusion areas, the presence of scotoma at the maximum luminance level were anticipated, since not only capillaries but arterial branches were involved in the etiology.

However, an almost normal sensitivity remained at some sites. Moreover, a comparison of retinal sensitivity among the different stages of diabetic retinopathy at the sites of lesions detected by fluorescein angiography revealed that the more advanced the stage, the more markedly the sensitivity decreased. The above findings suggest that visual function in diabetic retinopathy cannot be completely grasped by fluorescein angiography alone.

References

1 Bell JA, Feldon SE: Retinal microangiopathy correlation of OCTOPUS perimetry with fluorescein angiography Arch Ophthalmol 102: 1294–1298 (1984)

2 Gandolfo E, Zingirian M, Corrallo G, Piccolino FC: Diabetic retinopathy: Perimetric findings Doc Ophthalmol Proc Series 35: 443–448 (1982)

3 Greite JH: OCTOPUS-Perimetry in diabetic retinopathy (DR): Proceedings, First International Meeting on Automatic Perimetry System-OCTOPUS, pp 107–115 Interzeag, Schlieren, 1979

4 Greite JH, Zumbansen HP, Adamczyk R: Visual field in diabetic retinopathy (DR) Doc Ophthalmol Proc Series 26: 25–32 (1981)

5 Harrington DO: The visual fields (4th ed), p 169 CV Mosby, St Louis, 1976

6 Hasunuma T, Muraoka K, Kitagawa M, Niki T, Tsuji K, Awane H: Correlation between capillary non-perfusion and visual field in diabetic retinopathy Jpn J Clin Ophthalmol 36: 1053–1063 (1982)

7 Ishikawa K, Shimotori M, Oshitari M: Studies on the diabetic maculopathy [1] Acta Soc Ophthalmol Jpn 77: 1411–1421 (1973)

8 Tamura T, Fukuda M, Tamura M: Static perimetry and diabetic retinopathy Jpn J Clin Ophthalmol 28: 1123–1131 (1979)
9 Wisznia KI, Lieberman TW, Leopold IH: Visual fields in diabetic retinopathy Br J Ophthalmol 55 183–188 (1971)

Author's address:
Department of Ophthalmology,
Tokyo Medical College Hospital,
6-7-1, Nishishinjuku, Shinjuku-ku, Tokyo, Japan 160

VII.2 Early foveal dysfunction in glaucoma

K. MIZOKAMI, N. KATSUMORI and H. MIYAZAWA
Kobe, Japan

Abstract

In this study, we evaluated the correlation between foveal dysfunction and the atrophic appearance of retinal nerve fiber bundles in early to middle stage glaucoma by using a fundus perimeter (Quantitative Maculometer). Measurements of spatial contrast sensitivity function (SCSF) were also carried out.

Our study of ten patients with macular nerve fiber atrophy demonstrated that open angle glaucoma can involve the central field, including fixation, before the peripheral visual field is markedly distorted The grade of SCSF damage seemed to be well correlated with the degree of maculo-papillar nerve fiber bundle atrophy.

Introduction

Traditionally, it had been believed that foveal function was preserved until very late in the course of primary open angle glaucoma.

But recently, diffuse involvement of the field in the form of a generalized depression has been recognized as an early glaucomatous defect in spite of the presence of proceeding localized nerve fiber bundle atrophies [1, 2, 7].

In this study, we evaluated the correlation between foveal dysfunction and atrophic appearance of retinal nerve fiber bundle in early to middle stage glaucoma by using a fundus perimeter (Quantitative maculometer [4]), because a generalized depression might logically involve the point of fixation.

Materials and methods

We examined ten cases with early to middle stage primary open angle glaucoma, who had detectable retinal nerve fiber layer defects (NFL defects) within the

maculo-papillar bundles, in spite of normal visual acuities (over 1.0) (Tables 1–3) The NFL within the maculo-papillar bundles was determined by red-free, stereoscopic fundus photographs.

In every case, macular sensitivities were determined using a fundus perimeter (Quantitative maculometer [4]). By using this apparatus, while observing the fundus, we can examine the exact position at the fovea on the ring scale (Figs 1–3) very accurately and constantly.

The concentric circles in the ring scale indicate 2.5, 5.0 and 10° of visual angle and the meridional divisions are at every 45°.

In this study a 250 asb background was chosen; the stimulus was 6.37′ in diameter. A 250 msec duration was used for static measurements and continuous light for kinetic measurements. The measurement of spatial contrast sensitivity function (SCSF) were carried out by a modified [5] TV-display system. The spatial frequencies were 0.7, 1.4, 2.5, 3.5, 7.0 and 15 0 cpd.

Results

According to the appearance of NFL, the ten cases could be divided into three groups. In the first group slit like NFL defects were seen within the maculo-papillar nerve fiber bundles (Table 1, cases 1–3). In the second group, bundle-like atrophies were seen in the maculo-papillar nerve fiber layer (Table 2, cases 4–6). In the third group diffuse atrophic patterns were already evident, in spite of only moderate glaucomatous visual field damage (Table 3, cases 7–10). Case 1 (Fig. 1) showed macular slit-like NFL defects accompanied with lower arcuate nerve fiber layer defects. Corresponding to the defects, points with depressed sensitivity (up to 1.8.1.u. in two points) were seen using the quantitative maculometry. SCSFs were slightly altered at the lowest frequency (Table 1) Cases 2 and 3 also showed slit-like NFL defects within the upper and lower macular fiber bundles accompanied by one depressed point and slightly lowered at the lowest frequency SCSF (Table 1)

Table 1 The cases with slit-like macular nerve fiber atrophy

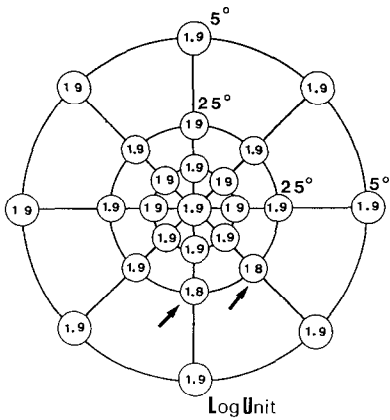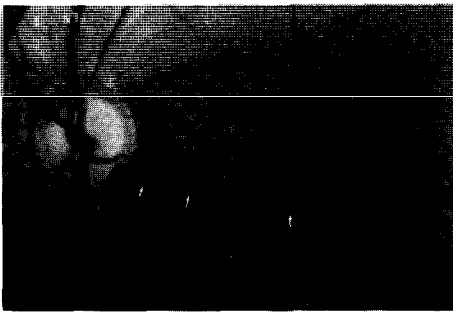| Slit Atrophy	Visual acuity	SCSF (Cpd)						VSF
		0 7	1 4	2 5	3 5	7 0	15 0	
Case 1, 51, F, left	1 2	45	88	118	145	152	99	Upper central nasal depres
Case 2, 49, M, left	1 0	31	70	93	83	98	59	Lower few scotomas
Case 3, 28, M, right	1 0 −7 0 D	32	82	114	118	101	63	Lower arcuate scotoma

Figure 1 Case 1, 51 y, F, macular slit-like nerve fiber atrophy (white arrows) accompanied by points with depressed sensitivity (black arrows) on quantitative maculometry

Table 2 The cases with bundle-like macular nerve fiber atrophy

Bundle Atrophy	Visual acuity	SCSF (Cpd)						VSF
		0 7	1 4	2 5	3 5	7 0	15 0	
Case 4, 48, M, left	1 5	27	77	104	102	87	66	Up cent nasal step & scotoma
Case 5, 58, F, left	1 5	33	55	82	82	93	51	Up cent nasal step
Case 6, 44, M, right	1 0	25	67	89	91	87	49	Up nasal depression

Table 3 The cases with diffuse macular nerve fiber atrophy

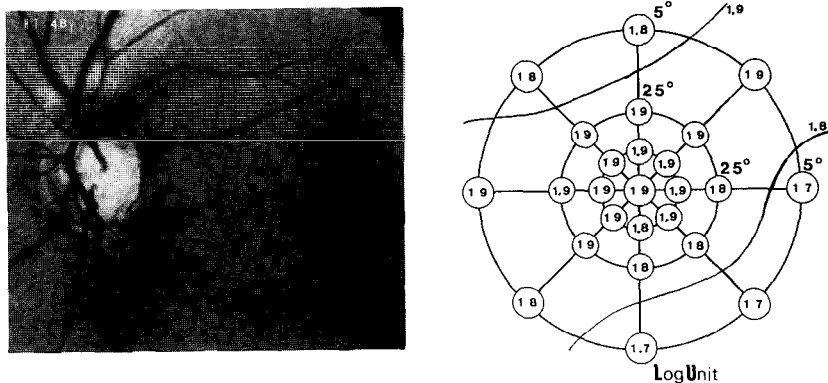| Diffuse Atrophy	Visual acuity	SCSF (Cpd)						VSF
		0 7	1 4	2 5	3 5	7 0	15 0	
Case 7, 36, M, left	1 0 −4 0 D	25	61	75	53	23	12	Double arc scotoma
Case 8, 38, M, right	1 0 −1 0 D	25	48	73	107	114	31	Double arc scotoma
Case 9, 57, M, right	1 2 −2 0	17	36	53	55	69	32	Up few scotomas
Case 10, 37, M, right	1 0	16	31	33	33	25	9	Double arc scotoma

LogUnit

Figure 2 Case 4, 48 y, M, macular bundle-like nerve fiber atrophies (arrows) are seen In accordance with the atrophy, a wide area with depressed points is seen

Case 4 (Fig. 2) showed macular bundle-like NFL defects in the lower and upper macular fiber bundles and foveal dysfunction was seen in accordance with the NFL defect using the quantitative maculometry.

In this case SCSF was slightly damaged especially at the lowest and highest spatial frequencies (Table 2). Cases 5 and 6 were similar to Case 4 (Table 2).

Case 7 (Fig. 3) already showed diffuse macular NFL defect and foveal sensitivity depression in spite of only moderate glaucomatous visual field damage (Fig. 4). SCSF was significantly lowered especially at the lowest and highest spatial frequencies (Table 3). Similar results were seen in Case 8, 9 and 10 (Table 3).
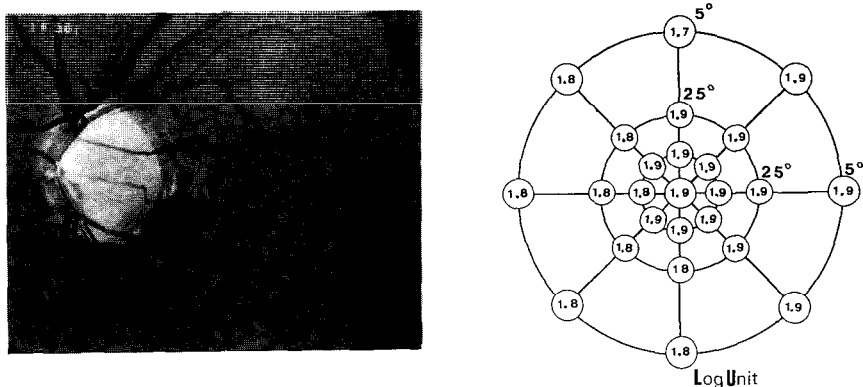

LogUnit

Figure 3 Case 7, 36 y, M, diffuse macular atrophy and sensitivity depressions are already seen in spite of only moderate glaucomatous visual field damage
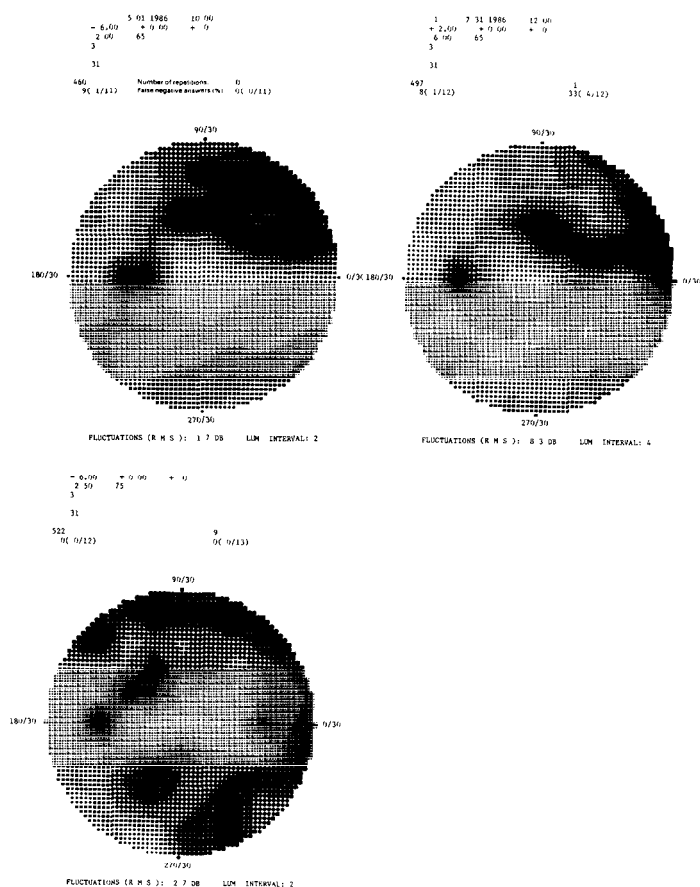
Figure 4 Results of computerized perimetry on the Octopus perimeter (program 31) in cases 1 (upper left), 4 (upper right), and 7 (below)

Discussion

In primary open angle glaucoma central vision is usually preserved until very late in the course of the disease. When central vision is involved marked peripheral field loss is often present as well.

In this study, by using the Quantitative maculometer [4], we evaluated the correlation between foveal dysfunction and the atrophic appearance of retinal nerve fiber bundle in early to middle stage glaucoma.

The brightness of the background in the Quantitative maculometer was chosen to 250 asb. At this level, the patient will not be dazzled under light adaptation and we can observe the fundus accurately.

By using this instrument, it is possible to point out the accurate position of areas

with depressed sensitivity in the macula.

Our study of ten patients demonstrated that foveal involvement in glaucoma was not limited to patients with severe glaucomatous optic nerve damage. Further, a close relationship was found between the depression of sensitivity and atrophic patterns in the papillo-macular nerve fiber bundles.

Employing a modified video display system [5], the spatial contrast sensitivity functions (SCSF) were also evaluated in this study. By studying the SCSF, it is possible to detect a visual function deficiency which cannot be found using conventional acuity tests. It was also documented that the SCSF damage develop almost in parallel to the grade of papillo-macular bundle atrophy. Our results show a depression of sensitivity to low and high frequencies in glaucoma, confirming previously published results [7].

According to a recent study [3], it has been believed that the ganglion cells whose dysfunction results in reduced SCSF are different from the cells whose death is responsible for the first glaucomatous field defects. So in some patients with macular nerve fiber atrophy already in early stage glaucoma it may occur that visual sensitivity to low and high spatial contrast frequency function is reduced, while visual acuity is still preserved.

Acknowledgement

References

1 Ancil JL, Anderson DR: Early foveal involvement and generalized depression of the visual field in glaucoma Arch Ophthalmol 102: 363–370 (1984)
2 Anderson DR: What happens to the optic disc and retina in glaucoma? Ophthalmology 90: 766–770 (1983)
3 Enroth Cugell C, Robson JG: The contrast sensitivity of retinal ganglion cells of the cat J Physiol 187: 517–552 (1966)
4 Isayama Y, Tagami Y: Quantitative maculometry using a new instrument in cases of optic neuropathies Doc Ophthal Proc Series 14: 237–242 (1976)
5 Isayama Y, Tagami Y, Ohnuma T: A new system for automatic measurements of contrast sensitivity functions with VEP pattern stimulator Acta Soc Ophthalmol Jpn 86: 1510–1515 (1982)
8 Pederson JE, Anderson DR: The mode of progressive disc cupping in ocular hypertension and glaucoma Arch Ophthalmol 98: 490–495 (1980)
7 Stamper RL: The effect of glaucoma on central visual function Tr Am Ophth 132: 792–826 (1984)

Author's address: Koke University,
Kuniyoshi Mizokami M D ,   Kusunoki-Cho, 7-Chome, Chuo-Ku, Kobe, Japan
Department of Ophthalmology,
School of Medicine,

VII.3 The measurement of normal retinal sensitivity in the central quantitative visual field using a fundus photo-perimeter

M. TOMONAGA, K. HAMANO and Y OHTA
Tokyo, Japan

Abstract

We previously reported the clinical application of the fundus photo-perimeter (Canon CPP-1) developed by our department. This report describes the results of measurement of normal retinal sensitivity in the quantitative visual field and changes in sensitivity with age measured using this fundus photo-perimeter.

In normal subjects (age ranging from 18 to 59), the quantitative kinetic visual field was measured in 33 eyes of 33 subjects; and the quantitative static visual field was measured in 45 eyes of 45 subjects. The 20, 19, 6.3 and 3.2 asb isopters of the quantitative kinetic visual field was found to be located 20°, 18°, 13° and 8° from the center, respectively

For the determination of the quantitative static visual field, the peak of retinal sensitivity threshold was calculated at the apex of 1.0 asb of the mean macular threshold using white 10-minute test targets determined by the Tübinger perimeter. As a result, the peak was about 0.5–0.6 log units higher than the threshold of the normal static visual field. There were no statistically significant differences in changes in the visual field with age.

Introduction

The authors previously reported the development on a trial basis of a fundus photo-perimeter (F.P.P.) that enables measurement of the visual field under direct observation of the fundus [4, 5], and also described its clinical applications. In the present study, the quantitative kinetic and static visual fields were measured using the Canon perimeter CPP-1, which is an improved version of the trial instrument developed earlier, and normal retinal sensitivity and its changes according to age were examined.

Materials and methods

Normal subjects between the ages of 18 and 59 with visual acuities of >1.0 were used in the present study. Kinetic perimetry was conducted in 33 eyes of 33 subjects. Static perimetry was conducted in 45 eyes of 45 subjects. The maximum luminance of the test targets was set at 1000 asb, with a visual angle of 6.5 minutes. The background luminance was set at 10 asb. The kinetic measurements were conducted along eight different meridians: 0°, 45°, 90°, 135°, 180°, 225°, 270° and 315°. The isopters were determined with four different luminances (20, 10, 6.3 and 3.2 asb). The results of the initial experiments revealed that an isopter of 10 asb with our instrument coincided with a 0/1 isopter on the Goldmann perimeter, therefore the luminance of the determined test targets were selected such that their luminance was within the range of fluctuation of the luminance of Goldmann perimeter, which was used as the standard. Static perimetry was performed along a meridian of 0°–180° at 2°, 4°, 6°, 10° and 14° of eccentricity.

Results

Figs 1–5 respectively illustrate the mean and S.D. values of the results of quantitative kinetic perimetry of subjects in their teens, twenties, thirties, forties and fifties. The values with a parentheses represent the S.D. All the kinetic visual fields were treated as right eye fields. The results of the measurements at 20 asb on the temporal side revealed that the output values often overlapped the optic disks. Thus the reliability of these results was assumed to be low. They therefore were excluded, but the isopters are shown with dotted lines as seen in the chart.

Table 1 shows the results of χ^2-test on the mean values of subjects belonging to the age groups between the teens and the fifties, excluding those in their twenties

Table 1 χ^2-test on the mean values of quantitative kinetic visual field of subjects in their twenties

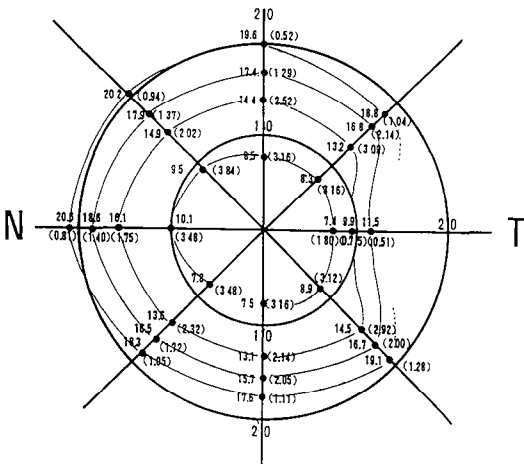|	20 asb (n = 7)	10 asb (n = 8)	6 3 asb (n = 8)	3 2 asb (n = 8)
10's	$\chi^2 = 0\ 36$ (P>0 99)	$\chi^2 = 2\ 27$ (P>0 9)	$\chi^2 = 11\ 08$ (0 2>P>0 1)	$\chi^2 = 13\ 43$ (0 1>P)
30's	$\chi^2 = 0\ 35$ (P>0 99)	$\chi^2 = 2\ 62$ (P>0 9)	$\chi^2 = 11\ 77$ (0 2>P>0 1)	$\chi^2 = 14\ 64$ (0 05>P)
40's	$\chi^2 = 0\ 10$ (P>0 99)	$\chi^2 = 1\ 07$ (P>0 99)	$\chi^2 = 5\ 92$ (0 7>P>0 5)	$\chi^2 = 10\ 86$ (0 2>P>0 1)
50's	$\chi^2 = 0\ 41$ (P>0 99)	$\chi^2 = 3\ 61$ (P>0 7)	$\chi^2 = 10\ 59$ (0 2>P>0 1)	$\chi^2 = 7\ 90$ (0 5>P>0 3)

Figure 1 Mean values and S D of the kinetic visual field of 4 eyes of subjects in their teens
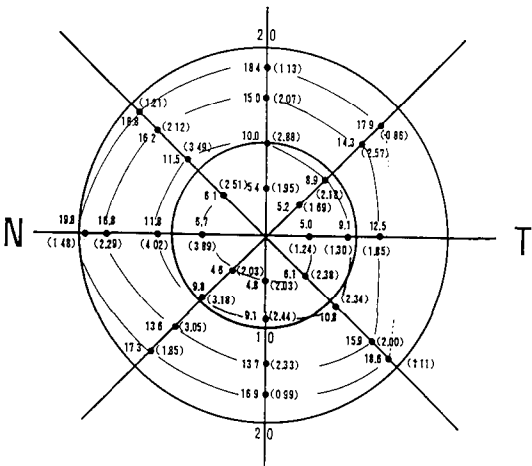

Figure 2 Mean values and S D of the kinetic visual field of 8 eyes of subjects in their twenties

Table 2 S D values of quantitative static visual field for each age group

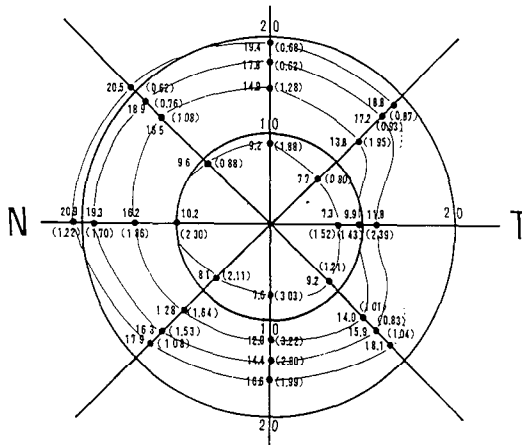|	14°	10°	6°	4°	2°	0°	2°	4°	6°	10°
10's	2 61	1 95	1 27	1 23	0 33	0 26	0 51	0 64	1 10	1 54
20's	3 06	1 67	1 45	0 97	0 53	0 36	0 43	0 81	1 38	1 75
30's	2 88	1 74	1 42	1 30	0 55	0 40	0 32	0 38	1 35	5 28
40's	2 68	0 92	0 99	0 74	0 28	0 36	0 47	0 84	1 31	1 77
50's	2 27	1 85	1 05	0 47	0 24	0 24	0 20	0 81	1 23	1 15

Figure 3 Mean values and S D of the quantitative kinetic visual field of 7 eyes of subjects in their thirties

against the standards of the mean values of subjects in their twenties in the kinetic visual fields. In the test on the mean values of each isopter of 20 asb and that of 10 asb, there was no significant difference between the values of subjects in their forties and those in their twenties, whereas there were marginally singificant differences between subjects in their twenties and those in their teens, thirties and fifties. Some significant differences were seen in the mean values of the 3.2 asb isopters between subjects in their twenties and those in the teens or thirties. There was a marginally significant difference apparent between subjects in their twenties and their forties.

Fig 6 shows the results of the mean values of the quantitative static visual fields for each age group which were plotted on the same recording paper as that used
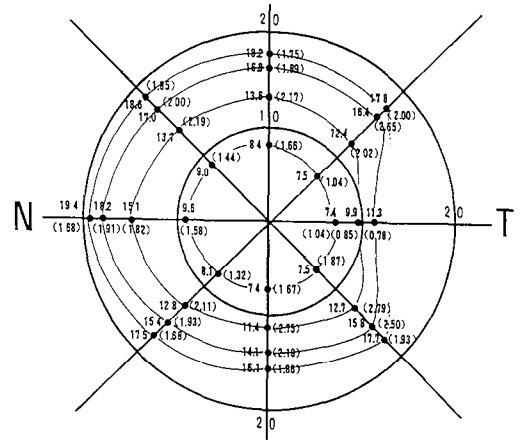

Figure 4 Mean values and S D of the quantitative kinetic visual field of 7 eyes of subjects in their forties

Figure 5 Mean values and S D of the quantitative kinetic visual field of 7 eyes of subjects in their fifties

for visual fields. There were hardly any differences in the retinal sensitivity in any of these age groups. The χ^2-test of the mean values with subjects in their twenties as the standard showed no significant difference between age groups, and had a confidence coefficient of 99%.

The peak of the threshold values of the retinal sensitivity in the quantitative static visual field in the present experiment was located approximately 0.5–0.6 log units higher than the threshold value of the normal static visual field measured obtained with a white 10' visual target on a Tübinger perimeter and a mean value at the fovea of 1.0 asb.

Table 2 shows the S.D. values of quantitative static perimetry of the subjects in

Figure 6 Mean values of quantitative static visual field for each age group ----- teens, p>0 99 ——— twenties –●–●–●– thirties, p>0 99 —————— fories, p>0 99 —●●—●●— fifties, p>0 99 (χ^2-test)

each age group. Within 6° from the center S.D. values among the subjects are small in all age groups. Outside of 10°, the S.D. values among the subjects were large, showing much variation.

Discussion

In the present experiment perimetry was conducted in order to investigate the normal values and changes according to age for both kinetic and static testing, utilizing the recently commercially available Canon perimeter CPP-1.

The data within 22° of the center revealed more fluctuations in kinetic perimetry than in static perimetry. Marginally significant differences were noted between the isopters of subjects in their twenties and those of each of the other age groups using kinetic perimetry at 6.3–3.2 asb, whereas, in static perimetry, no significant difference was observed between the data from subjects in their twenties and those of the other age groups, with a confidence coefficient of 99%.

The results of these experiments can be interpreted as being in agreement with the conventional opinion [1] that static perimetry has less fluctuations and is more accurate than kinetic perimetry because the visual cells are connected to ganglion cells via a single nerve fiber in the centre of the visual field.

Therefore, the difference in the obtained data between the kinetic perimetry and the static perimetry can be regarded atributable to the difference in the methods for determination. There was no significant difference in the data from the different age groups, between the teens and the fifties. The mean values of the foveal threshold values in the quantitative static visual field were obtained as the peak of a threshold, which is approximately 0.5–0.6 log unit higher with a maximum of 1.0 asb than the threshold value of the normal static visual field [6, 7], using a white 10′ visual target of the Tübinger perimeter. Kani et al. [2, 3], however, reported results almost identical to the threshold values for a white 10′ visual target on the Tübinger perimeter. It is assumed that, since Kani et al. used a measuring instrument with a Maxwell artificial pupil diameter of 1.5 mm while our instrument had a pupil diameter of 1.75 mm, the differences in the diameters of artificial pupils influence the results of their experiments.

Conclusion

We have statistically evaluated the normal values of the visual field and their changes according to age in the visual field of the recently commercially available Canon fundus photo perimeter CPP-1.

The results of evaluation of the quantitative kinetic visual field revealed that the 20 asb, 10 asb, 6.3 asb and 3.2 asb isopters were located at 20°, 18°, 13° and 5°, respectively. In the quantitative static visual field, the peak of the threshold value

of retinal sensitivity was generally 0.5–0.6 log units higher than the threshold value in the normal static visual field using a white 10′ visual target on a Tübinger perimeter with 1.0 asb of the mean fovea threshold value as maximum. There was no statistically significant change of the visual field with age.

References

1 Greve EL: Single and multiple stimulus static perimetry in glaucoma; the two phases of perimetry, pp 15–17 Dr W Junk, Dordrecht, 1973
2 Kani K, Eno N, Abe K, Ono T: Perimetry under television ophthalmoscopy Doc Ophthalmol Proc Ser 14: 231–236 (1977)
3 Kani K, Ogita Y: Fundus controlled perimetry Doc Ophthalmol Proc Ser 19: 341–350 (1978)
4 Ohta Y, Miyamoto T, Harasawa K: Experimental fundus photo-perimeter and its application Doc Ophthalmol Proc Ser 19: 351–358 (1978)
5 Ohta Y, Tomonaga M, Miyamoto T, Harasawa K: Visual field studies with fundus photo-perimeter in postchiasmatic lesion Doc Ophthalmol Proc Ser 26: 119–126 (1981)
6 Tomonaga M: The quantitative visual field of children Acta Soc Ophthalmol Jpn 78: 150–159 (1974)
7 Tomonaga M, Miyamoto T, Suzumura H, Ohta Y: Static perimetry in central serous retino-choroidopathy (MASUDA'S TYPE) using fundus photo-perimeter Doc Ophthalmol Proc Ser 35: 449–457 (1983)

Author's address:
Dr M Tomonaga,
Dept of Ophthalmology,
Tokyo Medical College Hospital,
Kasumigaura Hospital,
3-20-1, Chuoh, Ami-machi, Inashiki-gun, Ibaragi-ken 300-03, Japan

VII.4 Characteristics of two systems of human vision using fundus perimetry

Y. OKAMOTO, O. MIMURA, K. KANI and T. INUI
Hyogo, Japan

Abstract

Electrophysiological studies confirmed two different cells, X- and Y-cells, under-lying the visual system in primates. Furthermore, psycho-physical studies suggest existence of these two cells in human vision. However, these psycho-physical studies had many methodological and technical difficulties, and were not suitable for clinical application. In this study we applied the fundus perimeter to examine the spatial and temporal properties of the two different cells in human vision.
   The results were as follows:
1. The diameter of receptive field increased with retinal eccentricities from the fovea in both cells.
2. The diameter of the receptive field of Y-cells is always about three times the size of the receptive fields of X-cells at various retinal loci.
   These results are in agreement with the properties of the receptive field in primate's vision reported by electrophysiological and anatomical studies

Introduction

Since Kuffler's demonstration of the center-surround organization of the retinal ganglion cell's receptive field, the first main subdivision was that of Enroth-Cugell and Robson on the basis of the characteristics of spatial summation over the receptive field: X- and Y-cells.
   Later, Cleland and coworkers classified the cells in accordance with the dura-tion of their responses, sustained and transient, and these were probably equiva-lent to X- and Y-cells respectively of Enroth-Cugell and Robson [1].
   In the human visual system the existence of this subdivision seems quite reasonable. However, direct experimental support in electrophysiology has not been obtained due to methodological difficulties.
   In this study we employed a refined method of fundus perimetry using psycho-

physical techniques to detect the diameter of the receptive field of human retinal ganglion cell on the basis of the electrophysiological properties of X- and Y-cells.

Subjects and methods

Subjects

The experiments were carried out on five normal subjects for experiment 1 (Y-cells) and three normal subjects for experiment 2 (X-cells). Their visual acuity was more than 1.0 for both eyes.

Apparatus

Trials were conducted on a modified fundus perimeter which was originally designed by Kani and Ogita [5]. The subject's fundus picture and the target position on the retina could be monitored by means of an infrared television system. Therefore, the subjects never felt photophobic Stimulus, background and fixation light beams were set up in a Maxwellian view arrangement. The light passed through a central 1.5 mm diameter part of the subject's pupil. This arrangement minimizes the Stiles-Crawford effect. The circular background subtended 30 degrees in diameter and the luminance was 10 apostilbs. Target intensity could be changed with neutral density filters (Kodak Wratten No. 96) by steps of 0.1 log unit.

The principal experimental variables were target size, retinal locus and stimulus condition.

a) For experiment 1: the position of retinal eccentricities were 0, 1, 2, 4, 5 and 10 degrees on the horizontal meridian of the temporal part of the subject's retina. Target sizes used here were 1.2, 2.7, 3.1, 6.4, 10, 13, 21, 28, 33, 60 and 79 minutes in diameter. Duration of the stimulus was controlled by an electromechanical shutter and it was 200 ms in this experiment.

b) For experiment 2: the position of retinal eccentricities were 0, 1, 2, 4, 5, 7.5 and 10 degrees on the horizontal meridian of the temporal retina. Target sizes were 1.2, 1.58, 2.9, 3.6, 9.3, 11.5, 20, 32 and 41 minutes in diameter. The intensity of the stimulus increased monotonically by means of a rotating wedge neutral density filter inserted in the stimulus light beam and stimulus duration was 3 sec in this experiment.

Procedure

The subject was allowed approximately ten minutes for background adaptation.

At the start of the experiment, the subject was instructed to press the key if the target was seen, and to do nothing otherwise. The subject was in good focus before initiating each session and told to be sure of the fixation point.

The subjects participated in 11 (Exp. 1) or 9 (Exp. 2) experimental sessions, each of which corresponded to one of the randomly selected target sizes. A session consisted of 6 (Exp. 1), 7 (Exp. 2) blocks of 15 trials. Before each block, five trials were performed so that target intensity could be set in the vicinity of the threshold at each retinal locus. Fifteen sets of data were collected for each target size by a up-and-down method, and a 50% threshold as described above, was determined from the probability of seeing curve, similar to the method of constant stimuli.

Results

The results of Experiment 1 are illustrated in Figures 1 and 2. The details of these results have been described elsewhere [4]. The results of Experiment 2 are illustrated in Figures 3 and 4. Figures 1 and 3 show the spatial summation curves in a normal subject, in which log light energy of the increment threshold is plotted against log area of the stimulus at different eccentricities.

The increment threshold data of fig. 3 show a decided tendency as follows: for less than 1.58 minutes, they are parallel to the abcissa. For more than 3.6 minutes, they approach a slope of 45°. thus, the sensitivity curves have two asymptotes. The former shows complete spatial summation and the latter shows non-summation. We called the stimulus area at the intersection point of the two asymptotic lines the critical area. Figure 4 shows the diameter of the critical area plotted against the eccentricity from the fovea.
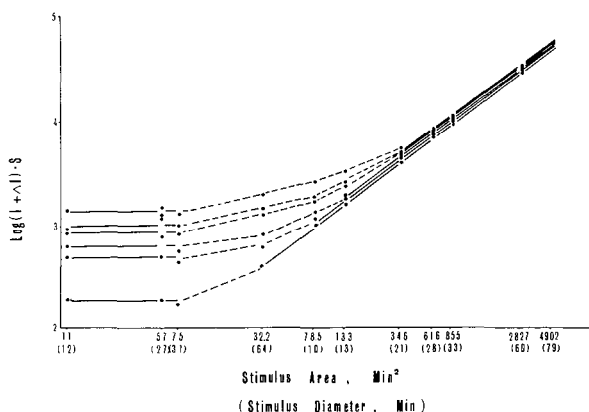
Figure 1 Relation between log light energy of increment threshold (ordinate) and log area of stimulus (abscissa) at six different eccentricities in a normal subject Critical area: intersecting point of two asymptotic lines (200 msec duration)
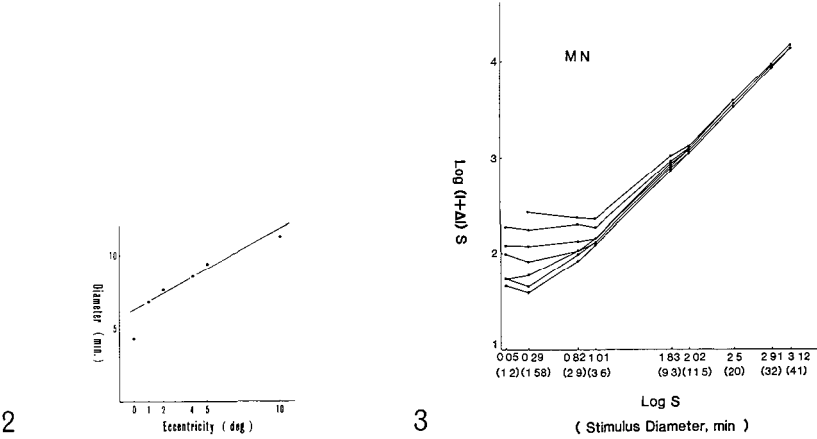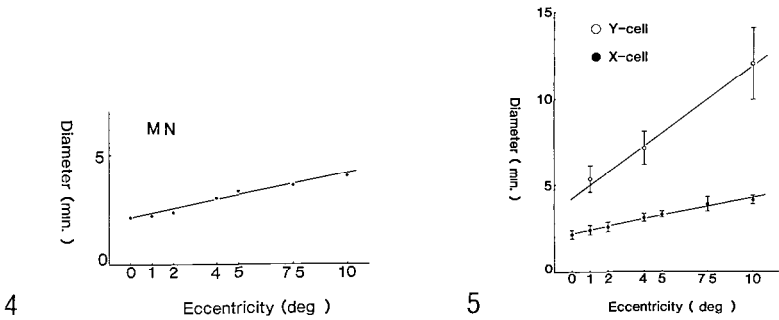
Figure 2 Relation between critical area diameter (ordinate) and retinal eccentricity from fovea (abscissa) on Y-cells in a normal subject

Figure 3 Relation between log light energy of increment threshold (ordinate) and log area of stimulus (abscissa) at seven different eccentricities in a normal subject (5 sec duration)

The results of Experiment 1 and 2 are summarized in Figure 5. The receptive field diameter of the Y-cells calculated from Experiment 1 is shown in the upper solid line, and that of X-cells from Experiment 2, in the lower solid line. The diameter of Y-cells increased considerably with retinal eccentricity. The diameter of X-cells increased only slightly with retinal eccentricity.

Figure 4 Relation between critical area diameter (ordinate) and retinal eccentricity from fovea (abscissa) on X-cells in a normal subject

Figure 5 Relationship between critical area diameter (ordinate) and retinal eccentricity from fovea (abscissa) for X- and Y-cells Means and standard deviations are given for the participatry subjects
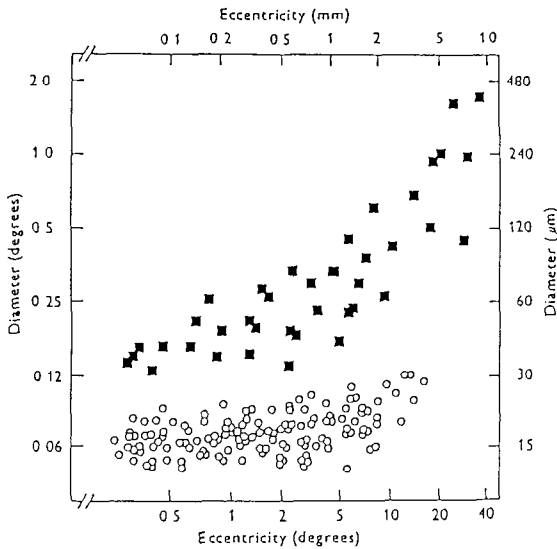
Figure 6 Distribution of receptive-field centers or activating areas in relation to retinal eccentricity ○: data from concentric colour-opponent cells, receiving input from one cone mechanism to the center ■: data from broad-band cells (Modified from De Monasterio, 1975)

Discussion

If the light stimuli are sufficiently small, the threshold luminance of an incremental stimulus on a constant background is inversely proportional to its area [8]. This relationship, 'spatial summation', is one of the most basic and essential mechanisms of the visual function, and has been studied electrophysiologically in animal models. Because of the impossibility of single unit study on the characteristics of the human retinal ganglion cells, numerous psychophysical studies have been performed.

Many psychophysical investigations on the properties of Y-cells (transient cells) have been reported. However, only a few extensive studies on the properties of X-cells (sustained cells) have been published because of technical difficulties.

The introduction of the fundus perimeter enabled us to measure the increment threshold of the retinal ganglion cells [4, 6]. In this study we applied a fundus perimeter to investigate properties of the X- and Y-cells in human retina.

Our results suggest the existence of these two subdivision in the human retina. In the primate retina De Monasterio and Gouras [3] have identified the retinal ganglion cells which they classified as either 'colour opponent' or 'broad band' (Figure 6). More recently De Monasterio [2] demonstrated that the majority of 'colour opponent' cells have X-like properties and that the majority of 'broad

band' cells have Y-like properties. As shown in Figure 6 the diameter of the receptive field increased monotonically with eccentricity up to 15 degrees. Furthermore, the diameter of the receptive field in broad band cells is always about three times as large as that in colour opponent cells on various retinal loci. Hence, our results seem to be in accordance with respect to the properties of the receptive field determined electrophysiologically.

Furthermore, Perry and Cowey [7] reported morphologically two types of ganglion cell of the monkey's retina. They filled the cell body and dendrites of retinal ganglion cells with horseradish peroxidase implanted in the optic nerve. Quantitative measurements of the dendritic trees of two types of ganglion cell suggest that they correspond to our psychophysically classified Y- and X-cells, respectively. Thus, our results are in nearly complete agreement with not only electrophysiological but also morphological studies.

Acknowledgement

References

1 Davson H: Electrophysiology of the retina – further aspects In: Physiology of the eye (4th ed), pp 284–297 Churchill Livingstone, Edinburgh, 1980
2 De Monasterio FM: Properties of concentrically organized X- and Y-ganglion cells of macaque retina J Neurophysiol 41: 1394–1417 (1978)
3 De Monasterio FM, Gouras P: Functional properties of ganglion cells of the rhesus monkey retina J Physiol 251: 167–195 (1975)
4 Inui T, Mimura O, Kani K: Retinal sensitivity and spatial summation in the foveal and parafoveal regions J Opt Soc Am 71: 151–154 (1981)
5 Kani K, Ogita Y: Fundus controlled perimetry – the relation between the position of a lesion in the fundus and in the visual field Doc Ophthalmol Proc Ser 19: 341–350 (1979)
6 Mimura O, Inui T, Kani K, Ohmi E: Retinal sensitivity and spatial summation in amblyopia Jpn J Ophthalmol 28: 389–400 (1984)
7 Perry VH, Cowey A: The morphological correlates of X- and Y-like retinal ganglion cells in the retina of monkeys Exp Brain Res 43: 226–228 (1981)
8 Wilson ME: Invariant features of spatial summation with changing locus in the visual field J Physiol 207: 611–612 (1970)

Author's address:
Department of Ophthalmology,
Hyogo College of Medicine,
1-1, Mukogawa-cho, Nishinomiya, Hyogo, Japan, 663

VII.5 Blind spots of normal and high myopic eyes measured by fundus photo-perimetry

H. MASUKAGAMI, F. FURUNO and H. MATSUO
Tokyo, Japan

Abstract

We measured the sensitivity of the retina around the optic disc of 60 normal and 15 high myopic eyes with the Fundus Photo-Perimeter. Kinetic perimetry is performed while observing the fundus of the eye.

In normal eyes we found an absolute scotoma in an area slightly larger than the optic disc. The area corresponding to the nasal-inferior juxtapapillary retina showed the largest defect. Angioscotomata were most frequently seen at the upper and lower ends of the optic disc.

In the high myopic eye, we found enlarged blind spots in all directions except in the superior and nasal-superior directions.

Introduction

This is a study on the relationship between the size of the blind spot and the size of the optic disc, the location of the blood vessels and the juxta-papillary retina.

The study was carried out with the Fundus Photo-Perimeter designed by Ohta [3]. Since 1668 there have been many studies about the size of the blind spot [2]. The absolute scotoma of the blind spot is generally considered to correspond to the optic disc and the conus. The relative defect around the absolute scotoma may enlarge with increasing age, with medial opacities or with refractive errors [1] Until now the blind spot has not been measured under direct observation of the retina.

Material and methods

Subjects

Seventy-five eyes of 52 persons were tested. These normal eyes had a visual acuity of 1.0 or better in each eye, normal findings on ophthalmological examination and a normal intraocular pressure level. Sixty of these eyes had an emmetropia that did not exceed 1 diopter for distance and 15 eyes had a myopia of -6.25 diopters or more (Table 1).

Apparatus

We used the Fundus Photo-Perimeter CRP-1 (Cannon In-corporation in Japan) and performed kinetic perimetry with it. The background illumination was 10 asb. The fixation point was red with a diameter of 10 minutes. The stimulus was a white spot with a diameter of 6.5 minutes and a luminance of 1000 asb to determine the size of the absolute scotoma and a luminance of 32 asb for the relative scotoma.

Methods

The size of the blind spot and the size of the optic disc were measured in 8 directions, i.e. temporal, temporal inferior, nasal-inferior, nasal, nasal-superior, superior, temporal superior and inferior. The findings were characterized by the diagonal dimensions of the optic disc in each of the measured directions. Furthermore the distance between the margin of the optic disc (a) and the luminance threshold at the opposite site of the diagonal was measured (Figure 1). The distance between those points was called M. Each M. was measured for 1000 asb and 32 asb. A M/D ratio was calculated which is in fact the ratio of the size of the blind spot to the size of the optic disc.

Table 1 Subjects

Normal group $< \pm 1\ 0$ Diopter,
60 eyes (39 persons)
10–60 years (mean 38 1 $\pm$ 14 2)

High myopic group $>-6\ 0$ Diopter,
15 eyes (13 persons)
16–60 years (mean 32 0 $\pm$ 14 5)

D=a b (diagonal of the optic disc)
M_{1000}=a c (c: detection point for 1000asb)
M_{32}=a d (d: detection point for 32asb)
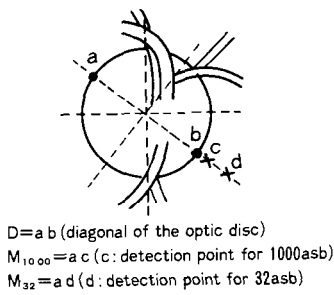
Figure 1 Methods

Results and discussion

Normal group

Table 2 indicates the mean values and standard-deviations of the M/D ratios in 8 directions in the normal group. The M/D ratios were greater than 1 both for the 1000 asb stimulus as well as for the 32 asb stimulus. The M/D ratios were larger in the vertical direction and specially so in the inferior direction. On the temporal side the margin of the conus, almost coincided with the rim of the blind spot. On the nasal side the size of the blind spot was somewhat larger than the size of the disc. Angioscotoma were detected in 37% of cases in the normal group. As expected they were concentrated in the superior or inferior direction (Figure 2). In some cases the defect did not have any relation to either the conus or the blood vessels. This suggests a true change in retinal sensitivity (Figure 3). Such a depression of a sensitivity was detected in 36 eyes (60%) In 27 of these 36 eyes the blind spot was enlarged in the nasal inferior and adjacent directions (Table 3). The retinal sensitivity seems to be poorer in these areas than in the other peripapillary areas. A satisfactory explanation for this decreased sensitivity is not available. An explanation maybe sought in the properties of the receptive fields or in the late closure of the inferior-peripapillary area in the fetal development.

Table 2 The mean and SD of M/D ratio in normal group

|	Temporal	Temporal-inferior	Inferior	Nasal-inferior	Nasal	Nasal-superior	Superior	Temporal-superior
M_{1000}/D	1 08	1 09	1 13	1 09	1 07	1 06	1 09	1 06
SD	0 09	0 07	0 11	0 09	0 08	0 07	0 08	0 08
M_{32}/D	1 12	1 16	1 24	1 18	1 15	1 19	1 21	1 12
SD	0 10	0 12	0 14	0 12	0 12	0 13	0 14	0 12

n = 60
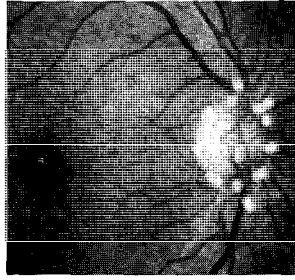
Figure 2 Angioscotomata 56-year-old man, Vd = 1 2 × + 0 37D Angioscotomata at 32 asb of the upper and lower poles of the optic disc
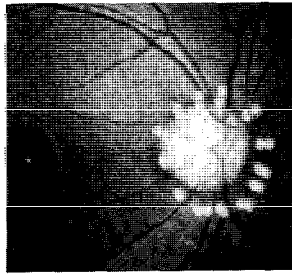
Figure 3 Retinal sensitivity depression 29-year-old woman, Vd = 1 5 × −0 25 D 1000 asb depression in the nasal-inferior and adjacent directions
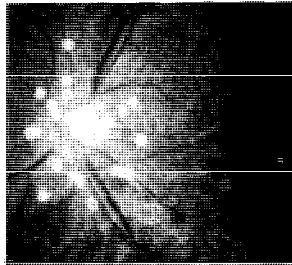
Figure 4 Boundary spread out from the temporal conus margin in high myopic eye 40-year-old man, Vs = 1 2p × −7 O D The temporal boundary of the blind spot did not agree with the conus margin

High myopic eyes

The mean value and standard deviation of the M/D ratio in each direction in the high myopic group is shown in Table 4. In the temporal, temporal-inferior, or temporal-superior direction the mean M/D ratio was larger than that of the normal group.

Table 3 Distribution of the depression of retinal sensitivity

	1000 & 32 asb	32 asb	(eyes)
Enlarged in the nasal, nasal-inf & inf directions	20	7	27 (75%)
Enlarged in the other directions	2	7	9 (25%)
	22	14	36 (100%)

Table 4 The mean and SD of M/D ratio in high myopic group

	Temporal	Temporal-inferior	Inferior	Nasal-inferior	Nasal	Nasal-superior	Superior	Temporal-superior
M_{1000}/D	1 36	1 33	1 19*	1 17*	1 12	1 07	1 08	1 22
SD	0.42	0 36	0 15	0 10	0 13	0 09	0 10	0 27
M_{32}/D	1 40	1 41	1 35	1 25*	1 19	1 20	1 20	1 29
SD	0 43	0 38	0 22	0 13	0 14	0 14	0 12	0 28

* v s (normal group) $p<0$ 05
n = 15.

Five eyes in this group had a big temporal conus which explained the M/D ratio in these directions. There was however also a significantly larger M/D ratio in the inferior or nasal-inferior direction in the higher myopic group. In 4 of the 15 eyes the temporal boundary of the blind spot was wider than the ophthalmoscopically observed margin of the temporal conus. A larger size of the blind spot as compared to the size of the optic disc and conus means that the retinal sensitivity in these areas is reduced. It is presumed that the retinal sensitivity is influenced by an increase of the axial length as previous studies have shown [4, 5].

References

1 Armaly MF: The size and location of the normal blind spot Arch Ophthalmol 81: 192 (1969)
2 Aulhorn E, Harms H: Early visual field defects in glaucoma Glaucoma Symp, Tutzing Castle, 1966, pp. 151–186 (1967)
3 Ohta Y, Miyamoto T, Harasawa K: Experimental Fundus Photo-Perimeter and its application Foria Ophthalmol Jpn 30: 148–153 (1979)
4 Sato Y, Yamashita M, Hayashi K, Tokoro T: Abnormality of visual field in pathological myopia Acta Soc Ophthalmol Jpn 88: 977–982 (1984)
5 Takizawa E: Retinal sensitivity in the papillomacular area in high myopia by fundus-controlled perimetry Jpn J Clin Ophthalmol 37: 495–501 (1983)

Author's address:
Dept of Ophthalmology,
Tokyo Medical College, Shinjuku, Tokyo 160, Japan

VII.6 A rapid technique for kinetic visual field determination in young children and adults with central retinal lesions

T.M. FAUSSET and J.M. ENOCH
Berkeley, U.S.A.

Abstract

Young children (in general) and adults with central retinal lesions are often difficult to assess visually. Because of fixational drift and/or eccentric viewing, visual fields are particularly hard to measure in these populations We describe a relatively simple and rapid technique to determine visual fields in these two groups using commercially available equipment.

With the Canon Fundus Photoperimeter, a 45° non-mydriatic infrared fundus camera-perimeter combination, we could directly view the fundus and relate stimulus location relative to fixation at the time of stimulus detection. A positive response was either through an audible buzzer or a fixational saccade. The video display terminal test record was recorded on a standard VCR (VHS or Betamax) After all data were collected, the tape could be replayed and the visual field plotted using a simple graphical technique Both the test itself and the data analysis prove to be rapid and simple.

Introduction

Because of the difficulty in stabilizing eye position, holding interest, and maintaining fixation, the testing and assessment of visual fields in all young children [1, 3–6] and in adults with central retinal lesions is difficult to perform. The task of the clinician may be further complicated by very low central acuity, nystagmus, mental retardation, and visual pathway lesions. Yet, these populations often require comprehensive visual assessment.

Using the Canon Fundus Photoperimeter, Model CPP-1, we measured and quantified monocular kinetic visual fields in children 4–10 years of age [2], and adults with central retinal disease. Both groups have unsteady and often wandering fixation.

The unique advantages offered by our technique are:

a) simplicity,

b) speed,

c) the ability to continuously view the fundus (monitor fixation) and stimulus position simultaneously on the retina during the perimetric exam,

d) the capability to record data and later to review the test and assess data through the use of a video recorder (VCR), and

e) the commercial availability of the equipment without modification.

Data analysis is conducted *after* testing. Thus, we feel we have developed a relatively simple and rapid procedure for determining kinetic visual field configurations in

a) young children and

b) adults with unsteady fixation and/or central field scotomas.

Hopefully, vision threatening diseases common to children can be detected and/or followed by application of our techniques and possibly aid in the diagnosis and rehabilitation of the visually impaired population.

Test subjects

The children tested were between the ages of 4 and 10 years. A complete visual examination was carried out prior to field testing, and only those children having visual acuity of about 20/20 or better and showing no ocular disease were tested in these trials. All guardians gave informed consent.

The adult low vision patients used in this study all had central retinal lesions due to age-related macular degeneration or macular holes. The Snellen visual acuity of those tested ranged from 20/80 to 20/500.

Experimental methods

The instrument used in this research, the Canon Fundus Photoperimeter, is a modified Canon 45° non-mydriatic infra-red fundus camera that provides the examiner with a TV video image of the patient's fundus (infrared projection). Images of the fixation and test targets are added for perimetric testing. A uniform white background is standardly set at a luminance level of 10 apostilbs, i.e., the same as the Tubingen perimeter (Oculus) of Harms and Aulhorn. The test target size is the equivalent of a Goldmann (Haag-Streit) Size I and target luminance can be varied between 0.1 and 1000 apostilbs.

Although a mydriatic is not necessary when using an infrared fundus camera, we found dilation of the pupil greatly simplified the task of the clinician when seeking to maintain proper alignment during fixational drifts. The Canon instrument was originally designed for photographic documentation of the kinetic isopters superimposed on the fundus photograph. We found it necessary to

videotape the test procedure in order to determine the isopter configuration and compensate for fixational drift.

The Canon Fundus Photoperimeter instrument was coupled to a VRC for recording the perimetric exam. The background illumination, red fixation target, and test target size were standardized according to specifications of the manufacturer. Only one fixation target size of 10′ (30′ for the adults with low vision) was used The subjects were dark-adapted to the light level of the examination room for five minutes before kinetic perimetry was performed Refractive errors were corrected by focusing the instrument. Pupil size was measured immediately before and after testing

Since our procedure required a dilated pupil, the medical history of subjects was evaluated. Anterior chamber angles were examined and tonometry was performed, generally on a separate occasion. After dilation and patching, the children were positioned before the instrument. They were given a response buzzer and were told that they will be playing a video game. They watched a red fixation spot, centered in the test field. This was identified to them as their 'home base'. In order to win the game, they were told to protect their home base from approaching space ships (the kinetic targets). We tell them the space ships may come from any direction and as soon as they see one, they are to push the buzzer (which causes us to extinguish it) The children are encouraged periodically to watch their home base if fixation wanders excessively Having the availability of the video tape and the auditory component of the tape recorder, we can note when the buzzer was pushed and/or when the child made a saccade in the direction of the target. The target was moved from not seeing to just seeing Their saccadic eye movement from fixation towards the object required no prompting. Thus, we could use either the buzzer cue on the tape or a readily detected saccade in the direction of the kinetic target as an indicator of test spot detection. The data was recorded on a VCR (VHS or Betamax).

A relatively simple modification of standard perimetric testing procedures was employed. Kinetic perimetry was carried out along 8 half meridians presented in random order The 6.5′ diameter test spot was moved from the mid-periphery towards the fixation point at approximately 5° per second using pre-selected test target luminance levels.

For the adult subjects, standard perimetric procedures were employed with the arrangement and conditions the same as for the children. The 6.5′ diameter test spot was used (if possible) although a 103′ diameter spot was available if needed The target was moved from the center (non-seeing) outward within scotomas Peripheral isopters were determined by moving the target inward from non-seeing to just detection The adults were instructed to hold fixation near the center of the field. They used the buzzer.

Precise fixation is not necessary because

a) the infrared camera provides a continuous view of the retina including the fovea (or locus of eccentric viewing) and

b) an eye movement towards a perceived moving target (or some other form of response, e.g., buzzer) indicates just detection of the kinetic target.

The recording capability of the VCR allowed continuous assessment of both the location of the target and the fixation point and made possible assessment of data after the subject completed the test. In order to plot the visual field, one merely overlaid a piece of graph paper (centered on the point of fixation) on the video display. The lack of reliability of fixation on the part of the child, or adult observer with low vision, can be readily detected by the examiner by repeat trials during the course of the examination and points of importance can be retested as often as desired.

Calibration was fairly straightforward, because of the availability of a visible fovea (in the child) and blind spot (in the low vision adult) as well as the capability of defining specific eye movements. Normal observers are tested on a separate occasion using a fixation point and defined stimuli (look 5° left, etc.). The internal correction of refraction by the fundus camera perimeter removes the need for wearing a refractive correction. If a special problem exists, e.g., an irregular cornea, the use of a contact lens would not interfere with these measurements.

Thus, either objective or subjective criteria for detection can be used in these patients. We have had no difficulty testing a number of four year old children and adults with severe low vision. We see no difficulty in extending the test to three year old children. It is not clear that the same procedure could be used with a (often extremely fidgety) two year old child. Sample test/retest data for the four year old child will be presented in order to indicate the essential reliability of the method.

Three or more measurements were taken in each half-meridian and the arithmetic mean was calculated in order to determine the isopter. Because data are recorded on the VCR, it is possible to accumulate data for analysis after the subject completes the test. Often, we completed the analysis of data before the subject left the premises in order to be sure that further testing was not required. The test takes approximately 10–15 minutes including set-up time and the analysis requires about 10 minutes.

Because the fixation of these patients wanders, we utilized the playback and freeze-frame ability of the VCR. For this reason the isopters were plotted by noting the target location, relative to the central fovea, just prior to when a response was first initiated (i.e., an audible buzzer response or fixational saccade). By placing an oriented transparent (or semi-transparent) graphical overlay over the TV monitor screen, the isopter can be directly plotted from the VCR recording The overlay was carefully oriented. We noted

a) the foveal position (to compensate for fixational drift),
b) the peripheral stimulus location, and
c) the stimulus intensity (for a given isopter).

It is important to point out that when making a graphical overlay we often utilized the optic nerve head and the vascular tree as a secondary reference to monitor
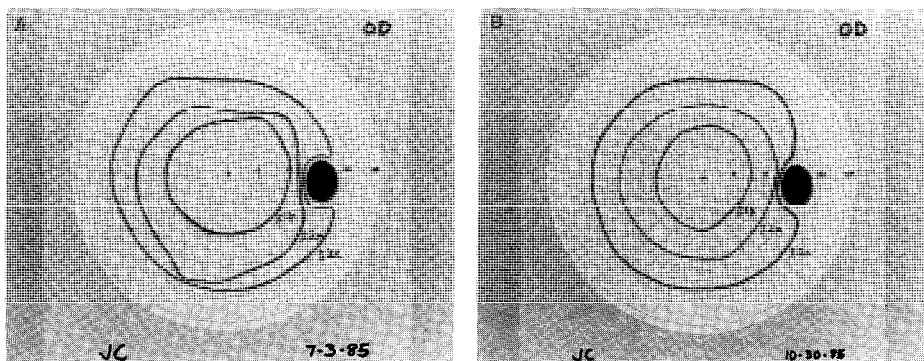
Figure 1 Sample kinetic fields are presented These data are (a) test, and (b) retest kinetic fields obtained on a four-year-old child There was a four month separation between the test and retest sessions Isopters correspond to the Goldmann (Haag-Streit) designation

fixation because of the occasional difficulty in following the precise center of the fovea and absence of fovea in the adults. By knowing the anatomical relationship between the fovea and optic nerve head, we were able to compensate for fixational drift by plotting where the fovea was just prior to the response. N such interpretations determined the isopter. In many subjects, a combination of both methods (fixational saccade or buzzer) was used based on the VCR interpretation of which response was recorded first.

Results

Of those tested, it was possible to obtain and record quite satisfactory visual field plots for 10 children out of 13 tested and all adults.

Sample data are presented for one eye of one child and one adult. These sets of data are in no way unique. The 4-year-old child was retested for reliability on a second test day. The second data set was obtained without reference to the prior data, although the same test targets were employed by the same examiner

In Figs 1a and b, data for JC, age 4, are presented. He was a +6.50 DS accommodative esotropic patient with 20/20⁻ visual acuity in each eye. Otherwise, his eyes were normal. The second set of data (Fig. 1b) was obtained several months after the first set.

Adult case: data of patient OK, age 79, are presented in Fig. 2. He had reduced vision due to age-related macular degeneration with 20/50 visual acuity.

We determined two or three 2–3 isopters on each subject.
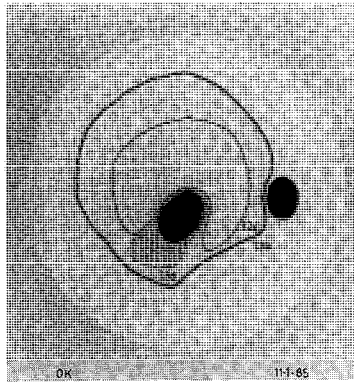
Figure 2 This is a kinetic field obtained in one eye of a 79-year-old adult with age-related macular degeneration Isopters correspond to the equivalent Goldmann (Haag-Streit) designations

Discussion

The Canon Fundus Photoperimeter coupled with a VCR makes possible the simplified testing and assessment of kinetic visual fields in young children where fixation stability, duration of the test, and attentiveness all are important factors. The same arguments that apply to young children clearly apply to adults with central lesions of poor fixation.

The adults were found to be more easily tested because of better communication between them and the experimenter and the knowledge of 'straight ahead' position. The photoperimetry field plots could be readily compared to previous tangent screen and Goldmann field plots. There was good correlation in size and location relative to the blind spot. We felt that more accurate multiple isopters were achieved using our techniques.

The children actually enjoy the game-like task and enter into the testing situation with considerable enthusiasm. Those who have had previous eye examinations are easier to handle. The greatest problem we encountered with the young children related to the use of the dilating drops The dilating drops burn for a brief period of time and of course, the children react adversely to that situation. Those who have had prior eye examinations know that the burning lasts only a short time. The fact that on the first trial we were able to successfully test 10 of 13 children we think is highly significant. It is probable that the other 3 would have cooperated given a bit more time and familiarity with the task. We need not tell those who work with young children that sometimes some patience is required when dealing with this population.

After our first trials with this technique, it is obvious that certain improvements in equipment could be made Obviously, it would be desirable to have more than a 45° field of view (Canon instrument) as this limits the eccentricity of retinal

testing. This can be quite important. Moving the fixation spot by 22° in any direction is possible, but this also often reduces the visibility of other retinal landmarks and makes tracking of the fovea a bit difficult in certain circumstances. The ability to introduce an additional or optional fixation display would be highly desirable. In the case of low vision patients, it would be desirable to be able to have a larger fixation target available on the current Canon instrument and one that would allow central foveal testing as well.

Acknowledgements

References

1 Aspinall PA: Peripheral vision in children Ophthalmologica 173: 364–374 (1976)
2 A Rapid, Simple Means of testing Kinetic Visual fields in Young Children *Technical Digest,* Topical Meeting on Noninvasive Assessment of The Visual System, Paper MB3, Optical Society of America, Monterey, CA , March 24–26, 1986
3 Howe JW: The causes of assessment of visual field defects in young children Br Orthopt J 34: 46–53 (1977)
4 Laio F: Perimetry in young children Jap J Ophthalmol 17: 277–289 (1973)
5 Lakowski R, Aspinall PA: Static perimetry in young children Vision Res 9: 305–312 (1969)
6 Verriest G: Visual field in childhood Bull Soc Belge Ophthal 202: 41–58 (1982)

Author's address:
Prof J M Enoch,
School of Optometry,
University of California, Berkeley,
Berkeley, CA 94720, U S A

Section VIII
Ergo-perimetry

VIII.1 Percentage impairment by visual field defects

G. VERRIEST
Ghent, Belgium

Abstract

This report[1] is a critical survey of different systems and of different national regulations which are or have been used for the percentage evaluation of functional impairment due to visual field losses. The scores of these several systems vary greatly.

The new Esterman binocular system is the one which is recommended, with certain precautions.

Introduction

This report is intended as the information to be supplied by the International Perimetric Society (IPS) Task Group on Functional Visual Field to the IPS Committee on Standards, to the IPS Directorial Board, to the Concilium Ophthalmologicum Internationale (COI) Visual Functions Committee and to the COI itself concerning an eventual recommendation of an Esterman system for scoring visual field disability.

Historical overview of the different systems which have been proposed for scoring disability percentages for visual field defects

Percentage estimation of disability for visual field defects developed first in Germany and later in other countries. Its original purpose was to calculate diminished earning power in the general work market; later on it was used to determine the amount of compensation.

For brevity the principal available percentage values of the different systems are given by the successive rows of Table 1. The visual acuity is normal in functioning eyes.

Table 1. Percentages of disability for visual field defects according to different systems.

System	Loss one eye	Loss both eyes	Complete hemianopsia						Concentric narrowing							
			heteron.		homon.		horiz.		in one eye				in both eyes			
			bin.	bit.	right	left	sup.	inf.	50°	30°	10°	5°	50°	30°	10°	5°
	1	2	3	4	5	6	7	8	9	10	11	12	13	14	15	16
Old German systems																
Schröter (1891)	1		0	20	45	30	30	45	>10							>75
Magnus (1894)	2		0	20	32	32	32	32	>10				>20	45		100
Groenouw (1896–1905)	3		0	20	40–60	40–60	40	40	>10							100
Derived																
Rintelen (1954)	4	25	100		20	45	45	30	50	5	10	15	20	15	40	80	90
Hambresin (1958)	5	27	100	10	20	35	35	20	60	0	0	5	12	0	0	20	80
Old French systems																
(1919)	6			10	70–80	35	35	15	50								
(1939)	7	30	100	10–15	70–80	30–35	30–35	10–15	30–50		3–5		10–15		5–20		70–80
Voisin (1974)	8			24	40	32	32	16	48								
Jonquères (1981)	9	25	85	12	55	25	25	16	38	0	3	10		0	20	65	
Proportional to radii																
Old AMA (1958)	10	24	85	42	53	44	44	42.5	51.5	5	12	20	22	19	49	79	85
New Zealand	11	50	100	43	57	50	50	48	52	14	29	43		29	57	86	
Colenbrander (1975)	12	21		4	26	39	31	18	48	12	14	16	16	19	40	56	63
Not proport. to radii																
Bracci Torsi (1933)	13	35	100	22	44	50	50		50	5	15	25	35	25	45	65	100
Furuno (1983)	14	50	100	38	64	51	51	44	55	12	30	48		24	60	96	
Dufour & Cuendet (1961)	15	30	100	33	33	33	33	33	33	3	5	8	11	11	21	32	44
Esterman systems																
Esterman I (1968) + AMA	16	24	85	38	57	42	42	33	67	6	13	23	24	22	51	85	85
Esterman II (1982)	17		100	0	30	50	50	32	68	12	12	12	12	32	62	95	100

Old german systems: systems based on thirds and sixths (rows [1] to [3] of Table 1)

A German law of July 6, 1884 defined the concept of indemnification for permanently diminished earning power resulting from a work accident Concerning vision, it was soon accepted that loss of vision of both eyes corresponds to a total (100%) loss of earning ability, while the functional loss of only one eye corresponds e.g. to only 33$^{1}/_{3}$% disability because, as explained by von Zehender [41], the remaining eye acquires a double value. (Later, the value of the remaining eye became to be considered as three or four times that of the lost eye). It was also soon accepted that practical blindness, corresponding to 100% disability, can be caused as well by visual field loss as by loss in visual acuity

Mooren [30] introduced in 1890 the (false) concept that a (homonymous) hemianopsia should correspond to 33$^{1}/_{3}$% disability because the total extent of the loss in both monocular fields is the same as for the total loss of one eye.

Schröter [36] showed in 1891 that more peripheral parts of the visual field are functionally less important. He subdivided the monocular visual field, by concentric circles at 30° and at 60°, into three zones of which the relative values from centre to periphery were 3, 2 and 1. Just as Groenouw [18–19] had introduced the notion of professional visual acuity in order to deny compensation for slight losses in central visual acuity which do not impair occupational activity, so other authors [18, 22, 26, 28, 39] created the concept of occupational peripheral field by denying functional importance to slight very peripheral perimetric losses.

An important feature of the German school [18–19, 26, 28, 36] is that it soon denied compensation for monocular visual field defects covered by the non-affected visual field of the other eye. Accordingly, it denied compensation for binasal hemianopsia and gave only 20% disability for bitemporal hemianopsia (two times 10%, the value of a temporal crescent according to the above-cited system of Schröter).

Another principle was that defects in the very central part of the visual field should be indemnified not as visual field defects but as visual acuity defects (Groenouw [18]).

Some authors like Schröter [36] assumed that a right homonymous hemianopsia is more harmful than a left one, while the disability percentage given for homonymous hemianopsia increased from 33$^{1}/_{3}$% to 50% by the assessment of its severity during the first World War [40]. Binasal hemianopsia became compensated by about 10%. In 1981 the German Ophthalmological Society reduced the percentages for hemianopsia and (on proposal of Aulhorn) it equated with blindness concentric narrowing to 5°.

Outside Germany the systems of Berry [1] and Percival [32] in England, of Rintelen [33] in Switzerland and of Hambresin [20] in Belgium (rows [4] and [5]), and many present regulations in Central Europe are also offsprings of the old German conceptions.

Old French systems: systems based on the relative values of the quadrants of the monocular fields (rows [6] and [7])

Genêt [16] subdivided in 1916 the normal monocular field into 10 equal parts, so that the whole of both normal monocular fields consists of 20 parts. As the loss of one eye corresponded to 30% disability, it was concluded that the value of each part is 3% when the total visual loss does not exceed 10 parts, and 7% when the total visual loss does exceed 10 parts (as e.g. in an one-eyed subject suffering from visual field loss in his remaining eye)

In 1916 the French Ophthalmological Society appointed a commission which was formed by Morax, Moreau and Genêt and which concluded that the functional importance of a temporal half field is twice (24%) that of a nasal half field (12%); there was no difference between the superior and inferior quadrants. However it was assumed in 1939 that the functional importance of an inferior half field is three times that of a superior half field.

All subsequent French systems are based on such appreciations of the relative values of the different quadrants of the monocular fields. They never took into account the eventual congruency of the visual field defects of both eyes. The result was that too big disability percentages were given for bitemporal hemianopsia even when it became accepted that the loss of all quadrants in whatever eye gives no more disability than the functional loss of one eye.

Systems in which ability is assumed to be in linear proportion to a sum of radii of the monocular fields

The older *American Medical Association (AMA) system* (1958, row [10]) is the most widespread system in this category. It is based on the fact that in the normal monocular visual field for a big target the sum of the radii along the 8 principal meridians (temporally, down temporally, down, down nasally etc.) is about 500 degrees. The percentage loss of a monocular visual field is simply obtained by adding the degrees lost in each of the 8 principal meridians and dividing the total by 5. Where there is a loss of a quadrant or a half field, it is necessary to add the total of the loss in each meridian to half the sum of the two boundary meridians. Visual field loss can be calculated for other defects in a similar manner. For visual field defects as for other visual losses, an 'impaiment of visual system' V is obtained from the percentage impairment of the better eye B and from the percentage impairment of the worse eye W by means of a formula assuming that the value of the better eye is 3 times that of the worse eye:

$$V = \frac{3B + W}{4}$$

Thereafter a conversion table allows to determine the 'impairment of the whole man' M contributed by the 'impairment of visual system' V. Total loss of vision in both eyes (V = 100%) gives only M = 85%, but is only for V>86% that the difference V-M exceeds 5%.

The system is easy and can be applied to many kinds of visual field defects. It does not take congruency into account and greatly overestimates the functional importance of more peripheral field losses in comparison to that of the more central ones.

In a somewhat similar system which has been used in *New-Zealand* (row [11]) the normal visual field of each eye is subdivided into 27 sectors and 2 half-sectors by means of meridians at each 30° and of parallels at each 30°. The disability percentage is obtained by multiplying by 100 the number of sectors not seen by the eyes separately and by dividing the result by 56.

Contrasting greatly with these simplistic assumptions is the very sophisticated system of *Colenbrander* [6] (1975, row [12])

In this system 5% of the validity depends on the visual acuity of the right eye, a further 5% depends on the visual acuity of the left eye, a further 5% depends on the visual field of the right eye, a further 5% depends on the visual field of the left eye, a further 20% depends on the binocular visual acuity, a further 20% depends on the binocular visual field, and the last 40% depends on the product of binocular visual acuity and binocular visual field indexes. The ability from a monocular visual field is obtained from the extent of the actual visual field for an intense target in 16 sectors, the sectors bordering the horizontal and vertical meridians covering 15° and the other sectors covering 30°. As the sum of the 16 normal values is 1000, the validity of a monocular visual field is obtained by dividing the sum of the 16 radii by 10. For the binocular visual field things are still more complicated as the sector just beneath the right horizontal meridian is counted twice while the extent of some less important sectors is limited to 10°.

Systems in which ability is assumed to be not linearly proportional to radii of the monocular fields

In an *Italian system*, which has been proposed by Valenti in Rome in 1920, and which has been described by Bracci Torsi [2] (row [13]), all disability percentages for visual field defects are derived from tables concerning concentric narrowing in one eye, in both eyes and in the sole functioning eye Only narrowings beyond 60° are considered. The disability percentages are not linearly related to the radius of the remaining field. The figures are reduced to a third for binasal hemianopia and to a two thirds for bitemporal heminaopia. This system is not very logical but can be applied to cases of incomplete hemianopsia.

Crick, Crick and Ripley [7] (1983) maintained that the decrease of functional importance of the visual field area towards the periphery can be represented by a

parabolic function. An 'unspecialized Average Functional Value for the whole of the (monocular) field under test' could be achieved in such a parabolic system by allotting to the centre of each unit of field a functional factor to be multiplied by the threshold expressed in 0.4 decibel units.

Dannheim [8] (1983) stated that a parabolic projection is a suitable compromise between invariant representation of the receptive fields and correct representation of the retinal areas.

In *Furuno's system* [14] (1983) the percentage functional value of the (monocular) visual field is calculated by a (micro-) computer on the basis of the volume of the 3-dimensional onion-shaped island of vision as projected on the surface of a sphere: row [14].

The *system of Haruta, Kani and Inui* [21] (1985) is based on the use of a visual field chart in which area is linearly proportional to the number of retinal ganglion cells (and also to the number of cortical visual cells). The value of the whole visual island is obtained by multiplying ganglion cell count by sensitivity. We will not consider further such systems because they were not conceived for functional purposes and because they cannot be used without a computer.

But we have to consider the very peculiar *system of Dufour and Cuendet* [10] (1961, row [15]) in which the functional loss due to a concentric narrowing of the visual field is considered to be proportional to the difference between the sum of the Goldmann area and luminance indexes for a normal isopter and the sum of the Goldmann area and luminance indexes for the isopter of the same extent obtained in the considered eye. Graphs enable one to calculate the disability by combining the visual acuity, visual field and light sense scores of both eyes. The disability percentage corresponding to the functional loss of one eye is 20% in the first graph, 25% in the second and 30% in the third. Hemianopic and quadrantopic defects are considered to concern the half or the quarter of the visual field of each eye. The system is somewhat difficult to apply, even for concentric narrowings, because in a normal subject all intense targets give about the same isopter and because 8 steps are too many.

Let us not forget the 1978 *WHO system*, in which the horizontal angular extent of the binocular visual field is the basis of a purely qualitative assessment of visual impairment due to visual field defect.

The Esterman systems

In the Esterman systems the visual field is subdivided into numerous unit areas of unequal sizes, these units being smaller and denser in the areas which were judged by the author as functionally more important. Each unit is centered by a dot. The functional score is obtained by a simple count of those dots that lie wholly within the outline of the field obtained by kinetic perimetry (or of the dots that were 'seen' in static and/or automatic perimetry). Accordingly such systems

can very easily take into account all possible differences in the functional value of the different parts of the visual field.

The *first (monocular) Esterman system* [11] (row [16]), presented in 1967, was based on the relative values of the different parts of the monocular visual field. Therefore the field was divided into a grid of 100 unequally sized units, each worth 1%. The sum of the 'seen' dots yields the functional percentage. As in the AMA system the visual field scores from both eyes can be converted into an 'impairment of visual system' (not taking congruency into account) and into the AMA 'impairment of the whole man'.

The *second (binocular) Esterman system* [12] (row [17]), presented in 1982, takes congruency into account by plotting the field binocularly (without occluding either eye), then scoring it on his binocular scale. This new scale is merely the 100-unit monocular grid expanded to a 120-unit binocular grid by overlapping the right and left monocular grids. Because this now creates 120 dots, we must multiply the number of 'seen' dots by 5/6 (100/120) to obtain directly the total, binocular score. This serves as the visual field component when calculating the 'impairment of the visual system'. Esterman emphasized that is better to measure really the visual field in binocular vision because 'binocular enhancement' yields a larger field (and higher score) than would result from merging of both separate monocular fields.

Geographical overview of the different systems used presently in different countries for scoring disability percentages for visual field defects

We asked information from ophthalmologists of a large number of countries around the world, but the response was poor as the countries mentioned in the list of contributors (p. 523) are the only ones for which we received recent data. However many of the non quoted countries, especially those of the Third World, may have no national regulations at all, or only an (often simplified) version of those from colonial times, or only a rough classification in different categories of visual impairment.

For brevity, the principal available percentage values for the different countries are given in the successive rows of Table 2. Visual acuity is again supposed to be normal in all seeing eyes.

Austria

The only precise data received are the 'Richtsätze für die Einschätzung der Minderung der Erwebsfähigkeit (MdE) gemäss §7 KOVG 1957' published in Vienna in 1983 by the 'Zentralorganisation der Kriegsopferverbände Öster-reichs': see 1 in Table 2. For court cases experts use the 1982 German book of Gramberg-Danielsen et al.

Table 2. Percentages of disability for visual field defects in different countries.

Country		Loss one eye	Loss both eyes	Complete hemianopsia						Concentric narrowing							
				heteron.		homon.		horiz.		in one eye				in both eyes			
				bin.	bit.	right	left	sup.	inf.	50°	30°	10°	5°	50°	30°	10°	5°
		1	2	3	4	5	6	7	8	9	10	11	12	13	14	15	16
Austria	1	30	100	20–30	30–40	60	40		80–90	5	5–10	15–20	30	20	20–30	50–60	100
Belgium	2	30	100	16	24	45	40	28	57	4	10	19	20	17	42	80	85
Finland	3	20	100	–	30	50	40	30	70	0	10	20	20	(20)	50	100	100
France	4	25–33	85–100	15–20	40–45	30–35	28–33	14–18	45–50	5–8	12–16	15–19	4–10	15–22	70–80		
	5	25	85	5–10	50–60	20–25	20–25	5–10	20–40	0	3–10	5–10	10	0	10–40	40	40–65
Germ. Dem. Rep.	6	30	100	15	25	55	50	30	60	5	15	25	30	15	50	95	100
Germ. Fed. Rep.	7	25	100	10	25	40	40	40	60	5	10	15	20	15	30	70	100
Hungary	8	30	100	50	67	67	67	67	67	15	20	30	30	40	67	100	100
Israel	9	30	100	10	30	30	30	30	30	0	10	30	30	10	20	40	100
Italy	10	30	100	10	50	25	25	10	25	0	5	20		0	15	50	
	11			15	70	35	35	15	35	0	7	30		0	20	70	
Norway	12	18	100	(15)	25–35	40–45	(30)	(30)	(60)	(2)	(5)	(12)	(18)	(8)	(20)	(80)	100
Sweden	13	20	100	(20)	30	40	40	(30)	(35)	(5)	(10)	(15)	(20)	(10)	(20)	(70)	
Switzerland	14	30	100	33	33	33	33	33	33	3	5	8	11	11	21	32	44
USA	15	24	85	42	53	44	44	42.5	51.5	5	12	20	22	19	49	79	85
	16		100	0	30	50	50	32	68	12	12	12	12	32	62	95	100
Yugoslavia	17	30	100	30	30	50	50	30	60						50	90	

Belgium

The last edition (1975/76) of the official table issued by the Ministry of Public Health is based on the paper of Hambresin (1958): see 2 in Table 2 However it allows the Esterman I system. It is now used for every purpose, except the determination of handicaps handled by the Ministry of Social Works, which still makes obligatory an older system from 1959.

Bulgaria

There are three degrees of disability. They correspond to bilateral concentric narrowings to 30–40°, 20° and 10°.

Canada

According to the Worker's Compensation Board the functional loss of one eye corresponds to 16% of wage, the functional loss of both eyes to 100%, and a (right or left) homonymous hemianopsia to 25%. There are no other rules which can be identified provincially or nationally in judging visual disability on a percentage basis.

   As a result of our enquiry Dr Gordon R. Douglas asked 7 ophthalmologists (glaucoma specialists and people working in low vision) to assess disability percentages for various field defects. Some of the results are given in Table 3. Only two individuals gave their opinions on the basis of Worker's Compensation Board estimates as mentioned above. A statistical analysis showed that the 7 means are very different at a very high level of significance (P<0.00001) and that the attempt at a consensus of opinion has failed.

Denmark

In the Danish pension legislation a three-step ladder is used, corresponding to 50%, 75% and 100% disability. Traditionally bilateral concentric narrowing to 10° corresponds to 100% disability. Combinations of a reduction of visual acuity to 6/18 with a complete hemianopsia or a concentric narrowing to 20° are scored at 50% disability. In this frame it is extremely difficult to determine disabilities amounting to less than 40%.

   However in the regulations of compensation for work accidents hemianopsia is rated to correspond to 40% disability. No other visual field defects are considered (Th. Rosenberg).

Table 3. Percentages of disability for visual field defects as rated in Canada by 7 ophthalmologists.

	Loss one eye	Loss both eyes	Complete hemianopsia						Concentric narrowing					
			heteron.		homon.		horiz.		in one eye			in both eyes		
			bin.	bit.	right	left	sup.	inf.	50°	30°	10°	50°	30°	10°
	1	2	3	4	5	6	7	8	9	10	11	13	14	15
A	16	100	20	25	20	20	12	25	0	5	16	10	16	75
B	45	100	30	30	30	30	20	30	5	10	15	20	25	30
C	35	100	60	75	80	75	45	75	6	18	25	20	45	85
D	16	100	35	10	8	8	30	14	1	8	16	30	14	16
E	30	100	40	50	50	50	60	60	7	15	25	12	25	50
F	20	100	20	25	50	50	50	60	4	20	20	20	40	80
G			60	50	45	40	25	55	9	14	20	25	55	85

Finland

The actual regulation is reproduced in row 3.

France

Many different systems are still applied, namely:
- for military pensions and for the victims of war: several systems succeeding to the laws of 1836, 1887, 1919 etc.
- for work accidents and for the occupational diseases: e g. the Journal Officiel of December 30, 1982, succeeding to laws from 1898, 1938, 1939 etc
- for civil cases (traffic accidents, assaults and so on). tables of the Concours médical, of the Société de Médecine Légale etc.

The military systems give as much as 65% disability for the loss of one eye and cannot be compared to the others, of which row 4 is an example for work accidents (established by Louis Guillaumat) while row 5 is an example for civil cases (established by Jean Vola). It is typically French that ranges of disabilities are given for each kind of defect.

German Democratic Republic

The system which is generally used nowadays is that which has been accepted by the Ministry of Public Health on April 29, 1961 on proposal of Velhagen and Sachsenweger. It can be found in the book of Sachsenweger [35]: see row 6

Another system in three grades based on visual acuity and visual field is used only for social insurance of the partially sighted.

German Federal Republic

The system which has been proposed by the German Ophthalmological Society on September 22, 1981 on proposal of Aulhorn, Pape, Schulte, Thomann, Waubke and Gramberg-Danielsen is now used for most purposes: row 7.

A special system expressed in twentieths of use for each eye is still valid for private accident insurance and is described by Burggraf and Burggraf [4]

Hungary

This country uses a three degrees system of disability, whereby homonymous hemianopsia and bilateral concentric narrowing to 20° correspond to the third degree.

The values on row 8 of Table 2 were based by Follmann on a methodological letter for internal use, approved by the Ministry of Health and the National Institute of Ophthalmology.

India

The All India Blind Relief Society uses the 1977 WHO classification in four categories of visual impairment: mild (50% disability), moderate (75%), severe (100%) and profound (100%). Bilateral concentric narrowing to 20° is considered as moderate, 10° as severe and 5° as profound.

Israel

Row 9 reproduces the actual regulation.

Italy

There is no official regulation. Most ophthalmologists use the book of Luvoni and Bernardi [25], in which the disability percentages are different for civil responsability (row 10) and for work accidents (row 11).

Japan

In the Workmen's Accident Compensation Insurance system there are 14 grades of physical handicap. Visual field impairment which is larger than 60% of the normal field area in both eyes (assessed on 8 meridians) gives access to subdivision 4 of the 9th grade. A similar defect in only one eye gives access to subdivision 4 of the 13th grade.

In the social welfare law of visual handicapped persons there are 7 grades of visual impairment. A binocular visual field smaller than half the normal binocular visual field corresponds to subdivision 3 of the 5th grade. A visual field smaller than 10° in both eyes corresponds to subdivision 2 of the 5th grade, while a bilateral contraction to less them 5° corresponds to subdivision 2 of the 4th grade.

The Netherlands

The somewhat complicated Colenbrander [6] system never achieved general acceptance. There are no national regulations. In many instances involving a

financial settlement the insuring agency seeks to judge disability according to such foreign systems as the AMA rules, the DOG rules or the book of Sachsenweger [34]. Most Dutch ophthalmologists also follow such foreign rules in cases where they are not specified.

Norway

The regulations of the official insurance system (concerning also work accidents and war damage) specifies that paracentral visual field defects are more disabling than peripheral ones, defects in the lower field more disabling than those in the upper field, temporal defects more disabling than nasal ones, congruent defects more disabling than non-congruent ones, and right homonymous defects more disabling than left ones. However it yields only a very small number of percentages: row 12, where the figures between brackets were interpolated by Hansen

Spain

In 1984 Spain and some countries of South America accepted the disability calculations of the Council on Industrial Health and thus the old American AMA system. Murube-del-Castillo et al [31] (1985) describe not only the old AMA system, but also the 1978 WHO system.

Sweden

There are no governmental rules. Some principles were accepted by private Swedish insurance companies as a base for economic compensation· row 13, where the figures within brackets were interpolated by Hedin.

Switzerland

By a new law on work accident insurance applied since January 1, 1984 the system of Dufour and Cuendet [10] is used with as basis 30% for the loss of one eye: row 14 of Table 2. Private insurances now use the same system.

United Kingdom

Great Britain does not have any national or private standards relating to disability percentages for visual field defects. Most of the approached colleagues added that they do not want to have any such standards.

518

United States of America

The older American Medical Association (AMA) system (row 15) was adapted from a report prepared by a committee of the Council on Industrial Health in 1955 and was much used until the monocular Esterman system became in April 1984 standard for the United States by publication in the AMA Guides to Impairment. The same two systems are still used by the Department of Health and Human Services. The binocular Esterman system (row 16) will probably soon become standard.

Yugoslavia

Row 17 gives the actual disability percentages prescribed by a law passed in 1975.

We have not considered the reduced disability percentages which are sometimes applied to lesser handicaps (Rintelen, [33]; often in France) or after a given time.

All reviewed standards imply that the extents of the visual fields have been measured kinetically by means of an intense target (at least III/3, generally III/4 and even V/4 in the case of the Goldmann perimeter).

Discussion

We will not discuss here the wisdom of trying to determine precise disability percentages on the general work market for visual field defects as well as for other handicaps. However we must stress that, if we do, we have to make it as uniformly as possible. Moreover, owing to the enormous differences between national regulations, as shown in Table 2, it seems evident that some standardization has to be proposed by a relevant international organization.

The first principle for such a standardization could be that disability percentages have to be rated on the basis of functional impairment and not merely on the size of lost field areas. This principle implies, taking into account what we know about the normal and pathological functional visual field (see Verriest et al. [37]), *that the disability assessment should be based on the binocular visual field* and not on the monocular visual fields. Indeed we look with both eyes together in the overwhelming majority of real life situations. Accordingly impairment is much less or even non existant for monocular defects when compared to binocular ones and for heteronymous defects when compared to homonymous ones.

This was not recognized by many systems and regulations, including the French ones and the old AMA system, but is a common feature of the old German systems (and their derivatives) and of the Esterman binocular system.

We asked several persons to rate, according to their own national rules, the

disability percentages corresponding to 64 pairs of monocular visual fields presenting many kinds of field defects. Fig. 1 shows that, with visual fields ordered according to the Esterman binocular scores, there is a better agreement among these scores and those derived from the old German school (GFR, GDR, Belgium) than with the figures from other countries.

On the other hand, it must be stressed that it is much more realistic to obtain the binocular field on which the disability percentage will be scored not by superimposing the two monocular fields but by actually measuring the binocular visual field in binocular vision (without any dissociation between the two eyes). The reasons are that there is in binocular vision an enhancement of perception, also in pathological cases [5, 12], and that otherwise we cannot guess how the binocular visual field behaves in cases of squint [27]. Technically it is not a problem to measure the visual field in binocular conditions with a perimeter of rather larger radius such as the Goldmann apparatus despite normal convergence on the fixation target and despite eventual lack of fixation control (especially since binocular fixation is steadier and more reliable than monocular).

What we know about the functional visual field implies that relatively more weight should be given to *central defects* than to peripheral ones, to *inferior defects* than to superior ones, and to *defects along the horizontal meridian* than to defects along other meridians The only systems which take account of these three principles alltogether are those of Colenbrander and of Esterman

The comparison in Tables 1 and 2 of the percentages for the different kinds of hemianopsia allows to detect easily in which systems superior defects are considered less disabling than inferior defects. We can also infer from Tables 1 and 2 that some systems and regulations imply that *right homonymous hemianopsia should be more disabling than the left one* The principal reason for this assumption is that (in occidental culture) one reads from left to right, while a subsidiary reason is that (in most Western countries) one drives in the right lane and has to watch right priority

Such a distinction is not provided by the Esterman binocular system. In fact, it is not necessary as the Esterman systems omit *visual function within the central 5 degree circle,* while it is well known that only a central visual field of 5° radius is needed for recognizing letters and for regulating the reading saccades to the right Visual field defects outside 5° could affect the return saccade to the beginning of the next line, but this pertains more to left hemianopsia than to right hemianopsia.

Ignoring defects in the very central part of the visual field is another similarity between the old German school and Esterman. Esterman wrote that examination by his grid system should be separate and distinct from the assessment of central visual acuity, which has always been quite properly and adequately expressed by the Snellen fraction. Let us add that it should also be (eventually) completed by the assessment of reading ability, as this can be impaired by paracentral scotomata affecting neither the more peripheral visual field nor central acuity. The

520
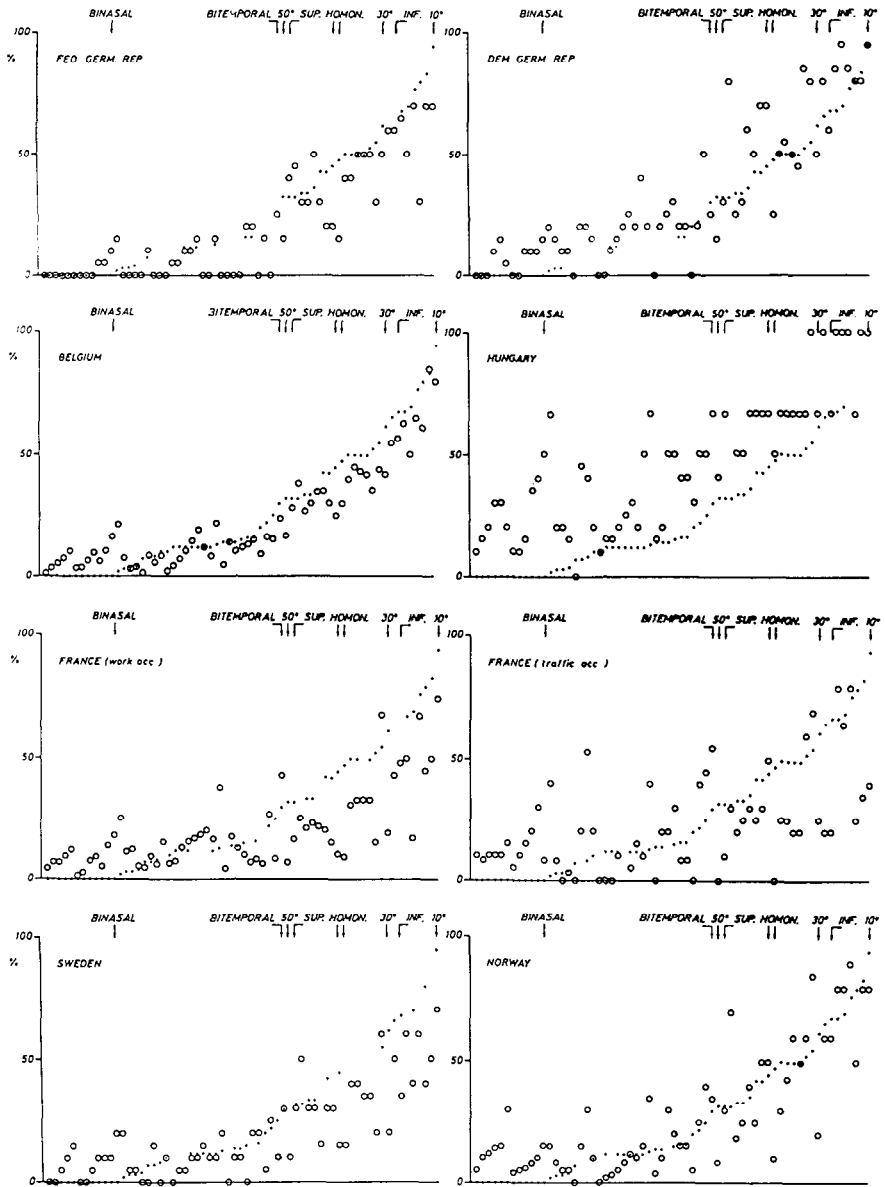
Figure 1 Comparison, for 64 pairs of monocular fields representing the usual kinds of perimetric defects, of the binocular Esterman scores (dots) with the scores obtained in various european countries according to national regulations (○) The fields are ranked according to increasing binocular Esterman scores The Esterman scores correlate better with those inspired from the old german authors (especially Belgium!) than with other systems (as in France)

belgian rule of 1976 assigns important disability percentages to such defects.

For driving in the right lane, right homonymous hemianopsia makes it difficult to take right priority into account, but left homonymous hemianopsia imperits overtakings. On the other hand it is better that a system for international use should not introduce geographically limited considerations (e.g. Japanese read vertically and drive left).

We should also discuss the relationship between the percentages for visual field defects according to the Esterman binocular system and that for the *total functional loss of one eye*. In most countries the loss of one eye is presently estimated to correspond to 25% or 30% disability. In fact there is in this condition (nearly) no loss in binocular visual acuity and the loss of only a (peripheral!) sixth of the binocular field: exactly 11% disability according to the Esterman binocular system. This is again in agreement with the old German school, for which the loss of the visual field of one eye (or of its temporal crescent) corresponds to 10% disability [18, 26, 36]. Loss of one eye also causes loss of stereopsis, but loss of binocular vision is practically never regarded in disability determination (because it should correspond to a disability percentage in concomitant strabismus and even to a supplementary disability percentage in heteronymous hemianopsia).

One could conclude that the major part of the 25–30% disability from the functional loss of one eye is in fact a compensation for a loss in the potential reserve of vision, which becomes a real disadvantage only in the rare monocular experiences of life and, of course, in the event of permanent loss of the second eye. Furthermore, if we accept this, we should also have to accept a (smaller) degree of disability for a visual field defect of one eye which is compensated by a sound field of the other. This has been done in Colenbrander's complicated system.

The other issue is to conclude that 25% is too much for the loss of an eye. One needs not be an ophthalmologist or a visual scientist to close one eye and realize that a 25% loss is a great exaggeration from the functional point of view. Moreover, the loss of an eye already corresponds to only 20% disability in Sweden, 18% in Norway and even 16% in Canada

We have also to consider that the target used in Esterman's systems is, as in most other systems, an intense one and that, accordingly, such systems take into account only *absolute defects*. It should not be impossible to take into account also *relative defects* as it was suggested by several authors [3, 7] and by Trutneva and Nemtseev (1985, pers. comm.). However we presently do not know to what extent relative defects could harm behavior, while testing with an unique intense target is less problematical as it does not imply correction of ametropia and presbyopia and as such a correction is practically impossible in the peripheral visual field. We should stress however that the examiner has not only to determine the peripheral limits (on at least 12 meridians) but also to check with the same target whether there are scotomata within the visual field (and to outline eventually such scotomata because the number of the corresponding Esterman dots has to be known).

As in other preceeding methods Esterman's grids have been conceived on the basis of a *kinetic* visual field determination. Kinetic perimetry is better than static perimetry for the assessment of the functional visual field because it permits easier detection of simulated or neurotic field narrowing, because in real life objects are generally in relative movement and because it shortens examination time. In principle the Esterman systems are those which are most easily adapted to (automated) *static* perimeters because they could present supraliminar stimuli (corresponding to the Goldmann target III4e) in all locations corresponding to the grid dots. In fact some automatic perimeters do not give access to the entire peripheral field; also it was found that, even with equivalent targets, one does not obtain the same Esterman scores by means of automated static perimetry as by means of conventional kinetic perimetry [13]. This could be foreseen as we know from Dubois-Poulsen [9] that successive lateral spatial summation makes a target of given intensity more visible peripherally when it is moving than when it is stationnary. Accordingly we must use in automatic perimeters a target which is somewhat more intense than Goldmann III4e so that it could be seen in static conditions even by older subjects.

Finally we must mention three further properties of the Esterman system that makes it still more proper to be chosen as an international standard:
1. the score, in percent, is obtained by a very simple count and does not require the use of a computer,
2. unlike all other systems, it produces a meaningful result even in very irregularly shaped visual field defects (as e.g. in glaucoma),
3. the grid could be *easily changed for special conditions*, e.g. certain specialized occupations, and given eye movements between the fixations.

Conclusion

A comparison of the different systems and of the different national regulations which were made in order to obtain disability percentages for visual field defects shows very different scores for the same defects and thus a real need of standardization.

It is the 1982 binocular Esterman system which has to be recommended because it offers all the combined advantages
1. of values which are based on the knowledge of the functional visual field and which are comparable to that of the better preceeding systems and
2. of great ease of obtaining the results even for the most complicated defects.
It should be understood that the original Esterman score is a positive figure, quantifying not the lost field but the seeing (retained) field. The percent functional loss considered here is the opposite: it equals the Esterman score subtracted from 100% (a 70% functional field = a 30% loss).

Furthermore it has to be recommended that:

1. the binocular visual field should be plotted and then measured binocularly, even in cases of squint, ignoring the misalignment of the eyes and without any dissociation between the two eyes;
2. the used perimeter permits the exploration of the visual field at least to 85° eccentricity;
3. the used target should be equivalent to the Goldmann target III4e in the case of kinetic perimetry and that it should be more intense, in order to be visible for all normal subjects in all Esterman locations, in the case of (automatic) static perimetry;
4. in the case of kinetic perimetry, the examiner should determine the peripheral limits as well as the outline of all scotomata within the visual field;
5. in the case of (automated) static perimetry, the stimulus should be presented at all 120 Esterman locations;
6. spectacles be worn only if the patient customarily wears them for everyday activity (i.e. aphakia, high myopia etc.);
7. the user should be aware that the system does not concern central and paracentral vision within 5 degrees eccentricity and, accordingly, that central and paracentral vision should be checked by other appropriate methods (central visual acuity and reading ability).

Notes

1 Data have been used from Elfriede Aulhorn (FGR), G Calabria (Italy), Emilio Campos (Italy), Gordon R Douglas (Canada), Ben Esterman (USA), Chr Faschinger (Austria), Piroska Follmann (Hungary), Fumio Furuno (Japan), B Gramberg-Danielsen (FGR), Louis Guillaumat (France), Egill Hansen (Norway), Anders Hedin (Sweden), Roger A Hitchings (UK), Lea Hyvärinen (Finland), Riri S Manor (Israel), Marion Marré (DGR), Juan Murube del Castillo (Spain), Anastassia Nakowa (Bulgaria), G I Nemtseev (Soviet Union), Tetsure Ogawa (Japan), Ajay Pathak (India), D F Rice (UK), André Roth (Switzerland), Thomas Rosenberg (Denmark), Slobodan Savic (Yugoslavia), P J Spierenburg (Nederland), K V Trutneva (Soviet Union) and Jean Vola (France)

Dr Jorge Benozzi (Buenos-Aires) wrote to me on September 3, 1986 that there is no official regulation in Argentina The ophthalmologists decide and generally take only visual acuity in account A recent joint paper of the lawyer M E Marsiletti and the ophthalmologist N Palermo give as much as 42% for the functional loss of one eye and 80% for bitemporal hemianopsia

References

1 Berry GA: On the relation between visual acuity and visual efficiency Trans Ophthalmol Soc UK 13: 233 (1983)
2 Bracci Torsi H: Sui criteri d'indennizzo globale nei danneggiamenti da infortunio della funzione visiva Ann Ottalmol Clin Ocul 61: 461–470 (1933)
3 Bronner A, Schalk Ph, Lambrou GN: Représentation tridimensionnelle et quantification du

champ visuel; Application aux névrites optiques Soc Fr Ophthalmol, May 13, 1986

4 Burggraf H, Burggraf A: Grundlagen augenärztlicher Begutachtung in der Bundesrepublik Deutschland Gustav Fischer, Stuttgart, 1984

5 Calabria G, Capris P, Burtolo C: Investigations on space behaviour of glaucomatous people with extensive visual field loss Docum Ophthalmol Proc Ser 35: 205–210 (1983)

6 Colenbrander MC: Visual acuity, visual field and physical ability, A proposal of a formula Ophthalmologica 171: 100–108 (1975)

7 Crick RP, Crick JCP, Ripley L: The representation of the visual field Docum Ophthalmol Proc Ser 35: 193–203 (1983)

8 Dannheim F: Non-linear projection in visual field charting Docum Ophthalmol Proc Ser 35: 217–223 (1983)

9 Dubois-Poulsen A et al : Le champ visuel, Topographie normale et pathologique de ses sensibilités Masson & Cie, Paris, 1952

10 Dufour R, Cuendet JF: Graphiques pour l'estimation des invalidités en ophtalmologie Ophthalmologica 141: 262–267 (1961)

11 Esterman B: Grid for scoring visual fields, I Tangent screen II Perimeter Arch Ophthalmol 77: 780–786 (1967); 79: 400–406 (1968)

12 Esterman B: Functional scoring of the binocular field Ophthalmology 89: 1226–1234 (1982)

13 Esterman B, Blanche E, Wallach M, Bonelli A: Computerized scoring of the functional field, Preliminary report Docum Ophthalmol Proc Ser 42: 333–339 (1985)

14 Furuno K: disc Verriest et al Docum Ophthalmol Proc Ser 35: 222–223 (1983)

15 Gasteiger H: Uber Bewertung von Gesichtsfeldstörungen in Gutachten Klin Mbl Augenheilk 116: 537–542 (1950)

16 Genêt L: Hémianopsies d'origine corticale, Evaluation des invalidités Ann Oculist (Paris) 153: 153–157 (1916)

17 Gramberg-Danielsen B et al : Augenärztliche Begutachtung im Versicherungswesen Bücherei d Augenarztes 91 Enke, Stuttgart, 1982

18 Groenouw: Anleitung zur Berechnung der Erwerbsfähigkeit bei Sehstörungen Bergman, Wiesbaden, 1896

19 Groenouw: Sehstörungen und Invalidenversicherungsgesetzgebung Klin Mbl Augenheilk 43 (Beilageh): 1–31 (1905)

20 Hambresin L: Essai d'uniformisation des taux d'invalidité en ophthalmologie Rapport présenté à la 3e réunion de l'Association Internationale des Médecins Oculistes, Bruxelles, 11 9 1958

21 Haruta R, Kani K, Inui T: A new numerical representation of the visual field in regard to the retinal ganglion cell density Docum Ophthalmol Proc Ser 42: 131–136 (1985)

22 Hummelsheim: Uber die Frage der Werteinschätzung des Verlustes, bzw der Sehschädigung eines Auges Klin Mbl Augenheilk 42: 265–273 (1904)

23 Jaeger W, Thomann H: Rechtsfragen und Begutachtung, Deutsche Ophthalmologische Gesellschaft, Empfehlungen zur Beurteilung der Minderung der Erwerbsfähigkeit durch Schäden des Sehvermögens, September 1981 Klin Mbl Augenheilk 180: 242–244 (1982)

24 Jonquères J: Projet de barême des invalidités ophthalmologiques en droit civil Bull Socs Ophtalmol France 81: 195–199 (1981)

25 Luvoni R, Bernardi O: Guida alla valutazione medico-legale dell' invalidità permanente, Infortunistica del lavoro e infortunistica privata, responsabilità civile Dott A Giuffre, Milano, 1970

26 Magnus: Leitfaden für Begutachtung und Berechnung von Unfallbeschädigung der Augen (2nd ed) J Kern, Breslau, 1897

27 Mahendrastari R, Verriest G: Monocular and binocular visual field in different types of strabismus Docum Ophthalmol Proc Ser 42: 507–509 (1985)

28 Maschke: Die augenärztliche Unfallpraxis JF Bergmann, Wiesbaden, 1899

29 Mills RP, Drance StM: Esterman disability rating in severe glaucoma Ophthalmology 93: 371–378 (1986)

30 Mooren: Nochmals das Capitel: 'Sehstörungen und Entschädigung' Klin Mbl Augenheilk 28: 336–342 (1890)

31 Murube-del-Castillo J, Emparan-Alvarez A, Mocorrea Roemmers M, Salazar Oliveros L, Viana Perez J: Oftalmologia legal, Deficiencias, menoscabos y desventajas visuales Ann Soc Ergof Esp 14: 1–23 (1985)

32 Percival ASt: Relation between visual acuity and efficiency Ophthalmic Rev: 211 (1899)

33 Rintelen F: Probleme der Unfallophthalmologie Ophthalmologica 128: 326–343 (1954)

34 Sachsenweger R: Augenärztliche Begutachtung Gustav Fischer Stuttgart, 1976

35 Sachsenweger R: Augenärztliche Begutachtung in der DDR VEB Georg Thieme, Leipzig, 1983

36 Schroeter P: Unfallentschädigungen des Sehvermögens und ihre Abschätzung, Antritts-vorlesung A Edelmann, Leipzig, 1891

37 Verriest G, et al : The occupational visual field I Theoretical aspects: The normal functional visual field II Practical aspects: The functional visual field in abnormal conditions and its relationship to visual ergonomics, visual impairment and job fitness Docum Ophthalmol Proc Ser 35: 165–185 (1983); 42: 281–326 (1985)

38 Voisin J: Comment peut-on envisager le taux d'invalidité secondaire à la perte d'un quadrant du champ visuel? 5e Symposium Int Ergophtalmol, Bordeaux, 23–24 Mai 1974

39 von Guillery: Über die Entschädigungsansprüche Einäugiger Klin Mbl Augenheilk 30: 206–218 (1892)

40 von Schleich G: Erwerbsbeschränkung bei gleichseitiger Hemianopsie Klin Mbl Augenheilk 58: 506–507 (1917)

41 von Zehender: Über den zahlenmässigen Ausdruck der Erwerbsunfähigkeit gegenüber den Unfallversicherungsgesellschaften Klin Mbl Augenheilk 27: 265–282 (1889)

Author's address:
Guy Verriest, M D ,
Dept of Ophthalmology,
Universitair Ziekenhuis,
De Pintelaan 185, B-9000 Gent, Belgium

VIII.2 Automated Esterman testing of disability in glaucoma

E.S. CHOY, R.P. MILLS and S.M. DRANCE
Seattle, U.S.A. and Vancouver, Canada

Abstract

Patients with severe glaucomatous visual loss were evaluated for visual field disability with the Esterman binocular program on an automated perimeter and with conventional manual testing on the Goldmann perimeter. The disability indices obtained from the two types of testing were highly correlated. A brief questionnaire, which rated patients' perceptions of their disability, correlated moderately well with the objective indices. The automated Esterman test was rapid, produced highly reproducible results, and offers an attractive alternative to the current standard manual method for visual disability estimation

Introduction

The evaluation of visual field disability is a new application of automated perimetry. Binocular testing has been advocated as more relevant in terms of the patient's functional disability than traditional monocular testing [1, 4, 5]. In a prior study, good correlation of visual disability scores generated by binocular automated Esterman perimetry and monocular testing with manual kinetic or automated Esterman perimetry was shown [8] The same study identified several questions relating to patient perceptions of their visual disability which correlated with objectively measured visual field loss The goals of the current study were to compare different methods of rating visual field disability, evaluate the previously refined questionnaire, and estimate the reliability of Esterman binocular suprathreshold automated perimetry with repeated testing

Methods

Patients with severe glaucomatous visual field loss were recruited from the clinic

populations of the University of Washington Hospitals and Vancouver General Hospital. Eligibility was determined by an absolute loss of over 50% of the visual field in one or both eyes on testing with Goldmann manual or Humphrey automated perimeters.

All study participants had visual fields evaluated by manual testing with the Goldmann perimeter using a III-4-e stimulus and by an Esterman binocular test on a CooperVision Diagnostics Dicon AP2000 perimeter with stimulus intensity = 10,000 apostilbs and background intensity = 31.5 apostilbs. The automated Esterman program calculated a residual visual function score as the percentage of points seen. As described previously [8], a visual disability index (percentage of visual field loss) was derived by subtracting the visual function score from 100. To simulate everyday conditions, the patients wore their glasses for testing only if glasses were always worn. Patients were then administered a brief questionnaire (Table 1) consisting of five items previously shown to correlate with the Esterman binocular disability index [8]; responses for each question were rated ordinally from one (least impairment) to three (greatest impairment). The question responses were summed into a 'Q score'. Corrected visual acuity in each eye was also recorded.

The fields done with the III-4-e stimulus at the Goldmann perimeter were analyzed by two methods·

Meridian

The meridian approach is the original method adopted by the American Medical Association (AMA) for visual field loss evaluation. The sum of the eccentricities of the isopter in the eight principal meridians was divided by five, and then subtracted from 100 [1]. The monocular results were combined by an AMA impairment values table [1] into a 'principal meridian binocular visual field loss score' Calculations were made both by ignoring scotomas central to the peripheral isopter and by subtracting any scotoma's width from the values of the meridians crossing through it.

Table 1 Visual disability questionnaire

1	Are your vision troubles mostly corrected by glasses?
2	Do you bump into or trip on things?
3	Have you had to give up any activities because of your vision?
4	Do you notice any variation in color richness from time to time?
5	Do you have trouble following a line of print or finding the next line of print?
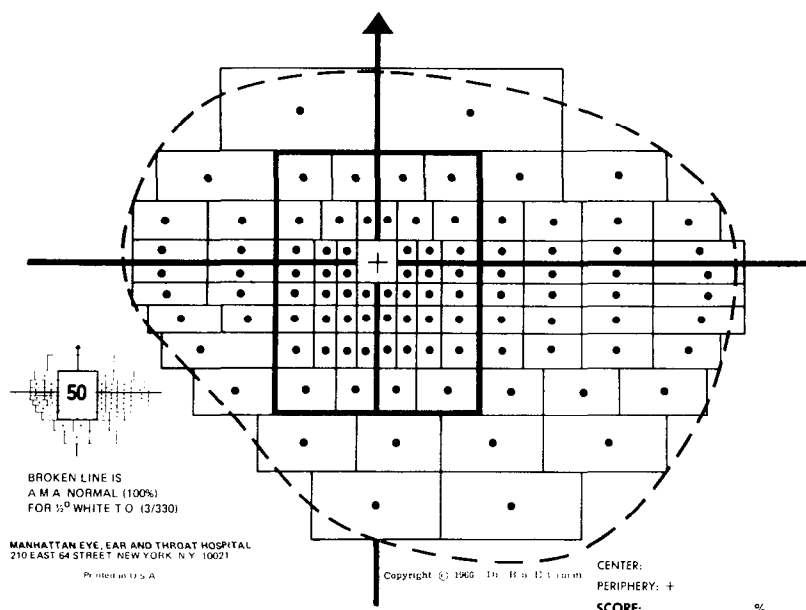
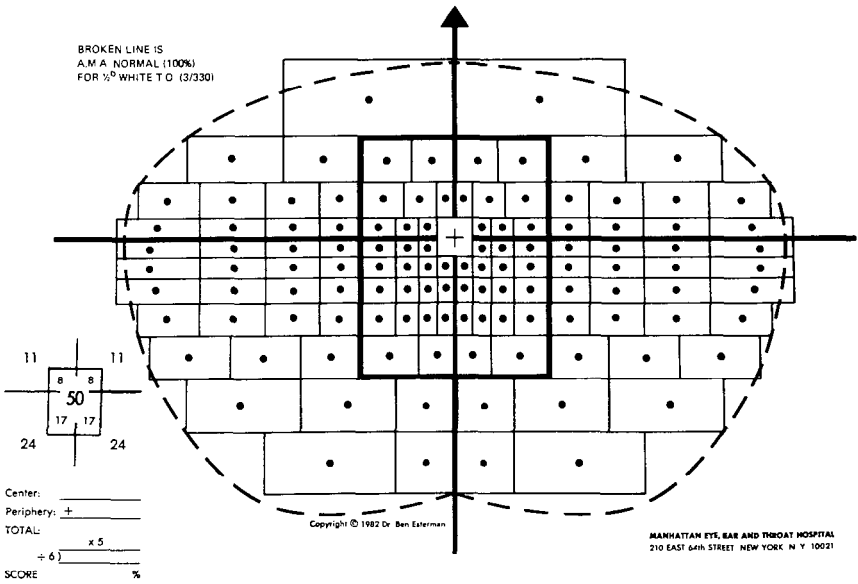*Figure 1* Esterman grid for scoring a manual monocular field This template is placed over a standard Goldmann perimeter chart One point is scored for each dot lying outside the III-4-e isopter line The result is a percent visual field disability

Grid

Field charts were overlaid with the Esterman 100-unit functional Relative Value Grid, which enabled a simple count of each grid square falling outside the isopter outline (Fig 1). Again, the monocular grid scores were combined by the AMA impairment values table to produce a calculated binocular score. The paracentral area, the zone alongside the horizontal meridian and the inferior field are weighted more heavily using this method [5] In addition, an Esterman 120-point binocular grid (Fig. 2) was used as an overlay of both monocular fields, grid squares falling outside both monocular isopters were counted to produce a binocular Esterman grid score [4].

Pearson's R correlation coefficient [9] was calculated for combinations of disability scores from the automated Esterman program, manual fields, and questionnaire. Some patients who were examined previously in a preliminary evaluation of the Esterman binocular quantitative field program [8] were retested in the current study; for this subset of patients, the correlation between current and previous disability scores was calculated to estimate reliability of the automated Esterman test

BROKEN LINE IS
A.M.A. NORMAL (100%)
FOR ½° WHITE T O (3/330)

11   11
8   8
50
17   17
24   24

Center:
Periphery: +
TOTAL
x 5
÷ 6)
SCORE   %

Copyright © 1982 Dr Ben Esterman

MANHATTAN EYE, EAR AND THROAT HOSPITAL
210 EAST 64th STREET NEW YORK N Y 10021

Figure 2 Esterman grid for scoring a manual binocular field This template is placed over a standard Goldmann perimeter chart on which a binocular III-4-e isopter has been plotted One point is scored for each dot lying outside the III-4-e isopter line. The score is multiplied by 5/6 to determine the percent visual field disability

Results

Forty-seven patients (21 male, 26 female) with severe glaucoma were enrolled in the study. Age distributions are noted in Fig. 3; the mean age was 70.0 years with a range from 32 to 97. Corrected visual acuity in the better eye ranged between 20/15 and finger counting, with a median of 20/40 (Fig. 4). Fifteen patients were functionally monocular with visual acuity in the worse eye HM, LP, or NLP. Automated Esterman Binocular Disability Index (EBDI), a measure of visual field loss, ranged from 0 to 88, with a mean of 32.1 (Fig. 5).

Correlations were high between EBDI and scores derived using four methods that combined monocular fields done with the III-4-e isopter on the Goldmann perimeter (Table 2). Correlations among these latter four methods were also very high The difference between meridian analyses with and without scotoma subtraction was minimal The mean and range of disability scores for each method are seen in Table 3.

Questionnaire scores (ranging from 5–15 with higher scores reflecting an increase in perceived disability) correlated moderately well with all disability scores and with visual acuity (Table 4). The highest correlations were observed with both EBDI and visual acuity score. However, visual acuity in the better eye correlated poorly with all visual field disability scores (Table 5).
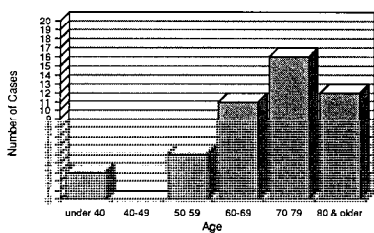
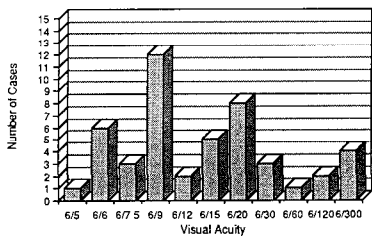*Figure 3* Age distribution of the 47 study patients with severe glaucoma

Figure 4 Best corrected visual acuity of the better eye of the 47 study patients

Table 2 Correlations* of visual field disability scores

	EBDI	Meridian 1	Meridian 2	Esterman grid monocular	Esterman grid binocular
EBDI[a]					
Meridian 1[b]	0 91				
Meridian 2[c]	0 91	0 98			
Esterman grid monocular[d]	0 92	0 97	0 97		
Esterman grid binocular[e]	0 89	0 94	0 91	0 96	

* Pearson's R, with 2-tailed p = 00000 for all correlations, n = 47
[a] Esterman binocular disability index (from automated Dicon perimetry)
[b] Principal meridian analysis including scotomas as visual field loss (from manual perimetry – Goldmann) Monocular scores were combined by use of AMA impairment values table [1]
[c] Principal meridian analysis ignoring scotomas (from manual perimetry – Goldmann) Monocular scores were combined by use of AMA impairment values table [1]
[d] Combination of monocular Esterman grids (from manual perimetry – Goldmann) Monocular scores were combined by use of AMA impairment values table [1]
[e] Binocular Esterman grid on superimposed monocular fields (from manual perimetry – Goldmann)

The automated Esterman disability scores obtained in this study were compared with similar scores obtained two years previously on the same subset of 21 patients with a resulting R = 0 97, p = 0.00000. Testing time averaged 4 5 minutes (range 3.0 to 6.7).

Table 3 Mean and ranges of visual field disability scores

Method	Mean	Range
EBDI[a]	32	0–88
meridian 1[b]	48	15–97
meridian 2[c]	46	15–97
Esterman grid monocular[d]	47	14–100
Esterman grid binocular[e]	40	4–100

N = 47

[a] Esterman binocular disability index (from automated Dicon perimetry)

[b] Principal meridian analysis including scotomas as visual field loss (from manual perimetry – Goldmann) Monocular scores were combined by use of AMA impairment values table [1]

[c] Principal meridian analysis ignoring scotomas (from manual perimetry – Goldmann) Monocular scores were combined by use of AMA impairment values table [1]

[d] Combination of monocular Esterman grids (from manual perimetry – Goldmann) Monocular scores were combined by use of AMA impairment values table [1]

[e] Binocular Esterman grid on superimposed monocular fields (from manual perimetry – Goldmann)

Table 4 Correlation of questionnaire score with visual field disability scores and visual acuity

	R*	2-tailed p
Q score* v EBDI[a]	0 71	0 00003
Meridian 1[b]	0 63	0 00034
Meridian 2[c]	0 65	0 00029
Esterman grid monocular[d]	0 67	0 00019
Esterman grid binocular[e]	0 65	0 00013
Visual acuity[f]	0 73	0 00001

* Q score may range from 5–15; higher scores indicate greater perceived disability

* Pearson's correlation coefficient, N = 47

[a] Esterman binocular disability index (from automated Dicon perimetry)

[b] Principal meridian analysis including scotomas as visual field loss (from manual perimetry – Goldmann) Monocular scores were combined by use of AMA impairment values table [1]

[c] Principal meridian analysis ignoring scotomas (from manual perimetry – Goldmann) Monocular scores were combined by use of AMA impairment values table [1]

[d] Combination of monocular Esterman grids (from manual perimetry – Goldmann) Monocular scores were combined by use of AMA impairment values table [1]

[e] Binocular Esterman grid on superimposed monocular fields (from manual perimetry – Goldmann)
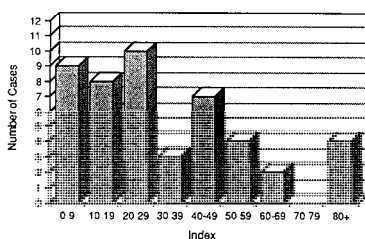
[f] Visual acuity in better eye

Figure 5 Esterman binocular disability index (% visual field loss) of the 47 study patients

Discussion

The automated Esterman binocular suprathreshold static program compares favorably to conventional monocular manual kinetic testing of visual field disability. Reports have begun to accumulate that consistently confirm such comparability [6, 8].

In the current study, the automated EBDI was highly correlated to both principal meridian and Esterman grid scoring of monocular fields done with the III-4-e isopter at the Goldmann perimeter. Intercorrelation between different scoring methods used on the same pair of monocular fields were, as expected, close to unity. In this patient series, most scotomas internal to the peripheral isopter were small, so meridian analyses with or without correction for scotomas were nearly perfectly correlated.

Table 5 Visual acuity correlations with visual field disability scores

	R*	2-tailed p
VA† v EBDI[a]	0 45	0 00070
Meridian 1[b]	0 39	0 00349
Meridian 2[c]	0 40	0 00248
Esterman grid monocular[d]	0 39	0 00335
Esterman grid binocular[e]	0 38	0 00378

† Corrected visual acuity in better eye
* Pearson's correlation coefficient, N = 47
[a] Esterman binocular disability index (from automated Dicon perimetry)
[b] Principal meridian analysis including scotomas as visual field loss (from manual perimetry – Goldmann) Monocular scores were combined by use of AMA impairment values table [1]
[c] Principal meridian analysis ignoring scotomas (from manual perimetry – Goldmann) Monocular scores were combined by use of AMA impairment values table [1]
[d] Combination of monocular Esterman grids (from manual perimetry – Goldmann) Monocular scores were combined by use of AMA impairment values table [1]
[e] Binocular Esterman grid on superimposed monocular fields (from manual perimetry – Goldmann)

The lower mean disability score of 32.1 for the automated method (EBDI), compared with scores derived from the manual charts (40–48, Table 3), suggests that the Dicon stimulus intensity of 10,000 asb was too strong. A lower intensity would have produced disability scores more comparable to those obtained from the manual fields done with the III-4-e isopter. Indeed, Esterman et al. [6] found a setting of 2500 asb on the Dicon perimeter to approximate the findings on a III-4-e isopter with the Goldmann perimeter in a general ophthalmology patient population. While our preliminary study suggested that the stronger 10,000 asb stimulus was a more appropriate choice, the Goldmann III-4-e isopter was not tested in a direct comparison as it was in this study. Accordingly, we are inclined to support Esterman's recommendation that 2500 asb (with 31.5 asb background) should be the standard stimulus strength. Currently available Dicon software incorporates this level as the default setting in the Esterman binocular test.

Subjective comparisons of visual field defect patterns showed good agreement between automated binocular Esterman and combined monocular manual testing methods.

Questionnaire results correlated better with objective visual field scores in this study than in the past report [8]. In contrast to the low predictive value of the five questions with visual acuity noted in our preliminary study [8], questionnaire scores in this group of patients correlated moderately well with visual acuity as well as with visual field disability scores. Since visual acuity and EBDI were poorly correlated with each other, the questionnaire seemed to be independently sensitive for field and acuity information.

A patient's perception of his visual disability may be influenced by many factors other than objective signs, including denial, adaptation, and secondary gain. Thus, moderate correlations between such perceptions and objective measures of disability such as EBDI are to be expected. Nonetheless, some assurance that the EBDI is, in fact, measuring functional disability can be obtained from the reasonably good correlation with the questionnaire score.

The reliability of the automated Esterman test (with $R = 0.97$) over a two-year interval may be regarded as excellent, especially given the potential changes in clinical history and the short- and long-term fluctuations inherent in perimetric testing. Eighty-one percent (17/21) of repeat scores were within 10% of the first score, with 13/21 deviating five or fewer points. This high degree of reproducibility, if confirmed in future investigations, is reassuring to those responsible for certifying disability levels on a continuing basis

As automated perimeters become more commonplace in clinical practices, agencies responsible for evaluating disability will feel increasing pressure to certify visual field test methodologies which do not require manual testing at the Goldmann or arc perimeter. These agencies are justifiably reluctant to do so without reasonable assurance that the results obtained with automated perimetry are comparable to those obtained with the previously acceptable standard. Automated strategies which test only the central 30 degrees of field are clearly not

acceptable for the application of disability testing. However, full field binocular testing using stimulus locations similar to those used in scoring fields with the Esterman binocular grid is an attractive automated alternative to conventional manual testing. The high correlation between the previously accepted manual standard and the Esterman test on the Dicon perimeter is evidence that the two methods can produce similar results, once comparable stimulus strengths can be determined. These results may also stimulate development of similar strategies by other manufacturers of automated perimeters

Acknowledgements

References

1 American Medical Association: Guides to the evaluation of permanent impairment (2nd Ed), pp 141–151 American Medical Association, Chicago, 1984
2 Calabria G, Capris P, Burtolo C: Investigations on space behaviour of glaucomatous people with extensive visual field loss Doc Ophthalmol Proc Ser 35: 205–210 (1983)
3 Calabria G, Gandolfo E, Rolando M, et al: Ergoperimetry in patients with severe visual field damage Doc Ophthalmol Proc Ser 42: 349–352 (1985)
4 Esterman B: Functional scoring of the binocular field Ophthalmology 89: 1226–1234 (1982)
5 Esterman B: Grid for scoring visual fields II Perimetry Aich Ophthalmol 79: 400–406 (1968)
6 Esterman B, Blanche E, Wallach M, Bonelli A: Computerized scoring of the functional field; preliminary report Doc Ophthalmol Proc Ser 42: 333–339 (1985)
7 Mills RP: A comparison of Goldmann, Fieldmaster 200, and Dicon AP2000 perimeters used in a screening mode Ophthalmology 91: 347–353 (1984)
8 Mills RP, Drance SM: Esterman disability rating in severe glaucoma Ophthalmology 93: 371–378 (1986)
9 SPSSX Edition 2, Appendix E: Scattergram, pp 928–933 McGraw Hill, New York, 1986

Authors' addresses:
Elizabeth S Choy, Richard P Mills,
Department of Ophthalmology, University of Washington, Seattle, Washington, U S A 98195

Stephen M Drance,
The University of British Columbia, Vancouver, Canada

VIII.3 Functional quantification of the visual field: a new scoring method

E. GANDOLFO
Genova, Italy

Abstract

Esterman's grid for visual field scoring is both well known and widely accepted as a valid system for evaluating perimetric defects. However, it does not offer a completely precise functional assessment, because the threshold inside the visual field areas studied is not evaluated. In order to overcome this drawback we studied a new scoring method based on the position of 100 points strategically placed on the perimetric diagram. This method permits the quantitative analysis of the results of manual or automatic perimetric examination performed utilizing four targets: IV/4, I/4, I/3 and I/2. The points arrangement has been studied on the basis of the physiological visual field width of elderly subjects. A correction index must be used with younger subjects.

Our method evaluates not only the defect's extention but also its depth. In such a manner a better quantification of the functional damage, useful for medical-legal and insurance purposes, is obtained

Introduction

The Esterman's grid for visual field quantitative evaluation is universally known [2, 3, 4]. This method offers important advantages regarding precision and speed of residual visual field evaluation. The most important disadvantage is represented by the lack of evaluation of the sensitivity inside the residual visual field. In such a way, the same score may be ascribed either to normal field charts or to pathological ones in which relative defects are present inside the normal peripheral limits.

According to these considerations we have devised a new method for functional visual field scoring.
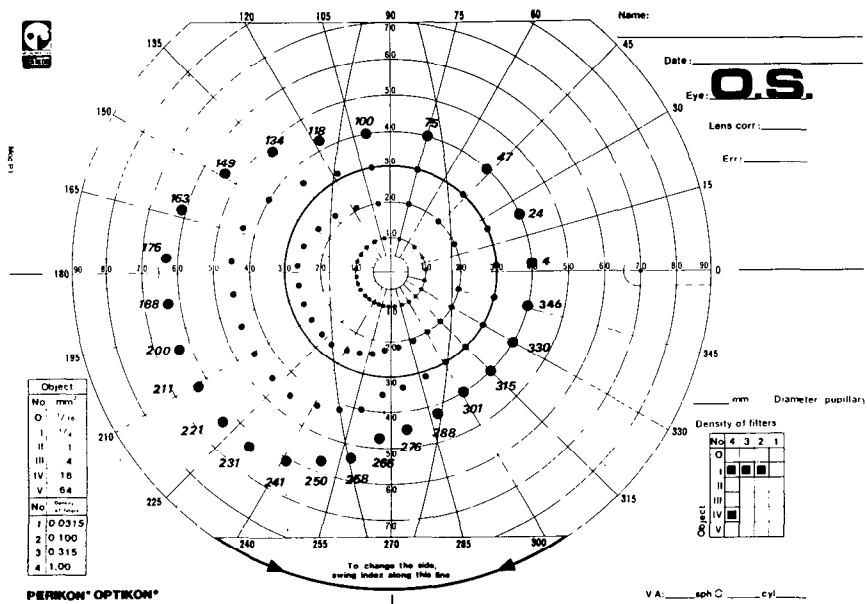
Figure 1 Scoring diagram for left eyes The 100 points are arranged in 4 concentric series of 25 points The numbers in the diagram indicate the meridians on which the points lie Every points series corresponds to an interisopteric space

Material and methods

We have elaborated a new method based on 100 points, strategically placed in order to emphasize the functionally most important areas (e.g. the inferior and temporal sectors of the visual field) (Fig. 1). Sixty points are placed in the lower and fourty in the upper visual field. The temporal visual field is covered by sixty points, while fourty are placed in the nasal visual field.

For the functional scoring, a standard manual or automatic kinetic examination with four isopters is required using the following stimuli: IV/4, I/4, I/3, I/2. The 100 points are arranged in four concentric series of 25 points. In relationship to a theoretical normal visual field, the most external series must lie between the two most peripheral isopters (IV/4 and I/4), the second series between the second and the third peripheral isopters (I/4 and I/3), the third series between the two most central isopters (I/3 and I/2), the fourth series inside the most central isopter (I/2).

This arrangement was studied on the basis of the physiological visual field width of elderly patients (older than 60 years) [1] A correction index must be adopted in the visual field scoring of younger people. This correction index is 0.8 for subjects under 40 years of age and 0.9 for ages between 40 and 60 years.

For the practical execution of our scoring test, we have elaborated two transparent diagrams (one for left eyes, the other for right eyes), reproducing the 100
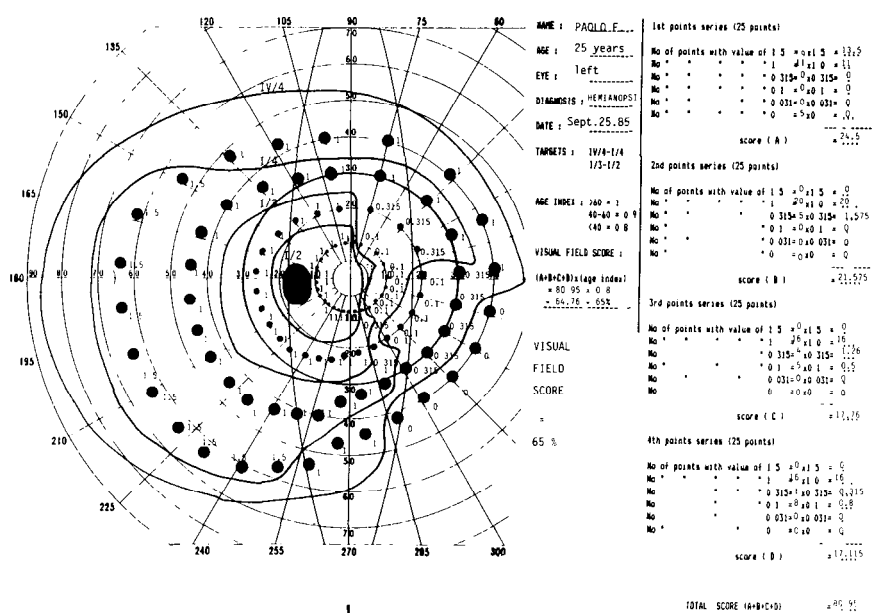
539

Figure 2 Example of the scoring strategy The position of every point is verified The values are assigned on the basis of the position of the points with respect to their own interisopteric spaces The final score must be calculated in relationship with the patient's age index

scoring points, which can easily be placed on the standard kinetic Goldmann charts in order to verify the position of every single point with respect to the corresponding interisopteric intervals.

The value of a point correctly positioned is 1 and the value of a point situated inside an absolute scotoma or outside the most peripheral isopter is 0. If a point is situated in an inner position in relationship to its own interisopteric interval, it is necessary to introduce an index of superevaluation that is in all cases equal to 1.5.

The value of every point situated more peripherally with respect to its physiological interisopteric space is modified according to the logarithmic scale of the Goldmann stimuli series (0.315; 0.1; 0.031). Following this criterion, the value 0.315 corresponds to a point situated outside its interisopteric space but inside the immediately more peripheral one. The value 0.1 refers to a point located two interisopteric steps outside its normal position and 0.031 is the value of a point that jumps three interisopteric steps. The same procedure must be performed in the case of relative defects, after their scotometric definition (Fig. 2).

These evaluation criteria have been adopted after a long series of perimetric tests. The same scoring step has been introduced between the most peripheral isopters (IV/4 and I/4) and between the most central ones, in order to give greater importance to the central and paracentral visual field in comparison with the periphery.

Results and comment

The proposed scoring strategy was verified in a large number of normal and pathological visual fields (50 cases with normal visual fields in people of different ages and 50 cases of pathological perimetric results in patients suffering from glaucoma, neurophthalmological disturbances, retinal detachment, etc) The score was rapidly and easily calculated (1 or 2 min. were required). Good compatibility with the Esterman grid results was found in normal visual fields or in cases of absolute defects (hemianopsias, severe central scotoma, etc.). The results appeared to be different when relative defects were present: in fact, this type of damage was not perfectly evaluated by the Esterman method.

Moreover, the proposed visual field scoring method can be easily automated utilizing computerized perimetry The positioning of the points along the visual field meridiands permits their automatic exploration with a simple static procedure. The results of automated kinetic perimetry performed by the computerized Goldmann perimeter 'Perikon' [5] can be easily scored utilizing our strategy, if standard targets are selected. In the future, we will elaborate further diagrams in order to evaluate binocular and functional visual fields for ergophthalmological and legal purposes.

References

1 Egge K: The visual field in normal subjects Acta Ophthalmol Suppl 169 (1984)
2 Esterman B: Grids for scoring visual fields I: tangent screen Arch Ophthalmol 77: 780–786 (1967)
3 Esterman B: Grids for scoring visual fields II: perimeter Arch Ophthalmol 79: 400–406 (1968)
4 Esterman B: Functional scoring of the binocular field Ophthalmology 89: 1226–1234 (1982)
5 Zingirian M, Gandolfo E, Orciuolo M: Automation of the Goldmann perimeter Doc Ophthalmol Proc Ser 35: 365–370 (1983)

Author's address:
Dr E Gandolfo,
Clinica Oculistica dell' Università,
Viale Benedetto XV, n° 5, I-16132, Genova, Italy

VIII.4 Effects of visual field defects on driving performance

A. HEDIN and P. LÖVSUND
Stockholm and Linköping, Sweden

Abstract

To elucidate the possible traffic safety risks induced by visual field defects, volunteers have been studied in a driving simulator In the traffic scene, stimuli randomly appeared in any of 24 different positions. The measured parameter was the latency between stimulus appearance and braking. Twenty younger and older normals served as controls. Only four out of 27 subjects with field defects showed compensation as did one of two one-eyed drivers. Contact lenses or glasses made no difference in two myopic persons. The results support the opinion that homonymous field defects should constitute an obstacle to licensing.

Introduction

Normal visual fields have long been considered essential for safe driving. In theory, a normal field makes possible the early detection of obstacles, other vehicles etc in the peripheral field. It has, however, been difficult to prove in practice that visual field defects constitute a risk and there are not sufficient data to support a standard for visual fields in drivers. It is very difficult to prove a correlation between a certain visual defect and an increased frequency of traffic accidents or violations The two main reasons are the low frequency and the multifactorial causes of these occurrences. When it comes to visual field defects, no correlation between the extent of the visual fields and the driving performance was found in several large-scale studies [1–4]. In these, non-standard perimetric techniques were used and only the horizontal meridian was tested.

In a more recent study, it was found that among over 17,000 volunteers those with bilateral visual field defects had a rate of accidents and convictions more than twice as high as the other subjects [5]. Here, a fast but nevertheless accurate perimetric procedure was followed. In another report, it was stated that the accident frequency of one-eyed drivers was increased and that these persons

tended to be involved in collisions to the anophthalmic side [6]. No study so far has been devoted to the possible compensatory mechanisms. It has been claimed, especially by the patients themselves, that they learn to see in the blind area by frequent head and eye movements. Drivers, almost without exception, deny any problems with detection in the direction of the blind zone (as related to the dominating fixation point straight ahead).

We considered that it was of great interest to study the detection capacity in a simulated driving situation. A computer-assisted program was designed for the driving simulator at VTI (Swedish Road and Traffic Research Institute) in Linköping, Sweden. The reaction time for randomly appearing stimuli was measured in normals and subjects with visual field defects as well as one-eyed drivers.

Methods

The subject was seated in a real car body. In front of this, the computer-controlled traffic scene was projected on a wide-angle screen with the aid of three TV-projectors; the luminance of the screen was 15–25 cd/m². The scene was a two-lane grey road on each side surrounded by a flat green-coloured landscape; above the horizon was the sky. The road wound through the landscape with a speed that was controlled by throttle commands, braking etc.; inside the car body, the speed was also evident from the 'motor' sound and the tachometer reading. The subject had to drive with a speed of 100 km/h, which was a difficult task that demanded constant attention. If he could not hold the car on the road, it seemed to skid out in the green ending up in a crash. Such an accident, as well as crossing to the left lane was recorded by the computer.

On the screen, quadratic yellow and black 6 Hz flickering stimuli of three different sizes were presented; they subtended an angle of 0.96° (large), 0.46° (medium) and 0 23° (small). The luminance contrast to the background made them clearly suprathreshold as was evident from the readings of peripheral small stimuli in normals. Stimuli appeared randomly, one at a time, in any of 24 positions within an area of 20° vertically and 120° horizontally. The stimuli were located in areas of traffic safety and ocular pathology interest (Fig. 1). The stimulus disappeared after braking or after 10 seconds. One test session lasted half an hour during which stimuli appeared in each position 10 times, ie, a total of 240 presentations. In the first and last sessions, the medium-sized stimuli were used, in the second the small and in the third the large objects.

The subjects had to respond to a stimulus by immediate braking; the measured parameter was the latency between the appearance of the stimulus and brake pedal movement, ie, *the detection capacity. The driving capacity* was recorded as the ability to drive with the specified speed on the right side of the road.
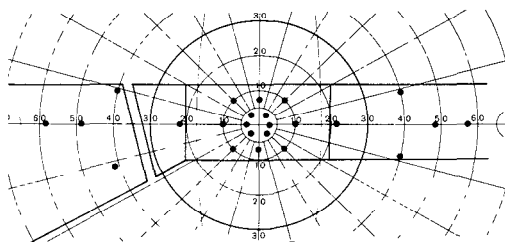
Figure 1 Location of the stimuli in the field of view The frame shows the boundaries of the windscreen and part of the left side window

Subjects

Twenty subjects with normal visual acuity and fields volunteered for the study; they were divided into two groups: 20–30 years and 50–60 years. Twenty-seven subjects with visual field defects have been studied so far. In all cases, the duration of the defect was at least one year. Most subjects had had brain lesions giving rise to homonymous field losses, a few had central/paracentral scotomas due to optic nerve disorders and a few had bilateral glaucoma.

Two one-eyed subjects who had lost the other eye several years ago were also tested. The single eye was normal. Two persons were tested with both contact lenses and spectacles. Their refraction was sphere $-8.5/-8,0$ D and $-8.5/-8.5$ D.

In the subjects with visual field defects, monocular kinetic perimetry was done with the Goldmann perimeter to define the extent of the absolute and relative visual field deficiencies.

Results

The subjects kept the speed required and the departures from the right lane were quite few.

Normals

There were 10 reaction times for each stimulus location in every test session. The reaction times of the 10 younger and the 10 older subjects were grouped together. Fig. 2 shows an example of the results obtained. The figure shows the medians of the reaction times and the 90th percentile. Median values were typically of the order of 0.8 seconds. There were small differences between the reaction times for central and peripheral stimuli; these differences were somewhat more outspoken
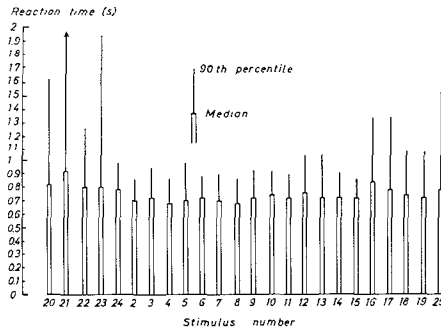
Figure 2 One example of reaction times obtained in the group of older normals: medium-sized stimuli, first presentation. Depicted are medians and 90th percentiles

for older subjects and small stimuli. The reaction times of the older subjects were a little longer than those of the younger.
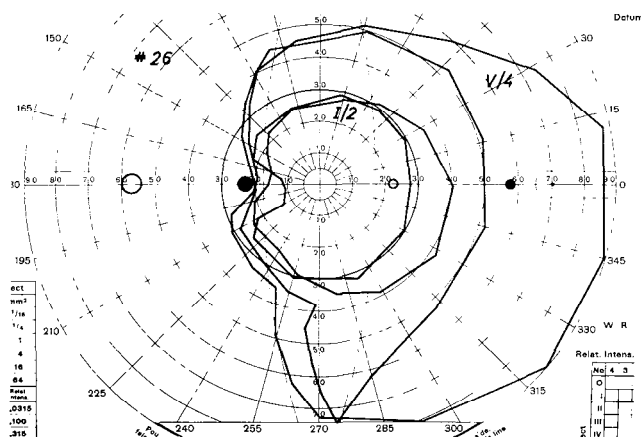
Subjects with visual field defects

For each stimulus location and session, the median reaction time (the 6th longest time) was compared to the results of the normals of corresponding age. If the value of the subject exceeded the 90th percentile of the normals, this was considered to mean an *overall increment of the reaction times* and marked on the perimetric chart (circles).

From the traffic safety point of view, it could also be of importance if *the reaction times of single presentations were prolonged.* A fourfold increment, ie, times exceeding 3.00 seconds was arbitrarily considered significant. Single delays were accepted (chance lack of attention?); thus two or more reaction times over 3.00 seconds were considered of importance and this was marked with filled dots on the charts.

Even more significant were reaction times over 10 seconds, ie, that *the subject did not observe the stimulus at all.* Two or more such misses were recorded and marked with filled triangles on the charts. Since we considered it more significant if larger stimuli were affected, circles, dots and triangles of three sizes were used to mark the abnormal reaction times.

A visual evaluation of the perimetric charts served to decide whether there was on overrepresentation of prolonged reaction times in the affected visual field areas. Single abnormal points often appeared in normal field areas, but could usually be explained by interference from the rear-view mirror or a wind-screen post. Several deviant points within the pathological field was taken to infer that the subject did not compensate for the defect; this point was strenghtened by increments over 3 or 10 seconds.

Figure 3 The result of one subject judged to compensate for the visual field defect Rings: abnormally long reaction times; Dots: two or more reaction times longer than 3 seconds; Triangles: two or more presentations not seen Small, medium-sized and large symbols correspond to stimulus size

Out of the 27 subjects with visual field defects, we found that only four compensated for their field loss (Table 1). Representative examples of compensation and non-compensation are given in Figs 3 and 4 Of the two subjects with only one eye, one performed as well as the normals whereas the other showed markedly prolonged reaction times in the periphery of the blind side.
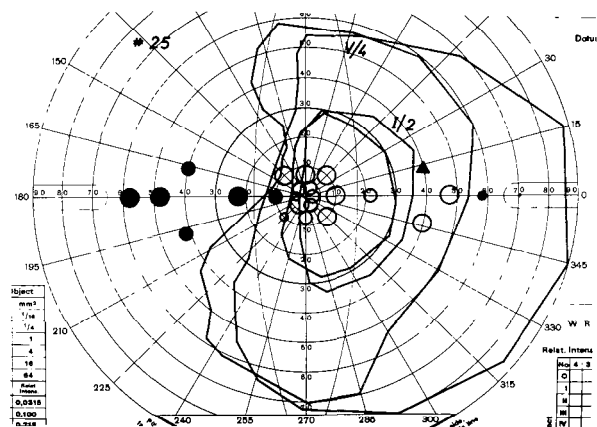
Figure 4 The result of one subject with prolonged reaction times especially in the abnormal visual field area Symbols as in Fig 3

Spectacles and contact lenses

The results of these two subjects were, except for a point corresponding to a window post, quite normal both with contact lenses and spectacles.

Discussion

Visual field defects are considered to impair the drivers' ability to detect objects in the traffic scene. Safety is at risk if other vehicles, children, etc are observed too late or not at all. However, several other factors probably have to play a part as well for an accident to occur; therefore drivers with field defects can drive for years without crashes and correlations between the visual impairment and the driving performance are hard to establish.

Measuring the detection capacity in the traffic would meet great methodological difficulties. The driving task in the simulator used in this study imitates real driving to a very high degree and sharp attention has to be paid to steering and speed control. In the simulator, controlled stimuli can easily be presented and a parameter related to detection capacity selected and measured. The chosen flickering stimuli were suprathreshold; no attempts to measure their size or luminance thresholds were made, however.

The data obtained in the normal groups showed little variation between stimulus locations and subjects. Somewhat longer reaction times were recorded in the periphery and with the older drivers. Median latency values were used to compensate for the possibility of pressing the brake pedal by chance. So far, we have operated with three arbitrary levels to denote important increases of the reaction times: median values exceeding the 90th percentile of the normals, two or more times longer than 3 seconds and two or more times longer than 10 seconds. Symbols for these occurrences were drawn on the perimetric charts. Single abnormal points could be explained by interference from structures in the car body if they coincided with the direction of the rear-view mirror or a window

Table 1 Types of visual field defects and degree of compensation

Number of subjects	Type of field defect	Result
2	Local scotoma	+ −
3	Irregular defects	+ + +
4	Partial quadrant	+ + − −
6	Quadrant	+ + + + + +
8	Partial hemidefect	+ + + + + + + +
4	Hemidefect	+ + + −

+ = impaired detection capacity
− = compensation

post. Four subjects were able to compensate for their defect: their performance was good in the whole area tested. In the other 23 pathological cases, it was easy to conclude that the deficient field areas comprised an excess of abnormal stimulus points. In all these cases, the total number of abnormal points was large (>8) and there were also at least two points with reaction times longer than three seconds.

The subjects that did compensate belonged to different types of field abnormality (Table 1). The way these subjects control their deficiency is as yet not known to us. Further studies are under way where the fixation pattern of compensating and non-compensating subjects will be recorded.

License standards for visual fields vary between countries. In many, a normal field in one eye or the two eyes together is required. Scientific support for this opinion has been hard to furnish but was brought forward by the recent Californian study [5]. Our study demonstrates that most subjects with homonymous visual field defects show impaired detection capacity in deficient field areas. From perimetry it is not possible to tell if a driver can compensate for the defect. If the abnormal area is located in a part of the visual field of relevance to driving, it seems justified to deny the subject a license

One-eyed persons are allowed to drive passenger cars in most countries; in Sweden after an adaptation period of half a year. Some patients claim that they get used to the condition in a short time, others that it takes months. Our study only includes two subjects so far; one compensating and the other not. More testees are required in order that one should get support for the opinion that these drivers could run into collisions more often than normals [6]. The experiments with myopic subjects do not prove that persons with a moderate degree of this refractive error are handicapped by wearing spectacles instead of contact lenses.

References

1 Cole DG: A follow-up investigation of the visual fields and accident experience among North Carolina drivers UNC Highway Safety Research Center, Chapel Hill, NC, 1979
2. Council FM, Allen JA: A study of the visual fields of North Carolina drivers and their relationship to accidents UNC Highway Safety Research Center, Chapel Hill, NC, 1974
3 Henderson RL, Burg A: Vision and audition in driving Report DOT-HS-801-265, Department of Transportation, National Highway Administration, Washington DC, 1974
4 Hills BL, Burg A: A reanalysis of California driver vision data: general findings TRRL Laboratory report 768, 1977
5 Johnson CA, Keltner, JL: Incidence of visual field loss in 20,000 eyes and its relationship to driving performance Arch Ophthalmol 101: 371–375 (1983)
6 Keeney AH, Garvey J: The dilemma of the monocular driver Am J Ophthalmol 91: 801–803 (1981)

Author's address:
Department of Ophthalmology,
Karolinska Sjukhuset,
S-104 01 Stockholm, Sweden

Section IX
Miscellaneous

IX.1 Standards of perimetry

T.J. SMITH and K.M. GOINS
Lexington, U.S.A.

Abstract

Skilled manual kinetic and static threshold perimetry is assumed to be the standard of practice. However, Trobe suggested that the actual standard in clinical practice may fall considerably short of this ideal [3]. We polled the ophthalmologists in the state of Kentucky. With some effort, we obtained replies from all 137 practicing ophthalmologists. This complete sample eliminates upward bias. Data was obtained on, among other things, age of the physicians, practice type, number of patients seen, type of perimeters utilized, types of visual fields obtained, and number of visual fields done. Eighty-eight percent of examinations were performed by technical staff. Automated fields were most commonly performed (34%) 41% of automated perimeters test supra-threshold only. Only 10 of 67 practitioners using the Goldmann used Armaly-Drance techniques and only one practitioner out of 137 utilized manual static threshold perimetry.

We believe that our sample is an accurate reflection of national standards. Clinical perimetry as practiced in no way approximates the ideal

Introduction

For the most part, two of the twenty-five definitions of 'standard' in the Oxford English Dictionary apply in medicine. One denotes correct or exemplary behavior and the other usual or normative practice. The exemplary standards of perimetric practice are clear and well documented [1]. Practitioners may vary in their approaches but multiple isopter kinetic testing with suprathreshold checks, threshold static perimetry, defined and appropriate testing strategies, skilled and well trained perimetrists, and state-of-the-art equipment, be it manual or automated, all find a place in the 'standard of practice'.

Normative or usual practice is less well documented. Based on the study of

perimetry in the community Trobe [2] has recently suggested that usual clinical practice may be unsatisfactory. In order to establish normative standards for perimetry in the community, we telephone surveyed the ophthalmologists of the State of Kentucky between April and August 1985

Material and methods

According to the Kentucky Academy of Eye Physicians and Surgeons, in the summer of 1985, there were 137 practicing ophthalmologists in the state. Demographic data is presented in Table 1. One hundred and thirty were men and 7 were women. Forty-one (30%) did their opthalmology residency training in Kentucky. One hundred and thirteen described themselves as general ophthalmologists, 24 as subspecialists The questions used in the survey are listed in Table 2

Table 1 Demographics of Kentucky ophthalmologists

Number	137
Average age	47
Practice population <100,000	65
Practice population >100,000	72

Table 2 Questionnaire

1	How many patients do you see each week?
2	What percent of these patients have glaucoma?
3	How often do you follow your well-controlled glaucoma patients?
4	What type of practice do you have? General or Specialty
5	How many surgical cases do you do per week?
6	How many visual fields do you do per week?
7	What types of visual fields do you do?
8	How often do you use each type of visual field?
9	Who does the visual field testing?
10	How was your technician trained to do visual field testing?
11	How long has your technician been doing the visual field testing?
12	What percent of your visual fields are for screening and for follow-up?
13	What visual field type is used for screening?

For those who use the Goldmann perimeter, the additional questions were asked:

14	What isopters do you routinely plot?
15	What target do you check the blind spot with?
16	Do you do static suprathreshold perimetry?
17	How many spot checks do you use?
18	Do you do static threshold perimetry?
19	Do you use the Armaly-Drance technique?

Results

We obtained answers from all (137/137) ophthalmologists with respect to the number and type of visual fields obtained. Automated fields (35.3%) were the most commonly performed followed by Goldmann (23.6%). Full results are given in Table 3.

Of the automated instruments, the Humphrey visual field analyzer was by far the most commonly used (49.2%). The other instruments are listed in Table 4.

Only 37% of manual visual field testing in Kentucky is done using the Goldmann perimeter. Thirty of 137 ophthalmologists do not have access to either a Goldmann or an automated perimeter.

Physicians performed 11.5% of visual field examinations and 88 5% were performed by technicians. However, only 9% of the physician fields are performed on the Goldmann perimeter This amounts to only 1 05% of all the visual fields tested The percentage of visual field examinations performed for follow-up of known disease was 62%. Thirty-eight percent were performed for screening purposes. This amounts to 24,544 screening examinations per year.

Discussion

Trobe suggested that 'visual field examination may not be fulfilling its diagnostic potential in the current practice of ophthalmology' [3] He suggested that there

Table 3 Visual field usage in Kentucky

1	Automated (all types)	35%
2	Goldmann	24%
3	Tangent	18%
4	Harrington-Flock	17%
5	Arc	5%
6	Amsler	1%

Table 4 Automated visual fields used

Humphrey	49%
Fieldmaster 101	22%
Dicon 200	11%
Fieldmaster 200	6 5%
Fieldmaster 50	3 75%
Digilab	3 75%
Octopus	3%
Autofield	1%

were six reasons for this: Stereotyped (non-selective approach); use of kinetic targets that were too bright or too large; movement of targets from seeing to non-seeing areas of the visual field in search of defects; failure to measure the physiological blind spot; lack of familiarity with suprathreshold static technique; and failure to measure the full extent depth and slope of defects. He estimated that approximately 10% of visual fields done were performed by ophthalmologists.

While we agreed with his findings, we felt that pessimistic as his report may have been his very small sample size (five technicians from one ophthalmic office) may have distorted the study. All of the technicians had access to a Goldmann perimeter and presumably had some interest in perimetry as is evidenced by their participation in the study. It is our experience that neither interest in perimetry nor access to Goldmann technology is universal.

In this study we obtained a 100% response rate. We feel that this is very important. A small percentage of replies to a postal survey biases results upward because it may fairly be assumed that those with an interest in perimetry would be more likely to respond. We obtained replies from all ophthalmologists in the state by virtue of persistence and, in many instances, dogged determination.

We feel that Kentucky may fairly be used as a measure of visual field practice in the United States in 1985. There is an even mix of urban (53%) and non-urban (47%) practitioners. There is one ophthalmologist per 26,330 population (3,660,777/137) in the state versus approximately 1 per 22,352 (260 million/11,362) nationally. Only 1 in 3 ophthalmologists in the state trained in Kentucky and the residencies and fellowships represent a cross-section of eastern, mid-western, southern and west coast programs. The average age is 47 years. We found, not surprisingly, that those younger than 40 years were more likely to perform Goldmann or automated field (78%) than those over 40 (52%). However, when we looked at practice location, we were surprised to find that the practitioners in communities less than 20,000 actually performed more visual fields per capita and of higher quality than their colleagues in larger cities.

The results of any questionnaire such as this must be considered soft data. We relied on the practitioners' estimates of the number, type and quality of visual fields performed; therefore there is likely to be some overestimation in all categories Nonetheless the results are sobering. Eighty percent of ophthalmologists, when they perform their own visual fields, still use the tangent screen or arc perimeters. Only 1.05% of all visual fields performed in the state are done by ophthalmologists using the Goldmann perimeter. Sixty-five percent of all Goldmann fields are performed with two or fewer isopters (with 4% done with one only!). Only 10 of the 71 practitioners who regularly utilize the Goldmann perimeter use the Armaly-Drance technique as described by Anderson [1]. Only one ophthalmologist attempts manual static threshold perimetry.

Although automated perimetry may be very useful in upgrading the quality of visual fields in the state, it is unfortunate that 41% of the instruments in use are

non-thresholding screeners. It is to be hoped that the increased availability of cheaper thresholding instruments will change this situation

Screening visual fields performed in 1985 totalled 24,544. While on the surface of it, this may seem impressive, it represents only 0.7% of the population of the state. No matter how sensitive or accurate the technique, any strategy which screens only this small number of those at risk is of limited use.

There is a double standard in the practice of perimetry. Trobe identified the tip of the iceberg and the extent of the problem is truly enormous. Screening for disease with visual fields is a myth. Quality manual perimetric practice is rare and exists only in isolated pockets. Automated perimetry is poorly understood by the general ophthalmologist but may be a source of optimism for the future.

References

1 Anderson D: Testing the field of vision CV Mosby Company, St Louis, 1982
2 Trobe JD, Acosta PC, Shuster JJ, Krischer JP: An evaluation of the accuracy of community-based perimetry Am J Ophthalmol 90: 654–660 (1980)
3 Trobe JD: How effective is perimetry in current practice? Ophthalmology 90: 1380–1383 (1983)

Author's address:
Department of Ophthalmology,
University of Kentucky,
Veterans Administration Hospital,
Lexington, KY, U S A

IX.2 Automated perimeter results: the need for a common language

E. AULHORN and W. DURST
Tübingen, F.R G.

Towards the end of the nineteen-fifties the Goldman Perimeter had established itself so completely that nearly all physicians doing perimetry used either this instrument or one similar to it. In those days, the results were recorded in a uniform manner and were easily understandable by every ophthalmologist.

Today's automation of perimetry allows very precise examinations with no increase in work for the examiner, since the perimetric examination can be delegated to trained assistants. Thanks to the advent of automation in clinic and practice, perimetric examination has become more common – to the patient's benefit! These are all advantages of the automated perimeter.

However, there are also disadvantages. One of the main problems is the large variability between automated perimeters, as far as examination conditions, examination strategy, and description of results are concerned Examination results for two different perimeters can only be matched with one another if one is familiar with all details of the programs used in both perimeters. Therefore, a practizing ophthalmologist often cannot understand perimetric results sent to him by a clinic.

This does not imply that today's automated perimeters should all function in the same way. The present multitude of procedures will naturally generate the best procedure for clinic and practice. But it would be beneficial to attempt to standardize the depiction of results immediately; otherwise there can be no communication between examiners who use different perimeters. The perimeters should communicate their findings to ophthalmologist in a common language, and this language should be neither complicated nor involved, but easy for every eye doctor to interpret.

The big differences in the graphical display of results cause difficulties in the following situations:
- Follow-up and determinations of improvement or deterioration of the visual field, even when the patient chooses a new ophthalmologist, and so another type of perimeter.
- Simultaneous scientific studies in different clinics, using different perimeters.
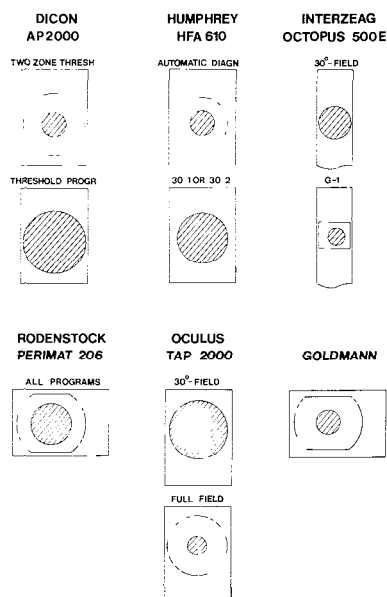
Figure 1 Demonstration of test result forms on scale from 5 automatic perimeters and the Goldman perimeter The shaded circles show the 30° visual field

- Comparing different strategies in order to find the best final strategy.
- Medical assessments of visual performance: Can the patient drive a car, for instance, or pilot an airplane?
- Medical assessments for insurance companies and courts.
- Certifications of blindness

There are four different factors which make it so difficult to compare the results: *first of all,* the large variation in the size of the visual field areas depicting equal visual angles on the different result charts. Among the five automated perimeters sold most often in West Germany, the 30-degree fields vary on paper between 5.3 and 18 centimeters in diameter (Fig. 1). The same visual field defect thus appears quite insignificant in one case, but large and ominous in another.

Secondly, on many charts it is impossible to determine the number and positions of the test points with which a specific visual field area has been examined. However, this information is absolutely essential, since the number and positions of the test points can differ widely from one perimeter to another (Figs 2 and 3).

When a small scotoma (Fig. 4) disappears during a follow-up examination with a different perimeter or program, this can mean that visual function has improved. However, it may also mean that a coarser or differently – distributed test – point grid was used the second time, so that the scotoma could not now be detected at all. This can have serious consequences for therapeutic management.

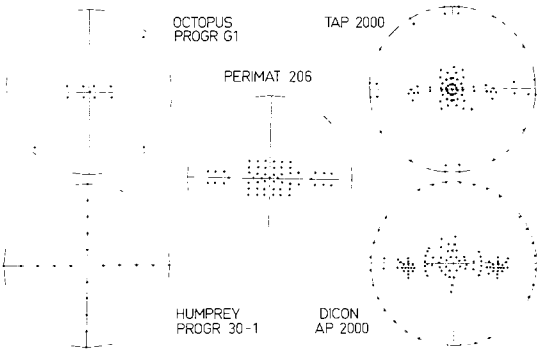Thirdly, the symbols used for quantifying different test point luminances, i.e.

Figure 2

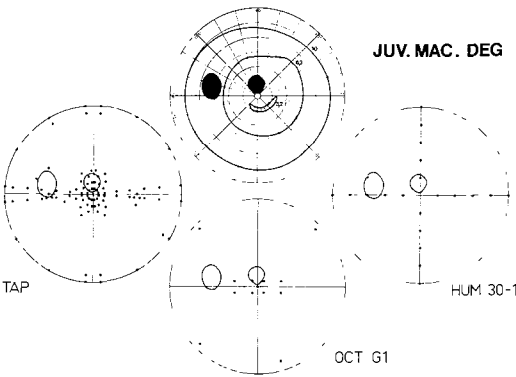*Figure 3* Test point grids of 5 automatic perimeters in the 30° visual field

Figure 4 A paracentrally located scotoma (juvenile macular dystrophy with eccentric fixation) Above: a Tübinger manual perimetry result The same scotoma was schematically depicted on test point grids of 3 different automatic perimeters It is evident that some perimeters the scotoma and the blind spot are only pinpointed by one test point, or are not pinpointed at all
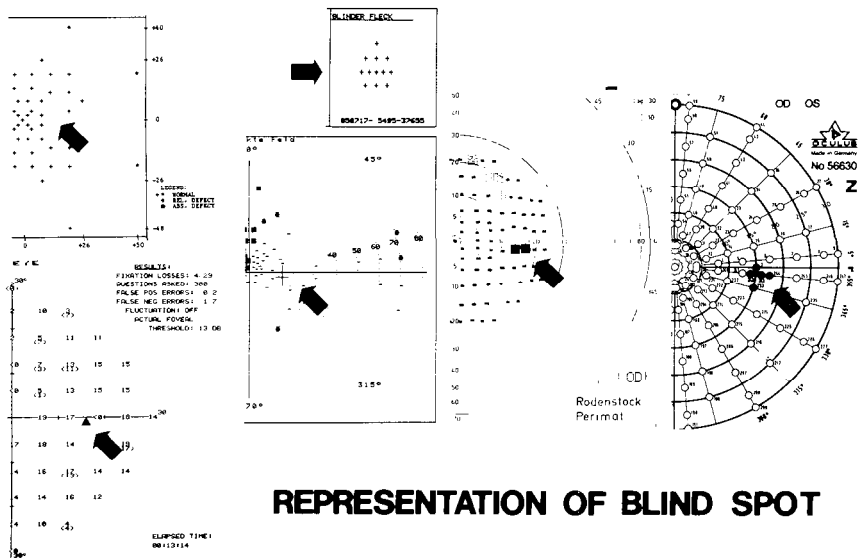
REPRESENTATION OF BLIND SPOT

Figure 5 There are widely varying degrees of accuracy when it comes to the determination of the blind spot (an important reference scotoma!), as can be seen on the original graphical display of 5 automatic perimeters

varying scotoma depths, are in some cases very different and therefore cannot be compared The reference system of some perimeters and programs is the individual threshold level. Thus, the depth of the defect in circumscribed scotomas is determined relative to this level. With other perimeters or programs, the scotoma depth is given in absolute luminance values, that is, in terms of a constant scale.

Moreover, in many perimeters, black symbols are used for visual field areas in which the brightest test point of the perimeter is not recognized – so-called absolute scotomas. At the same time, however, black symbols are also used for test points where only a relative but as yet undetermined defect was indentified. Gray-scale print-outs on the other hand, admittedly give a clear overview of the defect depths in the visual field; but since the test points are not identified, it is also impossible to draw a relationship between retinal location and measured light-difference sensitivity

Fourthly, the blind spot – an important reference scotoma – is purposely not represented by some perimeters. In others, it is examined separately and given special representation apart from the visual field chart, using a different scale. In another perimeter, only the midpoint of the blind spot is measured, so that the user has no idea whether it is enlarged, or could not be detected at all, because it is located in a larger scotoma (Fig 5).

If we really want to compare the results of perimetry from place to place, from clinic to clinic, from clinic to practice and practice to clinic, then different automated perimeters must yield comparable results. The methods of examin-
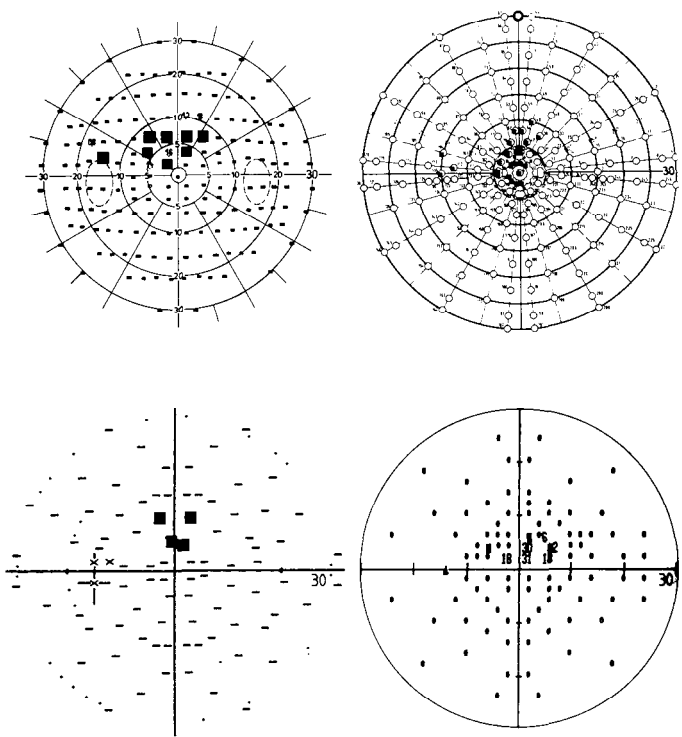
Figure 6 Demonstration of a paracentrally located scotoma (same scotoma as in Fig 4) on 4 different automatic perimeters The 30° visual fields have all been adjusted to scale

BLIND SPOT

NORMAL POSITION | ECCENTRIC FIXATION
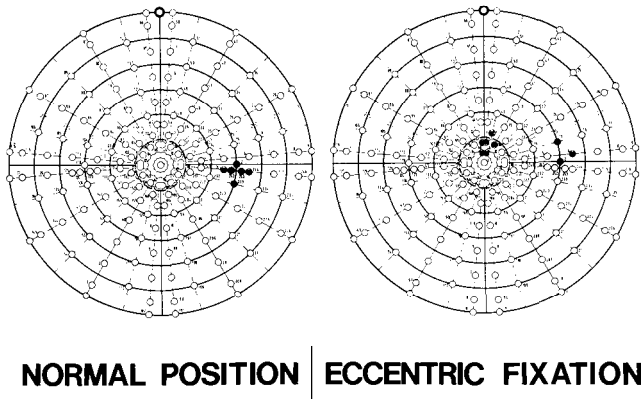
Figure 7 The blind spot must be demonstrated by at least 2 test points – if possible with more – especially when it is not in its normal location

ation themselves can differ widely; however, the manner in which results are displayed must show the examination method precisely and make comparison possible. This can be accomplished in four ways:

1. Identical visual field areas should have identical sizes on the perimetry charts (Fig. 6).
2. It should be possible to recognize the number and positions of the examined visual field points on every print-out of results.
3. The symbols for the light-difference sensitivity which was found at each location should be as uniform as possible The examination results should clearly state – possibly by means of a reference table or curve – what degree of sensitivity was found at each location.
4. The blind spot should be clearly displayed and have the same magnification on every print-out. In those areas in which the blind spot can appear, the test point grid should be dense enough to correctly demonstrate the blind spot even when it is shifted from its typical position (Fig. 7).

If these four conditions can be met in all representations, there will be a considerable general increase of understanding of perimetric results between ophthalmologists We will again be able to discuss our visual field results in detail with one another, and scientific studies can be understood by those working with different perimeters.

In the course of time and given this standardization the strategies and examination conditions which yield the best and most meaningful results will emerge, to the patients' benefit.

Author's address:
Prof Dr Med E Aulhorn,
University Eye Clinic,
Ophthalmology II: Neuroophthalmology and Pathophysiology, Tübingen, F R G

IX.3 JAWS (Joint Automated Weighting Statistic): a method of converting results between automated perimeters

C.A JOHNSON, J L. KELTNER and R A LEWIS
Davis, U.S.A.

Abstract

JAWS (Joint Automated Weighting Statistic) is a data conversion routine that has been developed to provide quantitative comparisons of visual field test results among different automated threshold static perimeters The procedure is based on a simple linear least-squares regression equation that is used to predict the test results on one automated perimeter from the data obtained on another auto-mated perimeter. Using data obtained from 12 normal eyes undergoing repeated testing, correlation coefficients of between 0.83 and 0.97 were obtained for comparisons of six automated perimeters (Humphrey Field Analyzer, Octopus 500, Squid, Fieldmaster 50, Dicon 2000 and Digilab 350) Preliminary evaluations indicate that the accuracy of the conversion procedure is mainly limited by the test-retest reliability of the individual devices. The procedure is computationally simple, and could be readily incorporated into existing data analysis procedures employed by automated perimeters. With further refinements, JAWS may be a useful clinical tool for comparison of visual field data obtained with different automated perimeters.

Introduction

The recent popularity of automated perimetry has stimulated the development of many commercial devices that perform automated static and suprathreshold static visual field testing [1]. In conjunction with the many advantages that automated perimetry has brought to ophthalmic practitioners, it has also intro-duced a new series of problems. One of these difficulties pertains to the ability to compare the results of visual field testing with one device to those obtained from a different device.

Among the various commercially-available automated perimeters, there are a variety of background luminance levels, target sizes, target presentation patterns,

test strategies, dynamic range of target luminances, staircase scoring procedures and other test parameters that are employed by different manufacturers. In addition, there are at least 4 different specifications for the 0 dB reference level of sensitivity values that are utilized by various devices. Direct comparisons of test results from different automated perimeters is therefore a difficult and frustrating clinical task.

In a previous investigation [2], we performed qualitative comparisons of numerical and graphical representations of visual field results obtained with various automated static perimeters This study extends this work to examine the feasibility of developing a simple conversion routine for conducting quantitative comparisons of test results obtained with different automated static perimeters.

Methods

The initial database for JAWS was established by testing 6 normal observers (12 eyes) a total of 4 times on each of the 6 automated perimeters (24 visual fields for each eye) Because each device had a different target presentation pattern, it was not possible to perform one-to-one correlations of threshold values for individual target locations The visual field was therefore divided into 12 sectors (0–10, 10–20, 20–30 degrees eccentricity for the superior nasal, superior temporal, inferior nasal and inferior temporal quadrants) and the average threshold values for each sector were used for comparisons.

For each eye, the average threshold values for the 12 visual field sectors (with the 4 tests combined) were compared for all 6 automated perimeters. Correlation coefficients and least-squares regression equations were then computed for each of the pairings of automated devices. In addition, data for both size II and size III targets were obtained for the Humphrey Field Analyzer to provide another comparison.

The basis of the JAWS conversion is thus a linear equation of the form $Y = A + BX$, where X is the sensitivity value of the device you are converting *from*, Y is the sensitivity of the device you are converting *to*, A is a constant that reflects uniform shifts in the sensitivity profile of the entire visual field, and B is a constant that reflects changes in the slope of the sensitivity profile.

Results

Table 1 presents the correlation coefficients and regression equation constants (y intercept A, and slope B) for all comparisons of pairs of automated perimeters. The correlation coefficients range from 0.83 to 0 97, and all are statistically significant. This suggests that our simple linear conversion is able to account for the majority of differences among various automated perimeters employing

Table 1 Conversion of automated perimetry threshold values

| From device	To device	Corr coeff	A (Y int)	B (slope)
Humphrey, Size III				
	Octopus 500	0 93	−12 16	1 20
	Squid	0 95	−21 11	1 30
	Fieldmaster 50	0 92	−17 08	1 22
	Dicon 2000	0 93	−19 09	1 31
	Digilab 350	0 85	−41 18	1 97
	Humphrey, Size II	0 95	−17 49	1 44
Humphrey, Size II				
	Octopus 500	0 97	2 65	0 83
	Squid	0 96	−4 49	0 87
	Fieldmaster 50	0 96	−1 93	0 84
	Dicon 2000	0 92	−1 56	0 85
	Digilab 350	0 87	−16 12	1 33
	Humphrey, Size III	0 95	14 13	0 62
Octopus 500				
	Humphrey, Size III	0 93	13 04	0 72
	Humphrey, Size II	0 97	−1 45	1 14
	Squid	0 95	−6 16	1 01
	Fieldmaster 50	0 95	−3 64	0 98
	Dicon 2000	0 93	−3 88	1 01
	Digilab 350	0 83	−17 08	1 48
Squid				
	Humphrey, Size III	0 95	17 91	0 69
	Humphrey, Size II	0 96	6 88	1 07
	Octopus 500	0 95	8 04	0 90
	Fieldmaster 50	0 93	3 84	0 90
	Dicon 2000	0 91	3 73	0 93
	Digilab 350	0 83	−6 78	1 41
Fieldmaster 50				
	Humphrey, Size III	0 92	16 56	0 70
	Humphrey, Size II	0 96	4 21	1 10
	Octopus 500	0 95	5 74	0 93
	Squid	0 93	−0 83	0 96
	Dicon 2000	0 95	0 59	1 00
	Digilab 350	0 88	−12 15	1 54
Dicon 2000				
	Humphrey, Size III	0 93	16 84	0 66
	Humphrey, Size II	0 92	5 93	1 00
	Octopus 500	0 93	6 75	0 86
	Squid	0 91	0 08	0 89
	Fieldmaster 50	0 95	1 75	0 90
	Digilab 350	0 90	−11 67	1 48

Table 1 Continued

From device	To device	Corr coeff	A (Y int)	B (slope)
Digilab 350				
	Humphrey, Size III	0 85	23 82	0 37
	Humphrey, Size II	0 87	15 95	0 57
	Octopus 500	0 83	16 07	0 46
	Squid	0 83	9 41	0 49
	Fieldmaster 50	0 88	10 93	0 51
	Dicon 2000	0 90	10 74	0 54

threshold static perimetry, in spite of their variations in background luminance, target size, target presentation pattern, test strategy, definition of 0 dB reference value for sensitivity, and other parameters As a general rule, the highest correlations were found for devices that had previously been shown to have the greatest test-retest reliability [3].

To conduct a preliminary test of the efficacy of this approach, we compared predicted vs empirically determined sensitivity values for converting Humphrey Field Analyzer Size III data to Octopus 500 sensitivity values. This comparison was selected for several reasons.

1 Both of these devices have high test-retest reliability.
2. The Octopus 500 and Humphrey Field Analyzer are among the most commonly used automated threshold static perimeters.
3 Both devices have undergone little or no changes in stimulus conditions and test strategy since our initial comparison study [2], whereas the other 4 automated perimeters in this study have been subsequently modified.

Figure 1 presents the comparison of predicted (Humphrey Size III to Octopus 500 JAWS conversion) vs empirically derived sensitivity values. The percentage of target locations for 12 normal eyes (small cross-hatch bars) and 12 eyes with visual field loss (large cross-hatch bars) are plotted as a function of the difference (in dB) between predicted and empirical sensitivity values As a comparison standard, the filled bars reflect the relationship between sensitivity values for test 1 vs test 2 for normal observers on the Humphrey Field Analyzer (i.e., the amount of variation expected on the basis of test-retest reliability). The Humphrey to Octopus 500 conversions for normal observers are essentially equivalent to those for the Humphrey Field Analyzer test-retest data. The results are only slightly worse for the conversions in eyes with visual field loss
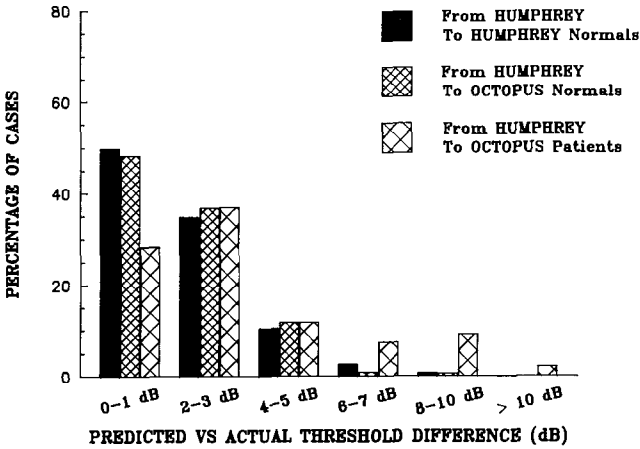
Figure 1 The percentage of threshold values for which predicted (JAWS conversion values) and empirical (actual threshold values) were within the amount shown by the categories on the abscissa Humphrey Field Analyzer (Size III) to Octopus 500 conversions are depicted for normal observers (small cross-hatch bars) and patients (large cross-hatch bars), with Humphrey exam 1 to Humphrey exam 2 comparisons presented as a control condition (filled bars)

Discussion

Our present findings indicate that it is possible to use a simple linear regression model to convert threshold values obtained with one automated perimeter to those of another automated perimeter with considerable accuracy Correlation coefficients for all comparisons of pairs of automated devices were between 0.83 and 0.97. The main limitation of the JAWS conversion process appears to be the test-retest reliability of the individual devices. The computational simplicity of JAWS makes it possible to readily incorporate this conversion process into the data analysis software of existing automated perimeters. For many ophthalmic practitioners, the availability of such conversion routines may be of great clinical benefit.

Although our preliminary findings are quite encouraging, there are two improvements that could be made to the JAWS conversion process. First, a larger database should enhance the accuracy of predicting test results for one automated perimeter on the basis of thresholds obtained with another automated perimeter In addition, the use of non-linear regression techniques may provide a better means of approximating the relationships among sensitivity values obtained with different automated perimeters These two potential enhancements are currently under investigation.

Acknowledgements

References

1 Keltner JL, Johnson CA: Comparative material on automated and semi-automated perimeters – 1985 Ophthalmol Instr Book Suppl 92: 34–57 (1985)
2 Keltner JL, Johnson CA, Lewis RA: Quantitative office perimetry Ophthalmology 92: 862–870 (1985)
3 Lewis RA, Johnson CA, Keltner JL, Labermeier PK: Variability of quantitative automated perimetry in normal observers Ophthalmology 93: 878–881 (1986)

Authors' addresses:
Chris A Johnson, Ph D ,
Dept of Ophthalmology School of Medicine, University of California, Davis, CA95616, U S A

John L Keltner, M D ,
Dept of Ophthalmology and Depts of Neurology and Neurological Surgery

Richard A Lewis, M D ,
Dept of Ophthalmology

IX.4 Octopus visual field examination in Saudi Arabia: an assessment of patient performance

C.E. TRAVERSO, K F. TOMEY and R. FATANI
Riyadh, Saudi Arabia

Abstract

A total of 120 consecutive Octopus visual field tests using the Programs 31 or 32 were analyzed. All cases were exposed for their first time to computerized perimetry. The number of questions for the determination of threshold, the number of stimulus repetitions, the false positive and false negative answers and the short-term (RMS) fluctuations, were calculated Statistical significance for the difference between normal and pathological visual fields was present for all parameters considered except the number of the repeated stimuli and the percentage of cases requiring more than 15 repetitions From our study it is so far apparent that patient performance at Octopus perimetry, as quantifiable by routine reliability parameters was, in our environment, comparable to what is recorded for Western patients.

Introduction

Computerized perimetry is more effective than manual perimetry for the detection and assessment of visual field defects [6, 8, 9] Despite the availability of reasonably priced models which are simple to operate and with minimal maintenance needs, computerized perimeters are not commonly used in developing and industrializing countries. This may be due to the belief that patients belonging to cultures with less exposure to technology should have poorer understanding of the tests and are thus intimidated by the hardware. The purpose of our study was to verify the feasibility of Octopus visual field testing in our patient population

Patients and methods

A total of 120 consecutive Octopus visual field tests using the Program 31 or 32

were analyzed. All patients were exposed for their first time to computerized perimetry. In all cases vision was better than 20/60. Forty-two visual field examinations were found to be normal, and 76 showed pathological findings. Criteria for the definition of an abnormal visual field were the following:

a) Four or more tested points with sensitivity decreased by at least 3× the RMS value.
b) Four or more contiguous points with sensitivity decreased by at least 5 dB.
c) An absolute scotoma.

The blind spot and its four adjacent points were not considered.

The parameters analyzed were:

a) Number of stimulus presentations (questions) necessary to complete each test.
b) Percentage of cases requiring 550 or more questions.
c) Number of repeated stimuli.
d) Percentage of cases which had 15 or more stimulus repetitions.
e) False positive answers. Percentage and absolute number
f) False negative answers. Percentage and absolute number.
g) Short-term fluctuations (RMS).
h) Percentage of cases with more than 2.5 dB RMS.

Where appropriate a two-tailed t-test and z values were obtained

Results

All data is shown in Table 1.

Number of questions

Patients with normal visual fields required 497 ($\pm$ 75) stimulus presentations for the definition of threshold at all points tested. In pathological visual fields, the questions required were 549 ($\pm$ 109). More than 550 stimulus presentations were needed in 12% of normal, and in 38% of pathological tests.

Repetitions

In normals, a mean of 20.4 ($\pm$ 25) stimuli had to be repeated during the test. In abnormal visual fields, 26.7 ($\pm$ 40) repetitions were necessary. Fifteen or more repeated stimuli were present in 45% and 42% of normal and pathological tests, respectively

False answers

Normal subjects showed 12.5% ($\pm$ 13.9) false positive answers and 3.2% ($\pm$ 4 9) false negative answers More than 3 false positive answers were given in 12% of the cases; in no case were there more than 3 false negative answers. Subjects with abnormal visual fields had 3.3% ($\pm$ 6.9) false positive answers, and 13.5% ($\pm$ 22.7) false negative answers. In no case were more than 3 false positive answers necessary, while more than 3 false negative answers were observed in 12% of the tests in this group

Table 1

	Normal N:42	Abnormal N:74	Significance
Age years (SD)	40 ($\pm$ 10)	43 ($\pm$ 14)	
Questions			
Mean N (SD)	497 ($\pm$ 75)	549 ($\pm$ 102)	$t = 2\ 99$ $p < 0\ 01$
% above 550$\times$ exam	12	38	$z = 2\ 97$ $p < 0\ 01$
RMS			
Mean Db (SD)	2 0 ($\pm$ 0 95)	3 84 ($\pm$ 2)	$t = 9\ 2$ $p < 0\ 001$
%>2 5 Db	7	76	$z = 7\ 09$ $p < 0\ 001$
Repetitions			
Mean N (SD)	20 4 ($\pm$ 25)	26 7 ($\pm$ 40)	$t = 0\ 25$ $p > 0\ 5$
%>15$\times$ exam	45	42	$z = 0\ 35$ $p > 0\ 5$
False positives			
Mean % (SD)	12 5 ($\pm$ 13 9)	3 26 ($\pm$ 6 9)	$t = 3\ 31$ $p < 0\ 01$
%>3$\times$ exam	12	0	$z = 3\ 02$ $p < 0\ 01$
False negatives			
Mean % (SD)	3 2 ($\pm$ 4 9)	13 5 ($\pm$ 22 7)	$t = 1\ 33$ $0\ 1 < p < 0\ 5$
%>3$\times$ exam	0	12	$z = 3\ 02$ $p < 0\ 01$

Tests interrupted: N 4 (3 3%)

Short-term fluctuations (RMS)

Mean RMS values of 2.0 ($\pm$ 0.95) dB were recorded in normal visual fields. Abnormal subjects had 3.84 ($\pm$ 2.0) dB of RMS A value above 2.5 dB was observed in 7% of normals and 76% of abnormal visual fields.

Statistical significance for the difference between normal and pathological visual fields was present for all parameters considered except the number of the repeated stimuli and the percentage of cases requiring more than 15 repetitions (Table 1).

Discussion

The detection and assessment of visual field defects is based upon the comparison between actual retinal threshold values obtained during the test and values which are considered normal for age and eccentricity It is extremely important for the ophthalmologist, before making diagnostic decisions based on the raw data obtained, to be able to weigh the patient's ability to cope with the examination, his/her understanding of the test, as well as his/her final performance.

It is widely believed that patients with rural cultural backgrounds and overall non-technological education are poorer performers at psycho-physical tests. The physical facility where the patient is examined, the hardware of the instrument used and the complexity of the tests can be intimidating and confusing. Manual perimetry is considered to be simpler for most patients; moreover, it can be adapted by modifying the number of the isopters plotted or the number of threshold determinations The operator can thus tailor the complexity of the examination to each patient individually, changing strategy at any time during the test. Usually, a comment on the overall patient performance will be added at the end to the bottom of the chart. The extensive interaction between the patient and perimetrist has a reassuring effect, but does not give any guarantee as to the reliability of each test, the evaluation of patient performance will always be qualitative and not quantitative.

The measurement of differential light thresholds is accomplished more precisely with automated computerized perimetry than with manual perimetry [6, 8, 9]. With automated computerized visual field testing the interaction between patient and operator is minimal The patient's understanding of the test and his/her alertness and ability to cope with the task should not rely only on an operator's own evaluation. During quantitative Octopus visual field testing of the central 30°, several standard reliability parameters are obtained and printed in a numerical form; each of them, when considered as an isolated factor, can have quite a precise implication. The number of questions necessary to determine the threshold reflects the patient's ability to respond accurately to the light stimulus, while the number of repetitions is related to patient fixation and blinking patterns

[10]. False positive answers are more frequent with anxious and over-eager patients; false negative answers indicate lack of concentration [2, 10]. Short-term fluctuations (RMS) are higher in abnormal areas of visual field [3, 7]. Overall, fluctuation rates indicate how accurate the individual threshold determinations are for a given examination [1, 3, 4, 5]. Variations of reliability parameters are seldom isolated. Even when considering that reliability parameters with lower scores, in general, reflect a better understanding of the test, the interaction among them and their interpretation are not well established and appear to be very complex [1, 2, 4]. We have analyzed the reliability parameters obtained during visual field testing using Octopus Programs 31 or 32 in patients exposed for the first time to computerized automated perimetry In our sample, eyes with normal visual fields scored significantly better than those with pathological findings. An increased number of questions in order to assess the differential light threshold and a higher short-term fluctuation rate are both associated with abnormal visual fields [3, 7]. The patient's attitude toward the testing situation can be altered by his/her level of instruction Our sample size did not allow us to consider separately illiterate patients from the rest. It is relevant though to outline that the composition of our two groups was not homogenous· normal patients had overall higher education. This might explain the difference in false positive and false negative answers observed in the two groups. It is possible that patients who were more aware of the clinical implications of not answering to a stimulus could have been more prone to fail the false positive trials. On the other hand, an illiterate patient might take the test in a more playful and relaxed way, with a consequent decrease in the level of attentiveness and an increased likelihood of failure to respond when tested for false negative answers

The values observed in our patients are within reasonable limits of reliability for quantitative Octopus visual field testing [10]. In the pathological visual fields the range of variation was, for the parameter studied, wider than in normal examinations (Table 1). Although higher short term fluctuations and a larger number of questions are expected during the testing of abnormal visual fields, an overall poor performance could be assumed in some of our cases [1, 2, 3]. On the whole, very few patients could not complete the test (Table 1).

The advantages of computerized perimetry go beyond the exactness of data collection; the possibility of operating the instrument with minimal training and the reproducibility of the test are important factors. Our study was performed on a population of patients with a high incidence of illiteracy and very low proportion of highly educated subjects. A more detailed analysis of the influence of these cultural factors is mandatory; from our study it is so far apparent that patient performance at Octopus perimetry, as quantifiable by routine reliability parameters was, in our environment, comparable to what is reported for Western patients [1, 3, 7, 10].

References

1 Bebie M, Fankhauser F, Spahr J: Static perimetry: accuracy and fluctuations Acta Ophthalmol 54: 339–348 (1976)

2 Flammer J, Drance SM, Fankhauser F, Augustiny L: Differential light-threshold in automated static perimetry: factors influencing short-term fluctuation Arch Ophthalmol 102: 876–879 (1984)

3 Flammer J, Drance SM, Zulauf N: Differential light threshold: short- and long-term fluctuations in patients with glaucoma, normal controls and patients with suspected glaucoma Arch Ophthalmol 102: 704–706 (1984)

4 Heijl A: Time changes of contrast thresholds during automated perimetry Acta Ophthal 55: 696–708 (1977)

5 Heijl A, Drance SM: Changes in differential threshold in patients with glaucoma during prolonged perimetry Br J Ophthal 67: 512–516 (1983)

6 Krieglstein GK, Schrems E, Gramer E, Leydmecker W: Detectability of early glaucomatous visual field defects: a comparison of Goldmann and Octopus perimetry In: Greve EL (ed) 4th International Visual Field Symposium, Bristol Docum Ophthal Proc Series Vol 26 Dr W Junk Publ, Dordrecht, 1981

7 Le Blanc RP: Abnormal values in computerized perimetry In: Whalen WR, Spaeth GL (eds) Computerized visual fields, p 174 Slack Thorofare, NJ, 1985

8 Li SG, Spaeth GL, Scimeca MA, Schatz NJ: Clinical experiences with the use of an automated perimeter (Octopus) in the diagnosis and management of patients with glaucoma and neurological diseases Ophthalmology 86: 1302–1312 (1979)

9 Schmied U: Automatic (Octopus) and manual (Goldmann) perimetry in glaucoma Albrecht v Graefes Arch Klin Ophthalmol 213: 239–244 (1980)

10 Whalen WR: Routine reliability parameters In: Whalen WR, Spaeth GL (eds) Computerized visual fields, pp 81–88 Slack, Thorofare, NJ, 1985

Author's address:
Carlo E Traverso, M D
King Khaled Eye Specialist Hospital,
P O Box 7191, Riyadh, Saudi Arabia 11462

IX.5 Staircase scoring procedures for automated perimetry

C.A. JOHNSON and R.A. LEWIS
Davis, U.S.A.

Abstract

Conventional psychophysical studies have used a variety of analysis methods for
determining thresholds from staircase procedures In general, these methods
demonstrate very good agreement in their threshold estimates when a large
number of stimulus presentations (50–200) are employed However, staircases in
automated perimetry typically employ between 4 and 12 stimulus presentations.
The present study compared five different analysis procedures (average of all
presentations, median of all presentations, mode of all presentations, average of
reversals at the minimum step size, and the value of the last seen target) for
staircases used in automated static perimetry. Test-retest data for 14 normal eyes
and 14 eyes with moderate visual field loss were obtained using a 6-3-3 staircase
procedure on the Digilab 750 automated perimeter. Threshold estimates were
determined for the five analysis procedures for 66 target locations in each visual
field (blind spot region excluded). All of the analysis procedures exhibited good
agreement in threshold estimates, except for the 'last seen' procedure, which was
approximately 1.5 dB different from all other threshold estimates. The average of
all stimulus presentations and the average of reversals at the minimum step size
both displayed the best test-retest reliability. This was a small but consistent
effect, suggesting that these staircase analysis procedures should be employed to
improve the test-retest reliability of automated perimetry tests.

Introduction

Although staircase procedures have been used for many years in visual psycho-
physical experiments, they were not introduced to visual field testing until the
recent advent of automated perimetry. There are a variety of methods available
for analyzing and scoring staircase procedures, and their statistical properties
have been well documented [1, 2, 4]. Some of the more common analysis
techniques include determining:

1. the average of all stimulus presentations,
2. the median of all stimulus presentations,
3. the mode of all stimulus presentations, and
4. the average of all stimulus reversals at the minimum step size of the staircase.

All of these analysis methods yield substantially equivalent results in standard psychophysical experiments [1, 2], which typically utilize highly practiced observers and a large number of trials per staircase (50–200) for establishing threshold measurements.

In contrast, automated perimetry is usually performed on patients with minimal practice as psychophysical observers, and threshold measurements are obtained with a small number of stimulus presentations (typically 4–12). An additional consideration is that some automated perimeters have adopted a different staircase analysis procedure that uses the value of the last target in the staircase that was seen as the basis for the threshold value. In view of the differences between automated perimetric methods and standard psychophysical procedures, it is not clear how these analysis methods compare with each other for automated perimetry, or whether they influence the test-retest reliability of the devices. The present study was therefore conducted to determine the influence of various staircase analysis and scoring procedures on automated perimetric threshold measurements We compared the sensitivity values derived from the average of all stimulus presentations (AVE), the median of all stimulus presentations (MED), the mode of all stimulus presentations (MODE), the average of all stimulus reversals at the minimum step size (REVS), and the target that was last seen (SEEN)

Methods

All testing was performed with the Digilab 750 automated perimeter (Bio-Rad Inc , Cambridge, MA), using their standard central 30 degree test program consisting of 72 target locations. Two modifications were made to the test procedure:
1 A 6-3-3 staircase (6 dB initial step size, 3 dB final step size, 2 reversals at the final step size) was employed, since previous simulation studies [3] indicate that this strategy provides an optimal compromise between accuracy and efficiency of staircase procedures.
2. A 'trace' of all stimulus presentations and responses was retained for each staircase, so that they could be analyzed according to the five different methods.

Visual field evaluations were performed on 14 normal eyes and 14 eyes with moderate visual field loss Each eye was examined twice (test-retest) within a period of 1 to 7 days. For all tests, an optimal refractive correction was placed before the eye being tested. Sensitivity values were calculated for each staircase trace according to the 5 analysis procedures:

(A)

MEAN DIFFERENCES AMONG STAIRCASE ANALYSES
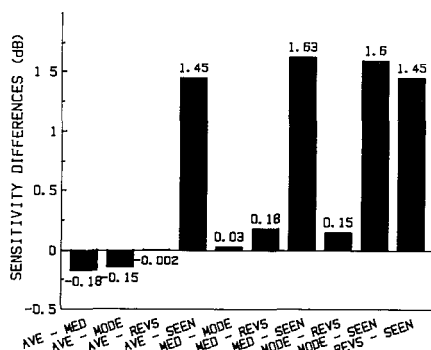
(B)

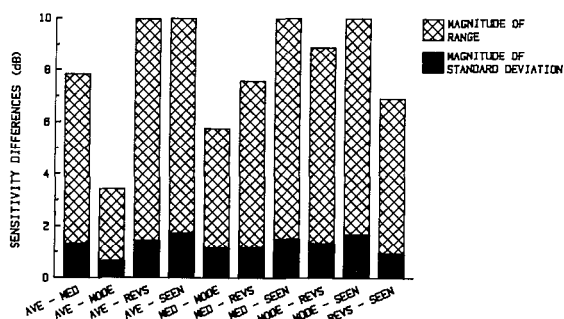S. D. AND RANGE OF STAIRCASE ANALYSIS DIFFERENCES

Figure 1 A The mean difference in sensitivity estimates for all paired comparisons of the five staircase analysis procedures B The standard deviation and range of sensitivity differences for all paired comparisons of the five staircase analysis procedures AVE represents the average of all stimulus presentations MED represents the median of all staircase presentations MODE represents the mode of all staircase presentations REVS represents the average of all staircase reversals at the minimum step size of the staircase SEEN represents the value of the last seen target for the staircase

1. the average of all stimulus presentations (AVE),
2. the median of all stimulus presentations (MED),
3. the mode of all stimulus presentations (MODE),
4. the average of all staircase reversals at the minimum step size (REVS), and
5. the target that was last seen (SEEN).

Targets in and around the blind-spot region were excluded from the analysis, leaving a total of 66 target locations per eye for which comparisons could be made among the staircase analysis procedures.
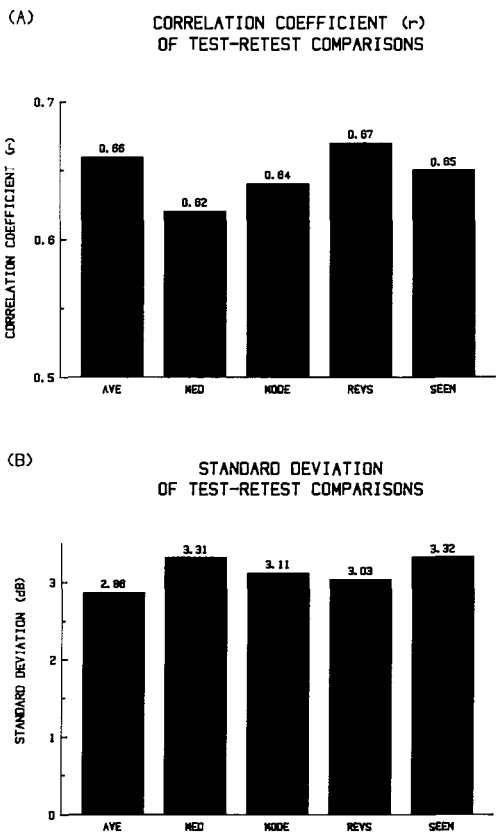
(A)   CORRELATION COEFFICIENT (r)
OF TEST-RETEST COMPARISONS

(B)   STANDARD DEVIATION
OF TEST-RETEST COMPARISONS

Figure 2 The test-retest characteristics for each of the five staircase analysis procedures A Test-retest correlation coefficients for the five staircase analysis procedures B Standard deviations of test-retest differences in sensitivity estimates for the five staircase analysis procedures See legend of Figure 1 for a description of the AVE, MED, MODE, REVS and SEEN analysis procedures

Results

Figure 1A presents the mean differences in sensitivity estimates for all of the paired comparisons of the five staircase analysis procedures Each value is based on the mean of more than 3,500 threshold determinations. In general, there is good agreement among the various analysis procedures, with the exception of the estimates derived from the last target seen (SEEN) analysis. All of the other comparisons are close to 0 dB mean difference in sensitivity values, whereas the SEEN values are about 1.5 dB (half of the final step size interval) different from the other estimates. There also appears to be a tendency for the distribution of differences between the SEEN values and other estimates to have a greater standard deviation and range (Figure 1B).

Figure 2 indicates that the various staircase analysis procedures also have an influence on the test-retest reliability of automated visual field testing The average of all stimulus presentations (AVE) and the average of staircase reversals at the minimum step size (REVS) exhibit the greatest correlation coefficients (Figure 2A) and the lowest standard deviations (Figure 2B) for test-retest comparisons.

Discussion

The present findings indicate that the method of analyzing staircase data can affect both the absolute values of visual field sensitivity and the test-retest reliability for automated static perimetry. All of the analysis methods displayed reasonably good agreement in threshold estimates, with the exception of the 'last seen' procedure which was approximately 1.5 dB different from the other estimation methods. This difference (one half of the final step size) was expected, since all of the other methods attempt to define threshold on the basis of the *midpoint* between seeing and non-seeing rather than the *endpoint* of seeing.

Of greater significance is the test-retest reliability obtained for the five analysis procedures. The average of all stimulus presentations (AVE) and the average of reversals at the final step size (REVS) had the highest test-retest correlations and the lowest variability. Although these effects are small, they are quite consistent For example, a comparison of the test-retest reliability of REVS and SEEN, the two analysis procedures most commonly used in automated perimetry, 27 out of 28 eyes showed a higher test-retest correlation for REVS than for SEEN.

Our findings indicate that improvements in the reliability of automated perimetry results can be achieved by the use of appropriate data analysis procedures. The average of reversals at the minimum step size (REVS) appears to be the method of choice for automated perimetry, since it displays better test-retest reliability and is currently implemented on several automated devices. Because these analysis methods do not affect test strategies and other parameters that may be exclusive to a particular device, it should be possible to implement the averaging procedure on all threshold static perimeters. This would significantly enhance the standardization of automated perimeters and improve the ability to compare test results among various automated devices.

Acknowledgements

References

1 Cornsweet TN: The staircase method in psychophysics Am J Psychol 75: 485–491 (1962)
2 Feeny S, Kaiser PK, Thomas JP: An analysis of data gathered by the staircase method Am J Psychol 79: 652–654 (1966)
3 Johnson CA: Properties of staircases in automated perimetry (Abstract) Invest Ophthalmol Vis Sci (Suppl) 26: 217 (1985)
4 Rose RM, Teller DY, Rendleman P: Statistical properties of staircase estimates Perception Psychophys 8: 199–204 (1970)

Author's address:
Chris A Johnson, Ph D ,
Dept of Ophthalmology,
University of California, Davis,
1603 Alhambra Blvd,
Sacramento, CA 95816, U S A

IX.6 A new contingent algorithm for static automatic perimetry based upon chain pattern analysis

J.R. LYNN, R.L. FELLMAN and R J STARITA
Dallas, U S A.

Abstract

This communication introduces the term, 'Chain Pattern', and shows how analysis of the static automatic perimetric data embedded in chain patterns can help
1. use all equally valid and relevant data to find thresholds which are reproducible enough to serve as standards for comparison,
2. quantitate the rate of internal inconsistencies during static automatic perimetry,
3. design and refine a more efficient algorithm, and
4. provide a 'report card' on the accuracy and short-term stability of each threshold on the numerical printout

Background

Deterioration of the glaucoma patient's visual field during the brief course of a clinical test session was reported by Heijl and Drance in 1983 [1] We found two minute rest periods after each 5 minutes of perimetry was not sufficient to avoid this decay [2]. Until the deterioration itself has been studied adequately, it appears clear that all testing must be accomplished quickly if it is to be accurate. The testing of any given location also needs to be brief so a critical number of locations can be evaluated because in glaucoma, small defects can be missed altogether if the test pattern leaves large areas untested Rapid testing of individual locations is usually accomplished by crossing threshold a few times, often using progressively smaller steps and reporting only the last seen or the mean of the last seen and unseen tests. The data leading up to the last test or two is discarded, yet each test presentation is as valid as any other. We hope to illustrate what can be gained by retaining for immediate and later analysis the initial and intermediate data as well as the last test or two.

Categories of Visual Response

	Not Reported Seen	Reported Seen
Dimmer	Correct Rejection	False Alarm
Threshold →		
Brighter	Miss	Hit

Figure 1 Classification of responses relative to threshold. The response types hit and correct rejection usually apply respectively to stimuli which are brighter and dimmer than threshold. When tests are reported seen yet they are dimmer than threshold, these are called false alarms. Others which are not reported seen despite stimulus values greater than threshold are called misses. False alarms and misses are the internal inconsistencies, booboos, or errors which make accurate measurements of thresholds challenging

Classification of response types

If one treats threshold as a precise limit between what is truly visible and what is not, and subjects can only report the test was seen or not, four classifications are possible (see Figure 1). A perfect subject would always report seeing all tests which are brighter than thresholds (hits) and never report seeing tests which are dimmer than threshold (correct rejections). Reports of seeing tests which are dimmer than threshold (false alarms) and failure to see tests which are brighter than thresholds (misses) constitute the internal inconsistencies which make us human

Algorithm defined

Any rational process which seeks a goal may be called an algorithm. The first rule of any threshold-seeking algorithm in static automatic perimetry is to increase the intensity (↓ decibel value) of the next test at a given location if the most recent test there was not seen. The second rule is to decrease intensity (↑ decibel value) next time if the former test was seen. A third rule often used is to change intensities by large increments early (usually 3, 4, or 6 dB), by smaller ones (usually $1\frac{1}{2}$, 2, or 3 dB) once a change in response type (seen or not seen) occurs.

Rules of 4-2 and 4-2-2 algorithms

These rules are illustrated in Figure 2 with sequential responses of the same type (all seen or all not seen) grouped in vertical columns, called chains. The algorithm 4-2 is named by the step sizes in decibels before and after the first change in response type. The 4-2 algorithm shows a 4 decibel difference between all the
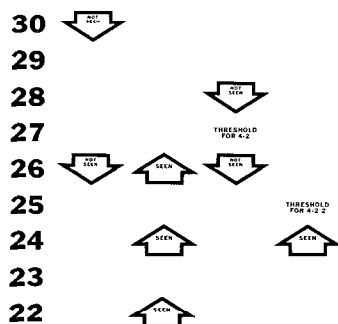
Figure 2 Serial responses to stimulus attempts at one location. Arrows represent responses to eight attempts at various decibel levels. The first two attempts were at 30 and 26 decibels (dB) respectively, and neither was seen. The next three were at 22, 24, and 26 dB, and all were seen. The next two, at 28 and 26 dB, were not seen but the last stimulus, at 24 dB, was seen. The not seen arrows always point downward because the next stimulus attempt must use more light, a smaller decibel value. Seen arrows point upward because the next stimulus must be presented with less light, a larger number of decibels. The arrow count in vertical columns, called chains, is 2, 3, 2, and 1. These numbers constitute a chain pattern. If this pattern and the underlying logic, a 4-2 or 4-2-2 algorithm, are known along with the dB level and response type of the initial test, threshold is easily calculated.

members of chain I and the first change in response and a 2 decibel difference between all the members of chain II and the second (and final) response reversal. The 4-2-2 algorithm is a continuation of the 4-2, still using 2 decibel steps to a third reversal of response.

Chain pattern definition

The chain pattern at a given location is the number of serial responses of identical type within each vertical column leading up to threshold. In Figure 2, the chain pattern is 2-3-2-1 with the initial stimulus of 30 dB not seen.

Composite threshold

Frequency of seeing curves from classical psychometrics should serve as the ideal standards of threshold accuracy. Since glaucoma patients' thresholds deteriorate before these curves can be measured in only 10 locations [2], an alternative 'composite threshold' was chosen. This assumes each stimulus response is equally valid, not just the final test or two. It uses all available tests of threshold, combining them as shown in Figure 3. In essence, a threshold range is chosen to
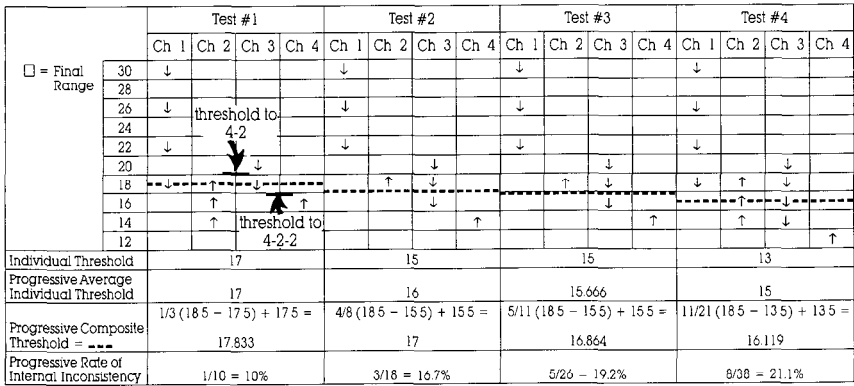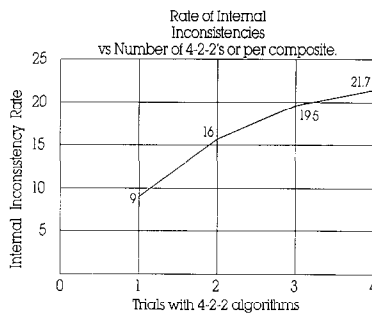
		Test #1				Test #2				Test #3				Test #4			
		Ch 1	Ch 2	Ch 3	Ch 4	Ch 1	Ch 2	Ch 3	Ch 4	Ch 1	Ch 2	Ch 3	Ch 4	Ch 1	Ch 2	Ch 3	Ch 4
□ = Final Range	30	↓				↓				↓				↓			
	28																
	26	↓	threshold to 4-2			↓				↓				↓			
	24																
	22	↓				↓				↓				↓			
	20			↓				↓				↓				↓	
	18	↓	↑	↓			↑	↓			↑	↓		↓	↑	↓	
	16		↑	↑				↓				↓			↑	↓	
	14		↑	threshold to 4-2-2					↑				↑		↑	↓	
	12																↑
Individual Threshold		17				15				15				13			
Progressive Average Individual Threshold		17				16				15.666				15			
Progressive Composite Threshold = ---		1/3 (18.5 – 17.5) + 17.5 = 17.833				4/8 (18.5 – 15.5) + 15.5 = 17				5/11 (18.5 – 15.5) + 15.5 = 16.864				11/21 (18.5 – 13.5) + 13.5 = 16.119			
Progressive Rate of Internal Inconsistency		1/10 = 10%				3/18 = 16.7%				5/26 = 19.2%				8/38 = 21.1%			

Figure 3 Calculation of composite threshold Four tests of threshold at one location by the 4-2-2 algorithm are shown, all starting at 30 dB, not seen The four tests have chain patterns of 4-3-2-1, 3-1-3-1, 3-1-3-1, and 4-3-4-1 respectively These patterns are symbolized on one decibel scale by 38 response arrows The dimmest test which is seen in any chain (higher decibel number) is identified along with the brightest which is not (lower decibel number) In test 1, these are at 18 dB, the top of chain II and also at 18 dB, the bottom of chains I and III In tests 2, 3, and 4 the 18 at the top of chain II remains the dimmest test seen The brightest not seen is at 16 dB in chain III of tests 2 and 3 and at 14 dB in chain III of test 4 One fourth the interval between sequential tests in chain II, or 0 5 dB in this example, is added to the larger dB value and the same amount is subtracted from the smaller value to find the limits of the threshold range Within that range, all seen and unseen stimuli are counted and the proportion seen is multiplied times the difference between limits of the range, then added to the lower end of the range The individual threshold to 4-2-2 is shown in the first row beneath the arrows for each test In the second row, the mean value of the current 4-2-2 threshold with all prior 4-2-2 thresholds is shown The third row shows how composite thresholds are calculated, progressively adding all data which falls within the collective range of the tests which are chosen The number of arrows pointing upward and located above the composite threshold plus the number of arrows pointing downward and located below the composite threshold are summed and then divided by the total number of arrows to calculate the progressive rate of internal inconsistency

encompass all contradictory data and the proportion of responses of each type within that range is used to strike the appropriate level, a composite threshold.

Inconsistency rate

False alarm and miss classifications have been lumped together and called errors, booboos, or internal inconsistencies. The percentage of internal inconsistences is larger with a 4-2-2 algorithm than with a 4-2. The number and percentage of responses subject to error is larger when more tests are given because the first three stimuli in both algorithms are originally immune from internal inconsistency. As indicated in Figure 4, the internal inconsistency rate rises toward 25% of responses as more data is added.

Rate of Internal
Inconsistencies
vs Number of 4-2-2's or per composite.

25

20

Internal Inconsistency Rate

15

10

5

21.7

19.5

16

9

0   1   2   3   4

Trials with 4-2-2 algorithms

Figure 4 Rate of internal inconsistencies The Squid automatic perimeter was programmed with the 4-2-2 algorithm to retest two locations to three independent thresholds and two more loci to four independent thresholds This test system was applied to 39 eyes with glaucoma, all of which were analysed to learn the rate of internal inconsistency The method is illustrated in Figure 3 and calculates in its last row The results of the 78 spots tested three times and the 78 tested fourfold are shown here The rate appears to approach 25% as immunity from error is eliminated

Chain pattern frequency in glaucoma patients

Figure 5 shows the percentage of various chain patterns among 8,860 complete 4-2-2 algorithms found in 10,000 patterns from 105 glaucomatous eyes The remaining 1,140 threshold attempts were incomplete because they tested blind. The initial presentation was seen in 4,452 cases and unseen in 4,408. Of the 112 unique chain patterns found and classified, 18 were only found in the initially unseen group, 16 were exclusively found among the initially seen, and 78 patterns were represented in both groups.

As indicated in the upper half of the outer ring of Figure 5, the frequency of chain patterns with any length chain I, a single response in chain II, and 1, 2, or 3 responses in chain 3 is 37.1% of the completed patterns. The 4-2-2 algorithm is recommended to improve accuracy by its third reversal to compensate for the single response in chain II.

The length of chain III exceeds 3 in the lower half of the outermost circle Because two or more contradictory responses cast significant doubt on the validity of the single response in chain II, the action recommended is 'jumping', a return to large step sizes.

The second ring includes all instances where chain II equals 2 or 3. Along with the right half of the third ring where chain II = 4 and chain 1 is longer than 1, it totals 55%. The 4-2 algorithm is recommended for all these circumstances

The left half of the third ring (chain II = 4) is combined with the left half of the inner circle (chain II >4) totalling 4.8% of the completed tests. In this circumstance, chain I is suspected of being a false alarm because it has been contradicted twice. For this reason, resumption of the maximal step size is recommended,

Chain III = 1 2, or 3
Chain I = 1

Ch II = 1

Chain III = 1, 2, or 3
Chain I > 1

Ch II = 2 or 3

Uses
4 2-2

37 1%

Ch II = 4

4 8%

1 4%

55%

Ch II > 4

Stops in Ch II

Uses 4 2

Jumps in
Ch II

1 8%

Chain III > 3
Chain I = 1

Jumps in Ch III
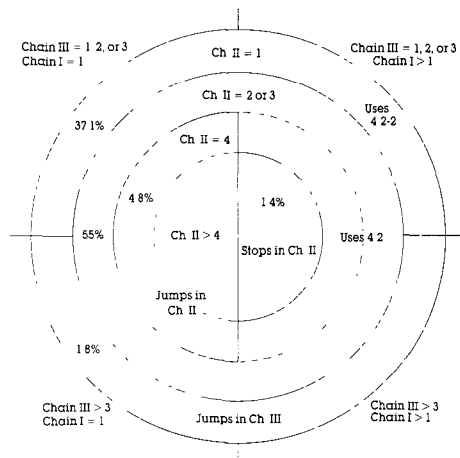
Chain III > 3
Chain I > 1

Figure 5 Chain patterns found at 8860 locations in 105 glaucomatous eyes All possible 4-2-2 chain patterns are shown in this generic schematic diagram The outermost ring of Figure 5 indicates chain II is 1 in length; the next ring shows chain II is either 2 or 3 in length; the third layer shows chain II contains 4 responses, and the innermost circle signifies second chains longer than 4 The left half of the pic applies to situations where the length of chain I = 1 while the right half shows chain I is greater than 1 The upper half of the pie shows chain III is 3 or less and the lower half indicates chain III is greater than 3 Frequencies observed are noted on the figure and in the text, not proportional to area

along with another intermediate stimulus after the response change, as in the other jumping algorithms.

The right half of the inner circle represents chain I greater than 1 and chain II greater than 4. This occurs in only 1.4% of the chain patterns, resulting in a recommendation that the test be stopped after the fifth stimulus response of the same type in chain II.

Rules for application and grading of the 4-2-c algorithm

If a 4-2-2 algorithm has single steps in chains II and III or a 4-2 has 2 steps in chain II, double confirmation is present on both sides of threshold without any conflict. This is called grade J

If a 4-2-2 algorithm has two steps in chain III or a 4-2 has 3 steps in chain II, a single conflict exists a half step from calculated threshold. This is resolved by shifting to the conflict level, calling it threshold, and the mechanism is grade K.

When a single conflict cannot be eliminated by a half-step threshold shift, this is a grade L. An example is a chain III length of 3, which would only occur when chain II = 1.

The 'jumping' algorithms can occur in chain II or III after a single step in the preceding chain. They occur after four single steps in the chain have not yet

Graded Numerical Threshold Plot of Glaucoma Patient's Left Eye

Figure 6 Clinical example of the 3-1½-c algorithm with grades The 4-2-c algorithm was programmed in the Digilab 750 perimeter as a 3-1½-c to use existing hardware Thresholds are thus reported to quarters of a decibel Some of the grades which are shown beneath each decibel score have greater validity and predictability than others, as shown in Table 2

shown a change in response type. After the fourth attempt, each additional trial in the chain is separated by the same size steps as in chain I. When a change in response occurs, constituting a new chain, one final trial occurs at an intensity between the last two stimuli. If the response to that trial is a different type from the one before, threshold is the mean of those two tests, and the grade is M. If both of the final two tests show the same response type, threshold is between the last two which are of different response types and the grade is N.

When two or more responses are recorded in chain I and the tests number four in chain II, jumping is not done. The last stimulus is presented in the same sequence as the four before it. If it is a change in response type, threshold is the mean of the last two stimuli and the test is graded O. If it is the same response type as the four before it, threshold is the same as the last stimulus and the algorithm grade is P.

The clinical results of a 3-1½-c algorithm are shown in Figure 6, with sub-algorithm grades beneath each reported threshold The validity and reproducibility of each threshold is only as accurate as its grade indicates (see Table 2)

Comparison of 4-2-c with existing algorithm

Two versions of the 4-2-c with initial step sizes of 6 dB and 3 dB were available for trial against the 3-c and 3-c-m algorithms used normally on the Digilab 750

perimeter where step size remains 3 dB in the first and all subsequent chains. The accuracy and reproducibility of the 3-1$^1/_2$-c algorithm appear to be best, as shown by their lower root mean squares (RMS) when compared with the other clinical algorithms (see Table 1).

While the composite threshold is not a clinical test because of its undesirable duration, the composite threshold not only serves as a standard for current comparison, but proves its superiority by predicting the standard threshold on another day better than any of the clinical algorithms. The 3-c-m is 1$^1/_2$ dB closer to the composite threshold than the 3-c so the 3-c-m was chosen for comparison with the 3-1$^1/_2$-c in Table 2. The 3-c algorithm uses the last seen test as threshold and the 3-c-m uses the mean of the last seen and the last unseen tests. The 3-c algorithms test an initial spot in each quadrant to a triple reversal threshold, using the thresholds of recently determined locations for calculating starting intensities of their neighbors. The number of response reversals then varies during the remainder of the test, contingent upon patient response In 13 patients with glaucoma, a single reversal algorithm occurred in about 25.58%, double reversal in 45 08%, and triple reversal in 23 62%. In 5.73%, the locations tested were blind

When these three different subalgorithms were compared to the composite threshold on the same day, the triple reversal was most accurate with an RMS of 1.47; the double reversal less so with an RMS of 1 82, and the single reversal was least accurate with an RMS of 2.84, as shown in Table 2. This same table also shows an apparent correlation between accuracy of a given subalgorithm and its ability to predict threshold by the same algorithm or the composite threshold on another day. The correlation is suggested by similar magnitudes of numbers in the first two data columns as compared with numbers in the same row and the third and fourth columns.

Using the three best subalgorithms of the 3-1$^1/_2$-c algorithm (K, J, and L), 81.6% of glaucomatous loci and 88.4% of normal spots (84 6% overall) showed closer correlation with the composite threshold (RMS = 1.27 to 1.32) than the best (triple reversal) subalgorithm of the 3-c-m. Refinement of the remaining grades and steps to reduce duration without loss of accuracy require further research by chain pattern analysis.

Conclusions

The authors hope this communication will encourage others to use the chain pattern data which is usually discarded before threshold is determined. The benefits of using chain pattern data include calculation of a better standard threshold for accuracy comparisons, identification of false alarms and misses, the creation and critique of new algorithms for static automatic perimetry, and graded numerical printouts which indicate the accuracy and stability of each threshold shown

Table 1. Accuracy and reproducibility of algorithms (dB) in 13 glaucomas and 10 normals.

	RMS to same day's composite	RMS to composite another day	RMS to same algorithm another day	Mean threshold	Time	Average # of presentations
6-3-C						
Abnormal	1.73	3.10	3.57	22.0	9 35	454
Normal	1.82	2.57	3.10	25.8	10 04	460
3-1½-C						
Abnormal	1.57	2.91	3.17	21.6	11 26	542
Normal	1.41	2.23	2.44	25.8	11 56	545
3-C						
Abnormal	2.59	3.48	3.25	19 1	9 19	441
Normal	2.84	3.34	3.21	22.8	10 08	455
3-C-M						
Abnormal	2.06	3.13	3.31	20.6	9 19	441
Normal	2.23	2.84	3.22	24.3	10 02	455
Composite						
Abnormal	Std.	2.52	2.52	21.7	30 20	1437
Normal	Std.	1.95	1.95	25.7	32 02	1460

Table 2. Frequency, duration, and accuracy of subalgorithms compared with current and future thresholds at the same 100 locations in 13 glaucomatous and 10 normal eyes.

Grade	Same day				Different day				Occur-rence in %	Mean # of presenta-tions	Overall rank
	Average difference to composite threshold	Rank	RMS to composite threshold	Rank	RMS to composite threshold	Rank	RMS to same algorithm	Rank			
3-1¹/₂-C											
J	1.15	2	1.32	3	2.42	3	2.85	3	55.7	4.86	2
K	1.06	1	1.27	1	2.20	1	2.51	1	26.3	5.86	1
L	1.61	5	1.31	2	2.35	2	3.11	4	2.6	6.90	3
M	2.97	8	2.67	7	3.87	7	4.16	6	1.4	7 79	7
N	2.92	7	2.80	8	3.52	5	3.65	5	3.2	7.68	6
O	1.54	3	1.56	4	2.57	4	2.67	2	4.9	7.69	4
P	1.57	4	1.90	5	3.54	6	4.31	7	2.2	7.90	5
Blind	1.68	6	2.47	6	5.31	8	4.89	8	3.6	2.66	8
3-C-M											
3	2.88	4	2.84	3	3.73	3	3.71	3	26.9	2.08	3
3-3	1.86	2	1.82	2	2.54	2	2.81	1	45.1	4.74	2
3-3-3	1.54	1	1.47	1	2.39	1	3.34	2	24.3	6.98	1
Blind	2.19	3	3.17	4	5.17	4	4.57	4	3.7	2.39	4

Acknowledgements

References

1 Heijl A, Drance S: Changes in differential threshold in patients with glaucoma during prolonged perimetry Br J Ophthalmol 67: 512 (1983)
2 Lynn JR, Batson EP, Fellman RL: Internal inconsistencies versus root mean square as measures of threshold variability Doc Ophthalmol Proc Series 42: 7–15 (1984)

Author's address:
Glaucoma Associates of Texas,
7150 Greenville Avenue, Suite 300,
Dallas, Texas 75231, U S A

IX.7 Reliability parameters in computerized perimetry

A. HEIJL, G. LINDGREN and J. OLSSON
Malmö and Lund, Sweden

Abstract

The distribution of results of perimetric reliability tests, false positive and false negative answers, fixation losses and short-term fluctuation, was studied in a material of 84 healthy normal subjects, randomly selected from the population, and in 45 patients with glaucoma All subjects were tested with the 30-2 programme of the Humphrey Field Analyzer We further investigated the influence of perimetric reliability on the measured visual field, as expressed by the visual field indices Mean Deviation and Pattern Standard Deviation. Sample multiple correlation coefficients were calculated for a number of combinations of reliability parameters and visual field indices.

False negative answers were more common and short-term fluctuation higher in glaucomatous than in normal subjects False positive answers and fixation losses did not differ between groups Among glaucoma patients false negative answers were significantly more common than false positive answers No such difference was found in the group of normals The results showed no age-dependence. A large part of inter-individual field variability, particularly among normals, could be explained by perimetric reliability False negative answers and short-term fluctuation had the largest predictive value

Normal inter-individual variation decreased considerably when stricter criteria for minimum results at reliability testing were applied Naturally the number of fields meeting these criteria decreased at the same time Therefore, when establishing limits for normality, a compromise must be made resulting in reasonably narrow prediction limits without excluding a large percentage of normal and pathological fields from analysis

Introduction

Several computerized perimeters display the results of various reliability tests in

their field charts. These tests are designed to help estimate the behaviour of the patient in the perimetric situation.

The inclination of the patient to press the response button of the intrument without having perceived a stimulus is examined by so-called false positive (FP) catch trials. The perimeter produces the same sound as when displaying a stimulus without showing one and registers whether the patient responds or not. The opposite is tested by false negative (FN) trials. A strong, supraliminal stimulus is exposed at a location where the threshold has already been measured. The ability of the patient to maintain fixation is monitored by exposing stimuli in the blind spot of the tested eye at random intervals [4]. The number of perceived stimuli divided by the total number of such presentations is the fixation loss (FL) ratio.

Catch trials for false positive and false negative answers and blind spot stimulus presentations test basic components of the patient's behaviour in the perimetric test situation The short-term fluctuation (SF) on the other hand is a more complex function, and represents the measurement error of the threshold determination of a test [5]. SF is influenced by perimetric reliability as tested by FP, FN and FL. SF is an estimate of the intra-test standard deviation of the threshold measurements and is calculated by performing double threshold measurements at a number of pre-determined locations.

It is obvious that the results of visual field testing is influenced by the patient's reliability and that therefore results of reliability tests may be clinically helpful. More detailed knowledge on the normal outcome of such tests, and on the dependence of perimetric test results on perimetric reliability should make it easier to use these results effectively.

The aim of the present investigation was to study the distributions of the results of reliability tests in normal eyes and in eyes with glaucomatous field loss, and the influence of perimetric reliability on the measured visual field. A further aim was to investigate whether normal threshold limits can be narrowed if accepting only field tests meeting certain minimum reliability criteria.

Material and methods

Two groups of subjects were studied, normals and patients with glaucoma. The *normals* were randomly selected from a normal population. Abnormal subjects were excluded according to predetermined criteria [6]. The *glaucoma group* consisted of patients with elevated IOP and visual field defects demonstrated by computerized threshold-measuring perimetry and/or optic discs judged to be glaucomatous or highly suspected of being glaucomatous. Those eyes where earlier perimetry had failed to demonstrate clear field defects but where glaucoma was evident or suspected because of the optic disc, usually had fellow eyes with clear, often advanced, glaucoma. Eyes with large visual field defects were avoided.

One eye of each subject was tested with the threshold-measuring 30-2 pro-gramme of the Humphrey Field Analyzer [3] using appropriate correction for refractive error and near. The patients were instructed according to a standard protocol and a demonstration subroutine was used at the beginning of each test They were moderately supervised during the test. They were encouraged, re-instructed and realigned when necessary but the operator avoided constant interference.

The normals were subjected to repeated field testing. The result from the first tested eye from the second test session was chosen for the study. When taking this test the large majority of the normal subjects therefore had experience of one previous session of automatic perimetry, involving both eyes. Out of 88 thus selected tests 84 met the inclusion criteria requiring the following minimum number of performed tests: $\geqslant 1$ FP plus $\geqslant 1$ FN plus $\geqslant 10$ FL tests and SF testing on.

The great majority of the glaucoma patients had previous experience of com-puterized perimetry. All 45 tests from these patients met the inclusion criteria regarding reliability testing stated above.

The ratio of perceived to exposed blind spot check stimuli gave the fixation loss (FL) ratio. Similarly the FP ratio was defined as the number of patient answers on FP catch trials divided by the total number of such trials, and the FN ratio as the number of FN catch trials on which the patient did not respond divided by the total number of FN trials, FN, FP and FL, displayed as ratios by the perimeter, were converted into %. SF, in dB, was used as calculated by the perimeter [5].

When studying the influence of perimetric reliability on the measured visual field, the latter was represented by the global field indices mean deviation (MD) and pattern standard devation (PSD), as calculated by the Statpac programme of the Humphrey perimeter [5] MD estimates the uniform part of the deviation of the measured field from the age-corrected normal reference field. With increas-ing field defects MD becomes an increasing negative number. PSD estimates the non-uniform part of this deviation, the deviation of shape of the measured field from the shape of the reference field. PSD is always positive and increases when field defects develop and progress.

Sample multiple correlation coefficients R^2 were calculated for a number of combinations of reliability parameters and visual field indices. The coefficients estimate the percentage of inter-individual variance which may be explained by one or several reliability parameters. Measured PSD and MD values were plotted versus results of reliability tests.

Dependence of normal variation on perimetric reliability was studied by divid-ing the normal subjects into groups according to the results at reliability testing and calculating 5% limits for PSD and MD in the different groups.
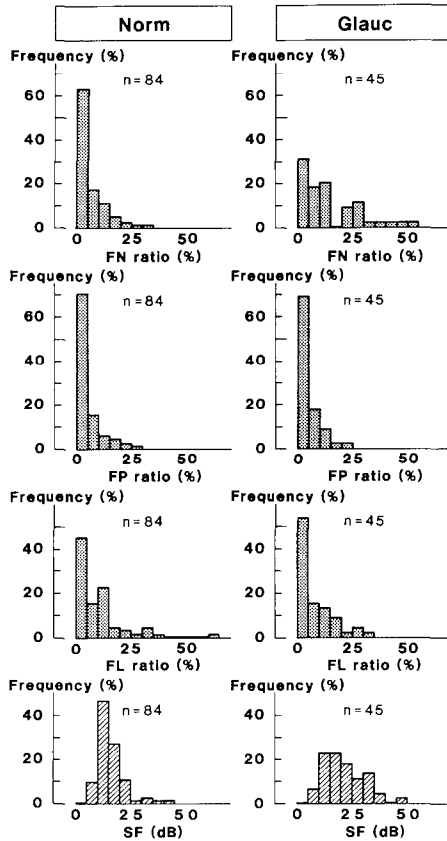
Figure 1 Percentages of false negative (FN), false positive (FP) answers and of fixation losses (FL) and short-term fluctuation (SF) in normal and glaucomatous eyes. High ratios of FN answers and high SF are both more common in pathological than in normal eyes.

Results

The distributions of the results of the reliability tests are shown in Fig. 1. Means and standard deviations are shown in Table 1. The results were not identical in the two groups of subjects (p<0.0001; Hotelling's T^2, test for equal means between groups [7]). False negative answers were more common (p<0.0002; t-test of separate variances [1]) and short-term fluctuation higher (p<0.0002; same test) in glaucomatous than in normal eyes. False positive answers and fixation losses did not differ significantly between groups.

Among the glaucoma patients false negative answers were significantly more common than false positive answers (p<0.0001; Student's t-test, test for equal means). In normals the frequency of these two types of false answers did not differ significantly. Regression analyses failed to show any influence of age on any
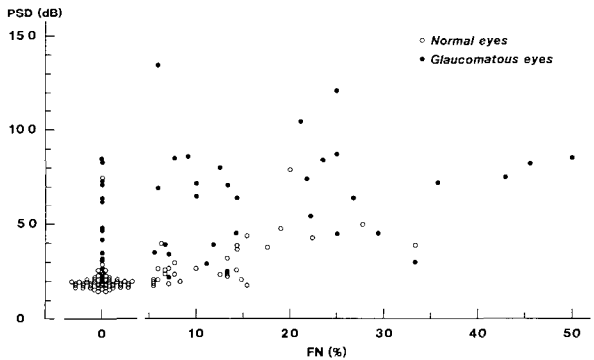
Figure 2 Influence of percentage of false negative answers on PSD

of the four reliability parameters in both groups of subjects. The correlations between measured visual field and measured reliability are shown in Table 2. A large part of inter-individual variance of MD and PSD could be explained by differences in perimetric reliability. Short-term fluctuation and false negative answers had largest predictive value, PSD increasing and MD moving in negative direction with increasing SF and FN. The dependence of PSD on the frequency of false negative answers is illustrated in Fig. 2.

Inter-individual variation, and therefore 5% limits for PSD and MD, decreased when stricter reliability criteria were applied when selecting the fields forming the normal data base (Examples in Table 3) Increasing the demands on perimetric reliability also, of course, meant increasing the number of fields not meeting these stricter criteria.

Table 1 Means and standard deviations of FN and FP answers, FL (in %) and SF (in dB) The mean number of FN, FP and FL trials per test was 13 5, 13 5 and 48 2 respectively, differing very little between the two groups of subjects Means and standard deviations are given for PSD and MD in order to provide a numeric description of the material

	Normal eyes		Glaucomatous eyes	
	Mean	SD	Mean	SD
FN (%)	4 6	7 3	13 2	13 6
FP (%)	3 5	6 2	3 3	5 5
FL (%)	9 6	10 5	7 6	8 6
SF (dB)	1 57	0 65	2 18	0 91
PSD (dB)	2 42	1 13	6 12	2 65
MD (dB)	− 0 05	1 73	− 7 28	4 28

Table 2 The correlation (R^2) between measured visual field (as represented by MD and PSD) and measured perimetric reliability (FN, FP, FL and SF) Many correlations are significant as indicated by * (F-test, p<5%) FN and SF are most important (cf text) R = multiple correlation coefficient

	PSD		MD	
	Norm (%)	Glauc (%)	Norm (%)	Glauc (%)
FN	37*	8	36*	21*
FP	0 2	2	6*	2
FL	0 2	0 8	0 7	0 1
SF	30*	30*	39*	31*
FN, FP, FL	37*	12	43*	22*
FN, FP, FL, SF	43*	30*	52*	42*

Table 3 Increasing minimum acceptable results at reliability testing effectively narrows limits of normal visual field variation (here shown as normal limits of MD and PSD) At the same time, however, the number of field tests meeting these stricter criteria diminishes This is particularly so for field tests from abnormal eyes The 5% limits for normality corresponds to the 5th percentile in that part of the normal material, which fulfills the reliability criteria

Maximum allowed % errors at reliability testing			Number of subjects meeting criteria		5% limits for normality		Means in normal group	
FN	FP	FL	Normal	Glauc	PSD	MD	PSD	MD
100	100	100	84	45	4 7	− 3 8	2 42	− 0 05
20	20	20	72	29	4 0	− 4 2	2 36	0 11
0	10	5	30	12	3 3	− 0 9	2 03	0 02
0	0	0	9	2	−	−	1 88	0 71

Discussion

Fig. 1 gives a clear indication of the outcome of reliability tests in normals and in patients with glaucoma with subtle to medium-sized field defects.

In the present results the rate of false positive answers did not differ between the normal and glaucomatous groups False negative answers, on the other hand, were considerably more prevalent in glaucomatous than in normal eyes. This is clearly a problem when interpreting computerized visual fields. Increasing visual field defects seem to lead to an increased ratio of FN answers. Results from pathological eyes may therefore be hard to distinguish from those of normal patients with a high frequency of FN answers, since in such non-reliable normal patients measured sensitivity levels often are considerably lower than those of the age-corrected normal reference field (cf below). Our observation that SF is

higher in pathological than in normal eyes is of course in agreement with previous findings [2].

The FL ratio is influenced both by faulty fixation (leading to positive responses to stimuli which should have been placed in the patient's blind spot, had he maintained fixation) and by FP answers (positive responses without stimulus perception). The instrument of course cannot separate between these two reasons for a faulty positive response. The FN ratio also influences FL, but to a much smaller degree. It is therefore expected and logical that the observed FL ratios are considerably higher than the FP ratios.

The size of the ratios may partly be instrument-specific. Different perimeters might be expected to yield somewhat different results, e.g. due to the existence or non-existence of an audible stimulus in conjunction with the perimetric stimulus or due to the method of fixation control.

It is encouraging to see that such a substantial part of normal variance among individuals can be explained by differences in perimetric reliability. The ratio of false negative answers and the short-term fluctuation are both clearly important. This means that it should be possible to improve interpretation of computerized visual fields if the results of these tests are taken into account. One might wonder why the results did not show false positive answers to have the same effect on MD and PSD as false negative answers. Theoretically one would expect false positive answers to affect MD to about the same extent as false negative answers, although in the opposite direction One explanation to this surprising difference might be the fact that the test sequence in most points starts 2 dB brighter than the expected threshold. Another possible explanation is that FN and FP answers influence test results in a non-linear fashion so that the effect is quite small until the frequency of erroneous answers becomes high, when the effect increases drastically. If high FN ratios are more common than high FP ratios the encountered large differences in R^2 coefficients may be partly explained Our data suggest such a difference.

In a non-fixating eye the stimulus may happen to fall in areas which are either more or less sensitive than the area where the stimulus would have fallen if fixation was maintained. It is therefore understandable if the influence of FL on MD is small. The small influence of FL on PSD is more difficult to explain.

In the glaucoma group R^2 coefficients were generally smaller than in the group of normals. This is both expected and natural. Inter-individual field differences are of course larger among eyes with glaucoma than among normal eyes. Therefore, in glaucomatous eyes a proportionally smaller part of the pathological variation is caused by variation in perimetric reliability. It is obvious, however, that perimetric reliability significantly influences perimetric results also in abnormal eyes.

Table 3 shows that narrower limits of normality may be used for tests with good results at reliability testing than if results of reliability tests are not taken into account at all. Thus in 'reliable' field charts pathological field loss may be

detected at an earlier stage than in 'non-reliable' charts If, however, narrower normal limits (and therefore more demanding requirements on reliability test results) are selected when limits of normality are calculated, an increasing percentage of measured field tests will not meet these stricter criteria. This percentage increases particularly rapidly in the glaucoma group, largely due to the increment of FN with increasing field defects Obviously a compromise must be made giving reasonable narrow prediction limits without excluding a large part of normal and pathological fields from analysis. Even an arbitrary compromise requiring only reasonable results at reliability testing can narrow the limits of normality considerably thus facilitating early detection of pathological field loss.

Further studies of results of reliability testing in normal and pathological eyes should make it possible to use results of such tests more efficiently in visual field interpretation It is e g. conceivable to correct individual threshold estimates according to the results obtained at reliability testing.

References

1 Brownlee KA: Statistical theory and methodology in science and engineering, p 299 Wiley, New York, 1965

2 Flammer J, Drance SM, Zulauf M Differential light threshold Short- and long-term fluctuation in patients with glaucoma, normal controls and patients with suspected glaucoma Arch Ophthalmol 102: 704–705 (1984)

3 Heijl A: The Humphrey Field Analyzer In: Drance SM, Anderson D (eds) Automatic perimetry in glaucoma A practical guide, pp 43–54 Grune & Stratton, Orlando, 1985

4 Heijl A, Krakau CET: An automatic static perimeter Design and pilot study Acta Ophthalmol 53: 293–310 (1975)

5 Heijl A, Lindgren G, Olsson J: A package for the statistical analysis of visual fields Doc Ophthalmol Proc Series: 00: 153–168 (this volume) (1987)

6 Heijl A, Lindgren G, Olsson J: Variability of computerized threshold measurements across the central field in a normal population Doc Ophthalmol Proc Series 00: 91 (this volume) (1987)

7 Morrison DF: Multivariate statistical methods, p 120 McGraw-Hill, New York, 1967

Authors' addresses:
Anders Heijl, MD,
Dept of Ophthalmology, University of Lund, Malmö General Hospital, S-21401 Malmö, Sweden

Georg Lindgren, PhD, Jonny Olsson MSc,
Dept of Mathematical Statistics, University of Lund, PO Box 118, S-22100 Lund, Sweden

IX.8 Experience with the reliability parameters of the Octopus automated perimeter

F. JENNI and J FLAMMER
Berne, Switzerland

Abstract

To evaluate the reliability of automated perimetry results, fluctuation is one of the most important factors. This fluctuation is, however, influenced not only by the cooperation of the patient but also by the disease state and the defect depth. To estimate patient cooperation, an additional test is necessary In Octopus perimetry, this has always been performed with the so-called catch trials. In a large series of visual fields, we analyzed the rates of false responses in catch trials and the factors influencing them.

Introduction

The examination programs of the Octopus automated perimeter system contain catch trials which occur during the examination. The number of catch trials per examination is set to approximately 10% of the total number of questions (5% negative and 5% positive, if possible). A positive catch trial is a stimulus presented with 51 dB (0.008 asb), invisible for the patient. If the patient responds (i.e as if seen), a false positive answer is recorded Such catch trials are possible in all parts of the visual field [3]. Negative catch trials on the other hand are only made in those regions of the visual field where the examination has already proved that a minimal sensitivity of 5 dB (315 asb) exists. Negative catch trials are presented with 0 dB (= max luminance). If the patient does not respond a false negative answer is recorded [3]

At the end of an examination, false negative and false positive answers are printed out as percentual rates of the catch trials and also as absolute values In the G1 glaucoma program [1] a new parameter called RF is added. It represents the sum of the false responses as percentual rate of the total number of catch trials, negative and positive together. The rate of false responses to the catch trials is a measure of patient reliability and thereby provides information about the quality of the examination.

Materials

The influence of age and mean sensitivity on the rate of false responses was investigated by means of 756 normal and 130 glaucomatous visual fields measured with the OCTOPUS G1 glaucoma program [1].

Results

In the normal fields the rate of false negative responses (RFN) was $0.28\% \pm 1.22$, the rate of false positive responses (RFP) was $3.1\% \pm 4.59$. For the RF an average value of $1.81\% \pm 2.6$ was found. The rate of false answers in normals did not increase with increasing age Surprisingly, with the RFP, the reliability appeared to improve with age of the subject. The actual numerical values are presented in Table 1. In pathological visual fields, a fairly strong negative relationship was found between the mean sensitivity and RFN ($R = 0.62$, $p = 0.0001$), while RFP displayed no particular tendency. Moreover, in a comparison, normal and pathological visual fields displayed roughly the same behaviour for the RFP. For the RFN, on the other hand, in pathological fields, the average value increased considerably.

Discussion

For more than a decade, the catch trials have proven their usefulness and worth for clinical routine. The present analysis should help in the interpretation of catch trial results as obtained with the OCTOPUS automated perimeter. Both RFP and RFN are not age related. This contradicts the widely held assumption that older patients do less well in automated perimetry.

In normals the rate of false positive responses is clearly higher than the rate of false negative responses. The rate of false negative responses increases, however,

Table 1

Age	Mean values			Number of visual fields
	RF	RFN	RFP	
20	2 11	0 17 ± 0 84	4 04 ± 4 60	76
30	2 02	0 28 ± 1 26	3 76 ± 5 43	237
40	1 56	0 22 ± 0 99	2 90 ± 3 82	122
50	1 33	0 21 ± 0 99	2 46 ± 3 83	149
60	1 43	0 41 ± 1 69	2 45 ± 4 48	135
70	1 51	0 43 ± 1 25	2 59 ± 3 34	37

as the mean sensitivity is decreased. As a 'rule of thumb' for clinical practice, a rate of false responses exceeding 15% cannot be tolerated unless we are dealing with an advanced defect where a larger rate can be expected and accepted. Further details of this study will be published elsewhere [2].

Acknowledgements

References

1 Flammer J, Jenni F, Bebie H, Keller B: The Octopus glaucoma program G1 Glaucoma 9, 67 (1987)
2 Jenni F, Flammer J: Factors influencing the reliability parameters (in preparation)
3 Octopus manual model 201, Ch 3 4 Interzeag AG, Schlieren, Switzerland

Author's address:
Piof Dr J Flammer,
University Eye Clinic,
Insel Hospital,
CH-3010 Berne, Switzerland

IX.9 Primate arcuate nerve fiber bundle anatomy

D.S MINCKLER and T. OGDEN

Abstract

The primary injury in glaucoma probably involves axonal transport block in the lamina cribrosa. Topographic correlations between visual field damage and axon injury in the lamina are dependent on anatomical dispersion of ascending axons. Lateral and vertical dispersion of axons is partially due to intermixing of axon bundles in the peripapillary retina and is accentuated by further intermixing in the nerve head. Morphometric studies of nerve fiber layer axons demonstrate mirror image symmetry in fiber populations in arcuate bundles between paired normal eyes, but with a preponderance of large axons in the inferior relative to the superior bundles. In glaucomatous monkey eyes, large axons in arcuate bundles are especially vulnerable to injury. Dispersion of axons and selective vulnerability of subpopulations of axons are potentially important factors in the pathogenesis of glaucomatous visual field defects

Introduction

Visual field damage in glaucoma often evolves to include arcuate defects correlating with damage to ganglion cell axons between ten and twenty degrees of visual angle from fixation [1, 6] These typical scotomas encountered in moderately advanced disease often expand both peripherally and centrally toward end-stage fields. Expanding arcuate scotomas usually correlate with typical optic disc changes and are widely accepted as resulting from progressive damage in the lamina cribrosa, especially in the polar regions of the optic nerve head [8, 21, 22] Arcuate scotomas are more likely to be in the visual field superiorly corresponding to the anatomical array of ganglion cell projections into the inferior polar portion of the optic nerve. Typical arcuate scotomas may be preceded by retinal dysfunctions, including generalized depression [2], alterations in short and long term fluctuations in quantitative perimetry [4, 25], decreases in contrast sen-

sitivity [1] decrease in macular function, including color vision and decreased eccentric visual acuity [19, 20]

This report summarizes new, quantitative studies of the axonal population in the arcuate portion of the nerve fiber layer of the monkey, and describes other anatomical features potentially relating to arcuate scotomas in man. Our studies suggest that relatively greater numbers of large diameter fibers are present inferiorly and that they have increased vulnerability to glaucomatous damage. Other features of the nerve fiber layer and optic nerve head may underlie some of the clinical variations in visual fields and define the limits of the anatomic correspondence between field and nerve damage.

Materials and methods

The new data summarized here were obtained from experimental studies of five normal adult male cynomologus monkeys and five additional animals with unilateral experimental glaucoma [9, 14] The methods used conform to the ARVO Resolution on the Use of Animals in Research. Eye pressures were obtained under thiopental anesthesia using a Perkins hand-held applanation tonometer. All eyes were examined before use under atropine dilation to ensure the absence of pre-existing disease by indirect ophthalmoscopy, fundus photography, and fluorescein angiography.

Retinal tissues were obtained by enucleation under general anesthesia, immediate hemisection of the eye and immersion fixation of the posterior portion of the globe. The fixative, cold 1% glutaraldehyde and 1% osmium tetroxide, was replaced after five minutes with fresh solution and changed to Karnovsky's dialdehyde solution after thirty minutes. Retinal and choroidal flat mounts were obtained after careful dissection in the latter solution Tissues were dehydrated in graded alcohols and propylene oxide and embedded as flat mounts in plastic. Marking holes were placed in the disc and fovea with glass needles prior to osmification and were easily visible for subsequent orientation of blocks.

The retinas of the first animal were studied in great detail to determine the most efficient method for study of additional eyes. These retinas were studied at fifteen locations between the vertical meridian through the fovea and the optic disc edge along the superior and inferior arcuate ridges. Based on these initial samplings, subsequent retinas were studied only at four locations along the superior and inferior arcuate ridges.

The blocks of plastic containing the flat mounts were inscribed using the disc and foveal marks as guides to define the arcuate ridges and specific areas for study (Fig. 1). Target blocks were removed, re-mounted to ensure accurate cross sectioning of the nerve fiber layer and sectioned at one micron for light microscopic study The crest or thickest portion of the arcuate ridge was identified and the block trimmed for ultrathin sectioning centered on the same area (Fig. 2).
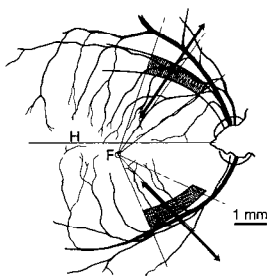
Figure 1 Diagrammatic illustration of the tissue blocking method for maintaining orientation of samples The flat, plastic embedded retina was sub-divided using disc and foveal marks as guides into upper and lower quadrants Insofar as the area sampled was equidistant from the fovea, its fiber spectra were the same The shaded area indicates the region sampled to localize the arcuate ridge

Thin sections were mounted on slot grids, stained with uranyl acetate and lead citrate and examined with a Zeiss 10B electron microscope.

Montage electron micrographs, including the entire nerve fiber layer, were prepared using a magnification of 12,500 diameters The largest montage was four by twelve feet when completed and corresponded to approximately a 0.5 millimeter sampling across the arcuate ridge. The nerve fiber layer montage was divided into square grids eleven inches on each side, corresponding to the active area on the digitizing tablet.

The diameter of every axon profile in a square chosen was measured without regard to axon bundle boundaries. All axon profiles were round or slightly elliptical. Pen marks were made on each measured profile as measurements proceeded. The technicians were trained to select the smallest diameter of the profile for digitization and to consistently use the outer membrane edge as the axon boundary. Every fiber through the entire thickness of the nerve fiber layer was sampled in each montage, but the number of squares measured varied with the location of the montage and the thickness of the nerve fiber layer. During the
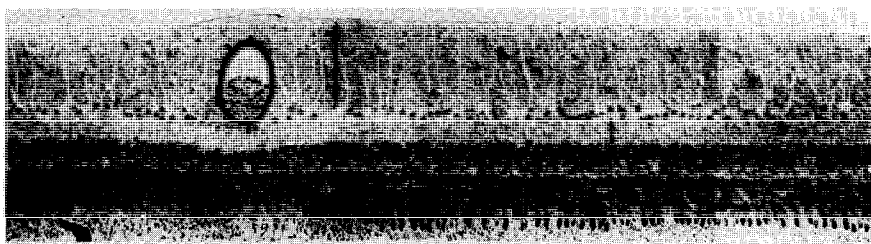
Figure 2 Photomicrograph of the arcuate ridge crest (double arrow) from the shaded area in Figure 1 The ganglion cell layer is a single cell in thickness in this area and the nerve fiber layer thinner to either side Glaucomatous eye demonstrated collapse of the nerve fiber layer relative to control eyes (Toluidine blue, ×100)
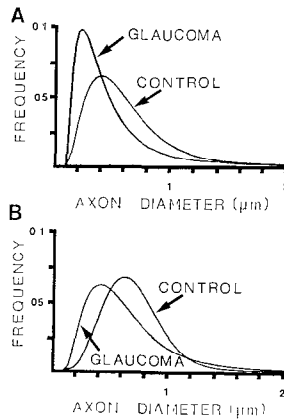
Figure 3 Weibull curves representing the relative frequency of fibers of different sizes in the arcuate ridges of a normal and of a glaucomatous eye Comparisons between normotensive and glaucomatous eyes of the same animal are illustrated for upper and lower arcuate ridges The shift in population fiber spectra indicates preferential loss of large diameter fibers in the glaucomatous eye, especially inferiorly

course of developing the measuring technique, some montages were re-measured to judge technician consistency and data accuracy. Software converted the diameter line length to microns and stored the X/Y coordinates of its center. Near the disc, a square contained about 1000 profiles. Because of the thickness of the nerve fiber layer (up to 100 microns), digitization of the entire thickness of the peripapillary nerve fiber layer required about one week of entry time. Peripheral retina contained fewer squares and could be digitized in a few hours.

Studies of the normal retinal tissues in these experiments involved analysis of 54 montages and digitization of 1.5 million axon profiles [14]. Data reduction consisted of fiber spectrum histogram plots fit to log-Weibull distributions to enable comparison of fiber spectra from different locations (Fig. 3). The method of curve fitting is described elsewhere [17, 18], as is its application to retinal nerve fiber populations [15]. The log-Weibull curves better describe a skew population than do histograms, which are dominated by the modal value and often show marked irregularity in the overall population profile. Systematic variation of the shape parameters in a series of Weibull curves are likely to reveal subtle trends in population statistics, often obscured by noise in histograms.

Five sets of eyes from five additional animals were also studied after inducing experimental glaucoma in one eye of each animal (Fig. 3) [9]. Glaucoma was produced using argon laser pangoniophotocoagulation [5] and the animals were followed clinically for several weeks before sacrifice to ensure that disc changes indicating optic nerve injury typical of glaucoma had occurred Tissue recovery and processing were identical to that described above. Measurements in the glaucomatous eyes were compared only to measurements in mirror image areas
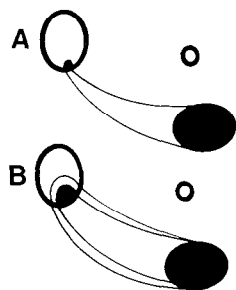
Figure 4 Diagrammatic illustrations of the traditional (A) and our modified (B) projection of nerve fibers into the disc from an area of retina corresponding to 6 degrees of visual angle in the arcuate zone between 10 and 20 degrees of visual angle from fixation The primary route of projection (inner lines) narrows approaching the disc (B), but outlying fibers (outer lines) considerably expand the actual projection area The fiber population projecting into the disc from the 6 degree retinal area probably disperses over at least one-quarter of the nerve head at the level of the lamina

from the opposite normotensive eye of the same animal (Fig. 3)

Besides the above new quantitative measurements, materials from previous experiments relevant to furthering our understanding of arcuate scotomas are also summarized herein (Fig 4).

Results

With great care taken to assure anatomical symmetry in sample position, corresponding portions of the nerve fiber layer in companion eyes were symmetrical in nerve fiber diameter spectra. Superior and inferior arcuate ridges in the same eye had significant differences in fiber spectra, and variations among different animals was also very significant.

Variations across a montage were not significant provided the samples were all from the arcuate ridge (Fig. 1). If the sample included portions of the central or peripheral slopes of the ridge, disproportionate numbers of small or large fibers were found. Errors in register along the arcuate ridge were relatively more likely adjacent to the disc, where the packing of fibers was most dense. Variations due to sampling error were minimized by concentrating measurements where the arcuate ridge was best defined (Fig 1), and values from these locations were emphasized in final comparisons between superior and inferior ridges, between eyes and among animals. Comparisons of samples obtained from multiple sites along the same ridge indicated that the diameter spectra of the population of fibers remained unchanged as the disc was approached, even though the total number of fibers in a given bundle and the nerve fiber layer thickness increased by as much as ten times The nerve fiber spectra of upper and lower arcuate bundles from the same eye consistently demonstrated more large fibers in the lower bundles (Fig. 3).

Histological study of eyes with laser-induced glaucoma, using the opposite normotensive eye as a control, demonstrated thinning of the nerve fiber layer along the arcuate ridge. Quantitative studies of the fiber spectra in glaucomatous eyes compared to the companion normal eye consistently indicated a shift toward smaller fibers in the eye with glaucoma (Fig. 3).

Discussion

Quantitative study of axon fiber spectra in the normal monkey retina indicated that only the opposite eye of the same animal could be used as a control to detect subtle damage to the arcuate nerve fibers in early glaucomatous injury. Assuming the same symmetry is true of man, the use of one eye as a clinical control for the other seems valid. However, the large variations between eyes of different animals should make us cautious about generalizing with regard to the significance of quantitative measurements of disc tissues among humans. Additionally, assuming that monkey and man are similar, the discrepancy between upper and lower arcuate bundles in the normal eye [14] may provide an anatomical basis for the relatively greater vulnerability of the superior field in glaucoma. The relatively greater population of large axons in the inferior arcuate bundles, and our suspicion that they are especially vulnerable to pressure-induced injury, also makes the large axons prime candidates as indicators of early injury in glaucoma. The apparent heightened sensitivity of large diameter axons to glaucomatous injury must also have implications as to the pathogenesis of the injury in the nerve head [9]. Evidence supporting the greater vulnerability of large diameter axons in glaucoma has been reported previously from studies of the lateral geniculate body in chronic glaucoma in monkeys [23].

In addition to the possible vulnerability of large diameter axons to glaucomatous injury, other anatomical features of the nerve fiber layer and optic nerve head have implications for the development of arcuate scotomas. Significant vertical and lateral dispersion of ganglion cell axons in the peripapillary retina and optic disc has been described. Axons from the peripheral retina have been found in recent studies to travel on the surface of the nerve fiber layer. These peripheral axons cross over axons of peripapillary origin to take a position on the edge of the optic nerve [12]. These peripapillary ganglion cells project their axons through those from more peripheral cells to a superficial position at the disc margin and a more central position in the optic disc [10]. Inter-species variation may account for discrepancies in findings related to the layering of nerve fibers in the retina and peripapillary tissues [14, 24]. Regardless of the degree of dispersion of axons from a given retinal locale at the disc margin, further dispersion clearly occurs during transit of the nerve head.

Individual axons meander within bundles of axons and the bundles themselves branch extensively as they course through the pre-laminar and laminar regions [3,

9, 11]. Studies in the same animal used for the above experiments indicated that degenerating fibers from a single 100 micron argon laser burn in the retina were dispersed over an entire quadrant of the optic nerve head [25].

Based on present information, we can speculate that a range of injury from diffuse damage over an entire quadrant to total destruction of less than a quadrant of the laminar nerve could produce an arcuate scotoma involving approximately six degrees of visual angle (Fig. 4). Such a scotoma would correspond roughly to the minimum defect detectable with modern quantitative perimeters as commonly employed. Retinal and optic nerve head dispersion of ganglion cell axons in the primate necessarily limit the resolution of such correlations, even without consideration of physiological factors

References

1　Drance S: The early structural and functional disturbances of chronic open-angle glaucoma Ophthalmol 42: 852–857 (1985)
2　Drance S: Visual field defects In: Duane TD, Jaeger EA (eds) Clinical ophthalmology, Vol 3, Ch 49 Harper and Row, Philadelphia, 1985
3　Ogden T, Duggan J, Danly K, Wilcox M and Minckler DS: Morphometry of nerve fiber bundle pores in the optic nerve head of the human Submitted to Am J Ophthalmol 1987
4　Flammer J, Drance SM, Zulauf M: Differential light threshold: short- and long-term fluctuation in patients with glaucoma, normal controls, and patients with suspected glaucoma Arch Ophthalmol 102: 704–706 (1984)
5　Gaasterland D, Kupfer C: Experimental glaucoma in the rhesus monkey Invest Ophthalmol Vis Sci 13: 455–457 (1974)
6　Kolker AE, Hetherington J Jr: Becker-Shaffer's diagnosis and therapy of the glaucomas (5th ed), pp 141–183 CV Mosby, St Louis, 1983
7　Marmion VJ: A comparison of contrast sensitivity function and field loss in glaucoma In: Heijl A, Greve EL (eds) Doc Ophthalmol Proc Series 42, pp 443–446 Dr W Junk, Dordrecht, 1985
8　Minckler DS, Bunt AH, Johanson GW: Orthograde and retrograde axoplasmic transport during acute ocular hypertension in the monkey Invest Ophthalmol Vis Sci 16: 426–441 (1977)
9　Minckler DS, Ogden TE: Experimental glaucoma in the primate: selective loss of larger nerve fibers In preparation, 1987
10　Minckler DS: The organization of nerve fiber bundles in the primate optic nerve head Arch Ophthalmol 98: 1630–1636 (1980)
11　Minckler DS: Correlations between anatomic features and axonal transport in primate optic nerve head Am Ophthalmol Soc Thesis, submitted as partial fulfillment of membership requirements, April 1986
12　Ogden TE: Nerve fiber layer of the macaque retina: retinotopic organization Invest Ophthalmol Vis Sci 24: 85–98 (1983)
13　Ogden TE: Nerve fiber layer of the owl monkey retina: retinotopic organization Invest Ophthalmol Vis Sci 24: 265–269 (1983)
14　Ogden TE, Minckler DS: Nerve fiber layer of the primate retina: size spectra of the arcuate fibers Submitted to Inv Ophthalmol Vis Sci 1987
15　Ogden TE: Nerve fiber layer of the primate retina: morphometric analysis Invest Ophthalmol Vis Sci 25: 19–29 (1984)
16　Ogden TE: The nerve-fiber layer of the primate retina: an autoradiographic study Invest Ophthalmol Vis Sci 13: 95–100 (1974)

17 Oyster CW, Takahashi ES, Hurst DC: Density, soma size, and regional distribution of rabbit retinal ganglion cells J Neurosci 1: 1331–1346 (1981)

18 Oyster CW, Takahashi ES, Hurst DC: Analysis of neuronal soma size distributions J Neurosci Methods 6: 311–326 (1982)

19 Phelps CD, Blondeau P, Carney B: Acuity perimetry: a sensitive test for the detection of glaucomatous optic nerve damage In: Heijl A, Greve EL (eds) Doc Ophthalmol Proc Series 42, pp 359–363 Dr W Junk, Dordrecht, 1985

20 Polizzi A, Gandolfo E, Grillo N, Calabria G: Early macular damage in glaucoma and suspected glaucoma patients In: Heijl A, Greve EL (eds) Doc Ophthalmol Proc Series 42, pp 453–456 Dr W Junk, Dordrecht, 1985

21 Quigley HA, Green WR: The histology of human glaucoma cupping and optic nerve damage: clinicopathologic correlation in 21 eyes Ophthalmology 86: 1803–1827 (1979)

22 Quigley HA, Addicks EM, Green WR, Maumenee AE: Optic nerve damage in human glaucoma II The site of injury and susceptibility to damage Arch Ophthalmol 99: 635–649 (1981)

23 Quigley HA, Hendrickson A: Personal communication

24 Radius RL, Anderson DR: The course of axons through the retina and optic nerve head Arch Ophthalmol 97: 1154–1158 (1979)

25 Ryu DT, Minckler DS: The retinal nerve fibers in the primate optic nervehead Proc Jap Acad 59: (B) 328 (1983)

26 Sturmer J, Gloor JS, Tobler HJ The glaucomatous visual field in detail as revealed by the Octopus F-programs In: Heijl A, Greve EL (eds) Doc Ophthalmol Proc Series 42, pp 391–401 Dr W Junk, Dordrecht, 1985

IX.10 A new numerical representation of the visual field in cases of chiasmal tumor

R. HARUTA, K. KANI, O. MIMURA, M SHIMO-OKU, K SAKATANI and T. OHTA
Hyogo and Osaka, Japan

Abstract

We have developed a new numerical representation of the visual field, in which the visual field is shown by the equation of retinal ganglion cell count multiplied by retinal sensitivity. This representation also presents the visual field defects directly in relation to the visual cortex. The relationship between the visual field defects shown in this representation and various neuroradiological factors were studied in case of chiasmal tumor using multivariate analysis. The preoperative visual field was found to be influenced significantly by the shape of the tumor, the presence A1 (A1 portion of anterior cerebral artery) elevation, and the depth of the sella turcica; the postoperative visual field was influenced by the depth of the sella turcica and by the height and transverse diameter of the tumor

Introduction

The term visual field refers essentially to the photosensitivity of a certain retinal locus. The photosensitivity of the retinal locus is projected to the striate cortex as the output of excitation of retinal ganglion cells. Great interest has arisen recently regarding the functional role of the density of retinal ganglion cells with respect to the visual field However, conventional perimetric charts are not suitable for a quantitative estimation of the visual field from the viewpoint of retinal ganglion cell density. The principal difficulty till quite recently has been the lack of a formula adequate for representing the relationship between retinal ganglion cell density and eccentricity from the fovea In 1977 Drasdo calculated the neural representation of visual space and formulated an equation expressing the number and density of human retinal ganglion cells [1]

Our new perimetric chart based on Drasdo's formula for estimating the visual field taking into account the retinal ganglion cell density (Figure 1) was first reported in 1983 [3]. In this study, our new numerical representation of the visual
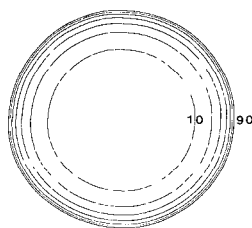
Figure 1 Our new perimetric chart in which the area represents the count of retinal ganglion cells

field was applied to evaluate the relationship between visual field defects and various neuroradiological factors in patients with chiasmal tumor.

Subjects and methods

Thirty-seven patients with a chiasmal tumor who were proved to have good central fixation were examined by kinetic perimetry using Goldmann's perimeter and who underwent long-term follow-up. They consisted of 29 cases with pituitary adenoma, 4 cases of meningioma and 4 cases of craniopharyngioma. The isopters on Goldmann's perimeter were converted to the new isopters of our chart based on Drasdo's formula using a SORD M-343 computer and a digitizer (Bit Pad One). The numerical value of the visual field was calculated from the visual island in both Goldmann's scale and our new scale. These calculations have been reported in detail elsewhere [3].

Then the relationship between the numerical value of the visual island and the following neuroradiological factors were studied using multivariate analysis: the size of the tumor, the size of the sella turcica and the shape of the tumor determined by CT-image, the presence of a double floor or pocket formation detected by plain skull X-ray photography; and the presence of A1 elevation, determined by carotid angiography.

Results

After surgical removal of the chiasmal tumor, most cases demonstrated more or less improvement of the visual field. The numerical value of the postoperative visual field was generally greater than that of the preoperative visual field in both Goldmann's and our scales. In a few cases, however, the results indicated on our scale were opposite to those on Goldmann's scale. For example, Figures 2 and 3 show this discrepancy in perimeter charts of a case of pituitary adenoma. Figure 2 shows the temporal visual field defects at the time of the first examination (Before surgical operation). The numerical value was 6.6×10^{-2} on Goldmann's scale and

Preoperation

Ordinary scale   Our scale

V-4-e
I-4-e
I-3-e
I-2-e

Numerical value

6.6×10^{-2} 0.68×10^{6}
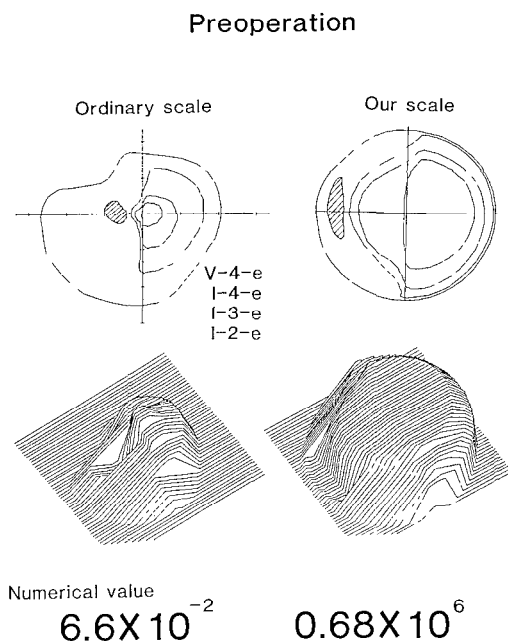
Figure 2 Two representations, the conventional one and ours, of the preoperative visual field in a pituitary adenoma case The upper left figure represents the ordinary scale, the upper right figure represents the same visual field converted to our scale The lower figures are the respective three-dimensional computer graphics representations and numerical values

0.68×10^{6} on our scale. Figure 3 shows the visual field defects after surgical operation. The numerical value on Goldmann's scale was 7.8×10^{-2}, greater than that calculated at the time of the first examination, whereas the numerical value on our scale was 0.51×10^{6}, slightly less than that calculated at the time of the first examination.

Figure 4 shows the relationship between the numerical values indicated on our scale for the preoperative and postoperative visual fields of patients who underwent long-term follow-up. No significant difference in the values of the visual fields was noticed between patients whose operations used the intracranial approach and those whose operations used the transsphenoidal approach. When the value of the preoperative visual field was less than 0.7×10^{6}, a value indicative of total temporal hemianopsia for all stimuli, the numerical value of postoperative visual field never reached 1.5×10^{6}, the average value of normal visual fields of patients examined in our clinic. On the other hand, in about one-third of patients with a preoperative value greater than 0.7×10^{6}, the visual field was restored to normal, resulting in values of 1.5×10^{6} and higher.

Multivariate analysis demonstrated that the preoperative visual field was influenced significantly by the shape of the tumor, the presence of A1 elevation, and

Postoperation

Ordinary scale   Our scale

V-4-e
I-4-e
I-3-e
I-3-c

Numerical value

$$7.8 \times 10^{-2} \qquad 0.51 \times 10^{6}$$
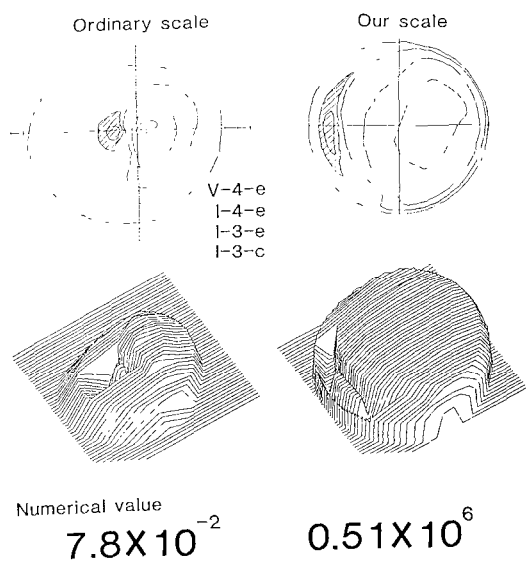
Figure 3 The conventional representation and our representation of the postoperative visual field in the same case shown in Fig 2

Numerical value
of visual field
$\times 10^6$

● Intracranial approach
○ Transsphenoidal approach

Postoperation

2.0

1.5

1 0

0.5

0   0.5   1 0   1.5   Numerical value
                                              of visual field
              Preoperation $\times 10^6$
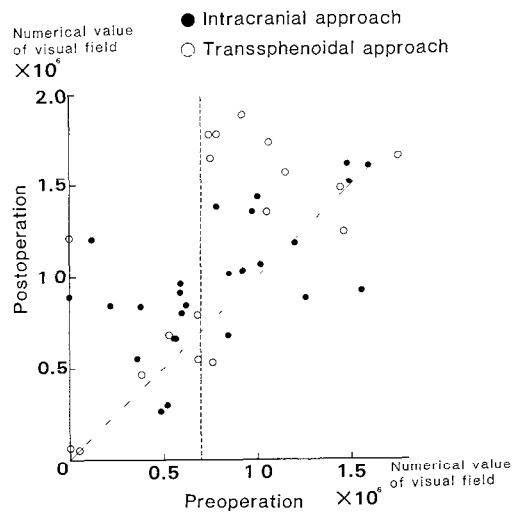
Figure 4 The relationship between the numerical values of the preoperative and postoperative visual fields on our scale The dashed line shows the numerical value calculated in cases of total temporal hemianopsia for all stimuli

the depth of the sella turcica and that the postoperative visual field was influenced by the depth of the sella turcica and by the height and transverse diameter of the tumor

Discussion

Studies of the effects of surgical removal of a chiasmal tumor on the visual field have long been of interest in neurosurgery and neuro-ophthalmology [2, 4]. Numerous reports have demonstrated the effectiveness of surgery for the improvement of the visual field, but extensive evaluation of neuroradiological factors affecting changes in the visual field is lacking. We think that the difficulty in evaluating these factors is due primarily to the method of estimating the visual field Conventional perimetry does not reflect the cortical magnification factor in their consideration of the anatomy of the central visual pathway; one degree of arc in the visual space does not correspond to the extent of the striate cortex in millmeters-that is the small actual importance of a depression in the central vision is likely to be easily undervaluated against less important but more noticeable changes in the peripheral vision.

Various studies emphasizing the central visual field have been performed. These studies, however, have neither anatomical nor physiological bases We developed a new perimetric chart representing the retinal ganglion cell density based on Drasdo's equation [3] Each ganglion cell, regardless of its retinal position, affects a specific area of the striate cortex. Consequently, an area in our chart directly represents a definite cortical area In this chart the isopters are drawn using a computer program in which the volume of the visual island represents the numerical value of the whole visual field. With this chart we can easily estimate the temporal change of a visual field and the influence of neuroradiological factors.

References

1 Drasdo N: The representation of visual space Nature 266: 544–556 (1977)
2 Findlay G, McFadzean RM, Teasdale G: Recovery of vision following treatment of pituitary tumors; Application of a new system of assessment to patients treated by transsphenoidal operation Acta Neurochir 68: 175–186 (1983)
3 Haruta R, Kani K, Inui T: A new numerical representation of the visual field in regard to the retinal ganglion cell density Doc Ophthalmol Proc Series 42: 131–136 (1983)
4 Lennerstrand G: Visual recovery after treatment for pituitary adenoma Acta Ophthalmol 61: 1104–1117 (1983)

Authors' addresses:
Ryugo Haruta, Kazutaka Kani, Osamu Mimura, Masashi Shimo-Oku,
Dept of Ophthalmology, Hyogo College of Medicine, 1-1, Mukogawa-cho, Nishinomiya, Japan, 663

Kaoru Sakatani, Tomio Ohta,
Dept of Neurosurgery, Osaka Medical College, Japan

IX.11 Pituitary adenomas with ocular manifestations: incidence of cases and clinical findings 1946–1984

H. BYNKE
Lund, Sweden

Abstract*

Originally, visual dysfunction constituted the main indication for treatment of pituitary adenomas, but today an increasing number of adenomas with isolated endocrine dysfunction are subjected to treatment Hence, some authors have argued that the incidence of large adenomas with visual dysfunction is declining and that the diagnostic role of the ophthalmologists is diminishing.

In the University Hospital, Lund, Sweden, 339 new patients with pituitary adenomas and visual dysfunction were subjected to surgical treatment in 1946 through 1984. Surprisingly, it was found that the mean annual incidence of treated cases had increased gradually from 4.07 per million inhabitants in 1946–55 to 6.93 in 1976–84, *i.e.* by no less than 70%.

Consecutive cases treated during different periods were compared. The mean duration of the visual impairment before treatment decreased from about 3 years before 1961 to about 10 months after 1970. In addition, visual function before and after treatment was significantly better in patients treated during late periods than during early periods. For example, the preoperative bitemporal hemianopsia was complete in 44% of cases treated before 1961 but only in 13% of cases treated after 1970. Thus, the majority of the patients are now diagnosed and treated at an earlier stage than before, reflecting an expanding ophthalmic service. Modern endocrinological tools played a minor role, since 52% of the patients lacked endocrine symptoms and many others suppressed these symptoms when they sought medical advice for visual complaints.

As a matter of fact, small pituitary adenomas with isolated endocrine symptoms should not be regarded as precursors of large adenomas with visual dysfunction. On the contrary, these groups constitute more or less separate entities

In the light of this study it seems unlikely that the diagnostic role of the ophthalmologists will diminish in the future.

Author's address:
Dr Hans Bynke,
University Eye Clinic,
S-221 85 Lund, Sweden

IX.12 Computerized perimetry in neuro-ophthalmlogy: comparison of different test patterns by an 'information index'

J. WEBER
Cologne, F.R.G.

Abstract

121 visual fields of 67 patients with chiasmal and suprageniculate lesions of the visual pathway were examined with the Humphrey Field Analyzer, using a 6° or 4.2° pattern in the 30° central field Different patterns were simulated and the informational gain by additional points was evaluated For detection, the mid periphery (20°–30°) was most important, for other additional information the center was more effective. An equally distributed 6° pattern seems to be optimal for detection, a condensed 4.2° pattern in the center (<10°) useful for assessment and follow-up

Introduction

Suprageniculate lesions of the visual pathway mainly produce absolute scotomata [8]. They are located in the center as well as in the mid peripheral area of the visual field, but are somewhat deeper in the area of 15°–20° eccentricity [1]. The chiasmal lesions more often show slight depressions [17] and relative scotomata [8]. 30% of them are atypical [7]. Although at the beginning the defect depth is greater and more progressive in the mid periphery (35°) [1], other authors find the earliest defects with kinetic methods in an area of 8°–12° eccentricity [4] and don't find isolated defects outside 30° with this diagnosis [15].

In automated static perimetry of neuro-ophthalmological cases strategy has an influence on the result [8, 16]. The second main factor of automated perimetry, the spatial resolution of the test point pattern, might have an influence as well. So far, an influence is only reported for glaucoma patients [5, 11, 12, 13, 14] This study wants to investigate the influence of patterns in cases of chiasmal and suprageniculate lesions of the visual pathway in order to give recommendations for the optimal pattern in this type of visual field loss

Methods

From the visual field chart records of the last 2 years (Oct. 1984 to Aug. 1986) all automatic visual fields of patients with chiasmal and suprageniculate lesions of the visual pathway were selected. Diseases or mainly involvement of the optic nerve were excluded, as well as ocular diseases with the possibility of field defects. 132 fields were found. All of them were central field tests (up to 30° eccentricity) with a paraaxial 6° or a 4.2° grid pattern and full threshold strategy on the Humphrey Field Analyzer 620 (30-2 and 30-1 central threshold tests), using Stimulus size 3.

After excluding those with bad fixation, correcting glass scotomata and sus-pected functional visual field constriction, 121 fields of 67 patients could be analyzed for this study Table 1 shows the diagnosis of these patients. 5 eyes of 3 patients were twice in the study, because the defect changed considerably due to deterioration or operation. 99 visual fields were pathological. Table 2 shows the types of defects. 50 of them were tested with a 4.2° pattern, 49 with a 6° pattern.

The defect* pattern of each field was reduced step by step to 6°, 8.5° and 12° grid patterns with a symmetric paraaxial geometry. This was performed by a simple deletion of points from the result, thus simulating the other patterns. Each grid

Table 1 The diagnosis of the 67 patients of this study

Diagnosis	n = 67
Tumors	50
– Pituitary tumors	21
– Other chiasmal tumors	21
– Other regions	8
Cerebro-vascular accidents	10
Trauma	4
Miscellaneous	3

Table 2 Frequency and type of visual field defects

Visual fields	n = 121
Normal	22
Pathological	99
– Heteronymous defects	39
– Homonymous defects	41
– Not classified	19

* The calculations were made by the Humphrey Field Analyzer according to the physiological shape of the hill of vision and individual central expected threshold (software version Dec 1985)

was compared to the next finer grid, evaluating the new information gained by the additional points. The occurrence of 'informational events' was counted separately for 3 areas, center (<10°), 'Bjerrum' (10°–20°) and mid periphery (20°–30°). According to an earlier study on glaucoma fields [13, 14], we distinguished 3 types of information:

- detection of a scotoma
- modification of size, number and extension
- refinement of representation

The criteria for detection are given in Table 3. Criteria for modification is the involvement or second scotoma in another quadrant of a significant change of size (at least 2 : 3 of 3 : 2). The criterion for refinement was the exceeding of a size of 5 defect points. In a few cases of extensive field loss we did not evaluate the size and extension of defects, but the size of the 'isle of vision' (sensitivity 10 dB or more) and its change. All criteria are similar to our previous study [13, 14] and illustrated in detail there.

For each step and area the 'informational events' were weighted according to their importance (detection = 3, modification = 2, refinement = 1) and summed up. Because the number of new points is very different (see Table 4), the sum was divided by this number. To transform the result into a predictive value and keep comparability of different groups, it was also devided by the number of pathological fields. A multiplication with 1000 produced handy figures The so-called 'information index' (Table 5) therefore represents the probability of new information per 1000 additional tested points in pathological fields As the testing of a point takes an definite time, the information index is also a benefit/time-relation.

Table 3 Criteria for the detection of a scotoma

Area	0°–10°	10°–20°	20°–30°
At least 1 defect point deeper than	9 dB	13 dB	18 dB
3 or more neighboured defect points deeper than	6 dB	9 dB	12 dB

Table 4 Number of new points in the specific areas and steps of pattern condensation In the step 12° → 8 5° there are no new points in the center

New points	Step		
	12°–>8 5°	8 5°–>6°	6°–>4 2°
Area			
0°–10°	–	8	8
10°–20°	4	8	28
20°–30°	8	24	36

Results

Table 6 gives the result of the information indices in the different areas, Fig. 1 shows the graphic representation. First, all areas show a decrease of the information index with increase of spatial resolution. The higher the density of a pattern is, the smaller is the chance of new information by additinal points. Second, the information indices are higher towards the center (except Bjerrum area and mid periphery in the 6°->4.2° step).

The number of false negative fields is given in Table 7 separate for the two groups. It shows two interesting facts: First, a 12° pattern (only consisting of 20 Pts.) would have missed 12 of 99 pathological fields (12%), meaning a remarkable sensitivity of 88%. And second, all of the pathological fields in the group examined with a 4.2° grid were already identified with the 6° pattern.

Table 5 The formula of the 'information index'

Information index
$$\frac{(3 \ D + 2 \ M + 1 \ R) \ 1000}{\text{no of path fields new points}}$$

D = detection   M = modification   R = refinement

Table 6 Information index in the specific areas and steps of pattern condensation For the step 6°->4 2° n = 50, for the other steps n = 99

Information index	Step		
	12°->8 5°	8 5°->6°	6°->4 2°
Area			
0°–10°	–	107 3	50 0
10°–20°	60 6	54 2	7 1
20°–30°	44 19	26 5	8 3

Table 7 False negative fields in different patterns

	6° group n = 49	4 2° group n = 50
12° pattern	7	5
8 5° pattern	5	4
6° pattern	0	0
4 2° pattern	–	0
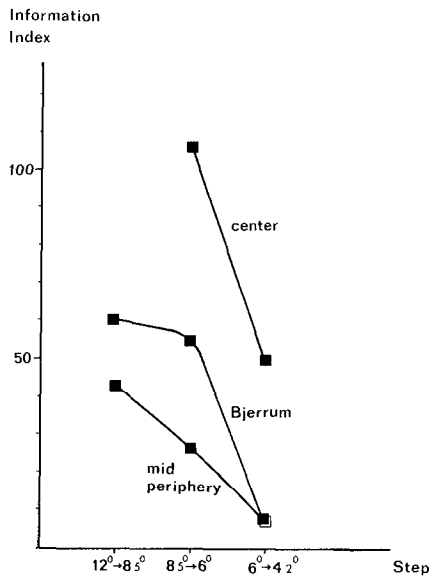
Figure 1 The information index as a function of spatial resolution

The 12 fields that appeared normal in the 12° grid were reviewed to see in which area the first defects were detected (Table 8). 8 of them were detected in the mid periphery (20°–30°), 1 in the center, and 3 in more than one area. −9 of these 12 fields where chiasmal tumors. In this group, 6 of the first defects appeared in the mid periphery, 1 in the center and 2 in more than 1 area.

Table 8 Detection of the 'first defect' (see also text)

pattern	area + detections		false negative
12° pattern			12
↓	mid peripheral	3	
8 5° pattern			9
	mid peripheral	5	
	mid periph + Bjerrum	1	
	mid per + Bje + cent	2	
	center	1	
6° pattern			0

Discussion

The decrease of the information index with increasing spatial resolution seems to be a general rule, as it was also found in glaucoma patients [13, 14]. But while the graph for glaucoma fields showed a smooth, exponential decrease, the graph for neurological fields shows a crooking in the 'Bjerrum' area. To proof whether the number of cases was to small and the crooking was an accidental variation, we calculated the information index also separately for the 6° and 4.2° group. These smaller groups ($n_1 = 49$, $n_2 = 50$) gave nearly identical figures meaning that the size of the whole group (n = 99) was sufficient So the crooking appears to be a characteristic of this diagnostic group.

In neuro-ophthalmological visual fields the information index values of the center are smaller than the central values in glaucoma. Those of the mid periphery are about double as high as in glaucoma cases, but still values are significantly increasing towards the center. In this small area important details, such as macular sparing or central quadrantanopsia, are detected and described only with few test points. This explains well the remarkable benefit/time-relation. But considering the detection of first defects it clearly comes out that the informational events in the center are mainly additional informations important for assessment and follow-up, but not vital for detection. Examination of the mid periphery was more effective for detection purposes. A higher resolution than 6° had no effect on detection in all 3 areas.

The area, where the first defect of chiasmal lesions appeared, coincides well with the area of the deepest defects of BYNKE's report [1]. But if the 'first detected defects' are defined as 'early defects', our findings differ from those of FRISÉN [4], who used kinetic perimetry and found the area between 8°–12° to be of greatest interest. This may be caused by fundamental differences between static and kinetic perimetry, which are even increased in pathological fields [2]. Concerning cerebral lesions, this phenomenon was described by RIDDOCH [9] and recently reported again [10] It is possible that this effect varies in different locations.

There are theoretical ways to set a mathematical relation between scotoma size and probability of detection [6, 3] However, we did not analyze the size of scotomata in our study, as most of them are not sharply cut, round, absolute scotomata, but relative and irregular defects. Therefore, detection is both a function of size and depth (see definition of our limits, Table 3) and calculation becomes nearly impossible.

Conclusions

There are three conclusions from this study:
– A regular 6° pattern seems to be sufficient to detect all field defects by chiasmal and suprageniculate lesions.

- A pattern with higher density in the center (<10°) can be useful to get additional information with minimal increase of test time.
- A coarser pattern than 6° in the mid periphery (20°–30°) increases the rate of false negatives considerably

This study is only valid for the central 30°. Although the importance of peripheral visual fields was questioned recently [15, 4], other results are possible if examination of the periphery is added. Careful investigations using threshold strategies for both central and peripheral visual fields should be carried out to answer this question.

Acknowledgement

References

1   Bynke H: A study of the depth of hemianopic field defects for optimizing computerized perimetry Neuro-Ophthalmology 4: 237–247 (1984)
2   Fankhauser F: Kinetische Perimetrie Ophthalmologica (Basel) 158: 406–418 (1969)
3   Fankhauser F, Bebie H: Threshold fluctuations, interpolations and spatial resolution in perimetry Doc Ophthal Proc Ser 19: 295–309 (1979)
4   Frisén L: The earliest visual field defects in mid-chiasmal compression Docum Ophthal Proc Ser 42: 191–195 (1985)
5   Gloor B, Stürmer J, Vökt B: Was hat die automatisierte Perimetrie mit dem Octopus für neue Kenntnisse über glaukomatöse Gesichtsfeldveränderungen gebracht? Klin Mbl Augenheilk 184: 249–253 (1984)
6   Greve EL: Static Perimetry Netherl Ophthal Soc, 166th Meeting, Eindhoven 1971 Ophthalmologica (Basel) 171: 26–38 (1975)
7   Greve EL, Raakman M: On atypical chiasmal visual field defects Doc Ophthal Proc Ser 14: 315–325 (1977)
8   Meienberg O, Mattle H, Jenni A, Flammer J: Quantitative versus semiquantitative perimetry in neurological disorders Docum Ophthal Proc Ser 42: 233–237 (1985)
9   Riddoch G: Dissociation in visual perception due to appreciation of movement Brain 40: 15–57 (1917)
10 Safran AB, Glaser JS: Statokinetic dissociation in lesions of the anterior visual pathways A reappraisal of the Riddoch phenomenon Arch Ophthal 98: 291–295 (1980)
11 Stürmer J: What do glaucomatous visual field really look like in fine-grid computerized profile perimetry? Dev Ophthal 12: 1–47 (1985)
12 Weber J, Dobek K: What is the most suitable grid for computer perimetry in glaucoma patients? Ophthalmologica (Basel) 192: 88–96 (1986)
13 Weber J, Kosel J: A new, glaucoma-specific test pattern, optimized by an 'Information Index' 25th Int Congr Ophthal, Rome, 4 –10 5 86
14 Weber J, Kosel J: Glaukomperimetrie – die Optimierung von Prüfpunktrastern mit einem Informationsindex Klin Mbl Augenheilk 189: 110–117 (1986)

15 Wirtschafter JD, Hard-Boberg AL, Coffman SM: Evaluating the usefulness in neuro-ophthalmology of visual field examinations peripherial to 30 degrees Trans Am Ophthal Soc 82: 329–357 (1984)
16 Wirtschafter JD, Coffman SM: Comparison of manual Goldmann and automated static visual fields using the Dicon 2000 perimeter in the detection of chiasmal tumors Ann Ophthal 16: 733–741 (1984)
17 Younge BR: Computerized perimetry in neuro-ophthalmology In: Whalen WR, Spaeth GL (eds) Computerized visual fields, pp 241–276 Slack, Grove, 1985

Author's address:
Dr Jörg Weber,
Universitäts-Augenklinik,
Joseph-Stelzmann-Str 9,
D-5000 Köln 41, F R G

IX.13 Selective retests in automated perimetry: an experimental study for the evaluation of the effect of the regression towards the mean

C. RUTISHAUSER and J. FLAMMER
Berne, Switzerland

Abstract

Selective retests were compared to global retests using a large pool of visual fields measured with program JO on the Octopus automated perimeter. The results of this investigation are that in selective retests, the mean sensitivity (MS) is increased, while the number of pathological test locations (NP) is decreased To obtain as objective an impression as possible of a visual field, therefore, selective retests should be avoided. It is better to retest every test location or none

Introduction

In manual, as well as in automated perimetry, retests are often performed at those test locations which are out of the expected range. Although this seems to be very reasonable, such an approach is subject to a statistical bias which is called 'regression toward the mean'.

It was Sir Francis Galton who, in his studies of hereditary traits in the nineteenth century, first pointed out the apparent regression toward the mean in the prediction of natural characteristics [4]. Regression toward the mean designates the phenomenon that, for example, on the average very tall fathers tend to have sons who are smaller than they are, and, on the other hand, very small fathers tend to have sons who exceed them in size With respect to visual field measurements, this means that in retesting outcomes which lie out of the normal range, the probability is high that in the retest they will be closer to normal. The purpose of this study was to compare the effects of global retesting with those of selective retests, in order to examine how the regression toward the mean influences visual field outcomes obtained with retests at selected test locations only

Material and methods

For this analysis, 1885 visual fields measured with the Octopus glaucoma program JO were used [1, 5]. This program measures every test location twice, once in an initial phase, and then again in a second one. The visual field is examined out to an eccentricity of 26 degrees. In order to simulate selective retests, the measured values of the second phase were taken into account only at those test locations with pathological values in the first measurement phase. For the other test locations, the values of the first phase were retained. Pathological values were defined as lying more than 6 dB below the age-corrected normal values. The second phase as measured by the program JO represents a global retest.

The differences in mean sensitivity (MS) and the number of pathological test locations (NP) between the second and the first phase were calculated in global as well as in selective retests.

In order to compare the effects of selective retests in normal and in pathological visual fields, pathological visual fields were selected with the help of the visual field indices [2], using the following rule: mean deviation (MD) >3 and corrected loss variation (CLV) >6 and short-term fluctuation (SF) >2. If all the indices were equal to or less than the values just indicated, the visual field was considered as being normal. The number of normals was 1138, the number of pathological visual fields was 189. There were 558 visual fields which were neither in the pahological nor in the normal group, because one or two of the indices lay in the normal range, while the remainder lay in the pathological one. In both groups, the differences of MS and NP between the first and the second phase were calculated in global as well as in selective retests

Results

The differences in MS between the second and the first phase were different between global and selective retests. A calculation of the means of these differences for normal and pathological visual fields makes evident that in the selective retests MS is higher than in the first phase (the difference between second and first phase is positive: MS = 0.03), whereas in the global retest MS is lower than in the first phase (difference negative. MS = -0 15). These effects are much stronger in pathological than in normal visual fields (selective retest: MS = 0.22, global retest: MS = -0.30). Both differences are highly significant (p = 0.0001).

The differences in NP between the second and the first phase between global and selective retests are considerable. A calculation of the means of these differences for normal and pathological visual fields shows that the number of pathological test locations in the selective retest approach is markedly lower than in the first phase (the difference between second and first phase is negative: NP = -0 35), and with the global retest method, it is somewhat higher than in the first

phase (difference positive NP = 0.21). These effects are, as for MS, much stronger in pathological than in normal visual fields (selective retest: NP = −4 14, global retest: NP = 0 38). The differences between global and selective retests are highly significant as well (p = 0.0001)

From the whole pool of data (1885 visual fields), only 50 observations contained values lying more than 6 dB above the normal ones. A slight negative correlation (R = −0.2) was found between the number of those values and the number lying below the normal values.

Discussion

The comparisons between global and selective retests prove that in automated perimetry there exists the phenomenon of the regression toward the mean When retests are performed at test locations which are out of normal range, the outcomes of the retests, in the average, are closer to normal. This fact is illustrated by the increasing MS and the decreasing NP in the retest, compared to MS and NP of the first phase If a global retest is performed, the contrary is true· MS is lower and NP is higher in the second phase. An explanation for this fact could be the fatigue effect, which probably is greater in pathologial visual fields than in normals, in agreement with the differences for MS and NP which were presented above.

The results show that selective retests can distort visual field outcomes in the sense described above, and this even more in pathological than in normal visual fields. This means that there is, especially in pathological cases, a risk of overlooking visual field damage that, apparently, can have quite severe consequences. One could object that these results are based upon one-sided retests only and expect that double-sided retests – where values lying above the normal values would be retested as well – would compensate for the differences found in this study. The influence of the very small number of above normal values is negligible in a statistical analysis When considering an individual case, double-sided retests would also not correct the regression effect, due to the negative correlation between above and below-normal values

There is a further problem when doing selective retests which arises in follow-up examinations· There are not necessarily the same test locations to be retested because of the short- and long-term fluctuations in the visual field This would impede the comparability of follow-up examinations

In view of these results, one can conclude that to obtain as objective an impression as possible of a visual field, we should avoid selective retests It is better to retest every test location or none, as it is done e g. in the Octopus glaucoma program G1 [3].

Detailed results of this study will be published elsewhere [6].

References

1 Flammer J, Drance SM, Jenni A, Bebie H: JO and STATJO: Programs for investigating the visual field with the Octopus automated perimeter Can J Ophthalmol 18: 115–117 (1983)
2 Flammer J, Drance SM, Augustiny L, Funkhouser A: Quantification of glaucomatous visual field defects with automated perimetry Inv Ophthalmol & Vis Sci 26: 176–181 (1985)
3 Flammer J, Jenni A, Bebie H, Keller B: The Octopus glaucoma program G1 (in print)
4 Hays WL: Statistics for the social sciences Holt, Rinehart and Winston, Plymouth, 1977, p 627
5 Jenni A, Flammer J, Funkhauser A, Fankhouser F: Special Octopus software for clinical investigations Doc Ophthalmol Proc Series 35: 351–356 (1983)
6 Rutishauser Ch, Flammer J: Selective versus global retests in automated perimetry (in preparation)

Author's address:
Charlotte Rutishauser,
University Eye Clinic, Inselspital,
CH-3010 Berne, Switzerland

IX.14 Binocular threshold campimetry in the amblyopic syndrome

G.P. FAVA, P. CAPRIS, M. FIORETTO and E GANDOLFO
Genova, Italy

Abstract

A binocular static campimetric study was carried out on normal and amblyopic subjects. The examination was performed without any device to separate the individual perception of each eye. Comparison between the light threshold levels, monocular and binocular conditions, revealed an increase of sensitivity in binocular vision both in normal and amblyopic subjects, suggesting a valid cooperation between the two eyes also in monocular amblyopia.

Introduction

In order to study binocular vision both in normal and amblyopic subjects, perimetry had been utilized by numerous authors [1, 2, 3, 4, 7, 8, 9, 10, 12]. Several different methods have been suggested to separate the perception of the two eyes: colored filters, polarized filters, Bagolini's striated glasses and phase difference haploscopy.

The dissociating effect of such systems is extremely variable and only in some cases it is possible to consider it of modest importance. Moreover, a particularly good cooperation is required from the subject to obtain reliable responses

We have set up a perimetric method based on the comparison between monocular and binocular static thresholds in normal and amblyopic eyes In this manner we have avoided the artificial separation utilized by several other authors for separating the perception of each eye [5, 13].

Kinetic perimetric investigations of monocular and binocular vision in strabismus were carried out without dissociating devices, utilizing the Goldmann perimeter [11].

In the present study, we used a projection campimeter based on the Goldmann Standards, that required only slight accomodation and convergence due to the great distance between the screen and the patient's eye (2 meters) [6].

Materials and methods

Thirty subjects, whose ages ranged from seven to fourteen years, were examined. Ten were normal, ten were affected by anisometropic amblyopia, and ten by strabismic amblyopia, with a visual acuity better than 0.6.

For every subject, after a routine ophthalmological and orthoptic examination, static threshold determinations along the 0–180° and the 0–90° hemimeridians were performed

Thresholds were tested in the fixation point and at every three degrees of eccentricity first under monocular circumstances and then under binocular conditions. In a second phase of the study the threshold was retested, in normal subjects, stimulating only one eye, while in front of the other one a mirror reflecting a section of the screen was positioned

All perimetric tests were performed using the giant projection campimeter of Grignolo-Tagliasco-Zingirian [6]. This instrument, derived from previous prototypes, consists of a concave hemispherical screen, with a radius of 200 cm. and a width of 200 cm, corresponding to 30° of eccentricity. The same light source provides luminance for both background and target, so that contrast constancy is guaranteed The background luminance can be set to values ranging from definitely photopic to scotopic values The luminance values of the target are those of the Goldmann perimeter, while continuous regulation is possible. The surfaces of the target correspond in angular value to those of the Goldmann perimeter, and retain their nominal value The fixation point is obtained by projecting on the centre of the back-ground a circular-shaped target whose diameter can be varied. To explore the central threshold, a particular pattern is projected which consists of four radially arranged oblique segments, ranging from 2° to 10° in eccentricity.

For the evaluation of the results we calculated, for all the tested eccentricities, the mean difference between the threshold value obtained under binocular conditions, and the better one of the two obtained under monocular conditions.

Results

The comparison between the results of the monocular tests and the binocular one permitted us to formulate the following considerations:
– In normal subjects, the binocular threshold was slightly lower (better sensitivity) than in monocular conditions, considering the values of the best eye (Fig 1). This behaviour was present at all eccentricities: only in the blind spot area, in each subject, the binocular sensitivity overlapped with that of the contralateral eye. Analyzing the static profiles, only at 15° of eccentricity (i.e. in the center of the blind spot) the monocular and binocular results were equal, while outside of this point the binocular sensitivity progressively increased, in comparison with the monocular threshold profiles As a consequence of this
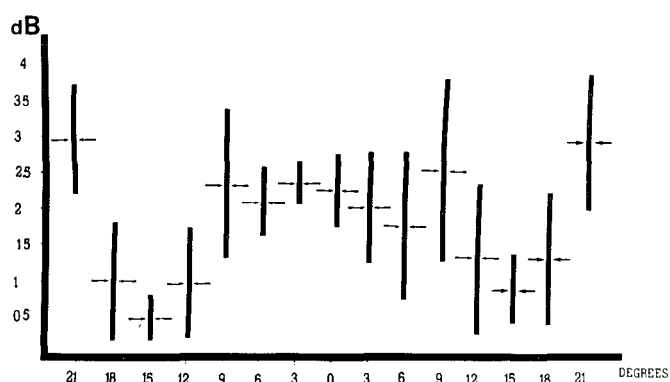
Figure 1 Normal subjects [10]
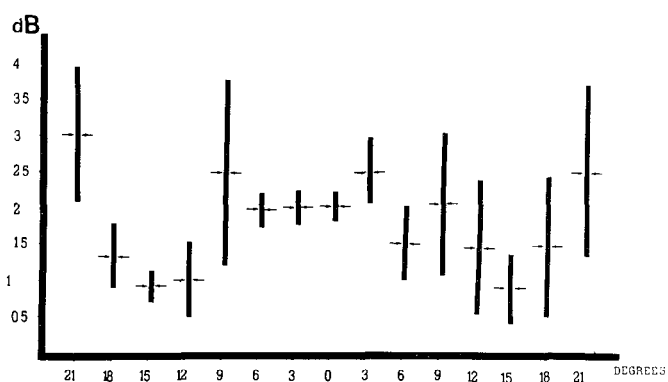
Figure 2 Anisometropic amblyopic subjects [10]
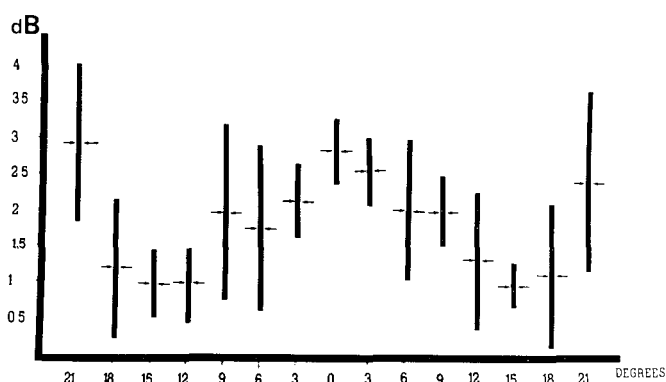
Figure 3 Strabismic amblyopic subjects [10]

636

fact, the static binocular profiles presented two symmetric depressions between 9° and 21° of eccentricity, due to the presence of the blind spots.
- The monocular retest, performed by using the mirror in front of the non-stimulated eye, confirmed the results obtained with monocular occlusion.
- In amblyopic subjects a similar increase of light sensitivity was detected in binocular vision. No significant differences were found in comparison with normals.

Such a behaviour was present also in those areas in which monocular tests showed a depression in the static profile with the characteristics of an amblyopic scotoma, as described in the literature. No significant difference was found between the two kinds of amblyopia

Conclusions

In normal subjects light sensitivity is better, even if only slightly, under binocular conditions than under monocular conditions.

The absence of a sensitivity increase in the blind spot area suggests that the threshold improvement observed is due to a bilateral summation phenomenon.

The monocular test performed after the positioning of a mirror in front of the non-examined eye, confirms the hypothesis that the sensitivity improvement in binocular vision acts through mechanisms other than inhibitory phenomena due to eye occlusion.

In amblyopic subjects the summation phenomena are evident, too.

These facts suggest the presence of a valid cooperation between the two eyes, at least as far as light sensitivity is concerned. The binocular sensitivity increase is not proportional to the performance of the amblyopic eye, which cooperates in a way that has no relation with its own visual acuity.

References

1 Bagolini B, Campos EC: Binocular campimetry in small-angle concomitant esotropia Doc Ophthalmol Proc Series 14: 405–409 (1977)
2 Bagolini B: Vision binoculaire dans les esotropies à petite angle (demonstration campimétrique et électrophysiologique) Bull Soc Belge Ophthalmol 196: 7–18 (1981)
3 Bisio RA, Capris P, Terrile R, Fava GP: Perimetria binoculare mediante vetri striati di Bagolini Indicazioni e limiti Boll Oculist 63: Suppl 11/12: 319–324 (1984)
4 Brewitt H, Honegger H, Peppendieck N: Gesichtsfeld Prüfung bei monokularer und binokularer Fixation A v Graefes Arch Ophthalmol 206: 11–15 (1978)
5 Capris P, Fava GP: Esplorazione del campo visivo binoculare mediante soglie statiche G It Ortott e Tec Strum Oft 9: 153–156 (1982)
6 Capris P, Spinelli G, Zingirian M: Comparing continuous and stepwise luminance variation in static campimetry using the Grignolo-Tagliasco projection campimeter Int Ophthalmol 8: 55–58 (1985)

7   Dubois-Poulsen A: The enlargement of the blind spot in binocular vision Doc Ophthalmol Proc Series 19: 423–426 (1979)

8   Engel FL: Visual cospicuity, directed attention and retinal locus Vision Res 11: 563–576 (1971)

9   Fava GP, Capris P, Bisio R, Fioretto M: L'ambliopia da inibizione e da anopsia: studio perimetrico e campimetrico Boll Oculist 63: Suppl 11/12: 325–333 (1984)

10 Levi DM, Ronald S, Harwerth, Ruth EM: Suprathreshold spatial frequency detection and binocular interaction in strabismic and anisometropic amblyopia

11 Mahendrastari R, Verriest G: Monocular and binocular visual fields in different types of strabismus Doc Ophthalmol Proc Series 42: 507–509 (1985)

12 Merzav V: Perimetry of suppression scotomas with phase difference haploscopy Doc Ophthalmol Proc Series 14: 399–403 (1977)

13 Zingirian M, Molfino A, Levialdi S, Trillo M: Monocular and binocular responses to liminal and subliminal stimuli Ophthalmologica 162: 41–50 (1971)

Authors' address:
FAVA G P ,
Via dei Landi 10/23, Genova, Italy

IX.15 Centro-coecal field examination in chronic alcoholism

P BRUSINI, P. DAL MAS, G. DELLA MEA, C. TOSONI and B. LUCCI
Udine, Italy

Abstract

The Humphrey Field Analyzer automatic perimeter was employed to examine the differential luminosity threshold of the centro-coecal area in 33 alcoholic patients with normal visual acuity. A specific grid custom test was designed for this purpose. The results were compared with values found in a control group of 50 normal subjects of the same age. In 39.4% of patients one or both eyes showed a significant reduction in sensitivity in the examined area, probably due to sub-clinical optic nerve damage.

The static computerized centro-coecal field examination seems to be a valid test for the identification of sub-clinical involvement of the optic nerve in chronic alcoholism.

Introduction

Retrobulbar optic neuritis is a relatively common complication in chronic alcoholism [8]. Thiamine and vitamin B 12 deficiency appears to have a more determinant role in the development of optic neuropathy than the toxic effects of alcohol; tobacco abuse, which is often connected with alcoholism, also being an important factor.

While manifest optic neuritis poses no diagnostic problems, little is known about the sub-clinical involvement of the optic nerve in chronic alcoholism [1, 4] Early optic nerve damage can be identified through visual evoked potentials [4, 7, 9, 10, 11] and by means of colour vision [5, 10] and contrast sensitivity examination [3, 12]. Manual and automatic static perimetry has also been employed to study initial losses in the visual field in retrobulbar optic neuritis [7, 9, 10, 11].

The growth of automatic computerized perimetry now allows us to carry out accurate and reproducible examinations under rigorously standardized conditions. This eliminates any possibility of human testing error, due to operator

subjectivity. The aim of this research is to study the centro-coecal area in a group of chronic alcoholics with good visual acuity by means of an automatic threshold perimeter in order to enable the early diagnosis of sub-clinical optic neuritis.

Materials and methods

64 eyes were tested from 33 different patients (26 male and 7 female) ranging from 29 to 68 years of age (average 44.7) They all suffered from 'pathology and alcohol-related disabilities', according to the definition given by the WHO [2]. 19 of them were smokers (57 6%) and 11 (33.3%) showed signs of peripheral neuropathy. In each of the cases taken into consideration the visual acuity was 20/20 and the fundus examination and the intraocular pressure were normal.

A control group of 61 eyes from 50 normal subjects, from 29 to 67 years of age (average 43.4), was also examined All the subjects were divided into 3 groups according to age (<40, from 40 to 50 and >50 years of age).

The visual field examination was carried out with the aid of the Humphrey Field Analyzer, a fully automatic, static projection-type perimeter, complete with various suprathreshold and threshold programs [6]. Special custom tests can be designed for the study of specific areas in the visual field.

For the centro-coecal area examination we designed a grid of 50 points with a 3° interstimulus space (Fig. 1) The stimulus size was 4 mm² (III Goldmann) with a background luminance of 31.5 asb The full threshold strategy was used. At each point the stimulus brightness is changed in steps of 0.4 log. unit until the first reversal. The process then changes direction at steps of 0.2 log. unit until the second reversal.

A double-threshold measurement is automatically carried out in the points which differ by more than 0.4 log unit from the expected value. The results are expressed in decibels (Figs 2, 3). The average test time is 8 minutes. The following were taken into consideration for each test: 1) foveal threshold; 2) mean threshold (sum of the values obtained in the fifty points tested/50; 3) mean threshold of
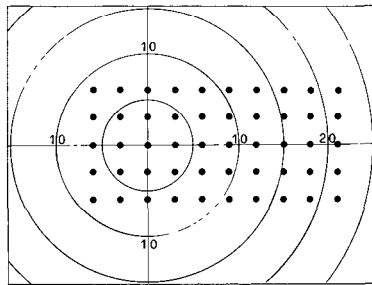
Figure 1 Arrangement of test locations for the centro-coecal field examination (Grid Custom Test)
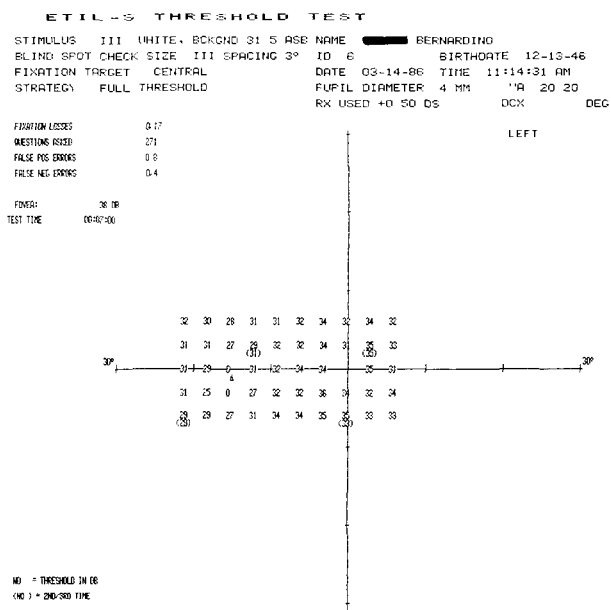
Figure 2 Example of results in a normal subject (foveal threshold = 38; mean threshold = 30 6; mean threshold of points on 0–180° meridian = 29 5; No of points depressed >10 dB = 2)
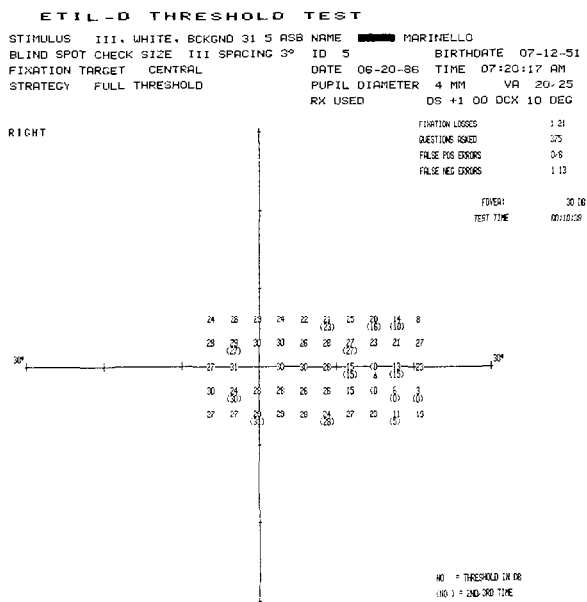
Figure 3 Example of results in an alcoholic patient with sub-clinical optic neuritis (foveal threshold = 30; mean threshold = 22 7; mean threshold of points on 0–180° meridian = 22 8; No of points depressed >10 dB = 7)

the 10 points along the 0–180° meridian, 4) number of points with a sensitivity reduction >10 decibels compared to the mean threshold.

When there were different results with the double-threshold measurement, the average of the 2 values was taken. Any results which fell within ± 2.0 SD of the mean values obtained from the control group were considered normal, taking into account the age of the subject. Student's t-test was used for the statistical analysis of the results.

Table 1 Results in normal subjects (mean values in dB ± 1 SD)

Age (years)	No of eyes	Foveal threshold	Mean threshold	Mean thr mer 0–180°	No of points depressed >10 dB
<40	20	37 1 ± 1 7	29 8 ± 1 3	29 4 ± 2 0	3 1 ± 1 1
40–50	22	36 3 ± 1 8	28 6 ± 1 8	28 0 ± 2 2	4 0 ± 1 4
>50	19	35 6 ± 2 8	27 8 ± 1 7	27 2 ± 2 5	3 2 ± 1 0

Table 2 Results in alcoholic patients (mean values in dB ± 1 SD)

Age (years)	No of eyes	Foveal threshold	Mean threshold	Mean thr mer 0–180°	No of points depressed >10 dB
<40	22	37 3[a] ± 1 7	29 2[a] ± 1 2	28 9[a] ± 2 1	3 6[a] ± 1 3
40–50	27	34 3[c] ± 3 3	28 1[a] ± 2 6	27 4[a] ± 2 8	3 3[a] ± 1 3
>50	15	35 1[a] ± 2 4	26 1[b] ± 3 0	25 0[b] ± 2 8	4 7[b] ± 2 6

Statistical significance vs corresponding normal values: a = not significant; b = p<0 05; c = p<0 02

Table 3 Eyes with abnormal values in alcoholic patients

Age (years)	No of eyes	A foveal threshold*	%	A mean threshold*	%	A mean threshold meridian 0–180°*	%	A No of points depressed >10 dB*	%
<40	22	0	–	2	9 1	2	9 1	1	4 5
40–50	27	6	22 2	4	14 8	4	14 8	0	–
> 50	15	1	6 7	4	26 7	2	13 3	5	33 3
Total	64	7	10 1	10	15 6	8	12 5	6	9 4

* No of eyes   A = abnormal

Results

The mean values from the normal subjects are recorded in Table 1. A slight loss of sensitivity with increasing age can be noted. The mean values from the alcoholics and the statistical significance of the differences as compared to normal subjects of the same age, are recorded in Table 2.

The abnormal values taken from the alcoholics are recorded in Table 3. In total, 17 eyes from 13 different patients showed one or more abnormal values. 8 of these patients were smokers (61.5%) and 5 (38.5%) showed signs of peripheral neuropathy.

Discussion and conclusions

The analytical study of the differential luminosity threshold in centro-coecal area in alcoholic patients with normal visual acuity shows in almost 40% of the subjects a significant alteration in at least one of the parameters studied. The most sensitive appears to be the mean threshold (abnormal in 15.6% of the eyes tested), followed by the mean threshold of the points on the horizontal meridian (12.5%), the foveal threshold (10.1%) and the points depressed >10 dB (9 4%).

The very high specificity of the test makes it relatively easy to distinguish between the normal and the pathological results A limitation of this test is the necessity of a good co-operation on the part of the patient, which is not always readily forthcoming from an alcoholic

The sensibility appears to be good and can be compared to that of the colour vision test. In a small sample group of 12 alcoholic patients (24 eyes) the Farnsworth 100 Hue test showed significant changes in 9 eyes (37 5%); in the same group the centro-coecal field examination gave abnormal results in 8 eyes (33.3%). A comparative research programme is now in progress, making use of the VEP, whose high level of sensitivity in optic neuropathy has already been demonstrated The presence of peripheral neuropathy, tobacco abuse, drug usage and the co-existence of other diseases are important factors which should be taken into account in valuating the development of optic neuropathy. However, the static computerized perimetry in the centro-coecal area is a valid test to identify the initial sub-clinical involvement of the optic nerve. In this way it is possible to collect useful information on the conditions of the patient and on the follow-up.

References

1   Dally S, Dephus S, Delvert S, Buisine A, Hispard E, Girre C: Névrites optiques alcooliques infra-
    cliniques sans carences vitaminiques J Fr Ophthal 8: 345–348 (1985)

2   Edwards G, Gross MM, Keller M et al : Alcohol-related disabilities, p 32 Offset publ, World Health Organization, Geneve, 1977
3   Foulds WS: Optic nerve function in the toxic amblyopias and related conditions Doc Ophthalmol Proc Series 26: 269–278 (1981)
4   Franck H, Meyer F, Bronner A: Les potentiels évoqués visuels dans le diagnostic précoce de la névrite optique alcoolo-tabagique (Comparaison de deux méthodes de stimulation, damier et flash) Bull Soc Ophthalmol Fr 80: 1067–1070 (1980)
5   Francq P, Piérart P, Verriest G: Résultats d'épreuves de la vision des couleurs chez les alcooliques et chez les malades mentaux Bull Belge Ophtalmol 186: 73–86 (1979)
6   Heijl A: The Humphrey Field Analyzer, construction and concepts Doc Ophthalmol Proc Series 42: 77–84 (1985)
7   Ohnuma T, Tagami Y, Isayama Y: Visual fields versus visual evoked potentials in optic nerve disorders Doc Ophthalmol Proc Series 35: 239–244 (1983)
8   Saraux H, Labet R, Biais B: Aspects actuels de la névrite optique de l'étilique Ann Ocul 199: 943–954 (1966)
9   Van Dalen JTW, Spekreyse H, Greve EL: Visual field (VF) versus visual evoked cortical potential (VECP) in multiple sclerosis patients Doc Ophthalmol Proc Series 26: 79–83 (1981)
10 Wildberger H: Neuropathies of the optic nerve and visual evoked potentials with special reference to color vision and differential light threshold measured with the computer perimeter Octopus Doc Ophthalmol 58: 147–227 (1984)
11 Wildberger H: Zum Nachweis der zentralen Empfindlichkeitsverminderung bei Optikus-Neuropathien mit der Computerperimetrie (Octopus) und mit den visuell evozierten Potenzialen (VEP) Klin Mbl Augenheilk 184: 377–381 (1984)
12 Wildberger H: Zur Untersuchung erworbener Störungen des Kontrastsehens und der Farbwahrnehmung bei milden Optikusneuropathien Klin Mbl Augenheilk 186: 194–199 (1985)

Authors' addresses:
Brusini P, Dal Mas P, Della Mea G, Tosoni C,
Divisione Oculistica,

Lucci B,
Divisione Neurologica,

Ospedale Civile, 33100 Udine, Italy

IX.16 The effect of miosis on visual field indices

F.S. MIKELBERG, S.M. DRANCE, M. SCHULZER and K. WIJSMAN
Vancouver, Canada

Abstract

Visual field examination is important in monitoring patients with glaucoma. It is necessary to determine whether deterioration in the field of vision is due to glaucoma or other factors. A prospective study to determine the relationship of change in pupillary size to the visual field indices in 22 eyes of 22 normal volunteers was performed. All individuals were tested using Octopus program G1 after having received two drops of placebo or thymoxamine eye drops in random order. Statistical analysis consisted of correlating changes in pupil size with corresponding changes in the visual field indices after adjustment for placebo values by proportionate adjustments. Proportionate change in pupil size was strongly positively correlated with proportionate change in mean sensitivity. No other significant relationships were found.

Introduction

Visual field examination is important in monitoring patients with glaucoma Therapeutic decisions are often made on the basis of the assessment of deterioration in the field of vision. It is important to determine whether such change in the field of vision is due to deterioration in the glaucomatous state or due to extrinsic factors. Some factors which effect the field of vision are pupil size, the adequacy of the refractive correction, and lens clarity The pupil diameter can affect the clarity of the retinal image through diffraction and refraction. As the pupil diminishes the refractive effect sharpens the retinal image however diffraction acts to degrade the image. The eyes optimal performance occurs at a pupil size of 2.4 millimeters [5].

Decrease in pupil size causes less illumination of the retina. This change may be enough to shift the retinal adaptation from photopic to mesopic or mesopic to scotopic. Greve described a normal 20 year old subject in whom a change of the

pupil diameter from six millimeters to two millimeters produced no noticeable influence on the level of the sensitivity curve [3] De Natale et al. have described a patient in whom total sensitivity loss, expressed in decibels as measured with Octopus Program 31, varied from 450 decibels with a pupillary diameter of one millimeter to 259 decibels with a pupillary diameter of 4.5 millimeters [1], McCluskey et al. have recently demonstrated a statistically significant correlation of percent change in pupillary area with percent change in visual field area with pilocarpine induced miosis [4]. Because the determination of change in the field of vision is so important in the management of patients with glaucoma we performed a prospective study to determine the relationship of change in pupillary size to the visual field indices previously described by Flammer et al. [2].

Materials and methods

Twenty-two eyes of 22 normal volunteers were studied. Their age ranged from 24 to 67 years with a mean of 46.7 ± 14.0. All individuals were tested using Octopus Program G1. The mean sensitivity, mean defect, corrected loss variance, and short term fluctuation were calculated [2]. The mean sensitivity is the sum of all the threshold measurements divided by the number of loci tested. The mean defect is the mean deviation of the patient from the normal age corrected values stored in the Octopus computer. In normals it is scattered around zero. The corrected loss variance is an index of the local nonuniformity of the visual field defect. It also hovers around zero in the normal individual or when the visual field is uniformly depressed. It is increased with localized field loss. The short term fluctuation is the scatter observed during one visual field test All eyes were tested on two separate occasions, thirty minutes after having received two drops of either placebo or thymoxamine 0.5% at 5 minute intervals. The order of testing with placebo or thymoxamine was determined randomly Pupillary diameter was measured using a millimeter rule. Statistical analysis consisted of correlating changes in pupil size with corresponding changes in the visual field indices after adjustment for untreated (placebo) values by proportionate adjustments.

Results

The mean untreated (placebo) and thymoxamine values for pupillary diameter, mean sensitivity, mean defect, corrected loss variance, and short term fluctuation are summarized in Table 1. The untreated (placebo) pupil diameter ranged from two to ten millimeters whereas after thymoxamine it ranged from one to seven millimeters.

Change in visual field indices and pupillary diameter was defined as the untreated (placebo) value minus the value after thymoxamine instillation.
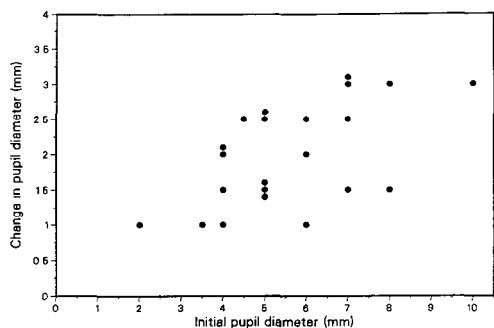
Figure 1 Scattergram illustrating the relationship between initial pupil diameter and change in pupil diameter after thymoxamine drops

We regressed the change in visual field indices on the change in pupillary diameter. No significant relationship was found We noted however that the change of the pupillary diameter was highly correlated with the untreated (placebo) diameter of the pupil (r = 0 59, p = 0.0021). (Figure 1)

We therefore re-expressed the changes in pupil diameter as well as in the visual field indices as proportionate changes relative to the corresponding untreated (placebo) level of the parameters. With this technique we found a highly significant positive relationship between change in pupillary diameter and change in mean sensitivity (r = 0.70, p = 0.0019). Figure 2 No significant relationships were found between the proportionate change in the mean defect, corrected loss variance, or short term fluctuation and the proportionate change in pupil diameter. The addition of age as a covariate did not show a significant relationship in this analysis. Similar analysis were performed correlating visual field indices with pupil area. The proportionate change in mean sensitivity was highly correlated with proportionate change in pupil area (r = 0 52, p = 0.0083).

Table 1 Means of pupil diameter and visual field indices

	Placebo	Thymoxamine	Change (Placebo-Thymoxamine)
Pupil diameter (mm)	5 6 ± 1 8	3 6 ± 1 5	2 0 ± 0 7
MS (dB)	27 8 ± 1 6	27 3 ± 1 9	0 5 ± 0 9
MD (dB)	0 10 ± 1 09	0 65 ± 1 29	−0 55 ± 0 96
CLV (dB)^2	1 5 ± 0 7	1 8 ± 1 0	−0 3 ± 0 8
SF (dB)	1 3 ± 0 2	1 4 ± 0 2	−0 1 ± 0 3

MS = Mean Sensitivity, MD = Mean Defect, CLV = Corrected Loss Variance, SF = Short Term Fluctuation
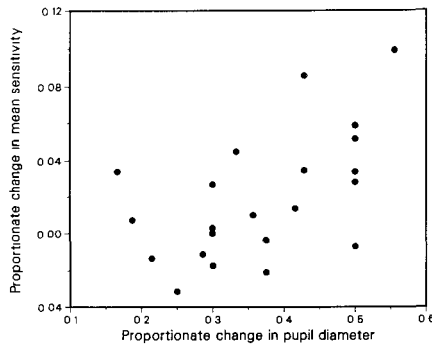
Figure 2 Scattergram illustrating a highly statistically significant positive relationship between the proportionate change in pupillary diameter and the proportionate change in mean sensitivity The regression formula is proportionate change in mean sensitivity equals $-0\ 04825 + 0\ 20940 \times$ proportionate change in pupillary diameter

Discussion

In order to determine true change in the visual field in patients with glaucoma the effect of changes in pupillary diameter must be understood. Although simple regression of change in pupillary diameter on change in the visual field indices does not show any statistically significant relationship it is of interest that when the effect of initial pupil size is taken into account that a statistically significant relationship does exist between change in pupil diameter and change in mean sensitivity. Proportionate change in pupil size is positively correlated with proportionate change in mean sensitivity. Because equal changes in pupil size are proportionately greater with small pupils, greater proportionate changes in mean sensitivity will tend to occur in individuals with small pupils Pupil size must be carefully noted in assessing individuals for the presence of change in the visual field defects

Acknowledgement

References

1 De Natale R, Glaab-Schrems E, Krieglstein GK: The prognosis of glaucoma investigated with computerized perimetry Documenta Ophthalmologica 58: 385–392 (1984)
2 Flammer J, Drance SM, Augustiny L, Funkhouser A: Quantification of glaucomatous visual field defects with automated perimetry Invest Ophthalmol Vis Sci 26: 176–181 (1985)

3 Greve EL: Simple and multiple stimulus static perimetry in glaucoma; the two phases of perimetry Documenta Ophthalmologica 36: 1–346 (1973)

4 McCluskey DJ, Douglas JP, O'Connor PS, Story K, Ivy LM, Harvey JS: The effect of pilocarpine on the visual field in normals Ophthalmology 93: 843–846 (1986)

5 Tate Jr GW: Physiological basis for perimetry In: Drance SM, Anderson DR, (eds): Automatic perimetry in Glaucoma, pp 1–29 A practical guide Grune and Stratton, Orlando, 1985

Authors' address:
Dr F S Mikelberg,
Department of Ophthalmology,
St Paul's Hospital,
1081 Burrard Street,
Vancouver, B C , V6Z 1Y6, Canada

IX.17 Spectral sensitivities on a white background as a function of retinal eccentricity

K. KITAHARA, A. KANDATSU, R TAMAKI and H MATSUZAKI
Tokyo, Japan

Abstract

The spectral sensitivities for a 1°, 200-ms test flash on a white background were studied for up to 15° from the fovea on two normal observers as a basis for color perimetry. The results showed the usual three maxima of sensitivities, about 430 nm, 530 nm and 610 nm, at the fovea. However, the two peaks above 480 nm gradually decreased with increasing retinal eccentricity and at the 15° temporal retina, the curve showed one broad maximum in the region above 480 nm. That is, no R/G opponent color system could be detected However, the peak at about 430 nm remained prominent even at 15° from the fovea.

   As a result, to study the opponent system outside the fovea, the sensitivity measurements when using a 1° test flash with green and red test lights on a white background are not appropriate, while the sensitivity measurements for a blue (say, λ max = 430 nm) test on a white background might be useful in assessing clinial cases by means of color perimetry

Introduction

It has been found that the spectral sensitivity curve for a low temporal frequency test on an intense white background shows three peaks which are at about 440 nm, 530 nm and 610 nm. The peak near 440 nm can be accounted for by the action of a single class of cones that contain a photopigment with peak absorption at 445 nm (P_{445}) without interaction with another class of cones The narrowed peaks above 500 nm have been attributed to linear subtractive interaction between the cones containing a photopigment with absorption at 540 nm (P_{540}) and at 570 nm (P_{570}) [2, 5, 6]. King-Smith, Kranda & Wood [1] and later on others applied this technique to demonstrate a selective loss of opponent system in clinical cases.

   In this experiment, the spectral sensitivities for a 1°, 200-ms test flash on a white

background were studied for up to 15° from the fovea. As a result, it was determined that sensitivity measurements on a white background are useful in detecting opponent color channels even outside the fovea.

Method

A two-channel Maxwellian view optical system with a 150 watt xenon arc as a light source was used in this experiment A 1° diameter circular test light was superimposed in the center of an 8° circular 'xenon white' background field. Narrow-band (6 to 10 nm half-band width) interference filters were used for the test light which was exposed for 200 ms every two seconds.

Measurements were made on the right eye of two normal male trichromats. Their pupils were dilated with 1% tropicamide. The biting board was adjusted at each eccentric position in order to allow the test and background light to pass directly through the center of the pupil. Prior to measurements the observers were adapted to the background for 5 min and test thresholds on this adapting field were measured along the horizontal meridian in the temporal retina for up to 15° from the fovea at least five times for each test wavelength.

Results

Fig. 1 illustrates the spectral sensitivities on a white background of luminance 1000 td for observer A.K. (on the left) and T.O. (on the right) The test sensitivities (log photons^{-1}sec deg^2) were plotted as a function of wavenumber (cm^{-1}). The curves for both observers obtained at the fovea are positioned absolutely in units of log photons^{-1}sec deg^2. Each successive curve is displaced downward by 1.0 log unit for clarity The results at the fovea showed the usual three maxima of sensitivities, about 430 nm, 530 nm and 610 nm. The solid lines are the fits of the single opponent red/green (R/G) model: $|P_{540}(\lambda)-kP_{570}(\lambda)|$ proposed by Thornton & Pugh [6]. The values of k were 1.4 for both observers. For this prediction, the relative spectral absorption characteristics of cones proposed by Smith & Pokorny [4] were used. However, the two maxima in the long wavelength region gradually decreased with an increase in retinal eccentricity and at 15° temporal retina for both observers the curves above 480 nm showed only one broad maximum with shapes similar to that of a CIE photopic curve.

It has been said that the three maxima at the fovea become more prominent with an increase in the intensity of the background. Therefore, we experimented using a higher intensity background to determine whether or not the three maxima could be detected outside the fovea. Fig 2 shows the spectral sensitivities for a 1°, 200-ms test flash on 1000, 10,000 and 100,000 td white backgrounds
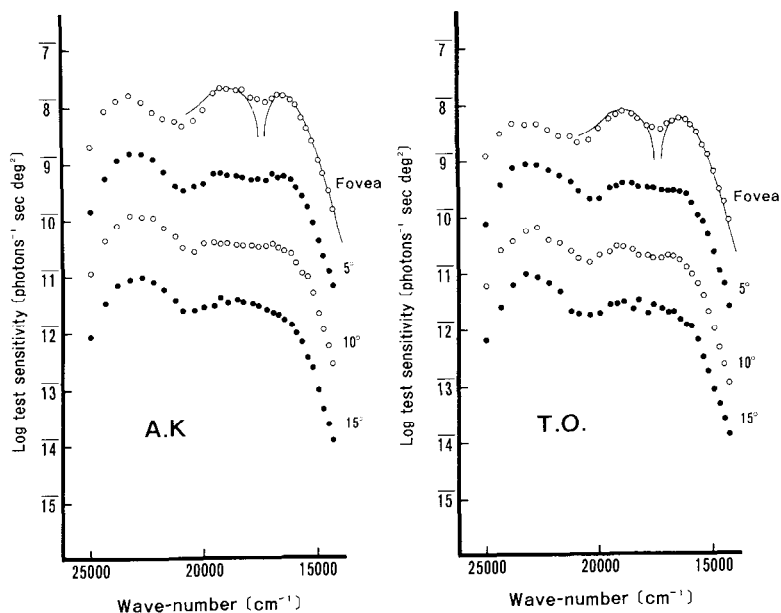
Figure 1 The spectral sensitivities for a 1°, 200-ms test flash on a 1000 td white background for observer A K (on the left) and T O (on the right) The test sensitivities (log photons⁻¹ sec deg²) were plotted as a function of wavenumber (cm⁻¹) Each successive curve is displaced downward by 1 0 log unit for clarity The solid lines are the fits of the single opponent (R/G) model: $| P_{540} (\lambda) - k P_{570} (\lambda) |$ proposed by Thornton & Pugh [6]
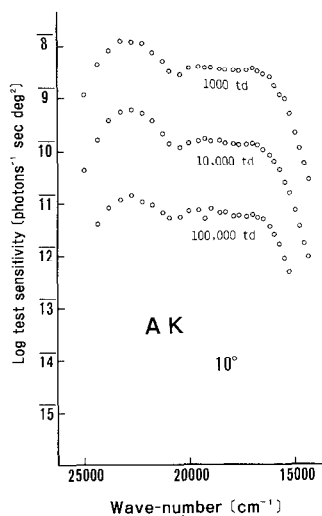
Figure 2 The spectral sensitivities for a 1°, 200-ms test flash on 1000, 10,000 and 100,000 td white backgrounds measured at 10° temporal retina for observer A K Each successive curve is displaced downward by 0 5 log unit for clarity

measured at 10° temporal retina for observer A.K. Each successive curve is displaced downward by 0.5 log unit for clarity. Even with the higher intensities of the background, the sensitivities above 480 nm showed characteristics similar to those obtained on a 1000 td background.

Discussion

The spectral sensitivities for 1°, 200-ms test flash on a white background were studied for up to 15° from the fovea. The data from both observers showed the same tendency of change, that is, the results at the fovea showed the usual three maxima of sensitivities, and the single opponent R/G model proposed by Thornton & Pugh [4] can account for the data reasonably well. However, the two maxima in the long wavelength region gradually decreased with increasing retinal eccentricity At the 15° temporal retina the curve above 480 nm shows the only one broad peak. That is, these two maxima which accounted for the R/G opponent color system at the fovea could not be detected even with the higher intensity of the background. However, below 500 nm the prominent peak attributed to the action of a single class of cones containing P_{445} could be detected even at the 15° temporal retina. Similar results were reported by Kuyk [3] when the spectral sensitivities for a 1° test flash on a 1000 td white background were measured extrafoveally at 20°, 30° and 40° As a result, to study the opponent system outside the fovea, the test sensitivity measurements when using a 1° test flash with green and red test lights on a white background are not appropriate, while the test sensitivity measurements for a blue test light with a maximum wavelength at about 430 nm on a white background might be useful in assessing clinical cases by means of color perimetry

Acknowledgement

References

1 King-Smith PE, Kianda K, Wood ICJ: An acquired color defect of the opponent-color system Invest Ophthalmol 15: 584–587 (1976)
2 Kianda K, King-Smith PE: Detection of coloured stimuli by independent linear systems Vision Res 9: 733–745 (1979)
3 Kuyk TK: The effects of stimulus size and retinal location of the increment-threshold spectral sensitivity of humans Invest Ophthal Vis Sci Suppl 19: 136 (1980)
4 Smith VC, Pokorny J: Spectral sensitivity of the foveal cone photopigments between 400 and 500 nm Vision Res 15: 161–171 (1975)

5 Sperling HG, Harwerth RS: Red-green cone interactions in the increment-threshold spectral sensitivity of primates Science 172: 180–184 (1971)

6 Thornton JE, Pugh Jr EN: Red/green color oppornency at detection threshold Science 219 191–193 (1983)

Authors' address:
Kenji Kitahara,
Dept of Ophthalmology,
The Jikei University School of Medicine,
19-18 Nishi-Shinbashi 3-chome, Minato-Ku, Tokyo, Japan

IX.18 Population study of global and local fatigue with prolonged threshold testing in automated perimetry

C.T. LANGERHORST, T.J.T.P. VAN DEN BERG, E. VELDMAN
and E.L. GREVE
Amsterdam, The Netherlands

Abstract

In 144 subjects (normals, ocular hypertensives, other glaucoma suspects and glaucoma patients) we investigated whether the fatigue-phenomenon that occurs during prolonged static threshold testing could be a useful diagnostic tool On average the glaucoma patients had higher fatiguability than the other groups, but there was a large overlap between the 4 groups of subjects. We did not find a relation between fatigue and pathologic condition within the visual field It seems unlikely that fatigue testing will become important for the detection of early glaucomatous damage.

Introduction

The *FATIGUE*-phenomenon that we have studied is the decrease of differential light sensitivity during more than 15 minutes continuous visual field testing in automated static perimetry. Enoch [2] proposed fatigue measurements to differentiate between glaucoma and other diseases of the optic nerve. He used a method rather different from our technique, which is not dealt with here. The literature dealing with the effect of prolonged perimetric testing on the behavior of the differential threshold in normal and glaucomatous subjects, has reported that glaucomatous visual fields might be more prone to fatigue than normal fields [3, 4, 5]. On the basis of a larger population we wanted to study whether this effect can be useful as a diagnostic tool. We examined a total of 144 subjects with two fatigue techniques in order to get an answer to the following questions·
- Is there a difference in fatigue between glaucoma patients and normals, or glaucomatous visual field areas and normal areas?
- Does fatigue testing help to detect early loss of visual function in ocular hypertensives or glaucoma suspects?
- Does the technique of testing i.e. localized versus more global testing influence the results?

Materials and methods

We examined 144 subjects divided over four groups·

group 1.   Normals: visual acuity ≥0.5, Intraocular pressure (IOP) ≤22 mm Hg, normal optic disc, no visual field defects, no other known eye disease

group 2   Ocular Hypertensives· as normals but IOP>22 mm Hg.

group 3.   Glaucoma Suspects· no visual field defects but suspect disc and/or glaucoma in the other eye, and/or family history of glaucoma. No IOP criteria.

group 4.   Glaucoma Patients: Primary Open Angle Glaucoma with visual field defects

We used two different fatigue testing techniques, both executed with the Scoperimeter automatic perimeter [1]. The stimulus duration was 0.1 sec.

– *Global fatigue* a threshold program of 60 locations within the 25° visual field was measured 5 times in succession without a break, totalling 30 minutes of continuous testing. Fatigue was defined as the loss of mean sensitivity in dB/hour. It was computed for the whole field, and for different areas of the visual field (upper half, lower half, central part, pheripheral part).

– *Local fatigue:* thresholds were tested with an up-down strategy at 4 different locations in the visual field between 5° and 15° of eccentricity for 20 minutes continuously In glaucoma patients the locations were chosen in such a manner as to be in normal area, in a defect or close to a defect. In the other groups we tested at either 5° and 15° or at 15° only. The presentations in the 4 locations were given in random order. For each location the fatigue value in dB/hour was defined as the slope of a straight line through the threshold values at each

Table 1 Number of subjects and their mean age for each group and each technique of fatigue testing

	Normals	Ocular Hypertensives	Glaucoma Suspects	Glaucoma Patients	Total number and age
Global fatigue only	Number 11	0	14	9	34
	Age 64 8 ± 4 3		61 1 ± 14 5	68 7 ± 9 3	64 3 ± 10 9
Local fatigue only	Number 16	18	4	6	44
	Age 40 9 ± 17 9	63 6 ± 13 3	54 8 ± 7 8	66 8 ± 5 7	55 0 ± 17 7
Both global and local fatigue tested	Number 17	8	20	21	66
	Age 59 9 ± 7 9	61 5 ± 8 6	63 3 ± 12 9	61 8 ± 8 7	61 7 ± 9 8
Total Number and age	44 54 2 ± 15 7	26 62 9 ± 11 9	38 61 6 ± 13 1	36 64 3 ± 8 8	144

moment in time. The slope values of the 4 locations were also averaged per subject (mean local fatigue).

The number of subjects in each group is shown in Table 1, as well as the mean age and fatigue technique used.

Results

– *Comparison between groups.* Figure 1 shows the distribution for the 4 groups of three representative fatigue scores, i.e global central (ie the mean over the 4 positions at 2° eccentricity), global whole field and mean local fatigue. The distributions show considerable overlap. The mean fatigue-values for the glaucoma group are the greatest except for central global fatigue values (Table 2). This reaches significance at the 5% level for the mean local values
– *Comparison local vs global fatigue.* We compared mean local and global whole field values for those subjects investigated with both techniques. Although the scatter was appreciable, there is a significant correlation ($r = 0\ 48$). The mean local fatigue is twice as large as the global fatigue.
– *Coherence of fatigue behavior within the visual field.* For the global fatigue we found a rather good correlation between fatigue of the upper and lower half of the visual field ($r = 0.82$). No correlation was found between the 4 central locations and the whole field scores. The correlation between mean local and individual local fatigue scores showed an $r = 0.81$
– *Age-dependency of fatigue behavior.* We computed the regression lines of

Table 2 Mean and standard deviation of the global central, global whole field and mean local fatigue values for the 4 different groups, expressed in dB/hour

	Central global fatigue	Whole field global fatigue	Mean local fatigue
Normals	$-3\ 6 \pm 5\ 1$ dB/hour	$-4\ 2 \pm 6\ 5$ dB/hour	$-6\ 4 \pm 8\ 5$ dB/hour
Number of subjects	28	28	34
Ocular hypertensives	$-0\ 6 \pm 2\ 3$	$-2\ 6 \pm 2\ 5$	$-7\ 6 \pm 8\ 3$
Number of subjects	8	8	34
Glaucoma suspects	$-2\ 4 \pm 4\ 5$	$-4\ 2 \pm 5\ 2$	$-11\ 0 \pm 10\ 4$
Number of subjects	34	34	24
Glaucoma patients	$-3\ 4 \pm 6\ 8$	$-6\ 3 \pm 6\ 2$	$-16\ 9 \pm 9\ 0$
Number of subjects	30	30	28
Significance of differences between pairs	n s	n s	glaucoma versus all other 3 groups

660
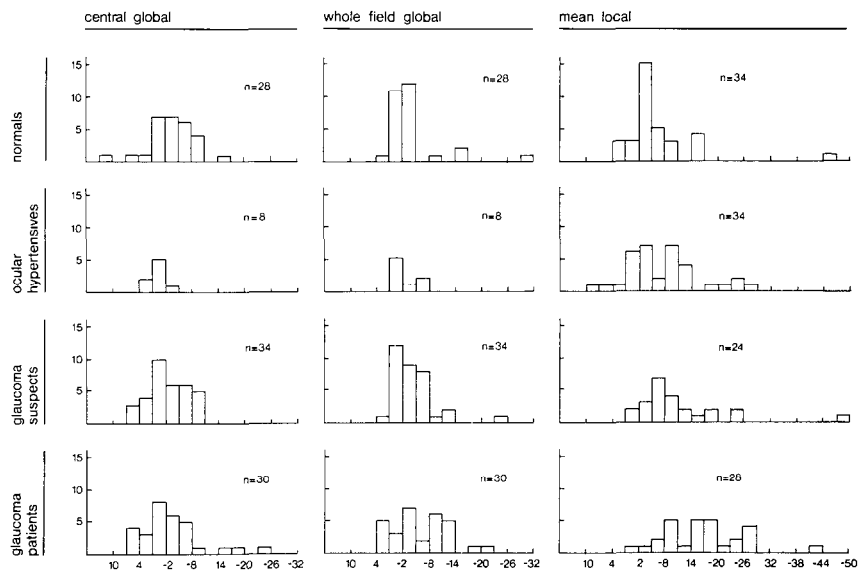
Figure 1 Frequency distribution of global central, global whole field, and mean local fatigue values for the 4 different groups The X-axis shows the fatigue values in dB/hour The Y-axis the number of subjects per interval

global and of local fatigue vs age and found a small but significant age-dependency of −0 18 and −0 17 dB/hour per year of age respectively. There was no difference in age dependency between groups.
− *Relation between local fatigue and pathology in glaucomatous visual fields.* We compared the local fatigue scores of positions in normal visual field areas, positions situated close to a defect, and positions in relative defects As shown in table 3, we found no difference in fatigue behavior.

Table 3 Relationship between local fatigue and pathology in glaucoma patients; fatigue expressed in dB/hour

POAG	Mean local fatigue	Mean local fatigue adjusted for age	Standard error
Location in normal field area	−0 28	−0 28	0 03
Location near defect	−0 26	−0 26	0 04
Location in defect	−0 31	−0 30	0 03
Probability		n s	

Discussion

Our results in this larger population generally confirm the findings reported in the literature [2, 3, 4] in that local fatigue is in the mean higher in glaucoma patients than in normals, ocular hypertensives or glaucoma suspects. Our results also show such a difference for the global fatigue, though this did not reach the 5% significance level. This could indicate that glaucoma suspects (including ocular hypertensives) with a high fatigue score have more chance of actually having some early form of glaucoma This interesting possibility however has several practical problems. In our suspects we found a fatigue distribution which was not different from the normals. This might be understood in the following way· suppose that the suspect-population consists of two subpopulations, one that will never develop glaucoma and one that will develop glaucoma. The second sub-population can be assumed to be much smaller. Suppose further that the two subpopulations have the same fatigue characteristics as the normal and glaucoma-groups respectively Since the glaucoma subpopulation is small and its fatigue characteristics not much different from that of the normal population, it is not to be expected that the suspect group as a whole shows a behavior clearly different from normal. Another question is whether in the glaucomatous distribution the low fatigue scores occur in early stage glaucomas and the high scores in late stage glaucoma or not Only if the glaucoma fatigue distribution is also valid as a whole for early cases, could fatigue be used as an early diagnostic test. However, in practice it will remain a test with low sensitivity, because of the large overlap of fatigue scores between groups. In order to find out whether one fatigue para-meter could be used as representative for the whole field, we looked at the coherence of the visual field We found good coherence between the upper and lower half of the visual field. There could be a certain eccentricity dependency, as suggested by the lack of correlation between the central and whole field scores We will have to analyse our data further to see whether there might be a gradual change in fatigue toward the periphery of the visual field

In one respect our results differ from the literature: we found no relation between local fatigue and the location in, near to, or away from a defect in 27 glaucoma patients.

Holmin and Krakau [4] reported that fatigue may increase as the stimulus duration decreases, especially in relative defects. Our stimulus duration was 0.1 sec. compared to their 0.5 sec. The absence of a difference of fatigue-values in normal and defect areas in our study cannot have been underestimated because of the stimulus duration

Conclusions

- The mean local fatigue is twice as high as global fatigue.
- There is considerable overlap in global as well as local fatigue between the four groups, however the glaucoma group has higher mean fatigue values.
- Fatiguability seems to be for a large part a behavior of the visual field as a whole, judging by the correlation between global upper and lower field fatigue values, and between mean local and individual local values. The central visual field may be an exception.
- There is a slight age-dependency, not different between groups.
- Local fatiguability in POAG patients does not seem to depend on the condition of the tested location.
- Our results do not allow us to advocate fatigue measurements as a diagnostic tool. Moreover the fatigue examinations were rather exacting for the patient. Of course the fatigue-phenomenon could be of importance as a cause of fluctuation in perimetry.

Acknowledgement

References

1 De Boer RW, Van den Berg TJTP, Greve EL, de Waal BJ: Concepts for automatic perimetry, as applied to the Scoperimeter, an experimental perimeter Int Ophthalmol 5: 181–191 (1982)
2 Enoch JM, Berger R, Birns R: A static perimetric technique to test receptive field properties: extension and verification of the analysis Doc Ophthalmol 29: 127–153 (1970)
3 Heijl A: Time changes of contrast thresholds during automatic perimetry Arch Ophthalmol 55: 696–708 (1977)
4 Heijl A, Drance SM: Changes in differential threshold in patients with glaucoma during prolonged perimetry Brit J Ophthalmol 67: 512–516 (1983)
5 Holmin C, Krakau CET: Variability of glaucomatous field defects in computerized perimetry Graefes Arch clin + exp Ophthalmol 210: 235–250 (1979)

Author's address:
Eye Clinic of the University of Amsterdam,
Academic Medical Center,
Meibergdreef 9,
1105 AZ Amsterdam, The Netherlands

IX.19 The correlation of the physiological blind spot and the disc area

R.J. BRITTON, S.M DRANCE, G.R DOUGLAS and M SCHULZER
Vancouver, Canada

Abstract

Peripapillary crescents of choroidal atrophy occur commonly in patients with glaucoma [6], particularly in those with low tension glaucoma [4] and may indicate the part of the optic nervehead that seems to be susceptible to glaucomatous damage [1]. It has been suggested that the absence of a peripapillary choroidal atrophy may indicate a more resistant optic nervehead in which much higher levels of intraocular pressure elevation are required to produce damage. In such resistant discs it is thought that the damage may be manifested by a generalized enlargement of the cup with diminution of the neuroretinal rim indicating diffuse as opposed to localized damage of the nerve. It has not yet been worked out whether peripapillary atrophy occurs as an acquired change together with localized damage, or whether it constitutes a congenital misalignment which makes the tissue more susceptible to the subsequent effects of intraocular pressure. Peripapillary crescents were found to be more common in patients with glaucoma than in normal controls or ocular hypertensives [7] Some degree of peripapillary chorioretinal atrophy was even reported to be present in all cases of glaucoma [3].

Peripapillary choroidal atrophy also occurs in myopia and is known to occur with age. It has not yet been shown whether the area of peripapillary choroidal atrophy changes with aging, but changes in the peripapillary choroidal crescents in glaucoma are known to occur.

Not all peripapillary crescents are alike as there are several tissue layers which can overlap in a variety of ways. The details of these variations may be important as they may denote various factors that make optic nerveheads susceptible. Such dfferences have not yet been clearly analyzed.

It was the purpose of this paper to correlate the size of the optic nervehead with the size of the physiological blind spot and to see whether the relationship between them breaks down with age which might indicate a change of size of the peripapillary chorioretinal atrophy with aging.

Methods

One eye of 97 normal people was studied. All of the subjects had a visual acuity of 6/6 or better; intraocular pressures less than 21 mm Hg; normal visual fields (Humphries screening program 120, sixty degrees, Octopus Program 7 or Goldmann perimetry performed by the modified Armaly technique), absence of anterior segment pathology on slit lamp examination, normal retinal examination including an absence of focal defects on retinal nerve fibre layer photography. The ages of the subjects were between twenty and eighty-one years. No exclusions were made on the basis of refractive error. In binocularly normal individuals, only one eye was selected for study on a random basis.

All eyes had their axial length measured by ultrasound and the refraction was ascertained Photography with a Zeiss 30° fundus camera, with an Allen stereo separator in both colour and black and white were obtained. Black and white prints were englarged to a 1 : 9 negative to print magnification. The area of the discs was determined by computerized planimetry. The measurement of the disc of each eye was corrected for the magnification of that eye, using its axial length and refraction according to the method described by Littman [5], and software supplied by Dr. Alanko, Department of Ophthalmology, Oulu, Finland.

The area of the disc was defined as the area that lies inside the inner circumference of the white scleral lip, best identified in the colour stereo photographs. Where the scleral rim was obscured by blood vessels or a thick nerve fibre layer, it was usually easy to extrapolate between well identified points.

All blind spots were plotted on an Oculus perimeter by the principal investigator. The blind spot was plotted with a 10 minute stimulus and 1000 apostilbs of illumination. The instrument was carefully calibrated before each use. At least fifteen blind spot boundary locations were determined using a static technique every degree from the centre of the blind spot outwards. The resultant blind spot was projected on to a screen using an acetate sheet and photographic enlarger to achieve a 4.5 times magnification. The blind spot area was then planimetrized with the computerized planimeter.

Results

The size of the blind spot was closely related to the size of the disc area corrected for the magnification of the eye ($R = .70$, $P = .000$) (Fig 1). The blind spot area had a slightly negative relationship with age which was not significant statistically at the 5% level of confidence ($R = -19$, $P = .062$) (Fig. 2).

Figure 1. N= 97 R= 0 70 P= 0 000

Disc Area (mm2)

4 2, 3 6, 3 0, 2 4, 1 8, 1 2

80 160 240 320 400
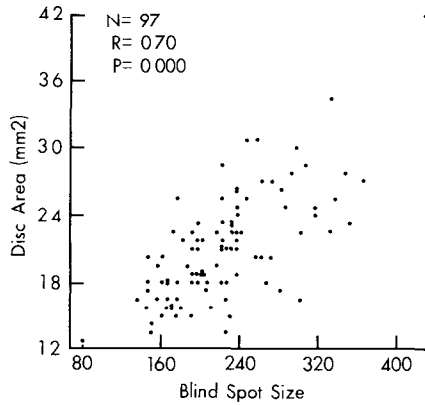
Blind Spot Size

Figure 1 Scattergram showing the linear relationship between the blind spot size and the disc area

Figure 2. N= 97 R= −019 P= 0 062

Blind Spot Area

420, 350, 280, 210, 140, 70

21 35 49 63 77

Age (yrs)
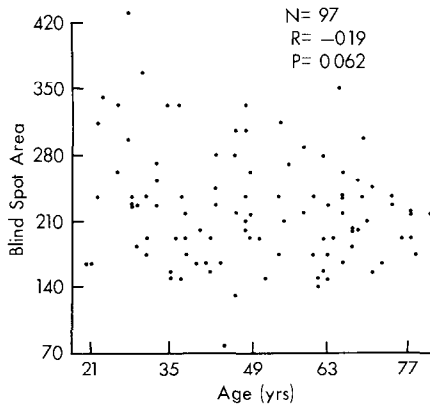
Figure 2 Scattergram showing the lack of relationship between the blind spot area and age

Discussion

In view of the obvious relationship of a peripapillary choriodal atrophy with the localized forms of disc damage in chronic open angle glaucoma and low tension glaucoma, it is possible that in some individuals these peripapillary chorioretinal disturbances may be acquired. It is known that chorioretinal peripapillary atrophy occurs in old normal individuals and it is therefore important to be able to determine whether the aging process itself increases the size of the peripapillary choriodal atrophy and whether the glaucomatous process accelerates this enlargement. It may be that some congenital chorioretinal misalignments may in fact remain stationary throughout life while in others acquired peripapillary atrophy may mimic the congenital appearances. The present study shows a good

correlation between the size of the optic nervehead and the physiological blind spot which was expected, but we also showed no relationship between the blind spot size and age and previous studies [2] showed that there was also no relationship between the disc area and age. It may well be that our present perimetric methods do not allow for subtle acquired changes in the peripapillary chorioretinal atrophy to be detected. The occurrence of such acquired changes would have resulted in the breakdown of the correlation between the physiological blind spot and the normal optic nervehead with age.

References

1 Anderson DR: Correlation of the peripapillary anatomy with the disc damage and field abnormalities in glaucoma In: Greve EL, Heijl A (eds) Fifth Int Visual Field Symposium Dr W Junk Publishers, Dordrecht, 1983
2 Britton RJ, Drance SM, Schulzer M, Douglas GR, Mawson DK: The area of the normal neuroretinal rim In preparation
3 Heijl A, Samander C: Peripapillary atrophy and glaucomatous visual field defects In: Heijl A, and Greve EL (eds) Proceedings of the 6th Int Visual Field Symposium Dr W Junk Publishers, Dordrecht, 1985
4 Laatikainen L: Fluorescein angiographic studies of the peripapillary and perilimbal regions in simple, capsular and low-tension glaucoma Acta Ophthalmol, Supplementum 111, (1981)
5 Littman H: Zur Bestimmung der wahren Grösses eines Objektes auf dem Hintergrund des lebenden Auges Klin Mbl Augenheilkd 180: 286–289 (1982)
6 Primrose J: The incidence of the peripapillary halo glaucomatosus Trans Ophthalmol Soc UK 89: 585–587 (1969)
7 Wilensky JT, Kolker AE: Peripapillary changes in glaucoma Amer J Ophthalmol 81: 341–345 (1976)

Authors' address:
University of British Columbia, Vancouver, B C , Canada

IX.20 Anomalous visual response in Tourette's syndrome

J.M ENOCH, G.L. SAVAGE and V LAKSHMINARAYANAN
Berkeley, U.S.A.

Abstract

Because haloperidol, a dopamine antagonist, is often successfully used in Tou-
rette's syndrome, this condition is commonly thought to involve an anomaly of
dopamine neurotransmission. It is also believed that the human retina contains
dopaminergic amacrine, interamacrine, and interplexiform cells Since these
retinal cells could represent the neural substrate of the psychophysical transient-
like response, we conducted a detailed visual study of a Tourette's patient. Our
subject is a 23-year-old male who has been on haloperidol medication since being
diagnosed as having Tourette's syndrome at age 10. He exhibited very good visual
acuity, essentially normal visual fields, and steady fixation.

Quantitative layer-by-layer perimetric testing was performed at fixation and
different parafoveal eccentricities. All loci tested revealed normal sustained-like
response. The transient-like response was often subnormal at 10 degrees eccen-
tricity for random, noncongruous loci in each eye. During a brief gastrointestinal
illness which caused interruption of his haloperidol medication, the patient's
transient-like response became supranormal at certain affected test sites. These
same data points became subnormal responses after the patient resumed therapy.

Introduction

In recent years there has been great interest in the analysis of neurotransmitter
substances and their role in vision and other central nervous system processes.
Much evidence has accumulated implicating dopamine as a neurotransmitter in
the retina. It is present in certain amacrine, interamacrine and interplexiform
cells [1–5, 8–10]. As our knowledge about the role of dopamine in visual process-
ing is limited, a key question to ask is, 'are there functional visual effects due to
anomalies of the dopamine system in the retina?'.

The quantitative layer-by-layer perimetric techniques developed by Enoch and

co-workers (e.g., references 6,7) provide means by which one can study local anomalies affecting discrete retinal response mechanisms. A psychophysical test cannot test one cell or groups of cells, but in its design, it can be biased in such a manner as to greatly excite a specific set of cells or functional responses at specific loci along the visual pathway. Thus, layer-by-layer test techniques offer a means of testing for anomalous retinal responses in patients exhibiting local anomalies of the dopamine system. Prof. John Dowling of Harvard University encouraged this research group to pursue this particular avenue of research.

We present preliminary results based upon a year-long, in-depth study and analysis of a patient manifesting Guy de la Tourette's syndrome. Tourette's syndrome is often controlled successfully by haloperidol, a butyrophenone derivative, known to be a dopamine antagonist. Because of this, it is thought that this condition is (at least, in part) an anomaly of the dopamine system.

Tourette's syndrome and subject

Tourette's patients often exhibit intermittent jerky head and body movements and an affliction known as coprolalia, i.e , a periodic or steady stream of obscenities and invectives. As noted, haloperidol, a dopamine antagonist, is used to treat this condition.

Our subject was a twenty three-year old white male in good physical condition. He had been on haloperidol therapy for his condition for many years. He manifested remarkably good visual acuity (20/15$^+$ O.U.), near normal visual fields and good fixation. He manifests the typical symptoms described above.

Method

The layer-by-layer perimetry test battery includes two tests of spatial interaction which probe different aspects of inner retinal function [6, 7]. These two operationally defined tests are: (a) the sustained-like test (also known as the Westheimer effect) and (b) the transient-like test. The sustained-like test measures the desensitizing and sensitizing effects of a steady bright background superimposed and centered upon a smaller, flashing test stimulus [11]. Since the sustained-like test results were essentially normal in the present study and in related cases, we will discuss only the method and results of the transient-like tests which were found to be affected in this patient.

A rotating windmill (Maltese cross) stimulus is particularly effective in eliciting responses which are most probably biased towards cells in the inner plexiform layer of the retina. Responses to this test have been shown to be anomalous in patients with known inner retinal pathology (e.g., [6, 7]). This test pattern specifically elicits responses from cells responding to onset and offset of this
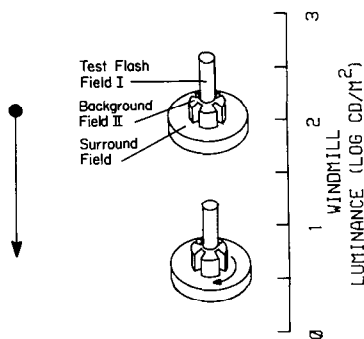
Figure 1 The transient-like test paradigm

spatially distributed stimulus. This test paradigm is shown in Figure 1.

After correcting refraction to the cupola surface at the point tested, the threshold at this test locus is determined for Field I, a small pulsed (200 msec, two times per second) target. The luminance of Field I is then increased by 0.8 log units above threshold and the projected windmill target is superimposed. Field I, at the adjusted setting, is now brought to threshold by varying the luminance of the stationary windmill target (Field II). Field III (the surround field) is maintained at 31.5 apostilbs (10 cd/m²). The threshold determination is then repeated with the windmill rotating. The difference in threshold found ranges from 0 4 to 1.0 log units in normal eyes in the central (radial 15°) field area and is found to be reduced or eliminated in anomalies or diseases of the inner plexiform layer. The greater distance the stimulus pattern is located from fixation, the larger the magnitude of the threshold difference in normal observers (Fig 2). The measured threshold difference (windmill not rotating minus windmill rotating) is called the transient-like function.
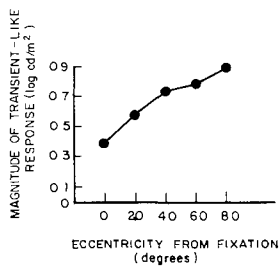
Figure 2 The magnitude of the transient-like function increases as a function of eccentricity of the test array from point of fixation Data points obtained from normal observers
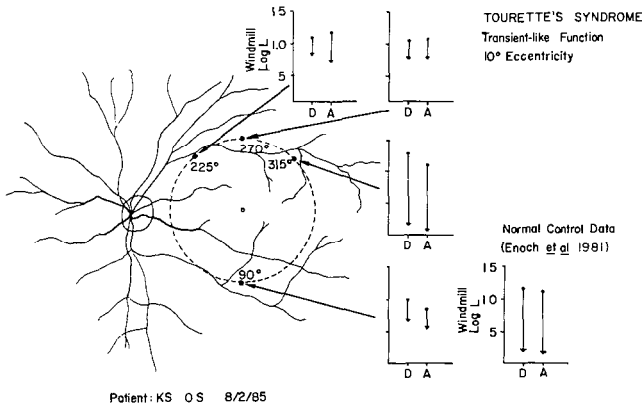
Figure 3 Sample transient-like funtion obtained from the subject with Tourette's syndrome Patient was *on* haloperidol at time of testing Note subnormal responses Control subject data at the same eccentricity [7]

Results

The subject was tested at numerous visual field loci in a radial zone of about 20° about fixation in both eyes. At many locations *outside* the fixation point, the transient-like function was found to be either reduced or essentially absent (e.g., Fig. 3). Both eyes exhibited markedly reduced transient-like responses in an idiosyncratic manner. These points were not located in congruent or equivalent areas in the two eyes and occurred in both halves of the visual field. The vertical did not serve as divider. This pattern of irregular responses was found to be stable over a period of several months.

When haloperidol therapy was interrupted for a week due to gastrointestinal
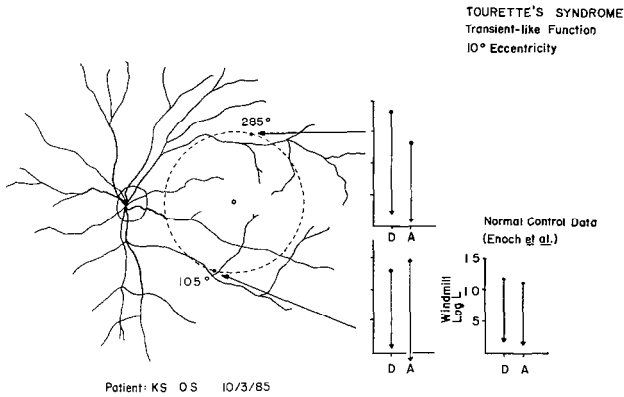
Figure 4 Transient-like functions from the same subject when he was *off* haloperidol Note supranormal responses
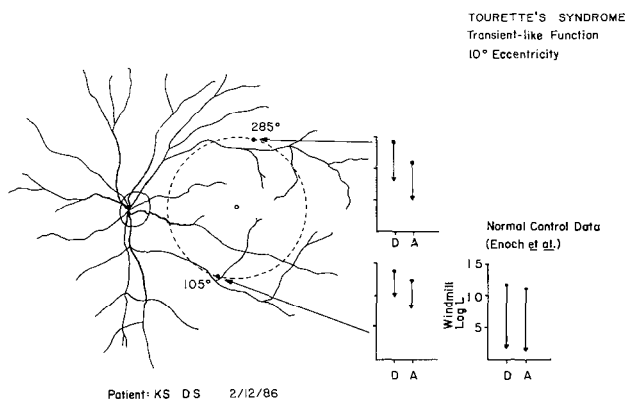
Figure 5 Transient-like functions at same loci as in Fig 4 Data were taken more than one month after subject resumed haloperidol medication

distress, within a few days the subject showed a *supranormal* transient-like function at several test points near those which previously exhibited subnormal functions (Fig. 4). Such supranormal effects have not been reported previously for this test. Testing was resumed about one month after haloperidol therapy was resumed. When the same test loci as shown in Fig. 4 were tested, we found that the responses were again subnormal (Fig. 5)

Discussion

The distribution of reduced amplitude transient-like function responses in both eyes (described above) suggests that the measured functional effects have origin prior to the point where the input from the two eyes combines. This suggests a retinal locus for these functional changes and further supports previous analyses on the localization of the dominant response to this test paradigm

Because haloperidol, a dopamine antagonist, is effective in treatment of Tourette's syndrome, this disease process is thought to cause anomalous responses in dopaminergic cells. From these data, one might surmise that an untreated patient with Tourette's syndrome shows a *greater* than normal functional response in affected neural units. In this condition, haloperidol, apparently reduces the measured response to this test pattern at affected retinal loci

At present we are studying patients with other dopamine anomalies and/or on haloperidol therapy, e.g., Parkinson's disease, schizophrenia as well as other patients with Tourette's syndrome. Our intial results on schizophrenic subjects on haloperidol therapy also show reduced transient-like functional responses Preliminary studies on patients with Parkinson's disease (receiving L-Dopa, etc , therapy) suggest somewhat different results. It is too early to comment on these findings. We plan to pursue avidly this exciting area of study.

672

Acknowledgements

References

1 Dowling JE, Ehinger B: Synaptic organization of the dopaminergic neurons in the rabbit retina J Comp Neurol 180: 203–220 (1978)
2 Dowling JE, Ehinger B: The interplexiform cell system I Synapses of the dopaminergic neurons in the goldfish retina Proc R Soc Lond B 201: 7–26 (1978)
3 Dowling JE, Ehinger B, Floren I: Fluorescence and election microscopic observations of the amacrine accumulating neurons of the cebus monkey retina J Comp Neurol 192: 665–685 (1980)
4 Ehinger B: Connexions between retinal neurons with identified neurotransmitters Vision Res 23: 1281–1291 (1983)
5 Ehinger B: Functional role of dopamine in the retina In: Osborne NN, Chader GJ (eds) Progress in retinal research, Volume 2, pp 213–232 Pergamon Press, Oxford, 1984
6 Enoch JM: Quantitative layer-by-layer perimetry Francis I Proctor Lecture, 1977 Invest Ophthalmol Vis Sci 17: 208–257 (1978)
7 Enoch JM, Fitzgerald CR, Campos EC: Quantitative layer-by-layer perimetry: An extended analysis Current Ophthalmology Monographs, Grune and Stratton, New York, 1981
8 Jensen RJ, Daw NW: Towards an understanding of the role of dopamine in the mammalian retina Vision res 23: 1293–1298 (1983)
9 Jensen RJ, Daw NW: Effects of dopamine antagonists on receptive fields of brisk cells and directionally selective cells in the rabbit retina Neurosci 4: 2972–2985 (1984)
10 Pourcho RG: Dopaminergic amacrine cells in the cat retina Brain Res 252: 101–109 (1982)
11 Westheimer G: Spatial interaction in human cone vision J Physiol 190: 139–154 (1967)

Author's address:
Prof J M Enoch,
School of Optometry,
University of California,
Berkeley, CA 94720, U S A

Authors index